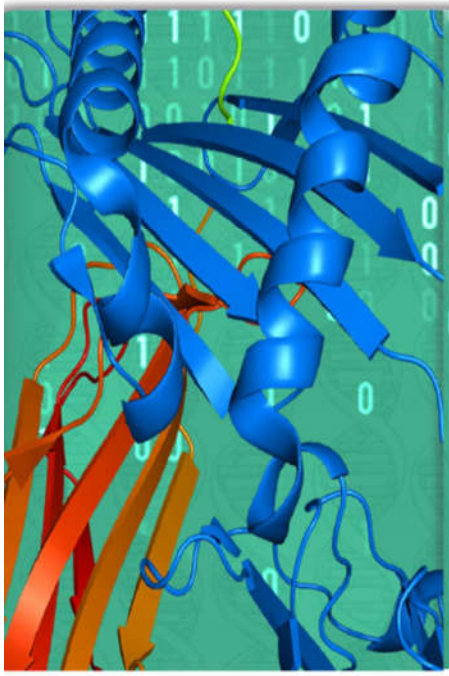

International Conference on Applications of Advanced Technologies: Biological Sciences

ICAAT 2nd

January 27-28, 2021
Namin, Ardabil, Iran

The Second International Conference on *Application of Advanced Technologies: Biological Sciences*

University of Mohaghegh Ardabili
Faculty of Advanced Technologies

1978
University of Mohaghegh Ardabili

January 27-28 2021

Namin, Ardabil, Iran

Preface

This proceeding contains papers presented at the 2nd International Conference on Applications of Advanced Technologies: Biological Sciences, Namin, Iran.

The purpose of the conference is to provide a community for academicians, scientists and engineers from various fields to share the application of their achievements in biological sciences.

Papers and posters presented at the conference and included in the proceeding are intended to provide information to both practical and theoretical researcher.

The keynote speakers were Dr. Abdolreza Mesgar, Dr. Hussein A. Ghanimi, Dr. K. Gurushankar, and Dr. Yasin Panahi.

Finally, it is appropriate that we record our thanks to our fellow members of the department of Advanced Technologies, scientific and organizing committee Dr. Arash Abdolmaleki, Dr. Araz Siabi, Dr. Hamid Safavi, Fatemeh Alizadeh, Dr. Abolfazl Bezatpour, Dr. Reza Hasanzade, Dr. Yashar Azizian, Dr Asadollah Asadi, Dr Kamel Sabahi Odlou, Payam Azizian, Latif Rezaei, and Gholamhassan Yousefi.

Each contributed paper was refereed before being accepted for publication in these proceedings. The papers were accepted for publication based on their interest, relevance, innovation, and application to biological sciences.

Dr. Farzad Sedaghati

January 2021

Contents

Committees

Conference President

Prof Aziz Habibi-Yangjeh	University of Mohaghegh Ardabili

Conference Chair

Dr. Farzad Sedaghati	University of Mohaghegh Ardabili

Scientific Committee

Dr. Farzad Sedaghati	University of Mohaghegh Ardabili
Dr. Arash Abdolmaleki	University of Mohaghegh Ardabili
Dr. Solmaz Kia	University of Mohaghegh Ardabili
Dr. Reza Hasanzade	University of Mohaghegh Ardabili
Dr Asadollah Asadi	University of Mohaghegh Ardabili
Dr Kamel Sabahi Odlou	University of Mohaghegh Ardabili
Dr. Yashar Azizian	University of Mohaghegh Ardabili
Dr. Hussein A. Ghanimi	University of Al-Ameed

Executive Committee

Dr. Farzad Sedaghati	University of Mohaghegh Ardabili
Dr. Arash Abdolmaleki	University of Mohaghegh Ardabili
Dr. Hamid Safavi	University of Mohaghegh Ardabili
Dr. Araz Siabi	University of Mohaghegh Ardabili
Dr. Maryam Moazedi	University of Mohaghegh Ardabili
Fatemeh Alizadeh	University of Mohaghegh Ardabili
Negar Azari	
Payam Azizian	

Invited Talks

Biocomposites containing bioactive glasses with potential application in wound repair and regeneration

Tina Mehrabi, Abdorreza S. Mesgar*

Biomaterials Laboratory, Division of Biomedical Engineering, Department of Life Science Engineering, Faculty of New Sciences and Technologies, University of Tehran, Tehran, Iran

*Email: asmesgar@ut.ac.ir

Abstract

The healing of burn injuries and chronic wounds associated with the prolonged hospital stay and mortality of patients following the extensive skin damages have always been among the healthcare issues. Despite the emerging of several advanced wound dressings and skin substitutes over time, shortcomings of these wound care products have led to the ongoing development of novel therapeutic strategies, specifically biomaterial-based approaches. Bioactive glasses are one of the most widely used subgroups of bioceramics that have been extensively studied for hard tissue replacement. In recent years, this class of materials has shown specific therapeutic effects on soft tissue regeneration, including skin tissue. The promising potential of bioactive glasses in distinct but overlapping stages of wound healing, including hemostasis, inflammation, proliferation, and remodeling, as well as participating in the early stages of repair with their antibacterial activity has been proved. The incorporation of bioactive glass nano/microparticles into the polymeric matrix enables the fabrication of multi-functional biocomposites, which may be used at the wound site to address the requirements of the wound healing process. This review highlights the biological effects of bioactive glasses in healing phases and summarizes the current progress of bioactive glass-containing composites in the field of wound healing.

Keywords: Biocomposites, Bioactive glass, Wound Healing, Skin Tissue Engineering.

Maternal separation induces recognition memory deficit in rats

Hussein A. Ghanimi[1, 2]* and Ali Moghimi[2]

1. College of Nursing, University of Al-Ameed, Karbala, PO Box 198, Iraq

2. Rayan Research Center for Neuroscience and Behavior, Department of Biology, Faculty of Science, Ferdowsi University of Mashhad, Mashhad, Iran

*Email: husseinalawi86@gmail.com

Abstract

Background & objectives: Maternal separation (MS) has harmful consequences on the hippocampal neurons of rat neonates. It has been reported to impair memory behaviors. Therefore, we conducted this study in order to assess the effects of MS on recognition memory deficit in the hippocampus of rat neonates.

Methods: Male Wistar rat neonates were divided into two experimental groups (n=20 in each). One group of rat neonates exposed to MS; they were reared with 1hour maternal separation (MS) for 8 consecutive days (P2-P9). On other hand, control group was reared normally.

Results: Novel object recognition task (NORT) test was used to evaluate the effects of MS on recognition memory deficit. NORT indicated that rat neonates experienced MS had long-term memory deficits ($P<0.01$).
Conclusion: The present results indicated that MS could induce recognition memory deficit in the hippocampus of rat neonate during adulthood.

Keywords: Maternal separation, hippocampus, rat, memory.

Applied Spectroscopy in Biological filed

K. Gurushankar[1], Asadollah Asadi[2], K. Chinnaiah[1], Karthik Kannan[3], Vivek Maik[4], M. Gohulkumar[5]

[1]Department of Physics, School of Advanced Sciences, Kalasalingam Academy of Research and Education, Krishnankoil, Virudhunagar, Tamilnadu - 626 126.

[2]Department of Biology, Faculty of Science, University of Mohaghegh Ardabili, Ardabil, Iran.

[3]Center for Advanced Materials, Qatar University, P O Box 2713, Qatar

[4]Research Assistant Professor, Department of Electronics & Communication Engineering, Kattankulathur Campus, SRM Institute of Science and Technology, Chennai.

[4]PG and Research Department of Physics, Vivekanandha College of Arts and Sciences for Women (Autonomous), Elayampalayam – 637 205, Tiruchengode, Namakkal, Tamil Nadu, India

*E-mail: gurushankar01051987@gmail.com

Abstract

FT-IR is a high-resolution, rapid, non-destructive analytical method that provides chemical sample formulation to classify the existence of functional groups responsible for their biological efficacy. Fluorescence spectroscopy is one of the non-invasive methods for detecting diseases and encouraging the advancement of medical diagnostic knowledge. Fluorophores have been identified by the use of applied fluorescence techniques in the microstructure and composition of biological tissues, accompanied by a description of chromophores. An optical molecular detective, Raman spectroscopy is a vibrational spectroscopic technique that has potential not only in the diagnosis of cancer but also in the understanding of disease progression. This paper discusses the contribution of spectroscopy in the present analysis and how it is very helpful in the biological field.

Keywords: FT-IR, RAMAN, Fluorescence, Natural drug

Reference gene selection to normalize RT-qPCR data

Yasin Panahi[1]

[1]Dept. of pharmacology and Toxicology, School of pharmacy, Ardabil University of Medical Sciences (ArUMS), Ardabil, Iran.

Abstract

Despite the advent of new methods for quantifying transcripts in clinical specimens, RT-qPCR is still the most widely used method. However, to control errors between samples, it is necessary to use the housekeeping gene/reference to detect this discrepancy. First, in this interactive lecture, I will try to summarize the concept of using the gene /reference in a clinical context, then I will describe the software used for this meaning. Finally, let me give you an example of what we did in childhood non-syndromic autism to discover the right reference gene.

Application of magnetic sporopollenin for magnetic dispersive solid phase extraction of sulfonamides from water samples

Mahboube Shirani*

*Department of Chemistry, Faculty of Science, University of Jiroft, Jiroft, P. O. Box 7867161167, Iran

*Email: m.shirani@ujiroft.ac.ir

Abstract

In this study, magnetic coupled with Magnetic dispersive micro-solid phase extraction was applied for simultaneous separation and preconcentration of sulfadiazine, sulfamethoxazole, and sulfamethazine and determination by HPLC-UV. The effect of important parameters including amount of magnetic sorbent, type and volume of elution solvent, extraction time, sample volume, and desorption time were assessed. At the optimum conditions, the linear ranges of 5-250 (µg L^{-1}) were for three analytes. Moreover, the LODs (S/N = 3) of 1.8, 1.6, and 1.7 (µg L^{-1}), and the LOQ (S/N = 10) of 6.1, 5.5, and 5.9 (µg L^{-1}) were acquired for sulfadiazine, sulfamethoxazole, and sulfamethazine respectively. The efficiencies of ≤ 97.3 % and the relative standard deviations of less than 3.5 % were also obtained for application of the method in complex matrixes.

Keywords: Magnetic sporopollenin, Magnetic dispersive solid phase extraction, Sulfonamides.

1. Introduction

In antibacterial implementation, sulfonamides (SAs) are widely used in human therapy and animal growth. The immense usage of SAs with inappropriate waste management would result in serious environmental problems because the SAs residues are evacuated from the waste water treatment plants and enter the aquatic environment [1, 2]. Moreover, application of SAs in animals' treatment leads to the accumulation of SAs residues in food matrices of animal origin such as water, chicken, honey, milk. The reported studies have been proved that the residual SAs have toxic impact on humans and the aquatic organisms [3]. Hence, development of a potent analytical method for sensitive and efficient separation and determination of SAs are really essential. Solid phase extraction (SPE) is one of the most common pretreatment techniques which suffers from some disadvantages such as time consuming process, consumption of large volumes of toxic organic solvents [4]. Magnetic dispersive micro-solid phase extraction (MD-µ-SPE) is one of the miniaturized forms of SPE which conquers all the SPE disadvantages which is based on the dispersion of a magnetic sorbent in the solution which accelerates the interface and the interaction of analyte and the sorbent [5, 6]. Then, the analyte would be desorbed from the sorbent and analyzed with a proper instrumental technique. In this study, sporopollenin as a natural biological polymer has been selected due its high porous structure and high adsorption capacity and surface area which definitely would lead to high potential to adsorb trace levels of analyte in the solution. Therefore, some sulfonamides including sulfadiazine, sulfamethoxazole, and sulfamethazine were preconcentrated via MD-µ-SPE and determined by HPLC in water samples.

2. Material and Methods

2.1 Chemicals

Sulfadiazine (SDZ) (≥99%, Sigma-Aldrich, USA), sulfamethoxazole (SMO) (≥98%, Sigma-Aldrich, USA), and sulfamethazine (SMZ) (≥98%, Sigma-Aldrich, USA) were prepared as sulphonamide family group. HPLC grade methanol, acetonitrile, acetone and water were purchased from Merck. Sporopollenin (Lycopodium clavatum) with particle size of 25 um was obtained from Fluka chemicals.

2.2 Instrumentation

The HPLC apparatus, having an Aliance Waters multisolvent delivery system, a manual 1177 Rehodyne injection port, and a Waters 481 variable-wavelength UV-Vis detector was set at 270 nm.(Waters Associates, Inc., Milford, MA, USA) A mobile phase consisted of methanol and phosphate buffer solution (0.05 mol L^{-1}, pH 8.0) at a ratio of 60:40 (v/v) was pumped at a flow rate of 0.6 mL min^{-1} in isocratic mode. 20 µL of analytes solution was introduced into the HPLC-UV system.

2.4 Sample preparation

Before extraction, the water samples were filtered using 0.45 mm micropore polyether sulfone membranes.

2.5 MD-µ-SPE procedure

The pH of the 10 mL sample solution was adjusted at pH 4.0 using 0.1 mol L^{-1} HCl and the ionic strength was adjusted to 5.0% (w/v) by addition of suitable amount of NaCl. Then 10 mg of the MS was added to the solution and sonicated for 4 min. Then, the MS containing the analytes was separated by an external magnet. The MS was eluted by 100 µL methanol under sonication. Methanol was evaporated to 60 µL under nitrogen process. 20 µL of methanol containing analytes was analysed with HPLC-UV.

3. Results and Discussions

2.5 Characterization

The SEM images of the prepared nanocomposite was shown in Fig. 1 in which indicates the depicts the sporopollenin with pictorial hexagonal holes and walls. Fig. 1 (b) shows the magnetic nanoparticles inside the sporopollenin holes.

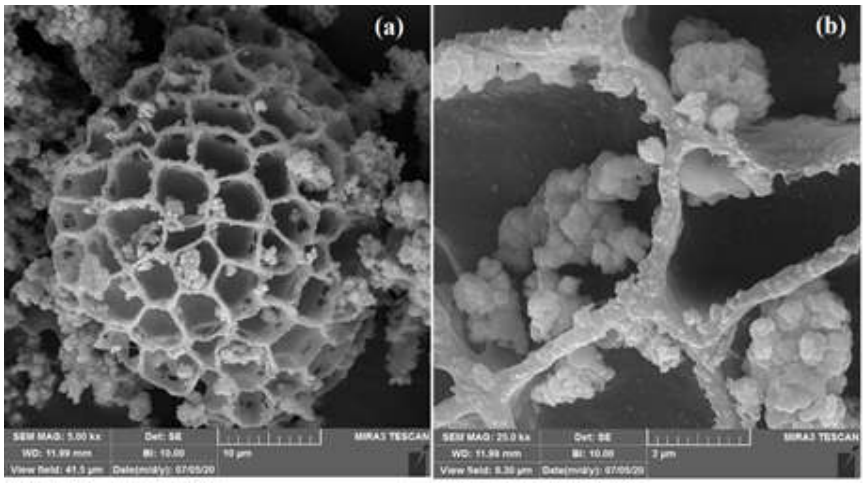

Fig. 2 The SEM-EDX images of tough outer (exine) walls of plant spores and pollen grains, a) the image of pictorial hexagonal holes and walls in MPSP nanocomposite, b) the micrograph of the magnetic nanoparticles inside the sporopollenin holes,

2.6 Optimization of the process

Sulfonamides are ampholytes which contain one basic amine group and one acidic group. The pH of sample solution plays an important role in the extraction of sulfonamides because the pH value of the solution determines the ionization status and solubility of sulfonamides. Therefore, the effect of pH value of sample solution in the range of 2–9 was investigated. sulfonamides would be slightly protonated or existed as neutral species under acidic condition and could adsorb on the MS through hydrogen bond. The maximum efficiencies were obtained at the pH of 3.

The amount of sorbent plays an important role in separation and adsorption of analyte which prepares sufficient active sites for immobilization of the analytes. The amount of MS in the range of 3-15 mg was studied and the amount of 10 mg was chosen as optimum.

The proper extraction time can provide equilibrium in the adsorption of analyte on the MS surface. In fact there should be enough time for the analyte to adsorb on the MS. Therefore, the sonication time in the range of 1-10 min was investigated and the time of 4 min was obtained as optimum.

The elution solvent volume and type are important factors. Selection of a proper elution solvent can directly affect the efficiencies of the analytes. To this aim different elution solvents including methanol, ethanol, and acetonitrile were studied and methanol had the highest extraction efficiencies. The volume of elution solvent affects the preconcentration factor and it is really noticeable. The volume of methanol in the range of 25-125 µL was considered and the volume of 100 µL could sufficiently elute the analyte from the MS with maximum efficiencies and after that the EEs were constant.

Adjustment of the ionic strength of the solution can decrease the solubility of the analyte in aqueous solution which intensifies the analyte partitioning into the extraction phase and defines as salting-out effect. The effect of NaCl concentration on the extraction of analytes was investigated in the range of 0-2 %. The EEs increase as the NaCl concentration augments to 1 % (w/v) owing to the salting-out effect. A decreasing trend is observed after 1 % (w/v) which may refer to the enhancement of the solution viscosity.

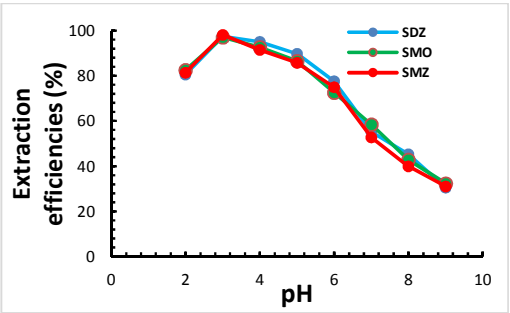

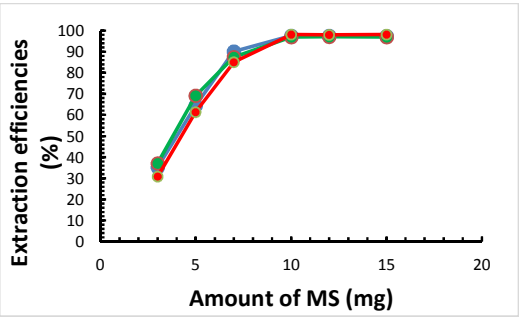

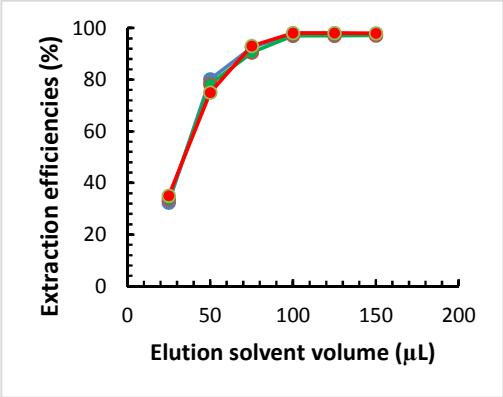

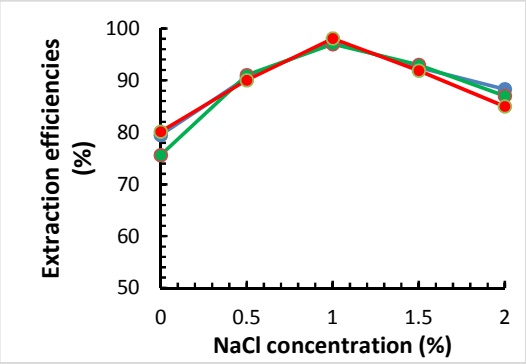

2.7 Figures of merits and method validation

The analytical performance of the method including limits of detection (LODs), limits of quantifications (LOQs), and relative standard deviations (RSDs) were evaluated at optimum conditions. The LODs (S/N = 3) of 1.8, 1.6, and 1.7 (µg L^{-1}), and the LOQ (S/N = 10) of 6.1, 5.5, and 5.9 (µg L^{-1}) were acquired for sulfadiazine, sulfamethoxazole, and sulfamethazine respectively. The efficiencies of ≤ 97.3 % and the relative standard deviations of less than 3.5 % were also obtained for application of the method in complex matrixes.

2.8 Conclusion

In this study magnetic sporopollenin was prepared as an efficient sorbent which combined with dispersive magnetic solid phase extraction for extraction of three sulfonamides from aqueous solutions. Short extraction time, ease of operation, facile extraction process, good enrichment factor, acceptable precision are the advantages of the proposed method.

Acknowledgements

The authors gratefully appreciate the Research Council of University of Jiroft.

References

[1] T. Yao, K. Du, Simultaneous determination of sulfonamides in milk: In-situ magnetic ionic liquid dispersive liquid-liquid microextraction coupled with HPLC, Food Chemistry, 331 (2020) 127342. https://doi.org/10.1016/j.foodchem.2020.127342

[2] A. Ait Lahcen, S. Ait Errayess, A. Amine, Voltammetric determination of sulfonamides using paste electrodes based on various carbon nanomaterials, Microchimica Acta, 183 (2016) 2169-2176. 10.1007/s00604-016-1850-3

[3] A. Shishov, A. Gorbunov, E. Baranovskii, A. Bulatov, Microextraction of sulfonamides from chicken meat samples in three-component deep eutectic solvent, Microchemical Journal, 158 (2020) 105274. https://doi.org/10.1016/j.microc.2020.105274

[4] F. Pourbahman, M. Zeeb, A. Monzavi, S.S. Homami, Simultaneous trace monitoring of prokinetic drugs in human plasma using magnetic dispersive micro-solid phase extraction based on a new graphene oxide/metal–organic framework-74/Fe3O4/polytyramine nanoporous composite in combination with HPLC, Chemical Papers, 73 (2019) 3135-3150. 10.1007/s11696-019-00855-1

[5] V.C. Fernandes, M. Freitas, J.P.G. Pacheco, J.M. Oliveira, V.F. Domingues, C. Delerue-Matos, Magnetic dispersive micro solid-phase extraction and gas chromatography determination of organophosphorus pesticides in strawberries, Journal of Chromatography A, 1566 (2018) 1-12. https://doi.org/10.1016/j.chroma.2018.06.045

[6] A. Chisvert, S. Cárdenas, R. Lucena, Dispersive micro-solid phase extraction, TrAC Trends in Analytical Chemistry, 112 (2019) 226-233. https://doi.org/10.1016/j.trac.2018.12.005

Possible Applications of Memristor in Bio-Amplifiers

Vahideh Sadat Sadeghi[1*]

[1] Department of Electrical Engineering, Golpayegan University of Technology, Golpayegan, Iran

*Email: vs_sadeghi@gut.ac.ir

Abstract

Memristor as the 4th passive elements in electrical circuits which relates electric charge to magnetic flux has some unique properties that makes researchers interested in using it in different electronic circuits. Smaller size, less power dissipation and more feasibility for integrity are some predicted advantages. These advantages make memristive circuits usable in different applications specially in biological applications. In this paper we presented a memristor based differential pair amplifier as the basic unit for most of the bioelectrical amplifiers.

Keywords: Memristor, Amplifier, biosignal..

1. Introduction

The usual analogue electronics uses three fundamental passive elements including resistors, capacitors and inductors . Figure.1 shows the typical characteristics of linear resistors, capacitors and inductors [1].

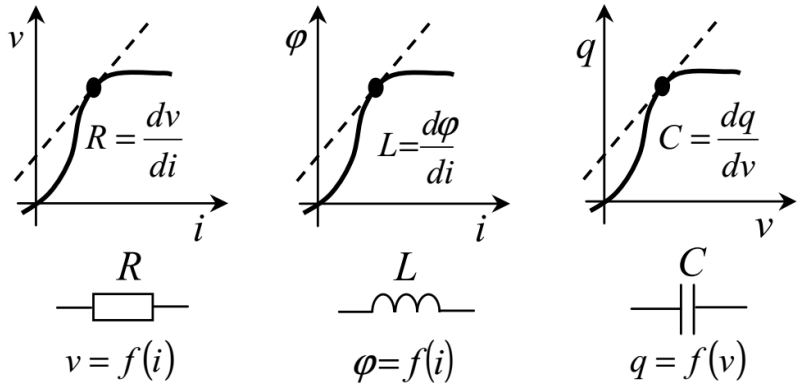

Figure 1. Typical illustration of the traditional passive element parameters [1].

according to the square symmetry, Leon Chua, accomplished the number of the elementary passive elements to four in 1971 by introducing the fourth element called memristor [2]. The basic function of memristor (Memory Resistor) is memristance M. It is a bond of the charge and the flux. In fact, the

resistance of a memristor depends on the passing charge. This fact leads to the idea of using it as a special analogue memory element which consumes no energy to conserve the information. In other words, resistance can be continuously changed within certain boundaries according to the passing current [1]. Figure 2. Shows the fundamental concept of the memristor.

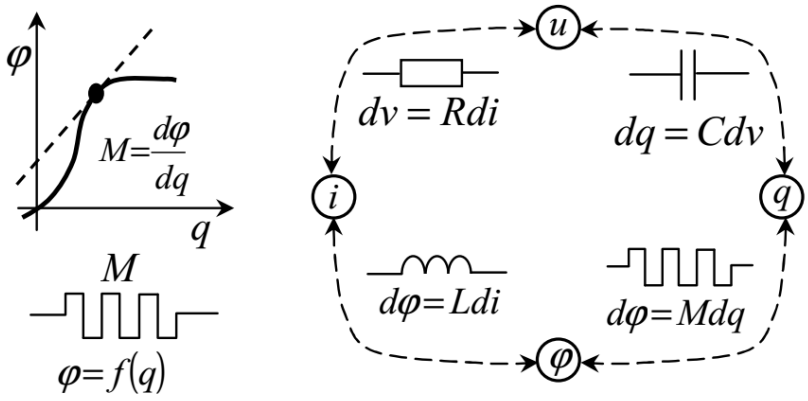

Figure 2. The memristor and a passive elements quaternion [1]

2. Material and Methods

2.1 Need for Bio-Amplifiers

Most of biological signals and especially bioelectric signals have low amplitude and low frequency. Hence, we need amplifiers to increase the amplitude level of these biosignals. ECG, EMG and any other bioelectric signals in human bodies or animals need amplifiers so-called bio amplifiers or biomedical amplifiers to be used for more analysis. There are different types of Bio Amplifiers including differential amplifiers, instrumentation amplifiers *etc.* [3].

2.2 Bio-Amplifiers Requirements

The biological amplifier should have a high input impedance value depending on the applications. Higher impedance value reduces distortion of the signal. The voltage gain value of the amplifier should be high enough to amplify bioelectric signals which are namely in millivolts or microvolt range and also , a constant gain should be maintained entire the bandwidth range. In addition, A bio-amplifier should have a small output impedance and should be free from noise and distortion. Also, a great Common Mode Rejection Ratio (CMRR) should be meet. On the other hand, with the development of

amplifiers, one challenge has been reducing its size for better feasibility, as well as making them implantable on the body or skin for recording and analysing the signals. Also, they should dissipate heat well. Heat dissipation is a challenging issue, because extra heat may cause in the temperature of nearby tissue to rise, potentially causing a change in the physiology of the tissue or lead to misunderstanding the problem [3], [4].

2.3 Memristor Properties

A memristor is considered as a proper candidate for low power circuit designs because it can use any value between 0 and 1, unlike traditional devices which use only 0 and 1. It is a passive element similar to elementary devices such as the resistor, inductor, and capacitor, in which these express the relations between voltage and current, flux and current, and voltage and charge, respectively [5].

For example, researchers have shown that a piece of a wire, which warming up by its inherent current, meets the typical definition of the generic memristor [6] or a new mutator has been proposed by making use of varactor diode with variable capacitance to achieve the desired features. It is shown that memristor emulation can be achieved by properly configuring the elements of the mutator circuit and is suitable for integrated circuit implementation and design [7].

We have used the model discussed in [8] to get Figure 2. Which models i-v characteristics of a generic memristor in different frequencies. We performed the simulation for different frequencies to verify memristor behavior. As the frequency increases the hysteresis loop becomes narrower and for the higher frequencies it becomes straight line on the graph like a typical resistor.

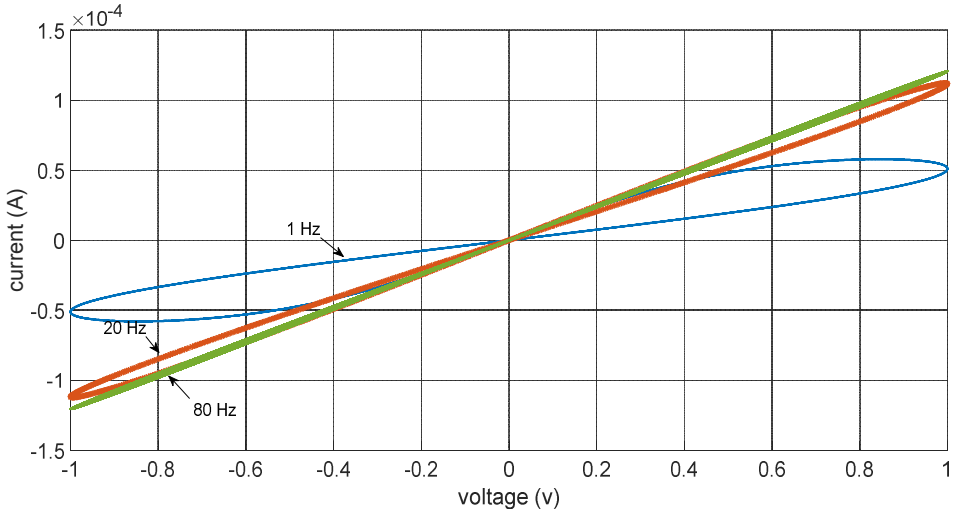

Figure 3. current-voltage characteristic for a typical memristor and its variations with frequency

Using the model described in [8], the pinched hysteresis demonstrates some time shifting between voltage and current which is shown in Figure 3.

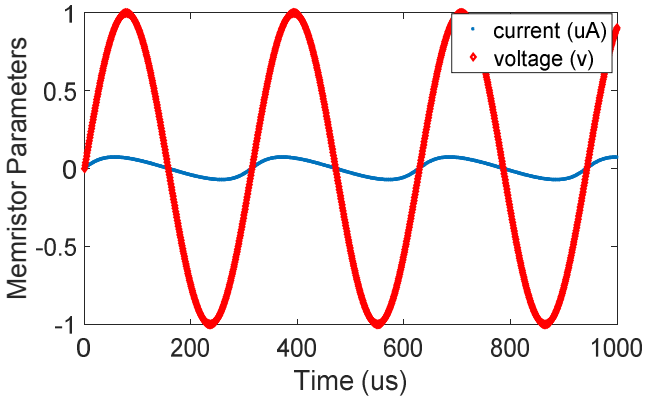

Figure 4. time shifting between voltage and current in low frequencies

We used Matlab/Simulink/Simscape for simulating the proposed circuit which uses model described in [9] for modelling the memristor.

2.4 Differential Pair Amplifiers

As mentioned above, there are different types of amplifiers that widely used in biology, biotechnology and biomedical sciences. Most of these amplifiers as can be easily accessed in literatures are based on operational amplifiers which in turn are based on differential pair amplifiers. Hence, here we have tried to present the possibility of use of memristors in this basic circuit as a good elementary example. Figure. 5 shows the basic balanced differential pair amplifier in the common and differential mode [10].

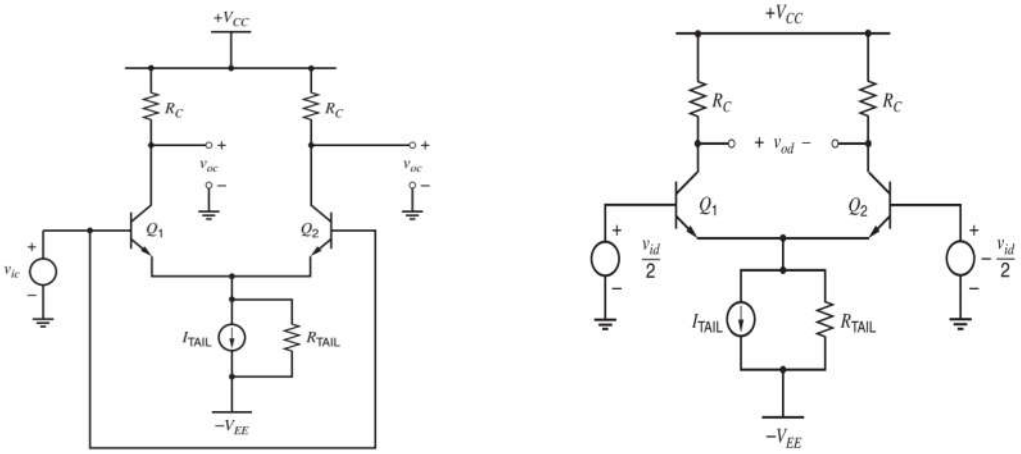

Figure 5. The basic balanced differential pair amplifier in a- common mode and b- differential mode [10]

3. Modelling and simulation

Figure 6 and Figure 7 are the complete model we implemented in Matlab/Simulink by replacing common resistors with memristors. The circuit in Figure 6 and Figure 8 show a differential pair amplifier circuit which uses memristors as collector loads. Figure 7 and 9 show the input and output signals related to common mode and differential mode respectively. The proposed model tested using differential and common-mode inputs. As we have used identical transistors and memristors, the balanced output has gain equal to zero in the common-mode.Transistor Qt is used as a constant tail current source that enhances differential-mode gain. The combination of the diode and other resistor connected to this transistor, sets the base voltage to about 1V above the negative bias voltage. The base-emitter voltage here is about 0.4V, and other parameters are set so that an emitter current of about 2.5 mA is obtained.

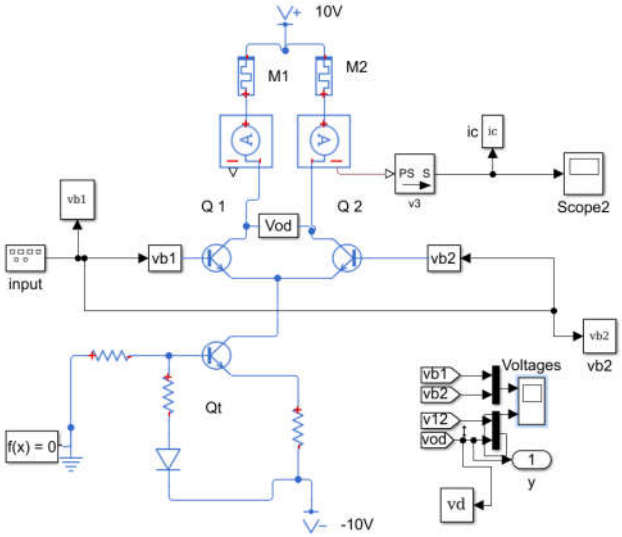

Figure 6. Our simulated memristor based balanced differential pair amplifier in common mode

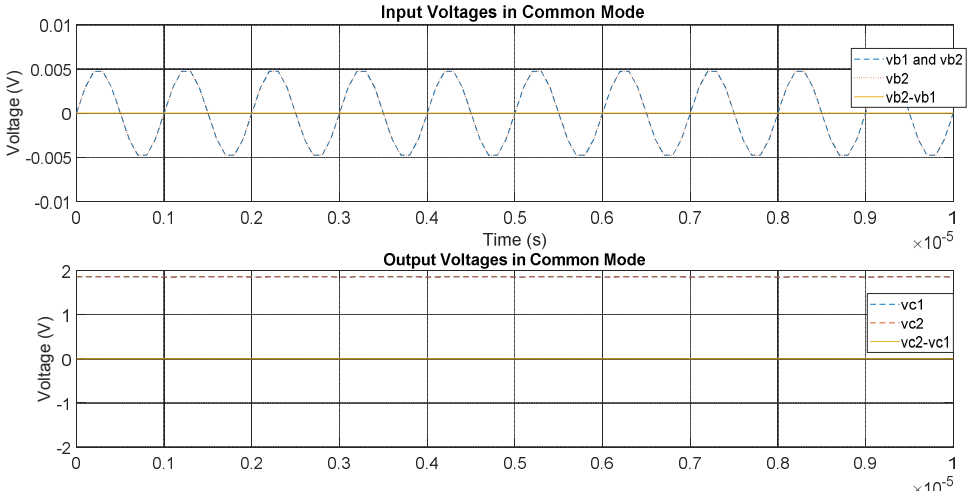

Figure 7. The simulation results of memristor based balanced differential pair amplifier in common mode

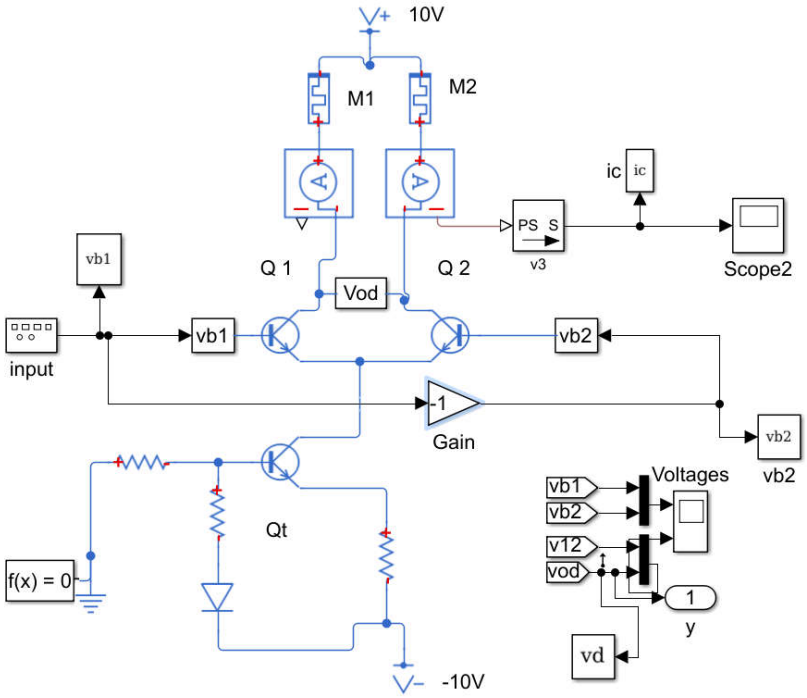

Figure 8. Our simulated memristor based balanced differential pair amplifier in differential mode

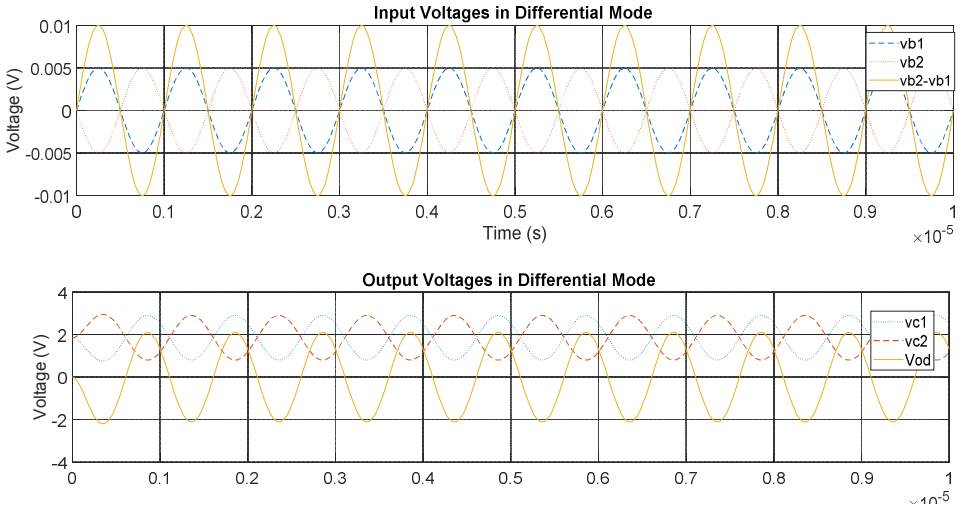

Figure 9. The simulation results of memristor based balanced differential pair amplifier in differential mode

As mentioned above and illustrated in Figure 3, the memristor works so similar to a resistor when the frequency is increased. So in our work frequency which is typical for biological applications, almost all the features of the circuit are completely similar to what we expect from typical differential pair amplifier.

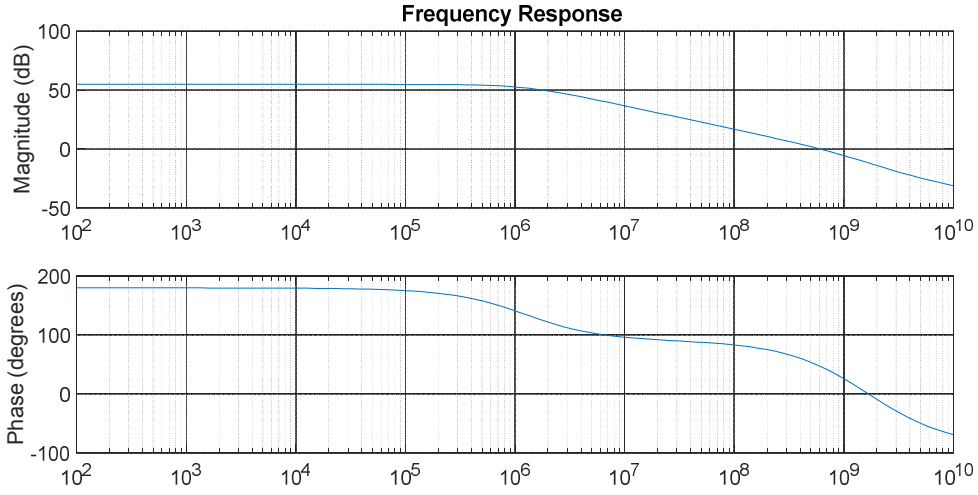

Figure 10. Frequency Response of the memristor based differential pair

Also, as expected we have similar behavior in frequency domain that makes us satisfied to use the memristor in a wide range of biological applications.

So it is predicted that using memristors in differential amplifiers as well as other important circuits in biological amplifiers can lead to new useful advantages. These benefits can be very helpful in the close future and helps engineers to design circuit which uses less power, produces less heat and occupy smaller space on chips. It is also

has been shown that using memristor can increase the linear range of the differential pair that can be useful in bio amplifiers [11].

To get better gain it is also possible to use a memristive active load in the differential pair amplifier instead of common active load which leads to get the advantage of low on-chip area, and lower leakage currents [12].

4. Conclusion

In this paper we suggested using memristors instead of resistors in bio-amplifiers in order to get the advantages of memristor including low power dissipation, smaller chip area and also the larger linear input range.

These advantages make memristive circuits usable in different applications specially in biological applications. In this paper we presented and simulated a memristor based differential pair amplifier as the basic unit for most of the bioelectrical amplifiers. Our simulations showed that desired features of the differential pair amplifier remain constant while some good advantages related to memristor can be obtained.

References

[1] K. Zaplatilek (2011, April). Memristor modeling in MATLAB & SIMULINK. In Proceedings of the European computing conference (pp. 62-67).

[2] L. Chua (1971). Memristor-the missing circuit element. IEEE Transactions on circuit theory, 18(5), 507-519.

[3] https://www.electrical4u.com/biological-amplifiers. Retrieved October 14, 2020

[4] https://en.wikipedia.org/wiki/Bioamplifier Retrieved October 12, 2020

[5] N. O. Adesina, A. Srivastava (2019). Memristor-Based Loop Filter Design for Phase Locked Loop. Journal of Low Power Electronics and Applications, 9(3), 24.

[6] Z. Biolek, , D. Biolek, , J. Vavra, , V. Biolková, Z. Kolka, (2016, May). The simplest memristor in the world. In 2016 IEEE International Symposium on Circuits and Systems (ISCAS) (pp. 1854-1857). IEEE.

[7] D.Yu, , X. Zhao, T. Sun, H. H. Iu, T. Fernando (2019). A Simple Floating Mutator for Emulating Memristor, Memcapacitor, and Meminductor. IEEE Transactions on Circuits and Systems II: Express Briefs.

[8] T. Hoang (2020) Memristor model (https://www.mathworks.com /matlabcentral /fileexchange /25082-memristor-model), MATLAB Central File Exchange. Retrieved October 18, 2020.

[9] Y. N. Joglekar, S. J. Wolf (2009). The elusive memristor: properties of basic electrical circuits. European Journal of physics, 30(4), 661.

[10] Gray, P. R., Hurst, P., Meyer, R. G., & Lewis, S. (2001). Analysis and design of analog integrated circuits. Wiley.

[11] D. Varghese, G. Gandhi, (2009, July). Memristor based high linear range differential pair. In 2009 International Conference on Communications, Circuits and Systems (pp. 935-938). IEEE.

[12] O. Krestinskaya, I. Fedorova, & A. P. James, (2015, August). Memristor load current mirror circuit. In 2015 International Conference on Advances in Computing, Communications and Informatics (ICACCI) (pp. 538-542). IEEE.

Exploiting Well-tempered metadynamics to explore the adsorption behaviour of small biomolecules on inorganics surfaces

Zeynab Mohammad Hosseini Naveh

Assistant professor, Kashmar Higher Education Institute

Email: z.mohammadhosseininaveh@kashmar.ac.ir

Abstract

Reconstructing the free energy surface underlying the bimolecular adsorption processes is of great significant in probing the molecular mechanisms governing many biological functions. Employing molecular dynamics (MD) techniques, the study of dynamics of macro-molecules containing thousands of atoms is feasible owing to the high-speed growth of computating resources. Present research aims at exploring the free energy surface directing the interactions at an organic-inorganic interface using an enhanced sampling techniques which is called the well-tempered metadynamics (WT-MTD). The factors affecting the convergence of the WT-MTD method are discussed too.

Keywords: Free energy surface, adsorption energy, molecular dynamics simulation, bio-molecules, well-tempered metadynamics.

1. Introduction

The spontaneous adsorption of organic molecules on the inorganic nano-materials such as carbon nano particles/nanotubes (CNTs) and graphene lies at the centre of numeric applications ranging from medicine and pharmacology to bio-sensors and water desalination [1-4]. Due to the increased surface to volume ratio, carbon nano-materials such CNTs have demonstrated excellent electronic, chemical, optical and mechanical properties. Many applications are reported through which an organic molecule/macro-molecule interfaces the CNT surface specifically in the drug delivery [5,6] and bio-sensing utilizations [1,2].

Computational techniques such as molecular dynamics (MD) simulation [7] could provide valuable information on the interactions of organic molecules with the inorganic surfaces at the atomic details. Rapid advances in the high performance calculations and computational resources as well as developing the reliable force fields makes the MD technique a very powerful tool to predict the free energy surface governing the dynamic behaviour of the biomolecules-nanomaterial interactions. Utilizing the MD simulation, the spontaneous adsorption of the biomolecule on the surface is reconstructed. The biomolecule spends most of the time constrained to the surface as the adsorbed state is a local free energy minimum. The observation of the escaped state in a standard MD simulation is a rare-event due to the limitation in the computational resources. Hence, modelling the free energy landscape is not feasible because of the poor sampling of phase space. The enhanced

sampling methods such as metadynamics (MTD) [8] bias the potential energy of the system to accelerate the rare-event. In MTD, an extra history-dependent bias potential is added to the system potential, forcing the system to leave the local minima and visiting the low-probability regions of the free energy landscape. In the present work, a variance of the MTD, which is called the well-tempered MTD (WT-MTD) is employed to reconstruct the adsorption free energy surface of an amino acid (Serine, SER) on the CNT surface.

2. Material and Methods

2.1 Molecular dynamics simulation

The MD simulation of the CNT–SER hybrid system was run for 5 ns, in the explicit water, using the NAMD software (NAMD2.13b1) [9], and the CHARMM36 force field [10]. The CNT–SER hybrid systems were solvated in a cubic box of TIP3P [11] water molecules. The initial distance between the mass centers of CNT and SER was set to 20 Å. Each solvated system underwent the preparation protocol including 1 ns of energy minimization, using the conjugate gradient may cause problems during processing. method [12], followed by a gradual temperature increase, using the Langevin dynamics, from 25 to 325 K. The system was then equilibrated over 1 ns at constant pressure (1 bar) and temperature (T = 310 K) by using the Langevin–Hoover pressure control method as implemented in the NAMD [13]. The simulations for the data collection (after minimization and equilibration) were then performed at the constant temperature of 310 K by using the Langevin dynamics (friction constant 22 ps−1). Periodic boundary conditions were used [14]; van derWaals interactions were cut off beyond 12 Å. Electrostatic interactions were calculated by the Ewald sum using the particle mesh Ewald (PME) method [15]. The time step of 1 fs was considered.

2.2 Well-tempered metadynamics

Metadynamics which was introduced by Laio et al [16] on 2002, is an efficient method to sample the rare events. The system evolves based on the potential energy which is composed of the real system potential V(x) plus an iteratively-added Gaussian bias (B(S(x))) centered at the value of the collective variables (CVs), eq. (1). The CVs (S(x)) are functions of atomic coordinates (x) capable of monitoring the event progress.

$$B\left(S\left(x,t\right)\right)=w\sum_{t'=\tau_G,2\tau_G}^{t}\exp\left(-\frac{\left(S-s\left(t'\right)\right)^2}{2\delta s^2}\right) \quad (1)$$

Where, w is the Gaussian height, δs is the Gaussian width, τ_G is the time interval of the Gaussian deposition. s(t)=S(x(t)) is the value of the CV at time t. As the simulation advances, the Gaussians are accumulated suppressing the system to revisit the same place in the CV space. Consequently, if the simulation starts at a local free energy minimum, the Gaussian biases fill in the well and directing the system towards a close-by minimum,

then enhancing the probability to sample the rare-event. When all the wells are stuffed with the Gaussians, for sufficiently long simulation, the accumulated bias potential is assumed to provide an estimate of the underlying free energy [17]:

$$\lim_{t\to\infty} B(S,t) = -F(S) + C \tag{2}$$

Metadynamics exist in many flavors, all sharing the same basic idea. In the standard metadynamis, constant hill weight Gaussian are added to the bias potential. As a result, in a long time simulation the estimated free energies oscillate around the real value of free energy. A variant of metadynamics is called well-tempered metadynamics [16] in which the height of the Gaussian is reduced over the simulation time according to:

$$w(t) = w_0 \exp\left(-\frac{V(S(x,t))}{k_B \Delta T}\right) \tag{3}$$

where W_0 is the initial Gaussian height, ΔT is and input parameter with the dimension of the temperature, and k_B is the Boltzmann constant. With this decreasing hill weight, the bias potential is then smoothly converged in the long time limit, although it does not entirely gratify the underlying free energy:

$$B(S,t \to \infty) = -\frac{\Delta T}{T + \Delta T} F(S) + C \tag{4}$$

where T is the system temperature. Eventually, the CVs sample an ensemble at a temperature $T + \Delta T$ which is higher than the system temperature. The parameter ΔT could be regulated through a bias factor (γ) to determine the extent of free energy exploration:

$$\gamma = \frac{T + \Delta T}{T} \tag{5}$$

3. Results and Discussions

The well-tempered metadynamics simulation were carried out using the Colvars package [] employed within the NAMD configuration file. The collective variable is the radial distance of carbon alpha (C_α) atom of the SER from the central axis of the CNT. One dimensional adsorption profiles as a function of CV was calculated for several bias factors. Gaussian were added every 0.5ps. Initial height was 0.01 kcal/mol. The Gaussian hill height as a function of time is plotted in Figure 1 for the bias factor 2. The potential of mean force (PMF) was calculated for several bias factors. The results for the bias factor of 6 and the hill width of 1 are displayed in Figure 1 for 4ns, 16ns and 40ns of simulation time. The CV values over time is plotted in Figure 2, where it is observed that the CV is correctly exploring all the collective variable space starting from 6.8Å till 32Å. The hills height over the simulation time is shown in Figure 3. It is inferred that Gaussian hill height reduces as the simulation

progresses and in the long time it is expected the hill weight becomes smaller and smaller while the system diffuses in the entire CVs space.

The initial hill height, hill width and the bias factor parameters are of great importance to the WT-MTD convergence. E.g. in Figure 4, the CV values versus time is shown for two WT-MTD simulations with two different hill widths of 1 and 0.1. It is observed that the CV for the second simulation (blue curve) is not capable of efficiently exploration of the phase space, especially after 40ns the CV is trapped in one state.

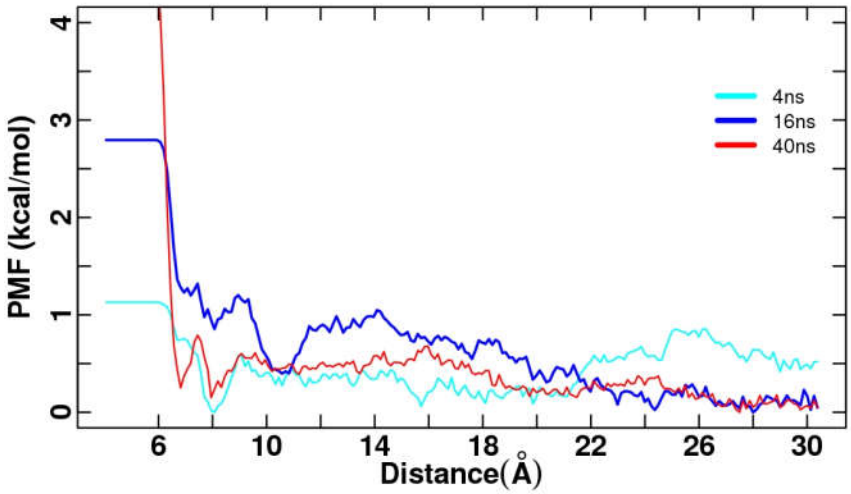

Figure 1: The potential of mean force (PMF) versus collective variable (CV) for the WT-MTD simulation. The bias factor is 6; initial hill weight 0.01 kcal/mol; hill width 1. CV is radial distance of carbon alpha atom of amino acid from the central axis of carbon nanotube.

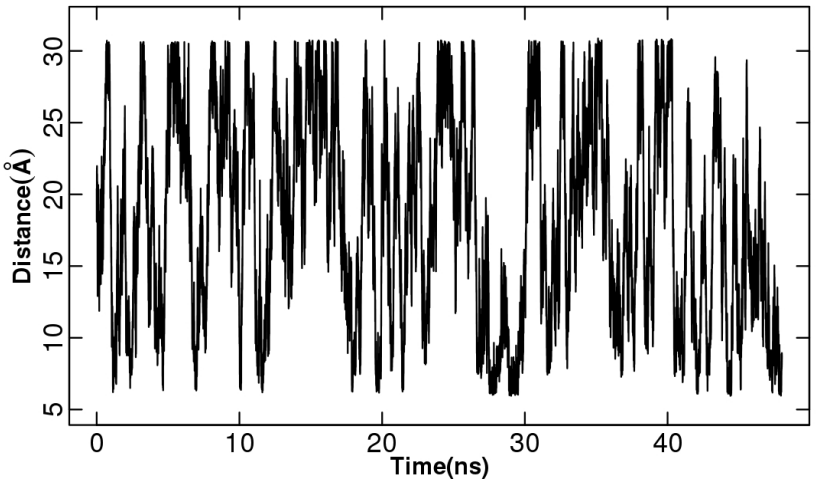

Figure 2: The collective variable (CV) values versus metadynamics simulation time for the WT-MTD simulation. The bias factor is 6; initial hill weight 0.01 kcal/mol; hill width 1. CV is radial distance of carbon alpha atom of amino acid from the central axis of carbon nanotube.

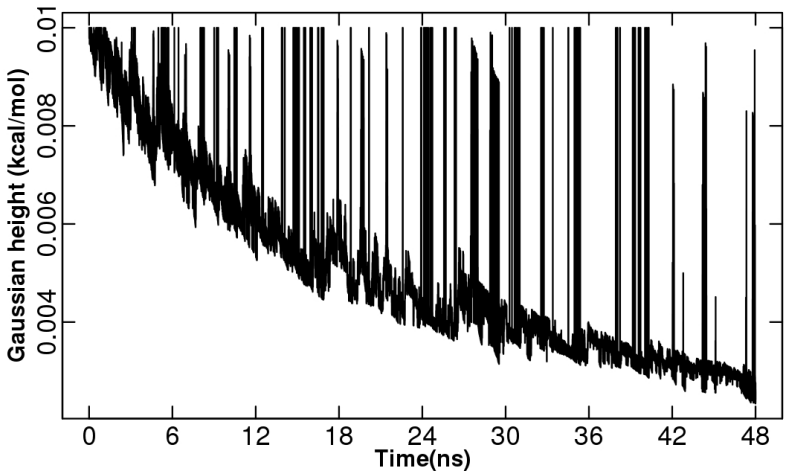

Figure 3: Gaussian hills height as a function of time rescaled according to the WT-MTD simulation. The bias factor is 6; initial hill weight 0.01 kcal/mol; hill width 1. CV is radial distance of carbon alpha atom of amino acid from the central axis of carbon nanotube.

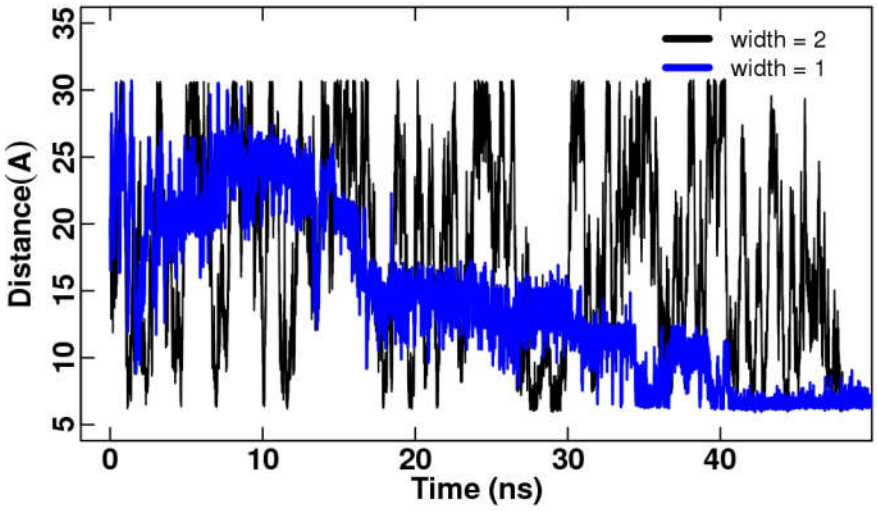

Figure 4: The collective variable along the WT-MTD simulation time, for hill width 1 (black curve) and hill width 0.1 (blue curve). The bias factor and the initial hill weight are 6 and 0.01 kcal/mol, respectively.

References

[1] S. Han, W. Liu, M. Zheng and R. Wang, (2020) Label-Free and Ultrasensitive Electrochemical DNA Biosensor Based on Urchinlike Carbon Nanotube-Gold Nanoparticle Nanoclusters, *Anal. Chem.* 92, 7, 4780–4787.

[2] Tran NH Nguyen, Xin Jin, James K Nolan, Jian Xu, Khanh Vy H Le, Stephanie Lam, Yi Wang, Muhammad A Alam, Hyowon Lee, (2020) Printable Nonenzymatic Glucose Biosensors Using Carbon Nanotube-PtNP Nanocomposites Modified with AuRu for Improved Selectivity, ACS Biomater. Sci. Eng. , 6, 9, 5315–5325.

[3] Tanaka, M., Aoki, K., Haniu, H., Kamanaka, T., Takizawa, T., Sobajima, A., Yoshida, K., Okamoto, M., Kato, H., Saito, N. (2020) Applications of Carbon Nanotubes in Bone Regenerative Medicine. Nanomaterials, 10, 659.

[4] Wang, R., Chen, J., Chen, L., Ye, Z., Cui, W., Gao, W., Xie, L., & Ying, Y. (2020). Ultrathin and ultradense aligned carbon nanotube membranes for water purification with enhanced rejection performance. *Desalination, 494*, 114671.

[5] Y. Hu and Christof M. Niemeyer, (2020) Designer DNA–silica/carbon nanotube nanocomposites for traceable and targeted drug delivery, J. Mater. Chem. B, 8, 2250-2255.

[6] Maleki R, Afrouzi HH, Hosseini M, Toghraie D, Rostami S. (2020) Molecular dynamics simulation of Doxorubicin loading with N-isopropyl acrylamide carbon nanotube in a drug delivery system. Computer Methods and Programs in Biomedicine. 184:105303.

[7] Ciccotti G, Ferrario M, Schuette C, (2014). Molecular Dynamics Simulation, MDPI AG, ISBN 978-3-906980-66-9.

[8] A Barducci, G Bussi, and M Parrinello. (2008) Well-tempered metadynamics: A smoothly converging and tunable free-energy method. Phys. Rev. Lett., 100(2):020603.

[9] Phillips JC, Braun R, Wang W, Gumbart J, Tajkhorshid E, Villa E, Chipot C, Skeel RD, Kale L, Schulten K (2005) Scalable molecular dynamics with NAMD. J Comput Chem 26:1781–1802.

[10] Brooks BR, Bruccoleri RE, Olafson BD, States DJ, Swaminathan S, Karplus M (1983) Charmm: a program for macromolecular energy, minimization, and dynamics calculations. J Comput Chem 4: 187–217.

[11] JorgensenW, Chandrasekhar J,Madura J, Impey R,KleinM(1983) Comparison of simple potential functions for simulating liquid water. J Chem Phys 79:926–935.

[12] Lasdon LS, Mitter SK, Waren AD (1967) The conjugate gradient method for optimal control problems. IEEE Trans Autom Control 12:132–138.

[13] Quigley D, Probert MIJ (2004) Langevin dynamics in constant pressure extended systems. J Chem Phys 120:11432–11441.

[14] Allen MP, Tildesley DJ (1989) Computer simulation of liquids. Oxford Science publications, Oxford University Press, USA.

[15] Darden T, York D, Pedersen L (1993) Particle mesh ewald: an nlog(n) method for ewald sums in large systems. J Chem Phys 98: 10089–10093.

[16] A. Laio and M. Parrinello. (2002) Escaping free-energy minima. Proceedings of the National Academy of Sciences, 99(20):12562–12566.

[17] A. Laio and F.L. Gervasio. (2008) Metadynamics: a method to simulate rare events and reconstruct the free energy in biophysics, chemistry and material science. Reports on Progress in Physics, 71(12):126601.

Effects of different de-binding condition on the final properties of biomedical dental system implant parts

M.Moradjoy [1], H.Khorsand [2*]

[1] PhD Candidate, Faculty of Material Science and Engineering, K. N. Toosi University of Technology,Tehran,Iran..

[2] Assistant Professor, Faculty of Material Science and Engineering, K. N. Toosi University of Technology,Tehran,Iran.

*Email: hkhorsand@kntu.ac.ir

Abstract

Homogeneity of the feedstock was evaluated by DSC and TGA test. The results reveal the injection molding temperature should be set above 138 °C in order to improve the rheological properties of feedstock and decrease the degradation of the binder, and the mold temperature should be set below 60 °C. Backbone polymer in the binder start degrading at 360 °C until 550 °C, which indicates that in the thermal de-binding stage, the temperature should exceed 550 °C. Biocompatible metals have been developing the biomedical and biological field, predominantly in human implant applications, where these metals widely used as a substitute to or as function restoration of degenerated tissues or organs. A systematic considerate of thermoplastic polymer in the wax-based binder is necessary for ensuring the dimensions and mechanical properties of 316L stainless steel metal injection molding parts. Metal injection molding (MIM) is considered as a novel technology for producing metal parts with complex geometry. The present work is focused on producing a homogeneous SS 316L feedstock for MIM process by optimizing chemical properties of polymeric and surfactant material. A horizontal mixing machine of capacity 4500 cc is used and Taguchi technique has been used for optimizing the process parameters to produce a homogeneous feedstock of SS 316L.

Keywords: Binder, Biomedical, Dental Implant, Metal Injection Moulding, Biocompatible Metals; Sintering; Powder Metallurgy.

1. Introduction

The binder should possess the characteristic of fast removal during debinding, without forming defects in the injection molded component [1-5]. The green part is most susceptible to formation of defects during the debinding stage. The binder, which provides strength, is removed, gradually increasing the susceptibility of the green part to formation of defects. The absence of open porosity during the initial stages of thermal debinding results in the formation of defects such as cracking, blistering, etc [6-10]. The stresses arising owing to trapped degradation products as a result of polymer burnout will lead to the formation of defects. To avoid this scenario, the binders are typically designed to have multiple components which undergo decomposition at different temperatures. In this case the debinding process occurs in two stages. In the first stage, one component of the binder system is

removed, initially resulting in creation of open pores in the green component [11]. During this stage the remaining components of the binder system will provide strength to the metal particles and retain the shape [12]. The remaining components of the binder system are gradually removed during the second stage of the debinding process. The two-stage debinding process results in faster removal of binders from the green components. The binder should also possess the characteristic of complete burnout without leaving any residual carbon. The products formed due to thermal debinding should also be non-corrosive to the manufacturing equipment. Binders used for metal injection molding must be easily available, low in cost, and should have a long shelf life [13-15]. The sprues and gates are reused in the MIM process and the binder should have good recyclability and must not degrade on cyclic reheating. The binders should have high thermal conductivity and a low thermal coefficient of expansion in order to prevent defects formed as a result of thermal stresses. It is very hard for a single binder to fulfil all the characteristics of feedstock. The binder system used in the injection molding process typically contains multiple components, each performing a specialized task. The binder system contains a major constituent and other components are mixed as additives to obtain the desired characteristics of the feedstock [16-20].

Dispersants, plasticizers, stabilizers and inter-molecular lubricants are some common additives added to binders in the MIM process.[2] Dispersants are added to the binder to enhance the distribution of the powder in the system. Dispersants have the unique ability to replace the powder/powder and powder/air interfaces with a powder/binder interface [21]. The addition of dispersants enhances the solids loading. The dispersants create locations for the binder to react and bond with the powder. Zinc stearate is a commonly used dispersant in the MIM process. The plasticizers are added to the binder system to enhance the flow behavior in MIM. Camphor, dimethyl phthalate, and dibutyl phthalate are some of examples of plasticizers used in MIM. The molecules of the plasticizers contain ring-like atom groups. These ring-like atom groups will reduce the inter-molecular friction between the binder molecules and increase the flowability of the binder system.[4] Stabilizers are added to the binder system with the main aim of preventing agglomeration of the particles. The stabilizers must strongly bond to the powder particles and they should have sufficient extension in the binder blend to prevent agglomeration due to approaching particles. The metal powder particles' surface should also be completely covered by the stabilizer [22-27]. In addition, the stabilizers should mix completely in the binder media used for MIM. The inter-molecular lubricants enhance the flow of the feedstock [28-33]. The inter-molecular lubricants have a much lower molecular weight than the polymer and thus possess very much lower viscosity than the base polymer at the processing temperature. The inter-molecular lubricants decrease the friction between the adsorbed layer on the particles and the binder molecules. Stearic acid and wax are some common examples of intermolecular lubricants.

2. Material and Methods

2.1 Binder chemistry

Thermoplastic and thermosetting are two common types of polymers. Thermoplastic polymers are formed due to repetition of small monomer groups along the chain length without cross linking. Polyethylene, polypropylene, polystyrene, and wax are some examples of thermoplastic polymers. The crystalline polymers have smaller chain

lengths and amorphous polymers contain longer chain lengths. The amorphous polymers are more ductile in nature than crystalline polymers [34-37]. The crystalline and amorphous polymers show different behaviors on exposure to high temperature (Figure 1). Polymers with relative mass lower than M1 will display a narrow melting point, which will result in shape loss during the debinding process. Polymers with relative mass greater than M2 will require a high temperature to become viscous. The high temperature will cause degradation of the polymer. Thus, ideally, the relative mass of the polymer to be used as a binder should fall between M_1 and M_2

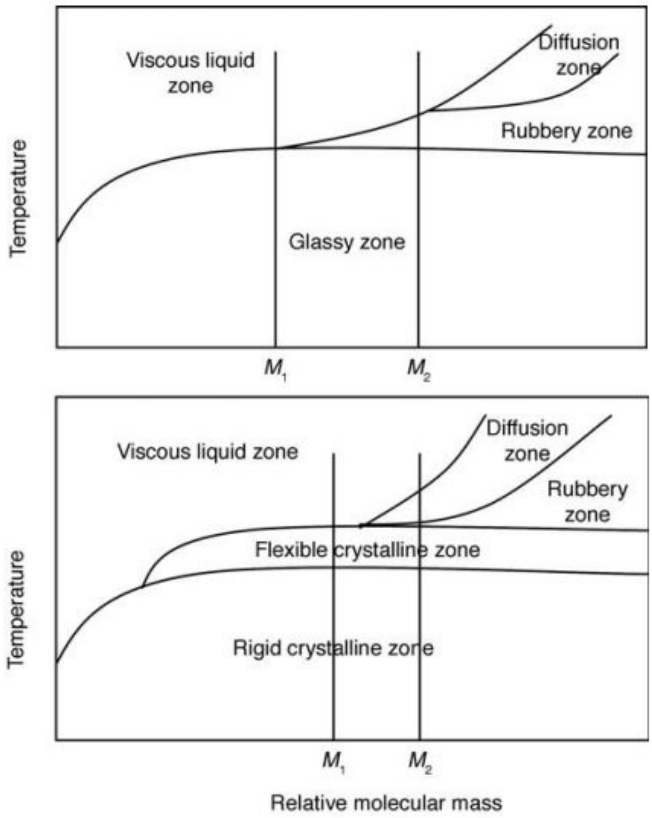

Figure 1. Temperature in relation to relative molecular mass plots for amorphous (top) and crystalline (bottom) polymers.

In this study the metallic powder used was 316L SS, with a particle average diameter of about 20 μm, and pycnometer density of 7.93 g/cm3. All the metal particles as approximately spherical well suited for powder flow ability and dense particle packing in the injection molding stage. The selected appropriate binder system that has been reported in the literature was composed of 68% paraffin wax (PW), 15% high density polypropylene (HDPE), 15% Polypropylene (PP) and 2% stearic acid (SA) (volume fraction). PW was used as a filler to decrease the viscosity of the feedstock and increase the flow ability of this, so it contributed to the feedstock filling the die cavity [38]. The surfactant SA aims to enhance the adhesion between powder and binder, preventing the separation of them [38]. HDPE and PP based backbone polymer ensure the strength of the green parts from injection molding and maintain the shape of the compacts in the de-binding stage [40]. In the blending stage, to avoid PW and SA degrading, the feedstock was prepared by mixing the metal powder with HDPE and PP backbone polymers in a

screw mixer at 290 °C for 60 min at 40 r/min. Then the PW and SA were added as filler and surfactant to the mixture and blended at 210 °C for 30 min at 40 r/min. To obtain the feedstock, metal powder (70 vol. %) and binder (30 vol. %) were mixed in a screw.

3. Results and Discussions

3.1 Effects of different de-binding condition on final MIM parts

Two stages were performed in the de-binding process: solvent and thermal de-binding to remove the binder shows the detailed experimental condition during thermal de-binding and sintering processes. Which is includes the temperature and the keeping time and the heating and cooling rates. The sintering was performed in hydrogen atmosphere at 1380°C. For debinding and sintering the parts were placed on top of a ceramic Al_2O_3 plate to ensure that no major diffusion occurred, which would cause the migration of the alloy elements between the sample and the supporting plate. The entire debinding and sintering processes took 36 hours to be completed. Figure 2 schematically represents the layout for sintering process. Temperature oscillation in the chamber was 1380°C within ±3°C.

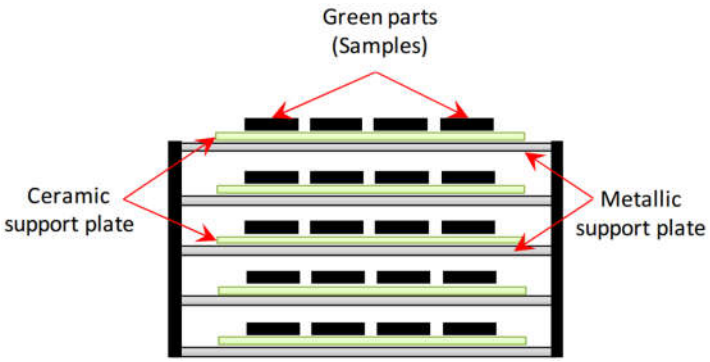

Figure 2. Schematic representations of stacks of green parts inside the chamber for debinding and sintering.

Solvent debinding is an important process that soluble part in binder is dissolved and open pore channels are formed. It can shorten heating and holding time of thermal debinding, thereby reducing the total time of debinding. Meanwhile, the defect produced by solvent debinding is less than that by thermal debinding. In this study, the removal of binders based on three backbone polymers in the solvent debinding stage was also investigated in n-heptane solvent at 60 °C. The backbone polymer has an effect on the leaching rate of PW and SA in the binder. Figure 3 displays the percentage of PW and SA removed in the binders based on three backbone polymers with the extension of time [20]. It can be seen that the percentage of removal of PW and SA gradually increases with the extension of time, but the rate of the removal gradually slows down and finally stabilizes. Furthermore, PW and SA in HDPE/PP binder are easier to remove. Most of PW and SA in the binder close to 92% are removed in

70 min, which is advantageous to optimize the solvent debinding process and shorten the time of solvent debinding. The stabilizers must strongly bond to the powder particles and they should have sufficient extension in the binder blend to prevent agglomeration due to approaching particles. The metal powder particles' surface should also be completely covered by the stabilizer. In addition, the stabilizers should mix completely in the binder media used for MIM. The inter-molecular lubricants enhance the flow of the feedstock. The inter-molecular lubricants have a much lower molecular weight than the polymer and thus possess very much lower viscosity than the base polymer at the processing temperature. The inter-molecular lubricants decrease the friction between the adsorbed layer on the particles and the binder molecules. Stearic acid and wax are some common examples of intermolecular lubricants.

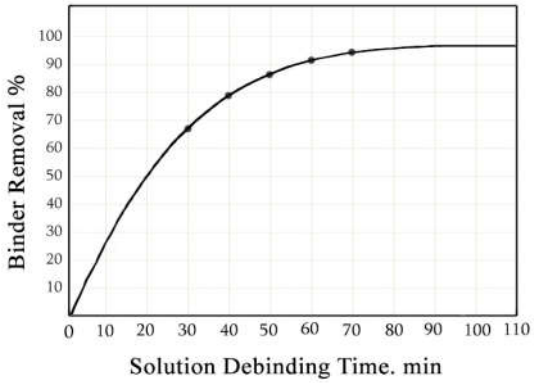

Figure 3. Solution de-binding of MIM parts in an n-heptane bath as a function of time.

Figure 4 presents the micrograph of injection molding green part before and after solvent debinding at 70 for 70 min respectively. It can be clearly seen from Figure 4a that the binder surrounds the powder particles in the green part. Due to the removal of PW and SA in solvent debinding, the powder particles are not fully surrounded by binder and the open pore channels are formed in Fig.4b. The binder in Fig.4b is the backbone polymer and remains of PW and SA. The formation of open pore channels is favorable for the rapid removal of the remaining binder without cracking, blistering or swelling during subsequent thermal debinding stage. The residual binder forms a porous network to provide the strength of debound part.

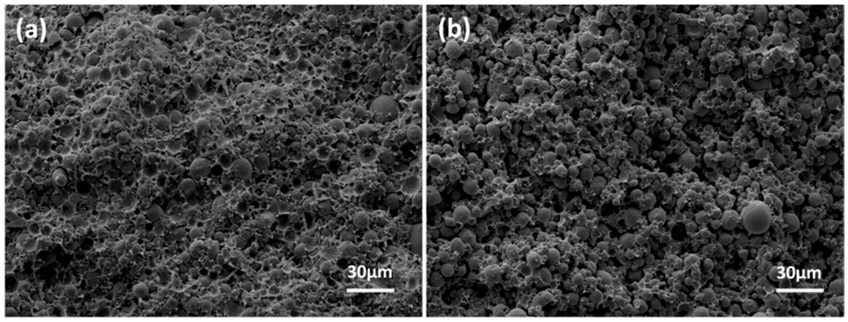

Figure 4. SEM image of cross section of specimens: (a) before and (b) after solvent de-binding.

In this study, the thermal debinding process was performed at 600 °C. Figure 5 illustrate the thermal debinding and sintering conditions in detail. Finally, the total mass loss of feedstock is about 6.6% lower than the ratio before blending from TGA results. This may be due to sampling error in experimentation during selection of specimen

in TGA [21]. Figure 5 show the microstructure after different thermal debinding condition. The above mentioned results and the extrapolation could be con□rmed from the microstructures of the samples at different temperatures (Fig. 5). It can be seen that the paraffin was gradually removed and the regular spherical copper particles became clearer with an increase in temperature. When it reached 500 ℃, powder with smaller diameter particles began to deform, slowly forming a sintered neck. On further increasing the temperature, all copper particles were sintered together and a large number of gaps could be observed in the structure. In the early stage of debinding, with the removal of paraffin, the initially dense microstructure of the sample became loose when the particles were simply physically bound. Subsequently, with the formation of the sintering neck the microstructure of the sample became dense again and the microstructure of the metal exhibited a metallurgical bonding mode.

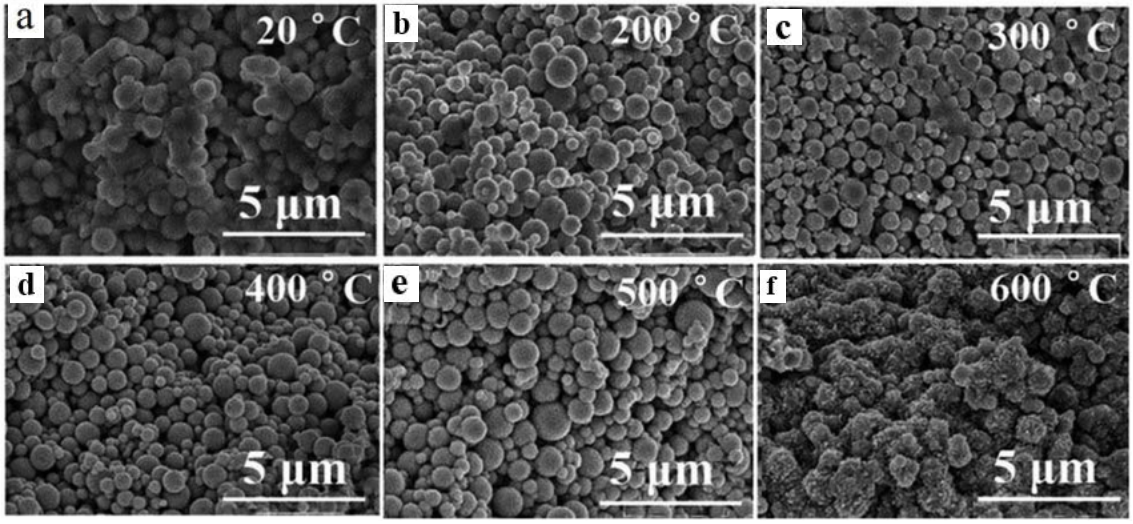

Figure 5. SEM image of cross section of specimens: (a)20℃ , (b)200℃ , (d)300℃ , (e)400℃ , (f)500℃ and (g)600℃.

Conclusions

The HDPE/PP backbone polymer shortens the time of solvent debinding and optimizes the solvent debinding process. Use of a HDPE/PP backbone polymer performs better in terms of the dimensional stabilities of green parts and sintered parts than those of HDPE and PP. Threedimensional stabilities of sintered parts with HDPE/ PP are 46%, 40%, 20% better than those of PP. The binder with HDPE/PP backbone polymer provides better density stability and hardness stability of 316L stainless steel sintered parts than with HDPE and PP. Meanwhile, the binder with HDPE/PP backbone polymer improves the mechanical properties of sintered parts.

References

[1] Y. Li, L. Li, and K. Khalil, Journal of Materials Processing Technology, 2007, 183(2-3), 432-439, DOI:.1016/j.2006.10.039.

[2] M. Wright, L. Hughes, and S. Gressel, Journal of materials engineering and performance, 1994, 3(2), 300-306, DOI:10.1007/BF02645856.

[3] M. Ibrahim, N. Muhamad, A. B. Sulong, S. Ahmad, and N. Nor, International Journal of Mechanical and Materials Engineering, 2010, 5(2), 282-289, DOI:10.4028264-265.135.

[4] K. Essa, P. Jamshidi, J. Zou, M. M. Attallah, and H. Hassanin, Materials & Design, 2018, 138, 21-29, DOI:10.1016/j.matdes.2017.10.025.

[5] S. Yu, P. Zhang, K. Qiu, W. Zhang, J. Li, S. Yao, D. Zhou, N. Yao, and J. Li, Ferroelectrics, 2018, 530(1), 25-31, DOI:10.1080/00150193.2018.1454071.

[6] H. Ö. Gülsoy and R. M. German, Scripta Materialia, 2008, 58(4), 295-298, DOI:10.1016/j.scriptamat.2007.10.004.

[7] R. German, Materials, 2013, 6(8), 3641-3662, DOI:10.3390/ma6083641.

[8] N. Loh, S. Tor, and K. Khor, Journal of Materials Processing Technology, 2001, 108(3), 398-407, DOI:10.1016/S0924-0136(00)00855-4.

[9] K. Tam, S. Yap, M. Foong, and N. Loh, Journal of Materials Processing Technology, 1997, 67(1-3), 120-125, DOI:10.1016/S0924-0136(96)02830-0.

[10] H. Youhua, L. Yimin, H. Hao, L. Jia, and T. Xiao, Rare Metal Materials and Engineering, 2010, 39(5), 775-780, DOI:10.1016/S1875-5372(10)60100-2.

[11] A. Abdullahi, I. Choudhury, and M. Azuddin, Materials and Manufacturing Processes, 2015, 30(11), 1377-1390, DOI:10.1080/10426914.2015.1025977.

[12] E. Sachs, E. Wylonis, S. Allen, M. Cima, and H. Guo, Polymer Engineering & Science, 2000, 40(5), 1232-1247, DOI: 10.1002/pen.11251.

[13] B. Huang, S. Liang, and X. Qu, Journal of Materials Processing Technology, 2003, 137(1-3), 132-137, DOI:10.1016/S0924-0136(02)01100-7.

[14] H. Chen, X. Jing, Y. Deng, T. Wu, and S. Cao: 'Study on the Production Process of 304L Stainless Steel Injection Molding', IOP Conference Series: Materials Science and Engineering, 2018, IOP Publishing, 032022, DOI:10.1007/s00170-016-9256-2.

[15] S. Zinelis, O. Annousaki, M. Makou, and T. Eliades, The Angle Orthodontist, 2005, 75(6), 1024-1031, DOI:10.1043/0003-3219(2005)752.0. 2.

[16] B. Suharno, F. Mawardi, S. Dewantoro, B. Irawan, M. Doloksaribu, and S. Supriadi: 'Effect of powder loading on local feedstock injection behavior for fabrication process of orthodontic bracket SS 17-4 PH using metal injection molding', AIP Conference Proceedings, 2019, AIP Publishing, 020030, DOI:10426914.2018.1544709.

[17] M. Hamidi, W. Harun, M. Samykano, S. Ghani, Z. Ghazalli, F. Ahmad, and A. B. Sulong, Materials Science and Engineering: C, 2017, 78, 1263-1276, DOI:10.1016/j.msec.2017.05.016.

[18] N. Loh and R. German, Journal of materials processing technology, 1996, 59(3), 278-284, DOI:10.1016/0924-0136(95)02158-2.

[19] H. He, Y. Li, J. Lou, D. Li, and C. Liu, Powder technology, 2016, 291, 52-59, DOI:10.1016/j.powtec.2015.12.009.

[20] H. Ö. Gülsoy, Ö. Özgün, and S. Bilketay, Materials Science and Engineering: A, 2016, 651, 914-924, DOI:10.1016/j.msea.2015.11.058.

[21] A. Safarian, M. Subaşi, and Ç. Karataş, The International Journal of Advanced Manufacturing Technology, 2017, 89(5-8), 2165-2173, DOI:10.1007/s00170-016-9256-2.

[22] A. Dehghan-Manshadi, M. Bermingham, M. Dargusch, D. StJohn, and M. Qian, Powder technology, 2017, 319, 289-301, DOI:10.1016/j.powtec.2017.06.053.

[23] D. Sanétrník, B. Hausnerová, P. Filip, and E. Hnátková, Powder Technology, 2018, 325, 615-619, https://doi.org/10.1016/j.powtec.2017.11.041.

[24] J. W. Oh, W. S. Lee, and S. J. Park, Powder Technology, 2017, 311, 18-24, DOI:10.1016/j.powtec.2017.01.081.

[25] M. Seerane, P. Ndlangamandla, and R. Machaka, Journal of the Southern African Institute of Mining and Metallurgy, 2016, 116(10), 935-940, DOI:7159/2411-9717/2016/v116n10a7

[26] Y. Li, L. Li, and K. Khalil, Journal of Materials Processing Technology, 2007, 183(2-3), 432-439, DOI:.1016/j.2006.10.039.

[27] M.-W. Wu, Z.-K. Huang, C.-F. Tseng, and K.-S. Hwang, Metals and Materials International, 2015, 21(3), 531-537, DOI: 10.1007/s12540-015-4369-y.

[28] J. W. Oh, J. M. Park, D. S. Shin, J. Noh, and S. J. Park, Materials and Manufacturing Processes, 2019, 34(4), 414-421, DOI:10426914.2018.1544709.

[29] H. Abolhasani and N. Muhamad, Journal of materials processing Technology, 2010, 210(6-7), 961-968, DOI:10.1016/j.jmatprotec.2010.02.008.

[30] S. Li, B. Huang, Y. Li, X. Qu, S. Liu, and J. Fan, Journal of Materials Processing Technology, 2003, 137(1-3), 70-73, DOI:10.1016/S0924-0136(02)01069-5.

[31] Y. Zhang, E. Feng, W. Mo, Y. Lv, R. Ma, S. Ye, X. Wang, and P. Yu, Metals, 2018, 8(11), 893, DOI:10.3390/met8110893.

[32] L. V. Dihoru, L. N. Smith, R. Orban, and R. M. German, Materials and manufacturing processes, 2000, 15(3), 419-438. DOI:10426914.2018.1544709.

[33] L. Yu, C. G. Koh, L. J. Lee, K. W. Koelling, and M. J. Madou, Polymer Engineering & Science, 2002, 42(5), 871-888. DOI:.1016/j.2006.10.039.

[34] R. Pantani, I. Coccorullo, V. Speranza, and G. Titomanlio, Progress in polymer science, 2005, 30(12), 1185-1222. DOI:10426914.2018.1544709.

[35] J. Gonzalez-Gutierrez, I. Duretek, C. Kukla, A. Poljšak, M. Bek, I. Emri, and C. Holzer, Metals, 2016, 6(6), 129. DOI:.1016/j.2006.10.039.

[36] S. H. Kim, S. J. Park, S. J. Kim, T. G. Kang, and J. M. Park, Powder technology, 2014, 262, 198-202. DOI:10426914.2018.1544709.

[37] R. Aluru, M. Keefe, and S. Advani, Rapid Prototyping Journal, 2001, 7(1), 42-51. DOI:.1016/j.2006.10.039.

[38] M. Aslam, F. Ahmad, P. S. M. B. M. Yusoff, K. Altaf, M. A. Omar, and R. M. German, Powder Technology, 2016, 295, 84-95.

[39] J.-P. Choi, G.-Y. Lee, J.-I. Song, W.-S. Lee, and J.-S. Lee, Powder technology, 2015, 279, 196-202.

[40] Y. Li, L. Li, and K. Khalil, Journal of Materials Processing Technology, 2007, 183(2-3), 432-439, DOI:.1016/j.2006.10.039.

Synthesis and Characterization of Novel Anticancer Drug (DADMBTZ)

Akram Hosseinian*

* *Department of Engineering Science, College of Engineering, University of Tehran, P.O. Box 11365-4563, Tehran, Iran*

E-mail address: Hoseinian@ut.ac.ir

Abstract

Bithiazole is considered as a domain of bleomycin which countered as a chemotherapeutic drug to treat many types of cancers. Hence, trend towards the design of the model compounds containing bithiazole moiety has been increased, recently. In this regard, we describes the synthesis of a novel anticancer drug of *DADMBTZ = 2,2'-diamino-5,5'-dimethyl-* 4,4'-bithiazole using simple method. The characterization of this anticancer drug was done by IR, ^{1}H, ^{13}C NMR spectroscopy and elemental analyses. This anticancer drug was structurally characterized by single crystal X-ray diffraction. Single X-ray crystal analysis reveals that anticancer drug crystallizes in the triclinic space group $P\text{-}_{1}$. The crystal packing is mainly stabilized by intermolecular hydrogen bonding interactions. The anticancer drug was further characterized by UV-visible spectrophotometric measurements and fluorescence spectra. Anti cancer drugs, making use of this method, is a novel approach in the literature.

Keywords: Bithiazole, Heterocycle, Synthesis, Spectroscopy, X-ray diffraction.

1. Introduction

Bleomycins are natural glycopeptide antibiotics clinically used in the treatment of malignant tumors. Their structure, determined by Takita et al consists of four well-defined parts:

a sugar moiety, which may be required for the passage of the drugs through the cell membranes;

(i) a β-aminoalanine-pyrimidine-β-hydroxyhistidine unit which is capable of dioxygen activation by chelation with ferrous ion generating reactive species responsible for DNA cleavage;

(ii) a linear peptidic linker; and

(iii) a bithiazole containing moiety, which is believed to contribute significantly to the binding of the drugs to DNA.

The importance of the latter portion of the molecule to the biological properties of bleomycins has been confirmed recently by the study of synthetic models in the structure of which the bithiazole ring is lacking or is linked to a model metal complexing moiety of the molecules either by a connecting peptidic chain or by a glycopeptide spacer.

The precise role of the bithiazole group in the DNA-binding process of bleomycins has been the subject of controversy. Whether the bithiazole intercalates wedges in between the bases at a bending point of DNA or simply

binds in the minor groove seems to depend upon the nature of the bulky peptide chain to which it is linked. Nevertheless, although DNA sequences have been established to be specific sites for deoxyribose cleavage, no preferential binding directly induced by the bithiazole ring has been reported. Therefore, it could be of interest to couple to this heterocyclic moiety a molecule known to bind to double-stranded DNA in a sequence-specific way in order to systematically explore its binding characteristics.

In the present study we report the synthesis, DNA binding properties and biological valuation of a bithiazole molecules.

2. Material and Methods

All reagents for the synthesis and analysis were commercially available from Merck Company and used as received. Doubly-distilled water was used to prepare aqueous solutions. Ultrasonic generators were carried out on a SONICA-2200 EP, input: 50–60 Hz/ 305 W. Melting points were measured on an Electrothermal 9100 apparatus. Microanalyses were carried out using a Heraeus CHNO- Rapid analyzer. IR spectra were recorded using Perkin–Elmer 597 and Nicolet 510P spectrophotometers. Crystallographic data of polymer is given in Table 1. X-ray diffraction measurements were performed at low temperature (120 K) using a Bruker SMART CCD diffractometer equipped with graphite mono chromated Mo Kα radiation (λ = 0.71073 Å) using the φ–ω scan technique. Empirical absorption corrections were applied using program SADABS. Hydrogen atoms attached to carbon and nitrogen atoms were positioned geometrically, with Uiso values derived Ueq values of the corresponding carbon and nitrogen atoms. The structures of the title compounds were refined with SHELXL-97. The electronic absorption spectra were recorded on a Shimadzu UV–Vis 2100 recording spectrophotometer.

The 2,2'- diamino-5,5'- dimethyl- 4,4'-bithiazole (*DADMBTZ)* was prepared from 2,5-dibromo-3,4-hexandion and thiourea and recrystallized from $CHCl_3$. The single crystals suitable for X-ray analysis were then obtained by slow evaporation at room temperature. The light brown crystals were filtered off, washed with cold methanol and ethyl ether and dried.(yield 75 %, m.p. 437 K). Elemental analysis: found – C, 23.51 %; H, 3.45 %; N, 13.65 %; UV–Vis in DMSO (λ_{max}, nm):231.

3. Results and Discussions

The X-ray crystal structure of polymer is shown in Fig. 1. Single X-ray crystal analysis reveals that polymer crystallizes in the triclinic system and space group P-1. The crystal structure of the title compound have approximately C2 symmetry. The C—N bond lengths in the bithiazole ring is shorter than the single bond length of 1.48 Å and longer than the typical C-N distances of 1.28 Å indicating partial double-bond character. This can be interpreted in term of conjugation in the heterocycle.

TheC4-C4' bond length of is close to the standard value for a single bond between three bonded carbon atoms. The Unit cell packing of compound is given in Fig. 2.

The unit cell constituents form a network through intermolecular N–H…O bonds.

Table1.Crystal data and structure refinement for *DADMBTZ*

Emprical formula	$C_8H_{13}N_4OS_2$
Temperature	100(2) K
Wavelength	0.71073 Å
Crystal system	triclinic
Space group	P-$_1$
Unit cell dimensions	a = 7.6237(4)Å, α = 114.7620(10)º b = 114.6140(7) Å, β = 98.6730(10) c = 13.1084(7)Å, γ = 90.5560(10)
Z	4

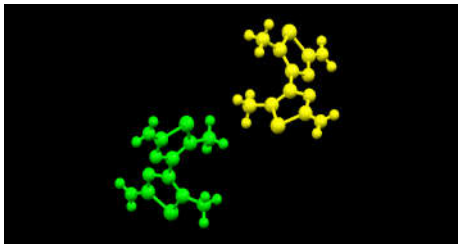

Fig.1. ORTEP drawing of *DADMBTZ*

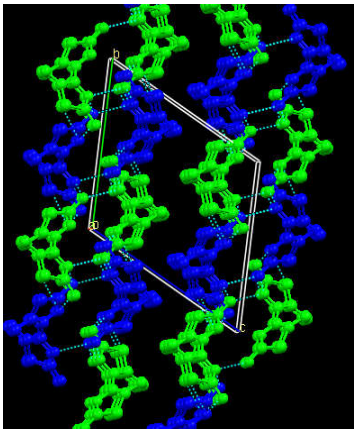

Fig.2. A view of unit cell of *DADMBTZ*

The IR spectrum, ^{1}H-NMR and ^{13}CNMR provide evidence of the anticancer drug (*DADMBTZ)*.(Fig.3-5)

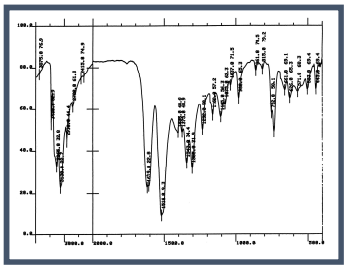

Fig.3. IR spectrum

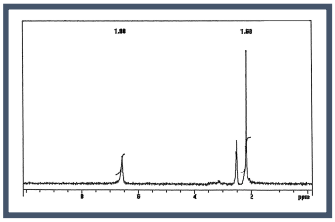

Fig.4. ^{1}H-NMR spectrum

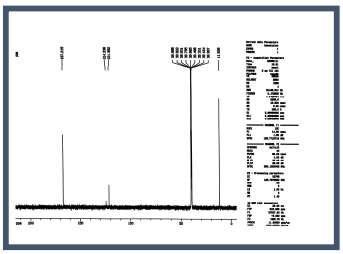

Fig.5. ^{13}CNMR spectrum

Conclusions

New bithiazole heterocycle polymer 2,2'- diamino- 5,5'-dimethyl- 4,4'-bithiazole was synthesized using simple method and characterized by IR spectroscopy and ^{1}H, ^{13}C NMR spectroscopy and elemental analyses. The polymer was further characterized by UV-visible spectrophotometric measurements and fluorescence spectra. Novel bithiazole polymer was structurally characterized by single crystal X-ray diffraction.Making use of this method, is a novel approach in the literature. This simple method is rarely used for syntheses of polymers, but can be easily controlled.

Acknowledgements

The authors would like to acknowledge the financial support Iran National Science Foundation (INSF) for this research.

References

[1] M. Laine, F. Richards, E. Tarnaud, C. Bied-Charreton, C. Verchere-Beaur, J. Biol.Inorg. Chem. 9 (2004) 550.

[2] R.S. Kumar, K. Sasikala, S. Arunachalam, J. Inorg. Biochem. 102 (2008) 234.

[3] M.E. Anderson, A.G.M. Barrett, B.M. Hoffman, J. Inorg. Biochem. 80 (2000) 257.

[4] T. Biver, F. Secco, M.R. Tine, M. Venturini, A. Bencini, A. Bianchi, C. Giorni, J.

[5] Inorg. Biochem. 98 (2004) 1531.

[6] K. Lassoued, J.-P. Clauvel, C. Katlama, M. Janier, C. Picard, S. Matheron, Cancer 66 (1990) 1869.

[7] James C. Quada, Jr, Didier Boturyn and Sidney M. HechtBioorganic & Medicinal Chemistry 9 (2001) 2303–2314

[8] R. Yu, Y. Zheng, Y. Li, Z. Wu, C. Yan, Syntheses and structures of copper(II) and nickel(II) complexes with N,N'-(4,4'-bithiazole-2,2'-diyl)diacetimidamide ligands: in vitro cytotoxicities and DNA-binding properties, Transition Met Chem (2012) 37:399–406 DOI 10.1007/s11243-012-9603-6.

Phylogeny and genetic diversity of Compsobuthus mattensii based on mitochondrial cytochrome oxidase subunit I gene

Hedieh Jafari[1], Fatemeh Salabi[1]

[1]Razi Vaccine and Serum Research Institute, Agricultural Research, Education and Extension Organization (AREEO), Ahvaz, Iran.

*Email: hedieh_jafari@yahoo.com

Abstract

Scorpions are widely distributed throughout Iran and scorpion species in Khuzestan province is one of the most diverse fauna of West Asia region. Estimates of variation among sequences were based on a COXI gene. The results obtained from the tree had two clusters A and B. Cluster A was also divided into two sub-clusters A1 (C.M4, C.M 1, C.M10, C.M8, C.M9, CM2), (C.M6, C.M5, A2 (C.M3) and B (C.M7) which the samples in these sub-branches showed 65-95% similarity. Sample C.M7 was placed in cluster B, which, although similar to other specimens in cluster A, was completely different from the rest of the specimens. Nucleotide variations found in the current work constitute the first descriptive report for *Compsobuthus mattensii*. Moreover, future studies may enlighten the genetic and venom composition variations for this scorpion species

Keywords: scorpion, *Compsobuthus mattensiii* COXI gene, phylogeny.

1. Introduction

Scorpions have medical importance roles as hunter arthropods and widely distributed in different regions with various climatic conditions, especially in tropical regions (Chippax et al., 2008; Rafeeazadeh et al., 2009). The family Buthidae is the most diverse family of scorpions and in this family (Navidpour 2015). Scorpions, as living fossils, have highly conserved morphology. The Compsobuthus mattensii is a scorpion of Buthidae family which can be found in Iran, Farzanpay (1988) and Akbari (2007) reported only C. matthiesseni from South and South-West parts of Iran and Dehghani et al (2009) identification of C. matthiesseni with the prevalence of 20.6% as one of the major species responsible for scorpion sting in Iran. Study of the behavior of this scorpion has shown that the monthly activity of this species started from Apr and ended in Mar with a peak in Jun. The evidence shows the adaptation of this species to tem-perate conditions than to higher tempera-tures. The sampled scorpions were collect-ed from rock crevices and bark of trees, where having the high humidity.

According to initial taxonomic studies Vachon (1949) described Compsobuthus, its species had been placed in Buthus Leach, 1818. More recently several specialists studied this genus in some detail (Levy & Amitai, 1980, Sissom & Fet 1998, Lorenco & Monod 1998, Lorenco 1999, Vignoli, 2005), and in addition to introducing new species also elaborated on new characters and new understanding of species-group taxa. Although evidence of inappropriate morphological characteristics for species and subspecies detection has been observed, result of nuclear and mitochondrial markers used in solving these challenges (Gantenbein and Largiadèr 2002; Vignoli et

al. 2005; Salomone et al. 2007). Molecular study and nucleotide sequences of these genes are used to characterize phylogenetic tree and determine the degree of affinities.

Therefore, the C. matthiesseni collected from Khuzestan province were identified molecular analysis and evaluated based on cytochrome c oxidase subunit I. The results were applied in the biosystematics approaches of this genus in Khuzestan and genetic divergence measurement of the studied species based on the sequence data of the mentioned genes.

2. Material and Methods

2.1 Sampling and PCR amplification

Compsobuthus mattensii is the small scorpions which live on sandy heights. The specimens of this genus were collected in the Khuzestan region based on the dispersion and diversity in different regions from April to September 2016 and April to June 2017. The morphological analysis of the specimens was based on the terminology presented by Vashon 1974. Genomic DNA was extracted using extraction kit (Sina PureTM Tehran,Iran) according to the Kit's instruction. Polymerase chain reaction was performed for duplicating one segment about 700 nucleotides of cytochrome c oxidase subunit I (COXI) from the primers 5'GGTCAACAAATATATAATAGATAT and 5'CCGGTAAAATTAAAATATAAA, amplification of this primer was carried out in 25 µl reaction volumes containing 1–5 µl of DNA template, 2.0 mM MgCl2, 200 mM of each dNTP, 25 pmol of each forward and reverse primer, 0.5 Unit of Taq DNA polymerase. The cycling protocol included an initial hot start (94 _C for 3 min), 35 PCR cycles of 94 °C for 30 s, 58 °C for 30 s, 72 °C for 60s and final extension was 72 °C for 7 min.

2.2 Phylogenetic analyses

PCR product, along with the designed primers, was sent to Tekapozist Co., Tehran for sequencing the COXI gene and determining the sequences of the product by using primers. Phylogenetic analyses were performed on individual COXI datasets using Maximum Likelihood (ML) method. The ML analysis was performed using MEGA 7.0 and the nodes were tested for robustness with 10,000 bootstrap replicates. *Androctonus crassicauda* was used as outgroup.

3. Results and Discussions

Eight new species of genus Compsobuthus sp. were described by Kovarı´k (2003). C. matthiesseni belongs to Buthidae family being bright yellow and 40–50 mm in length. C. matthiesseni has robust metasomal segments, pectinal tooth counts (males 27–29 teeth, females 20–23 teeth), a broad telson, and fused central median and posterior median carapacial carinae (Sissom et al., 1998). C. matthiesseni has some dark spots, which are considered diagnostic for this taxon (Fig. 2). This scorpion is reported from central Iran (Kashan), southeastern Turkey and eastern Iraq which are all in the Tigris–Euphrates region (Sissom and Fet, 1998; Vignoli et al., 2003). C. matthiesseni is common with a very high ensity in Khuzestan (Navidpour et al., 2008). It is usually found in warm and moist places like stone gaps and tree crusts.

In present study total 10 female specimens including Compsobuthus mattensii and a specimen of Androctonus crassicauda as an external group were sequenced. In order to investigate the molecular diversity of nucleotide sequences of COXI gene fragments obtained from scorpions of the genus Campusobutus mattensii in Khuzestan province, MEGA7 software was used. In this way, first the prepared sequence file was loaded in the program and after the alignment operation, the phylogenetic tree was drawn. The results obtained from the tree had two clusters A and B. Cluster A was also divided into two sub-clusters A1 (C.M4, C.M 1, C.M10, C.M8, C.M9, CM2), (C.M6, C.M5, A2 (C.M3) and B (C.M7) which the samples in these sub-branches showed 65-95% similarity. Sample C.M7 was placed in cluster B, which, although similar to other specimens in cluster A, was completely different from the rest of the specimens. This phenomenon indicates the existence of intra-population differences in the studied specimens are Compsobuthus mattensii scorpion in different regions of Khuzestan province.

3.1 Table 1. The average genetic distance of Compsobuthus mattensii from Khuzestan province

	1	2	3	4	5	6	7	8	9	10
1.CM1										
2.CM2	0.005									
3.CM3	0.035	0.039								
4.CM4	0.002	0.005	0.038							
5.CM5	0.040	0.057	0.000	0.026						
6.CM6	0.053	0047	0.049	0.033	0.052					
7.CM7	0.090	0.101	0.088	0.089	0.073	0.096				
8.CM8	0.002	0.001	0.003	0.005	0.024	0.031	0.102			
9.CM9	0.004	0.003	0.025	0.001	0.034	0.027	0.097	0.004		
10.CM10	0.004	0.000	0.035	0.003	0.042	0.021	0.110	0.008	0.005	

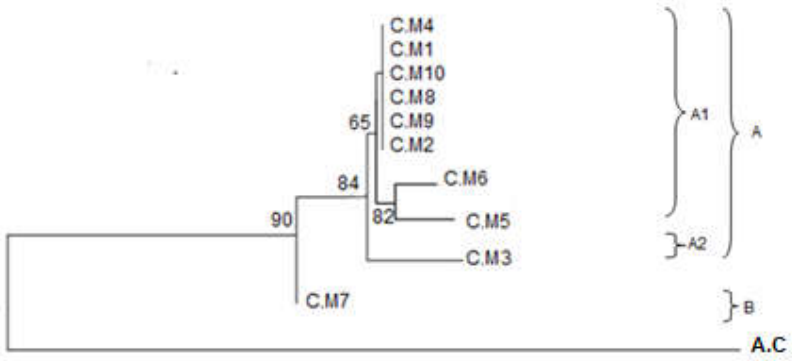

3.2 Figure 1. ML tree resulting from the analysis of the combined sequences of COXI of Compsobuthus mattensii from Khuzestan province Androctonus crassicuda was selected as out-group

Identification of scorpion and determine relationships between them based on analyzing of molecular studies and phylogenic tree showed that the branching order of Buthidae family of genera strongly supports Compsobuthus sp. as a sister group with Mesobuthus, Liobuthus, Kraepelinia.

According to new perspectives in systematic animal science, molecular study and determination of intraspecific changes can be a new achievement in the classification of animals.

Acknowledgment

We are thankful to Razi vaccine and serum research institute, for providing infrastructural facilities.

References

[1] A. Akbari, A. Study of scorpion fauna of iran, *Project report publication of razi vaccine & serum research institute, (*2007) 96 (in farsi).

[2] B. Gantenbein, C.R. Largiadèr, *Mesobuthus gibbosus* (Scorpiones: Buthidae) on the island of Rhodes—hybridisation between Ulysses'stowaways and native scorpions? Mol Ecol (2002) 11:925–938. doi: org/10.1046/j.1365-294X.2002.01494.

[3] F. Kovařík, Eight new species of *compsobuthus* vachon, 1949 from africa and asia (scorpiones: buthidae), *Serket (2003)* 8(3): 87–112.

[4] J.P. Chippaux, M. Goyffon, Epidemiology of scorpionism: a global appraisal, Acta Trop (2008) 107(2):71-9.

[5] Navidpour S., f. Kovařík, M. E. Soleglad & V. Fet. (2008). Scorpions of iran (arachnida, scorpiones), Part iii. Bushehr province. *Euscorpius* 69: 1–29.

[6] N. Salomone, V. Vignoli, F. Frati, F. Bernini, Species boundaries and phylogeography of the "*Euscorpius carpathicus* complex" (Scorpiones: Euscorpiidae) in Italy, Mol Phylogenet Evol (2007) 43:502–514. doi.org/10.1016/j.ympev.2006.08.023.

[7] M. Vachon,). Sur la systématique des scorpions, *Mémoires du muséum national d'histoire naturelle, paris*, (1940b) 13(2): 241–259.

[8] R, Dehghani, N, Dinparast djadid, D, Shahabzadeh, and S, Bigdeli, Introducing compsobuthus matthesseni (birula,1905) scorpion as one of the major stinging scorpions in khuzestan ,iran, T*oxicon (2009)* 54(3):272-275.

[9] R. Farzanpay, *Knowing scorpions.* Teheran: central university publications, no. 312, biology (1987) 4, 231 pp. (in farsi, with latin index).

[10] SH, Navidpour, An annotated checklist of scorpions in south and southwestern parts of Iran, Int J *Fauna* Biol Stud (2015) 2 (3): 09-15.

[11] S. Rafeeazadeh, Report of scorpion sting In Iran during 2009. Center of management of preventing and fighting with the diseases (2009) 1-15 (in Farsi).

[12] V, Fet, M.E. Braunwalder, The scorpions (Arachnida: Scorpiones) of the Aegean area: current problems in taxonomy and biogeography, Belg J Zool (2000) 130(1):15-20.

[13] V. Vignoli, Description of a new species of *compsobuthus* vachon, 1949 (scorpiones: buthidae) from southern Iran, *Zoology in the Middle East* (2005) 34: 79–86.

[14] WD, Sissom V. Fet. Redescription of *compsobuthus matthiesseni* (scorpiones, buthidae) from southwestern Asia, *The journal of arachnology* (1998) 26:1–8.

[15] W.R. Lourenco, Two new species of *compsobuthus* vachon, 1948 (scorpiones, buthidae,. Entomol. Mitt. Zool. Mus. Hamburg, (1999) 13(164):315-319.

[16] W.R. Lourenco, L. Monod, Rediscription of *compsobuthus rugosulus* (pocock, 1900) (scorpiones, buthidae) based on speciemens from Pakistan, Rev. Suisse zoology (1998) 105(4):789-796.

Study of Antimicrobial Peptides Encapsulation into the Polymeric and Phospholipid Nanoparticles using Molecular Dynamics Simulation

Faramarz Mehrnejad

Department of Life Sciences Engineering, Faculty of New Sciences and Technologies, University of Tehran, Tehran, Iran.

Mehrnejad@ut.ac.ir

Abstract

Antimicrobial peptides drugs can be encapsulated by nanoparticles and then deliver to the target cell and tissues. Herein, the effects of encapsulation on antimicrobial peptides' structure and stability have been studied using molecular dynamics (MD) simulations. Magainin-2, Pleurocidin, and Pardaxin have been selected as the antimicrobial peptide models. Furthermore, the PEG, PLGA polymers, and cell membranes have been chosen as the molecules encapsulating the antimicrobial peptide models. The polymers could keep the peptide's secondary structure content, considering the results of Magainin2 in pure water. The polymers were non-covalently bound to Magainin 2. The more efficient encapsulation of the peptide occurred in the PEG polymers' presence and specific concentrations of the PLGA polymers. The results have indicated that the N-terminal region of Pleurocidin has a crucial role in the peptide interactions with the bilayer models. Pleurocidin has more proper interactions with the DOPC/DOPG (3:1) bilayer than with the other bilayers. The results also revealed that antimicrobial peptide Pardaxin keeps its structure in DPC micelles. The analyses have shown that the phenylalanine residues of Pardaxin play a crucial role in the peptide activity. This research will provide an excellent opportunity to design polymer and bilayer surfaces for drug delivery applications such as controlled-release peptide delivery systems.

Keywords: Antimicrobial peptides; Polymeric nanoparticles; Molecular dynamics simulation

1. Introduction

Nanoparticles are essential in drug delivery and can transport various drugs to different parts of the body at the right time[1, 2]. Biodegradable polymeric micellar nanoparticles, such as polylactic-co-glycolic acid (PLGA) and polyethylene glycol (PEG), and have been extensively attracted as carriers in pharmaceutical science[3, 4]. The molecules are safe, biodegradable polymers and copolymers with various medical applications, particularly in drug delivery. AMPs are the overriding component of the innate immune systems in all domains of life and kill a broad range of targets consist of parasites, viruses, and bacteria. Encapsulation of the peptide in the safe, biodegradable polymers and copolymers could maximize their therapeutic effects and minimize their harmful side

effects[5]. Magainin2, the antimicrobial peptide, has an amphipathic α-helix with 23 amino acids. The peptide has extensive antimicrobial activity and is the only AMP that can enhance drug molecules' transdermal transport. Pleurocidin, an antimicrobial peptide with 25 residues length, has attracted a lot of attention because of its desirable characteristics. The most crucial trait of Pleurocidin is the deficient hemolytic activity against eukaryotic cells and high activity against prokaryotic cells. In this work, the encapsulation of Magainin, Pardaxin and Pleurocidin into the polymeric and phospholipid nanoparticles were investigated using molecular dynamics simulation.

2. Material and Methods

The GROMACS package, version 5.1.4, was used to run MD simulations[6]. The initial coordinates of Magainin2 (PDB ID: 2MAG), Pardaxin (PDB ID: 1XC0), and Pleurocidin (PDB ID: 1Z64) were obtained from the RCSB protein data bank. The lipid bilayer models and the polymers topology files were made by the CHARMM-GUI web tool and the automated force field topology builder database (ATB). The simulation systems solvated with the TIP3P water model and then neutralized by 0.15 M sodium and chloride counterions. In the next step, all MD simulation systems were energy minimized using the steepest descent algorithm. The simulation systems were continuously equilibrated under three consecutive NVT ensemble and two NPT ensemble. Each of the NVT and NPT ensembles performed for 1000 ps and 1000 ps, respectively. Over the NVT and NPT ensembles, the Berendsen thermostat was employed to maintain the temperature at 303 K. The Berendsen weak coupling method was used to keep the simulation systems' pressure 1 bar in NPT ensembles[7]. All H-bonds were constrained with the LINCS algorithm[8], and the electrostatic interactions were calculated by the particle-mesh Ewald (PME) algorithm[9].

3. Results and Discussions

The root means square deviation (RMSD) of the structure of the peptides in the presence of all types of polymers and cell membranes were analyzed. The RMSD of Magainin indicated the peptide kept the secondary structure content in the PEG and PLGA nanoparticles (Figure 1). Generally, considering the results of the peptides in pure water, the polymeric nanoparticles could keep the peptide's NMR structure in good agreement with the mentioned experimental and theoretical researches. The dictionary of protein secondary structure (DSSP) analysis was done for the peptides to show the nanoparticles' effect on the peptide's secondary structure content.

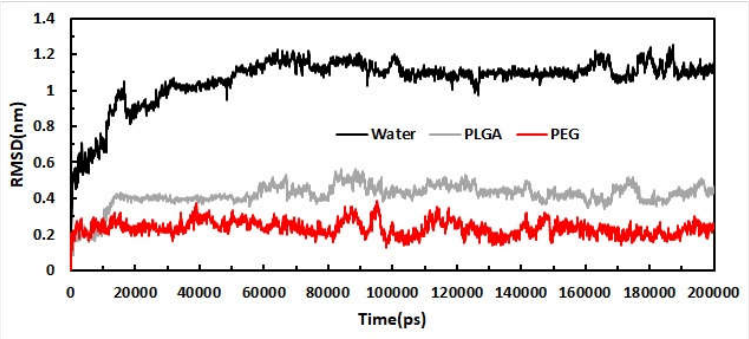

Figure 1. Root means square deviation (RMSD) of Magainin in water, PEG, and PLGA environments.

The RMSD result of Pardaxin in water and DPC micelles was shown in Figure 2. As shown in the results, the peptide keeps its most helical content when the micelles fully entrap it.

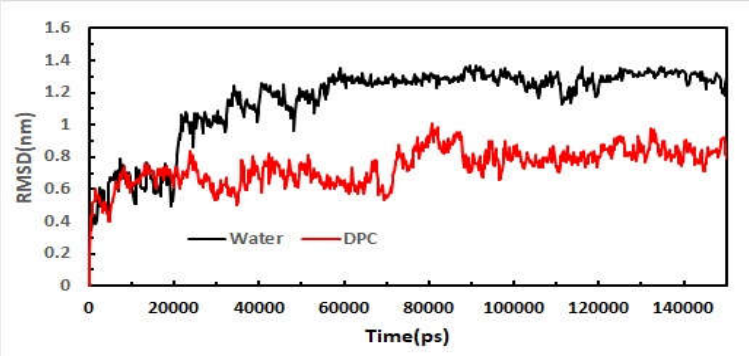

Figure 2. Root means square deviation (RMSD) of Pardaxin in water and DPC environments.

The Circular dichroism (CD), fluorescence spectroscopy, NMR, and MD simulations studies have shown that the peptides have more than 90 percent helical structure in the presence of hydrophobic environments[10-12]. Interestingly, the peptides have remarkably kept their helical structure in all MD simulations. Our results indicated that the polymers and lipid nanoparticles were non-covalently bound to the peptides. Therefore, almost all the secondary structures were kept during the MD simulations.

The radial distribution of function (RDF) results show that the polymers and lipid distribution around the peptides gradually increased; therefore, the maximum distribution can be detected from 0.4 to 0.6 nm. The number of contacts between the peptides and water molecules in the presence and absence of the nanoparticles was computed. The results revealed that, compared to the pure water ambient, the number of peptide contacts with water molecules decreased in nanoparticles' presence. It means the peptides bind to the nanoparticles over the simulation time. Besides, the number of contacts between the polymers in the micellar aggregations was analyzed. The results show that the number of contacts for all polymers was increased during the MD simulation. The MD results demonstrated that the dominant deriving force for aggregation of the polymers and lipid molecules into micelles and vesicles is the hydrophobic interactions. Therefore, the number of contacts may indicate the number of hydrophobic interactions between the polymers in their micellar aggregations. All micelles had hydrophobic interactions with the peptides, whereas they made hydrogen bonds with water molecules. The MD results show that the peptide's number of contacts with water molecules reduces during the MD simulation time, and the

peptides keep their helical structure. According to the energy analyses, the hydrophobic interactions are essential in the polymers' aggregation and the nanoparticles' peptides encapsulation.

References

[1]. P. Couvreur, Nanoparticles in drug delivery: past, present and future, Advanced drug delivery reviews 65(1) (2013) 21-23.

[2]. M. Yu, et al., Silica-based nanoparticles for therapeutic protein delivery, Journal of Materials Chemistry B 5(18) (2017) 3241-3252.

[3]. M. Jafari, F. Doustdar, and F. Mehrnejad, Molecular Self-Assembly Strategy for Encapsulation of an Amphipathic α-Helical Antimicrobial Peptide into the Different Polymeric and Copolymeric Nanoparticles, Journal of chemical information and modeling 59(1) (2018) 550-563.

[4]. Z. Lotfi-Sousefi, et al., Insight into the Microcosm of the Human Growth Hormone and Its Interactions with Polymers and Copolymers: A Molecular Dynamics Perspective, Langmuir (2020).

[5]. H.-H. Han, et al., Protein encapsulation: a new approach for improving the capability of small-molecule fluorogenic probes, Chemical Science 11(4) (2020) 1107-1113.

[6]. D. Van Der Spoel, et al., GROMACS: fast, flexible, and free, Journal of computational chemistry 26(16) (2005) 1701-1718.

[7]. H. Berendsen, J. Grigera, and T. Straatsma, The missing term in effective pair potentials, Journal of Physical Chemistry 91(24) (1987) 6269-6271.

[8]. B. Hess, et al., LINCS: a linear constraint solver for molecular simulations, Journal of computational chemistry 18(12) (1997) 1463-1472.

[9]. T. Darden, D. York, and L. Pedersen, Particle mesh Ewald: An N· log (N) method for Ewald sums in large systems, The Journal of chemical physics 98(12) (1993) 10089-10092.

[10]. F. Porcelli, et al., Structure and orientation of pardaxin determined by NMR experiments in model membranes, Journal of Biological Chemistry 279(44) (2004) 45815-45823.

[11]. J. Gesell, M. Zasloff, and S.J. Opella, Two-dimensional 1H NMR experiments show that the 23-residue magainin antibiotic peptide is an α-helix in dodecylphosphocholine micelles,

sodium dodecylsulfate micelles, and trifluoroethanol/water solution, Journal of biomolecular NMR 9(2) (1997) 127-135.

[12]. R. Talandashti, et al., Molecular basis for membrane selectivity of antimicrobial peptide pleurocidin in the presence of different eukaryotic and prokaryotic model membranes, Journal of chemical information and modeling 59(7) (2019) 3262-3276.

The simulation of the effect of Wi-Fi electromagnetic waves on testis temperature and spermatogenesis in human

Mahmoud Feizipour Namaghi [1*], Hesameddin Hadiani [2]

[1] Biochemistry and biophysics department, Biological Institution, Malek Ashtar University of Technology, Tehran, Iran

[2] Biology department, Faculty of science, Islamic Azad University branch of Mashhad, Mashhad, Iran

*Email:. mhd.feyzi97@gmail.com

Abstract

As humankind uses devices which produce electromagnetic waves, it seems essential to study the effect of such waves on human body tissue. One of these tissues is testis that is responsible for reproduction in men. A currently used source which release electromagnetic waves is Wi-Fi technology. The spermatogenesis is defined as the process of producing the male gametes which is called spermatozoa or simply the sperm. This process is done in testis organ which located in scrotum out body, because the optimum temperature of spermatogenesis process is 2 to 3 °C lower than physiologic body temperature. When a tissue is exposed to electromagnetic waves, it may cause heat stress, and this may affect spermatogenesis in testis. In the present article, considering the medical ethics, it was preferred to do the experiment through a simulation. The largest 2D testis section was designed and the thermal effect of the Wi-Fi waves (with determined properties) was studied in different distances by simulating. The results suggest that such waves may cause a slight increase in testis temperature (about 0.10°C to 0.16°C). Therefore, testis exposure to the Wi-Fi may not cause any significant alter in spermatogenesis rate.

Keywords: Testicle, Spermatogenesis, Bioelectromagnetic, Hyperthermia, Infertility

1. Introduction

1.1 Male reproduction organ

The male reproduction organ in human includes penis and testicles (testis). Testicles are located in scrotum in a pair form. Testicles is the responsible for producing sperms. The reason of locating the testicles in the scrotum out of body is that spermatogenesis should be done in a temperature lower than physiological body temperature. This temperature is usually 35°C (about 2 to 3 °C lower than body temperature) [1]. Any increase may cause a great deal of influence on spermatogenesis and causes decrease in sperm quantity and also the decrease in male fertility [2].

1.1.1 Testis anatomy

After the birth, the testis sizes of infants are about 1.5cm length and 1cm width. In an adult male, these dimensions are about 3cm for diameter, 3-5 cm length and 2-4 cm width. However, these dimensions decrease during the aging.[3] The epididymis which is responsible to keep and maturation of the sperms is located on the testis. The end of epididymis is connected deferent duct, which mediates sperms into seminal vesicle during the ejaculation, in order to flow into ejaculatory duct. [4]

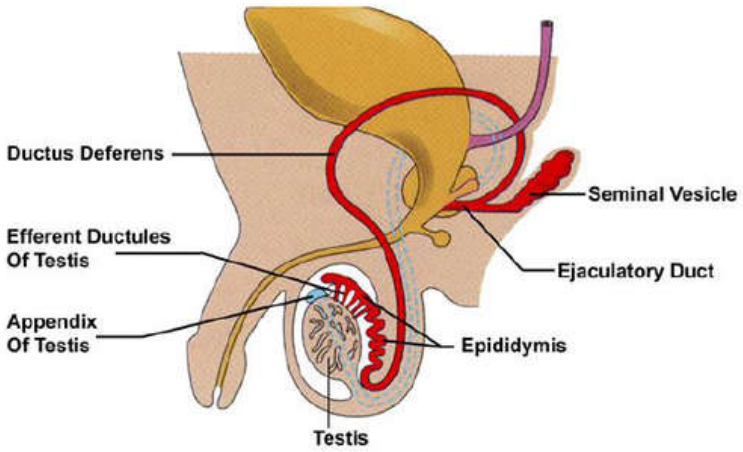

Figure 1-1 Testis, epididymis, deferent duct, ejaculatory duct and vesicle seminal locations

The outer layers of the testis are about 6-8 mm and includes some cutaneous and muscular layers:

1- a highly wrinkle skin

2- dartos muscle

3- spermatic fascia

4- cremasteric fascia

5- tonica vaginalis

6- tonica albuginea (which covers the testis) [5].

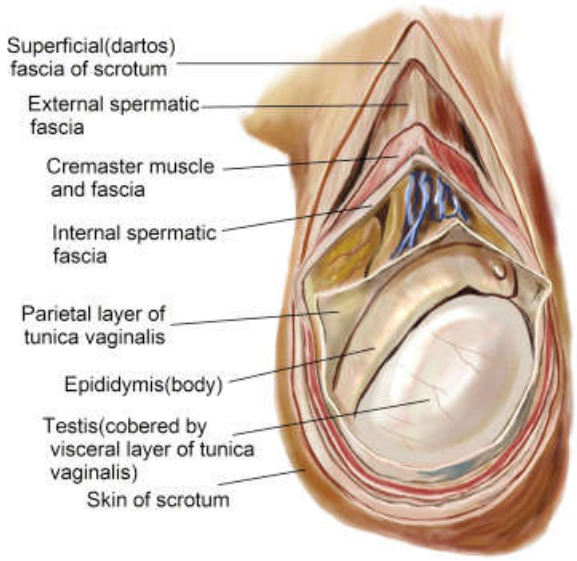

Figure 1-2 Testis layers

The tonica albuginea and tonica vaginalis are respectively blood serous layer and fibrous layer which are located all around the testis. Only tunica vaginalis is connected to the testis, in the posterior part (Greene,2016).

1.1.2 Spermatogenesis process and temperature

The spermatogenesis is defined as the process of producing the male gametes which is called spermatozoa or simply the sperm. In the result of this process, a haploid cell is produced using a diploid cell, which can fertilize another haploid cell (ovum) .This process is initiated in the testis and is completed in the epididymis. One of the most important factor in the spermatogenesis is the temperature. This temperature should be lower than the body temperature, in order that the spermatogenesis reach the end perfectly. Any increase in temperature may cause affect the produced sperm quantity negatively. The optimum temperature for the human is about 2°C lower than body temperature (about 35°C) and it is about 8°C lower than body temperature for the mouse. Maintain the testis temperature is done through adjusting the blood circulation, and using the dartos and cremaster muscles.[6]

1.2 Wi-Fi wave

The Wi-Fi is a wireless technology which provides internet connection in a determined regional domain. The Wi-Fi uses electromagnetic waves to create communications. The Wi-Fi connection range may be so much little (some rooms) to some kilometers. In order to cover large areas, some access points are used, this method is called Wi-Fi overlap [7].

1.2.1 Electromagnetic properties of Wi-Fi

1.2.1.1 Power

Wi-Fi routers use different bandwidth depending on different technologies. Major facilities are manufactured according to the predefined standards. These Wi-Fi access points are usually near the individuals. But considering the inverse-square law, the more the distance increases, the more the wave powers decrease significantly. This law is applicable for major waves including electromagnetic waves. According to this law: the power is inversely proportional to the square of distance from the source (equation 1). Electromagnetic waves are radiated in a sphere shape, and regarding the mentioned law, it is expected that by increasing the distance from the source, the power (in that point) decrease significantly.

Equation 1

$$i \propto \frac{1}{r^2}$$

In which: *i* is the power intensity and *r* is the distance from the source.

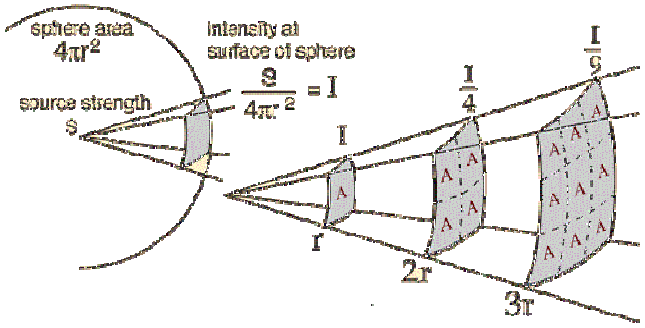

Figure 1-3 The intensity of the waves which are radiated in a sphere shape is proportional to square of the distance from any point toward the radiation axis

Considering the mentioned explanations and sphere surface formula ($4\pi r^2$), the wave intensity on a determined surface of an imaginary sphere equals the ratio of power/intense of the radiation source to the determined surface (equation 2):

Equation 2

$$i = \frac{S}{4\pi r^2}$$

In which *i* represents the wave intensity, *S* is the radiation source power intensity and *r* is the distance from the source. (Jeffrey, 2014)

1.2.1.2 Wi-Fi frequency

The Wi-Fi frequency depends on the application of the router. In the following table, you can observe the different frequency values of the different generations of the Wi-Fi technology.

Table 1-1 Wi-Fi frequency ranges in different technology generations [9]

Generation/IEEE Standard	Frequency
Wi-Fi 6 (802.11ax)	6 GHz
Wi-Fi 5 (802.11ac)	5 GHz
Wi-Fi 4 (802.11n)	2.45 GHz
Wi-Fi 3 (802.11g)	2.4 GHz
Wi-Fi 2 (802.11a)	5 GHz
Wi-Fi 1 (802.11b)	2.4 GHz

The newest Wi-Fi generation for the domestic application, is the IEEE 802.11x which is commercially named Wi-Fi 6. The frequency of this generation, which was presented by the end of 2019, is varied between 1-6 GHz, while in the domestic application, the frequency which is widely used is about 2.45 GHz.[9].

2. Material and Methods

In order to commit the experiment (simulation), we used COMSOL Multiphysics Version 5.2a.
The source parameters including power and frequency were set 8.2 W and 2.45 GHz respectively. Physical properties of the tissue and ambiance (air) are indicated in the Table 2-1. (the values are extracted according to the source parameters: 8.2 W and 2.45 GHz)

Table 2-1 Physical properties of the tissue and ambiance. The values for muscle indicates the common values of Dartos and Cremaster tissues (which are muscle) [10].

Material	**Thermal Conductivity (W/(m.k))**	**Density (Kg/m^3)**	**Specific heat capacity (J/(Kg.k))**	**Relative permittivity**	**Loss tangent (Rad)**
Air	0.03	1	1004	1	0
Skin	0.37	1109	3391	38	0.272
Muscle	0.49	1090	3421	52.7	0.241
Testis	0.52	1082	3778	57.6	0.276

The electromagnetic field is considered as full field, and the ambiance pressure is set to 1 atm. The port type is supposed rectangular and the mode is transverse electromagnetics (TEM).

The thickness and dimensions of each tissue layers are mentioned in the Introduction. The ambiance temperature is set on 298.15 K and the tissue temperature is set in 308.15 K. Also the blood properties including specific heat, blood perfusion and density are considered 3639 J/(kg/k), 0.0036 (1/s) and 1050 kg/m^3 respectively.[10] The tissue layers which have extremely low effect on the experiment are ignored in this simulation.

For the present simulation, two modules were used namely electromagnetic wave and bioheat, to study wave radiation and the thermal effect on living tissue respectively. The aim of the simulation is to experiment and obtain the amount of heat created while a testis is disposed to a Wi-Fi source (with before-mentioned parameters) in a period of 2 hours. We considered the distances of 1 m, 2m and 3m.

The Wi-Fi model that we supposed in this simulation is a TP-link Archer AX6000, which is included in the family of IEEE 802.11 standards. The maximum value of the power known for such a Wi-Fi router is 11.2 W, but we considered the average amount which is 8.2 W. (Man et al., 2016)

3. Results and Discussions

After simulation, we obtained the following results. The heat map results (after 2 hours) are demonstrated in the Figures 3-1, 3-2, 3-3.

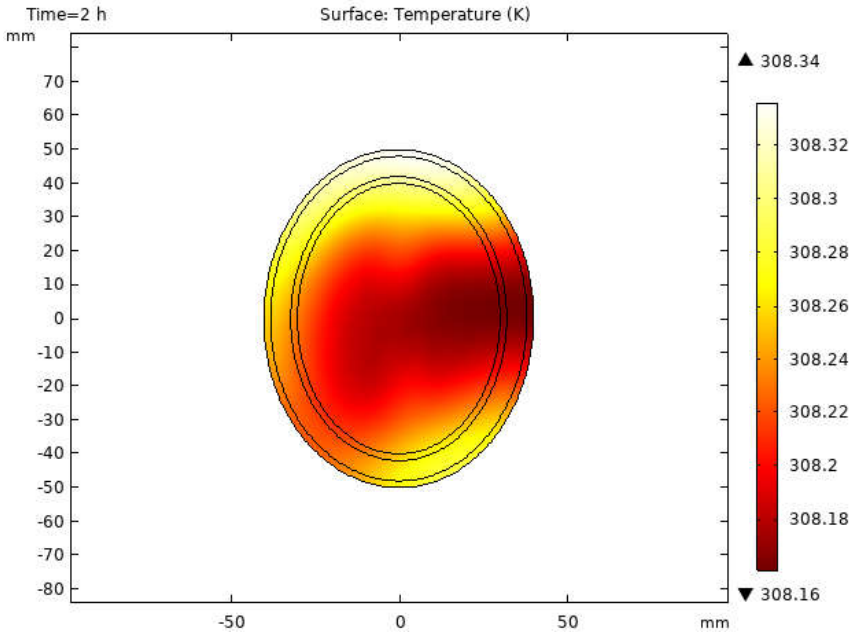

Figure 3-1 The heat map, in the distance of 1m from the source

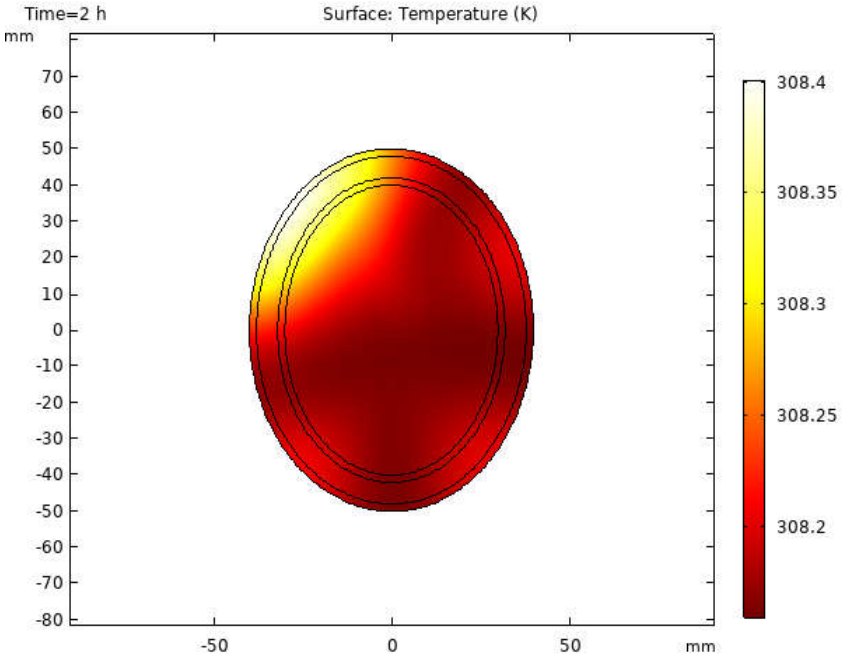

Figure 3-2 The heat map, in the distance of 2m from the source

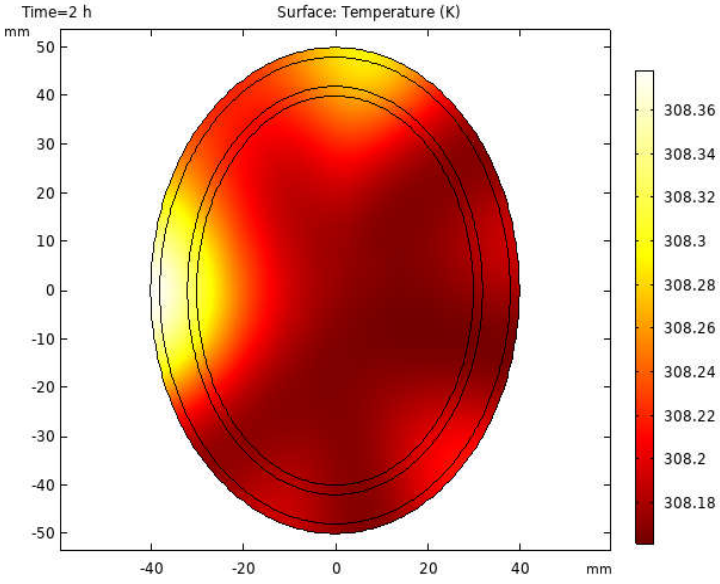

Figure 3-3 The heat map, in the distance of 3m from the source

To investigate the effect of Wi-Fi waves on spermatogenesis, it is necessary to consider the testicular layer, which is involved in sperm production.

The following figures demonstrate the variation of the heat in the vertical cutline of testis (from the lowest point to the highest point figure 3-4) .

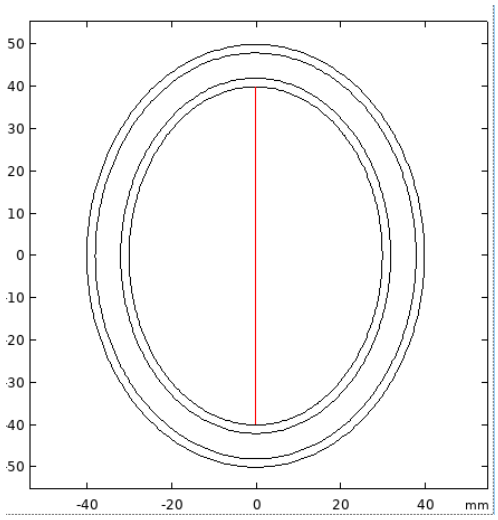

Figure 3-4 The vertical cutline

The x-axis (in the following graphs) represents the lowest point of the testis (-40) to the highest point (+40) which are demonstrated from 0 to 80.

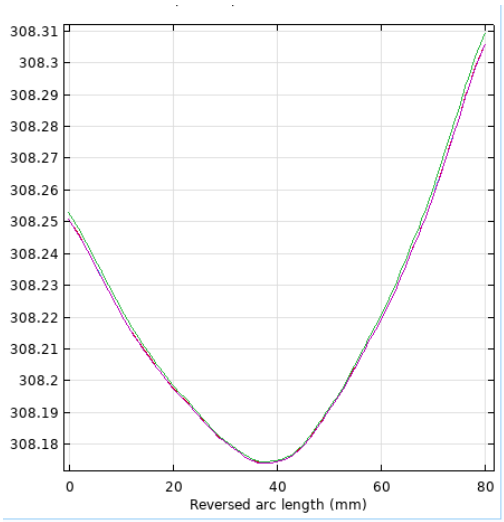

Figure 3-5 The vertical temperature variation vs length, in the distance of 1m (purple line = 1 hour, green line = 2 hours)

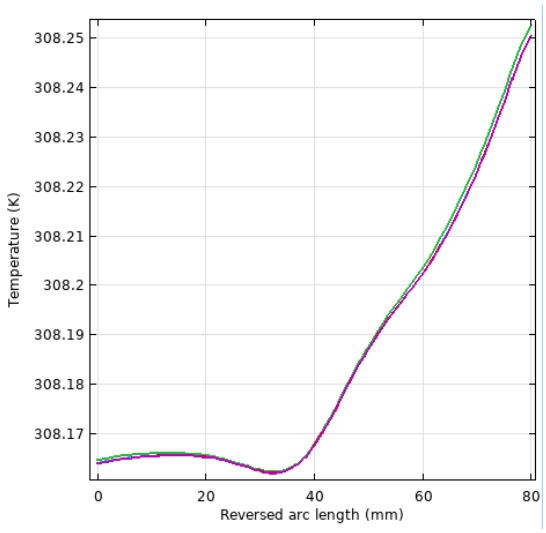

Figure 3-6 The vertical temperature variation vs length, in the distance of 2m (purple line = 1 hour, green line = 2 hours)

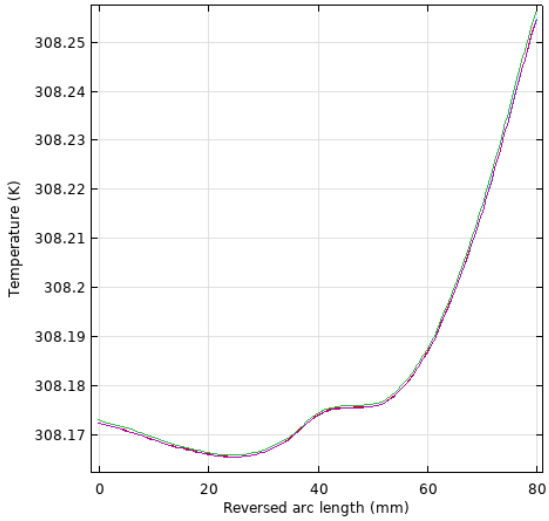

Figure 3-7 The vertical temperature variation vs length, in the distance of 3m (purple line = 1 hour, green line = 2 hours)

The table 3-1 and table 3-2 display the temperature variation after the radiation in the testis tissue. As we said before, the initial temperature of the testis is 308.15 K (35°C).

Table 3-1 maximum temperature in the first interval (1 hour) and the variation

Distance	Maximum temperature (k)	Temperature increase value
1m	308.30	0.15
2m	308.25	0.10
3m	308.25	0.10

Table 3-2 1maximum temperature in the second interval (2 hours) and the variation

Distance	Maximum temperature (k)	Temperature increase value
1m	308.31	0.16
2m	308.25	0.10
3m	308.25	0.10

According to the results obtained through the simulation (table 3-1 and 3-2) it is indicated that the temperature does not increase significantly after 1 hour till the second interval in 2 and 3 meters.

According to a study done by Wang et al (1997), An increase of 1°C entails a 14% drop in spermatogenesis, and consequently poorer sperm production. Our analysis in the present article is done according to the results of the mentioned study. [12]

As said before, no significant heat increase is observed after one hour till the second one in the distances of 2 and 3 meters, which can be explained by power decrease that was mentioned in the **Introduction** (inverse-square law).

In the table 4-1, the spermatogenesis drop percentages are obtained using the scale that Wang et al (1997) have deducted, which is 14% drop during a 1°C increase in the testis temperature.[12][13]. In this results, we suppose that the spermatogenesis decrease is a linear trend and the distances of 2m and 3m are considered as same parameters, because they showed no significant temperature difference after one hour in the simulation processes.

Table 4-1 The spermatogenesis drop percentage after 1 and 2 hours in the distances of 1m and 2m or 3m.

Distance	Spermatogenesis drop after 1 hour (%)	Spermatogenesis drop after 2 hours (%)
1m	2.10%	2.24%
2m and 3m	1.40%	1.40%

The average sperms that are produced during the spermatogenesis process per second is about 1000 unique sperms, and about 3600000 sperms per hours. Considering this rate, it is concluded that disposing testis to Wi-Fi radiation (with the mentioned parameters) may cause a drop in spermatogenesis process output, because of an increase in temperature. The approximate spermatogenesis production is indicated in the Table 4-2, supposing that these values are obtained, regarding the maximum heat created in the largest testis cross-section.

Table 4-2 The estimated decrease in sperm quantity after 1 and 2 hours in the distances of 1m and 2m or 3m

Distance	Decrease in sperm quantity after 1 hour	Decrease in sperm quantity after 2 hour
1m	75600	80640
2m and 3m	50400	50400

The results show that disposing testis to a Wi-Fi source (which is used in this simulation) may cause a drop of maximum 75600 and 80640 unique sperms respectively after 1 and 2 hours of radiation in a 1m distance. Also, this condition may cause a drop of maximum 50400 unique sperm quantity after 1 or 2 hours in a distance of 2 or 3 meters, supposing that regarding the simulation results, no significant heat difference is observed between the last two distances during the two intervals (1 and 2 hours). It should be stated that these values are estimated considering the maximum heat created in the largest cross-section of testis, also assumed that the testis is stable in the determined distances of the simulation.

References

[1] R. Ivell, "Lifestyle impact and the biology of the human scrotum," vol. 8, pp. 1–8, 2007. doi: 10.1186/1477-7827-5-15

[2] M. Rao et al., "Effect of transient scrotal hyperthermia on sperm parameters , seminal plasma biochemical markers , and oxidative stress in men," 2015. DOI: 10.4103/1008-682X.146967

[3] P. J. Craig Hacking, "radiopaedia, https://radiopaedia.org/articles/testis-1 Last modified: 2020." .

[4] K. Saladin, Anatomy & Physiology: The Unity of Form and Function. McGraw-Hill Science/Engineering/Math, 2003.

[5] D. J. Greene, Testes and Epididymis Anatomy. Medscape, 2016.

[6] M. Nakamura et al., "TEMPERATURE SENSITIVITY OF HUMAN SPERMATOGONIA AND SPERMATOCYTES IN VITRO," vol. 132, pp. 127–132, 1987 https://doi.org/10.3109/01485018708986808

[7] J. Epstein, "Introduction to Wi-Fi CHAPTER 5," Newnes, 2010, pp. 101–151.

[8] R.S, "Laws of light CHAPTER 3," in Solar Energy Conversion Systems, Academic press, 2014, pp. 55–58.

[9] Scott Blanchard, "Understanding IEEE 802.11 and Wi-Fi Standards,https://www.microwavejournal.com/," 2020. .

[10] TISSUE PROPERTIES/database/https://itis.swiss/virtual population/tissue-properties/database/Last modified: 2020." .

[11]LAN/MAN Standards Committee of the IEEE Computer Society "Wireless LAN Medium Access Control (MAC) and Physical Layer (PHY) Specifications," vol. 2016,**doi:** 10.1109/IEEESTD.2000.90914

[12]C. Wang and V. Mcdonald, "Effect of increased scrotal temperature on sperm production in normal men," vol. 0282, no. 3, 1997.doi: 10.1016/s0015-0282(97)81525-7

[13]R. S. Swerdloff, "Role of temperature in regulation of spermatogenesis and the use of heating as a method for contraception," vol. 49, no. 1, 1988. doi: 10.1016/s0015-0282(16)59640-x

New Zinc (II) Complex with *2,2'-diamino-5,5'-dimethyl-* 4,4'-bithiazole, Synthesis, Crystal Structure and DNA-binding studies

Akram Hosseinian*

* *Department of Engineering Science, College of Engineering, University of Tehran, P.O. Box 11365-4563, Tehran, Iran*

E-mail address: Hoseinian@ut.ac.ir

Abstract

New zinc (II) complex with 2,2'-diamino-5,5'-dimethyl- 4,4'-bithiazole (L), $[Zn(L)_3](NO_3)_2.CH_3OH$ (**ZnL_3**), was synthesized and subsequently characterized by means of various analytical techniques including; Infrared spectroscopy (IR), proton nuclear magnetic resonance (^{1}H -NMR), carbon nuclear magnetic resonance (^{13}C-NMR and single crystal X-ray determination. Based on X-ray single crystal data, the **ZnL_3** complex is belongs to orthorhombic system with space group Fdd2. In **ZnL_3**, one of **L** ligands acts as a monodentate ligand to form the five-coordinated Zn (II) complex, giving distorted trigonal bipyramidal geometry around the metal. Finally, UV-Vis and fluorescence spectroscopy was used to investigate the material's photophysical properties. The interaction ability of the two complexes with native calf thymus DNA (CT-DNA) has been monitored as a function of the metal complex–DNA molar ratio by UV–Vis absorption spectrophotometry, fluorescence spectroscopy.

***Keywords*:** Bithiazole; Metal complex; Synthesis; X-Ray.

1. Introduction

Over the past years, the recognition of specific DNA sequences by new metal complexes, which might contain nuclease attack or access of activators and repressor to regulate gene expression processes, has been a subject of interest from the viewpoint of the gene-targeted improvement drugs or the artificial modification of DNA [8, 9]. From the biological activity point of view, the origin of anticancer activity of BLM is ability to cleave deoxyribonucleic acid (DNA). A series of BLM analogs having identical bithiazole terminal regions but differing structurally in the geometry of the metal binding domain exhibited altered sequence selectivity and strand selectivity of DNA cleavage[4]. Based on these, there has been a growing trend towards the design and synthesis of the model compounds that can specifically recognize and cleave DNA [5-7].

Zinc(II) complexes play enormous and important roles in biological systems and have received considerable attention as potential anticancer agents[12]. On the other hand, in coordination chemistry there is many studies on

the interaction of Zn(II) ion with biomolecules[13].Understanding coordination modes of these biomolecules and metal ion makes us able to improve their biological properties[14].

It was found that aromatic heterocyclic compounds containing bithiazole rings are good ligands because the two nitrogen atoms in the bithiazole rings are able to chelate metal ions to form stable five-member rings[21, 22]. In addition, transition metal complexes of bithiazole derivative ligands have found increasing application. For instance, Ni and Co complexes of 2,2'-diamino-4,4'-bithiazole have been found to be effective inhibitors of DNA synthesis in tumor cells [23-26] and Fe(II), Fe(III),Cu(II), and platinum complexes have found effective and applicable in magnetic and photoactive materials[23, 27-31].Therefore, the comparison of coordination geometries Zn(II) complexes with 2,2'-diamino-5,5'-dimethyl-4,4'-bithiazole (**L**) is very interesting and so important.

Herein, we present the synthesis and structural characterization zinc (II) complex, $[Zn(L)_3](NO_3)_2.CH_3OH$ (**ZnL₃**), was done by single-crystal X-ray diffraction, IR, ^{1}H-NMR, ^{13}C-NMR, UV-Vis, fluorescence spectroscopy.

2. Material and Methods

2.1. Synthesis of $[Zn(L)_3](NO_3)_2.CH_3OH$ (ZnL_3).

The complex was procured by the reaction of a methanolic solution of $Zn(NO_3)_2.4H_2O$ with a methanolic solution of **L** and excess amount of ammonium acetate .It settled 6 days at room temperature after purifying. The complex is soluble in DMSO and insoluble in water, methanol, ether and $CHCl_3$. $[Zn(L)_3](NO_3)_2.CH_3OH$ (**ZnL₃**) complex with bigger crystals are separated from a mixture containing smaller crystals in media.*Anal.* Calc. for $C_{25}H_{34}N_{14}O_7S_6Zn$ (**ZnL₃**) (900.39): C, 33.34, H, 3.80, N, 21.77. Found: C, 33.32, H, 3.90, N, 21.80.IR data ((KBr, cm^{-1}): 3270s- 3135s ν(N-H),2920wν(C-H)$_{al}$, 607sν(C=C),1515sν(C=N), 1427w and 1301sν (Skeletal vibration), 1301vs, 821w and 749wν(NO_3^-),1119wν(C-S),749wν(C-S-C), 673wν(C=S), 407wν(Zn-N).^{1}H–NMR (d_6-DMSO, 25ºC, TMS) δppm: 7.0 (4H, $2NH_2$), 2.2 (6H, $2CH_3$). ^{13}C-NMR (d_6-DMSO, 25ºC, TMS) δppm: 168.22, 137.97, 116.36, 12.95. UV-Vis in DMSO (λmax: 275 nm).

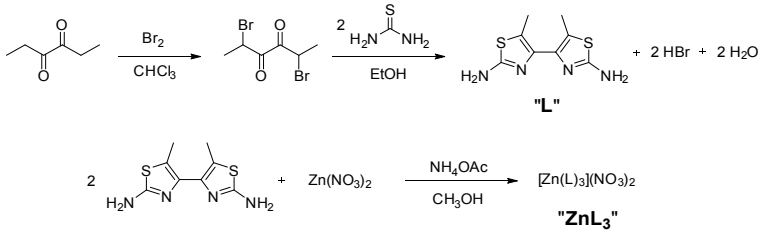

2.2.Crystal structure determinations.

X-ray diffraction measurements were performed at low temperature (120 K) using a Siemens P3 four-circle diffractometer equipped with graphite monochromated Mo-K_α radiation (λ = 0.71073 Å) using the φ–ω scan techniques. The structures of the title compounds were refined with SHELXL-97 [32, 33].

2.3.Characterization

Chemical analyses of carbon, hydrogen and nitrogen were performed by microanalytical methods using a Heraeus CHN-O-RAPID apparatus. NMR spectra were recorded on a Bruker Avance DRS 500 spectrometer. ^{1}H and ^{13}C chemical shifts were determined relative to internal TMS. Infrared spectra were recorded on a Shimadzu model IR-60 spectrometer, from KBr pellets in the 4000–400cm^{-1} range. The electronic absorption spectra were recorded on a Shimadzu UV-Vis 2100 recording spectrophotometer. Emission and excitation spectra of complexes were determined in DMSO solution using a Shimadzu-RS-5000 fluorescence spectrum photometer at room temperature.

3. Results and Discussions

3.1.Structure description

The pentacoordinated geometry suggests that this coordination is energetically favored and may be important in biological systems.

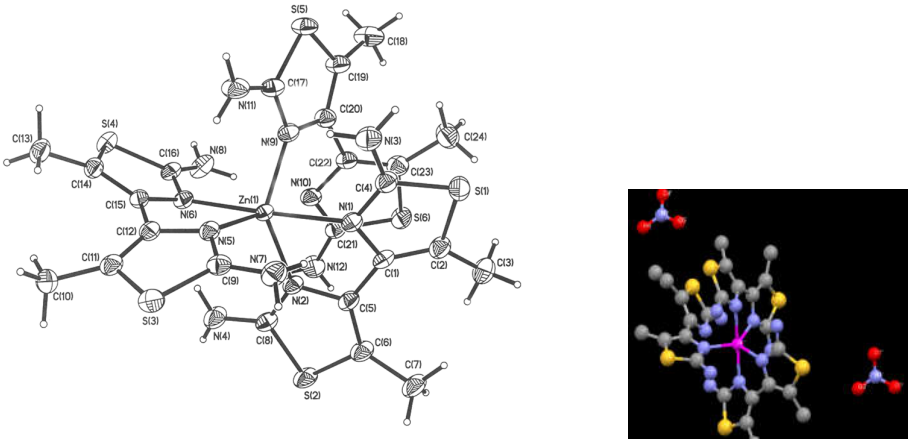

Fig.1. ORTEP drawing of polymer

X-ray crystallography analysis revealed **ZnL_3** crystallizes in orthorhombic (Fdd2 space group). Structure determination showed **ZnL_3**consists of one discrete cation $[Zn(L)_3]^{2+}$, two $[NO_3]^-$anions and one methanol molecule (Fig. 1). There are 14 types of N-H…O, N-H…N and O-H…O hydrogen bonds in a 3-D network between $[Zn(L)_3]^{2+}$ cations, two symmetrically independent nitrate anions and solvated methanol

3.2.DNA-binding mode and affinity

Electronic absorption spectroscopy is universally employed to examine the binding characteristics of metal complexes with DNA. The UV-Vis spectra of compounds in DMSO display intense absorption bands ranging from 227 to 275 nm, have been ascribed to the bithiazole π -π* and n-π* transitions.

The luminescence spectra of the all compounds in DMSO exhibit an emission at 298 K upon excitation at 250 nm. These spectral characteristics obviously suggest that the titled complex most likely interact with DNA through a mode of stacking interaction between the aromatic bithiazole ligand of the complexes and the base pairs of DNA.

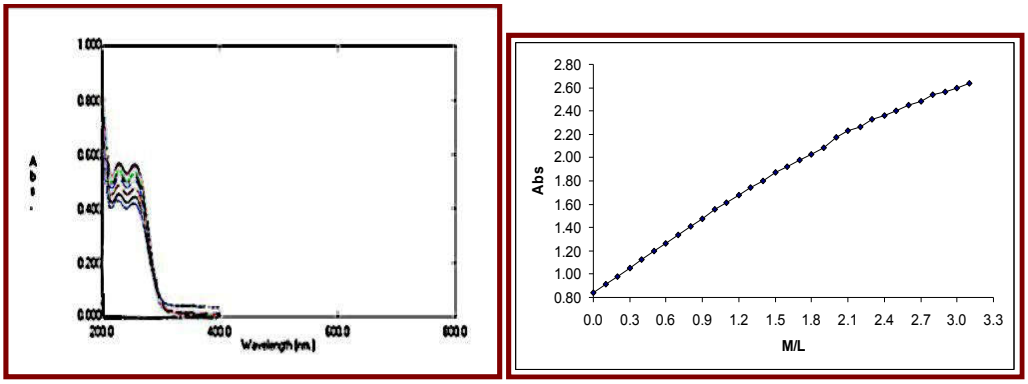

Fig.2. UV–Vis absorption spectra of complex in the presence of increasing amounts of CT-DNA

Conclusions

In conclusion, a new zinc (II) complex of $[Zn(L)_3](NO_3)_2.CH_3OH$ which **L** is 2,2'-diamino-5,5'-dimethyl-4,4'-bithiazolium nitrate ligand was synthesized and characterized. The complex shows distorted trigonal bipyramidal geometry around zinc (II) because one of the **L** ligands acts as a monodentate ligand to form the five coordinated Zn (II) complex. The results obtained from Uv-vis spectra revealed that bithiazole π -π* transition increases from 229.5 nm for **L** to 275.0 nm for **ZnL_3.** The interaction ability of the complex with native calf thymus DNA (CT-DNA) has been monitored as a function of the metal complex–DNA molar ratio by UV–Vis absorption spectrophotometry, fluorescence spectroscopy.

Acknowledgements

The authors would like to acknowledge the financial support Iran National Science Foundation (INSF) for this research.

References

[1] J.F. Da Silva and R.J.P. Williams. The biological chemistry of the elements: the inorganic chemistry of life, Oxford University Press, 2001.

[2] G. Schneider. *Nat. Rev.Drug Discov.*, 2018, *17*, 97.

[3] R. Yu, Y. Zheng, Y. Li, Z. Wu, C. Yan, Syntheses and structures of copper(II) and nickel(II) complexes with N,N'-(4,4'-bithiazole-2,2'-diyl)diacetimidamide ligands: in vitro cytotoxicities and DNA-binding properties, Transition Met Chem (2012) 37:399–406 DOI 10.1007/s11243-012-9603-6.

Applications of PCR-DGGE method in plant pathology

Nahid Moarrefzadeh [1], Hadi Khateri[2]
Razi University, Kermanshah, Iran, email: n.moarrefzadeh@razi.ac.ir
Razi University, Kermanshah, Iran, email: hkhateri@razi.ac.ir

Abstract

Plant diseases play an important role in reducing the quality and quantity of agricultural products. One of the most important strategies to improve the decision making process for plant diseases control and management is the fast and accurate identification and detection of phytopathogens. Investigating the genetic diversity in the populations of plant pathogens and detecting the changes in these populations is also important in understanding their dynamics and spread and helps for their better management. On the other hand, the application of integrated pest management control methods including agricultural, biological, physical and chemical methods may cause major changes in the structure and diversity of soil microbial communities and finally affect the level of soil inhibition against pathogens and the incidence and severity of plant diseases. Nowadays, culture-independent molecular approaches such as polymerase chain reaction (PCR)-based methods are being widely used for identification, detection and quantitative assessment as well as studying the genetic diversity of pathogen populations and in comparison with the conventional cultivation techniques, they are faster, more specific, more reliable and more sensitive. Among these methods, PCR- denaturing gradient gel electrophoresis (PCR-DGGE) is a well-known and widely used molecular tool that has been used successfully in various aspects such as identification and detection of various microorganisms, including plant pathogens, and examining the existence of diversity and changes in their community structure, as well as determining the effect of various factors such as control measures and management practices on the diversity and structure of soil microbial communities. The results of these studies can help us to select the best environmentally friendly management strategies and pave the way for achieving the goals of sustainable agriculture. Considering the various capabilities of PCR-DGGE technique, the efficiency of this method in plant pathology and some related researches, the principles of this technique and some of its advantages and limitations have been discussed in this review.

Keywords: Microbial Communities, Detection, Phytopathogens, Disease Management, Biocontrol

Introduction

Plant diseases cause great damage to plants and play a major role in reducing the quality and yield of agricultural products [23]. According to some reports, the total damage caused by plant pathogens in developing countries has been more than 40% of total production [40]. One of the first and most important strategies to improve the decision process for sustainable control and management of plant diseases and initiation of preventive or curative measures is the rapid and accurate identification and detection of phytopathogens [11, 76]. In plant quarantine, early detection of pathogens in seeds and plant propagation material is necessary to prevent further entry and spread of a new pathogen in a growing area where the pathogen did not already exist [11]. In addition, some species of mycotoxigenic fungi cause chronic risks to human and animal health by producing strong

mycotoxins in agricultural products, especially storage products. Therefore their rapid detection in food and agricultural products is vital [21]. Also due to the accelerated emergence of virulence, which leads to an increase in the prevalence of plant pathogens, the use of advanced molecular methods for timely detecting of these populations is necessary for management practices [40].

The FAO's definition of Integrated Pest Management (IPM) states:"IPM means the careful consideration of all available pest control techniques and subsequent integration of appropriate measures that discourage the development of pest populations and keep pesticides and other interventions to levels that are economically justified and reduce or minimizethe risks to human health and the environment. IPM places emphasis on the growth of a healthy crop with the least possible disruption to agro-ecosystems and encourages natural pest control mechanisms" [22]. Various management and control practices (e.g. agricultural, biological, physical and chemical methods) are part of integrated pest management that can make major changes in abundance, structure and diversity of both harmful and beneficial organisms and thus affect the level of soil suppresssion against pathogens and the incidence and severity of plant diseases. [3, 4, 12, 30, 43, 67, 81]. Due to the involvement of soil microorganisms in various processes such as decomposition of soil residues, nutrient cycle [3, 25, 28] and mineralization and stabilization of these materials for plant growth, biological fixation of nitrogen [28, 43], biodegradation of environmental pollutants [43] and biocontrol of plant pathogens to protect the crop and plant health and growth [56, 74], these organisms play very important roles in the performance of agricultural ecosystems [25]. The mentioned definition of IPM emphasizes the growth of a healthy crop with minimal disruption to agricultural ecosystems. Therefore, before applying any control method it is necessary to carefully study its effects on microbial communities.

In the past, the most common techniques used to identify plant pathogens have been culture-based morphological methods, which are often time consuming, tedious, and require extensive knowledge of classical taxonomy [11]. They may also not be able to detect low microbial populations. Moreover, the faster growth of saprophytic organisms may inhibit the growth of latent endophytes and in latent pathogen infections or their low concentrations, cultural or serological methods may not be effective. Today, several methods are being used to detect, identify and quantify plant diseases, as well as to study the genetic diversity of pathogenic populations and to characterize new species [11]. Among these, culture-independent molecular approaches based on DNA directly extracted from environmental samples such as rhizosphere and soil, have several advantages over conventional cultivation techniques; Including being faster, more specific, more reliable and more sensitive [3]. And due to the lack of culture restrictions [75] provide the possibility of detection and identification of non-cultured microorganisms [11]. Also, these methods are more suitable than conventional methods in understanding microbial ecology and studying the dynamics of microbial communities [57] and they may even reveal the presence of previously unknown microorganisms associated with plant diseases. The most common DNA amplification technologies are polymerase chain reaction (PCR)-based methods that have been used to identify various plant pathogens [76] and to study the diversity and structure of soil microorganisms [20 , 57, 83]. Among these methods, PCR- denaturing gradient gel electrophoresis (PCR-DGGE) is one of the most well-known and widely used molecular tools that is being used widely in many research laboratories for ecological studies and soil microbial communities [49, 80] and successfully in various fields such as diagnosis and detection of different microorganisms and study the existence of diversity and changes in their structure in laboratory samples and

natural environments, determine the effect of various factors such as agronomic, chemical and biological management methods on the diversity and structure of beneficial and harmful soil microbial communities and monitoring changes or differences without (or with) cultivation-based methods [8, 19, 36, 46, 57, 58, 75, 85]. In this review, the various applications of PCR-DGGE method in plant pathology and related fields have been discussed. The principles of this method and some of its advantages and limitations are also mentioned.

Principles and steps of PCR-DGGE method

PCR-DGGE is a molecular tool first used in medicine to detect gene mutations [9]. The first people to use this method to analyze soil microbial communities were Muyzer *et al*. [54]. PCR-DGGE consists of several main steps; After collecting the sample, the nucleic acid is extracted and then the desired gene is amplified by PCR to allow tracing on the gel. In the next step, DGGE separates PCR amplicons that are approximately the same size but with different DNA sequences. The polyacrylamide gels used in DGGE contain denaturing agents (a mixture of urea and formamide). The differences in DNA sequences cause different denaturing properties. Thus, the DNA fragments begin to denature when they reach their melting point, and their movement in the gel stops [21, 57]. Because GC content is a major factor in the PCR-DGGE separation mechanism, a clamp of approximately 40 bp with high GC content that does not melt, is being attached to the 5' end of one of the primers used in PCR to keep together the PCR-amplified fragments [21, 31, 78]. The difference of even a single nucleotide between fragments changes their relative melting behaviors and allows them to be detected by PCR-DGGE [51]. PCR-DGGE gel images include a set of bands with different intensities [5], which is usually used to estimate species richness, and the band intensity corresponds to the frequency or relative density of different PCR products in a sample [14]. After revealing the profiles, PCR-DGGE fingerprinting can be followed by statistical analysis and calculation of biodiversity indices such as PCA (principal component analysis), Simpson and Shannon diversity indices, cluster analysis, etc.., to analyze the data and compare the structure and diversity of microbial communities in different samples [17, 49].

Advantages of PCR-DGGE

PCR-DGGE is a cost-effective, reliable, powerful, fast, reproducible, yet very sensitive fingerprinting method [8, 13, 20, 21, 61, 86] which theoretically can distinguish two molecules that differ only in a single base [6, 57, 58]. This method can be used to identify organisms that make up only 1% of the total microbial community. This technique is very suitable for identifying new or unknown creatures. Most prevalent species in microbial communities can be easily identified by this method. Due to its high throughput capabilities, PCR-DGGE can analyze a large number of samples (more than 30 samples) in one gel and allow comparison between samples and their statistical analysis [6, 11, 31, 57]. Since this method is culture-independent, it reveals more microbial diversity than conventional culture methods [8, 57]. PCR-DGGE by using specific primers for different arrays or functional groups can increase the specificity of the analysis [65] and provide access to less frequent microbial groups [26]. The differential bands of PCR-DGGE gels can be cut, re-amplified and cloned, therefore populations related to these changes or differences in the community can be identified by determining the nucleotide sequence of the respective bands [6, 20, 57, 58]. Due to the mentioned advantages, PCR-DGGE has not only been effective in identifying microbes in environmental samples [50] but has also been the most widely used method for studying microbial communities for a long time [39]. Therefore, PCR-DGGE seems to be an appropriate method in studies where we try to identify and detect the pathogens, the diversity of pathogen populations or evaluate the effect of

different management strategies on the diversity or structure of the microbial community. The following are some studies that have used PCR-DGGE capabilities in plant pathology.

PCR-DGGE for the diagnosis of plant diseases and discrimination of pathogenic species

As mentioned earlier, rapid and accurate identification and detection of plant pathogens is very important in plant disease management [11] and PCR-DGGE is an efficient method in this field. *Pyrenophora* species are plant pathogens that, in addition to causing leaf and kernel diseases in cereals, raise food safety concerns by producing mycotoxins. There are no registered fungicides for use during seed development to control diseases caused by *Pyrenophora*. Therefore, we need to look for other ways to limit their negative effects [50]. *Pyrenophora* fungi are usually identified under a microscope after an incubation period on culture media, but morphological features are difficult to identify. In a study of six different species of *Pyrenophora*, PCR-DGGE was able to efficiently differentiate between these species after the amplification of DNA extracted from their pure cultures. When *Pyrenophora*-infected wheat seeds were analysed by this technique and amplicons of known *Pyrenophora* species were used as molecular markers, PCR-DGGE was able to detect different species of *Pyrenophora* directly from infected plant materials. This study showed that PCR-DGGE is a fast and accurate method that detects different species of *Pyrenophora* very efficiently in plant tissues infected with various fungal taxa without the need for isolation and culture [50]. The genus *Phytophthora* is composed of many species and includes some of the most important plant pathogens in the world that have a wide host range among plants. Species of this genus have an economically significant impact on agricultural products and natural ecosystems around the world. To prevent the spread of *Phytophthora*, strong and sensitive detection and identification tools are needed that can identify the pathogen at a relatively low cost. In one study, ITS amplification-based PCR-DGGE was used to directly detect and identify several species of *Phytophthora* in infected plant tissues. This method was able to successfully detect more than 16 species of *Phytophthora* tested in eight different plant tissues with high efficiency [68].

PCR-DGGE for studying the genetic diversity in the populations of plant pathogens

Better knowledge of the population genetics of different pathogens is important in understanding the dynamics and spread of their populations and can ultimately help to better manage them [64]. One suitable option for this purpose is to pool DNA from a significant number of individuals and analyze the variants of a polymorphic genetic region by PCR-DGGE fingerprinting, because this method is suitable for separating pooled DNA fragments of the same length but with different sequences [55]. Beet cyst nematode (*Heterodera schachtii*) causes significant economic damage to sugar beet (*Beta vulgaris*). Geographical populations of *H. schachtii* are inconsistent because they may differ significantly in terms of aggressiveness and virulence towards sugar beet cultivars, biological traits such as host range, hatching dynamics or rate of natural decline in the field, and all of these differences are related to genetic diversity within and between indigenous populations [32, 33, 53, 64]. A PCR-DGGE study based on the *vap1* effector gene of *H. schachtii* has identified genetic variation within and between beet cyst nematode populations [64]. PCR-DGGE has also been successfully used to analyze the genetic heterogeneity of

Meloidogyne incognita populations in different regions based on the comparison and determination of effector gene (*msp1*) [2].

PCR-DGGE for studying the changes in microbial communities and their frequency, diversity and structure in pathosystems

Insufficient knowledge of the microbial ecology of the rhizosphere and the restrictions that exist in identifying and describing microbial communications related to the healthy and infected plants are the important limitations for monitoring and promoting the disease suppressing microflora in the rhizosphere. Currently, PCR-DGGE can be used as a rapid method to assess and detect changes in the structure of culturable and non-culturable microbial communities (in response to various environmental factors) in many pathosystems [46, 85] . For example, Yang *et al.* [85] used 16S rDNA profiles generated by PCR-DGGE to investigate changes in the structure of rhizosphere bacterial community from avocado trees during infection by *Phytophthora cinnamomi* and the effect of repeated bioaugmentation with suppressive fluorescent *Pseudomonas*. Profiles of microbial communities in healthy and infected roots were differentiated by multivariate analysis procedures, indicating that the structure of the rhizosphere bacterial community may be a complementary indicator of changes in chemical and biological conditions in the plant rhizosphere during the infestation process. DNA band profiles in bacterial communities of healthy roots were also simple, indicating that the roots were colonized by a few dominant species that were almost structurally similar. In contrast, *Phytophthora* infected roots which did not yet show visible symptoms of disease, were colonized by much more diverse bacterial communities with completely different community structures than healthy roots. Therefore, there were significant changes in the bacterial community of avocado root rhizosphere before any visible contamination by *Phytophthora* root rot. On the other hand, root samples of trees that had frequently received *Pseudomonas fluorescens* st. 513, were free of *Phytophthora* infection, and their bacterial community structures resembled those of non-treated healthy roots. Therefore, bioaugmentation did not affect the structure of the bacterial community to such an extent that it was significantly different from healthy roots [85]. In another study, the relationship between density levels of different populations of soybean cyst nematode (SCN), the most destructive pathogen of soybean, with soil microbial properties on soybean roots and contaminated soils was investigated. A commercial soybean farm with different levels of density of this nematode (low, medium and high) was sampled and microbial communities were determined using dilution plating assays and PCR-DGGE. The population densities of *Trichoderma*, Actinomycetes, *Pseudomonas* and other bacteria in soils with low SCN were significantly higher compared to the high and medium populations of SCN. According to PCR-DGGE, the diversity indices of *Trichoderma* communities in roots in soils with low SCN were also significantly higher compared to the high and medium density of this nematode. According to both methods used, in soils with low SCN, more diverse species of Trichoderma, actinomycetes, *Pseudomonas* and Bacillus were found on the roots, indicating that the presence of these microbes in soybean roots may improve plant health and be related to reduced SCN. It is possible that a mixture of these microorganisms could be a promising combination to boost plant growth and protect soybean roots from SCN colonization [46]. PCR-DGGE has also been used to detect and determin the diversity of bacteria colonizing SCN cysts, suggesting that these bacteria may play a role

in suppressing SCN in soybean fields [63, 89]. Overall, the information obtained from such studies can be important for the ecological management of plant pathogens as well as the development of biological control agents against them.

PCR-DGGE for studying the existence and structure of plant endophytes

Endophytes are microorganisms that usually live inside the tissue of the host plant, without adversely affecting it or causing obvious signs of disease, and have symbiotic or mutualistic relationship with it [29, 42, 66]. Some endophytic microorganisms may be involved in plant disease control, either alone or in combination. Therefore, studying the internal tissues of plants that grow in different environments and soils can be a way to find potential candidates for biological control agents [41]. Most of our current information about the existence and structure of the endophytic community comes from cultivation-related methods. One of the major problems with these methods is the severe inherent error associated with the use of limited culture media and growth conditions, as many endophytic agents may be viable but non-culturable or may be non-culturable due to unknown growth needs. Thes make a comprehensive analysis of the endophytic community impossible. To overcome this problem, methods such as PCR-DGGE, which do not require the culture of microorganisms, have shown high potential for the study of endophytic bacteria in various plant species [41]; In one study, culture-dependent and culture-independent methods (16SrRNA PCR-DGGE) were simultaneously used to investigate endophytic bacterial communities in strawberry (*Fragaria ananassa*). Species of *B. subtilis*, *Enterobacter* sp. and *Pseudomonas* sp. were detected by both methods but *Arthrobacter* sp. and an unculturable *Erythrobacter* were not recovered using culture techniques. The acceptable detection limit of bacterial cells by PCR-DGGE (approximately 10^5 CFU g^{-1} of fresh plant tissue), indicates that a large portion of the bacterial population normally found in strawberries could be detected by this method. PCR-DGGE also provided an overview of bacterial community profiles that may be involved in a range of basic processes related to ecosystem functions such as decomposition of organic matter, nutrient cycle and plant growth stimulation and biocontrol of plant diseases [18].

PCR-DGGE for the detection of mycotoxigenic fungi in agricultural products

Some fungal species have the ability to produce mycotoxins in agricultural products, especially storage products. Mycotoxins are invisible, odorless toxins produced by fungi that are often undetectable by smell and taste [7]. Several species of *Aspergillus*, *Penicillium*, and *Fusarium* have been identified as sources of potent mycotoxins such as aflatoxins, ochratoxins, patulin, deoxynivalenol, and fumonisins. Because mycotoxins cause chronic health risks such as immunosuppression, cancer, and gastrointestinal, blood, and neurological defects [82], the rapid and accurate detection of mycotoxigenic contaminants in agricultural products and materials is very important for ensuring the safety of consumers and management methods of storage products. Due to the many limitations of classical culture-dependent methods for detection and identification of mycotoxin-producing fungi such as time-consuming and labor-intensive aspects, standardization problems and low reliability of results, PCR-DGGE is a promising, powerful and practical molecular tool for the detection of mycotoxigenic fungi and

their quantification in foods [21] as it has been effective in monitoring the dynamics of mycotoxin-producing fungi in grapes and coffee [44, 60].

PCR-DGGE for studying the effect of bioinoculants on soil microbial communities

Adding bioinoculants to soil is done with the aim of improving soil fertility [72], promoting plant growth and also biocontrol of plant diseases [1]. Although the positive effects of bioinoculants in the form of seed inoculation or direct application to plants have been confirmed, the introduction of formulations containing microorganisms into the soil environment may ultimately lead to safety concerns with minor to severe changes in the structure and diversity of soil microbial communities [25, 72]. Therefore, before the widespread use of such microorganisms, their effects on these communities should be investigated by efficient methods such as PCR-DGGE. In one study, the effect of inoculation of peanut seeds with biocontrol agent *Trichoderma harzianum* ITEM 3636 on the structure of bacterial and fungal communities of agricultural soils was investigated by PCR-DGGE and next-generation sequencing (NGS). The results of both methods showed that *T. harzianum* ITEM 3636 reduced the incidence and severity of plant diseases, without causing significant changes in the abundance and diversity of microbial communities [25]. In another study, co-inoculation of antagonistic isolates of *Bacillus subtilis* and *Trichoderma harzianum* against Fusarium wilt caused significant changes in the structure of the resident bacterial community in tomato rhizosphere compared to the uninoculated control. Phylogenetic analysis of PCR-DGGE bands obtained from rhizosphere soil samples of plants undergoing dual inoculation revealed the existence of ecologically important species related to potentially beneficial microorganisms and clearly shows the good effect of these biocontrol agents as a positive change in the abundance of beneficial bacteria and improving soil health against Fusarium wilt. In addition, compared to the single inoculation of these isolates, the highest values of diversity indices were observed in the combined treatment of these two factors, indicating the positive effect of simultaneous inoculation of these two biocontrol agents on the abundance of rhizosphere bacterial community [38].

PCR-DGGE for evaluating the effect of biological and chemical pesticides on soil microorganisms

Despite the positive effects of biological and chemical pesticides in the control of pests, plant diseases and weeds and the increasing use of these compounds in agriculture, there has always been a concern that with non-targeted effects on beneficial soil microbial communities they may ultimately lead to damages to the important functions, health and quality of the soil [15, 87]. Some studies have used PCR-DGGE to investigated the effect of various pesticides on soil microbial communities. In one of these, the effects of two systemic pesticides, metalaxyl and imidacloprid, applied to foliage or soil, on epiphytic fungal and bacterial communities was studied through PCR-DGGE and cloning. The results showed that these pesticides caused slight changes in the structure of fungal and bacterial communities [52]. In another study, the effect of carbendazim fungicide and several biological pesticides (azadirachtin, spinosad, pyrethrum and terpens) on the community structure of arbuscular

mycorrhizal fungi (AMF) was studied in pots and fields by PCR-DGGE and cloning. Compared to its field use, which had a transient and unstable effect on the colonization ability and community structure of native AMF, carbendazim completely prevented mycorrhizal colonization in pots. Spinosad, pyrethrum and terpenes had no effect on colonization and community structure of AMF. In contrast, the pot application of azadirachtin led to the selective inhibition of *Glomus etunicatum* strain, and its field application also brought about significant and persistent changes in the AMF community [37]. In another study, azadirachtin and chlorpyrifos had an adverse effect on the abundance and structure of soil bacterial populations, even at the recommended doses. These results indicate that due to the adverse effects of some biological and chemical pesticides on microbial communities, it is necessary to conduct appropriate studies and analyzes to assess the risk of all compounds used in agriculture before their release into the environment [73].

PCR-DGGE for evaluating the effeciency of fungicidal treatments in soil

Some studies have shown that fungal diversity evaluated by PCR-DGGE analysis can be useful to evaluate the control effect of fungicidal treatments in soil. In other words, PCR-DGGE diagnosis enables the effective use of fungicides [77].

PCR-DGGE for studying the effect of agricultural activities on soil microbial communities

As mentioned earlier, different methods of agricultural land management may directly and indirectly affect the soil environment and its various properties, change the composition and diversity of microbial communities in it and ultimately reduce or increase the incidence of plant diseases [3, 4 , 34, 43, 84]. The results of PCR-DGGE studies conducted on the effect of rotation or cultivated plant species on microorganisms could be used to manipulate microbial communities in the rhizosphere to increase plant health. In a study conducted by PCR-DGGE and qPCR, it was found that by converting fields with a long history of wheat cultivation into Jerusalem artichoke fields in a short period (one to three years), positive changes occurred in the structure and abundance of soil fungal communities because it reduced some fungal pathogens of wheat and stimulated beneficial fungal species [88]. The use of different fertilizers, in addition to improving plant nutrition, may affect microbial growth and competition [48] and the structure and activity of various soil-inhabiting microorganisms [71] and affect the occurrence of plant diseases. Adding a bioorganic fertilizer (containing antagonistic bacterium *Bacillus amyloliquefaciens* NJN-6 added to the organic mixture of amino acid fertilizer and pig manure compost) not only increased the richness and diversity of the rhizobacterial community compared to the untreated control but also significantly reduced the incidence of Fusarium wilt disease of bananas in newly cultivated lands and increased crop yield [24]. This study confirms the results of other studies in which there is a positive relationship between microbial diversity and disease inhibition in soil [10, 27, 79]. Organic amendments with effect on the whole microbial communities [69] or manipulation of soil antagonistic communities can provide a potentially effective combination for biocontrol of soil-borne plant pathogens [35]. On the other hand, the use of amendments such as

compost can have risks due to the presence of populations of plant and animal pathogens that may have survived the composting process [62]. So far, various methods have been used to monitor the change of microbial community structures in soils amended with organic compounds, of which PCR-DGGE is of the most reliable metyhods [62] In an experiment, the effects of using composted cotton gin trash as an organic amendment compared to the application of a synthetic fertilizer on the microbial community was investigated. Compost not only reduced southern blight (caused by *Sclerotium rolfsii*), but also kept the diversity of the bacterial community significantly higher than that of artificial modifiers. Interestingly, there was a significant negative correlation between the prevalence of southern blight and the PCR-DGGE diversity index [45]. In another study, the addition of compost and soil solarization alone and in combination reduced the frequency of *Ralstonia solanacearum*. Also in the mentioned treatments, changes in the structure of native soil bacterial communities (β-proteobacteria and eubacteria) were observed. The authors stated that the observed effect on the pathogen not only depended on the presence of compost but could also be due to changes in the structure and increase of soil microbial community resulting from the above treatments which lead to inhibition of pathogens [69].

PCR-DGGE limitations

PCR-DGGE is one of the most widely used techniques for studying soil microbial communities [39] but like other molecular techniques it has several drawbacks that can taint the analysis of microbial diversity in a sample [21]. One of the problems with PCR-DGGE is that with a single gel, only a limited number of samples can be tested and not all samples can be loaded on a single gel [20]. There are also no reliable instructions for comparing different gels. In addition, in some cases there is low resolution power and background clutter in the gels, which makes it difficult to interpret the results [39]. On the other hand, the number and intensity of bands observed in a PCR-DGGE profile cannot always be interpreted as the exact number and status of populations in a community, as a microorganism may produce more than one band with several rDNA gene operons [47] or because DNA molecules with different sequences move at the same time and are in the same position, a single band does not always represent a single microbial strain and may represent several populations [31, 57, 70]. Therefore the parameters calculated with PCR-DGGE fingerprinting should be interpreted as a representative of the microbial community and not a definitive measure [47]. PCR-DGGE also has its own limitations in separating relatively small pieces of DNA and sensitivity in detecting rare members of the community [24]. For this reason, it should be noted that the PCR-DGGE profile represents the dominant organisms of a community [31]. On the other hand, because this method is based on PCR, errors related to PCR amplification may also be included in DGGE analysis [21]. To overcome this and other potential problems, the skill of using PCR-DGGE as a tool for analyzing microbial communities has been enhanced. For example, combining this method with other methods such as band sequencing or hybridization with probes can reduce the ambiguity of band identification [57]. The use of fluorophore-labeled primers facilitates the normalization of PCR-DGGE profiles inside and between gels [59]. Application of *Pfu* enzyme DNA polymerase can also greatly reduce amplification errors during PCR [16]. The availability of several software options for comparing PCR-DGGE profiles for cluster analysis also reinforces

comparisons possible for PCR-DGGE fingerprints and enhances the integration of PCR-DGGE profiles with additional datasets [31].

Conclusion

Plant diseases are very important in reducing the quality and quantity of agricultural products. Timely and accurate identification and detection of plant pathogens or changes in their population is essential in improving the decision-making process for sustainable and successful management of plant diseases. On the other hand, control measures applied in agricultural lands due to their impact on soil microbial communities can greatly affect the prevalence of plant diseases caused by soil fungi. Therefore, by adopting proper management methods, these communities can be managed towards the growth and optimal health of the plant and reduce the impact of plant diseases. Nowadays, advances in plant pathology in various fields along with the development of biotechnology, bioinformatics and molecular biology have provided powerful tools for accurately identifying and detection of plant pathogens down to species level and detecting genetic diversity among their populations. These provide the ability to study the effect of different methods of integrated pest management on microbial communities in the soil, even its unculturable part. One of these valuable tools is PCR-DGGE, which, despite some limitations, has been successfully used for research in various fields of soil microbial ecology for more than two decades due to its outstanding features and numerous applications. Even today, despite the development of a new generation of high throughput sequencing technologies in detecting and studying soil microorganisms, this method is still an important method for various researches in the field of phytopathology due to its many advantages and many researchers use the capabilities of this technique to obtain valuable information that helps select the best environmentally friendly management practices and thus pave the way for achieving the goals of sustainable agriculture.

References

[1] Abdel-Monaim, M., Application of date palm leaves compost (DPLC) and plant growth promoting rhizobacteria (PGPR) for controlling faba bean root rot disease in New Valley, Egypt. Agricultural Engineering International: CIGR Journal, 2017. 19(5): p. 138-146.

[2] Adam, M., J. Hallmann, and H. Heuer, Identification of *msp1* gene variants in populations of *Meloidogyne incognita* using PCR-DGGE. Journal of Nematology, 2014. 46(3): p. 275-280.

[3] Ahemad, M., A. Zaidi, M.S. Khan, and M. Oves, Factors affecting the variation of microbial communities in different agro-ecosystems, in Microbial Strategies for Crop Improvement, M.S. Khan, A. Zaidi, and J. Musarrat, Editors. 2009, Springer: Berlin, Heidelberg. p. 301-324.

[4] Alabouvette, C. and C. Steinberg, The soil as a reservoir for antagonists to plant diseases, in An Ecological and Societal Approach to Biological Control, J. Eilenberg and H.M.T. Hokkanen, Editors. 2006, Springer: Dordrecht, The Netherlands. p. 123-144.

[5] Andreote, F.D., J.L. Azevedo, and W.L. Araujo, Assessing the diversity of bacterial communities associated with plants. Braz J Microbiol, 2009. 40(3): p. 417-32.

[6] Bergsma-Vlami, M., M.E. Prins, M. Staats, and J.M. Raaijmakers, Assessment of genotypic diversity of antibiotic-producing pseudomonas species in the rhizosphere by denaturing gradient gel electrophoresis. Appl Environ Microbiol, 2005. 71(2): p. 993-1003.

[7] Binder, E.M., Managing the risk of mycotoxins in modern feed production. Animal Feed Science and Technology, 2007. 133(1-2): p. 149-166.

[8] Bonanomi, G., M. Chiurazzi, S. Caporaso, G. Del Sorbo, G. Moschetti, and S. Felice, Soil solarization with biodegradable materials and its impact on soil microbial communities. Soil Biology and Biochemistry, 2008. 40(8): p. 1989-1998.

[9] Borresen, A.L., E. Hovig, and A. Brogger, Detection of base mutations in genomic DNA using denaturing gradient gel electrophoresis (DGGE) followed by transfer and hybridization with gene-specific probes. Mutat Res, 1988. 202(1): p. 77-83.

[10] Brussaard, L., P.C. de Ruiter, and G.G. Brown, Soil biodiversity for agricultural sustainability. Agriculture, Ecosystems & Environment, 2007. 121(3): p. 233-244.

[11] Capote, N., A.M. Pastrana, A. Aguado, and P. Sánchez-Torres, Molecular tools for detection of plant pathogenic fungi and fungicide resistance, in Plant pathology. 2012, InTech. p. 151-202.

[12] Castro-Sowinski, S., Y. Herschkovitz, Y. Okon, and E. Jurkevitch, Effects of inoculation with plant growth-promoting rhizobacteria on resident rhizosphere microorganisms. FEMS Microbiol Lett, 2007. 276(1): p. 1-11.

[13] Ccoscco, R.A., V.H. Sarmiento, and G.K. Villena, Microbial diversity assessment by PCR-DGGE analysis in National Sanctuary of Ampay in Perú. Advances in Biotechnology & Microbiology, 2018. 11(3): p. 60-65.

[14] Chandler, D.P., J.K. Fredrickson, and F.J. Brockman, Effect of PCR template concentration on the composition and distribution of total community 16S rDNA clone libraries. Mol Ecol, 1997. 6(5): p. 475-82.

[15] Chen, Q., B. Yang, H. Wang, F. He, Y. Gao, and R.A. Scheel, Soil microbial community toxic response to atrazine and its residues under atrazine and lead contamination. Environ Sci Pollut Res Int, 2015. 22(2): p. 996-1007.

[16] Cline, J., J.C. Braman, and H.H. Hogrefe, PCR fidelity of *pfu* DNA polymerase and other thermostable DNA polymerases. Nucleic Acids Res, 1996. 24(18): p. 3546-51.

[17] de los Reyes, A.M.M., E.T.M. Ocampo, M.C.C. Manuel, and B.C. Mendoza, Analysis of the bacterial and fungal community profiles in bulk soil and rhizospheres of three mungbean [*Vigna radiata* (L.) R. Wilczek] genotypes through PCR-DGGE. International Letters of Natural Sciences, 2020. 77: p. 1-26.

[18] de Melo Pereira, G.V., K.T. Magalhães, E.R. Lorenzetii, T.P. Souza, and R.F. Schwan, A multiphasic approach for the identification of endophytic bacterial in strawberry fruit and their potential for plant growth promotion. Microbial Ecology, 2011. 63(2): p. 405-417.

[19] Doi, T., Y. Hagiwara, J. Abe, and S. Morita, Analysis of rhizosphere bacteria of rice cultivated in Andosol lowland and upland fields using molecular biological methods. Plant Root, 2007. 1: p. 66-74.

[20] Dubey, R.K., V. Tripathi, R. Prabha, R. Chaurasia, D.P. Singh, C.S. Rao, A. El-Keblawy, and P.C. Abhilash, Methods for exploring soil microbial diversity, in Unravelling the Soil Microbiome- Perspectives for Environmental Sustainability. 2020, Springer: Cham, Switzerland. p. 23-32.

[21] El Sheikha, A.F., Molecular detection of mycotoxigenic fungi in foods: The case for using PCR-DGGE. Food Biotechnology, 2019. 33(1): p. 54-108.

[22] FAO. AGP Integrated Pest Management. IPM definition. 2013; Available from: http://www.fao.org/agriculture/crops/thematic-sitemap/theme/pests/ipm/en/.

[23] Figuerola, E.L., L.D. Guerrero, S.M. Rosa, L. Simonetti, M.E. Duval, J.A. Galantini, J.C. Bedano, L.G. Wall, and L. Erijman, Bacterial indicator of agricultural management for soil under no-till crop production. PLoS One, 2012. 7(11): p. e51075.

[24] Fu, L., Y. Ruan, C. Tao, R. Li, and Q. Shen, Continous application of bioorganic fertilizer induced resilient culturable bacteria community associated with banana Fusarium wilt suppression. Scientific Reports, 2016. 6: p. 27731.

[25] Ganuza, M., N. Pastor, M. Boccolini, J. Erazo, S. Palacios, C. Oddino, M.M. Reynoso, M. Rovera, and A.M. Torres, Evaluating the impact of the biocontrol agent *Trichoderma*

harzianum ITEM 3636 on indigenous microbial communities from field soils. Journal of Applied Microbiology, 2019. 126(2): p. 608-623.

[26] Garbeva, P., J.A. van Veen, and J.D. van Elsas, Predominant *Bacillus* spp. in agricultural soil under different management regimes detected via PCR-DGGE. Microb Ecol, 2003. 45(3): p. 302-16.

[27] Garbeva, P., J. Van Veen, and J. Van Elsas, Microbial diversity in soil: selection of microbial populations by plant and soil type and implications for disease suppressiveness. Annu. Rev. Phytopathol., 2004. 42: p. 243-270.

[28] Goh, K.M., Important roles of soil micro-organisms in organic farming, in Seventh International Conference on Kyusei Nature Farming, U.R. Sangakkara and Y.D.A. Senanayake, Editors. 2002, INFRC: Christchurch, New Zealand. p. 38-49.

[29] Golinska, P., M. Wypij, G. Agarkar, D. Rathod, H. Dahm, and M. Rai, Endophytic actinobacteria of medicinal plants: diversity and bioactivity. Antonie van Leeuwenhoek, 2015. 108(2): p. 267-289.

[30] Govaerts, B., M. Mezzalama, Y. Unno, K.D. Sayre, M. Luna-Guido, K. Vanherck, L. Dendooven, and J. Deckers, Influence of tillage, residue management, and crop rotation on soil microbial biomass and catabolic diversity. Applied Soil Ecology, 2007. 37(1-2): p. 18-30.

[31] Green, S.J., M.B. Leigh, and J.D. Neufeld, Denaturing gradient gel electrophoresis (DGGE) for microbial community analysis, in Handbook of Hydrocarbon and Lipid Microbiology, K.N. Timmis, Editor. 2015, Springer: Berlin, Heidelberg. p. 4137-4158.

[32] Griffin, G., Pathological differences in *Heterodera schachtii* populations. Journal of Nematology, 1981. 13(2): p. 191-195.

[33] Griffin, G., Differences in the response of certain weed host populations to *Heterodera schachtii*. Journal of Nematology, 1982. 14(2): p. 174-182.

[34] Grossman, J.M., B.E. O'Neill, S.M. Tsai, B. Liang, E. Neves, J. Lehmann, and J.E. Thies, Amazonian anthrosols support similar microbial communities that differ distinctly from those extant in adjacent, unmodified soils of the same mineralogy. Microb Ecol, 2010. 60(1): p. 192-205.

[35] Hoitink, H. and M. Boehm, Biocontrol within the context of soil microbial communities: a substrate-dependent phenomenon. Annual review of phytopathology, 1999. 37(1): p. 427-446.

[36] Hovda, M.B., Application of PCR and DGGE to characterise the microflora of farmed fish. 2007, University of Bergen: Stavanger, Norway. p. 65.

[37] Ipsilantis, I., C. Samourelis, and D.G. Karpouzas, The impact of biological pesticides on arbuscular mycorrhizal fungi. Soil Biology and Biochemistry, 2012. 45: p. 147-155.

[38] Jangir, M., S. Sharma, and S. Sharma, Target and non-target effects of dual inoculation of biocontrol agents against *Fusarium* wilt in *Solanum lycopersicum*. Biological Control, 2019. 138: p. 104069.

[39] Jin, N., X. Lu, X. Wang, Q. Liu, D. Peng, and H. Jian, The effect of combined application of *Streptomyces rubrogriseus* HDZ-9-47 with soil biofumigation on soil microbial and nematode communities. Scientific Reports, 2019. 9(1): p. 16886.

[40] Jongman, M., P.C. Carmichael, and M. Bill, Technological advances in phytopathogen detection and metagenome profiling techniques. Current Microbiology, 2020. 77(4): p. 675-681.

[41] Kang, S.A., J.W. Han, and B.S. Kim, Community structures and antagonistic activities of the bacteria associated with surface-sterilized pepper plants grown in different field soils. Archives of Microbiology, 2016. 198(10): p. 1027-1034.

[42] Khan, A.L., S.A. Gilani, M. Waqas, K. Al-Hosni, S. Al-Khiziri, Y.-H. Kim, L. Ali, S.-M. Kang, S. Asaf, R. Shahzad, J. Hussain, I.-J. Lee, and A. Al-Harrasi, Endophytes from medicinal plants and their potential for producing indole acetic acid, improving seed germination and mitigating oxidative stress. Journal of Zhejiang University. Science. B, 2017. 18(2): p. 125-137.

[43] Krupinsky, J.M., K.L. Bailey, M.P. McMullen, B.D. Gossen, and T.K. Turkington, Managing plant disease risk in diversified cropping systems. Agronomy Journal, 2002. 94(2): p. 198-209.

[44] Laforgue, R., L. Guérin, J.J. Pernelle, C. Monnet, J. Dupont, and M. Bouix, Evaluation of PCR-DGGE methodology to monitor fungal communities on grapes. Journal of Applied Microbiology, 2009. 107(4): p. 1208-1218.

[45] Liu, B., M.L. Gumpertz, S. Hu, and J.B. Ristaino, Long-term effects of organic and synthetic soil fertility amendments on soil microbial communities and the development of southern blight. Soil Biology and Biochemistry, 2007. 39(9): p. 2302-2316.

[46] Liu, B., H. Wei, W. Shen, H. Smith, and J.C. Correll, Microbial communities in soils with different population densities of soybean cyst nematode. Canadian Journal of Plant Pathology, 2017. 40(1): p. 48-60.

[47] Lopez-Lozano, N.E., M.G. Carcaño-Montiel, and Y. Bashan, Using native trees and cacti to improve soil potential nitrogen fixation during long-term restoration of arid lands. Plant and Soil, 2016. 403(1-2): p. 317-329.

[48] Luo, P., X. Han, Y. Wang, M. Han, H. Shi, N. Liu, and H. Bai, Influence of long-term fertilization on soil microbial biomass, dehydrogenase activity, and bacterial and fungal community structure in a brown soil of northeast China. Ann Microbiol, 2015. 65(1): p. 533-542.

[49] Marzorati, M., L. Wittebolle, N. Boon, D. Daffonchio, and W. Verstraete, How to get more out of molecular fingerprints: practical tools for microbial ecology. Environ Microbiol, 2008. 10(6): p. 1571-81.

[50] Mavragani, D., C. Hamel, and V. Vujanovic, Species-specific PCR-DGGE markers to distinguish *Pyrenophora* species associated to cereal seeds. Fungal Biology, 2011. 115(2): p. 169–175.

[51] Miller, K.M., T.J. Ming, A.D. Schulze, and R.E. Withler, Denaturing gradient gel electrophoresis (DGGE): a rapid and sensitive technique to screen nucleotide sequence variation in populations. Biotechniques, 1999. 27(5): p. 1016-1030.

[52] Moulas, C., C. Petsoulas, K. Rousidou, C. Perruchon, P. Karas, and D.G. Karpouzas, Effects of systemic pesticides imidacloprid and metalaxyl on the phyllosphere of pepper plants. BioMed Research International, 2013. 2013: p. 1-8.

[53] Müller, J., New pathotypes of the beet cyst nematode *(Heterodera schachtii*) differentiated on alien genes for resistance in beet (*Beta vulgaris*). Fundamental and Applied Nematology, 1998. 21(5): p. 519-526.

[54] Muyzer, G., E.C. de Waal, and A.G. Uitterlinden, Profiling of complex microbial populations by denaturing gradient gel electrophoresis analysis of polymerase chain reaction-amplified genes coding for 16S rRNA. Appl Environ Microbiol, 1993. 59(3): p. 695-700.

[55] Muyzer, G. and K. Smalla, Application of denaturing gradient gel electrophoresis (DGGE) and temperature gradient gel electrophoresis (TGGE) in microbial ecology. Antonie van Leeuwenhoek, 1998. 73(1): p. 127-141.

[56] Nadeem, S.M., M. Ahmad, Z.A. Zahir, A. Javaid, and M. Ashraf, The role of mycorrhizae and plant growth promoting rhizobacteria (PGPR) in improving crop productivity under stressful environments. Biotechnol Adv, 2014. 32(2): p. 429-48.

[57] Nakatsu, C.H., Soil microbial community analysis using denaturing gradient gel electrophoresis. Soil Science Society of America Journal, 2007. 71(2): p. 562-571.

[58] Nannipieri, P., J. Ascher, M. Ceccherini, L. Landi, G. Pietramellara, and G.J.E.j.o.s.s. Renella, Microbial diversity and soil functions. European Journal of Soil Science, 2003. 54(4): p. 655-670.

[59] Neufeld, J.D. and W.W. Mohn, Fluorophore-labeled primers improve the sensitivity, versatility, and normalization of denaturing gradient gel electrophoresis. Appl Environ Microbiol, 2005. 71(8): p. 4893-6.

[60] Nganou Donkeng, N., N. Durand, N.L. Tatsadjieu, I. Metayer, D. Montet, and C.M. Mbofung, Fungal llora and ochratoxin a associated with coffee in Cameroon. British Microbiology Research Journal, 2014. 4(1): p. 1-17.

[61] Nicolaisen, M.H. and N.B. Ramsing, Denaturing gradient gel electrophoresis (DGGE) approaches to study the diversity of ammonia-oxidizing bacteria. J Microbiol Methods, 2002. 50(2): p. 189-203.

[62] Noble, R., Risks and benefits of soil amendment with composts in relation to plant pathogens. Australasian Plant Pathology, 2011. 40(2): p. 157-167.

[63] Nour, S.M., J.R. Lawrence, H. Zhu, G.D. Swerhone, M. Welsh, T.W. Welacky, and E. Topp, Bacteria associated with cysts of the soybean cyst nematode (*Heterodera glycines*). Applied and Environmental Microbiology, 2003. 69(1): p. 607-615.

[64] Nuaima, R.H., J. Roeb, J. Hallmann, M. Daub, S. Otte, and H. Heuer, Effector gene *vap1* based DGGE fingerprinting to assess variation within and among *Heterodera schachtii* populations. Journal of Nematology, 2018. 50(4): p. 517-528.

[65] O'Callaghan, M., N. Lorenz, and E.M. Gerard, Characterization of phylloplane and rhizosphere microbial populations using PCR and denaturing gradient gel electrophoresis (DGGE), in Molecular Approaches to Soil, Rhizosphere and Plant Microorganism Analysis, J.E. Cooper and J.R. Rao, Editors. 2006, CAB International: Wallingford. p. 99-115.

[66] Passari, A.K., V.K. Mishra, R. Saikia, V.K. Gupta, and B.P. Singh, Isolation, abundance and phylogenetic affiliation of endophytic actinomycetes associated with medicinal plants and

screening for their in vitro antimicrobial biosynthetic potential. Frontiers in microbiology, 2015. 6: p. 273-273.

[67] Picard, C. and M. Bosco, Genotypic and phenotypic diversity in populations of plant-probiotic *Pseudomonas* spp. colonizing roots. Naturwissenschaften, 2008. 95(1): p. 1-16.

[68] Rytkönen, A., A. Lilja, and J. Hantula, PCR–DGGE method for *in planta* detection and identification of *Phytophthora* species. Forest Pathology, 2012. 42(1): p. 22-27.

Schonfeld, J., A. Gelsomino, L.S. Overbeek, A. Gorissen, K. Smalla, and J.D. Elsas, Effects of compost addition and simulated solarisation on the fate of *Ralstonia solanacearum* biovar 2 and indigenous bacteria in soil. FEMS Microbiol Ecol, 2003. 43(1): p. 63-74.

[69] Sekiguchi, H., N. Tomioka, T. Nakahara, and H. Uchiyama, A single band does not always represent single bacterial strains in denaturing gradient gel electrophoresis analysis. Biotechnology letters, 2001. 23(15): p. 1205-1208.

[70] Sharma, R., V. Pooniya, V.S. Bisaria, K. Swarnalakshmi, and S. Sharma, Bioinoculants play a significant role in shaping the rhizospheric microbial community: a field study with *Cajanus cajan*. World J Microbiol Biotechnol, 2020. 36(3): p. 44.

[71] Sharma, S.K., A. Ramesh, M.P. Sharma, O.P. Joshi, B. Govaerts, K.L. Steenwerth, and D.L. Karlen, Microbial community structure and diversity as indicators for evaluating soil quality, in Biodiversity, Biofuels, Agroforestry and Conservation Agriculture, E. Lichtfouse, Editor. 2010, Springer: Dordrecht, Netherlands. p. 317-358.

[72] Singh, S., R. Gupta, and S. Sharma, Effects of chemical and biological pesticides on plant growth parameters and rhizospheric bacterial community structure in *Vigna radiata*. J Hazard Mater, 2015. 291: p. 102-10.

[73] Stafford, W.H., G.C. Baker, S.A. Brown, S.G. Burton, and D.A. Cowan, Bacterial diversity in the rhizosphere of Proteaceae species. Environ Microbiol, 2005. 7(11): p. 1755-68.

[74] Thanwalee, S.N., Comparison of bacterial activities and diversity in soil between conventional and the novel rice cultivation: SRI, in School of Biotechnology. 2006, Suranaree University of Technology: Nakhon Ratchasima, Thailand. p. 107.

[75] Tibebu, B. and B. Nuh, Biotechnological tools for detection, identification and management of plant diseases. African Journal of Biotechnology, 2019. 18(29): p. 797-807.

[76] Tsushima, S., Integrated control and integrated pest management in Japan: the need for various strategies in response to agricultural diversity. Journal of General Plant Pathology, 2014. 80(5): p. 389-400.

[77] Valášková, V. and P. Baldrian, Denaturing gradient gel electrophoresis as a fingerprinting method for the analysis of soil microbial communities. Plant, Soil and Environment, 2009. 55(10): p. 413-423.

[78] van Elsas, J.D., P. Garbeva, and J. Salles, Effects of agronomical measures on the microbial diversity of soils as related to the suppression of soil-borne plant pathogens. Biodegradation, 2002. 13(1): p. 29-40.

[79] van Elsas, J.D. and F.G.H. Boersma, A review of molecular methods to study the microbiota of soil and the mycosphere. European Journal of Soil Biology, 2011. 47(2): p. 77-87.

[80] Verhulst, N., B. Govaerts, E. Verachtert, A. Castellanos-Navarrete, M. Mezzalama, P. Wall, A. Chocobar, J. Deckers, and K. Sayre, Conservation Agriculture, Improving Soil Quality for Sustainable Production Systems, in Advances in Soil Science: Food Security and Soil Quality, R. Lal and B.A. Stewart, Editors. 2010, CRC Press: Boca Raton, FL, USA. p. 137–208.

[81] World Health Organization (WHO), Mycotoxins. Children's Health and the Environment- WHO Training Package for the Health Sector. 2011. p. 42.

[82] Wu, T., D.O. Chellemi, K.J. Martin, J.H. Graham, and E.N. Rosskopf, Discriminating the effects of agricultural land management practices on soil fungal communities. Soil Biology and Biochemistry, 2007. 39(5): p. 1139-1155.

[83] Wu, T., D.O. Chellemi, J.H. Graham, K.J. Martin, and E.N. Rosskopf, Comparison of soil bacterial communities under diverse agricultural land management and crop production practices. Microb Ecol, 2008. 55(2): p. 293-310.

[84] Yang, C.-H., D. Crowley, and J. Menge, 16S rDNA fingerprinting of rhizosphere bacterial communities associated with healthy and *Phytophthora* infected avocado roots. FEMS Microbiology Ecology, 2001. 35(2): p. 129-136.

[85] Yuan, X., J. Xu, H. Chai, H. Lin, Y. Yang, X. Wo, and J. Shi, Differences of rhizo-bacterial diversity and the content of peimine and peiminine of *Fritillaria thunbergii* among different habits. Journal of Medicinal Plants Research, 2010. 4(6): p. 465–470.

[86] Zhang, J., J. Qin, C. Zhao, C. Liu, H. Xie, and S. Liang, Response of bacteria and fungi in soil microcosm under the presence of pesticide endosulfan. Water, Air, & Soil Pollution, 2015. 226(4): p. 226:109.

[87] Zhou, X., J. Zhang, D. Gao, H. Gao, M. Guo, L. Li, M. Zhao, and F. Wu, Conversion from long-term cultivated wheat field to Jerusalem artichoke plantation changed soil fungal communities. Scientific Reports, 2017. 7: p. 41502.

[88] Zhu, Y., F. Shi, J. Tian, J. Liu, S. Chen, M. Xiang, and X. Liu, Effect of soybean monoculture on the bacterial communities associated with cysts of *Heterodera glycines*. Journal of Nematology, 2013. 45(3): p. 228-235.

Electrochemical Aptasensors for Detection of *Salmonella Typhimurium*

Maryam Nazari[1*]

[1] Faculty of Chemistry, Razi University, Kermanshah, Iran

*Email: nazari.maryam@razi.ac.ir

Abstract

Foodborne illnesses pose a global public health challenge because of bacterial contaminants. In recent years, since concerns about food contaminants and the associated health problems have increased, controls on food safety and quality have become much more stringent. Establishing an infection, foodborne pathogens pose an important threat for the general population and, in severe cases, lead to death. *Salmonella* is contracted through the consumption of food contaminated with *Salmonella* bacteria and is a serious health concern and a main reason of many cases of food poisoning worldwide. It is a negative intestinal bacillus and one of the most common bacteria responsible for foodborne illness. *Salmonella* is typically transmitted to humans through animal feed or foodborne contaminants. Therefore, the development of sensitive, rapid, and reliable diagnostic methods for checking pathogens in food is very important to ensure a healthy diet and to diminish the prevalence of foodborne illnesses. Several methods are used to diagnose *Salmonella*, such as polymerase chain reaction (PCR), enzyme-linked immunosorbent assay (ELISA), and conventional culture methods, which are common and reliable but time-consuming and laborious. This study reviews *Salmonella Typhimurium* (*S. Typhimurium*) electrochemical aptasensors.

Keywords: Salmonella Typhimurium, Aptasensors, Electrochemical detection, Food contaminants.

1. Introduction

Foodborne illness is the second leading cause of death in the world because of the consumption of foods contaminated with pathogens such as *E. coli* O157: H7, *Listeria*, and *Salmonella*. According to the WHO, *Salmonella* is one of the four leading causes of diarrheal diseases in the world and ranks first among foodborne pathogens [1]. *Salmonella*, a gram-negative bacteria, is known to be a major cause of gastrointestinal infections and is associated with hospitalization and mortality worldwide. *Salmonella* can be found in beverages, milk, eggs, and meat. *Salmonella Typhimurium* (*S. typhimurium*) is one of the most common serotypes that is associated with human diseases among more than 2500 *Salmonella* serotypes [2]. *S. typhimurium* infection through food harms people and has become a life-threatening problem, emphasizing the serious need to develop cost-effective, sensitive, and rapid alternative technologies to control the spread of *S. typhimurium* [3]. Delicate and sensitive identification of this pathogen paves the way for timely monitoring, even preventing the spread of infection.

To date, traditional culture, enzyme-linked immunosorbent assay (ELISA), and polymerase chain reaction (PCR) are commonly applied in the food industry to identify foodborne pathogens. Cultivation is the gold standard procedure, but it takes 2 to 4 days for confirmation of results. PCR and ELISA diminish the recognition time to 3-6 hours, nevertheless, PCR involves complex nuclear extraction steps, and conventional ELISA is not enough sensitive. Over the past decade, many researches have been perfurmed on different biosensors, including electrochemical methods, optical methods, quartz microcrystal balance, surface plasmon resonance, etc., for sensitive and rapid recognition of pathogenic bacteria [1].

Aptamer-based diagnostic methods provide a simple, specific, rapid, and highly sensitive analytical technique for the quantitative determination of *S. typhimurium* [4]. Aptamers have been gaining enhancing attention as an attractive cognitive element that can be simply attached to the electrode surface to detect a complete cell. The aptamer is a single-stranded ribonucleic acid (RNA) or deoxyribonucleic acid (DNA) molecule that can bind exclusively to its complement target. The high binding affinity, ease of modification, high sensitivity, and small size of aptamers have led to its use in the development of biosensors. Aptamers are easily produced with high sensitivity and selectivity and are more stable in comparison to antibodies. When aptamers are used as recognizing components, aptamers can create specific three-dimensional structures by binding to the target [5].

In this study, the importance of diagnosing *S. typhimurium*, its detection methods, and its electrochemical aptasensors were reviewed.

2. Importance of diagnosing *S. typhimurium*

Foodborne illness is one of the leading causes of human deaths. *Salmonella* is a common pathogen that causes foodborne illness in animals and humans around the world. It is estimated that approximately 2,200 species of *Salmonella* infect humans, accounting for three-quarters of cases of salmonellosis each year [4]. Every year, according to the World Health Organization (WHO), approximately 21, 550, and 33 million cases of typhoid fever, diarrheal diseases, and deaths due to *Salmonella* are reported, respectively [5].

A number of outbreaks of foodborne illness have occurred where the source of *S. typhimurium* infection has been detected, which is the second most common serotype (after *S. enteritidis*) known to humans [6]. *S. typhimurium* is an anaerobic gram-negative bacillus bacterium belonging to the family of *Enterobacteriaceae*, which is one of the most important pathogens, because it is the leading cause of foburn bacterial diseases in humans at least in many countries [3]. *Salmonella* is estimated to cause 93.8 million human infections and 155,000 deaths worldwide annually [4]. In the United States, *Salmonella* causes approximately 1.2 million diseases, 23,000 hospitalizations, and 450 deaths annually. In China, *Salmonella* is responsible for more than 3 million times a year food poisoning, often associated with poultry products [1].

It is essential to develop a very specific and sensitive technique for the diagnosis of *Salmonella* in the field of clinical diagnosis, environmental monitoring, and food safety. Many procedures have been developed for the identification of pathogenic bacteria, including immunosorbent assay, and nucleic acid-based and conventional biochemical methods. All of these approaches can detect reliable, selective, and sensitive bacteria, but each method has its own disadvantages. To improve *Salmonella* recognition, new biosensor-based approaches have

been developed as potential alternatives to the bottleneck of conventional techniques, as they have the distinct advantages of inexpensive tools, low cost, rapid response, and ease of use [7].

Electrochemical sensors are procedures that allow the fast recognition of foodborne pathogens with high specificity and affinity. The most favorable capability of this type of biosensors is the low diagnostic range in that it is able to distinguish 1 to 5 mL of the sample up to one bacterial cell [8].

3. Methods of diagnosis of *S. typhimurium*

Over the past decades, conventional methods, including culture-based methods, ELISA, and nucleic acid or PCR, have been available to detect *S. typhimurium* infection. A common bacteriological method for assessing the presence of a pathogen and determining whether it is alive or dead is based on pre-enrichment in a non-selective culture medium followed by selective plating and subsequent biochemical and serological verification for possible outcomes. It takes 3 days and a maximum of 7-10 days to confirm photogene existence. This process is not valid for the diagnosis of uncultivated healthy strains and is time consuming [6]. It may also cause false negatives and enhance test costs, as some serotypes are not distinct enough, and they are lost in these environments. DNA probe and PCR serve/are regarded as two commercial nucleic acid delivery methods that require precise temperature cycle control, and advanced and expensive equipment, and are not able to detect living and dead cells and limit their use in the point-of-care testing [3].

Immunoassay methods including ELISA can sense *Salmonella* at the level of 10^4-10^5 cells per mL. Lower levels of detection can be attained by linking ELISA procedures to an enrichment stage that typically takes between 16 and 24 hours. The main disadvantages of ELISA are the complex washing method, insufficient sensitivity, and high-pressure analytical strategies. PCR assays are faster, simpler, and more sensitive than ELISA, but are not sufficient to sense low bacterial concentrations ($<10^5$ CFU (colony forming nit)/mL). PCR procedures have been displayed to considerably improve the limit of detection (LOD) to 5 CFU (colony forming unit) per mL, but these methods still need long and often complex preparation stages including cell lysis, and often DNA isolation is required. In addition, these procedures do not have the ability to determine the pathogen viability at the sampling time. Despite significant advances, current methods of diagnosing *Salmonella* are not fast and easily performed, nor are they reliable and sensitive enough [2]. Therefore, there is still an urgent need to produce biodegradable sensors for accurate, sensitive, and specific detection of *S. typhimurium* [3]. Other methods have been reported for *Salmonella* recognition, including surface plasmon resonance (SPR), optical methods, field effect transistors (FETs), quartz crystal microbalances (QCM), and electrochemical techniques. Biosensor techniques propose high specificity, and sensitivity but are limited in flexibility, stability, and production. To address these subjects, electrochemical biosensors have become increasingly attractive because of their high selectivity, and sensitivity, ease of operation without any pre-enrichment steps, fast response time, and low cost. Recent studies have shown that interest in developing biosensors as a rapid and accurate alternative method for detecting cell-borne pathogens specially *S. typhimurium* has increased [5].

4. Electrochemical biosensors and the use of nanomaterials in their construction

Recently, unparalleled attention and effort have been devoted to the production of new biosensors to promptly identify pathogens transmitted through food and water [8]. The electrochemical biological sensor, as a potential POCT platform with small sensitive detectors, has attracted good attention, works well in opaque environments, is inexpensive and easy to use. For direct bacterial detection, biosensors measure the biological signals of interactions between a biological detection element and whole-cell bacteria. Aptamers, microorganisms, enzymes, antibodies, and oligonucleotides are examples of biological cognitive elements utilized in the construction of biosensors. biological interactions are transmitted as an optical, electrical, or mechanical signal in a typical biosensing process,. In particular, electrochemical biosensors propose many advantages in the fields of medicine and biotechnology with the possibility of directly converting a biological reaction into a readable electrical signal. Electrochemical methods can be used in biosensors to detect the complete cell of bacteria due to being conductive layers of macromolecules with electrochemically active groups on the outer membrane of bacteria which can react with free ions in the electrolyte [8].

Electrochemical sensing techniques are extensively applied due to their high sensitivity, downsizing, ease of operation, and the production of portable devices. Labeled electrochemical sensing is a very attractive option [2].

Various materials have been used to develop highly sensitive electrochemical sensors. Among these reported materials, gold nanoparticles (AuNPs) have been extensively utilized to increase the sensitivity of sensors. The AuNPs are significant bio-functional materials with a large surface area, and excellent catalytic and electronic features [3]. Also, it has good conductivity, optimal biological compatibility, and unique physicochemical properties [7], and it has been widely used as labels of electrochemical sensors to increase sensitivity and stability [4]. For example, an electrochemical impedance sensor was developed based on graphene oxide/AuNPs and was capable to sense *S. Typhimurium* in the concentration range of 2.4–2.4×10^3 CFU/mL [2].

Carbon nanotubes (CNTs) are promising alternatives to glass and metal carbon electrodes for using in sensing instruments. CNTs have unique properties, including anti-fouling and fast electron transfer properties in aqueous and non-aqueous solutions. CNTs are useful as converters in electrochemical sensing to identify ions, metabolites, and biomarkers due to their electrical and electrochemical properties. As a result, CNT-based biosensors can attain a low sensing sensitivity threshold because of their high specific surface area and the large number of sites available for the connection of specific target analytes. Biosensors based on CNT demonstrated greatly improved the sensitivity and selectivity through the stabilization of cognitive elements, like metal nanoparticles, enzymes, and nucleic acids [5].

Inorganic nanomaterials (e.g., reduced graphene oxide (rGO), CNT, Ag and AuNPs) have been developed as measurement platforms in food diagnostics and forensics through the rapid revolution in nanotechnology. Though, the high cost of producing Ag and AuNPs and the incompatibility of CNTs limit their use in the biosensors fabrication.

rGO has excellent physicochemical properties, including high conductivity, large surface area, biocompatibility, and excellent mechanical strength. In addition, it is composed of hexagonal bonded sp^2 bonded carbon atoms that facilitate surface changes through non-covalent interactions such as π-π accumulation or hydrogen bonding between biomolecules and graphene for electroanalysis assay uses. Further improvement of

electrochemical biosensors sensitivity is achieved in the presence of functional groups including -CHO, -COOH, and -OH that permits interaction with biomolecules [8].

Studies on improving the performance of biosensors have developed from the use of metal oxides and pure metal as sensors to the fabrication of composite materials. For example, studies involving rGO with metal oxide nanoparticles like TiO_2 have been expanded to increase catalytic activity, electronic properties, and surface enhancement [9]. However, the electrochemical properties of rGO-TiO_2 nanocomposites have been extensively investigated, there is limited study on the use of this material as an electrochemical aptasensors for food-borne pathogens [9].

5. Electrochemical aptasensors for the detection of *S. typhimurium*

Aptamers are single-stranded RNA or DNA sequences that are screened from random RNA or DNA libraries by a laboratory evolution process called SELEX (systematic evolution of ligands with exponential enrichment), which usually has a high affinity and binds to a wide range. Compared to antibody-based biosensors, aptamer-based biosensors have unprecedented benefits with high efficiency, selectivity, affinity, and stability [10]. Aptamers can specifically bind to small organic molecules, antibiotics, proteins, cells, and bacteria [4]. Electrochemical decomposition assays using aptamers as a cognitive element have emerged as a cost-effective and rapid method with the potential to shrink the device [2, 9]. Aptamers have been produced and developed in a wide range of uses for the detection of microorganisms in the clinic, food, and environment [11].

Single-stranded DNA aptamers have been produced against various bacterial species, including *Shigella dysenteriae*, *Listeria monocytogenes*, *Salmonella paratyphi A*, *E. coli*, *Salmonella Enteritidis*, *Vibrio parahemolyticas*, and others. These aptamers have been used as cognitive components in various types of biosensor operating systems in combination with electrochemical transmission output to measure bacteria. For pathogens in need of modification, Preeti Pathania et al. demonstrated effective screening of selected DNA aptamers that are screened against *S. Typhimurium* as a specific molecule of the bio-detection pool of random oligonucleotide consequences. This process helps to improve the selection of aptamers produced by performing negative SELEX cycles with each control cell separately to eliminate the cross-reactive population that can be utilized for detection. Highly selective electrochemical biosensing platforms for the diagnosis of non-tuberculous salmonellosis can be developed by screened aptamers. The assay workflow was very simple to confine the properties of the selected aptamer produced using the affinity of gold with thiol groups [12]. Up-to-date and unlabeled electrochemical labels have undergone extensive research. Sheikhzadeh et al. developed an unlabeled electrochemical sensor (polypyrol polymer conjugated aptamers) to detect *S. typhimurium* through pre-measurements with a LOD of 3 CFU/mL. Guo et al. manufactured unlabeled graphene with electrically active aromatic dyes which improve the graphene solubility and retain its intrinsic properties (e.g., mechanical, electrical, and thermal properties) [8].

Specific DNA aptamers of *S. typhimurium* were selected based on SELEX from an 80 nt DNA library containing 40 nt random region, 5′-CTC CTC TGA CTG TAA CCA CG N40 GC ATA GGT AGT CCA GAA GCC-3 ′ (DNA Integrated Technologies, USA). Aptamer selection consisted of 12 rounds. Flow cytometry was

used for analyzing of the collected aptamer pools affinity for *S. typhimurium*. This was done by incubating the 100 nm aptamer pool labeled Alexa-488 with 50×10^3 CFU of bacteria and then flow cytometric analysis. It was perceived that the aptamer pool collected in the seventh round had the highest tendency to bind to bacteria (KD = 25 nM). The pool was then cloned, and the clones that showed the highest susceptibility to bacteria were sequenced. The ssDNA sequence (STYP-3, GAG TTA ATC AAT ACA AGG CGG GAA CAT CCT TGG CGG TGC), which shows the highest affinity for *S. typhimurium*, was modified at position 5 with the 6-hydroxyhexyl disulfide group. The DNA sequence, which shows the highest affinity for the bacterium, was integrated into a pre-pressure sensor by the automatic assembly on a carbon electrode printed with an AuNP-modified screen (GNP-SPCE). It is noteworthy that this aptasensor can successfully sense *S. typhimurium* up to 600 CFU/mL and distinguished it from other *Salmonella* species, including *S. enteritidis* and *S. choleraesuis* [6].

By combining target-induced aptamer displacement on AuNPs deposited electrodes deposited with a circular amplification (RCA), Ge et al. created a simple and easy aptasensor to determine the super-sensitivity of *S. typhimurium*.

Sheikhzadeh et al. 2016 reported a combination of poly [pyrrol-co-3-carboxyl-pyrrole] polycopolymer and aptamer to produce an unlabeled electrochemical biosensor suitable for *S. typhimurium* detection. Polypyrrole-based polymers have been proved as valuable candidates for manufacture biosensors because of their inherent electrical and chemical properties. Conductive polymer (CP) is a versatile and attractive material for the fabrication of functional interfaces and sensor surfaces. CPs combine the properties of ordinary metals and polymers and are used in a variety of fields, including extraction methods, fuel cells, artificial muscle, and medical engineering, as well as in sensor chemistry, biosensors, and functional surfaces for cell stimulation, tissue engineering, and bacterial differentiation [2]. Among CPs, polypyrrole has been widely used because of properties like high conductivity, good chemical stability, and ease of synthesis in various solvents and at room temperature. More interestingly, polypyrrole can be made by electrochemical methods, which provide high control over thickness, hydrophobicity, morphology, and shape. Nonetheless, polypyrrole suffers from lack of functional groups, and therefore the copolymerization of pyrrole with modified monomers has been investigated as a possible route for the preparation of polypyrrole films with new properties. Copolymers such as poly [[pyrrol-co-4- (3-pyrrolyl)] butanoic acid have been utilized to make hybrid DNA biosensors. In one study, Sheikhzadeh et al. used a bioconjugated poly [pyrroleco-3-carboxyl-pyrrole] copolymer-aptamer for an unlabeled electrochemical biological sensor to detect *S. Typhimurium*. Since most unlabeled electrochemical methods require a redox probe, often ferro/ferrocyanide, there is no need to add potential redox probes in this aptacensor [2].

In another study, a sensitive electrochemical sensor was fabricated utilizing a micro-electrode with an aptamer-coated digital gold to target and measure impedance and antibody-modified nickel nanowires (NiNWs) to separate the target and amplify the impedance. Biotinylated aptamers against *S. typhimurium* were used for the modification of microelectrode by electrostatic adsorption of streptavidin-biotin binding. The target *Salmonella* cells were then magnetically isolated by NiNWs modified with anti-*S. typhimurium* antibodies to form NiNW bacterial complexes and incubated on a microelectrode to form aptamer-bacterium-NiNW complexes. After generation of an external magnetic field, the change in advanced microelectrode impedance resistance was applied to obtain the amount of target bacteria [1].

Using multi-walled carbon nanotubes (MWCNTs) deposited on ITO electrodes, Rockibool Hassan developed and evaluated a modified amino aptasensor to identify *Salmonella* pathogens. DNA aptamer was used to detect *Salmonella* whole cells by binding to their outer membrane proteins. The development of a complete sensing process of bacterial cells eliminates the need for DNA extraction and significantly reduces analysis time. The results displayed that the impedance was measured at the surface of the ssDNA / MWCNT / ITO electrode after exposure to *Salmonella* cells, which indicates the successful binding of *Salmonella* to the surface of the aptamer [5].

In a further study, the rGO-azophloxine (AP) nanocomposite aptasensor was fabricated for the robust, rapid, and sensitive sensing of foodborne pathogens. In addition to providing a conductive rGO nanocomposite and an excellent solution, AP dye acts as an electrical indicator for redox reactions. In addition, an aptasensor developed with non-*Salmonella* bacteria and an artificial cluster chicken specimen with *S. typhimurium* were evaluated. The results showed that rGO-AP aptasensor has a high potential for rapid and effective specific food pathogen detection by an electrochemical method. Chemical doping of rGO with AP dye enriches its free charge carrier density, therefore increasing its electrical conductivity and solubility in hydrophilic medium. In addition, high-powered active electrical molecules remove the expensive and complex process of aptamers labeling and modifying. This electrochemical aptasensor offers a food sensing sensitivity system because of its unique potentials, including cost efficiency, good selection, high sensitivity, and simplicity [8].

An additional study focused on the production of an aptasensor based on rGO-TiO_2 nanocomposite for the sensing of *S. Typhimurium*. An unlabeled aptamer was stabilized via electrostatic interactions in the rGO-TiO_2 nanocomposite matrix. Changes in electrical conductivity on the surface of electrode were estimated via electrode analysis approaches. DNA aptamer adsorbed on the rGO-TiO_2 surface attached to bacterial cells at the electrode interface created a physical barrier to prevent electron transfer. The interaction reduced the DPV signal of the electrode in proportion to the decrease in the concentration of bacterial cells. This rGO-TiO_2 aptasensor is an excellent biosensing platform which propose a safe, fast, and sensitive option for detecting foodborne pathogens [9].

Lei et al. reported a sensitive, simple, and fast electrochemical sensor based on target-induced filament displacement and amplification of AuNPs to detect *Salmonella*. The thiol-recorded probe was fixed on the electrode interface via sulfur-gold affinity and hybridized with *Salmonella* aptamer containing a complementary sequence of the recording probe. Aptamer was isolated from the aptamer receptor-probe duplex in the presence of *Salmonella* due to strong interaction between *Salmonella* and aptamer. As the binding sites were re-exposed, the single-strand recording probe was hybridized with a biotinylated detection probe assembled on AuNPs and catalyzed by streptavidin-alkaline phosphatase, generating an electrically active product and an electrochemical response to *Salmonella*. As a consequence, a simple electrochemical biological sensor was considered to rapidly detect Salmonella with the expected application in the diagnosis of biotherapy and early detection of foodborne illness. AuNPs significantly amplify the diagnostic probe signal and increase sensitivity. This strategy was used to determine Salmonella in milk, representing its potential use in environmental monitoring, clinical diagnosis, and food safety [4].

6. Conclusion

Gram-negative bacterium *S. typhimurium* is a foodborne pathogen that is responsible for hospitalization and countless deaths worldwide. Conventional methods of detecting pathogens are time-consuming and laborious. Rapid recognition of food-borne pathogens is very important to prevent the spread of food-borne diseases. Traditional approaches of detecting this pathogen are based on a combination of pre-enrichment steps, culture on agar plates, and serological validation of suspected colonies. Though these methods can offer reliable consequences, they may take up to 5 days to achieve results and are relatively time-consuming. Given these drawbacks, developing faster and new methods to detecting bacteria is a major challenge in contemporary microbiology. Aptamer-based diagnostics provide a rapid, simple, highly sensitive, and specific analytical technique for quantifying *S. typhimurium*.

References

[1] L. Wang, X. Huo, W. Qi, Z. Xia, Y. Li, J. Lin, Rapid and sensitive detection of Salmonella Typhimurium using nickel nanowire bridge for electrochemical impedance amplification, Talanta 211 (2020) 120715. doi: 10.1016/j.talanta.2020.120715.

[2] E. Sheikhzadeh, M. CHamsaz, A. Turner, E. Jager, V. Beni, Label-free impedimetric biosensor for Salmonella Typhimurium detection based on poly [pyrrole-co-3-carboxyl-pyrrole] copolymer supported aptamer, Biosensors and bioelectronics 80 (2016) 194-200. doi: 10.1016/j.bios.2016.01.057.

[3] C. Ge, R. Yuan, L. Yi, J. Yang, H. Zhang, L. Li, W. Nian, G. Yi, Target-induced aptamer displacement on gold nanoparticles and rolling circle amplification for ultrasensitive live Salmonella typhimurium electrochemical biosensing, Journal of Electroanalytical Chemistry 826 (2018) 174-180. doi: 10.1016/j.jelechem.2018.07.002.

[4] X. Li, H. Fu, Y. He, Q. Zhai, J. Guo, K. Qing, G. Yi, Electrochemical aptasensor for rapid and sensitive determination of Salmonella based on target-induced strand displacement and gold nanoparticle amplification, Analytical Letters 49 (2016) 2405-2417. doi: 10.1080/00032719.2016.1151888.

[5] M.R. Hasan, T. Pulingam, J.N. Appaturi, A.N. Zifruddin, S.J. Teh, T.W. Lim, F. Ibrahim, B.F. Leo, K.L. Thong, Carbon nanotube-based aptasensor for sensitive electrochemical detection of whole-cell Salmonella, Analytical biochemistry, 554 (2018) 34-43. doi: 10.1016/j.ab.2018.06.001.

[6] M. Labib, A.S. Zamay, O.S. Kolovskaya, I.T. Reshetneva, G.S. Zamay, R.J. Kibbee, S.A. Sattar, T.N. Zamay, M.V. Berezovski, Aptamer-based viability impedimetric sensor for bacteria, Analytical chemistry 84 (2012) 8966-8969. doi: 10.1021/ac302902s.

[7] D. Zhu, Y. Yan, P. Lei, B. Shen, W. Cheng, H. Ju, S. Ding, A novel electrochemical sensing strategy for rapid and ultrasensitive detection of Salmonella by rolling circle amplification and DNA–AuNPs probe, Analytica Chimica Acta 846 (2014) 44-50. doi: 10.1016/j.aca.2014.07.024.

[8] S. Muniandy, I.J. Dinshaw, S.J. Teh, C.W. Lai, F. Ibrahim, K.L. Thong, B.F. Leo, Graphene-based label-free electrochemical aptasensor for rapid and sensitive detection of foodborne pathogen, Analytical and bioanalytical chemistry 409 (2017) 6893-6905. doi: 10.1007/s00216-017-0654-6.

[9] S. Muniandy, S.J. Teh, J.N. Appaturi, K.L. Thong, C.W. Lai, F. Ibrahim, B.F. Leo, A reduced graphene oxide-titanium dioxide nanocomposite based electrochemical aptasensor for rapid and sensitive detection of Salmonella enterica, Bioelectrochemistry 127 (2019) 136-144. doi: 10.1016/j.bioelechem.2019.02.005.

[10] W.-h. Wu, M. Li, Y. Wang, H.-x. Ouyang, L. Wang, C.-x. Li, Y.-c. Cao, Q.-h. Meng, J.-x. Lu, Aptasensors for rapid detection of Escherichia coli O157: H7 and Salmonella typhimurium, Nanoscale research letters 7 (2012) 658. doi: 10.1186/1556-276X-7-658.

[11] A.L. Furst, M.B. Francis, Impedance-based detection of bacteria, Chemical reviews 119 (2018) 700-726. doi: 10.1021/acs.chemrev.8b00381.

[12] P. Pathania, A. Sharma, B. Kumar, P. Rishi, C.R. Suri, Selective identification of specific aptamers for the detection of non-typhoidal salmonellosis in an apta-impedimetric sensing format, Microchimica Acta 184 (2017) 1499-1508. doi: 10.1007/s00604-017-2098-2.

Growth hormone signaling pathway in mature and immature scorpions: Androctonus Crassicauda

Fatemeh, Salabi*, Hedieh, Jafari and Alireza Forouzan

Razi Vaccine and Serum Research Institute, Ahvaz, Agricultural Research, Education and Extension Organization (AREEO), Iran. 2. Razi Vaccine and Serum Research Institute, Karaj, Agricultural Research, Education and Extension Organization (AREEO), Iran.

***Corresponding author:** Fatemeh Salabi, Department of Venomous Animals and Anti-venom Production, Razi Vaccine and Serum Research Institute, Agricultural Research, Education and Extension Organization (AREEO), Ahvaz-Iran. Telephone and Fax Numbers: 0098-613332504

Email: f.salabi@rvsri.ac.ir

Abstract

The scorpion of *Androctonus Crassicauda* is belong to Buthidae family that widely distributed in the Middle East, including Iran, Iraq, Turkey, Jordan and Arabia. However, no studies have been conducted on the venom of *Androctonus Crassicauda* species yet. In this work, we performed a transcriptomic approach for analyzing and compering the venom components from *Androctonus Crassicauda* scorpions in two different growth stages: immature and mature. After functional and pathway analysis, we employed protein annotation to identify genes related to growth and development of scorpion among the immature and mature scorpions. Enrichment analysis of KEGG indicated that some of differentially expressed genes were involved in growth hormone signaling pathway. Our study provides an archive for future studies on development of scorpions.

Keywords: Buthidae, *Androctonus Crassicauda,* Transcriptomic approach, immature and mature scorpions**.**

1. Introduction

Scorpions are ancient terrestrial animals that are considered as living fossils [1]. Recently, most of the studies have analyzed the components if scorpion venom. Venoms are the secretion of venom glands found in scorpions and other venomous animals which are complex mixture of water, salts, biogenic amines, mucoproteins, lipids, nucleotides, neurotoxins, enzymes and other components [2]. The number of discovered venom peptides were not as expected. It mainly due to the fact that the venom contains of heterogeneousity, complexity and high variability of components and in addition, the current venom protein separation methods have low resolution [3]. Nowadays, the emergence of new methods such as high-throughput RNA sequencing has revolutionized the identification of venom compounds [4]. The number of new venom components has significantly increased in recent years due to the rapid development of transcriptomic analysis.

The scorpion of *Androctonus Crassicauda* is belong to Buthidae family that widely distributed in the Middle East, including Iran, Iraq, Turkey, Jordan and Arabia [5]. The employment of transcriptomic analysis in scorpion is adding new insights about biological processes of the venom gland, as well as facilitating the identification of regulatory factors. Nevertheless, lack of transcriptomic information is evident in *A. Crassicauda*, therefore, in this

study, we used RNA sequencing to de novo assembled the scorpion transcriptome of the venom gland of *A. Crassicauda* scorpions in two different growth stages: immature and mature. Furthermore, KEGG pathway enrichment analyses were carried out to explore the potential function of the DE mRNAs. The most important differentially deregulated mRNAs of the scorpion venom gland associated with growth hormone signaling pathway were identified using the KEGG database.

2. Materials and Methods

2.1 Sequencing, assembly and bioinformatics analysis

The telsons of mature and immature males *A. Crassicauda* were removed 72 h after being milked by electrical stimulation. After total RNA extraction, all cDNA libraries were sequenced using an Illumina HiSeq 2000 platform (Illumina, San Diego, CA, USA) and 150 bp paired-end reads were produced.

Afterwards, in order to identify mRNA transcripts, we used annotation pipeline with *five search strategies.* The main step consists of the *identification of all* putative homologous sequences with sequence similarity searching against Swissprot, NCBI non-redundant (Nr), UniProtKB/TrEMBL and Pfam protein domain databases with an *E-value* threshold of 10^{-3}. Thereafter, RSEM software was used to estimate the gene expression levels in terms of FPKM (fragments per kilobase of transcript sequence per million base pairs sequenced).

[7]

2.2 Gene ontology and pathway enrichment analysis

Differentially expressed coding genes in both of growth stages were enriched for the Kyoto Encyclopedia of Genes and Genomes (KEGG) pathways to investigate the main functions of DE mRNA in growth hormone signaling pathway.

3. Results and Discussions

3.1 Differential expression analysis of mRNAs

To investigate the differential expression of mRNAs during development of *Androctonus crassicauda*, approximately 54Gb of high-quality data, were generated. Approximately average of 200,537,746 raw reads were gained for the mature and immature male scorpions. After filtering the raw reads and removing low quality, adapter and uncertain reads, a total of 200 million clean reads. In order to extract protein coding transcripts from the *A. Crassicauda* transcriptome, similarity searches using a blast against Swiss-Prot; NCBI nr; UniProtKB/TrEMBL, Pfam, UniProt proteins/toxins databases and TransDecoder predictions were done. *Finally, after removing non-coding RNAs from the assembled transcriptomes, we annotated 209951 coding sequences that they were classified as mRNA transcripts.*

To study the differential expression of mRNAs in the two developmental stages of *A. Crassicauda*, the expression levels of mRNA transcripts were measured and differential expression analysis was conducted using EdgeR. There were 963 mRNAs transcripts with differentially expression levels ($p< 0.01$).

3.2 KEGG pathway enrichment analysis of DE mRNAs

To further evaluate the role of differentially expressed (DE) genes in scorpion development, these genes were submitted to diverse databases for functional annotation including GO and KEGG.

KEGG analysis of the predicted DE mRNAs was used to enhance our knowledge of the biological functions of the DE mRNAs during development of *A. Crassicauda*. According to GO and KEGG analysis of differentially upregulated and downregulated mRNA transcripts, one of the most importantly enriched pathways was Growth hormone synthesis, secretion and action. More importantly, the GO and KEGG analyses revealed that many genes related to growth hormone signaling pathway were dysregulated. Therefore, in this study, altering the expression pattern of genes involved in this pathway suggested to be key development indicators in scorpion. According to our results, the upregulated genes Guanine nucleotide-binding protein (GNAS), Cyclic AMP-dependent transcription factor ATF-4 (CREB) and Phosphatidylinositol phospholipase C, beta (PLCB) the downregulated genes Voltage-dependent calcium channel L type alpha (CACNA) and Protein kinase A (PKA) were enriched in scorpion growth hormone signaling pathway. Growth hormone synthesis, secretion and actionare pathway illustrated in figure 1.

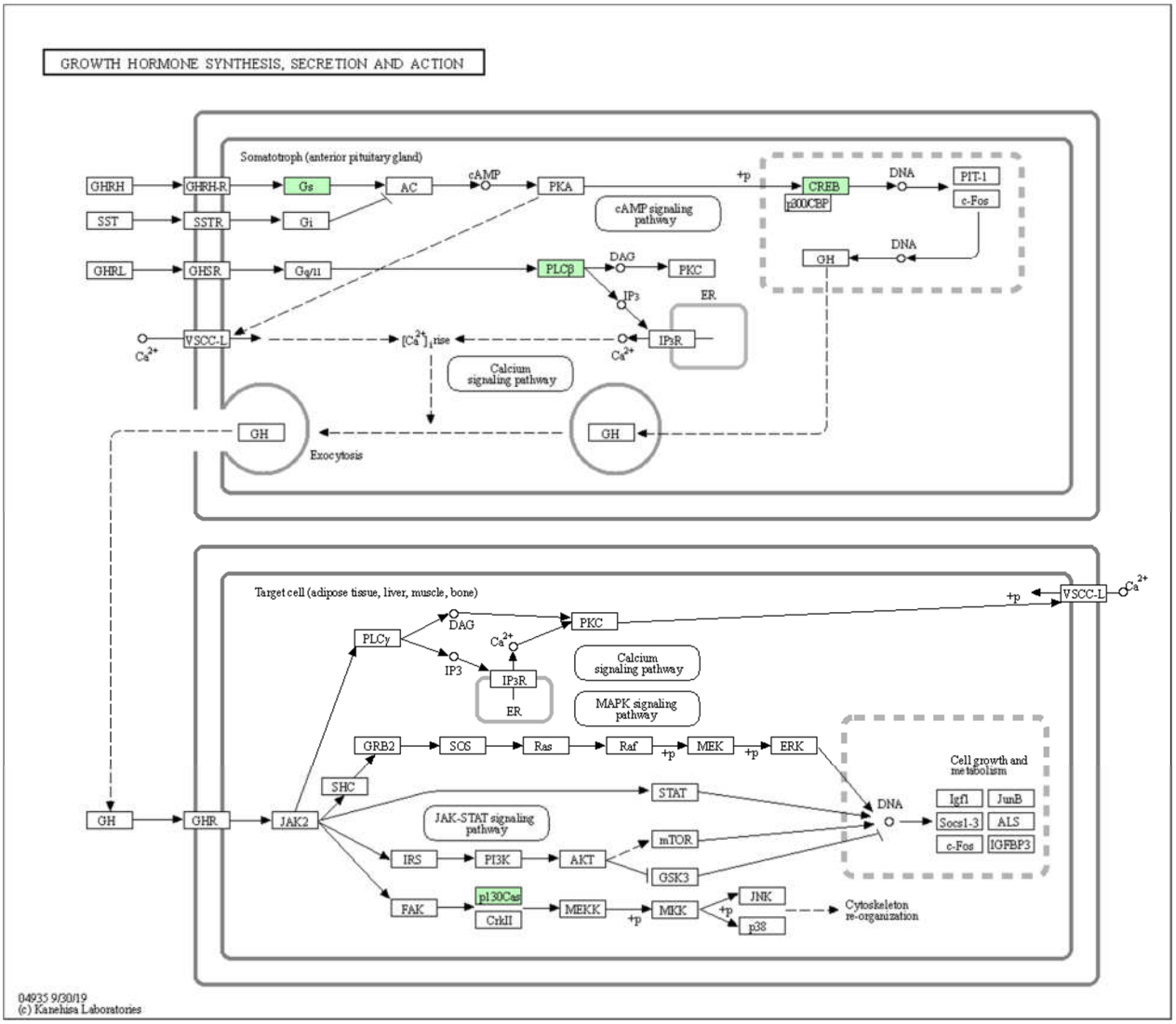

Figure1. Growth hormone signaling pathway. Green color indicate upregulated genes of matures.

Several studies were undertaken to elucidate the role of this important mediators in development of other animals. Protein kinase A (PKA) has been investigated to regulate cellular growth, differentiation, sperm maturation and function [6,7].

Overall, this study investigated dysregulated genes based on GO and KEGG pathways. *Our* functional study suggested that growth hormone signaling pathway to be associated with aging and development function of scorpions. Taking these results together, these findings broadened our knowledge about the differences between mature and immature scorpions venom.

Acknowledgements

We thank the Razi Vaccine and Serum Research Institute, of Iran for their financial support and our colleagues for many stimulating discussions.

References

[1] V. Quintero-Hernández, Jiménez-Vargas, J. M. Jiménez-Vargas, G. B. Gurrola, H. H. Valdivia, and L. D. Possani. "Scorpion venom components that affect ion-channels function." Toxicon 76 (2013) 328-342.

[2] A.K. Al-Asmari, F. Kunnathodi, K. Al Saadon, M.M. Idris. Elemental analysis of scorpion venoms. Journal of venom research, 7 (2016) p.16.

[3] S. Ahmadi, J.M. Knerr, L. Argemi, K.C. Bordon, M.B. Pucca, F.A. Cerni, E.C. Arantes, F. Çalışkan, A.H. Laustsen. Scorpion venom: detriments and benefits. Biomedicines, 8(5), (2020) p.118.

[4] J. Wen, A.N. Egan, R.B. Dikow, E.A. Zimmer. Utility of transcriptome sequencing for phylogenetic inference and character evolution. Next-generation sequencing in plant systematics (2015).

[5] P. Crucitti. The scorpions of Anatolia: biogeographical patterns. Biogeographica 20, (1999) 81–94.

[6] P. Jenardhanan, P.P. Mathur. Kinases as targets for chemical modulators: Structural aspects and their role in spermatogenesis. Spermatogenesis, 4(2), (2014) p.e979113.

[7] J.Y. Wu, T.J. Ribar, A.R. Means.. Spermatogenesis and the Regulation of Ca2+-Calmodulin-Dependent Protein Kinase IV Localization Are Not Dependent on Calspermin. Molecular and cellular biology, 21(17), (2001) pp.6066-6070.

Optical and electrochemical aptasensors for glycated human serum albumin

Maryam Nazari[1*]

[1] Faculty of Chemistry, Razi University, Kermanshah, Iran

*Email: nazari.maryam@razi.ac.ir

Abstract

Diabetes mellitus (DM) is known as a common disease. It has accurate markers like glycated proteins including glycated hemoglobin and glycated human serum albumin (GHSA). The average blood glucose level can be reflected by GHSA over the prior 2 to 3 weeks. GHSA is a good marker specially for patients who are having hematologic disorders or undergoing hemodialysis. At present available approaches for GHSA detection are limited in clinical use. Aptasensors has revealed great potential for the diagnostics of various diseases. Comparing of HbA1c and GHSA properties for controlling of diabetes glucose level and GHSA optical and electrochemical aptasensors were reviewed.

Keywords: Aptasensor, Glycated Human Serum Albumin, Optical, Electrochemical

1. Introduction

One of the most common metabolic diseases in the world is diabetes mellitus (DM). Diabetes results most cases of renal failure and blindness [1]. To avoid long-term complications, the blood glucose level of diabetes patients should be control at a normal level. Circulating glycated proteins are significant indicators of mean glycemic control for DM; they include, glycated human serum albumin (GHSA) and hemoglobin A1c (HbA1c). HbA1c is another name of glycated hemoglobin [2]. The proportion of GHSA concentration divided by the total albumin concentration quantifies GHSA values and normal individuals have GHSA values ranging from 11 to 16%. Also, a percentage of the total hemoglobin molecules that are glycated reveal HbA1c amounts. [2].

Aptasensor is a type of biosensor that is fabricated using aptamer as the analyte detection unit. It has revealed abundant potential for the detection of various diseases [1]. Biomolecular probes with specific biomolecule-analyte/target interaction were applied to improve biosensor selectivity. Previously, aptamer-target and antigen-antibody bindings as two typical biomolecular recognition systems, have been widely utilized for biosensors fabricatation. The aptamer-target system-based aptasensors have presented several advantages comparison with biosensors based on antigen-antibody system such as wider sensing application of analytes, higher sensitivity, easier fabrication, lower price, and higher affinity [3].

In this study, comparing of HbA1c and GHSA properties for diabetes controlling glucose level and then GHSA aptasensors including optical and electrochemical types will be discussed.

2. Comparing HbA1c and GHSA for Diabetes Controlling Glucose Level

The non-enzymatic reactions between various circulating blood proteins and glucose produce glycated proteins [1]. The β subunit N-terminal valine of hemoglobin can be glycated and originated HbA1c. [2]. Non-enzymatic glycation of HSA disturbs the normal HSA roles and it produces GHSA through by excess circulating sugar. The ε-amino group glycation of internal lysine residues of circulating albumin in plasma can originate GHSA and. 25 times higher levels of a typical diabetic GHSA in glucose metabolism of both skeletal muscle cells and adipocyte cells can be seen for diabetic patients and it has been confirmed that the GHSA formation has pathogenic implication [1]. HbA1c and GHSA reflected the mean blood glucose level over the prior 2-3 months and 2-3 weeks, respectively.

While HbA1c is the standard accepted indicator of glycemic control and the most extensively utilized mean glycemia marker in the world and, GHSA has two advantages over HbA1c including (i) HbA1c cannot precisely reveal glycemic status in the presence of conditions with genetic variations in the hemoglobin structure or altered erythrocyte life span, (ii) over a shorter period glycemic status than HbA1c can be reflected by GHSA; therefore, monitoring of mean glycemia is better followed when a patient's state is quickly altering. Specially, conditions with enhanced replacement of older erythrocytes with young erythrocytes and hemolysis can diminish HbA1c levels, whereas disease such as vitamin B12 and iron deficiencies that related to diminished red blood cell formation, can raise HbA1c levels. Nevertheless, all these circumstances can affect hemoglobin producing and cannot affect GHSA levels [2]. Furthermore, specially for patients who are having hematologic disorders or undergoing hemodialysis, GHSA is a much more accurate marker for DM [1].

3. GHSA Detection Methods

At present, there is no standardized procedure for GHSA detection. The existing determining methods for GHSA generally like high performance liquid chromatography (HPLC) [4], mass spectrometry [5], enzymatic method [6], fluorescence [7], affinity chromatography [8], colorimetry [9], Raman spectrum method [10], and electrochemiluminescence [11]. The limit of detections that have been obtained for GHSA detection by HPLC, enzymatic method, fluorescence, electrochemiluminescence, and colorimetry method, were 10.9 μM, 0.47 mg/mL, 0.81 mg/L, 50 μg/mL, and 0.1 μM, respectively. These procedures have some advantages and disadvantages. As fluorescence quenching affect the biochemical immunofluorescence protein marker, this method is only valid to GHSA qualitative investigations. The signals of Raman scattering spectral are meanwhile, faint, and the difficult sense of GHSA scattering signal. Hence, Raman spectrum process is difficult to be utilized for quantitative and qualitative study of GHSA. Furthermore, mass spectroscopy, HPLC, enzymatic method, affinity chromatography, electrochemistry, and colorimetry are considered by many disadvantages, like using of chemical reagents, and requiring time-consuming and complicated analytical procedures with training and specialized knowledge [12].

Currently offered approaches for GHSA determination are restricted in clinical practice since they implicate cumbersome and slow procedures of thermal incubation proteolytic digestion, and sample preparation, a lack of normalization to total albumin levels, and suffering from limited analytical performance [13].

4. GHSA Aptasensing

Apiwat et al., performed systematic evolution of ligands by exponential enrichment (SELEX) process for selecting of DNA aptamers bound GHSA from the DNA aptamer library of ~10^{15}. They found DNA aptamer (G8 aptamer) sequence plays an important role in GHSA binding. According to the Mfold prediction, G8 aptamer formed secondary structures with the long flexible region at the 3' end and 2 hairpin loops at the 5' end. Only the big hairpin loop plays a role in GHSA binding due to unstable small loop at room temperature, according to their results. It was demonstrated that after 9 removing of the small loop at the 5' end GHSA binding was still observed for the 23 nucleotides length structure related to the big hairpin loop that was comprised of 15-nucleotide loop and triple G-C hairpins with the affinity of 5.78 µM [7]. They used this sequence aptamer for optical GHSA detection. Also, various strategies are reviewed on the use of aptamers to construct aptasensors for using in optical, and electrochemical detection of GHSA in the following. Also, Table 1 shows the applicable properties of GHSA aptasensors.

Table 1. Optical and electrochemical aptasensors for GHSA

Aptasensor	Type	Aptamer sequence	LOD	Linear range	Stability	Ref
Complex of graphene and Cy5-labeled aptamer	Optical (Fluorescence)	5′-TGCGGTTGTAGTACTCGTGGCCG-3′	50 µg/mL	0-0.3 mg/mL	-	[7]
QD-aptamer-AuNP	Optical (Fluorescence)	5′Amino C_6/TGCGGTTGTAGTACTCGTGGCCG/Thiol C_6 SS 3′	1.008 nM	1.008-14500 nM	-	[14]
Biotinylated aptamer/STR/SPCE	Electrochemical (SWV)	5′-TGCGGTTGTAGTACTCGTGGCCG-3′	2.6×10^{-6} mg/mL	2×10^{-6}-16 mg/mL	87% after 1 month	[13]
Aptamer-MB/ RGO-AuNPs/GCE	Electrochemical (SWV)	5′-GGTGGCTGGAGGGGGCGCGAACGTTTTTTTTTT 3′- SH	0.07 µg/mL	2-10 µg/mL	-	[15]

4.1 GHSA Optical Aptasensors

As it was discussed in section 4, Apiwat et al., found that the hairpin-loop structure plays a key role in GHSA binding. Before the addition of the analyte, a large hairpin loop is formed by this aptamer, and after the addition of target, the hairpin loop is opened up to bind to GHSA. They analyzed GHSA through the sensitive graphene-based aptasensor. Cy5- labeled aptamer and fluorescent quenching graphene oxide (GO) were utilized for development of sensitive and simple aptasensor for GHSA recognition. The unique properties of GO cause to widely use GO for fluorescent biosensors fabrication and the fluorescence resonance energy transfer (FRET) technique. GO causes to fluorescence quenching of dyes and gets the energy from dyes in a facile manner, hence, it is well known that GO has being as an excellent energy acceptor in FRET. The limit of detection (LOD) was lower than other existing procedures. Also, the GHSA recognition platform can be applied in clinical samples with the nuclease resistance system. Notably, their method could considerably demonstrate the GHSA concentrations with higher levels in diabetes than normal serums [7]. In another work, Awang et al., used molecular dynamics simulations for investigation of the GHSA aptamer adsorption on a mobile graphene in salt-free solutions and electrolyte. This work was performed to develop the graphene-based fluorescent aptasensor, an aptamer could be quenched upon graphene binding and was fluorescent after binding to GHSA. Graphene flexibility cause to obtaining various DNA conformations. This indicates important roles of nucleobases and a phosphate backbone for graphene adsorption and binding analytes, respectively [16].

Ghosh et al. designed an optical sensor combined of GHSA aptamer, gold nanoparticle (AuNPs), and semiconductor quantum dot (QD) for GHSA recognition. The aptamer was functionalized by amine and thiol groups at two its ends, and AuNP and QD were added to aptamer though reaction with these functional groups. By the addition of GHSA, an enhance in photoluminescence intensity was detected and therefore, the system functioned as a “turn on” sensor. Aptamer was folded to form a large hairpin loop and opened up before and after the analyte addition, respectively, causing in the leaving of QD and the AuNPs and a responding enhance in photoluminescence. When a specific time period was considered for binding rate of the aptamer to the target, it was accompanied by a decline for time based photoluminescence studies. Compare to other control proteins, this sensor shown higher selectivity towards GHSA. When traditional techniques of glucose level checking are conjugated with this simple aptasensor via superior number of clinical samples for an effective sensing of DM the most number of ways can be opened up [14]. Also, Ghosh et al. presented the application of aptasensors in the intracellular environment based on their previous work for GHSA aptasensing fluorescence method. They developed sensing of antigens in the intracellular environment from previous studies of aptasensors operation in the extracellular environment. A crucial stage in this study was the use of a new means of attaining the aptasensors endocytosis [17].

4.2 GHSA Electrochemical Aptasensors

Several electrochemical techniques, such as electrochemical impedance spectroscopy (EIS), differential pulse voltammetry (DPV), cyclic voltammetry (CV), and square wave voltammetry (SWV) have been extensively applied for GHSA biomedical analysis.

Bunyarataphan et al., fabricated an electrochemical biosensor values based on two DNA aptamers that specially bind to human serum albumin (HSA) and GHSA and require no sample preparation, thermal incubation, or proteolytic digestion. Aptamers had been immobilized on separate screen-printed carbon electrodes (SPCEs) that were modified with streptavidin (STR). The binding of the target proteins to their specific biotinylated aptamers was sensed by SWV and ferricyanide ($Fe(CN)_6^{3-}$)) was used as redox mediator. High selectivity was achieved for GHSA over other molecules existing in the blood. GHSA in plasma samples could be determined by this developed sensor and when the plasma with raised GHSA levels in non-diabetic versus diabetic patients were used, a statistically significant difference was obtained. Furthermore, the trends in these GHSA levels were consistent with those attained via the HbA1c test. This reported detection method could be used as a point-of-care-testing (POCT) device to detect clinically GHSA value [13].

Farzadfard et al., designed an electrochemical label-free aptasensor for GHSA sensing via GHSA aptamer for modification of reduced GO (rGO)/AuNPs serface. The aptamer chain was thiolated for simple and fast of the electrode modification. Structural examination of nanomaterials displayed that AuNPs distributed uniformly on the graphene sheets surface; in addition, graphene sheets were produced satisfactory by the average thickness of 2.5 nm. EIS, CV, and SWV were applied to electrochemical investigation of the modified electrode. Electrochemical studies confirmed the potential of synthetized rGO/AuNPs-aptamer electrode to selectively detect GHSA appropriately in buffer solution at the low LOD [15].

5. Conclusion

GHSA is a diabetes marker with medium-term glycaemic controlling and can be applied as an alternative to or together with HbA1c and it. GHSA reveals a shorter timeframe than HbA1c since GHSA has a half-life of three weeks whereas erythrocytes have a lifespan of over three months. GHSA aptasensors have a potential for recognition and controlling of DM. GHSA aptamer plays a key role in GHSA binding; it conforms of the hairpin-loop structure with 23 nucleotides length comprising 15-nucleotide loop and triple G-C hairpins. The GHSA aptamer with high binding affinity was utilized in combination with graphene and AuNPs in flourimetry and electrochemical techniques with low detection limits.

References

[1] J. Zhang, Y. Cao, Aptasensors, Nano-Inspired Biosensors for Protein Assay with Clinical Applications, Elsevier2019, pp. 139-166. doi:10.1016/B978-0-12-815053-5.00006-4.

[2] M. Hatada, W. Tsugawa, E. Kamio, N. Loew, D.C. Klonoff, K. Sode, Development of a screen-printed carbon electrode based disposable enzyme sensor strip for the measurement of glycated albumin, Biosensors and Bioelectronics, 88 (2017) 167-173. doi:10.1016/j.bios.2016.08.005i.

[3] L. Wang, A. Wu, G. Wei, Graphene-based aptasensors: from molecule–interface interactions to sensor design and biomedical diagnostics, Analyst, 143 (2018) 1526-1543. doi:10.1039/C8AN00081F.

[4] D.S. Hage, J.A. Anguizola, C. Bi, R. Li, R. Matsuda, E. Papastavros, E. Pfaunmiller, J. Vargas, X. Zheng, Pharmaceutical and biomedical applications of affinity chromatography: recent trends and developments, Journal of pharmaceutical and biomedical analysis, 69 (2012) 93-105. doi:10.1016/j.jpba.2012.01.004.

[5] X. Bai, Z. Wang, C. Huang, Z. Wang, L. Chi, Investigation of non-enzymatic glycosylation of human serum albumin using ion trap-time of flight mass spectrometry, Molecules, 17 (2012) 8782-8794. doi:10.3390/molecules17088782.

[6] T. Kohzuma, T. Yamamoto, Y. Uematsu, Z.K. Shihabi, B.I. Freedman, Basic performance of an enzymatic method for glycated albumin and reference range determination, Journal of diabetes science and technology, 5 (2011) 1455-1462. doi:10.1177/193229681100500619.

[7] C. Apiwat, P. Luksirikul, P. Kankla, P. Pongprayoon, K. Treerattrakoon, K. Paiboonsukwong, S. Fucharoen, T. Dharakul, D. Japrung, Graphene based aptasensor for glycated albumin in diabetes mellitus diagnosis and monitoring, Biosensors and Bioelectronics, 82 (2016) 140-145. doi:10.1016/j.bios.2016.04.015.

[8] R. Paroni, F. Ceriotti, R. Galanello, G.B. Leoni, A. Panico, E. Scurati, R. Paleari, L. Chemello, V. Quaino, L. Scaldaferri, Performance characteristics and clinical utility of an enzymatic method for the measurement of glycated albumin in plasma, Clinical biochemistry, 40 (2007) 1398-1405. doi: 10.1016/j.clinbiochem.2007.08.001.

[9] H.V. Roohk, A.R. Zaidi, A review of glycated albumin as an intermediate glycation index for controlling diabetes, Journal of diabetes science and technology, 2 (2008) 1114-1121. doi: 10.1177/193229680800200620.

[10] N.C. Dingari, G.L. Horowitz, J.W. Kang, R.R. Dasari, I. Barman, Raman spectroscopy provides a powerful diagnostic tool for accurate determination of albumin glycation, PLoS One, 7 (2012) e32406. doi:10.1371/journal.pone.0032406.

[11] Y. Inoue, M. Inoue, M. Saito, H. Yoshikawa, E. Tamiya, Sensitive detection of glycated albumin in human serum albumin using electrochemiluminescence, Analytical chemistry, 89 (2017) 5909-5915. doi:10.1021/acs.analchem.7b00280.

[12] Y. Li, F. Li, X. Yang, L. Guo, F. Huang, Z. Chen, X. Chen, S. Zheng, Quantitative analysis of glycated albumin in serum based on ATR-FTIR spectrum combined with SiPLS and SVM, Spectrochimica Acta Part A: Molecular and Biomolecular Spectroscopy, 201 (2018) 249-257. doi:10.1016/j.saa.2018.05.022.

[13] S. Bunyarataphan, T. Dharakul, S. Fucharoen, K. Paiboonsukwong, D. Japrung, Glycated albumin measurement using an electrochemical aptasensor for screening and monitoring of diabetes mellitus, Electroanalysis, 31 (2019) 2254-2261. doi: 10.1002/elan.201900264.

[14] S. Ghosh, D. Datta, M. Cheema, M. Dutta, M.A. Stroscio, Aptasensor based optical detection of glycated albumin for diabetes mellitus diagnosis, Nanotechnology, 28 (2017) 435505. doi:10.1088/1361-6528/aa893a.

[15] A. Farzadfard, J.S. Shayeh, M. Habibi-Rezaei, M. Omidi, Modification of reduced graphene/Au-aptamer to develop an electrochemical based aptasensor for measurement of glycated albumin, Talanta, 211 (2020) 120722. doi:10.1016/j.talanta.2020.120722.

[16] T. Awang, P. Thangsan, P. Luksirikul, D. Japrung, P. Pongprayoon, The adsorption of glycated human serum albumin-selective aptamer onto a graphene sheet: simulation studies, Molecular Simulation, 45 (2019) 841-848. doi:10.1080/08927022.2019.1605599.

[17] S. Ghosh, Y. Chen, J. Sebastian, A. George, M. Dutta, M.A. Stroscio, A study on the response of FRET based DNA aptasensors in intracellular environment, Scientific reports, 10 (2020) 1-8. doi:10.1038/s41598-020-70261-1

Analysis of Biological Database of TCGA Using Relational Model

Hassan Nosrati Nahook[1*], Shayesteh Tabatabaei[1]
[1]Department of Computer Engineering, Higher Educational Complex of Saravan, Saravan, Iran.

*Email: hsn.nosrati@gmail.com

Abstract

TCGA is a comprehensive and coordinate attempt to accelerate our perception on molecular basis of cancer using technologies of genome analysis including genome sequencing in large scale. TCGA dataset, which includes more than two petabytes of genomic data, is accessible publicly, and this genomic information helps cancer research society to improve prevention, diagnosis and treatment of cancer. TCGA is one of the most important projects in biological database in the bioinformatics field. Our aim in this study is to assess various sections of database of TCGA which the entities and relations extracted are presented in result which show complicity of this large database, and it is easy to present and solve different queries depending on application of various biological fields

Keywords: Cancer, DNA, GDC, RNA, Genome.

1. Introduction

TCGA is the richest and most complete genomic dataset and is prepared for perception of molecular basis of cancers. Data gathering for TCGA at 2006 was initiated as common attempt of National Cancer Institute, National Human Genome Research Institute (NHGRI), National Institute of Health, and U.S. Department of Health and Human. Over the last decade, TCGA has grown and includes information related to 33 types of various tumour and more than 11000 cases (patients). Among 50 to 1500 cases were sampled for each type of tumour. For each case, several samples were analyzed using microarray technology for genomic characteristics and later technology to determine sequence.

TCGA data shows more than 2.5 petabyte information nowadays, and it is expected that it is grown by processing of new samples, which these genomic information helps cancer research society to improve prevention, diagnosis and treatment of cancer [1]. Genome is a fantasy word for your whole genome. From potato to puppies, all the live-beings have their own genome. Each genome includes required information to construct and preserve the organism over lifetime.

If all the DNA from a single human cell was stretched out end-to-end, it would make a six-foot-long strand comprised of a six billion letter code. It's hard to imagine how that much DNA can be packed into a cell's nucleus, which is so small it can only be seen with a specialized microscope. The secret lies in the highly structured and tightly packed nature of the genome.

TCGA applies techniques of genome analysis with high efficiency to improve our ability to diagnose, treat and prevent cancer by better perception on genetic basis of this disease. Researchers of TCGA network explains

molecular characteristics which classifies types of testicular basic cells tumours including a separate set of seminomas described by KIT mutation.

This set provides candidate biomarkers for classification of risk and potential therapeutic aim. A three-year experimental project which was initiated at 2006 was concentrated on characteristic of three types of human cancers: Glioblastoma multiforme, lung and ovarian cancer [3]. At 2009, it was spread at second stage, which was planned to complete genomic characteristics and analysis of sequences of 20-25 types of various tumours up to 2014.

This 500-patient project planned genomics much more than many studies and uses various methods to analyze patient's samples. Techniques include profile of gene expression, profile of changing the copy number of SNP genotype, profile of wide DNA-methylation of genome, analysis of microRNA, and exon sequence of at least 1200 gene. TCGA includes sequence of whole genome of some tumours, consisting of at least 6000 candidate genes and sequences of microRNA. This sequence aimed to be performed by all the three centers of determining sequence using hybrid-record technology.

At the second phase, TCGA performed whole exon and whole transcriptomic sequence in 100% of cases, and used sequence of whole genome in 10% of cases in the project [2].

2. Related Works

2.1 Cancer genomics

Whole DNA existed in your cells forms your genome. In most cells, genome was packaged into two groups of chromosomes: one sett you're your mother and one set from your father. These chromosomes consist of six billions of unique DNA letters. There are 26 letters in English alphabet: A to Z. in alphabet of genes, we have four letters of A, C, G and T. Exactly similar to letters of one book, it writes words for the story, therefore, we write the letters in our genomes[4].

In cancerous cells, small changes in genetic letters can change the meaning of genetic words or sentence. Cancer starts in our cells. Cells are tiny building blocks that make up the organs and tissues of our body. We have about 10 trillion cells in our bodies.

Usually, our cells divide to make new cells in a controlled way. This is how our bodies grow and repair. Inside almost every cell of your body is a copy of your genome, made of DNA. The genome can be thought of as the instructions for running a cell. It tells the cell what kind of cell to be – is it a skin cell or a liver cell? It also has the instructions that tell the cell when to grow and divide, and when to die. When a cell divides to become two cells, your genome is copied. Sometimes when our cells divide, mistakes happen when copying the genome. These are called mutations. They are caused by natural processes in our cells, or just by chance. They can be caused by external factors in our environment too – like radiation from sunlight.

Usually, cells can repair mutations in their genome. In fact most DNA damage is repaired immediately, with no ill effects. If the damage is very bad, cells may self destruct instead. Or the immune system may recognise them as abnormal and kill them. This helps to protect us from cancer.

But sometimes mutations in critical genes mean that a cell no longer understands its instructions, and starts to multiply out of control. It doesn't repair itself properly, and it doesn't die when it should. The abnormal cell keeps dividing and making more and more abnormal cells. These cells form a lump, which is called a tumour. In the 100,000 Genomes Project, we sequence the DNA from both the tumour and healthy cells. This means we can compare the two. Cancer whole genome sequencing allows us to detect two types of changes, germline mutations and somatic mutations.

A changed letter can produce protein cell which does not let the cell to work. These proteins can lead to rapid growth of cells and cause damage to neighboring cells. By cancer genome study, scientists can discover that changes in letter can transform a cell into cancer. In some cases, genome study in one cancer can help to recognize sub-type of cancer in that type such as breast cancer HER2+. Understanding cancer genome might also help physician to select best treatment for each patient.

2.2 Importance of histological samples

Biospecimens are histological and body liquid specimens which can be used to diagnose and analysis of cancer. Biospecimens are vital for cancer research, since they consist of considerable amount of biological information, which is written in language of cells, genes and proteins, and can recognize biological characteristic of cancerous cells. TCGA strategy provides the strongest dataset to gather quantity tissue along with quality:

1. TCGA assesses high number of samples up to 500 specimen for each type of tumour this provides statistical power required to produce comprehensive genomic profile for each cancer- information which is necessary to better recognize of objectives to develop medication.
2. All the research teams of TCGA read similar specimen. These show precise, complete and reliable results of cancer genome, since each specimen is analyzed for each platform.

For all cancerous read samples of TCGA, both specimen of cancerous and normal tissue were gathered.

This lets researchers to recognize genomic changes which might play role in progress of cancer study [5].

TCGA found large steps for assurance on that the study tissues have highest quality. However, for specific cancer, information gathering from patents is difficult and makes challenges for study using various analysis technologies of genome. Access to quality and quantity of adapted tumour and normal tissue is one of large factors in selection of study in TCGA.

There are at least 200 types of cancer and several other subtypes. Each of them is due to mistakes in DNA which causes uncontrolled growth of cells. TCGA makes a tube line of analysis of genomic information which can do gathering, selection, and analysis of human tissues for genetic changes in large scale effectively. Success of this national network of research and technology teams acts as one model for further projects and is a sample of huge power of team work in sciences.

3. GDC resources

In order to achieve a resource of information based on integrated standards, GDC provides society with several resources to retrieve and download of data from GDC, sends data to GDC, and processes data from GDC's bioinformatics tube lines. The resources are preserved in a safe data center which provides support and documentation f the user, figure (1).

Figure 1: GDC resources [6].

Types of data and Format of file

Access to sent data from new programs, provides data produced by GDC through GDC alignment and high level tube line of producing data and data entered from the present programs.

- **Submitted data:**

GDC now accepts data of DNA and RNA sequence in both formats of FASTQ (external link) and BAM (external link). Sequence data is sent by metadata sign in both formats of simple TSV or JSON (external link), or last version (1.5 now) of SRAXML format. Clinical data and biospecimen can be sent in format of TSV or JSON (external link) and/or as XML which is valid due to last version of documents of NCI Biospecimen Core Source XML Schema (External link)(Table 1) [7].

Table 1: Types of submitted data.

Entity Category	Entity Name	File Format	File Metadata Template
Administrative	Case	--	TSV, JSON
Biospecimen	Sample	--	TSV, JSON
	Portion	--	TSV, JSON
	Analyte	--	TSV, JSON
	Aliquot	--	TSV, JSON
	Read Group	--	TSV, JSON
	Slide	--	TSV, JSON
Clinical	Demographic	--	TSV, JSON
	Diagnosis	--	TSV, JSON
	Exposure	--	TSV, JSON
	Family History	--	TSV, JSON
	Follow Up	--	TSV, JSON
	Molecular Test	--	TSV, JSON
	Treatment	--	TSV, JSON
Data File	Analysis Metadata	SRA XML, MAGE-TAB (SDRF, IDF)	TSV, JSON

	Biospecimen Supplement	BCR XML, GDC-approved spreadsheet	TSV, JSON
	Clinical Supplement	BCR XML, GDC-approved spreadsheet	TSV, JSON
	Experiment Metadata	SRA XML	TSV, JSON
	Pathology Report	PDF	TSV, JSON
	Run Metadata	SRA XML	TSV, JSON
	Slide Image	JPEG, SVS, TIFF	TSV, JSON
	Submitted Unaligned Reads (Illumina Platform)	FASTQ, BAM(link is external)	TSV, JSON
	Submitted Aligned Reads (Illumina Platform)	BAM(link is external)	TSV, JSON
	Submitted Genomic Profile	MAF, TSV, VCF, XML	TSV, JSON
	Raw Methylation Array	IDAT	TSV, JSON

Generated data:

For all the sent sequence data, including alignment files, BAM sent new produced alignments of GDC format of BAM using last version of human reference of GRCH38 with standard pipeline line of classification. Using these standard alignments, GDC produces derived data at high level, including various and normal tumors and mutation recalls in formats of VCF and MAF, and gene expression and mi RNA and quantifying of connection of data crosslink in formats of TSV (Table 2) [8].

Table 2: Types of generated data.

Entity Category	Entity Name	Access (Open, Controlled)	File Format	File Metadata Template
Analysis	Read Group QC	--	--	TSV, JSON
	Alignment + Co-cleaning	--	--	TSV, JSON
	Alignment	--	--	TSV, JSON
	Genomic Profile Harmonization	--	--	TSV, JSON
	RNA Expression	--	--	TSV, JSON
	miRNA Expression	--	--	TSV, JSON
	Germline Mutation Calling	--	--	TSV, JSON
	Somatic Mutation Calling	--	--	TSV, JSON
	Structural Variation Calling	--	--	TSV, JSON
Data File	Aggregated Somatic Mutation	Controlled	MAF	TSV, JSON
	Aligned Reads	Controlled	BAM	TSV, JSON
	Gene Expression	Open	TSV	TSV, JSON
	Masked Somatic Mutation	Open	MAF	TSV, JSON
	miRNA Expression	Open	TSV	TSV, JSON
	Structural Variation	Controlled	TSV	TSV, JSON

Imported Data:

GDC is host and distributor of data pre-prepared from TARGET, TCGA, and other programs.

Alignments of the main sequence are saved in BAM format, and file of data derived in main formats are saved and presented (Table 3) [9].

Table 3: Types of imported data.

Data Type	Data Subtype	Format
Raw Sequencing data	Aligned Reads	BAM(link is external)
	Unaligned Reads	FASTQ(link is external)
	Coverage WIG	WIGGLE(link is external)
Simple Nucleotide Variation	Genotypes	TSV
	Simple Germline Variation	MAF, VCF
	Simple Somatic Mutation	
	Simple Nucleotide Variation	
Raw Microarray Data	Raw Intensities	TSV
	CGH Array QC	
	Intensities Log2Ratio	
	Expression Control	
	Intensities	
	Normalized Intensities	
	Probeset Summary	
	Methylation Array QC Metrics	
Gene Expression	Gene Expression Quantification	TSV
	miRNA Quantification	
	Isoform Expression Quantification	
	Exon Junction Quantification	
	Exon Quantification	
	Gene Expression Summary	
Structural Rearrangement	Structural Germline Variation	VCF, FASTA
	Structural Variation	VCF, FASTA
DNA Methylation	Bisulfite Sequence Alignment	BAM(link is external)
	Methylation Beta Value	TSV
	Methylation Percentage	
Clinical	Clinical Data	XML
	Biospecimen Data	
	Tissue Slide Image	SVS
	Diagnostic Image	
	Pathology Report	PDF
Copy Number Variation	Copy Number Segmentation	TSV
	Copy Number Estimate	
	Copy Number Germline Variation<	
	LOH	
	Copy Number QC Metrics	
	Copy Number Variation	
	Normalized Copy Numbers	
	Copy Number Summary	
	Probeset Call	
Protein Expression	Protein Expression Quantification	TSV
	Protein Expression Control	
Other	Microsatellite Instability	FSA
	ABI Sequence Trace	TR
	Auxiliary Test	

GDC produces high level data with last reference of human genome of GRCh38. This includes types of DNA genome derived from other Germline and somatic mutations, genes extracted from RNA-Seq and miRNA-Seq and measurement of miRNA and SNP Array based on Copy Number Segmentation.

GDC produces recalling of somatic mutations using DNA-Seq data from tumor tissues. As diagnosis, combinatory type of tumor tissue is a complicated process; there is no consensus on the nest scientific society in best diverse recalling algorithm. So that, GDC implements several recipient contact which implements more than one set of outputs for users. In the first stage, GDC focuses on alone nucleotide words of SNV and INDEL. GDC

expands attempts of diagnosis of social type to SV and CNV. Now, three-line tubelines which are executed by GDC (Figures 2 and 3).

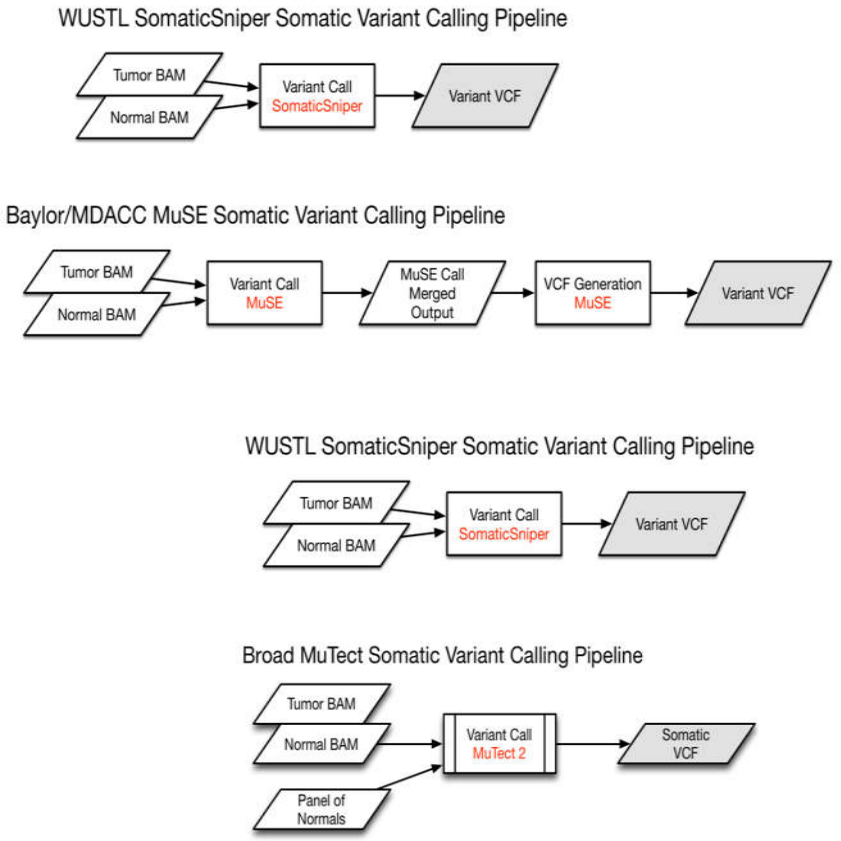

Figure 2: DNA-Seq Somatic Variation.

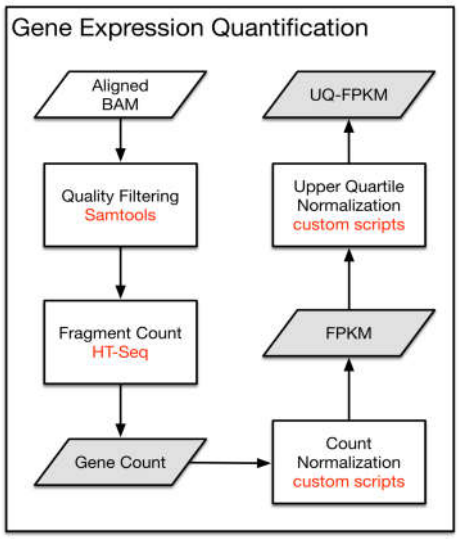

Figure 3: RNA-Seq Quantification.

4. Results

According to the information present in [6] all existences and relations of database of TCA with adjectives of their properties, relational model can be drawn which the information is presented in tables 4 and 5.

Relations of sent data include 25 types in table (4).

Table 4: relations of sent data.

Relational Name	
Case	Treatment
Sample	Analysis Metadata
Portion	Biospecimen Supplement
Analyte	Clinical Supplement
Aliquot	Experiment Metadata
Read Group	Pathology Report
Slide	Run Metadata
Demographic	Slide Image
Diagnosis	Submitted Unaligned Reads (Illumina Platform)
Exposure	Submitted Aligned Reads (Illumina Platform)
Family History	Submitted Genomic Profile
Follow Up	Raw Methylation Array
Molecular Test	Treatment

Relations of produced data includes 15 types presented in table 5.

Table 5: relations of produced data.

Relational Name
Read Group QC
Alignment + Co – cleaning
Alignment
Genomic Profile Harmonization
RNA Expression
miRNA Expression
Germline Mutation Calling
Somatic Mutation Calling
Structural Variation Calling
Aggregated Somatic Mutation
Aligned Reads
Gene Expression
Masked Somatic Mutation
miRNA Expression
Structural Variation

Figure 4 shows relational model obtained based on extracted information.

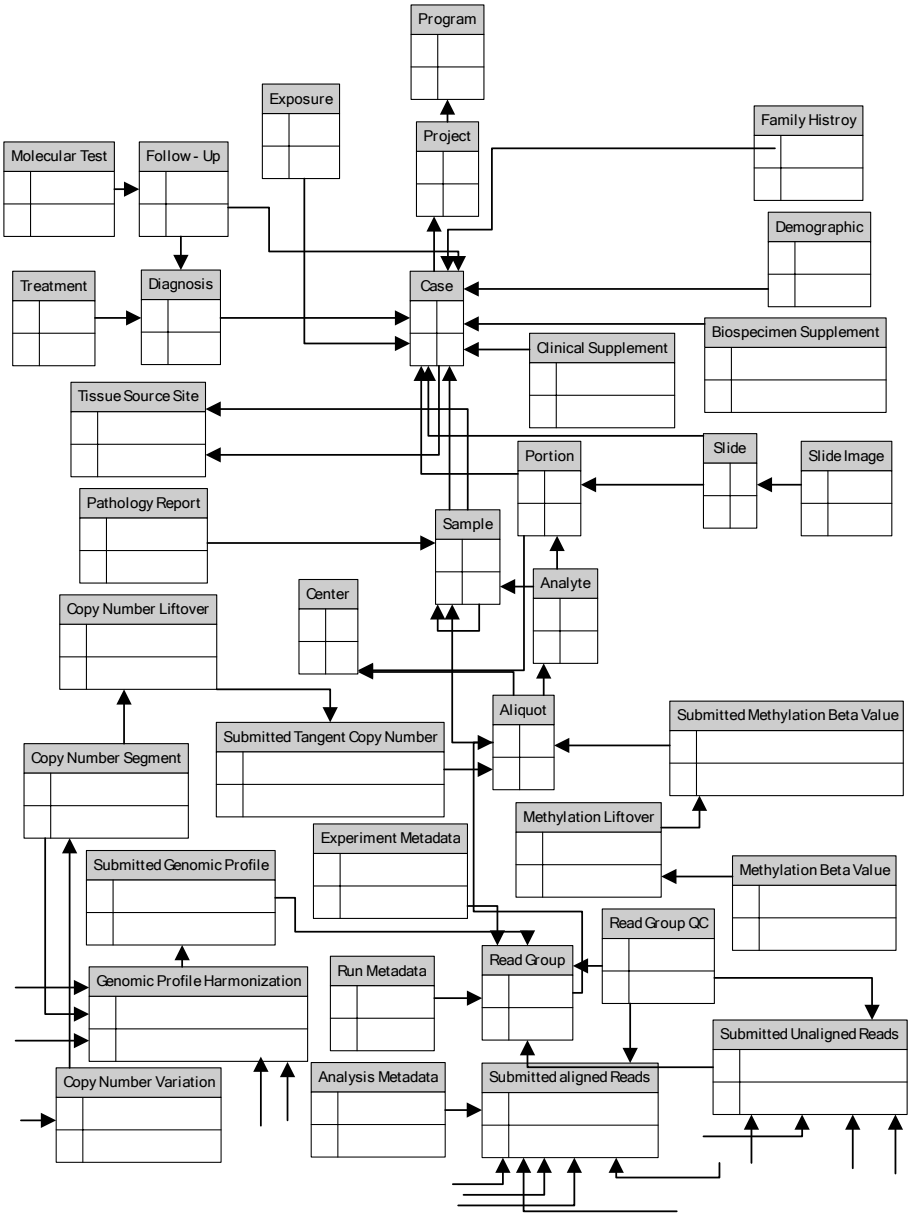

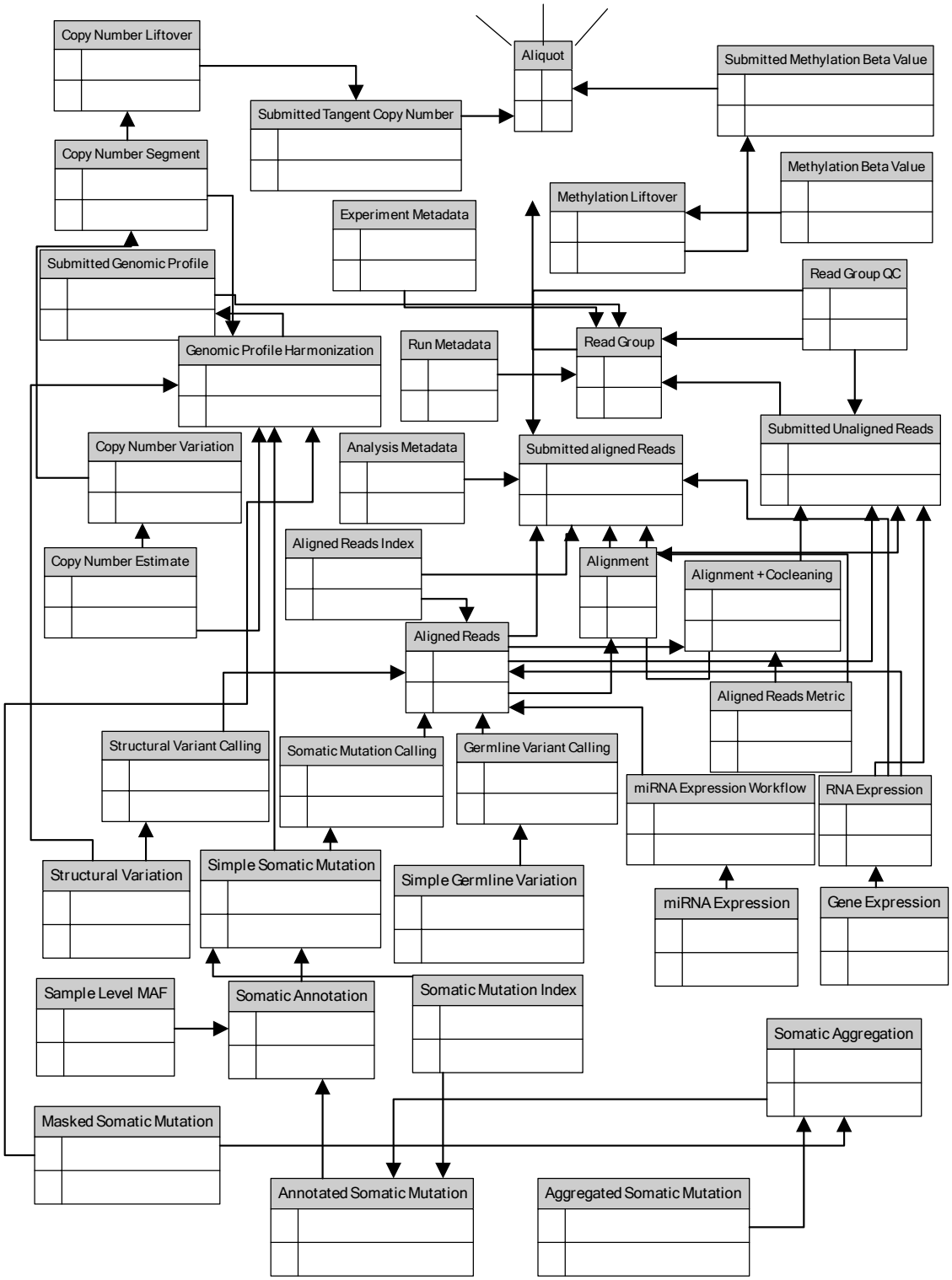

Figure 4: Extracted relational model.

Conclusion

In this article, various parts of biological database of TCGA are analyzed. The entities and relations present in input, sent and produced data are obtained and relation among them is identified. The extracted relational model indicates capabilities and relations present in database.

References

[1] "The Cancer Genome Atlas homepage", *(2009),* NCI *and the* NHGRI.

[2] NIH Launches Cancer Genome Project Washington Post December, 14 (2005).

[3] Daniela S. Gerhard, "TCGA Moving Molecular Oncology Forward", NCI cancer Bulletin, Director's Update. National Cancer Institute 5, 8(2009).

[4] "Cancers Selected for Study", The Cancer Genome Atlas – National Cancer Institute, 11(2015).

[5] Chu A, Robertson G, Brooks D, Mungall AJ, Birol I, Coope R, Ma Y, Jones S, Marra MA, Nucleic Acids Res. Large-scale profiling of microRNAs for The Cancer Genome Atlas 13(2015).

[6] "The Cancer Genome Atlas homepage".NCI *and the* NHGRI 4(2009), https://gdc.cancer.gov/about-data/data-types-and-file-formats .

[7] "The Cancer Genome Atlas homepage".NCI *and the* NHGRI 4(2009), https://gdc.cancer.gov/about-data/data-types-and-file-formats/submitted-data-types-and-file-formats.

[8] "The Cancer Genome Atlas homepage".NCI *and the* NHGRI 4(2009), https://gdc.cancer.gov/about-data/data-types-and-file-formats/generated-data-types-and-file-formats.

[9] "The Cancer Genome Atlas homepage".NCI *and the* NHGRI 4(2009), https://gdc.cancer.gov/about-data/data-types-and-file-formats/imported-data-types-and-file-formats.

Removal of lead as a toxic heavy metal from aqueous solutions by a novel biosorbent

Mahboube Shirani*

*Department of Chemistry, Faculty of Science, University of Jiroft, Jiroft, P. O. Box 7867161167, Iran

* E-mail: shirani.mahboubeh@gmail.com

Abstract

In this study, the dried quince stem as a novel biosorbent was applied for simultaneous adsorption of lead from aqueous solutions. The amount of biosorbent, pH, time, and temperature were studied. At optimum conditions of pH of 6.5, temperature of 25 □C, time of 8 min, amount of biosorbent of 10 mg, and the initial lead ion concentration of mg L^{-1}, the maximum removal (%) of 98.1 ± 0.5 was obtained. The potential of the method was considered in water samples including river water and tap water and the recoveries > 96 % indicate high capability of the method. The experimental data were adequately fitted into Fredluich model which proves that the adsorption occurs on a heterogeneous material. The maximum sorption capacity of mg g^{-1} was achieved for removal of lead ions by dried quince stem.

Keywords: Removal, Biosorbent, Lead

1. Introduction

Generally, water pollution is a principal cause of health disorders in the world. Increasing industrial activity, especially in developing countries, causes contamination of water with soluble toxic metal-ion pollutants that readily accumulate in body [1]. Lead and cadmium are widely applied in metallurgy, tannery, mining, electroplating, chemical manufacturing industries and thus inevitably released into the environment [3]. The main technologies for removal of heavy metals from wastewater include adsorption, ion-exchange, solvent extraction, membrane technology, electrostatic interaction, and chemical precipitation [3]. Adsorption is one of the simplest ones. Various sorbents including commercial sorbents, synthesis sorbents, and biosorbents are commonly used. biosorbents are environmentally friendly and in regards with green chemistry aspect. In recent years, considering the development of green, safe and economical processes, many biosorbents have been widely applied. Different biosorbents such as corn cob, eggshell [1], cellulose-metallothionein [2], luffa sponge [3], tomato waste [4], Tamarindus indica [5], Indian curry leaf [6], and lemon and bee shell [7] have been reported for adsorption of lead. In this study the dried quince stem as a novel biosorbent was applied for removal of lead from aqueous solutions. The amount of biosorbent, pH, time, and temperature were studied. At optimum conditions the thermodynamic and kinetic of the process was considered. The positive ΔH° and ΔS° values described endothermic nature of adsorption. The adsorption of lead followed the pseudo-second order kinetic model.

2. Material and Methods

2.1 Materials and instrumentation

The stock solution of lead nitrate (500 mg L^{-1}) was prepared by dissolving proper amount of lead nitrate (Sigma Aldrich, ≥99.0 %) in deionized water. standard solutions of lead were prepared daily by diluting of the stock solution. Hydrochloric acid (Merck, 37%) and nitric acid (Merck, 63%) were used for setting pH. The target metal analysis was carried out by Philps Atomic absorption spectrometer PU9100X (Netherlands).

2.2 Sample preparation

Water samples were filtered to remove any suspended contamination and were then used for analysis

2.3 Adsorption process

The pH of a 10 mL sample solution containing 10 mg L^{-1} of Pb^{2+} was adjusted to 6.5 by adding 0.1 mol L^{-1} nitric acid or sodium hydroxide. 10 mg of the biosorbent was added to the solution. The mixture was ultrasonicated for 8 min and then centrifuged for 3 min at 4000 rpm. The upper aqueous phase containing the residual cadmium in the solution was used for determination of Pb^{2+} by flame atomic adsorption spectrometry. The uptake of the adsorbate mathematically can be obtained as follows:

Removal (%) = $((C_0 - C_e)/C_0) \times 100$

In which C_0 and C_e are initial concentration and the equilibrium concentration of Pb^{2+} in the solution.

3. Results and Discussions

3.1 Optimization of the process

The effect of important parameters including pH, time, temperature, Pb^{2+} concentration, and amount of biosorbent were studied and optimized to obtain the maximum removal (%).

pH represents the acidity and basicity of the solution which can control the adsorption of lead on the surface of the biosorbent. Therefore, the pH of the solution in the range of 4.5-8.5 was studied and according to the obtained results the removal (%) increased from 4.5 to and it was maximum at 6.5 and the decreased.

The adsorption process can be endothermic or exothermic depending on the temperature of the solution. hence, the removal of lead was investigated in the range of 25-45 □C and according to the obtaining results by increasing the temperature a decreasing trend was observed. Therefore, the process was carried out at room temperature.

Appropriate contact time provides the equilibrium for the adsorption of lead on to the biosorbent. The sonication time in the range of 4-12 min was considered and as the results show the removal (%) increased from 4 to 8 min and then became constant.

The amount of biosorbent represents the active sites which have the opportunity to be occupied by the analyte molecules. The more the amount of biosorbent is the more the active sites are. The amount of biosorbent in the range of 5-15 mg was considered. And as the results show the removal (%) increased from 5 to 10 mg and then became constant. The amount of 10 mg was selected as optimum amount of biosorbent.

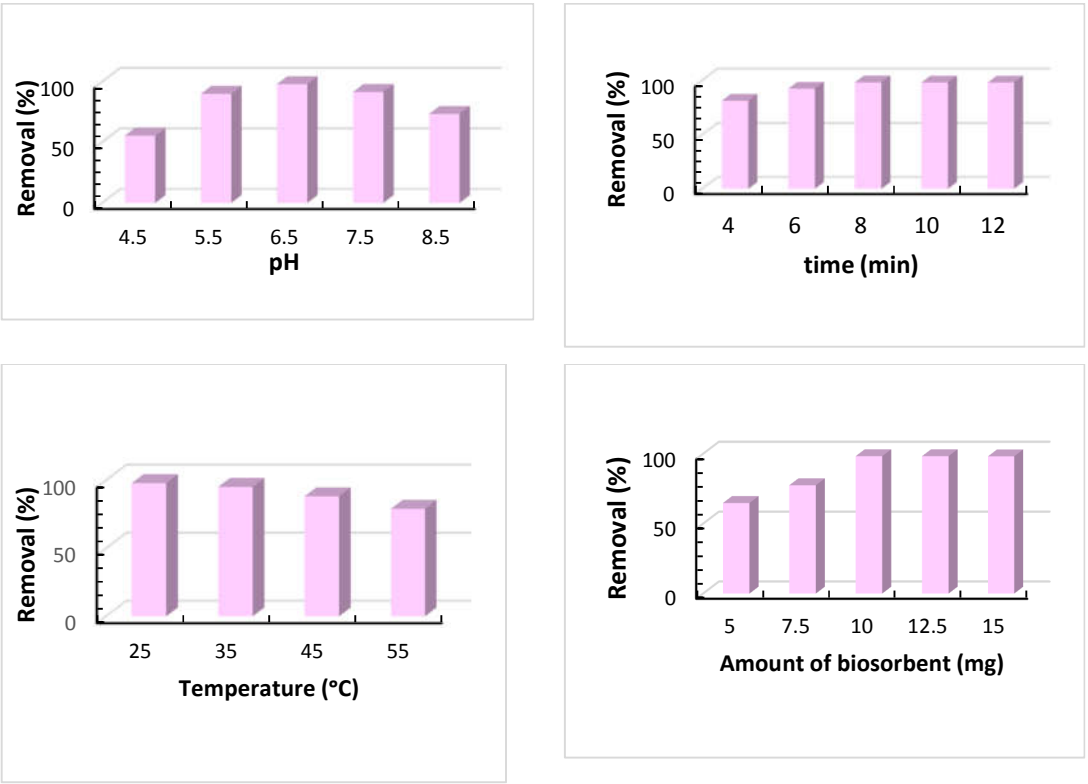

Fig. 1 The effect of influential parameters of pH, time, temperature, amount of biosorbent on the removal (%) of lead ions

3.2 Isotherm studies

The adsorption isotherms reveal the partition of the adsorbate molecules between the liquid sample solution and the solid sorbent in the adsorption process. the adsorption isotherms show the relationship between the adsorbent and the adsorbate at a special temperature. In order to evaluate the adsorption isotherm of the proposed method, two common isotherms of Langmuir and Fredluich models were studied at optimum conditions and at the concentration range of 10-300 mg g^{-1}. The Langmuir equation (1) and Fredluich equation (2) are as follow:

$$\frac{C_e}{q_e} = \frac{1}{q_m K_L} + \frac{C_e}{q_m} \qquad (1)$$

$$\log q_e = \log K_f + \frac{1}{n} logC_e \quad (2)$$

The linear regression analysis of C_e/q_e versus C_e for Langmuir model and log q_e versus logC_e for Freundlich model (Fig. 1). The n value n>1 shows the favorability of the adsorption process occurrence via physical forces. R_L is another factor to indicate the favorability of the adsorption of lead ions on to dried quince stem. The value of R_L implies the unfavorable ($R_L > 1$), linear ($R_L = 1$), favorable ($0 < R_L < 1$), and irreversible ($R_L = 0$) type of the adsorption isotherm. As the results show in Table 1, the value of R_L for lead ions is $0<R_L<1$ which are favorable for adsorption.

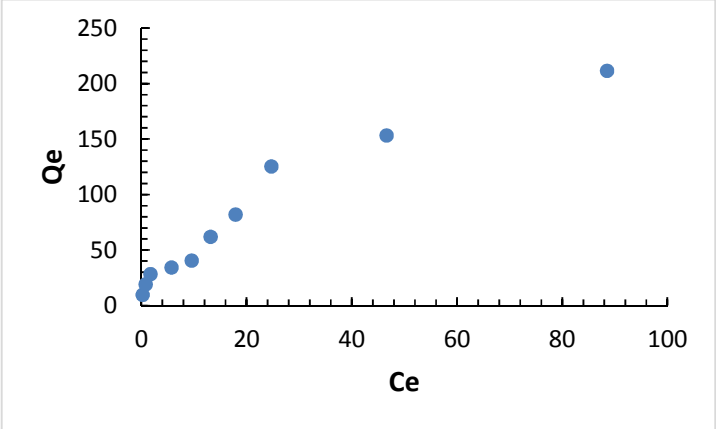

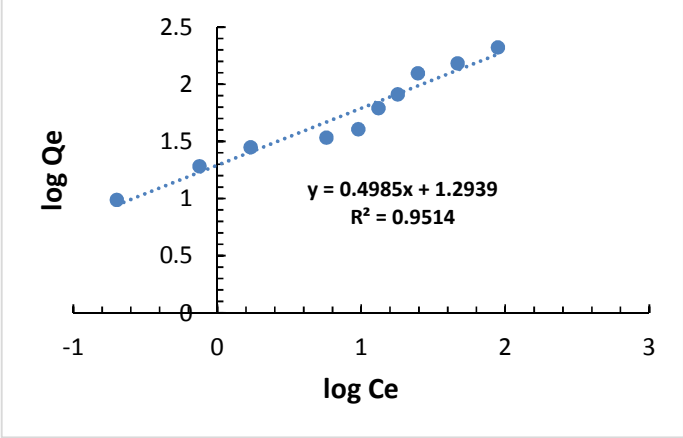

Langmuir isotherm

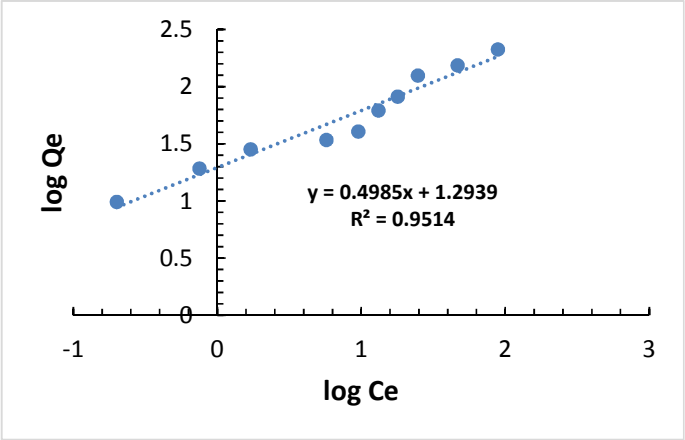

Fredluich isotherm

Fig. 2 The adsorption isotherms

Table 1

Isotherm parameters for adsorption of Pb^{2+} onto the quince stem at the optimum conditions

Analyte	Langmuir isotherm				Freundlich isotherm			
	Q_{max} (mg/g)	b (L/mg)	R^2	R_L	K_f	1/n	N	R^2
Pb^{2+}	256.41	0.037	0.774	0.082	19.67	0.4985	2.00	0.9514

3.3 Analysis of real sample

The proposed method was applied on the water samples. As the results show the present method was successfully applied to adsorb cadmium from water samples with perfect accuracy and precision. The results are shown in Table 2.

Table 2. Removal of lead ions from water samples with novel biosorbent at optimum conditions

Sample	Pb^{2+} concentration (mg L^{-1})	Added Pb^{2+} (mg L^{-1})	Founded Pb^{2+} (mg L^{-1})	Relative recovery (%)
Tap water [a]	N.D.[b]	20.0	19.3 ± 0.6	96.5
River water [c]	N.D.	20.0	19.5 ± 0.3	97.5

[*] For three replicates (n=3)

[a] Tap water from chemistry lab in university of Jiroft.

[b] Not detected

[c] River water from Halil Roud river in Jiroft.

4. Conclusion

In this research study, dried quince stem as a novel biosorbent was introduced for removal of lead ions from aqueous solution. the maximum removal (%) of 98.3 was obtained. The potential of the method was considered in water samples including river water, tap water, and sea water and the recoveries > 96 % indicate high capability of the method. Easy and facile operation, short extraction time, green and biodegradable sorbent, low consumption of biosorbent are the dominant features of the proposed method.

Acknowledgements

The authors gratefully appreciate the Research Council of University of Jiroft.

References

[1] M.A.R. Soares, S. Marto, M.J. Quina, L. Gando-Ferreira, R. Quinta-Ferreira, (2016) "Evaluation of Eggshell-Rich Compost as Biosorbent for Removal of Pb(II) from Aqueous Solutions", Water, Air, & Soil Pollution, 227, 150.

[2] W. Mwandira, K. Nakashima, Y. Togo, T. Sato, S. Kawasaki, (2020) "Cellulose-metallothionein biosorbent for removal of Pb(II) and Zn(II) from polluted water", Chemosphere, 246, 125733.

[3] S. D.V, L. Kumar R, S. J, (2017) "Immobilized fungi on Luffa cylindrica: An effective biosorbent for the removal of lead", Journal of the Taiwan Institute of Chemical Engineers, 80, 589-595.

[4] E. Heraldy, W.W. Lestari, D. Permatasari, D.D. Arimurti, (2018) "Biosorbent from tomato waste and apple juice residue for lead removal", Journal of Environmental Chemical Engineering, 6, 1201-1208.

[5] P. Bangaraiah, B. Sarath Babu, K. Abraham Peele, E. Rajeswara Reddy, T.C. Venkateswarulu, (2020) "Removal of multiple metals using Tamarindus indica as biosorbent through optimization of process variables: a statistical approach", International Journal of Environmental Science and Technology, 17, 1835-1846.

[6] S. Mukherjee, D. Kumari, M. Joshi, A.K. An, M. Kumar, (2020) "Low-cost bio-based sustainable removal of lead and cadmium using a polyphenolic bioactive Indian curry leaf (Murraya koengii) powder", International Journal of Hygiene and Environmental Health, 226, 113471.

[7] F. Ergüvenerler, Ş. Targan, V.N. Tirtom, (2020) "Removal of lead from aqueous solutions by low cost and waste biosorbents (lemon, bean and artichoke shells)", Water Science and Technology, 81, 159-169.

Effect of quadripartite Feedstock Chemical composition for Metal Injection Molding of Dental Implant System

M.Moradjoy [1], H.Khorsand [2*]

[1] PhD Candidate, Faculty of Material Science and Engineering, K. N. Toosi University of Technology,Tehran,Iran..

[2] Assistant Professor, Faculty of Material Science and Engineering, K. N. Toosi University of Technology,Tehran,Iran.

*Email: hkhorsand@kntu.ac.ir

Abstract

Biocompatible metals have been developing the biomedical and biological field, predominantly in human implant applications, where these metals widely used as a substitute to or as function restoration of degenerated tissues or organs. Powder metallurgy techniques, in specific the metal injection moulding (MIM) process, have been employed for the fabrication of controlled porous structures used for dental and orthopedic surgical implants. Binders play a very crucial role in processing of components by the metal injection molding (MIM) process. The porous metal implant allows bony tissue ingrowth on the implant surface, thereby enhancing fixation and recovery. The present study discusses critical aspects regarding the binders used in the MIM process. This study focus on the function and importance of binders in the MIM process and binder chemistries and constituents are discussed.

Keywords: Biomedical, Metal Injection Moulding; Biocompatible Metals; Sintering; Powder Metallurgy.

1. Introduction

The use of biomaterial can be dated from thousands of years ago. Archaeologists have discovered and evidenced the use of biomaterial as dental implants from as early as 200 A.D. However, the use of this implants came to glory after World War II [1]. Biomaterials were initially known as nonviable materials that widely used in biomedical applications. Predominantly in medical devices which aimed to interact with biological systems [2]. Biomaterials in the form of implants classically employed to ligaments, vascular grafts, intraocular lenses, heart valves, dental implants, and in medical devices like pacemakers, artificial hearts, and biosensors, which are widely used to replace and restore the function of traumatized or degenerated tissues and organs in the human body. The primary aim of these implants is to contribute to a better quality of life for the patients [3, 4]. The medical community started to accept metals as implant materials upon Lane's success of using metal plate for bone fracture fixation in 1895 (Lane, 1895) and later came to be known as biocompatible metal [5]. To date, biocompatible metals had become the most favoured materials for the commercial production of medical implants due to their outstanding mechanical, physical and chemical properties [6-11]. From the vast choice of metals and alloys available in the industry, only a handful are biologically compatible and have the aptitude to become long-term

implant materials [12]. These metals are principally used to replace and support parts of the damaged bones. Routinely also used as artificial joints, plates, screws, intramedullary nails, spinal and spacer fixations, external fixators, pacemaker casings, artificial heart valves, stents, and as dental implants. In comparison to ceramic and polymeric materials, biocompatible metals are ideal as implant since they exhibit greater fracture toughness, tensile strength, and fatigue strength [13-19]. Implants developed from stainless steel, titanium and its alloys, and cobalt based alloys are the most extensively used in the present-day biomedical applications [20-27]. They fit biomaterial prospects due to their outstanding mechanical, chemical properties and corrosion resistance. During the initial period of medical implant evolution, the key consideration criteria for implant material selection was the satisfactory physical properties and their non-toxicity nature [4]. At present date, the criteria have been broadened even to include the ability of the implant material to assist in the growth of human body tissues and its physical properties [28-33].

Powder metallurgy (PM) technology, in specific the MIM technique, has been recognized as one of the prominent methods to produce exceptional components or parts for numerous fields and industries in the past several years. Additionally, this technique had also been exploited in medicine field as an optional method for fabricating implants used in surgery and dentistry [12, 34-39] befitting for economical mass production. Also, MIM are known for its near net shaping technique that is particularly advantageous for the development of complex shapes of high density, and with excellent dimensional accuracy [40-48]. The MIM technique invented from the idea of plastic injection moulding, of which metal powder particles mixed with a binder and the mixture (usually in slurry form) injected into the cavity of the mold of desired shape [49-51]. The four major stages in MIM technique to produce a part are; (1) Mixing of powder and binders to produce feedstock; (2) Injection moulding process to get a green compact; (3) A de-binding process to extract away the binders; and (4) Produce a brown compact and sintering process to produce a sintered compact.

This paper summarizes the MIM process parameters for three groups of biocompatible metals which are stainless steel, titanium and its alloys, and cobalt based alloys, focusing primarily towards biomedical applications. This review covers pertaining research works that published between years of 2001 to 2016. Strengths and weaknesses respect to mechanical properties and corrosion resistance of these biocompatible metals systematically discussed. In MIM technique, it assumed that biocompatible metal feedstocks consist of multicomponent binders, and high powder loading will lead to successful injection process eventually deliver enhanced properties for green compacts. Where else, for the de-binding process, the binders expected to be fully removed when the de-binding temperature increased to the melting and decomposition temperatures. Finally, to attain higher relative density and full-dense compact, the brown compact is sintered at a higher temperature, close to the melting temperature of these alloys.

2. Material and Methods

2.1 feedstock preparation

In this study the metallic powder used was 316L SS, with a particle average diameter of about 20 µm, and pycnometer density of 7.93 g/cm3. All the metal particles as approximately spherical well suited for powder flow ability and dense particle packing in the injection molding stage. The selected appropriate binder system that has been reported in the literature was composed of 68% paraffin wax (PW), 15% high density polypropylene (HDPE), 15% Polypropylene (PP) and 2% stearic acid (SA) (volume fraction). PW was used as a filler to decrease the viscosity of the feedstock and increase the flow ability of this, so it contributed to the feedstock filling the die cavity [38]. The surfactant SA aims to enhance the adhesion between powder and binder, preventing the separation of them [38].

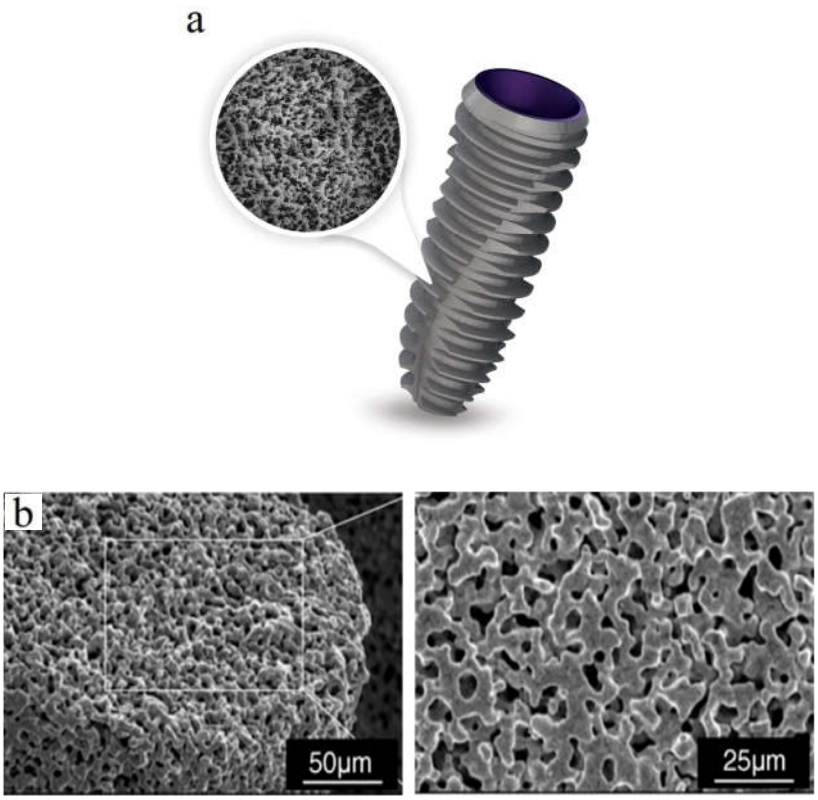

Figure 2. a) Biomedical surface of dental implant system and b) SEM image of specimen after de-binding of quadripartite binder system

HDPE and PP based backbone polymer ensure the strength of the green parts from injection molding and maintain the shape of the compacts in the de-binding stage [40].In the blending stage, to avoid PW and SA degrading, the feedstock was prepared by mixing the metal powder with HDPE and PP backbone polymers in a screw mixer at 290 °C for 60 min at 40 r/min. Then the PW and SA were added as filler and surfactant to the

mixture and blended at 210 °C for 30 min at 40 r/min. To obtain the feedstock, metal powder (70 vol. %) and binder (30 vol. %) were mixed in a screw. The turbo mixer that is used in this study is shown in Figure 2.

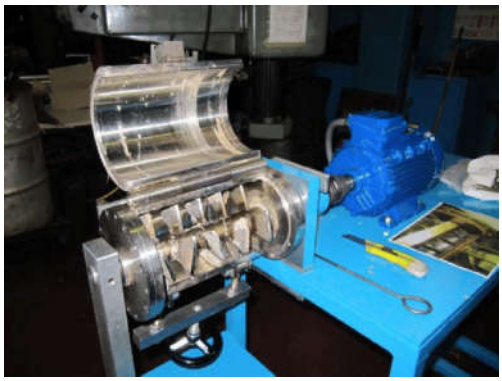

Figure 2. Scanning micrograph of initial 316L stainless steel powders.

2.2 Processing step

In the injection molding stage, prepared feedstock was injected into the standard tensile specimen mold die cavity to form the green parts. The geometric picture of the standard tensile specimen (according ASTM E8) and mold cavity are shown in Figure 3.

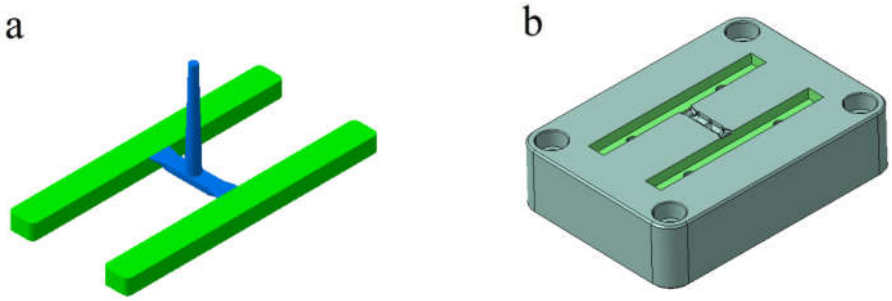

Figure 3. The schematic (a), and geometrics (mm) (b) of the standard tensile specimen.

Two stages were performed in the de-binding process: solvent and thermal de-binding to remove the binder shows the detailed experimental condition during thermal de-binding and sintering processes. Which is includes the temperature and the keeping time and the heating and cooling rates. The sintering was performed in hydrogen atmosphere at 1380°C. For debinding and sintering the parts were placed on top of a ceramic Al2O3 plate to ensure that no major diffusion occurred, which would cause the migration of the alloy elements between the sample and the supporting plate. The entire debinding and sintering processes took 36 hours to be completed.

Figure 2 schematically represents the layout for sintering process. Temperature oscillation in the chamber was 1380°C within ±3°C.

3. Results and Discussions

3.1 Biomedical Feedstock preparation

The melting and degradation temperatures of the components in the binder were measured by differential scanning calorimetry (DSC) and thermo gravimetry analysis (TGA). The temperature used for DSC ranged from 20 °C to 200 °C at 10 °C/min in a nitrogen atmosphere. And the experimental condition for TGA was the temperature heated from 20 °C to 600 °C at 10 °C/min in a nitrogen atmosphere. The melting temperature resulting from DSC is useful to set the barrel and mold temperature in the injection molding stage. Figure 4 provides the information about the DSC analyses of feedstock. It can be seen from this figure that the locations of the peaks in three feedstock are consistent, which indicates that each component in the feedstocks is stable. And the three peaks at 62, 120, 138 °C correspond to the melting temperatures of PW and SA, HDPE, PP, respectively. Accordingly, the injection molding temperature should be set above 138 °C, and the mold temperature should be set below 62 °C, which is the lowest temperature in binder from DSC results. In this investigation, the barrel temperature is set to 210 °C to improve the rheological properties of feedstock and decrease the degradation of the binder. The mold temperature is maintained 60 °C by circulating cooling water. The holding pressure is set to 1900 Bar for 7 s for proper mold filling. In addition, the melting temperatures of backbone polymers in binder from DSC results are lower than the corresponding melt temperatures of HDPE and PP (119 and 134 °C). The phenomenon of shifting of the melting temperature may be explained as follows: the mutual dissolution in the blending process restrains the crystallization of the backbone polymer, decreasing the melting temperature [19].

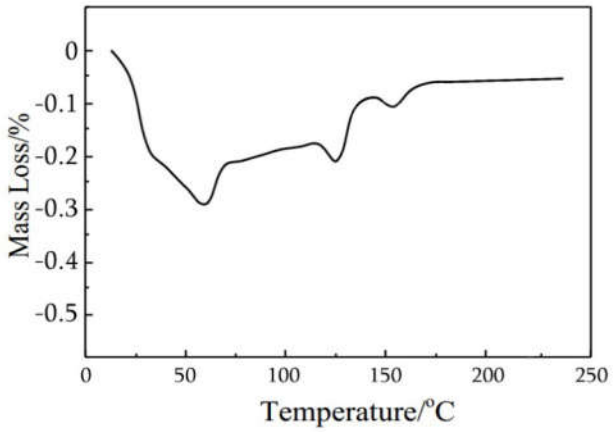

Figure 4. DSC curve analyses of feedstock.

TGA analyses of feedstock are displayed in Figure 5, which contribute to determine the blending process and the thermal debinding process. It can be seen that PW and SA in the binder start degrading at 225 °C until 360

°C, which indicates that the maximum injection molding temperature should be set below 225 °C. Then the backbone polymer starts evaporating at 360 °C until the temperature reaches 550 °C. Therefore, in the blending stage, to avoid PW and SA degrading, the feedstock was prepared by mixing the metal powder with HDPE and PP backbone polymers in a double screw mixer at 240 °C for 60 min at 40 r/min. Then the PW and SA were added as filler and surfactant to the mixture and blended at 190 °C for 30 min at 40 r/min. Meanwhile, in the thermal debinding stage, the temperature of thermal debinding should exceed 550 °C.

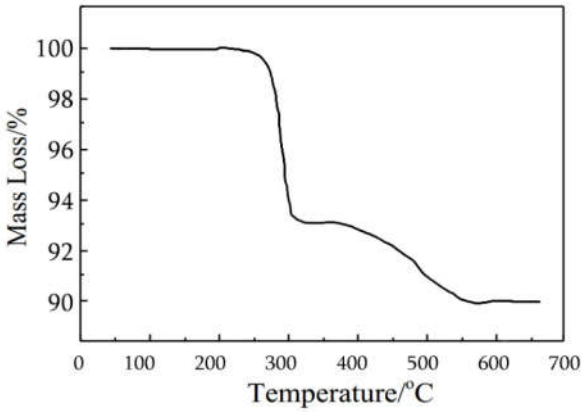

Figure 5. DSC curve analyses of feedstock.

3.2 Biomedical Feedstock removal for dental implant system

Solvent debinding is an important process that soluble part in binder is dissolved and open pore channels are formed. It can shorten heating and holding time of thermal debinding, thereby reducing the total time of debinding. Meanwhile, the defect produced by solvent debinding is less than that by thermal debinding. In this study, the removal of binders based on three backbone polymers in the solvent debinding stage was also investigated in n-heptane solvent at 60 °C. The backbone polymer has an effect on the leaching rate of PW and SA in the binder. Figure 6 displays the percentage of PW and SA removed in the binders based on three backbone polymers with the extension of time [20-25]. It can be seen that the percentage of removal of PW and SA gradually increases with the extension of time, but the rate of the removal gradually slows down and finally stabilizes [26-30]. Furthermore, PW and SA in HDPE/PP binder are easier to remove. Most of PW and SA in the binder close to 92% are removed in 70 min, which is advantageous to optimize the solvent debinding process and shorten the time of solvent debinding.

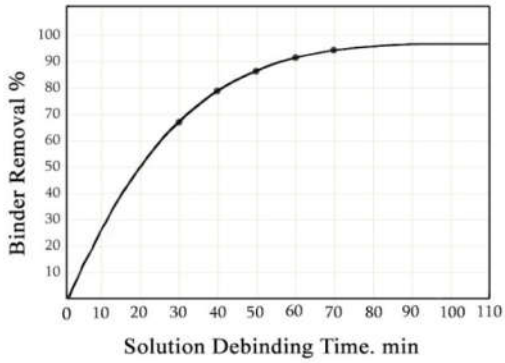

Figure 6. Solution de-binding of MIM parts in an n-heptane bath as a function of time.

Conclusions

The paper summarizes experimental and numerical results carried out on "Injection Molding Feedstock" during MIM process based on fine 316 L stainless steel powders. The findings can be summarized as follows:

- The selected binder system was composed of 68% paraffin wax (PW), 15% high density polypropylene (HDPE), 15% Polypropylene (PP) and 2% stearic acid (SA) (volume fraction).
- According to TGA & DSC result, the injection molding temperature should be set above 138 °C in order to improve the rheological properties of feedstock and decrease the degradation of the binder, and the mold temperature should be set below 62 °C.
- Backbone polymer in the binder start degrading at 360 °C until 550 °C, which indicates that in the thermal de-binding stage, the temperature should exceed 550 °C.
- The combination of temperature and pressure can serve as a promising injection condition, which leads to a relatively high sintered density.

References

[1] M. Wright, L. Hughes, and S. Gressel, Journal of materials engineering and performance, 1994, 3(2), 300-306, DOI:10.1007/BF02645856.

[2] B. Huang, S. Liang, and X. Qu, Journal of Materials Processing Technology, 2003, 137(1-3), 132-137, DOI:10.1016/S0924-0136(02)01100-7.

[3] H. Chen, X. Jing, Y. Deng, T. Wu, and S. Cao: 'Study on the Production Process of 304L Stainless Steel Injection Molding', IOP Conference Series: Materials Science and Engineering, 2018, IOP Publishing, 032022, DOI:10.1007/s00170-016-9256-2.

[4] S. Zinelis, O. Annousaki, M. Makou, and T. Eliades, The Angle Orthodontist, 2005, 75(6), 1024-1031, DOI:10.1043/0003-3219(2005)752.0. 2.

[5] B. Suharno, F. Mawardi, S. Dewantoro, B. Irawan, M. Doloksaribu, and S. Supriadi: 'Effect of powder loading on local feedstock injection behavior for fabrication process of orthodontic bracket SS 17-4 PH using metal injection molding', AIP Conference Proceedings, 2019, AIP Publishing, 020030, DOI:10426914.2018.1544709.

[6] M. Hamidi, W. Harun, M. Samykano, S. Ghani, Z. Ghazalli, F. Ahmad, and A. B. Sulong, Materials Science and Engineering: C, 2017, 78, 1263-1276, DOI:10.1016/j.msec.2017.05.016.

[7] N. Loh and R. German, Journal of materials processing technology, 1996, 59(3), 278-284, DOI:10.1016/0924-0136(95)02158-2.

[8] H. He, Y. Li, J. Lou, D. Li, and C. Liu, Powder technology, 2016, 291, 52-59, DOI:10.1016/j.powtec.2015.12.009.

[9] H. Ö. Gülsoy, Ö. Özgün, and S. Bilketay, Materials Science and Engineering: A, 2016, 651, 914-924, DOI:10.1016/j.msea.2015.11.058.

[10] A. Safarian, M. Subaşi, and Ç. Karataş, The International Journal of Advanced Manufacturing Technology, 2017, 89(5-8), 2165-2173, DOI:10.1007/s00170-016-9256-2.

[11] A. Dehghan-Manshadi, M. Bermingham, M. Dargusch, D. StJohn, and M. Qian, Powder technology, 2017, 319, 289-301, DOI:10.1016/j.powtec.2017.06.053.

[12] D. Sanétrník, B. Hausnerová, P. Filip, and E. Hnátková, Powder Technology, 2018, 325, 615-619, https://doi.org/10.1016/j.powtec.2017.11.041.

[13] J. W. Oh, W. S. Lee, and S. J. Park, Powder Technology, 2017, 311, 18-24, DOI:10.1016/j.powtec.2017.01.081.

[14] M. Seerane, P. Ndlangamandla, and R. Machaka, Journal of the Southern African Institute of Mining and Metallurgy, 2016, 116(10), 935-940, DOI:7159/2411-9717/2016/v116n10a7

[15] Y. Li, L. Li, and K. Khalil, Journal of Materials Processing Technology, 2007, 183(2-3), 432-439, DOI:.1016/j.2006.10.039.

[16] M.-W. Wu, Z.-K. Huang, C.-F. Tseng, and K.-S. Hwang, Metals and Materials International, 2015, 21(3), 531-537, DOI: 10.1007/s12540-015-4369-y.

[17] J. W. Oh, J. M. Park, D. S. Shin, J. Noh, and S. J. Park, Materials and Manufacturing Processes, 2019, 34(4), 414-421, DOI:10426914.2018.1544709.

[18] H. Abolhasani and N. Muhamad, Journal of materials processing Technology, 2010, 210(6-7), 961-968, DOI:10.1016/j.jmatprotec.2010.02.008.

[19] S. Li, B. Huang, Y. Li, X. Qu, S. Liu, and J. Fan, Journal of Materials Processing Technology, 2003, 137(1-3), 70-73, DOI:10.1016/S0924-0136(02)01069-5.

[20] Y. Zhang, E. Feng, W. Mo, Y. Lv, R. Ma, S. Ye, X. Wang, and P. Yu, Metals, 2018, 8(11), 893, DOI:10.3390/met8110893.

[21] M. Ibrahim, N. Muhamad, A. B. Sulong, S. Ahmad, and N. Nor, International Journal of Mechanical and Materials Engineering, 2010, 5(2), 282-289, DOI:10.4028264-265.135.

[22] K. Essa, P. Jamshidi, J. Zou, M. M. Attallah, and H. Hassanin, Materials & Design, 2018, 138, 21-29, DOI:10.1016/j.matdes.2017.10.025.

[23] S. Yu, P. Zhang, K. Qiu, W. Zhang, J. Li, S. Yao, D. Zhou, N. Yao, and J. Li, Ferroelectrics, 2018, 530(1), 25-31, DOI:10.1080/00150193.2018.1454071.

[24] H. Ö. Gülsoy and R. M. German, Scripta Materialia, 2008, 58(4), 295-298, DOI:10.1016/j.scriptamat.2007.10.004.

[25] R. German, Materials, 2013, 6(8), 3641-3662, DOI:10.3390/ma6083641.

[26] N. Loh, S. Tor, and K. Khor, Journal of Materials Processing Technology, 2001, 108(3), 398-407, DOI:10.1016/S0924-0136(00)00855-4.

[27] K. Tam, S. Yap, M. Foong, and N. Loh, Journal of Materials Processing Technology, 1997, 67(1-3), 120-125, DOI:10.1016/S0924-0136(96)02830-0.

[28] H. Youhua, L. Yimin, H. Hao, L. Jia, and T. Xiao, Rare Metal Materials and Engineering, 2010, 39(5), 775-780, DOI:10.1016/S1875-5372(10)60100-2.

[29] A. Abdullahi, I. Choudhury, and M. Azuddin, Materials and Manufacturing Processes, 2015, 30(11), 1377-1390, DOI:10.1080/10426914.2015.1025977.

[30] E. Sachs, E. Wylonis, S. Allen, M. Cima, and H. Guo, Polymer Engineering & Science, 2000, 40(5), 1232-1247, DOI: 10.1002/pen.11251.

Metal Injection Molding of Stainless Steel 316L for biomedical application: A Review

M.Moradjoy [1], H.Khorsand [2*]

[1] PhD Candidate, Faculty of Material Science and Engineering, K. N. Toosi University of Technology,Tehran,Iran..

[2] Assistant Professor, Faculty of Material Science and Engineering, K. N. Toosi University of Technology,Tehran,Iran.

*Email: hkhorsand@kntu.ac.ir

Abstract

The unique features of the process make it an attractive route for the fabrication of metal matrix composite materials.Metal injection molding (MIM) is a newly developed technology to form metals and alloys into desired shape. MIM is a combination of conventional plastic injection molding and powder metallurgy. The determination of optimal process parameters to produce parts by metal injection molding without defects and with required mechanical properties is discussed in the paperDetailed analysis of powders, binders, injection molding, binder removal process and parameter optimization process is discussed. Taguchi method can also be applied for optimal design configurations when significant interactions exist between and among the controlled variables. This paper provides an overview of MIM process, optimization of parameters using Taguchi method.

Keywords: Metal Injection Molding, Powder injection molding; sintering; Powder Metallurgy.

1. Introduction

Metal Injection Molding (MIM) is a newly developed technology to form metals and alloys into desired shape. MIM is a combination of convention plastic injection molding and powder metallurgy. The advantages of MIM have emerged as being able to produce cost-effective, complex shaped parts in both large and small volumes using almost all types of metals and intermetallic compound. MIM is a process that was developed from the combination of plastic injection molding and traditional powder metallurgy and is rightly regarded as a branch of both technologies. MIM is similar to plastic injection molding as the material is fed into a heated barrel, mixed and pushed into a mold cavity where it cools and then hardens to the mold cavity shape. Moreover, MIM is similar to traditional powder metallurgy in that procedure is able to compact a lubricated powder mix in a rigid die by uniaxial pressure, eject the compact from the die and sinter it. MIM is also a branch of powder injection molding (PIM), which is a subject that covers both metallic and non- metallic powder used in the manufacturing of small-to-medium-complex- shaped parts in large numbers [1-7].

The MIM process consists of four main steps which is mixing, injection molding, debinding and sintering as shown in Figure 1. During the mixing process, the metal powders is mixed with a binder at a selected volume ratio to form a homogenous feedstock. The molten feedstock is then allowed to cool down and solidify. The

attained feedstock after cool down and solidified is molded to produce a "green" compact and the binders hold particles together. The binder components are then removed to produce "brown" compact. Finally, sintering process is performed to give required mechanical properties for the sintered product also known as sintered body. Thus, the development and improvement of binders results in faster debinding procedures, cost reduction and less environmental defect. The flow diagram for the MIM process is shown in Figure 1.

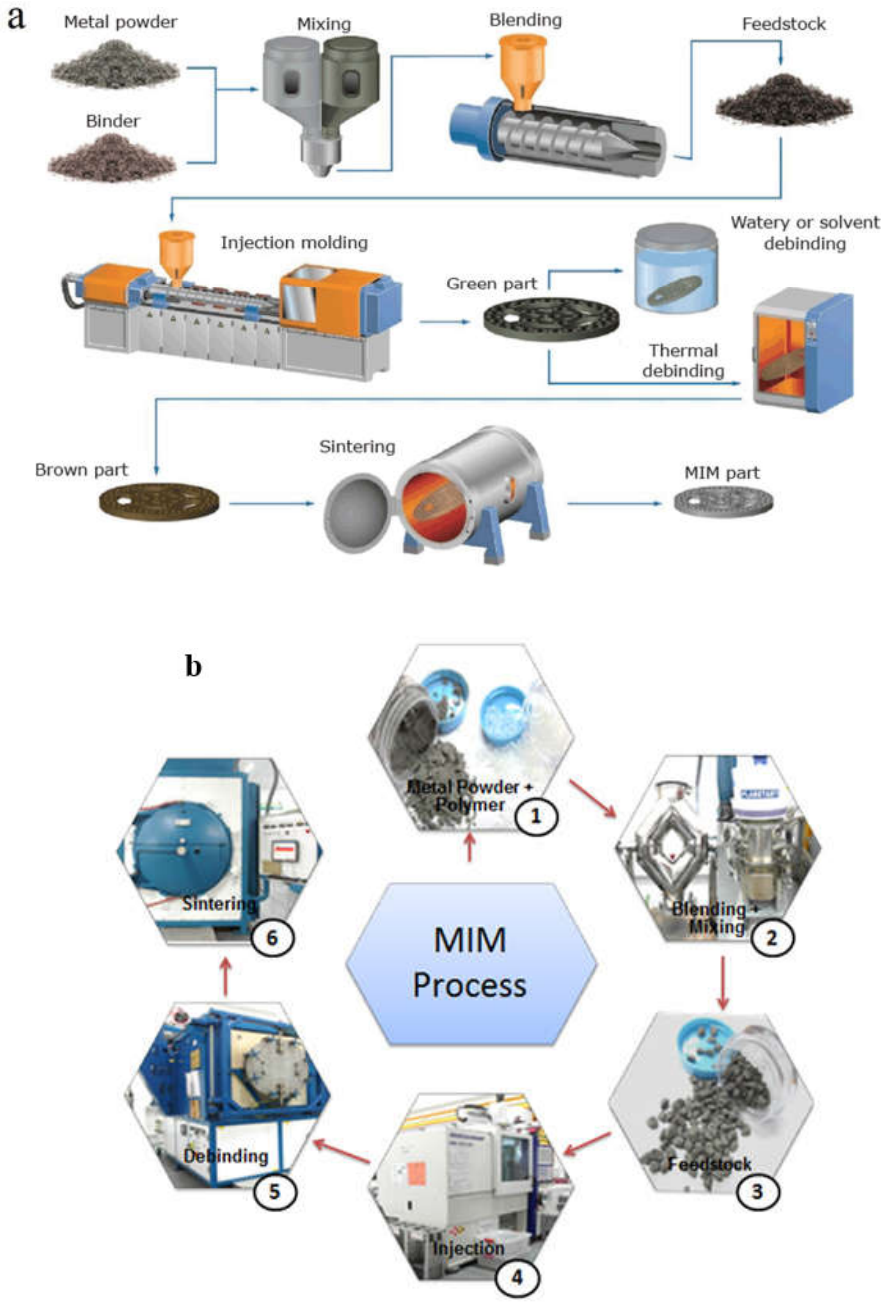

Figure 1: Flow Diagram for MIM process [4].

The rheological properties of the feedstock, which consists of the powder and binder mix, are of major importance. The requirement is that the mix flows smoothly into the die cavity without segregation at the molding temperature and therefore the viscosity should be as constant as possible over a range of temperature. The as-molded part, which is also called a green part, contains a high volume percentage of binder and the result is that during sintering a large shrinkage occurs. Therefore, a major requirement of the sintering process to ensure that this shrinkage is controlled because this affects the density as well as mechanical properties. It is in this regards that MIM has an advantage over traditional powder metallurgy because if the sintering is optimized the shrinkage should also be uniform [8-11].

1.1 Powders for Metal Injection Molding

The primary raw materials for MIM are metal powders and a thermoplastic binder. The properties of the powder determine the final properties of the MIM product and therefore the characteristics of the powder used in metal injection molding are important in the control of the process [13]. The properties that are considered in the powders used in MIM are:

- Particle shape: slightly non-spherical with an aspect ratio of 1:2 to 1:5
- Particle size: 0.1-20µm sizes are recommended
- Mean particle size: 2-8µm sizes are recommended
- Tap density: the recommended is at least 50% of the theoretical
- Dense, discrete particle free of voids
- Clean particle surface

All of these above characteristics and properties, the particle size distribution is the most important because it determines the sinter ability and surface quality of the final product. The finer powders sinter more readily than coarser powders and it is for this reason that the finer powders are preferred in MIM to coarser powders. The other powder property that is considered to be important is the particle shape of the powder because it is desirable to incorporate as high a proportion of metal as possible [14]. The choice of powder is in reality often determined by availability, but the growth in demand has encouraged powder manufacturers to produce powders that meet the requirements of MIM as desired. SEM image of the spherical iron oxide after granulation is shown in Figure 2.

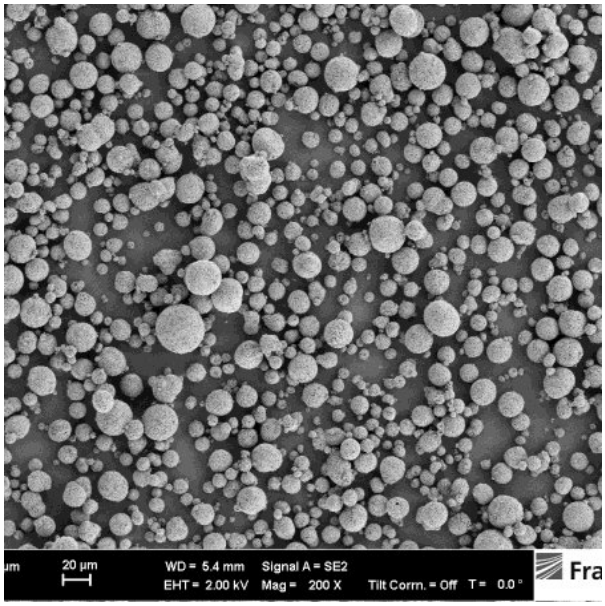

Figure 2: SEM image of the spherical iron oxide after granulation [4].

Even though almost any metal that can be produced in suitable powder form can be processed by MIM, there are some metals such as aluminium that are difficult to process via MIM. This is because they have an adherent oxide film that is always present on the surface and this inhibits sintering. For example, researchers found that mixing the aluminium with small quantities of magnesium overcomes the oxide barrier [15]. In general, the list of metals that are widely used in MIM includes many common and several less common metals and their alloys – plain and low alloy steels, high speed steels, stainless steels, super alloys, intermetallic, magnetic alloys and hard metals (cemented carbide) [14]. The more expensive materials like titanium offer better prospects for economic gain because, unlike alternative processes such as machining, there is practically no waste due to scrap which helps to offset the high cost of producing the powder in the required form.

1.2 Binders for Metal Injection Molding

The development of binder composition has been instrumental in the progress that MIM has made as a technology for manufacturing parts. The binder material is present in the green part to assist in processing by providing plasticity and it is removed from the products after injection molding in a process widely known as debinding [20,21]. SEM image of the spherical iron oxide after granulation is shown in Figure 3. One of the early challenges that presented itself during the early development of MIM was to find suitable compositions which fulfil several tasks as listed below:

- To be able to incorporate a high volume of fine metal powders, typically 60% by volume.
- To form a coherent mass that can be plastified and injection molded at elevated temperature.
- To allow removal of the main binder constituent in a reasonably short, environmentally friendly process.

- To provide enough strength after debinding by means of the 'backbone binder'.
- To be supplied in a regular granular form that can easily be fed into an injection molding machine.
- To be able to produce runners and green scrap which are easily recyclable.
- To be cost effective

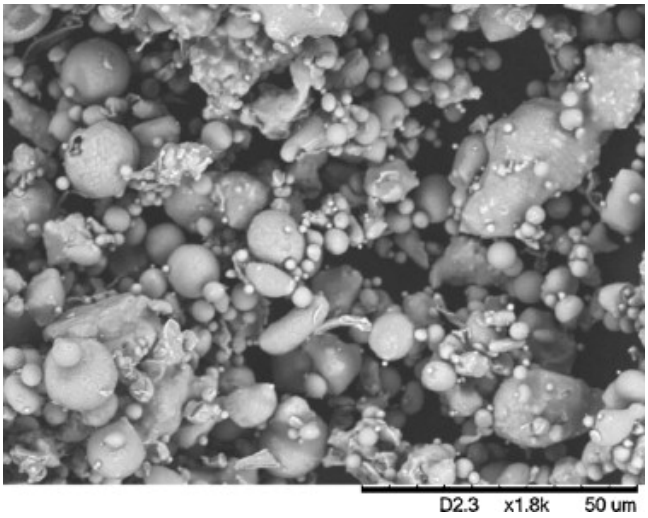

Figure 3: SEM image of the spherical iron oxide after granulation [5].

In general, there are five types of binder used in the MIM process and these are classified according to the following categories:

- Thermoplastic compounds
- Thermosetting compounds
- Water-based systems
- Gelation systems
- Inorganics

1.3 Binder Removal (Debinding)

The binder material in MIM green components is only an intermediate processing aid and it is always removed from the products after injection molding. Removal of the binder from the green part is also considered a key stage of the process and that one requires most careful control. The stage at which the binder is removed is known as debinding. The manner in which the binder is extracted consists of the heating of the green compact in order to melt, decompose, and/or evaporate the binder. This binder extraction has to be optimized so that there is no disruption of the as-molded part. The process normally takes several hours, depending on the thickness of the component. It has been the challenge for MIM developers to reduce and optimize the times for debinding. SEM image of the spherical iron oxide after granulation is shown in Figure 4. There are different methods which serve to obtain parts with the required interconnected pore network without destroying the shape of the components in

the shortest possible time. Different commonly used debinding methods applied in MIM industry are further explained.

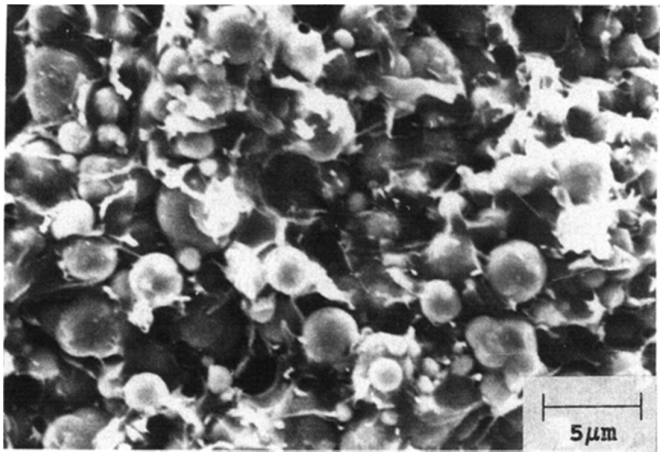

Figure 4: SEM image of the spherical iron oxide after granulation [8].

1.4 Thermal Debinding

Binders that usually lend themselves to this process are polymers such as polyethylene or polypropylene, a synthetic or natural wax and stearic acid [20, 21]. The MIM feedstocks based on these type of binders are easy to mold, but the removal of the binder requires very careful and slow heating in a thermal pyrolysis process. The debinding time lasts 24 or more hours and is therefore considered costly. In order to overcome the long and costly debinding times associated with thermal debinding, other methods have been adopted for use in conjunction with the process such that MIM components are debound in multi stages. Thermal debinding is now widely used as a second stage of debinding to remove organic binder material prior to sintering.

1.5 Solvent Debinding

Thermal debinding is now often used as a second stage of debinding in systems where the first stage is solvent debinding. Solvent debinding involves immersing the MIM compact in liquid that dissolves the binder material. The binder composition includes a constituent that can be dissolved in the liquid at low temperature. Acetone or heptane is sometimes used as the solvent although water-soluble binder compositions are preferred since it is easier to handle aqueous solvents than organic solvents. SEM micrographs of green compact before solvent debinding are shown in Figure 5. The times for debinding during solvent extraction are considered to be intermediate, which is shorter than thermal debinding times but take longer than catalytic binder removal. The investment and operating costs are lower so that total processing costs are competitive [20].

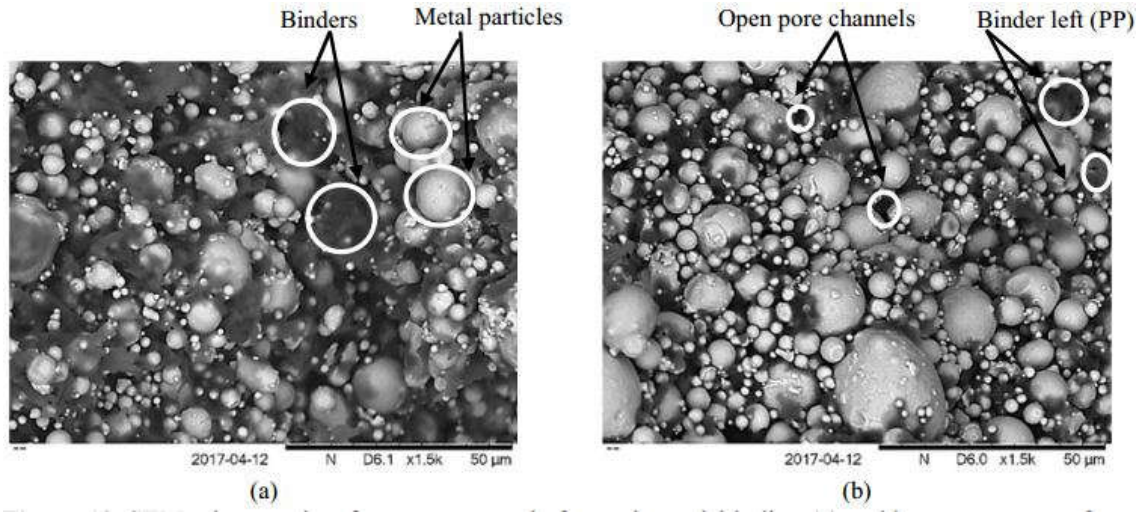

Figure 5: SEM micrographs of green compact before solvent debinding (a) and brown compact after solvent debinding (b)

1.6 Catalytic Debinding

Catalytic debinding of the binder is a process where most of the binder is attacked by a catalytic acid vapour [24] such as highly concentrated nitric or oxalic acid. Binder removal is done using a vapour catalyst at relatively low temperatures of approximately 120°C, which is below the softening temperature of the binder and has the advantage of reducing thermal defects. The acid acts as a catalyst in the decomposition of the polymer binder. Reaction products are burnt in a natural gas flame at temperatures above 600°C. The binder material is that is mainly used with this process is known as polyoxymethylene (POM) and it belongs to a grade of polymers known as polyacetals. These MIM feedstocks based on this binder are also easy to mold and possess excellent shape retention but there are hazards associated with acid catalysts and additional material costs.

1.7 Taguchi Method

Taguchi method is a capable of establishing an optimal design configuration, even when significant interactions exist between and among the controlled variables. The Taguchi method can also be applied to designing factorial experiments is an experiment whose design consist of two or more factors, each with discrete possible values or levels, and whose experimental units take on all possible combinations of these levels across all such factors [27]. Factorial experiments can be used when there are more than two levels of each factor. Taguchi parameter are used for optimizing the parameters and to obtain the minimum warpage. Huang and Tai [28] determined the most effective factors regarding warpage in injection molding of a thin shell part such as packing pressure, mold temperature, melt temperature and packing time injection parameters. Taguchi method is also strong tool for the design of high quality systems. To optimize designs for quality, performance and cost, Taguchi method presents

a systematic approach that is easy to use and effective. Taguchi extensively uses experimental design primarily as a tool to design products more robust (which mean less sensitive) to noise factors.

Robust design is an engineering methodology for optimizing the product and process conditions which are minimally sensitive to the various causes of variation, and which produce high-quality products with low development and manufacturing costs [29]. Hence, Taguchi developed manufacturing system that were robust or insensitive to daily or seasonal variations of environment, machine wear, and other external factors. Taguchi's parameter design is an important tool for robust design. His tolerance design can also be classified as a robust design. Robust optimization methods account for the effects of process variation by simultaneously optimizing the objective function and minimizing its sensitivity to parameter variation. Figure 6 demonstrate the step of taguchi parameter design.

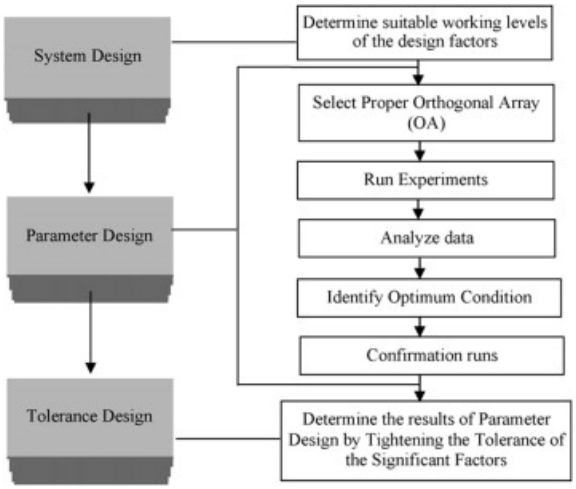

Figure 6: Steps of Taguchi parameter design [33].

1.8 Taguchi Approach

Two important tools are also used in parameter design are signal-to-noise (S/N) ratios and orthogonal arrays. Orthogonal arrays allow researcher or designer to study many type of design parameters and can be used to estimate the effects of each factor independent of the other factors. Orthogonal Arrays (OA) are a special set of Latin squares, constructed by Taguchi to lay out the product design experiments. By using this table, an orthogonal array of standard procedure can be used for a number of experimental situations. Consider a common 2-level factors OA as shown in Table 1 below: This array is designated by the symbol L8, involving seven 2-level factors, zeroes and ones. The array has a size of 8 rows and 7 columns. The number (zeroes/ones) in the row indicate the factor levels (be it fluid viscosity, chemical compositions, voltage levels, etc.) and each row represents a trial condition. The vertical columns represents the experimental factors to be studied. Each of assigned columns contain four levels of zeroes (0), and four levels of ones (1), these conditions can combine in four possible ways, such as (0,0), (0,1), (1,0), (1,1), with 27 possible combinations of level. The columns are said to be orthogonal or balanced, since the combination of the levels occurred the same number of times, when two or more columns, of

an array are formed. Thus, all seven columns of an L array, are orthogonal to each other [27]. Orthogonal Array L8 (2^7)

Table 1: An orthogonal array of L8 [33].

Trial No.	A	B	C	D	E	F	G
1	0	0	0	0	0	0	0
2	0	0	0	1	1	1	1
3	0	1	1	0	0	1	1
4	0	1	1	1	1	0	0
5	1	0	1	0	1	0	1
6	1	0	1	1	0	1	0
7	1	1	0	0	1	1	0
8	1	1	0	1	0	0	1

The signal-to-noise ratio is a quality indicator by which the experimenters and designers can evaluate the effect of changing a particular design parameter on the performance of product. There are 3 Signal-to-Noise ratios of common interest for optimization of Static Problems:

Smaller-the-Better

$n = -10 \text{ Log}_{10}$ [mean of sum of squares of measured data]

This is usually the chosen S/N ratio for all undesirable characteristics like "defects" etc. for which the ideal value is zero. Also, when an ideal value is finite and its maximum or minimum value is defined then the difference between measured data and ideal value is expected to be as small as possible. The generic form of S/N ration then becomes,

$n = -10 \text{ Log}_{10}$ [mean of sum squares of {measured – ideal}]

Larger-the-Better

$n = -10 \text{ Log}_{10}$ [mean of sum squares of reciprocal of measured data]

This case has been converted to Smaller-the-Better by taking the reciprocals of measured data and then taking the S/N ratio as in the smaller-the-better case.

Nominal-the-Best

$n = 10 \text{ Log}_{10}$ (square of mean / variance)

This case arises when a specified value is most desired, meaning neither a smaller nor a larger value is desirable. [30-34]. The Taguchi Approach is popular not only in the design stage, but also applicable during manufacturing stage for improving processes which reduce the variation. Having a certain degree of refinement without being too mathematical, the methodology should be readily understandable to engineers.

1.9 Process Parameters in Metal Injection Molding

In the MIM process the most critical step is the molding phase and more often many problems arise during this stage and lead to various kinds of defects such as voids, sinks, distortion and cracks. These defects can be avoided by proper selection of process parameters such as held pressure, temperature of the mold and melt. High injection

pressure is needed to force the melted powder mixture of high viscosity into the mold within a short period of time. On the other hand, higher pressure would lead to residual stresses which result distortion or cracking. Even though the increase of melt temperature can reduce viscosity and make mold filling easier, too low viscosity may result in problems with mold filling such as jetting, splashing or air entrapment. Increasing the mold temperature reduces heat losses and the maximum temperature difference at the end of the mold filling stage. This improves the quality of the part, but increases cooling time consequently the production time. Hence it can realized that the relationship between process parameter for MIM process is very complex and most of these parameters are inter-connected. Few examples of parameter optimization of few researchers are explained. Key process parameters and their ranges of operation are shown in Figure 7.

Parameter	Variable	Initial value	Range of operation
Injection time	INT (x_1)	1 s	0.5 to 1.5 s
Injection pressure	INP (x_2)	120 MPa	100 to 140 MPa
Packing pressure	PP (x_3)	100 MPa	80 to 120 MPa
Packing time	PT (x_4)	10 s	7.5 to 12.5 s
Cooling time	COTI (x_5)	19 s	14 to 24 s
Coolant temperature	COTE (x_6)	25°C	20°C to 30°C
Mold open time	MOO (x_7)	5 s	4 to 6 s
Melt temperature	MET (x_8)	275°C	270°C to 280°C
Mold surface temperature	MOTE (x_9)	70°C	65°C to 75°C

Figure 7: Key process parameters and their ranges of operation [35].

Parameter optimization of Natural Hydroxyapatite/SS316L via injection molding process is an important process in order to produce the higher strength and great quality green part. The injection parameters are nominated based on the most significant parameter via screening trial by using classical analysis of variance (ANOVA). From ANOVA results the whole control factors are orthogonal, hence interactions effects are neglected [5] and preferred injection parameters are injection temperature, mold temperature, pressure and speed [35]. The optimization process are conducted by using L9. (3^4) Orthogonal Array (OA) which is proposed of three level designs of experiment with 4 selected parameter in 9 trial. Table 3 demonstrates the three level of injection parameter design.

Table 2: Three level of injection parameter design [35].

Indicator	Parameter	0	1	2
A	Injection Temperature (°C)	165	170	175
B	Mold Temperature (°C)	40	45	50
C	Injection Pressure (%)	55	60	65
D	Speed (%)	55	60	65

Table 3: Taguchi's L9 (3^4) orthogonal arrays demonstrate the value of experimental trials (strength) and quality characteristic [35].

	Factors				S/N Ratio Larger is better	
Trial	A	B	C	D	Average	S/N ratios
1	0	0	0	0	4.996	13.973
2	0	1	1	1	4.893	13.792
3	0	2	2	2	5.045	14.058
4	1	0	1	2	5.465	14.752
5	1	1	2	0	5.374	14.605
6	1	2	0	1	5.983	15.538
7	2	0	2	1	5.372	14.603
8	2	1	0	2	5.155	14.245
9	2	2	1	0	5.146	14.229
					Σ	**129.75**
					T	**14.422**

As mentioned before, Taguchi method optimizes the performance characteristics over the setting of design parameters. A model based on L9 orthogonal array of Taguchi method was created by employing the S/N ratio optimization process [17]. Table 3 exhibit L9 (34) orthogonal arrays and demonstrates the value of experimental trials (strength) and quality characteristic. In simple explanation based from table 4, A1, Injection Temperature 170°C, B2, Mold Temperature 150°C, C0, Pressure 55%, and D1, Speed 60% is the optimum configuration.

Besides that this researcher [5] chose, L18 orthogonal array (OA) as the experimental design for this study. The OA is sufficient enough since the system has 1 control factor with 2 level, and another 3 control factors with 3 levels (Table 4), and because all the control factors are orthogonal, so interactions effects are not studied. The output response is the green density, because not only it reflects the green strength of the part, but also the best green density could lead to the best sintered density of the final part. The P-diagram and the ideal function are shown in Figure 8.

Table 4: Control Parameters for injection molding-step [5].

Factors (unit)		Level 1	Level 2	Level 3
Injection rate (cm/s)	A	10	20	-
Powder Loading (% vol)	B	59	61	63
Injection Temperature (°C)	C	140	150	160
Holding Pressure (bar)	D	1700	1800	1900

Based from the results obtained, factor D (holding pressure) contributed the most from each factor. This is by the fact that the holding pressure compresses the melt and fills the cavity, and has an effect until the gate solidifies. If the holding pressure is not enough sufficiently, slumps can occur on the surface [36]. Thus, the highest holding pressure could lead to the highest density of the green part. The second largest contribution is factor B (powder loading). The higher the powder loading, the bonding between powder particles increased within feedstock and make the green part to pack more densely due to the less void age created [37]. Thus, the density of the green parts increases.

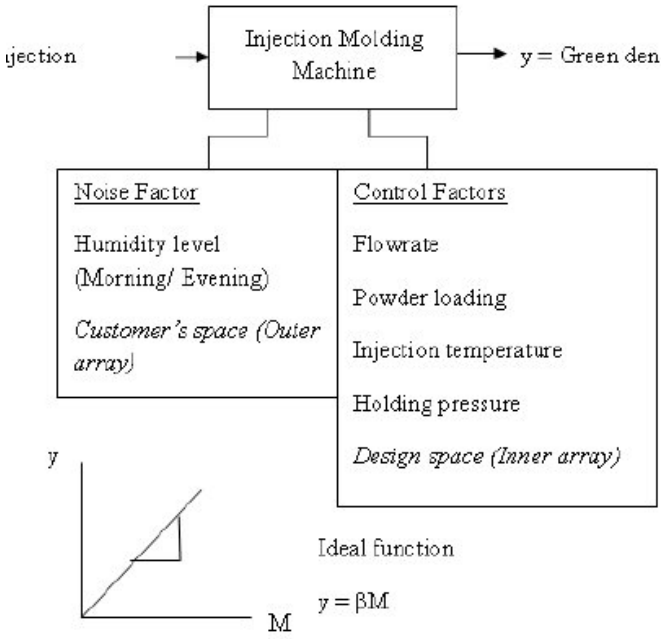

Figure 8: P-Diagram and Ideal Function [5].

This finding is quite similar with work [38], which also got powder loading as the second most influencing factor after optimization process done on stainless steel based feedstock. Injection temperature (factor

C) is still important since the temperature of materials has an effect on the viscosity of the melt, and consequently on the ability of the melt to fill up the cavity [36]. The parts will be unfilled if the viscosity of the melt is too high. Meanwhile for factor A (injection rate), the significance is too low and the effect can be neglected. This is because the injection rate only controls the time and amount of melt to fill up uniformly into the die cavity.

Table 5: The optimal condition for injection-molding step (5).

Factor		Parameter
Injection rate	A2	20ccm/s
Powder loading	B3	63% vol.
Injection Temperature	C1	140°C
Holding Pressure	D1	1700 bar

Table 6: Injection Parameters for 3 Level Taguchi Design [39].

Level	Injection Pressure (bar) A	Injection Temperature (°C) B	Mold Temperature (°C) C	Injection Time (s) D	Holding Time (s) E
0	10	150	55	5	5
1	11	155	60	6	6
2	12	160	65	7	7

Optimization of injection parameter to achieve highest green strength will be investigated using design of experiment (DOE) at which injection molding parameter are optimized using L_{27} (313) Taguchi orthogonal array [39]. The injection parameters that will be used are injection pressure, injection temperature, mold temperature, injection time and holding time, refer Table 7. Three–level designs of experiment with 5 parameters mentioned above are considered in the injection molding. With total 24 DOF for both single and interactions parameter, L_{27}'s Taguchi orthogonal array is the most suitable for design of experiment. L_{27} means 27 runs will be conducted with 5 replications at each run in order to guarantee statistical accuracy. In other words, based from 3 Level Taguchi Design optimization for L27 (313) results in injection pressure 11 bar, injection temperature 155°C, mold temperature 65°C, injection time 5s and holding time 5s.

2. Conclusions

Metal Injection Molding (MIM) is a newly developed technology to form metals and alloys into desired shape. Optimization of process parameters of MIM has been thoroughly discussed in the paper. Few parameters that are considered during optimization process such as injection pressure, injection temperature, mold temperature, injection time, holding time, holding pressure, injection rate and powder loading has been discussed. Besides that, there are still few factors for example cooling time, screw feeding speed, and etc. need to be studied further. Taguchi method is proven to be suitable for optimization process parameters of MIM.

References

[1] Prathabrao, M., Sri Yulis M. Amin, and M. H. I. Ibrahim. "Review on Sintering Process of WC-Co Cemented Carbide in Metal Injection Molding Technology." IOP Conference Series: Materials Science and Engineering. Vol. 165. No. 1. IOP Publishing, 2017.

[2] German, R. M. "Bose A." Injection Molding of Metals and Ceramics 1 (1997).

[3] Todd, I., and A. T. Sidambe. Developments in metal injection moulding (MIM). Eds. I. Chang, and Y. Zhao. Woodhead Publishing Limited: Sawston, UK, 2013.

[4] Todd, I., and A. T. Sidambe. Developments in metal injection moulding (MIM). Eds. I. Chang, and Y. Zhao. Woodhead Publishing Limited: Sawston, UK, 2013.

[5] Amin, Sri Yulis M., Norhamidi Muhamad, and Khairur Rijal Jamaludin. "Optimization of injection molding parameters for WC-Co feedstocks." Jurnal Teknologi (Sciences and Engineering) 63.1 (2013): 51-54.

[6] Liu, Z. Y., et al. "Micro-powder injection molding." Journal of Materials Processing Technology 127.2 (2002): 165-168.

[7] Abolhasani, H., and Norhamidi Muhamad. "A new starch-based binder for metal injection molding." Journal of Materials Processing Technology 210.6 (2010): 961-968.

[8] Nayar, Harbhajan S., and Bohdan Wasiczko. "Nitrogen absorption control during sintering of stainless steel parts." Metal Powder Report 45.9 (1990): 611-614.

[9] Cai, L., and R. M. German. "Powder injection molding using water- atomized 316L stainless steel." International journal of powder metallurgy 31.3 (1995): 257-264.

[10] Rawers, J., et al. "Tensile characteristics of nitrogen enhanced powder injection moulded 316L stainless steel." Powder Metallurgy 39.2 (1996): 125-129.

[11] Khor, K. "Dilatometry studies on water atomised stainless steel 316 L powders." Powder Metallurgy World Congress (PM'94). Vol. 2. 1994.

[12] Froes, FH Sam. "Getting better: big boost for titanium MIM prospects." Metal Powder Report 61.11 (2006): 20-23.

[13] Vervoort, P. J., R. Vetter, and J. Duszczyk. "Overview of powder injection molding." Advanced Performance Materials 3.2 (1996): 121-151.

[14] Todd, I., and A. T. Sidambe. Developments in metal injection moulding (MIM). Eds. I. Chang, and Y. Zhao. Woodhead Publishing Limited: Sawston, UK, 2013.

[15] Lumley, R. N., T. B. Sercombe, and G. M. Schaffer. "Surface oxide and the role of magnesium during the sintering of aluminum." Metallurgical and Materials Transactions A 30.2 (1999): 457-463.

[16] Schlieper, G. Metal Injection Moulding (MIM), Ceramic Injection Molding (CIM): An introduction [Online]. Shrewsbury, UK: Innovar Communications Ltd. (2009a)

[17]Schlieper, G. Powders for Metal Injection Moulding [Online]. Shrewsbury, UK. (2009b)

[18] German, Randall M. Powder injection molding. Princeton, NJ: Metal Powder Industries Federation, 1990.

[19] Froes, F. H., and D. Eylon. "Developments in titanium P/M." Moscow, ID: University of Idaho website (2005).

[20] Krug, Steffen, Julian RG Evans, and Johan HH ter Maat. "Reaction and transport kinetics for depolymerization within a porous body." American Institute of Chemical Engineers. AIChE Journal 48.7 (2002): 1533.

[21] Jorge, Hélio Rui Caldeira da Silva. "Compounding and processing of a water soluble binder for powder injection moulding." (2008).

[22] Chartier, Thierry, Marc Ferrato, and Jean F. Baumard. "Supercritical debinding of injection molded ceramics." Journal of the American Ceramic Society 78.7 (1995): 1787-1792.

[23] Jain, Kalpit, Deepak Kumar, and Sanjay Kumawat. "Plastic Injection Molding with Taguchi Approach-A Review." Int. J Sci Res 2 (2013): 147-149.

[24] Huang, Ming-Chih, and Ching-Chih Tai. "The effective factors in the warpage problem of an injection-molded part with a thin shell feature." Journal of Materials Processing Technology 110.1 (2001): 1-9.

[25] Alam, Kevin, and Musa R. Kamal. "A robust optimization of injection molding runner balancing." Computers & chemical engineering 29.9 (2005): 1934-1944.

[26] Antony, Jiju, and Mike Kaye. Experimental quality: a strategic approach to achieve and improve quality. Springer Science & Business Media, 2012.

[27] Foster, W. Tad. "Basic Taguchi design of experiments." National Association of Industrial Technology Conference, Pittsburgh, PA. 2000.

[28] Phadke, M. S. "Quality engineering using robust design, 1989." Englewood Cliffs, New Jersey: PTR Prentice-Hall Inc.

[29] Jain, Kalpit, Deepak Kumar, and Sanjay Kumawat. "Plastic Injection Molding with Taguchi Approach-A Review." Int. J Sci Res 2 (2013): 147-149.

[30] Torng, Chau-Chen, Chao-Yu Chou, and Hui-Rong Liu. "Applying quality engineering technique to improve wastewater treatment." Journal of Industrial Technology 15.1 (1999): 1-7.

[31] Mustafa, N., et al. "Parameter Optimization of Natural Hydroxyapatite/SS316l via Metal Injection Molding (MIM)." IOP Conference Series: Materials Science and Engineering. Vol. 165. No.

[32] Berginc, Boštjan, Z. Kampus, and B. Sustarsic. "Influence of feedstock characteristics and process parameters on properties of MIM parts made of 316L." Powder metallurgy 50.2 (2007): 172-183.

[33] Chuankrerkkul, Nutthita, Peter F. Messer, and Hywel A. Davies. "Application of polyethylene glycol and polymethyl methacrylate as a binder for powder injection moulding of hardmetals." Chiang Mai J. Sci 35.1 (2008): 188-195.

[34] Jamaludina, K. R., et al. "Injection molding parameter optimization using the Taguchi method for highest green strength for bimodal powder mixture with SS316L in PEG and PMMA." (2008).

[35] Ibrahim, M. H. I., et al. "Optimization of Micro Metal Injection Molding for Highest Green Strength by Using Taguchi Method." International Journal of Mechanical and Materials Engineering 5.2 (2010): 282-289.

A Review study of Biomedical and Surgical production by Metal Injection Molding (MIM) process

M.Moradjoy 1, H.Khorsand 2*

[1] PhD Candidate, Faculty of Material Science and Engineering, K. N. Toosi University of Technology,Tehran,Iran..

[2] Assistant Professor, Faculty of Material Science and Engineering, K. N. Toosi University of Technology,Tehran,Iran.

*Email: hkhorsand@kntu.ac.ir

Abstract

Metal injection moulding is gaining more and more importance over the time and needs more research to be done to understand the sensitivity of process to different process parameters. The current paper makes an attempt to better understand the effects of holding pressure and process temperatures on the moulded metallic parts. Stainless steel 316L is used in the investigation to produce the specimen by metal injection moulding (MIM) and multiple analyses were carried out on samples produced with different combinations of holding pressure, mould temperature and melt temperature. This review discusses the suitability of the MIM technology from the perspectives of both design and manufacture for the fabrication of medical devices using a variety of biocompatible materials including stainless steels, titanium alloys, iron and magnesium alloys. Recent progresses in the application of the MIM technology in the medical sector and challenges are reviewed and discussed. Future trends are suggested. It is concluded that MIM is better positioned today for wider application in the biomedical sector due to the benefits of reduced powder price and easy and fast supply of intricate dies brought by metal additive manufacturing (AM).

Keywords: Surgical devices, Biomedical, Metal Injection Molding; Biocompatible Metals; Sintering; Powder Metallurgy.

1. Introduction

T Research in biomaterials and medical implants is becoming increasingly important, as the life expectancy of an aging population is increasing. As early as 4000 years ago, the Egyptians and Romans used linen as sutures, gold and iron pieces for dental applications and wood for toe replacement [1]. Today the selection of biomaterials and implants has shifted towards more biocompatible and/or biomimetic options, thanks to our much- improved understanding of the biocompatibility of different materials and ever-advancing medical science and engineering. The selection of a proper biomaterial is very dependent on the application, expectations and requirement for the performance of the implanted material in the body. In general, polymeric materials are the candidate of the choice for soft tissue engineering, while metallic materials are a better choice for load-bearing applications. Particularly, biocompatible metallic materials have found significant applications in today's medical industry as orthopedic

implants, medical devices as well as surgical tools. New biocompatible metallic alloys and biomimetic metal implant designs enabled by advanced manufacturing technologies are the current focuses of the field.

With development of novel medical devices and surgical tools with micro and nano scaled features, clinical procedures are now possible to perform with greater precision and safety in addition to monitoring physiological and biomechanical parameters [2]. They are often manufactured from specific metallic materials, such as stainless steel, titanium and cobalt alloys, mainly due to their mechanical strength, biocompatibility and manufacturability. However, the manufacture of such devices and tools can be challenging due to geometrical complexity or low machinability in the case of Ti alloys. To address such manufacturing challenges, a few advanced techniques for metallic biomaterials and devices have been developed over the years.

Metal injection molding (MIM) is one such development. This process combines the most valuable manufacturing characteristics such as low cost, design simplicity, materials selection flexibility and low-cost raw materials from powder metallurgy, with those of plastic injection molding such as design freedom and rapid production, to offer an economic manufacturing technique for small intricate components (maximum dimension < 100 mm in most cases)[3]. MIM is particularly suited to mass production as illustrated in Figure 1 [3, 4]. As clear, MIM is a suitable technique for manufacturing of highly complex components in very high quantities. In term of complexity, additive manufacturing is the only common technique that able to manufacture more complex parts compared with MIM.

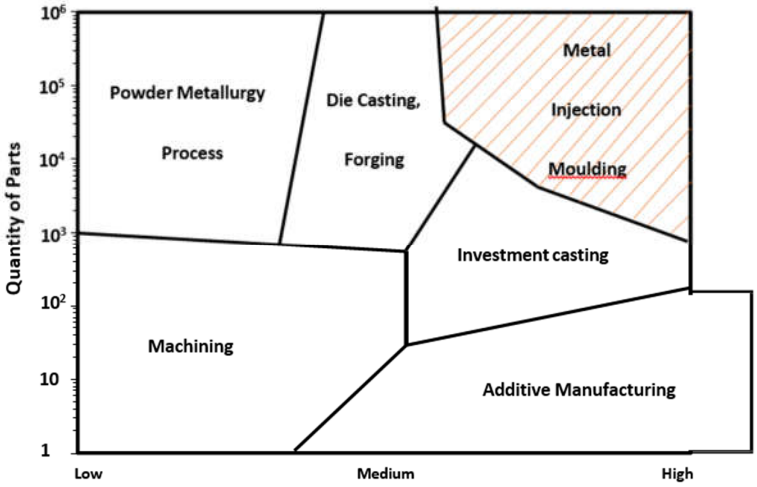

Figure 1 Suitability of different manufacturing process as function of geometric complexity and quantity (Adopted from [5]).

MIM has gained wide popularity in the defense sector, consumer goods, sports, communication devices, automotive, hand and power tools, as well as in the global medical sector. In fact, the more geometrically complex the part is, the stronger the rationale becomes to manufacture it through MIM technology. Consequently, new applications of MIM to manufacture instruments and reusable tools to assist surgical procedures as well as implants are playing an increasingly important role in the broad medical sector. This study reviews recent developments in the application of the MIM technology for the manufacture of medical related tools, instruments and implants. The review begins by providing an overview of MIM including its benefits to manufacture medical

tools and devices. Then, it discusses the emergence of MIM technology for a diverse range of biomedical tools and implants. This is followed by the latest trend in the application of MIM for different metallic biomaterials such as stainless steel, titanium, iron and magnesium. Finally, we conclude this review by considering the emerging research and the future directions for the application of MIM in the medical device manufacturing sector.

1.1 Powder Characterization for MIM of Biomedical Materials

The first step for a successful MIM process is selection of appropriate metal powder. Many parameters such as price, availability and suitability for MIM need to be considered for powder selection. While, economic considerations are extremely important for successful application of MIM as a manufacturing technique, for biomedical implants and devices the purity and performance of powders are more important than their economic factors due to high sensitivity of the product. An ideal powder for MIM of biomaterial and medical devices should have some specific characteristics [6, 7]:

- High purity; as small amount of impurities may negatively affect performance and biocompatibility of a metal, using high purity metal powder is essential for MIM of biomaterials and medical devices.
- Particle size and distribution; smaller sizes and tighter distribution are preferred for MIM but the recommended particles size are less than 22µm with d90 < 22µm for stainless steel and 45µm with d90 < 45µm for titanium and its alloys.
- Spherical shape; the best MIM performance obtain with spherical powder as can provide lower binder ratio, higher packing density, better flow-ability, less sintered shrinkage and lower dimensional instability.
- Void- free particles; particles with internal porosity can interfere sintering performance of the MIM products resulting poor mechanical properties.
- High packing density; to increase the powder loading (the ratio of metal powder to binder).

1.2 Metal Injection Molding Process

A typical MIM process consists of four main steps: feedstock preparation, injection molding, debinding and sintering as shown in Figure 2. Resizing is often needed as the fifth step to reach a tighter dimensional tolerance that the MIM process can offer for many MIM- fabricated parts, although not for every design and application. In addition, extra secondary metal working processes such as hot isostatic pressing (HIP), welding, machining, and heat treating or cleaning may be necessary to eliminate defects, optimize the properties and geometry of certain MIM-fabricated parts.

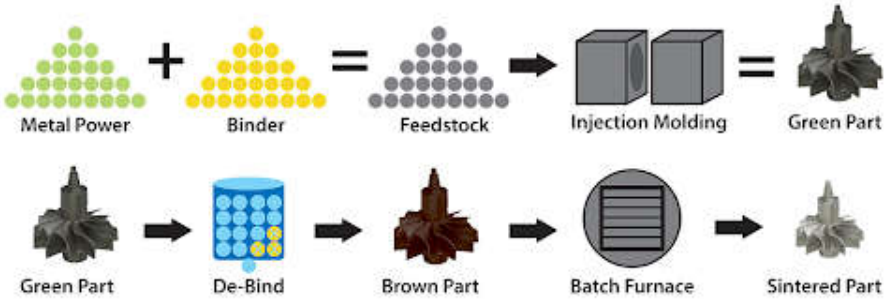

Figure 2. Schematic Diagram of Metal Injection Molding Process.

1.3 Feedstock preparation

To form feedstock, fine metallic powders are mixed with a binder, which is often composed of a few different polymeric materials. Such feedstock, which is fluid at temperatures of above 150℃, can be used in conventional plastic injection molding machines to manufacture desired components [3]. The selection of an appropriate binder system is essential for a successful MIM process. The binder system should provide sufficient fluidity when thoroughly mixed with the metal powder and leaves a minimum amount of oxygen and carbon residues after the debinding process. The ideal characteristics of a binder are expected to offer [3, 8]:

- good bonding with metal powder;
- low melting temperature (e.g. < 180 °C) suitable for the injection molding process;
- dimensional stability;
- complete decomposition and leaving little residue after thermal binder removal;
- no reaction with the metal powder during the thermal debinding stage;
- good green strength suitable for transport to sintering furnace; and
- being environmentally friendly

There is no single polymeric material that satisfies all of the above criteria. Therefore, different polymers mixed together to prepare a suitable binder system. A large number of binder systems have been tailored for MIM of different metallic materials over the years [8- 16]. While, the main components for most of the binder systems are based on wax such as paraffin and Carnauba wax, to manufacture biomedical implants and devices, specific binder systems based on water soluble polymers such Polyethylene Glycol (PEG), have been developed to reduce toxicological concerns [12, 15, 17]. Table 1 lists a few common binder systems developed for MIM of metallic biomaterials. While there have been many common binders suggested for both Ti and stainless steel (as the most important biomaterials), the selection of a binder for Ti is more critical due to the higher reaction rate of Ti to oxygen, carbon and nitrogen. In this regard, binders with less oxygen and lower decomposition temperature (such as polyethylene and polypropylene) are recommended to be used for Ti [18, 19].

Table 1. Common binder systems developed for MIM of metallic biomaterials

Binder System	References
Paraffin wax – Low Density Polyethylene – Stearic acid	[20, 21]
Paraffin wax – High Density Polyethylene – Stearic acid	[22]
Paraffin wax – Polyethylene – Stearic acid	[23, 24]
Paraffin wax – Polyethylene Glycol - Low Density Polyethylene – stearic acid	[25]
Polyethylene Glycol - polymethyl methacrylate – Stearic acid	[26, 27]
Paraffin wax – polyvinyl acetate – Stearic acid	[28]
Paraffin wax – polyethylene Vinyl Acetate – Stearic acid	[29, 30]

The selected binder and metal powder are then mixed and kneaded at a temperature slightly above the melting point of the binder (typically in the range of 140-170 °C). The "solid loading", which refers to the ratio of metal powder to the binder, should be selected to ensure good flow-ability whilst minimising binder use. At the end of mixing process, a thin layer of the binder should cover every individual metal powder to give the feedstock a good flow- ability [3]. Therefore, using high shear mixers such as Sigma or Z-blade kneaders are preferred. For reactive metals, such as Ti, the mixing process should be performed under a protected environment to prevent oxidation. The last step of feedstock preparation is to granulate the mixture into small pieces of less than 3.0 mm for easy and smooth injection molding.

1.4 Injection Molding

Most of the conventional plastic injection molding machines can be used for metal injection molding process as well. However, the surfaces of the cylinder and screws of the injection molding machines need to be specially hardened, and the selection of dies and tools including the design of gating and runner systems still needs detailed attention with respect to the part geometry and specific characteristics of the feedstock material. The injection molding parameters, such as injection speed, temperature and pressure as well as die temperature and clamping pressure, should be selected so that they provide proper die filling whilst preventing any metal powder and binder separation. Trial and error are necessary in most cases, and it is also common to refine the die and gating and runner systems. However, the injection process typically perform at a nozzle temperature of 120-180℃, mold temperature of 30-120℃, injection speed of 20-60 mm/s and injection pressure of 70-100 MPa [18, 31].

1.5 Debinding process

As previously mentioned, debinding process has two steps of solvent and thermal debinding. The main binder component, which is usually a wax-based (such as paraffin wax) or a water- based (e.g polyethylene glycol, PEG) polymer, is firstly removed by a solvent debinding process. During this step, more than 95% of the main binder

need to be removed from the components. The porosity left in the sample after removal of the main binder, facilitates the second component removal during the subsequent thermal debinding stage. In this stage, the green part is heated to a temperature range of 500-650°C, which is higher than the decomposition temperature of the remaining binder. The thermal debinding time and temperature are typically between 30-120 min and 400-600°C, respectively. However, if a separate furnace is going to be used for the final sintering stage, the debound parts need to be pre-sintered at the debinding furnace to even higher temperatures (in the range of 900°C for Ti or 800°C for stainless steel), to provide handling strength to the samples. A high purity inert gas should continuously flow over the samples in order to flush out the decomposed polymer from the furnace.

1.6 Sintering

The sintering stage has significant influence of quality and mechanical properties of the final products. For MIM-fabricated stainless steel parts, sintering is typically done under a moderate vacuum (< 10-3 mbar) or argon gas and at a temperature range of 1100-1250°C for 1-3 h. Sintering of MIM-fabricated titanium parts is different and selection of the appropriate temperature, holding time, vacuum level and substrate material is critical [19]. MIM- fabricated Ti samples usually sinter at a higher temperature (1200-1400 °C) for a longer period (2-6 h). A high vacuum (<10-5mbar) or high purity argon atmosphere is recommended. However, the optimal sintering cycle depends on powder characteristics, alloying approach (pre-alloyed or mixed elemental powders), and requirements for final desired density, microstructure and impurity level. For example, it has been recommended to use a lower sintering temperature (<1250°C) and a shorter sintering time (< 3 h), followed by a secondary step of hot isostatic pressing for parts that require a pore-free microstructure [19]. However, without HIP, the sintered density can easily exceed 97% of the theoretical density when sintered properly due to the fine powder used.

1.7 History of MIM application in biomedical industry

Metal injection molding process is relatively new technology compared with most tradition manufacturing methods such as powder metallurgy, casting and forging. After its early development in 1920's it was first applied to manufacturing of ceramic components (known as powder injection molding) followed by automotive and firearm parts [32]. The MIM process then showed its suitability in electronic industry for manufacturing of small and intricate mobile phone and notebook parts, where they traditionally produce by die casting process. The geometrical complexity of biomedical comments, urged scientists and manufacturers towards MIM as a reliable and prominent alternative manufacturing technique. Therefore, from early 2000's massive research and development activities on application of MIM for manufacturing of biomedical implants and devices were performs. In this regards many articles were published and patents were filed. These works concentrated of application of MIM for manufacturing of many biocompatible materials especially stainless steel, titanium, CoCrMo allys, Mg and Fe alloys. Table 2 summarizes examples of patents and remarkable publications in this area. As seen, MIM confirmed its suitability for manufacturing of many biomedical implants, devices and tools.

Table 2. Examples of publications and patents on application of MIM for manufacturing of biomedical components

Material	Description	Ref or Patent
CP-Ti	Metal injection molding of CP-Ti components for biomedical applications	[33]
Ti-Nb	Metal injection molding of low modulus Ti–Nb alloys for biomedical applications	[34]
Ti-Mn	Fabrication of low-cost beta-type Ti–Mn alloys for biomedical applications by metal injection molding process and their mechanical properties	[35]
Ti-Nb-Zr	Development of Ti-22Nb-Xzr using metal injection molding for biomedical applications	[28]
Stainless steel	Powder injection molding of biocompatible stainless steel Bio devices	[36]
Co-Cr-Mo	Effect of sintering temperature on density, hardness and strength of MIM Co30Cr6Mo biomedical alloy	[37]
Mg	Magnesium Powder Injection Molding (MIM) of Orthopedic Implants for Biomedical Applications	[38]

1.8 Applications of MIM in biomaterials and biomedical devices

As materials and labor costs for medical manufacturing continue to rise, reduction in manufacturing cost of component becomes increasingly important to control the overall cost issue. MIM is suitable for a large number of materials for medical applications such as stainless steel [36, 40-42], titanium alloys [3, 43, 44], Co-Cr alloys [45] as well as biodegradable metals such as iron [46], zinc and magnesium alloys [38]. It offers a massive reduction in manufacturing cost for high volume production of these components by reducing materials waste and machining processes. An excellent example of the benefits of MIM to manufacture an intricate biomedical part is that of a bone tissue engineering scaffold. The idea of such scaffolds is to mimic the porous and permeable hierarchical architecture of the human bone and also provide tissue support in- vivo through the porous structure. MIM in conjunction with the use of a temporary space holder can produce porous artificial bone scaffolds with a controlled porosity fraction and high pore interconnectivity [22, 47-49]. Numerous research and development activities have been carried out to enhance the capability of the MIM technique for the manufacture of different medical devices and tools. Typical examples include, metallic orthodontic brackets, surgical tools and instruments, miniaturized graspers, scissors and sewing units, drug delivery devices, surgical implants, hearing aids, dental equipment and implants, and joint replacements. A number of selected examples is discussed below.

1.9 Minimally invasive surgery (MIS) tools

MIM could be used for the manufacture of many small and geometrically complex MIS tools such as laparoscopic and endoscopic jaws, graspers, scissors, cutting and suturing tools [50]. These tools, are usually made from different grades of stainless steels due to their sufficient strength and hardness, outstanding corrosion

resistance, and ease of sterilization. Many of these surgical tools are traditionally manufactured through Computer Numerical Control (CNC) machining of wrought blanks, which is a costly process. Indeed, many attempts were made to reduce the machining cost, such as sulphur addition to the stainless steel to improve its machinability for high- volume production. Nowadays, MIS instruments are seeking new design ideas that allow open surgery to be replaced by minimally invasive procedures. Such new designs make the geometry of such components even more complex. Manufacturing of such small and geometrically complex tools is no longer possible with traditional machining methods, while metal additive manufacturing remains costly. Therefore, the MIM technology provides an important, if not the only, pathway for the affordable manufacture of those components (Figure 3).

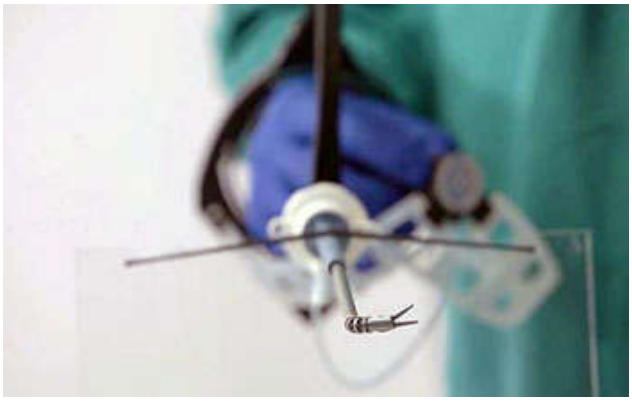

Figure 3. Minimally invasive surgery (MIS) instrument parts manufacture using MIM of stainless steel

1.10 General surgical tools

MIM has the capability to manufacture many general surgical tools such as scalpel handles, nippers, forceps and instrument mechanism parts. While, these parts are traditionally manufactured by forging and machining processes, MIM offers a much better and more affordable manufacturing pathway. Nowadays many such surgical tools are already manufactured using MIM of stainless steels and titanium alloys. For instance, surgical forceps were successfully fabricated using MIM. The products, as shown in Figure 4, have a length of ~30mm and feature many delicate structures that are difficult to manufacture by other methods. Both commercially pure Ti and stainless steel 17-4PH were used in the production of the forceps.

Figure 4. Forceps for medical applications using the MIM technique (Courtesy of ElementPlus, Shenzhen, China)

MIM also has the capability to manufacture large and geometrically complicated components for some advanced surgical tools. For instance, Figure 5 shows a cutting block with very complicated and detail shape, non-uniform wall thickness as well as large overall size (nearly 450g) recently manufactured by MIM of 17-4 HP stainless steel. These blocks are used in an advanced knee-replacement surgery instrument. Manufacture of such highly challenging medical components by MIM, which leads to an estimated cost reduction of 60% over traditional manufacturing methods, testifying to the suitability of MIM to manufacture many complicated medical surgical tools and devices.

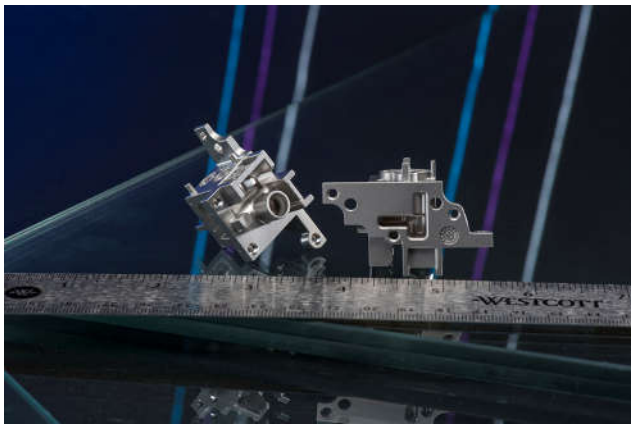

Figure 5. Cutting block made from MIM of 17-4 PH stainless steel uses in a knee- replacement surgery device (Image is courtesy MPIF). The overall weigh of block is 450g.

1.11 Orthopaedic Surgery

Another group of potential MIM candidates is the family of trauma plates, blades, screws and fixation devices used for fracture fixation, reconstruction or arthrodesis of small bones, including those in the forefoot, midfoot and hind foot. While these components are usually manufactured by CNC machining of stainless steel or Ti alloys, MIM can be a better technique for their production. For instance, recently, a Retractor Blade and Ring set used in a spinal surgery procedure was manufactured by Indo-MIM via MIM of 17-4PH stainless steel. This part is traditionally manufactured through extensive multi-axis CNC machining as well as wire EDM of wrought stainless steel bars to achieve the intricate detail. The MIM technique allowed for a dramatic reduction in manufacturing cost without sacrificing product quality or function.

1.12 Orthodontic

Probably the first major application area for MIM in the medical sector, which still is the major product of the industry, was for manufacturing of orthodontic brackets and hooks. 316L stainless steel is the main material for manufacturing of these extremely small precision parts, however MIM is being used to fabricate these components

more economically from stainless steel (Figure 6) as well as from Ti alloys [51-53]. A range of dental surgery tools may also be economically manufactured using the MIM technique.

Figure 6. Parts from an orthodontic tooth positioning system manufactured by Flomet LLC, USA. (Image courtesy MPIF, USA).

For instance, Ahn et al. [54] reported the manufacture of ultrasonic endodontic and scalar tips through MIM of 316L stainless steel powders. MIM has the potential for the manufacture of dental implants, due to the highly complex geometry and quality requirements of these components. Several studies have confirmed the potential of the MIM process for the manufacture of stainless steel [55], titanium [52] and magnesium [38] implants. For instance, Ferreira et al. [55] successfully developed a procedure capable of injection molding complex 3D dental implants from 316L stainless steel and polyolefin wax as binder with micro details, aiming for better bio compatibility and less expensive dental implants (Figure 7). In that regard, they coated the micro-cavity surfaces of the mould with dichalcogenides sulphides (W-S-C). This coating allowed a reduction of around 50% of the force needed in the ejection step to separate the parts from the micro mould surface. Accordingly, it improved the surface quality of the final products in both threads (Figure 7b) and the top of the implants (Figure 7C).

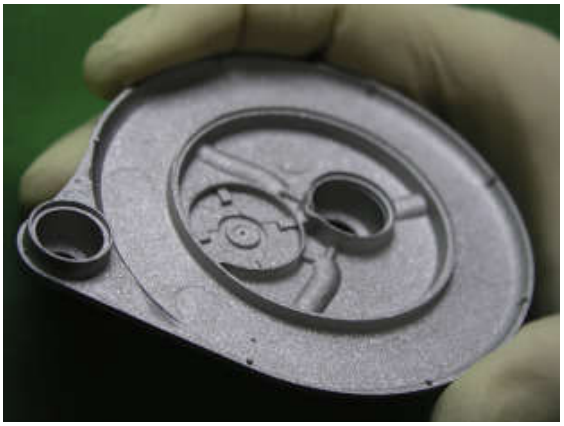

Figure 7. a) Stainless Steel implants fabricated using MIM, b) implant thread and c) top of the surface cavity of the implant [55].

1.13 Drug Delivery Equipment

Research has approved the successful application of MIM in the manufacture of micro needles for drug delivery purposes. Hollow or porous Micro needle Arrays (MAs), are excellent pain- free transdermal drug delivery devices with low skin trauma and reduced risk of infection [56]. Solid MAs are traditionally produced by different techniques such as lithography and etching, micro- molding, micromachining or laser cutting. Such solid MAs can only provide a limited dosage of drug into body. Therefore, replacing the solids MAs with single channel hollow needles offers great benefit as they can transfer drugs into the skin continuously via their holes, providing an unlimited dose of drugs. However, manufacturing of such hollow needles is possible only through very complicated and costly techniques. In this regard porous micro needles with many randomly distributed and interconnected pores are a far better option than single channel needles. In these needles, drug can be stored into the pores and diffused from the micro needle matrix into the skin. The interconnecting pores guarantee continuous drug delivery. MIM has been successful for the manufacture such porous micro needles. Li et al. [56] reported the successful fabrication of a Ti porous micro needle array by metal injection molding of a transdermal drug delivery device (Figure 8).

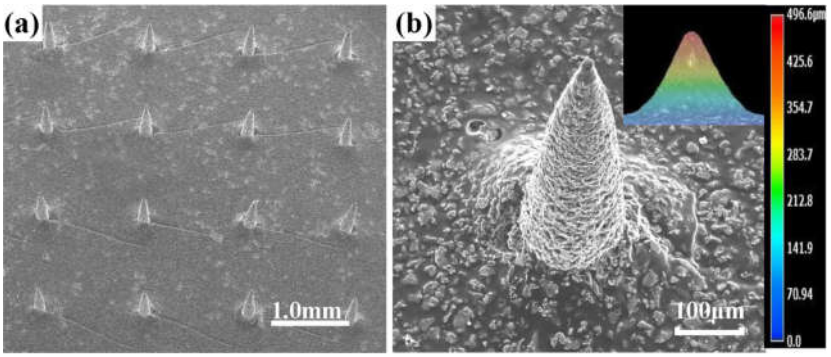

Figure 8. Morphology of porous Ti micro needle arrays manufactured by MIM [56].

1.14 Hearing aids: metal hook, tube element and various other parts

Components for hearing aids such as metal hooks and tube elements have been successfully manufactured by the MIM process. These components have very complicated geometry and are traditionally manufactured by CNC machining of smaller parts and gluing them together. However, MIM offers much higher finished quality and an affordable cost to manufacture these parts (Figure 9). Figure 9 Hearing aid sound tube manufactured using MIM of 316 stainless steel (Curtesy of Metal Powder Industries Federation, MPIF)

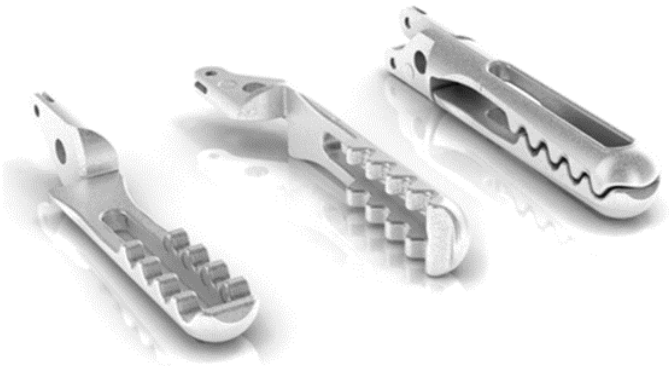

Figure 9. Hearing aid sound tube manufactured using MIM of 316 stainless steel (Curtesy of Metal Powder Industries Federation, MPIF)

1.15 Human implant materials stent and spinal implants

MIM can be used to fabricate stents, which can be implanted into the blood vessel of human bodies to treat cardiovascular diseases. The stents, having a large-sized thin- wall structure and an extremely complicated surface, were fabricated by sophisticated machining before MIM was introduced. Due to the complex structures, the fabrication cost is extremely high. Figure 10 shows the stents fabricated by MIM, reported by Dr. He in the WORLDPM2018 Congress. Currently, stents of different materials can be made by MIM, including stainless steels and NiTi. Both materials have reasonably high density and low interstitial contents, imparting good biocompatibility and mechanical properties to the sintered products.

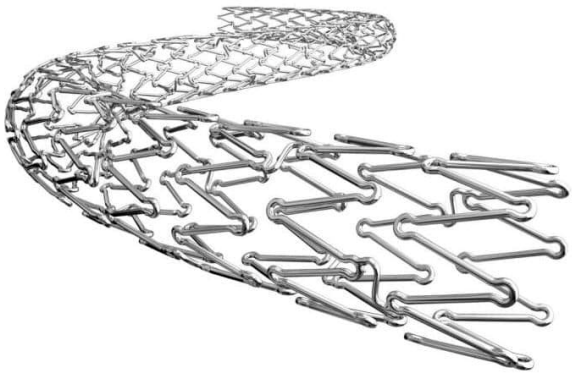

Figure 10. 316L SS stents fabricated by MIM (manufactured by Guangxi University of Science and Technology, China).

1.16 Advances in MIM of biocompatible metallic materials

Since the first use of MIM in medical device applications, the technology has advanced dramatically in terms of material choice, process control and reproducible quality across all end-user sectors [57]. MIM is now

considered to be a reliable process with excellent repeatability and this has driven the growth of MIM in the medical industry. A few important metallic biomaterials that are suitable for fabrication by MIM are discussed below.

1.17 MIM of Stainless Steel

17-4PH, 420 and 440C stainless steels (SS) are the most common metallic materials for medical tools and devices due to a combination of high strength, good wear resistance, biocompatibility, affordability and manufacturability [36, 58-63]. In fact, the first application of stainless steel as surgical implants was in 1926, where a stainless steel containing 18% Cr and 8% Ni (type 316SS) exhibited attractive properties [64]. This material showed better strength and resistance to body fluid compared with vanadium containing steels. Since then, stainless steel is the most frequently used material for internal fracture fixation, joint replacement and traumatic segmental bone replacement. However, due to the toxicity effect of Ni ions on the human body, a new range of Ni- free stainless steels have been developed, which have been in clinical use for a number of years [41, 42, 65, 66].They offer the combined benefit of excellent mechanical properties and biocompatibility.

While, traditional techniques such as CNC machining of forged billets are still the main technology to manufacture stainless steel medical devices, MIM has already confirmed its suitability as an economic alternative. Much research has been performed to evaluate the suitability of stainless steel for MIM processing and the properties of manufactured components [40, 60, 67, and 68]. For instance, Ji et al [60] confirmed that by a proper selection of MIM parameters, a high density is easily achievable for 316L stainless steel components. Currently, most 316L products produced by MIM have densities higher than 98%. Such high density can provide satisfactory mechanical properties for any biomedical application.

1.18 MIM of Titanium Biomaterials

Among all metallic biomaterials, titanium offers several distinct benefits, including lower elastic modulus, excellent corrosion resistance and enhanced biocompatibility [69]. Low elastic modulus of Ti and its alloys is particularly important for hard tissue replacement to mitigate the stress shielding effect, a cause that can lead to revision surgeries [69]. Stress shielding is a phenomenon where the higher elastic modulus of the implant results in bone loss as a result of decreased physiologic loading of the bone [70]. Examples of biomedical applications of Ti and its alloys are dental and orthopedic implants, artificial hearts, pacemakers, knee cap joints, bone plates, cardiac valve prostheses, and screws for fracture fixation, artificial hip joints and cornea back-plates [71, 72]. However, Ti and its alloys have some drawbacks, which limit their application as an ideal biomaterial. For instance, their tribological performance is deficient.

Most important applications of Ti-based materials are for load-bearing implants such as total knee or hip replacement and bone scaffolds, where proper bonding between the human tissue and the new implant is essential. Such bonding can only happen when the body fluid can transfer through the implant so that body cells can grow through them. To adequately add such functionality to the metallic implants, introducing porosity into the metal

structure has been adopted. MIM can provide a solution in this regard when combined with the addition of a temporary space holder technique [22].

During last couple of decades, many researchers such as [18, 32, 73-80] have deeply studied the application of MIM to manufacture titanium implants and medical devices, but progress has still been slow. In fact, there is very limited established commercial activity to manufacture Ti implants by MIM, mainly due to the need to use expensive fine (□45µm), low-oxygen spherical Ti powder. This is the main reason behind the slow progress of MIM- Ti industry compared to the established manufacturing industry on MIM-stainless steel.

However, the market growth for general Ti-MIM components shows that interest in using low cost powders is increasing. The growth of titanium Additive Manufacturing (AM) has driven down the cost of MIM grade titanium powders. As most additive techniques use Ti powders with particle size larger than those used by MIM, MIM-grade titanium powder has become more available and less expensive [57]. Nonetheless, the high reactivity of titanium to oxygen and carbon still requires special consideration during the MIM process (including the requirement for a specialized binder system). These factors increases the cost of Ti-MIM production process. However, this additional cost is negligible compared to the cost of the raw powder. Despite this, the specific circumstances for medical devices, such as very complicated geometry, small size of components and high cost of traditional manufacturing techniques (i.e. casting and machining), make MIM an affordable process even if special powders are used. In this regard, ASTM [81, 82] published the first Standard Specification for the application of metal injection molding in the manufacture of surgical implants from Ti-6Al-4V and un-alloyed Ti.

Many researchers reported successful manufacture and improvement in the properties of Ti implants using the MIM technique. For instance, Aust et al [83] reported the manufacture of a bone screw implant by MIM of Ti-6Al-7Nb alloy for fixing and repair of a broken dens axis. This alloy is an alternative to the most common Ti biomaterial of Ti-6Al-4V, where biocompatible niobium metal has been used as a replacement to the vanadium due to the toxic effect of vanadium in the human body. One important property requirement for load-bearing biomaterial parts is related to the fatigue strength. Ferri et al. [84-86] studied the fatigue behavior of Ti-6Al-4V implants manufactured by the MIM. They found that while MIM offer significantly lower fatigue properties compared with other standard manufacturing methods, post processing techniques such as shot penning promoted an increase in the fatigue resistance. The main reason for such improvement was due to the change in surface roughness caused by local plastic deformation on the surface of the sintered samples, as seen in Figure 11 [86], and the introduction of compressive surface residual stress. Similarly, the surface roughness of Ti implants has been improved by plasma treatment [87] to increase the clinical success of those implants [88]. Table 3 summarizes examples of the most successful applications of MIM in the manufacture of Ti medical implants including their properties. The mechanical properties are well accepted compared with the properties obtained by traditional manufacturing techniques, indicating the suitability of the MIM process.

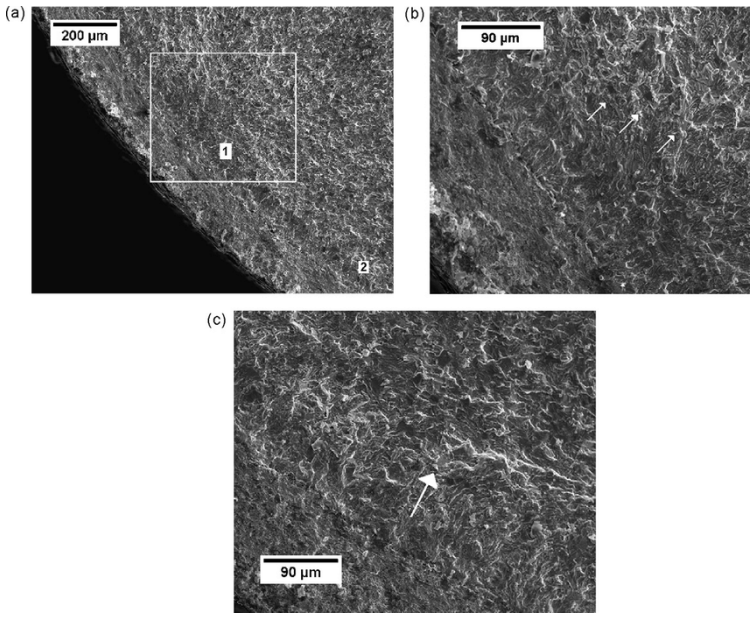

Figure 11. Effect of shot peening on the surface quality of Ti-6Al-4V samples manufactured by the MIM process. a) Without shot peening, and b,c) after shot penning application [86]

1.19 MIM of Porous Ti

Porous coatings were initially proposed in the late 1960's to increase the roughness of the implant surface aimed to increase the friction forces between the implant and the surrounding bone. This porous coating provided better initial stability to the implant leading to reduced implant failures. After implantation, the bone grows into the porous surface and helps to improve the long term stability of the implant [98]. Since then, porous coatings have been extensively used in various medical implant applications, but recent practice has changed to fully porous structures due to better biocompatibility of the metallic porous implants while offering sufficient mechanical properties.

In addition to established conventional manufacturing processes, research now focuses on the development of new processes and methods for porous metal fabrication, particularly for porous titanium and its alloys. As mentioned previously, despite the lower Young's modulus of Ti and its alloys, they are still much higher than those of human cortical bones, thereby increasing the risk of implant failure due to the stress shielding effect around the implant. The elastic modulus of titanium is about 114 GPa [99] while the values for cancellous and cortical human bone are in the range of 1-35 GPa [100]. The solution is to introduce porosity into titanium structures. These porous structures can be customized to have mechanical properties close to those of human bone and are usually designed to facilitate bone ingrowth [71]. The mechanical properties and Young's modulus of titanium implants can be tailored via the volume fraction, size and distribution of the pore structures. It has already been shown that the elastic modulus of porous titanium can be decreased to values very close to those of human cortical bone (i.e. < 35 GPa) with increasing pore size and pore fraction.

Table 3. Examples of Ti implants manufactured by the MIM process and their mechanical properties

Alloy	Application	Tensile Strength, MPa	Elongation, %	reference
Ti-6Al-4V	Implant	846	14.8	[89]
CP-Ti	Implant	483	21	[33]
Ti-6Al-7Nb	Bone screw implant	846	13.7	[83, 90]
Ti-6Al-4V-0.5B	Implant	902	11.8	[85, 91]
Ti-13Mn	Implant	888	1.0	[35]
Ti-9Mn	Implant	1046	4.7	[78]
Ti-10Nb Ti-16Nb Ti-22Nb	Implant	638 687 754	10.5 3.6 1.4	[30]
Ti-17Nb	Implant	641	5.1	[92]
Ti-12Mo	Implant	528	2.3	[93]
Ti-6Al-4V-2Fe Ti-6Ali-4V-4Cr	Implant	980 1030	14.8 15.1	[94]
Ti-24Nb-4Zr-8Sn	Implant	656	9.2	[95]
Ti-20Nb-10Zr-0.5Y	Implant	690	4.5	[96]
Ti-29Nb-13Ta-4.6Zr	Implant	630	2.8	[97]

As mentioned earlier, MIM together with the space holder techniques has been used to manufacture porous implants. A US patent filed in 2003 by Nelles et al. [101], described the principles to use MIM to fabricate different metallic materials with open porosity of at least 10%, assisted by the use of KCl or NaCl as space holders. Since then, research and development has evaluated the possibility of this technique to manufacture porous titanium [22, 47-49, 102-107] and stainless steel [108, 109] components. For example, Carreno- Morelli et al [47] applied the MIM of titanium hydride powders combined with the space holder technique, to produce highly porous Ti components with very low elastic modulus in the range of 4-22 GPa. In a similar attempt, porous Ti components with up to 72% porosity manufactured by Chen et al. [103] using HDH Ti powders and NaCl particles as the space holder. These microstructures indicate the development of well interconnected porosity, which is essential for biomedical applications [110]. Similarly, the current authors have manufactured Ti porous scaffolds using the

MIM technique with 40% porosity and a Young's modulus as low as 7.8 GPa [22]. Such research activities, demonstrate the capability of MIM process for manufacturing of many Ti porous implants and scaffolds.

For many specific biomedical applications, MIM also has the capability to manufacture porous components with a gradient in the amount of porosity across the specimen. For instance, using a two-component-MIM technique, Barbosa et al. [43] manufactured a titanium spinal implant component with a gradient in porosity. They proposed that the low porosity (or dense) part of the implant is responsible for its mechanical stability, while the high porosity part promotes Osseo integration by allowing cell ingrowth and body fluid circulation though the interconnected pores. Similarly, another extension of MIM is to manufacture components with two different materials joined together in a single process [111]. In this regard, Mulser and Petzoldt [112] studied the manufacture of biomedical implants with Ti-6Al-4V and stainless steel materials using the two-component-MIM technology.

1.20 MIM of Biodegradable Metallic Implant

MIM has the potential to be used as a suitable manufacturing technique for biodegradable metallic implants made from magnesium alloys. In addition to their application as a lightweight material, magnesium and its alloys are promising candidates for potential surgical implants for biomedical orthopedic and traumatology applications, considering their excellent biocompatibility and biodegradable properties [38, 118, and 132]. Although, currently Mg alloys are mainly considered for non- load- bearing applications such as stents [133], they also have the potential for load-bearing applications due to their much lower elastic modulus compared with more conventional biomaterials such as Ti and stainless steel. Similar to other metals, powder metallurgy could be an appropriate approach for the manufacture of Mg alloy implants. However, the strong affinity of Mg for oxygen is a major challenge for any PM routes. Considering such issues with PM of Mg alloys, special MIM processes have been designed as potential techniques for manufacturing small intricate biodegradable Mg implants with high reproducibility [38, 134- 136].

1.21 Future trends and concluding remarks

Since the first use of MIM in medical applications, the technology has advanced dramatically in terms of material choice, process control and reproducibility. It is clear from the literature that researchers have attempted to improve the suitability of MIM for the manufacture of porous and dense biomedical implants and devices and that many MIM products have acceptable properties and performance for use in clinical trials.

Among current important biocompatible metals, titanium and its alloys are preferred for medical applications due to their high biocompatibility, low weight, excellent corrosion resistance, low Young's modulus and high strength. However, they pose a significant challenge to manufacture by MIM due to their high affinity for impurities, especially oxygen and carbon. On the other hand, the increasing demand for small and intricate parts in the medical sector, is expected to boost the market demand over the coming years. In this context, MIM remains the most affordable and viable manufacturing technique for such small and complicated parts. In particular,

research is mature enough to progress towards industrial manufacturing and clinical use of MIM fabricated implants. At present, there are other manufacturing processes such as casting, machining, conventional powder metallurgy and metal additive manufacturing (AM), which are capable of fabricating biomedical devices and implants. However, most of these processes, especially the conventional processes, would not be able to compete with the feasibility promised by the MIM process in terms of both cost and manufacturability for geometrically complex parts in high quantities. Metal AM is scientifically attractive but cost-wise there is still a long way to go. However, in addition to the reduced powder-price benefit, metal AM has brought another significant benefit to the MIM business, i.e., it enables much faster and more cost-effective supply of intricate dies for MIM. Therefore, the future of MIM in biomedical implants and devices is encouraging.

Thanks to the high density achieved by MIM, most MIM-fabricated biomaterials have static mechanical properties comparable to those fabricated by conventional methods, such as casting or forging. However, the dynamic mechanical properties, especially fatigue life, are much inferior due to the presence of some small pores in the structure. The pores can be eliminated by hot isostatic pressing, therefore the fatigue properties of the MIM-fabricated materials are significantly improved. This improvement is crucial for many implants, which are expected to serve under cyclic loading in a human's body for their life time. The corrosion performance of the MIM-fabricated biomaterials and parts is an important area that still needs further attention. In fact, systematic experimental data are still missing on the in- vitro and in- vivo performance of MIM- fabricated implants. Such data are required to optimize the different aspects of the MIM process for the manufacture of biomedical implants and devices, including the development of fully biocompatible binder systems, optimized powder size and distribution, de-binding conditions, and sintering cycles.

As an overview for the current and future trend of MIM in medical industry, its application could be categorized in two important area of medical tools and implants. Currently MIM technology matured enough for manufacturing of medical tools compared with implants. Many medical tools and instrument components currently manufactured in industrial scale using MIM of stainless steel, titanium and other metallic materials. These include but not limited to: arthroscopic tools, bone drills, robotic arms for surgery, bone rasps, cutting jaws, biopsy jaws, needle guides, saw guides and hundreds of endoscopic instruments. However, using MIM for manufacturing of medical implants is still on its early development stage and not many clinically approved implants manufactured using this technique. Saying that, some fixation components such as orthodontic brackets manufactured using MIM for many years and MIM is still the major manufacturing route for such brackets. However, most of clinically approved implantable components still manufacture through traditional methods such as casting, forging and machining. Considering, increased demand for such implants with geometrically complex shapes, massive progress in optimizing MIM for manufacturing of medical implants and availability of raw materials (especially fine Ti powders), expected to boost up market demand for MIM technique in medical industry.

2. Conclusions

MIM has the full capability to meet the dimensional and material property requirements of medical instruments and devices as demonstrated by prototype applications. The technology has also shown the potential to produce porous implant materials. However, detailed assessments are required for metal- injection- moulded biomaterials to gain acceptance as implants. In addition, MIM can be used as a cost-effective production technique for novel designs, including micro-sized and functionally graded devices. Such developments may provide pathways for new solutions to current healthcare problems. Finally, the continuous healthy development of metal AM is expected to further drive the metal powder price lower and the supply of intricate and multifunctional ties for MIM easier and more affordable. Hence, MIM is better positioned today than before to play a premier role in the manufacture of small and intricate surgical devices and biomedical products.

3. References

[1] G. Manivasagam, D. Dhinasekaran, A. Rajamanickam, Biomedical implants: corrosion and its prevention-areview, Recent patents on corrosion science, (2010).

[2] W. Ahmed, M.J. Jackson, Surgical tools and medical devices, Springer2016.

[3] A. Dehghan-Manshadi, M. Bermingham, M. Dargusch, D. StJohn, M. Qian, Metal Injection Molding of Titanium and Titanium Alloys: Challenges and Recent Development, Powder Technol., 319 (2017) 289-301.

[4] E. Ergul, H.O. Gulsoy, V. Gunay, Effect of sintering parameters on mechanical properties of injection moulded Ti–6Al–4V alloys, Powder Metall., 52 (2009) 65-71.

[5] G.N. Levy, R. Schindel, J.-P. Kruth, Rapid manufacturing and rapid tooling with layer manufacturing (LM) technologies, state of the art and future perspectives, CIRP Annals- Manufacturing Technology, 52 (2003) 589-609.

[6] D.F. Heaney, Handbook of metal injection molding, Woodhead Publishing2018.

[7] D. Heaney, R. Zauner, C. Binet, K. Cowan, J. Piemme, Variability of powdercharacteristics and theireffect on dimensional variability of powderinjection moulded components, Powder Metall., 47 (2004) 144-149.

[8] G. Wen, P. Cao, B. Gabbitas, D. Zhang, N. Edmonds, Development and Design of Binder Systems for Titanium Metal Injection Molding: An Overview, Matall. Mater. Trans. A., 44 (2013) 1530-1547. [9] E. Nyberg, M. Miller, K. Simmons, K.S. Weil, Microstructure and mechanical properties of titanium components fabricated by anew powderinjection molding technique, Mater. Sci. Eng. C, 25 (2005) 336 – 342.

[10] M.D. Hayat, P. Cao, A new lubricant based bindersystem forfeedstock formulation from HDH-Ti powder, Adv. Powder Technol., 27 (2016) 255-261.

[11] M.D. Hayat, P. Cao, Development of PEG/PMMA Based Binders for Ti -Metal Injection Molding, Key Eng. Mater. 704 (2016) 130-138.

[12] G. Thavanayagam, K.L. Pickering, J.E. Swan, P. Cao, Analysis of rheological behaviourof titanium feedstocks formulated with awater-solublebindersystem forpowderinjection molding, Powder Technol., 269 (2015) 227-232.

[13] Y. Kaneko, K. Ameyama, S. Sakaguchi, Application of Injection Molding to Ti-5wt%Co and Ti- 6wt%Al-4wt%V Mixed Powders, J. Jpn. Soc. Powder Metall., 37 (1990) 605.

[14] K. Kato, Effect of Sintering Temperature on Density and Tensile Properties of Titanium Compacts by Metal Injection Molding, J. Jpn. Soc. Powder Metall., 46 (1999) 865-869.

[15] G. Chen, P. Cao, G. Wen, N. Edmonds, Debinding behaviourof awatersoluble PEG/PMMA binderfor Ti metal injection molding, Mater. Chem. Phys., 139 (2013) 557–565.

[16] G. Wen, P. Cao, Design Strategy of Binder Systems for Ti Injection Molding, Key Eng. Mater. 520 (2012) 161-166

[17] A.T. Sidambe, I.A. Figuero, H. Hamilton, I. Todd, Metal injection molding of Ti -64 components using a watersoluble binder, PIMInter., 4 (2010) 56-62.

[18] T. Ebel, Metal injection molding (MIM) of titanium and titanium alloys, in: D.F. Heaney (Ed.) Handbook of Metal Injection Molding, Woodhead Publishing Limited, Cambridge, 2012, pp. 415-445. [19] R.M. German, Titanium powderinjection molding: A review of the current status of materials, processing, properties and applications, PIMInter. 3 (2009) 21-37.

[20] E. Carren˜o-Morelli, J.-E. Bidaux, M. Rodrı´guez-Arbaizar, H. Girard, H. Hamdan, Production of titanium grade 4 components by powderinjection molding of titanium hydride, Powder Metall., 57 (2014) 89-92.

[21] M.-S. Huang, H.-C. Hsu, Effect of backbone polymeron properties of 316L stainless steel MIM compact, J Mater. Proc. Technol., 209 (2009) 5527-5535.

[22] A. Dehghan-Manshadi, Y. Chen, Z. Shi, M. Bermingham, D. StJohn, M. Dargusch, M. Qian, Porous Titanium Scaffolds Fabricated by Metal Injection Molding for Biomedical Applications, Mater., 11 (2018) 1573.

[23] V. Friederici, M. Ellerhorst, P. Imgrund, S. Kra¨mer, N. Ludwig, Metal injection molding of thin- walled titanium parts formedical applications, Powder Metall., 57 (2014) 5-8.

[24] R. Gerling, F.P. Schimansky, G. Wegmann, Metal Injection Molding Using Intermetallic γ-TiAl Alloy Powder, Adv. Eng. Mater., 3 (2001) 387-390.

[25] S. Guo, B. Duan, X. He, X. Qu, Powderinjection molding of pure titanium, Rare Met., 28 (2009) 261-269.

[26] M. Omar, H. Davies, P. Messer, B. Ellis, The influence of PMMA content on the properties of 316L stainless steel MIMcompact, J Mater. Proc. Technol., 113 (2001) 477-481.

[27] H. Bakan, Y. Jumadi, P. Messer, H. Davies, B. Ellis, Study of processing parameters for MIM feedstock based on composite PEG-PMMA binder, Powder Metall., 41 (1998) 289-291.

[28] A.B. Nagaram, T. Ebel, Development of Ti-22Nb-xZr Using Metal Injection Molding for Biomedical Applications, Key Eng. Mater., 704 (2016) 334-342.

[29] D. Zhao, K. Chang, T. Ebel, M. Qian, R. Willumeit, M. Yan, F. Pyczak, Titanium carbide precipitation in Ti–22Nb alloy fabricated by metal injection molding, Powder Metall., 57 (2014) 2-4. [30] D. Zhao, K. Chang, T. Ebel, M. Qian, R. Willumeit, M. Yan, FlorianPyczak, Microstructure and mechanical behaviorof metal injection molded Ti–Nb binary alloys as biomedical material, J Mech. Prop. Biomater., 28 (2013) 171-182.

[31] A. Dehghan-Manshadi, M. Qian, M. Dargusch, Y. Chen, D. StJohn, Optimisation of Processing Parameters for Metal Injection Molding of Titanium Using Non-Spherical Titanium Powders, J Manuf. Process., 31 (2018) 416-423.

[32] T. Ebel, Metal Injection Molding of Titanium, Mater. Sci. Forum, 690 (2011) 181-184 [33] A.T. Sidambe, I.A. Figueroa, H.G.C. Hamilton, I. Todd, Metal injection molding of CP -Ti components forbiomedical applications, J Mater. Proc. Technol., 212 (2012) 1591-1597.

[34] J. Bidaux, C. Closuit, M. Rodriguez-Arbaizar, D. Zufferey, E. Carreño-Morelli, Processing of a low modulus Ti–Nb biomaterialby Metal Injection Molding (MIM), PIMInter., 6 (2012) 72-75.

[35] K. Cho, M. Niinomi, M. Nakai, H. Liu, P.F. Santos, Y. Itoh, M. Ikeda, T. Narushima, Improvement in mechanical strength of low-cost β-type Ti–Mn alloys fabricated by metal injection molding through cold rolling, J Alloy Comp., 664 (2016) 272-283.

[36] M. Aslam, F. Ahmad, P.S.M.B.M. Yusoff, K. Altaf, M.A. Omar, R.M. German, Powderinjection molding of biocompatible stainless steel biodevices, Powder Technol., 295 (2016) 84-95.

[37] A. Wahi, N. Muhamad, A.B. Sulong, R.N. Ahmad, Effect of sintering temperature on density, hardness and strength of MIM Co30Cr6Mo biomedical alloy, J. Jpn. Soc. Powder Metall., 63 (2016) 434-437.

[38] M. Wolff, J. Schaper, M. Suckert, M. Dahms, T. Ebel, R. Willumeit-Römer, T. Klassen, Magnesium Powder Injection Molding (MIM) of Orthopedic Implants for Biomedical Applications, JOM, 68 (2016) 1191-1197.

[39] B. Williams, WORLDPM2018 Congress: Global MIM markets show healthy growth, PIMInter., 12 (2018) 67-75.

[40] H.O. Gulsoy, S. Pazarlioglu, N. Gulsoy, B. Gundede, O. Mutlu, Effect of Zr, Nb and Ti addition on injection molded 316L stainless steel forbio-applications: Mechanical, electrochemical and biocompatibility properties, J Mech. Prop. Biomater., 51 (2015) 215-224.

[41] M. Sumita, T. Hanawa, S. Teoh, Development of nitrogen-containing nickel-free austenitic

Stainless steels formetallicbiomaterials, Mater. Sci. Eng. C, 24 (2004) 753-760.

[42] G. Rondelli, P. Torricelli, M. Fini, R. Giardino, In vitro corrosion study by EIS of a nickel -free stainless steel fororthopaedicapplications, Biomater., 26 (2005) 739-744.

[43] A.P.C. Barbosa, M. Bram, D. Stöver, H.P. Buchkremer, Realization of a Titanium Spinal Implant with a Gradient in Porosity by 2-Component-Metal Injection Molding, Adv. Eng. Mater., 15 (2013) 510-521.

[44] R.M. German, Status of Metal Injection Molding of Titanium, Inter. J Powder Metall., 46 (2010) 11-17.

[45] V. Melli, M. Juszczyk, E. Sandrini, G. Bolelli, B. Bonferroni, L. Lusvarghi, A. Cigada, T. Manfredini,

L. De Nardo, Tribological and mechanical performance evaluation of metal prosthesis components manufactured viametal injection molding, Journalof Materials Science: Materials in Medicine, 26 (2015) 8.

[46] P. Mariot, M. Leeflang, L. Schaeffer, J. Zhou, An investigation on the properties of injection- molded pure iron potentially forbiodegradable stent application, Powder Technol., 294 (2016) 226- 235.

[47] E. Carren˜o-Morelli, M.R.g.-A.A. Amherd, J.-E. Bidaux, Porous titanium processed by powder injection molding of titanium hydrideand space holders, Powder Metall., 57 (2014) 93-97.

[48] N.d.F. Daudt, M. Bram, A.P.C. Barbosa, A.M. Laptev, C. Alves Jr, Manufacturing of highly porous titanium by metal injection molding in combination with plasma treatment, J Mater. Proc. Technol., 239 (2017) 202-209.

[49] N. Tuncer, M. Bram, A. Laptev, T. Beck, A. Moser, H.P. Buchkremer, Study of metal injection molding of highly porous titanium by physical modeling and direct experiments, J Mater. Proc. Technol., 214 (2014) 1352-1360.

[50] R. German, Metal powderinjection molding (MIM): key trends and markets, Handbook of metal injection molding, Elsevier2012, pp. 1-25.

[51] T. Deguchi, M. Ito, A. Obata, Y. Koh, T. Yamagishi, Y. Oshida, Trial production of titanium orthodonticbrackets fabricated by metal injection molding (MIM) with sintering, Journalof dental research, 75 (1996) 1491-1496.

[52] R.M. German, Progress in Titanium Metal Powder Injection Molding, Mater. 6 (2013) 3641- 3662.

[53] D. Gabriele Floria, L. Cand, Metal injection molding in orthodontics, Virtual J Orthod, 2 (1997) 1. [54] S. Ahn, C.J. Hwang, Y.-S. Kwon, S.J. Park, R.M. German, Development of Ultrasonic Dental Tips by Powder Injection Molding, Inter. J Powder Metall., 48 (2012) 11.

[55] F. TJ, V. MT, C. J, S. M, G. PT, Manufacturing Dental Implants using Powder Injection Molding, Journal of Orthodontics & Endodontics, 2 (2016) 1-7.

[56] J. Li, B. Liu, Y. Zhou, Z. Chen, L. Jiang, W. Yuan, L. Liang, Fabrication of a Ti porous microneedle array by metal injection molding fortransdermal drug delivery, PloS one, 12 (2017) e0172043.

[57] N. Williams, Metal Injection Molding: Building on solid foundations in the medical sector, PIM Inter., 11 (2017) 43-57.

[58] M. Hamidi, W. Harun, M. Samykano, S. Ghani, Z. Ghazalli, F. Ahmad, A. Sulong, A review of biocompatiblemetal injection molding process parameters forbiomedical applications, Mater. Sci. Eng. C, (2017).

[59] A. Dehghan-Manshadi, M.R. Barnett, P. Hodgson, Hot deformation and recrystallization of austeniticstainless steel: Part I. Dynamicrecrystallization, Matall. Mater. Trans. A., 39 (2008) 1359- 1370.

[60] C. Ji, N. Loh, K. Khor, S. Tor, Sintering study of 316L stainless steel metalinjection molding parts using Taguchi method: final density, Mater. Sci. Eng. A, 311 (2001) 74-82.

[61] P. Imgrund, A. Rota, A. Simchi, Microinjection molding of 316L/17-4PH and 316L/Fe powders for fabrication of magnetic–nonmagneticbimetals, J Mater. Proc. Technol., 200 (2008) 259-264. [62] P. Suri, R.P. Koseski, R.M. German, Microstructural evolution of injection molded gas- and

Water-atomized 316L stainless steelpowderduring sintering, Mater. Sci. Eng. A, 402 (2005) 341-348. [63] J. Torralba, Metal injection molding (MIM) of stainless steel, Handbook of Metal Injection Molding, Elsevier2012, pp. 393-414.

[64] J. Disegi, L. Eschbach, Stainless steelin bone surgery, Injury, 31 (2000) D2-D6.

[65] M. Fini, N.N. Aldini, P. Torricelli, G. Giavaresi, V. Borsari, H. Lenger, J. Bernauer, R. Giardino, R. Chiesa, A. Cigada, A new austeniticstainless steel with negligible nickel content: an in vitro and in vivo comparative investigation, Biomater., 24 (2003) 4929-4939.

[66] L. Montanaro, M. Cervellati, D. Campoccia, C. Prati, L. Breschi, C.R. Arciola, No genotoxicity of a new nickel-freestainless steel, The International journal of artificialorgans, 28 (2005) 58-65.

[67] Y. Li, L. Li, K. Khalil, Effect of powderloading on metal injection molding stainless steels, J Mater. Proc. Technol., 183 (2007) 432-439.

[68] E. Bayraktaroglu, H.O. Gulsoy, N. Gulsoy, O. Er, H. Kilic, Effect of boron addition on injection molded 316L stainless steel: Mechanical, corrosion properties and in vitro bioactivity, Biomed. Mater. Eng., 22 (2012) 333-349.

[69] H. Rack, J. Qazi, Titanium alloys forbiomedical applications, Mater. Sci. Eng. C, 26 (2006) 1269- 1277.

[70] M. Niinomi,M. Nakai, Titanium-based biomaterials forpreventing stress shielding between implant devices and bone, Inter. J Biomater., 2011 (2011).

[71] A. Sidambe, Biocompatibility of advanced manufactured titanium implants—A review, Mater. 7 (2014) 8168-8188.

[72] C. Elias, J.H. Lima, R. Valiev, M. Meyers, Biomedical applications of titanium and its al loys, JOM,

60 (2008) 46-49.

[73] T. Ebel, Advances in the Metal Injection Molding of Titanium at Euro PM2014, PIM Inter., 9 (2015) 51-61.

[74] F.H. Froes, Advances in Titanium Metal Injection Molding, Powder Metall. Met. Ceram. 46 (2007) 303-310.

[75] M. Scharvogel, Titanium Metal Injection Molding - A Commercial Overview, Key Eng. Mater. 704 (2016) 107-112.

[76] J.C. Piemme, J.A. Grohowski, Titanium Metal Injection Molding, a Qualified Manufacturing Process, Key Eng. Mater. 704 (2016) 122-129.

[77] T. Ebel, O.M. Ferri, Metal injection molding of advanced titanium alloys, Adv. Powder Metall. Part. Mater. 1 (2011) 45-47.

[78] P.F. Santos, M. Niinomi, H. Liu, K. Cho, M. Nakai, Y. Itoh, T. Narushima, M. Ikeda, Fabrication of low-cost beta-type Ti–Mn alloys forbiomedical applications by metal injection molding process and theirmechanical properties, J Mech. Prop. Biomater., 59 (2016) 497-507.

[79] T. Ebel, Titanium MIM for manufacturing of medical implants and devices, Titanium in Medical and Dental Applications, Elsevier2018, pp. 531-551.

[80] M.D. Hayat, G. Wena, T. Li, P. Cao, Compatibility improvement of Ti-MIMfeedstock using liquidsurfactant, J Mater. Proc. Technol., 224 (2015) 33-39.

[81] F2885-11, Standard Specification for Metal Injection Molded Titanium-6Aluminum-4Vanadium Components for Surgical Implant Applications, ASTMInternational, 2011.

[82] F2989-13, Standard Specification for Metal Injection Molded Unalloyed Titanium Components for Surgical Implant Applications, ASTMInternational, 2013.

[83] E. Aust, W. Limberg, R. Gerling, B. Oger, T. Ebel, Advanced TiAl6Nb7 bone screw implant fabricated by metal injection molding, Adv. Eng. Mater., 8 (2006) 365-370.

[84] O.M. Ferri, T. Ebel, R. Bormann, Influence of surface quality and porosity on fatigue behaviourof Ti–6Al–4V components processed by MIM, Mater. Sci. Eng. A, 527 (2010) 1800-1805.

[85] O.M. Ferri, T. Ebel, R. Bormann, The influenceof asmall boron addition on the microstructure an dmechanical properties of Ti-6Al-4V fabricated by Metal Injection molding, Adv. Eng. Mater., 13 (2011) 436-447.

[86] O.M. Ferri, T. Ebel, R. Bormannb, High cycle fatigue behaviourof Ti–6Al–4V fabricated by metal injection molding technology, Mater. Sci. Eng. A, 504 (2009) 107-113.

[87] N.F. Daudt, M. Bram, A.P.C. Barbosa, C.A. Jr., Surface modification of highly porous titanium by plasma treatment, Mater. Lett. 141 (2015) 194-197.

[88] A. Wennerberg, The importance of surface roughness for implant incorporation, International Journal of Machine Tools and Manufacture, 38 (1998) 657-662.

[89] G.C. Obasi, O.M. Ferri, T. Ebel, R. Bormann, Influence of processing parameters on mechanical properties of Ti–6Al–4V alloy fabricated by MIM Mater. Sci. Eng. A, 527 (2010) 3929-3935.

[90] L. Bolzoni, E.M. Ruiz-Navas, E. Gordo, Evaluation of the mechanical properties of powder metallurgy Ti-6Al-7Nb alloy, J Mech. Prop. Biomater. 67 (2017) 110-116.

[91] T. Ebel, C. Blawert, R. Willumeit, Ti–6Al–4V–0.5B---A Modified Alloy for Implants Produced by Metal Injection Molding, Adv. Eng. Mater. 13 (2011) B440-B453.

[92] J.-E. Bidaux, R. Pasquier, M. Rodriguez-Arbaizar, H. Girard, E. Carren˜o-Morelli, Low elastic modulus Ti–17Nb processed by powderinjection molding and post-sintering heat treatments, Powder Metall., 57 (2014) 320-323.

[93] W. Xu, X. Lu, L. Wang, Z. Shi, S. Lv, M. Qian, X. Qu, Mechanical properties, in vitro corrosion resistance and biocompatibility of metal injection molded Ti-12Mo alloy fordental applications, J Mech. Prop. Biomater. 88 (2018) 534-547.

[94] Y. Itoh, H. Miura, T. Uematsu, T. Osada, K. Sato, Effect of Fe or Cr addition on the strengthening Ti-6Al-4V alloy by metal injection molding, Journal of Solid Mechanics and Materials Engineering, 3 (2009) 921-930.

[95] F. Kafkas, T. Ebel, Metallurgical and mechanicalproperties of Ti–24Nb–4Zr–8Sn alloy fabricated by metal injection molding, J Alloy Comp., 617 (2014) 359-366.

[96] P. Xu, T. Ebel, W. Limberg, A. Amherd, A.A. Hidalgo, F. Pyczak, R. Willumeit-Römer, MIM- Processed High-Ductility β-type Ti-Nb-Zr-Y Alloy for Biomaterial Applications, Euro PM2018, European Powder Metallurgy Association (EPMA), Bilbao, Spain, 2018.

[97] B. Williams, World PM2016: PIM technical sessions review advances in novel titanium alloys for biomedical applications, PIMInter., 10 (2016) 51-58.

[98] L.P. Lefebvre, J. Banhart, D.C. Dunand, Porous metals and metallicfoams: current status and recent developments, Adv. Eng. Mater., 10 (2008) 775-787.

[99] G. Lütjering, J.C. Williams, Titanium, Engineering Materials and Processes, 2nd ed., Springer Science & Business Media, Berlin, Germany, 2007.

[100] X. Zhang, M. Leary, H. Tang, T. Song, M. Qian, Selectiveelectron beam manufactured Ti -6Al-4V lattice structures fororthopedicimplant applications: Current status and outstanding challenges, Current Opinion in Solid State and Materials Science, (2018).

[101] H. Nelles, M. Bram, H.P. Buchkremer, D. Stöver, Method forthe production of nearnet-shaped metallicand/orceramicparts, US Patent: 7351371, 2008.

[102] E. Carreño-Morelli, A. Amherd, M. Rodriguez-Arbaizar, D. Zufferey, A. Várez, J.-E. Bidaux, Porous titanium by powderinjection molding of titanium hydrideand PMMA space holders, Eur. Cells Mater., 26 (2013) 16.

[103] L.-j. Chen, T. Li, Y.-m. Li, H. He, Y.-h. Hu, Porous titanium implants fabricated by metal injection molding, Trans. Nonferr. Met. Soc. China, 19 (2009) 1174-1179.

[104] H. Guoxin, Z. Lixiang, F. Yunliang, L. Yanhong, Fabrication of high porous NiTi shape memory alloy by metal injection molding, J Mater Proc. Technol. , 206 (2008) 395-399.

[105] A.M. Laptev, N.a.F. Daudt, O. Guillon, M. Bram, Increased Shape Stability and Porosity of Highly Porous Injection-Molded Titanium Parts, Adv. Eng. Mater. 17 (2015) 1579-1587.

[106] C. Torres-Sanchez, F. Al Mushref, M. Norrito, K. Yendall, Y. Liu, P.P. Conway, The effect of pore size and porosity on mechanical properties and biological responseof porous titanium scaffolds, Mater. Sci. Eng. C, 77 (2017) 219-228.

[107] S. Özbilen, D. Liebert, T. Beck, M. Bram, Fatigue behaviorof highly porous titanium produced by powdermetallurgy with temporary space holders, Mater. Sci. Eng. C, 60 (2016) 446-457.

[108] H.Ö. Gülsoy, R.M. German, Production of micro-porous austeniticstainless steel by powder injection molding, Scrip. Mater. 58 (2008) 295-298.

[109] K. Nishiyabu, Powderspace holdermetal injection molding (PSH-MIM) of micro-porous metals, Handbook of Metal Injection Molding, Elsevier2012, pp. 349-390.

[110] Y. Chen, D. Kent, M. Bermingham, A. Dehghan-Manshadi, M. Dargusch, Manufacturing of biocompatibleporous titanium scaffolds using anovel spherical sugarpellet space holder, Mater. Lett., 195 (2017) 92-95.

[111] P. Suri, Two-material/two-colorpowdermetal injection molding (2C-PIM), Handbook of metal injection molding, Elsevier2012, pp. 338-348.

[112] M. Mulser, F. Petzoldt, Two-Component Metal Injection Molding of Ti-6Al-4V and Stainless Steel Bi-Material Parts, Key Eng. Mater. 704 (2016) 148-154.

[113] A.P.C. Barbosa, Development of the 2-component-injection Molding for Metal Powders, Forschungszentrum Jülich2011.

[114] R. German, The evolution of Powder Injection Molding: Past perspectives and future growth, PIM Inter., 13 (2019) 57-68.

[115] T. Ebel, PMTi 2017 Xi'an: Titanium MIM comes of age as Additive Manufacturing drives awareness, PIMInter., 11 (2017) 61-73.

[116] L. Machado, M. Savi, Medical applications of shape memory alloys, Brazilian journalof medical and biological research, 36 (2003) 683-691.

[117] T. Yoneyama, S. Miyazaki, Shape memory alloys forbiomedical applications, Elsevier2008. [118] M. Bram, T. Ebel, M. Wolff, A.C. Barbosa, N. Tuncer, Applications of powdermetallurgy in biomaterials, Advances in powdermetallurgy, Elsevier2013, pp. 520-554.

[119] M.H. Elahinia, M. Hashemi, M. Tabesh, S.B. Bhaduri, Manufacturing and processing of NiTi implants: A review, Prog Mater Sci, 57 (2012) 911-946.

[120] M. Chen, X. Yang, R. Hu, Z. Cui, H. Man, Bioactive NiTi shape memory alloy used as bone bonding implants, Mater. Sci. Eng. C, 24 (2004) 497-502.

[121] A. Bansiddhi, T. Sargeant, S. Stupp, D. Dunand, Porous NiTi forbone implants: areview, Acta Biomater., 4 (2008) 773-782.

[122] B.V. Krishna, S. Bose, A. Bandyopadhyay, Laserprocessing of net-shape NiTi shape memory alloy, Matall. Mater. Trans. A., 38 (2007) 1096-1103.

[123] I. Shishkovsky, Y. Morozov, I. Smurov, Nanofractal surface structure underlasersintering of titanium and nitinol forbone tissue engineering,Applied Surface Science, 254 (2007) 1145-1149.

[124] M. Es-Souni, M. Es-Souni, H. Fischer-Brandies, Assessing the biocompatibility of NiTi shape memory alloys used formedical applications, Analytical and bioanalytical chemistry, 381 (2005) 557- 567.

[125] M.H. Ismail, R. Razali, Z. Abdullah, I. Subuki, N. Muhamad, Shape Memory Behaviourof NiTi Alloy Produced by MIM using Palm Stearin Based Binder, Adv. Mater. Res., Trans Tech Publ, 2016, pp. 295-299.

[126] E. Schöller, L. Krone, M. Bram, H. Buchkremer, D. Ståaver, Metal injection molding of shape memory alloys using prealloyed NiTi powders, J. Mater. Sci., 40 (2005) 4231-4238.

[127] M. Bram, M. Bitzer, H. Buchkremer, D. Stöver, Reproducibility study of NiTi parts made by metal injection molding, J Mater. Eng. Perform. 21 (2012) 2701-2712.

[128] M. Bram, A. Ahmad-Khanlou, A. Heckmann, B. Fuchs, H. Buchkremer, D. Stöver, Powder metallurgical fabrication processes for NiTi shape memory alloy parts, Mater. Sci. Eng. A, 337 (2002) 254-263.

[129] L. Krone, J. Mentz, M. Bram, H.P. Buchkremer, D. Stöver, M. Wagner, G. Eggeler, D. Christ, S. Reese, D. Bogdanski, The Potential of Powder Metallurgy forthe Fabrication of Biomaterials on the Basis of Nickel-Titanium: A Case Study with a Staple Showing Shape Memory Behaviour, Adv. Eng. Mater., 7 (2005) 613-619.

[130] M. Köhl, T. Habijan, M. Bram, H.P. Buchkremer, D. Stöver, M. Köller, Powder Metallurgical Near-Net-Shape Fabrication of Porous NiTi Shape Memory Alloys for Use as Long-Term Implants by the Combination of the Metal Injection Molding Process with the Space-Holder Technique, Adv. Eng. Mater., 11 (2009) 959-968.

[131] M. Köhl, M. Bram, A. Moser, H. Buchkremer, T. Beck, D. Stöver, Characterization of porous, net-shaped NiTi alloy regarding its damping and energy-absorbing capacity, Mater. Sci. Eng. A, 528 (2011) 2454-2462.

[132] Z. Li, X. Gu, S. Lou, Y. Zheng, The development of binary Mg–Ca alloys foruse as biodegradable materials within bone, Biomater., 29 (2008) 1329-1344.

[133] F. Rosalbino, S. De Negri, A. Saccone, E. Angelini, S. Delfino, Bio-corrosion characterization of Mg–Zn–X (X= Ca, Mn, Si) alloys forbiomedical applications, Journalof Materials Science: Materials in Medicine, 21 (2010) 1091-1098.

[134] M. Wolff, J. Schaper, M. Dahms, T. Ebel, K. Kainer, T. Klassen, Magnesium powderinjection molding forbiomedical application, Powder Metall., 57 (2014) 331-340.

[135] M. Wolff, J. Schaper, M. Suckert, M. Dahms, F. Feyerabend, T. Ebel, R. Willumeit-Römer, T. Klassen, Metal injection molding (MIM) of magnesium and its alloys, Metals, 6 (2016) 118.

[136] J.G. Schaper, M. Wolff, B. Wiese, T. Ebel, R. Willumeit-Römer, Powdermetal injection molding and heat treatment of AZ81 Mg alloy, J Mater. Proc. Technol., 267 (2019) 241-246.

[137] M. Dargusch, A. Dehghan-Manshadi, M. Shahbazi, J. Venezuela, X. Tran, J. Song, N. Liu, C. Xu,

Q. Ye, C. Wen, Exploring the role of manganese on the microstructure, mechanical properties, biodegradability and biocompatibility of porous iron-based scaffolds, ACS Biomaterials Science & Engineering, (2019).

[138] M. Fontecave, J. Pierre, Iron: metabolism, toxicity and therapy, Biochimie, 75 (1993) 767-773. [139] Y. Zheng, X. Gu, F. Witte, Biodegradable metals, Mater. Sci. Eng., R, 77 (2014) 1-34.

[140] H. Hermawan, D. Dubé, D. Mantovani, Degradable metallicbiomaterials: design and development of Fe–Mn alloys forstents, J Biomed. Mater. Res. A, 93 (2010) 1-11.

[141] J. He, F.-L. He, D.-W. Li, Y.-L. Liu, Y.-Y. Liu, Y.-J. Ye, D.-C. Yin, Advances in Fe-based biodegradablemetallicmaterials, RSC Advances, 6 (2016) 112819-112838.

[142] M. Schinhammer, A.C. Hänzi, J.F. Löffler, P.J. Uggowitzer, Design strategy forbiodegradable Fe- based alloys formedical applications, Acta Biomater., 6 (2010) 1705-1713.

[143] A. Reindl, R. Borowsky, S.B. Hein, J. Geis-Gerstorfer, P. Imgrund, F. Petzoldt, Degradation behaviorof novel Fe/ß-TCP composites produced by powderinjection molding forcortical bone replacement, J. Mater. Sci., 49 (2014) 8234-8243.

Nonlinear Induced Heating in Biological Tissue for High Intensity Focused Ultrasound Using Comsol

Nastaran Faghihi[2*], Heydar Izadneshan[1]

[2]Department of engineering, Estahban Branch, Islamic Azad University, Estahban, Iran

[1]Department of Photonics, Marvdasht Branch, Islamic Azad University, Marvdasht, Iran

*n.faghihi78@gmail.com

Abstract

The present study aims to predict the induce of high intensity focused ultrasound (HIFU) in soft tissues to assess tissue damage during HIFU thermal therapies. With the help of a COMSOL software modules developed for HIFU simulation, the HIFU beam was simulated by solving the EMF equation from the frequency-domain perspective. In order to verify the simulation results, we performed in-vitro heating experiments on a tissue-mimicking phantom by employing a 1.1-MHz, single-element, spherically focused HIFU transducer. The temperature rises near the focal spot obtained from the HIFU simulator was in good agreement with that from the in-vitro experiments. Results can be show that measured and the simulated peak positive pressures are in good agreement along the beam axis.

Keywords: HIFU, COMSOL, ultrasound, SAR

1. Introduction

High intensity focused ultrasound applies high intensity focused ultrasound power to locally warmness and spoil diseased or broken tissue via ablation. Ultrasound beam may be targeted geometrically via lens or a spherically curved transducer, or electronically through adjusting the relative phases of elements in an array of transducer. Since HIFU penetrates the covering tissue adequately and best destroys the tissue at focal location deep with inside the body, it's far considered as a non-invasive modality of treatment. Compared with conventional surgical resection and chemotherapy, HIFU gives extremely good advantages.

The first research to analyze the bio-effect of focused ultrasound become mentioned in 1942[1]. A focused ultrasound generator become designed, built, and operated via way of means of Lynn et al. and nearby brain effect in animals produced by focused ultrasound of high intensity become demonstrated. In the 1950s and 1960s, HIFU become used to provide lesions (the broken tissue quantity is generally known as a 'lesion') in brain [2]. The first utility of HIFU in human become the treatment of Parkinson's disorder and painful neuromata mentioned in 1960[3]. However, this treatment become now no longer taken in addition likely due to the improvement of the drug L-dopa. What is more, the early research had been restrained due to the fact technology for specific photo

guidance and harm tracking become now no longer available. With the improvement of photo steering and phased array technology, ultrasound phased array transducer and computed tomography (CT) scans were used to attain a non-invasive adaptive focusing withinside the transcranial surgical procedure withinside the early twenty first century. In 2009, the primary report on a success medical utility of transcranial magnetic resonance-guided focused ultrasound (tcMRgFUS) in purposeful brain problems indicates all treatments had been properly tolerated, without side effects or neurological deficits [4,5].

The purpose of this work is to model the HIFU induced heating in a human tissue as a function of the properties of tissue by means of FEM using COMSOL software. As nonlinear propagation was neglected, tissue thermal conductivity temperature dependence was included in heating model in order to obtain both the temperature increment response at the focus and the axial temperature distribution after 120 s sonication [6].

2. Material and Methods

Theoretical predictions of the HIFU field and the HIFU-induced temperature rise were performed by using a freely-distributed, COMSOL software for simulating axisymmetric HIFU beams and their heating effects. The HIFU field was simulated by solving the axisymmetric KZK equation from the frequency domain perspective [7,8]. The KZK equation accounting for the effects of diffraction, absorption, and nonlinearity can be expressed as

$$\frac{\partial p}{\partial z} - \frac{\beta}{\rho_0 c_0^3}\frac{\partial p}{\partial r} - \frac{b}{2\rho_0 c_0^3}\frac{\partial^2 p}{\partial r^2} = \frac{c_0}{2}\int_{-\infty}^{\tau} \nabla_\perp p(\tau')d\tau' \quad (1)$$

where p is the acoustic pressure, z is the propagation coordinate along the beam axis, β is the coefficient of nonlinearity, ρ_0 is the mass density, c_0 is the small-signal sound speed, $\tau = t - z/c_0$ is the retarded time, b is the dissipative parameter, and $\nabla_\perp = \partial^2/\partial r^2 + r^{-1}\,\partial/\partial r$ is the Laplacian with respect to the transverse coordinate r. In the plane wave approximation of Eq. (1), the spatial distributions of the intensity I and the heating rate H can be written in terms of the harmonic amplitudes as

$$I(r.z) = \frac{1}{2\rho_0 c_0}\sum_{k=1}^{K}|\hat{p}_k| \quad (2)$$

and

$$H(r.z) = \frac{1}{\rho_0 c_0}\sum_{k=1}^{K} Re(\alpha_k)|\hat{p}_k|, \quad (3)$$

where $\hat{p}_k$ is the complex-valued pressure field of the kth harmonic and $Re(\alpha_k)$ is the absorption coefficient.

The KZK equation is solved by using a split-step method that permits the linear and the nonlinear terms to be integrated by using different techniques. The linear parts of Eq. (1) are solved in the frequency domain for each of the harmonics included in the calculation. At each integration step, the solution is converted to the time-domain representation via a fast Fourier transform, and the nonlinear part of Eq. (1) is solved by using the upwind method. After integration, the solution is converted back to the frequency-domain representation, and the cycle is repeated until the simulation is complete. The HIFU simulator also has provisions for layered media. If some of the

propagation path is through water and the rest through biological tissues, the code computes the incident beam and the transmitted beam, taking into account the impedance mismatch by using the standard formula.

The HIFU-induced temperature rise in a tissue mimicking phantom was simulated by solving Pennes' BHT equation [9]. The BHT equation accounting for the effects of heat diffusion, blood perfusion, and heat deposition can be expressed as

$$\rho_0 C \frac{\partial T}{\partial t} = \kappa \nabla^2 T + H - \omega C T, \tag{4}$$

where C is the heat capacity, T is the temperature, t is the time, κ is the thermal conductivity, H is the heating rate of Eq. (1), and w is the perfusion rate. The BHT equation is solved by using a second-order finite difference discretization with Dirichlet boundary conditions, and the temperature as a function of the time is evolved by using an efficient second-order implicit Runge Kutta method.

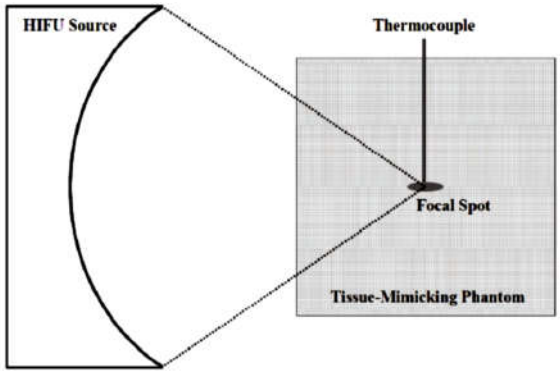

Fig. 1. Relative positions of the HIFU source, the target phantom, and the thermocouple.

a needle-type thermocouple with a diameter of 0.5 mm (HYP-21-1/2-E-G-48, OMEGA Engineering, Stamford, CT) that had been inserted into a position near the ultrasound focal spot.

Figure 1 shows the relative positions of the HIFU source, the target phantom, and the thermocouple. In order to prevent the temperature measurements from being influenced by the incident ultrasound, we embedded the thermocouple perpendicular to the acoustic axis approximately 1 mm away from the focal spot. The exact position of the thermocouple relative to the focal spot was determined off-line by analyzing the camera image. The thermocouple data were converted to a temperature scale as a function of time and was displayed on a temperature monitor (SR630, Stanford Research System, Sunnyvale, CA) and stored on a personal computer for off-line analysis.

The focusing of an ultrasonic signal is typically achieved either by using a phase delay or a focusing lens on the transducer side. In this model, a spherically focused ultrasound transducer with a concave lens is used to emit the signal. The transducer housing and the lens are assumed to be rigid. The model setup is shown in Figure 2. The model geometry is axially symmetric.

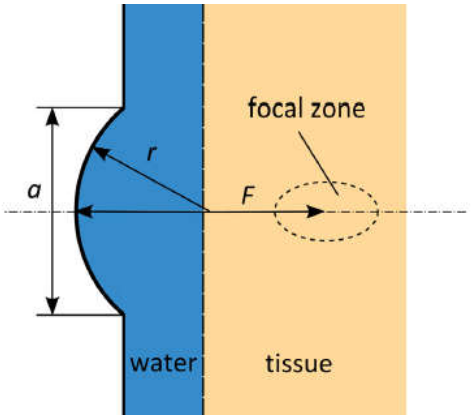

Fig2. Model geometry

The evolution of the signal traveling from the source is illustrated in Figure 3. The tone burst pulse has left the source at t = 10 μs and travels towards the boundary between the water and the tissue phantom domains, which it passes at t = 20 μs with some part being reflected back to the source. The focusing of the signal becomes visible at t = 30 μs and reaches its maximum at t = 40 μs.

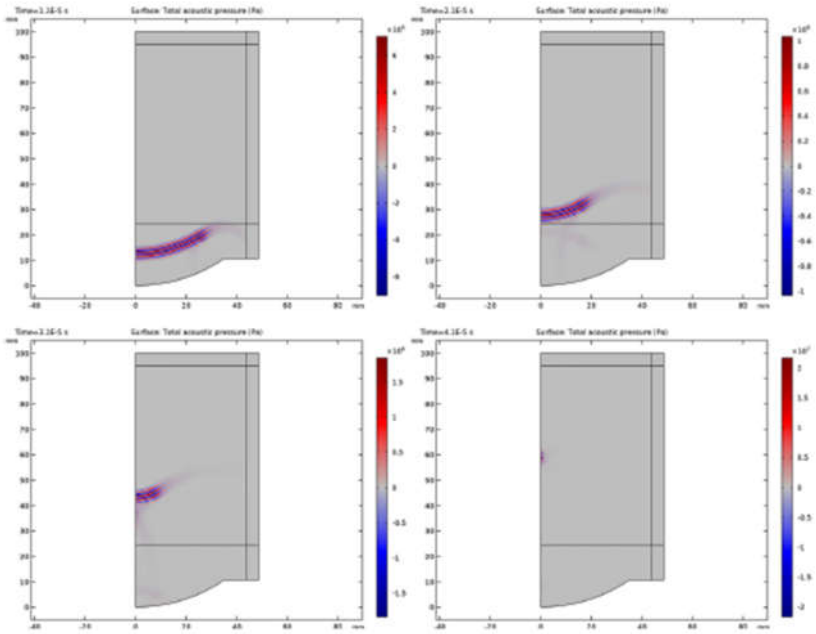

Fig.3 Propagation of the ultrasonic signal at times t = 10, 20, 30, and 40 μs.

It is worth selecting the time-stepping method to Adam-Bashforth 3 (local) and enabling the Update time levels option available in the General section of the time-explicit solver. Figure 4 shows the values of the cell wave time at different values. The smaller values are found for the smaller mesh elements in the vicinity of the signal, while the larger values are used in the rest of the computational domain.

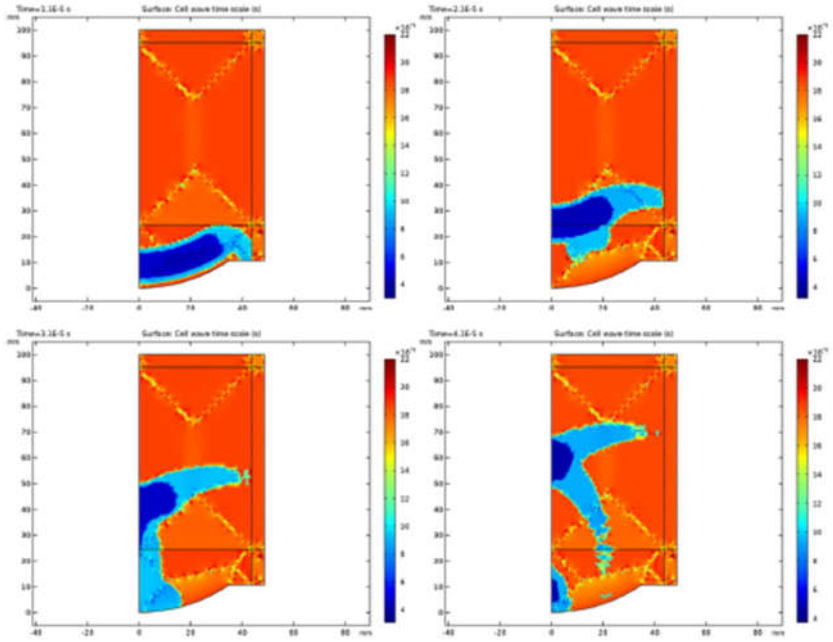

Figure 4: Cell wave time scale at times t = 10, 20, 30, and 40 μs.

3. Results and Discussions

In this paper the influence of HIFU beam on tissue by COMSOL modeling was investigated. Results show that the source pressure calibration was accomplished by comparing precise experimental and numerical results in water. Figure 5 shows the measured and the simulated peak positive (compressional) pressures at the focus without the phantom in water as functions of the source pressure. The asterisks and the solid line correspond to the measured and the simulated results, respectively. As seen in Fig. 5, a linear relationship between the source pressure and the focal peak positive pressure can be observed over the range of the source operation levels used in experiments and simulations. Three source pressures, 0.020, 0.034, and 0.039 MPa, were used in the in-vitro heating experiments. These correspond to driving voltages to the HIFU source of 30, 65, and 80 mV_{pp}, respectively.

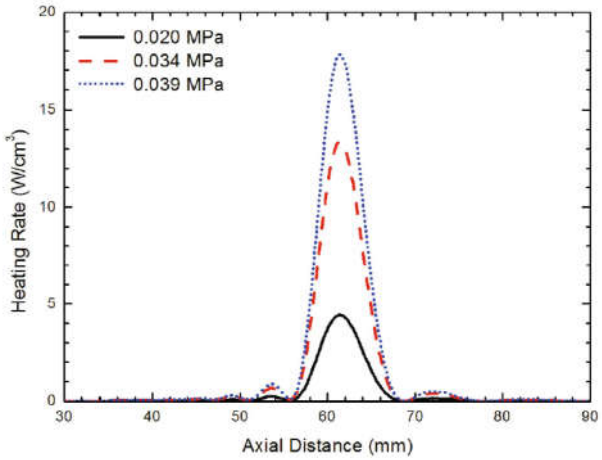

Fig.5. Simulated heating rate along the beam axis with the phantom in water for source pressures of 0.020, 0.034, and 0.039 MPa.

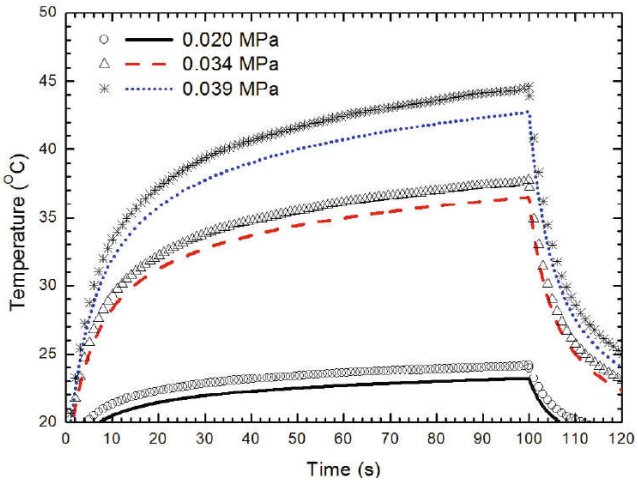

Fig.6. Measured and simulated temperature rise as functions of the time

Figure 6 shows the measured and the simulated temperature rises as functions of the time at a distance of 1 mm from the focal spot with the phantom in water for source pressures of 0.020, 0.034, and 0.039 MPa. The time duration of HIFU exposure was 100 s, and the time step for the temperature measurements was 1 s. One can observe that both the measured and the simulated temperatures increase with increasing time (heating) and rapidly decrease after reaching a maximum at 100 s (cooling). In addition, the peak temperature and the temperature rise rate are found to become larger with increasing source pressure.

References

[1] J.G. Lynn, R.L. Zwemer, A.J. Chick, A.E. Miller, A new method for the generation and use of focused ultrasound in experimental biology. The Journal of general physiology 26 (1942) 179-193.

[2] W.J. Fry, W.H. Mosberg, J.W. Barnard, F.J. Fry, Production of focal destructive lesions in the central nervous system with ultrasound. Journal of Neurosurgery 11 (1954) 471-478.

[3] D.J. Coleman, F.L. Lizzi, J. Driller, A.L. Rosado, S.E. Burgess, J.H. Torpey, M.E. Smith, R.H. Silverman, M.E. Yablonski, S. Chang, Therapeutic ultrasound in the treatment of glaucoma. II. Clinical applications. Ophthalmology 92 (1985a) 347-353.

[4] F. Bellemare, A. Jeanneret, J. Couture, Sex differences in thoracic dimensions and configuration. American Journal of Respiratory and Critical Care Medicine 168 (2003) 305-312.

[5] E. Martin, D. Jeanmonod, A. Morel, E. Zadicario, B. Werner, High-intensity focused ultrasound for noninvasive functional neurosurgery. Annals of Neurology 66 (2009) 858-861.

[6] J. Gao, S. Cochran, Z. Huang, Ultrasound beam distortion and pressure reduction in transcostal focused ultrasound surgery. Applied Acoustics 76 (2014) 337-345.

[7] R. Martínez, A. Vera L. Leija, HIFU induced heating modelling by using the finite element method, Physics Procedia 63 (2015) 127-133.

[8] T. Saliev, D. Begimbetova, A.R. Masoud, B. Matkarimov, Biological effects of non-ionizing electromagnetic fields: Two sides of a coin, Progress in Biophysics and Molecular Biology 141 (2019) 25-36.

[9] K. Lee, Prediction and measurement of temperature rise induced by high intensity focused ultrasound in a tissue-mimicking phantom, Journal of the Korean Physical Society 72 (2018) 1313-1319.

Effect of crosslinking time on the swelling degree of electrospun vancomycin-containing gelatin nanofibers

Mahan Mahdiyani1, Ali Nematollahzadeh2*

[1] Department of Chemical Engineering, University of Mohaghegh Ardabili, Ardabil, Iran

[2] Department of Chemical Engineering, University of Mohaghegh Ardabili, Ardabil, Iran

Nematollahzadeha@uma.ac.ir

Abstract

Nowadays, electrospinning is recognized as one of the best techniques for the production of nanofibers using a wide range of natural and synthetic polymers. The unique characteristics of electrospun nanofibers have given these structures great potential in biomedicine fields such as tissue engineering, drug delivery systems and wound dressing. This study aims to produce vancomycin containing gelatin nanofibers for wound dressing applications. To improve water-resistance properties of Electrospun gelatin nanofibers, these structures were crosslinked by exposing to saturated glutaraldehyde (GTA) vapor. Morphological properties and fiber diameter distribution were examined by field emission scanning electron microscope (FE-SEM). Also, the effect of crosslinking duration on the swelling degree of nanofibers was evaluated and the results showed that increasing the cross-linking duration could reduce the swelling degree of electrospun gelatin nanofibers.

Keywords: Electrospinning, Nanofibers, Swelling degree, Wound dressing, Crosslinking.

1. Introduction

Millions of people suffer from severe burns each year, and thousands of them die from wound injuries [1]. Current strategies for wound healing can limit the healing process of patients suffering from skin ulcers or chronic wounds. It is clear that a proper wound dressing will play an important role in the wound healing process. An ideal wound dressing not only provides favorable mechanical protection of the wound surface but also should has the ability of gas exchange, absorb excess wound secretions, antimicrobial activity, and creating a suitable moist environment to improve skin repairing process and it should be painless to remove [2]. Currently, different types of wound dressings that are produced from different materials and methods are commercially available [3-5], but due to the growing needs in this field, more studies need to be done on this subject.

Nanotechnology has made great strides over the past decade and nowadays, it covers a variety of areas. Generally, nanomaterials are highly regarded due to their small size, high surface to volume ratio, ability to load, and release bioactive molecules [6, 7]. Among them, nanofibers are known as one of the most important nanostructures and have been developed in various fields such as environment [8], health care [9], drug delivery systems [7], tissue engineering [10], and wound dressing [11]. Porous structure, very high surface-to-volume ratio, controllable loading, and release capacity of bioactive molecules are their specific features that have made

nanofibers even more important. Until now, various methods such as solution blowing [12], centrifugal spinning [13], phase inversion [14], and electrospinning have been proposed for the production of fibers. Among these methods, electrospinning due to the simplicity of the process and ease of operation attracted lots of attention. This technique employs a high potential difference (up to 30 kV) between a polymer solution flowing through a capillary niddle towards a. metallic collector to produce nanofibers [15]. (The schematic of the electrostatic process is shown in Figure 1). Electrospinning can control the properties of the produced fibers and became a reliable way to produce tissue engineering and drug delivery scaffolds. These fibers can mimic the extracellular matrix (ECM) which has led to improve cell proliferation and differentiation, and as a result, damaged tissue heals in less time [16]. So far, numerous articles have been published on the use of electrospun nanofibers to produce drug carriers or structures for repairing and regenerating damaged tissues, a combination of engineering and biological principles are required.

Gelatin has become one of the most widely used biopolymers in the biological fields due to its biocompatibility, biodegradation, and non-immunogenic properties [17]. So far, several studies have been conducted on the production of nanofibers using gelatin [18-20]. Gelatin nanofibers dissolve easily in water in a few seconds which limits the applications of these structures for long-term use. Therefore, it is necessary to cross-link the generated structures with the help of physical or chemical methods. Glutaraldehyde (GTA) is one of the most popular cross-linkers for proteins and has a high ability to cross-link collagenous materials such as collagen and gelatin [21]. Lysine, One of the structural amino acids of gelatin, reacts with glutaraldehyde and is the main cause of cross-linking of collagenous nanofibers [21].

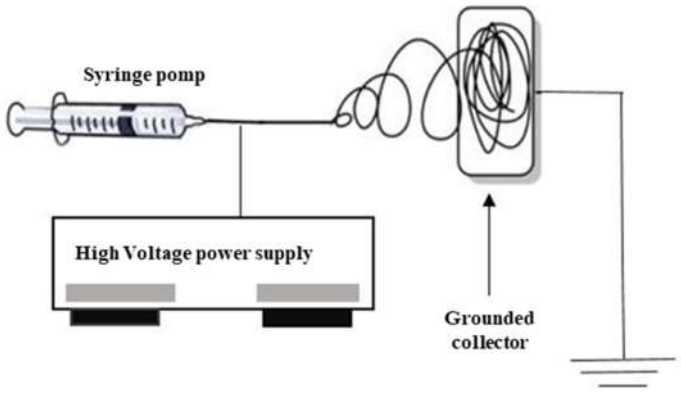

Figure 1: A schematic of the electrospinning process

This study aims to produce gelatin nanofibers containing a glycopeptide antibiotic (vancomycin) and investigating the ability of these structures to absorb physiological buffer. It should be noted that the degree of swelling of the produced structures can indicate the ability of these nanofibers to absorb excess wound secretions.

2. Material and Methods

2.1 Materials

Gelatin type A (food grade), dichloromethane (DCM), acetic acid (purity>%99), and aqueous glutaraldehyde (GTA) solution (25%) was purchased from Merck Co. Germany. Vancomycin hydrochloride (VAN) powder form was purchased from Behdaro Co. Iran. The polymer and the solvent were used without further purification.

2.2 Electrospinning

Gelatin solution with a concentration of 17.5% (w/v) was made in a mixture of acetic acid and DCM with a ratio of 8:2 by volume (v/v) and stirred at 25 ° C for 4 hours to ensure complete dissolution of the gelatin in a solvent medium. VAN does not dissolve directly in this solvent system due to its solubility properties. VAN aqueous solution was made with a concentration of 100 mg/ml in deionized water and stirred at room temperature for about one hour. The final electrospinning solution was obtained by adding gelatin and VAN solution in a ratio of 10:1(v/v) and stirring for half an hour to obtain a homogenous solution. A 2.5 ml plastic syringe with a metal capillary attached of gage 21 was set up in the electrospinning apparatus (Fanavaran Nano Meghyas, FNM, Iran). A stainless steel collector covered with aluminum foil was used to perform the electrospinning process. The distance between the needle and the collector was set to 10 cm and a potential difference of 12 kV was used to charge the solution and the collector. The electrospinning process was performed at room temperature and relative humidity in the range of 30–50%.

2.3 Morphology of electrospun nanofibers

Morphology of the electrospun nanofibers was examined by field emission scanning electron microscope (FE-SEM) (MIRA3, TESCAN, Czech). The specimen was coated with gold prior to observation. An accelerating voltage of 15 kV was used to capture SEM images. The diameter distribution and uniformity were measured with imageJ software. To investigate fiber diameter distribution, 60 measurements of random fibers were performed (n=60)

2.4 Crosslinking of gelatin nanofibers

Nanofibers made from gelatin or collagenous materials are extremely attractive due to their biocompatibility and biodegradability properties. However, due to their mechanical and water resistance properties, they need a suitable strategy to improve their physical characteristics. So far, various methods have been proposed for cross-linking of collagenous materials, and each of these methods in turn affects the morphology and physicochemical properties of structures [22-24]. In this study, Drug loaded gelatin nanofibers were cross-linked by exposing to

GTA vapor to improve their physical and mechanical properties. The resulting structures were cut to specific size of 3×3 cm and placed in a sealed desiccator. 5 ml of GTA (25%) was poured into a small glass container and placed on the bottom of the desiccator. In the present study, after cross-linking the structures with the use of GTA vapor, a slight shrinkage was observed in the nanofiber structures. The reason for this shrinkage can be attributed to the partial dissolution of the fibers in contact with the moist environment inside the desiccator. Besides, the fiber mats, after crosslinking, became darker. The reason for this phenomenon could be the attributed to forming new covalent bonds between the free amine groups present in the lysine and the aldehyde group of GTA that caused the formation of aldimine linkages (–CH=N–) [21]. The effectiveness of cross-linking was also investigated by examining the stability and degradability of structures in a physiological buffer (phosphate buffer saline) environment at 37 ° C. To investigate the effect of crosslinking duration on the swelling degree, the fibers were cross-linked at different time intervals of 7, 10, and 24 hours and were further investigated.

2.5 Degree of swelling

To investigate the degree of swelling of the structures, cross-linked nanofibers were immersed in 10 ml of phosphate buffer saline (PBS), pH 7.4 buffer, and placed in an incubator at 37 ° C with a rotational speed of 100 rpm. After 72 hours the swelling degree of these structures were calculated by the following equation:

$$\text{Degree of swelling (\%)} = \frac{Ws-Wd}{Wd} \qquad (1)$$

Where Ws is the weight of the swollen nanofiber sample which its excess water was removed with a neat tissue paper, Wd is the dried mass of the immersed sample in the PBS medium and measured by drying the swollen structures in a vacuum oven at 40 ° C to get a constant weight.

3. **Results and Discussions**

3.1 Morphology of electrospun nanofibers

One of the main challenges regarding the use of fibers as wound dressings and drug delivery systems is the morphology of the fibers. The gas exchange required for wound healing, the ability to absorb wound secretion, as well as the drug release profile are important examples of features that are directly affected by fiber morphology. Desirable and continuous VAN loaded gelatin nanofibers are presented in figure.3a. Various parameters such as applied voltage, flow rate, concentration, viscosity, and amount of drug in the electrospinning solution affect the morphology of the produced fibers [25, 26]. It is also necessary to investigate the interaction between different parameters such as the effect of the added drug on the electrospinning solution. The diameter distribution of produced fibers is shown in the figure.3.b. As shown in the figure, the average diameter of the fibers is 334±45 nm. In the current study, it was observed that when the drug was added directly to the electrospinning solution, it

caused the formation of a beaded structure (figure.2.a, b). To overcome this problem, the drug was first completely dissolved in deionized water and then added to an electrospinning solution, which improved the morphology of the fibers and created continuous fibers.

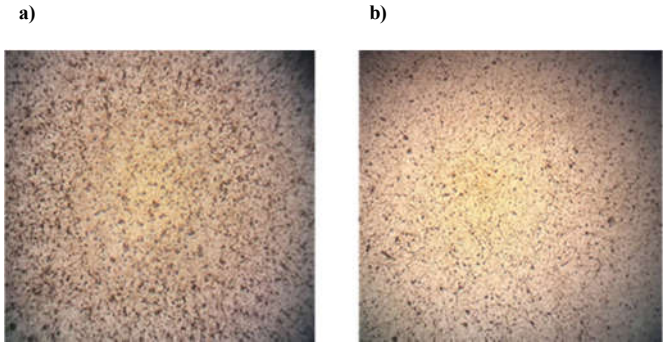

Figure 2: Optical microscope image of fibers to which the drug was added directly to the electrospinning solution at a similar concentration, (a) 12 kV of voltage, (b) 15 kV of voltage

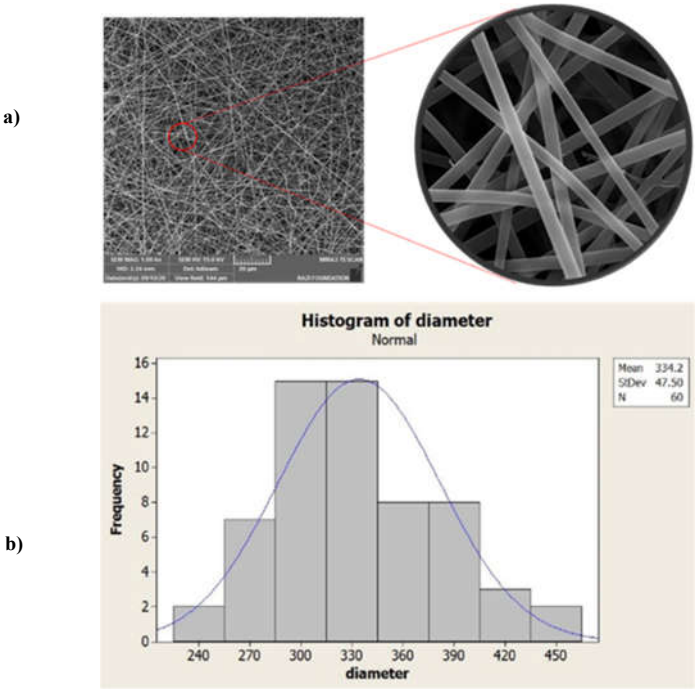

Figure 3: (a) SEM image of drug-containing gelatin nanofibers, (b) Fiber diameter distribution histogram

3.2 Degree of swelling

The swelling degree of the produced fibers is one of the key roles affecting the release of therapeutic molecules. On the other hand, this feature is directly related to the ability to absorb excess wound secretions, as well as maintaining a suitable moist environment for wound healing. To evaluate the degree of swelling, the fibers that

were produced under the same conditions were cross-linked at different time intervals of 7, 10, and 24 hours by exposure to GTA vapor, and then they were immersed in PBS solution at a constant temperature of 37 ° C. After 72 hours All samples wiped to dry and then and then their weight was measured again. The result of the measurements is shown in Figure 4. Based on the observations, it can be said that increasing the crosslinking duration can reduce the degree of swelling. The fibers that were crosslinked for 24 hours showed the lowest swelling degree of 450%. In another study, the swelling degree of gelatin/poly($_L$-lactide) (PLLA) composite nanofibers was reported to be about 346% [27]. Goutam et al. reported a swelling degree of about 170% of the cefazolin containing multilayer gelatin nanofibers [28]. According to previous researches and the degree of swelling of the fibers produced in this research, it can be said that the structures obtained from this research have a better ability in terms of the swelling degree.

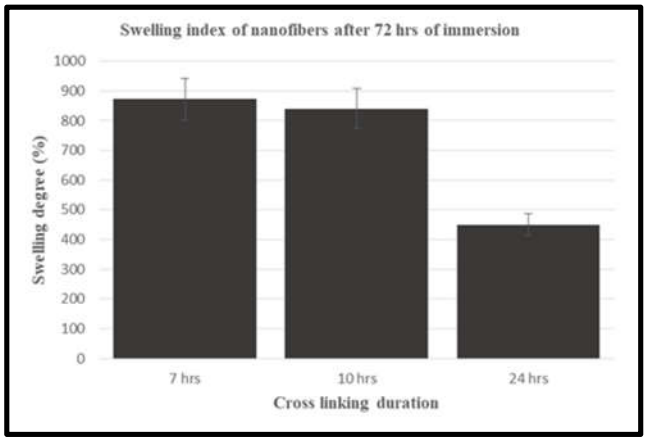

Figure 4: Comparison of the swelling degree of electrospun nanofibers that were cross-linked at different time intervals

4. Conclusion

Nowadays, electrospinning and fibers produced by this method have many applications in various fields such as wound dressing and drug delivery systems. In this study, vancomycin containing gelatin nanofibers with antibacterial properties were produced for use in wound dressing applications. SEM images showed desirable and continuous fibers. Also, the effect of cross-linking time on the ability to swell and absorb physiological buffer was investigated and the results showed that increasing the crosslinking duration could reduce the swelling degree of gelatin nanofibers.

Acknowledgements

The authors acknowledge the University of Mohaghegh Ardabili for providing the necessary research infrastructure to carry out this work.

References

[1] J.M. Torpy, C. Lynm, R.M. Glass, ″Burn injuries", JAMA, (2009), 302 1828-1828, doi: 10.1001/jama.302.16.1828.

[2] R. Lalani, L. Liu, ″Electrospun zwitterionic poly (sulfobetaine methacrylate) for nonadherent, superabsorbent, and antimicrobial wound dressing applications", Biomacromolecules, (2012), 13 1853-1863, doi: 10.1021/bm300345e.

[3] R. Thakur, C. Florek, J. Kohn, B. Michniak, ″Electrospun nanofibrous polymeric scaffold with targeted drug release profiles for potential application as wound dressing", International journal of pharmaceutics, (2008), 364 87-93, doi: 10.1016/j.ijpharm.2008.07.033.

[4] E.Y. Teo, S.-Y. Ong, M.S.K. Chong, Z. Zhang, J. Lu, S. Moochhala, B. Ho, S.-H. Teoh, ″Polycaprolactone-based fused deposition modeled mesh for delivery of antibacterial agents to infected wounds", Biomaterials, (2011), 32 279-287, doi: 10.1016/j.biomaterials.2010.08.089.

[5] R. Jayakumar, M. Prabaharan, P.S. Kumar, S. Nair, H. Tamura, ″Biomaterials based on chitin and chitosan in wound dressing applications", Biotechnology advances, (2011), 29 322-337, doi: 10.1016/j.biotechadv.2011.01.005.

[6] T. Miyahara, M. Nyan, A. Shimoda, Y. Yamamoto, S. Kuroda, M. Shiota, K. Akiyoshi, S. Kasugai, ″Exploitation of a novel polysaccharide nanogel cross□linking membrane for guided bone regeneration (GBR)", Journal of tissue engineering and regenerative medicine, (2012), 6 666-672, doi: 10.1002/term.475.

[7] N.M. Vacanti, H. Cheng, P.S. Hill, J.o.D. Guerreiro, T.T. Dang, M. Ma, S.e. Watson, N.S. Hwang, R. Langer, D.G. Anderson, ″Localized delivery of dexamethasone from electrospun fibers reduces the foreign body response", Biomacromolecules, (2012), 13 3031-3038, doi: 10.1021/bm300520u.

[8] S. Homaeigohar, M. Elbahri, ″Nanocomposite electrospun nanofiber membranes for environmental remediation", Materials, (2014), 7 1017-1045, doi: 10.3390/ma7021017.

[9] S. Chen, R. Li, X. Li, J. Xie, ″Electrospinning: An enabling nanotechnology platform for drug delivery and regenerative medicine", Advanced drug delivery reviews, (2018), 132 188-213, doi: 10.1016/j.addr.2018.05.001.

[10] X. Mo, B. Sun, T. Wu, D. Li, Electrospun nanofibers for tissue engineering, in: Electrospinning: Nanofabrication and Applications, Elsevier, pp. 719-734, (2019), doi: 10.3390/pharmaceutics11040182.

[11] M. Zhang, X. Li, S. Li, Y. Liu, L. Hao, ″Electrospun poly (l-lactide)/zein nanofiber mats loaded with Rana chensinensis skin peptides for wound dressing", Journal of Materials Science: Materials in Medicine, (2016), 27 136, doi: 10.1007/s10856-016-5749-7.

[12] Y. Polat, E.S. Pampal, E. Stojanovska, R. Simsek, A. Hassanin, A. Kilic, A. Demir, S. Yilmaz, "Solution blowing of thermoplastic polyurethane nanofibers: A facile method to produce flexible porous materials", Journal of Applied Polymer Science, (2016), 133, doi: 10.1002/app.43025.

[13] E. Stojanovska, E. Canbay, E.S. Pampal, M.D. Calisir, O. Agma, Y. Polat, R. Simsek, N.S. Gundogdu, Y. Akgul, A. Kilic, "A review on non-electro nanofibre spinning techniques", RSC advances, (2016), 6 83783-83801, doi: 10.1039/C6RA16986D.

[14] S. Kaiser, E. Reichelt, S.E. Gebhardt, M. Jahn, A. Michaelis, "Porous perovskite fibers–preparation by wet phase inversion spinning and catalytic activity", Chemical Engineering & Technology, (2014), 37 1146-1154, doi: 10.1002/ceat.201400097.

[15] J.M. Deitzel, J. Kleinmeyer, D. Harris, N.B. Tan, "The effect of processing variables on the morphology of electrospun nanofibers and textiles", Polymer, (2001), 42 261-272, doi: 10.1016/S0032-3861(00)00250-0.

[16] D.I. Braghirolli, D. Steffens, P. Pranke, "Electrospinning for regenerative medicine: a review of the main topics", Drug discovery today, (2014), 19 743-753, doi: 10.1016/j.drudis.2014.03.024.

[17] S. Young, M. Wong, Y. Tabata, A.G. Mikos, "Gelatin as a delivery vehicle for the controlled release of bioactive molecules", Journal of controlled release, (2005), 109 256-274, doi: 10.1016/j.jconrel.2005.09.023.

[18] S. Ebrahimi, M. Fathi, M. Kadivar, "Production and characterization of chitosan-gelatin nanofibers by nozzle-less electrospinning and their application to enhance edible film's properties", Food Packaging and Shelf Life, (2019), 22 100387, doi: 10.1016/j.fpsl.2019.100387.

[19] C.S. Ki, D.H. Baek, K.D. Gang, K.H. Lee, I.C. Um, Y.H. Park, "Characterization of gelatin nanofiber prepared from gelatin–formic acid solution", Polymer, (2005), 46 5094-5102, doi: 10.1016/j.polymer.2005.04.040.

[20] L. Maleknia, Z.R. Majdi, "Electrospinning of gelatin nanofiber for biomedical application", Oriental Journal of Chemistry, (2014), 30 2043-2048, doi: 10.13005/ojc/300470.

[21] Y. Zhang, J. Venugopal, Z.-M. Huang, C.T. Lim, S. Ramakrishna, "Crosslinking of the electrospun gelatin nanofibers", Polymer, (2006), 47 2911-2917, doi: 10.1016/j.polymer.2006.02.046.

[22] C.E. Campiglio, S. Ponzini, P. De Stefano, G. Ortoleva, L. Vignati, L. Draghi, "Cross-Linking Optimization for Electrospun Gelatin: Challenge of Preserving Fiber Topography", Polymers (Basel), (2020), 12, doi: 10.3390/polym12112472.

[23] A. Liguori, A. Bigi, V. Colombo, M.L. Focarete, M. Gherardi, C. Gualandi, M.C. Oleari, S. Panzavolta, "Atmospheric pressure non-equilibrium plasma as a green tool to crosslink gelatin nanofibers", Scientific Reports, (2016), 6 38542, doi: 10.1038/srep38542.

[24] J. Ratanavaraporn, R. Rangkupan, H. Jeeratawatchai, S. Kanokpanont, S. Damrongsakkul, ″Influences of physical and chemical crosslinking techniques on electrospun type A and B gelatin fiber mats", International journal of biological macromolecules, (2010), 47 431-438, doi: 10.1016/j.ijbiomac.2010.06.008.

[25] Z. Li, C. Wang, Effects of working parameters on electrospinning, in: One-dimensional nanostructures, Springer, pp. 15-28, (2013), doi: 10.1016/s0032-3861(00)00250-0.

[26] K. Matabola, R. Moutloali, ″The influence of electrospinning parameters on the morphology and diameter of poly (vinyledene fluoride) nanofibers-effect of sodium chloride", Journal of Materials Science, (2013), 48 5475-5482, doi: 10.1007/s10853-013-7341-6.

[27] S.-Y. Gu, Z.-M. Wang, J. Ren, C.-Y. Zhang, ″Electrospinning of gelatin and gelatin/poly(l-lactide) blend and its characteristics for wound dressing", Materials Science and Engineering: C, (2009), 29 1822-1828, doi: 10.1016/j.msec.2009.02.010.

[28] G. Rath, T. Hussain, G. Chauhan, T. Garg, A. Kumar Goyal, ″Fabrication and characterization of cefazolin-loaded nanofibrous mats for the recovery of post-surgical wound", Artificial cells, nanomedicine, and biotechnology, (2016), 44 1783-1792, doi: 10.3109/21691401.2015.1102741.

Biodegradation of Acid Red 88 dye using new bacterial strain A2 isolated from textile wastewater

Samira Eshghi[1], Fereshteh Jookar Kashi[2*]

1, 2 Department of Cell and Molecular Biology, Faculty of Chemistry, University of Kashan, Kashan, Islamic Republic of Iran

Email address: samiraeshghi@yahoo.com, Telephone number: 00989130928875

Corresponding author: jookar@kashanu.ac.ir

Abstract

Textile and dyestuffs industries release a considerable volume of dyes into the environment, which significantly have toxic effects on human health and aquatic organisms. The wastewater of the textile industry contains a variety of substances such as dyes, alkalis, acids, metals, starch, hydrogen peroxide, sodium hydroxide, agents used for surfactant dispersion, and various salts.

These dyes are extremely hard to decolorize since they are resistant to digestion due to their complex structure. Therefore, the removal of these dyes is necessary. This study aimed to isolate and identify dye degrading microorganisms from textile industry effluents. Twenty bacterial strains were isolated from the textile effluent, and one-strain A2 was selected. The strain A2 exhibited a remarkable ability to decolorize Acid Red 88. This gram-positive strain showed a great ability to decolorize at pH 7 and 37°C after 48 h. The results of UV–Vis analyses indicated that decolorization was due to biodegradation.

Keywords: Microorganism, Biodegradation, Wastewater, Disperse dye

1. Introduction

Most of the dyes used in the textile industry is synthetic dyes. These dyes are toxic and decompose slowly when they enter the environment, cause irreparable damage to the environment [1]. Some azo dyes or their decomposition compounds are toxic, carcinogenic, and mutagenic [2]. The microbial decontamination is valuable in terms of helping the health of the environment [3]. In the last two decades, microorganisms were applied as agents to clean up environmental pollution caused by colored effluents from textile factories. Various microorganisms, including fungi, aerobic bacteria, and some yeasts, can degrade various azo dyes [4]. The major constituents of textile effluents are dyes, stable organic compounds, toxic substances, surfactants, AOXs, and heavy metals. Dyes are one of the most important groups of contaminants to enter wastewater. They cannot be cleaned well, and their purification is due to their artificial origin and complex molecular structure. It makes them more durable and non-degradable, which will be very difficult [5]. This study investigates the decolorization ability of one bacterial strain isolated from the Kashan textile wastewater for Acid Red 88 dye.

2. Material and Methods

Textile effluent was collected from the Kashan textile industry. The bacterial isolates were taken by serial dilution technique. The colonies were selected and cultured several times to ensure purity on nutrient agar. The decolorization ability of Acid Red 88 dye was determined by a bacterial strain A2 isolated from the effluent. The decolorization screening was carried out in 5 ml of 0.7 g/l peptone, 0.35 g/l yeast extract, with 50 g/l glucose, Acid Red 88 dye at a concentration of 50 ppm and PH 7. Then, the bacterial suspensions (1% v/v) adjusted to 0.5 McFarland were inoculated in the medium, followed by incubation at 32 °C for 48 h. The color change was measured by ultraviolet spectroscopy at all three intervals of 24 hours, 48, and 72 during the color change process. At all three intervals, 1 ml of the samples was centrifuged for 7 min at 7000 rpm and analyzed using a UV-Vis spectrophotometer at λmax (530 nm) of the dye. The decolorization percentage was measured according to the following formula:

[8]

1. $$\textbf{Decolorization}\ (\%) = \frac{\textbf{initial absorbance} - \textbf{final absorbance}}{\textit{initial absorbance}} \times 100$$

3. Results and Discussions

This study was conducted to determine the ability of bacteria to decolorize. A bacterial strain A2, which had a high ability to decolorize Acid Red 88, was isolated from Kashan textile effluent. Decolorization efficiency was calculated at 91% after 48 hours of incubation. Decolorization analysis was investigated by UV-Vis spectroscopy. The gram-positive strain was able to decolorize Acid Red 88 (69.90 %) at 24h and (91%) at 48h, (91%) at 72h (Fig.1). Column diagrams are the percentage of decolorization at all three intervals (Fig.2.) Fig 3.A and Fig 3.B showed the absorbance analysis of Acid Red 88 dyes before and after

decolorizing by the strain. The disappearance of the peak from 530 nm is a decisive reason for molecular rearrangements in the dye structure and biodegradation. However, the results of this study suggest that the strain can be used to treatment dye-contaminated wastewaters.

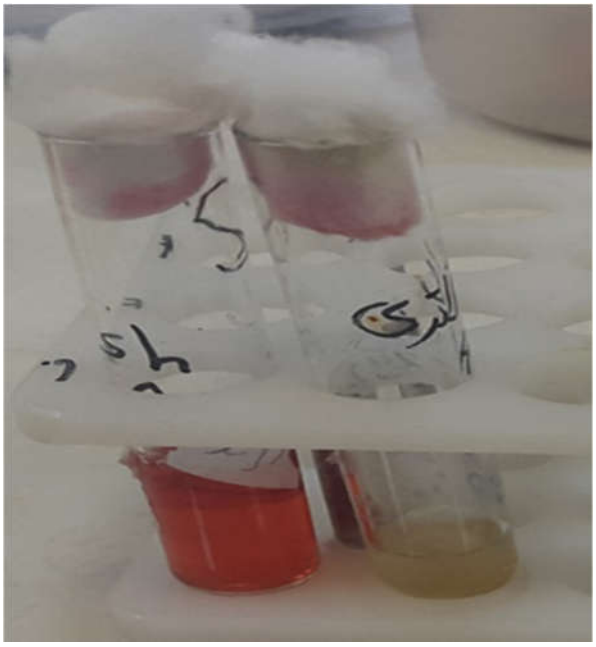

[9] **Fig. 1.** Decolorization of Acid Red 88 by a bacterial strain. Control culture (left) and culture after bacterial decolorization (right) after 72h

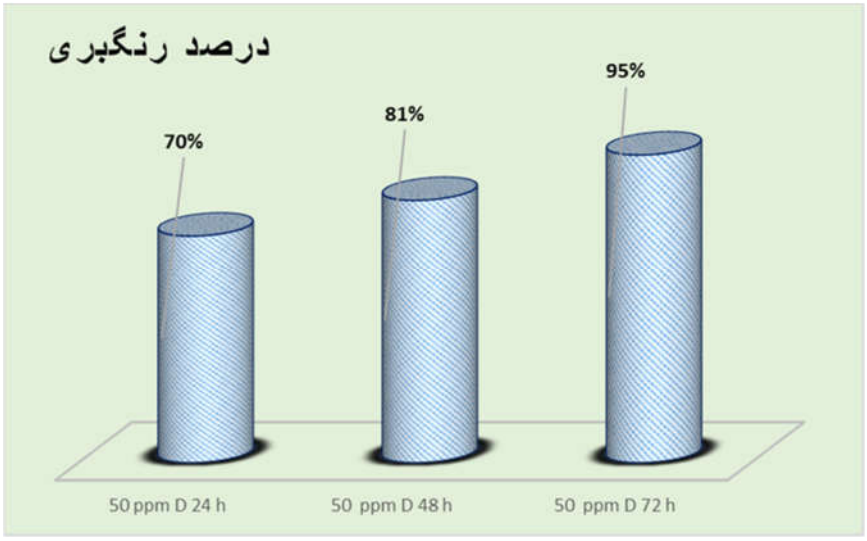

Fig. 2. The percentage of decolorization at 24, 48 and 72 h

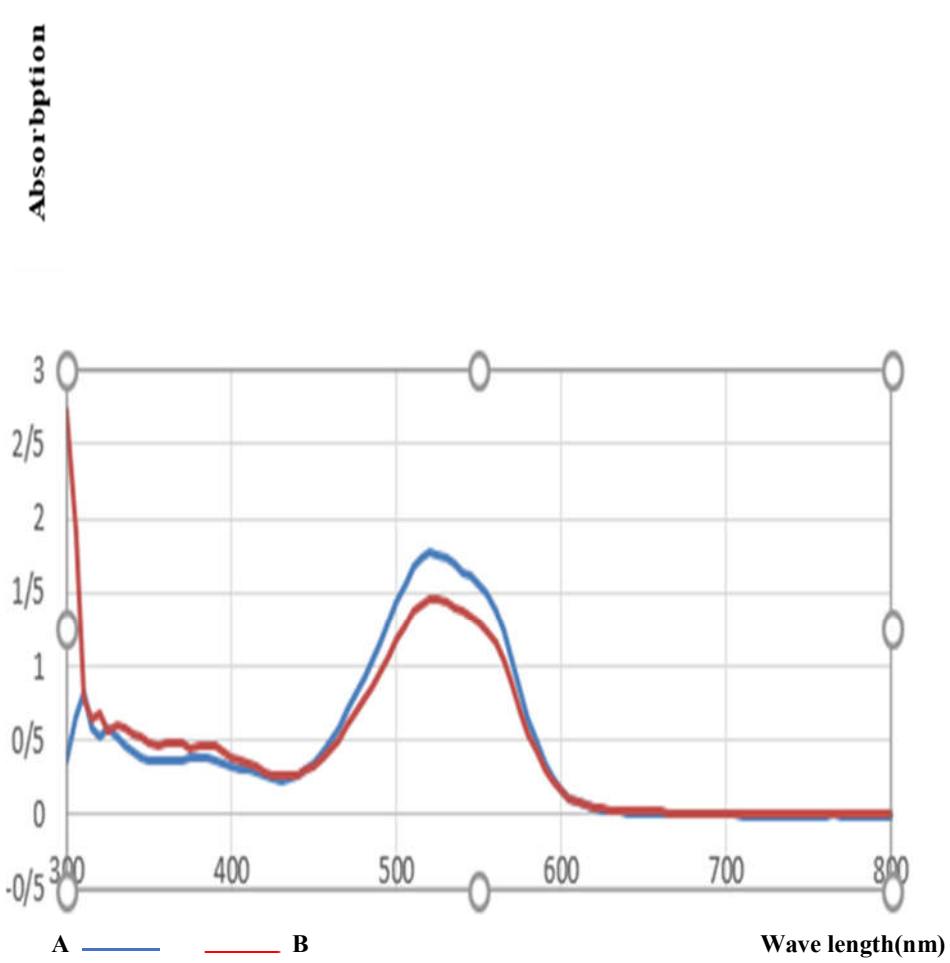

Fig.3. The variation in UV-Vis spectra of Disperse Acid Red 88 before (A) and after (B) decolorization by a bacterial strain

References

[1] علیرضا کیوانفرد، سال ۱۳۹۵، تصفیه پساب صنایع نساجی، (رنگرزی و چاپ)، چاپ اول کنکاش، صفحه ۱۳۰-۱۴۴

[2] Chung KT , Cerniglia CE, 1992. Mutagenicity of azo dyes: structure activity relationships. MutatRes, 277(3), 201-20.

[3] Moosvi,S. Keharia,H . Madamwar, D. 2005. Decolourization of Textile dye reactive violet 5 by a newly isolated bacterial consortium RVM 11.1. World Journal of Microbiology and Biotechnology **21**,667-672.

[4] Ramalho, P. A., H. Scholze, M. H. Cardoso, M. T. Ramalho, and A.M. Oliveira-Campos. 2002. Improved conditions for the aerobic reductive decolorisation of azo dyes by Candida zeylanoides. Enzyme Microb. Technol. **31 :** 848-854.

[5] Gupta, V. K, 2009. Application of low-cost adsorbents for dye removal-A review. Journal of environmental management 90, no. 8 :2313-2342.

Preparation, synthesis and characterization of multifunctional magnetic FeCO Chitosan-PLA-PEG-FA nanoparticles

Fatemeh Abedi Sarvestani[1] , Asadollah Asadi[1*], Saeid Latifi-Navid[1] , Saber Zahri[1]

[1]Department of Biology, Faculty of Science, University of Mohaghegh Ardabili, Ardabil, Iran

*Email: asad.asadi@gmail.com

Abstract

The magnetic nanoparticles for drug delivery are interesting in a variety of applications. These biocompatible nanoparticles moving towards a magnet, have been considered as the drug transporters. The cells detection using magnetic nanoparticles being visible with MRI offers a new practical method to cell therapies. This study synthesizes and investigates the morphological and physical properties of FeCO-Chitosan-PLA-PEG-FA magnetic nanoparticles and their capability to transmit into cancer cells. The nanoparticle based on FeCO-Chitosan can be used as an effective nanocarrier to transfer therapeutic agents and drugs to the cancerous cells due to the effective transferring capability of the therapeutic agents, the ability to move toward a magnet, and the high efficiency in the cellular absorption. Furthermore, the nanoparticles of FeCO-Chitosan have been blended with PLA-PEG-FA polymers to improve their properties such as permeability, biocompatibility, long circulation capability in the blood, and the targeted transfer of nanoparticles into cancerous cells.

Keywords: Chitosan, FeCo, Targeted Drug Delivery, Magnetic Nanoparticles

1. Introduction

Nowadays, the investigation in the area of drug delivery as a potential agent for the treatment of life-threatening human diseases such as cancer is rapidly growin [1]. Regarding the significance of drug delivery, it is required to design a potential system to transfer drugs to specific cells or tissues in the body with no immunological risks. Along with better understanding of cellular and molecular biology, the tremendous advances in materials science have resulted in the design of a variety of nano-scale materials developed as carriers with high capability in intracellular delivery and targeted drugs distribution [2]. The favorable drug delivery is a system with certain characteristics including efficient transferring of specific amount of drug to the target tissue, high drug loading capacity, biocompatible, safe from accidental release, and easy to synthesize, control, and remove [3]. The polymeric materials with the mentioned properties are suitable carriers in the area of nanomedicine. The biodegradable polymers are comprised of two groups of synthetic and natural polymers. The manufactured polymers include poly (lactide acid) (PLA), polyethylene glycol (PEG), poly (lactide-co-glycolic acid) copolymers (PLGA), polycaprolactone (PCL), poly (amino acids). The natural polymers include chitosan, alginate, gelatin, and albumin [4]. The biodegradable polymers category as drug carriers are highly effective due to their great biocompatibility [5] [6]. Three-block copolymers such as PEI-PLA-PEG three-block copolymers as gene delivery nano-vectors have been developed using PLA, PEI, and PEG polymers [7]. The hydrophobic PLA segments reach a degree of biodegradability to nanoparticles which increase nanocarrier stability through charge

shielding effects. In recent decades, many studies have been conducted on a multifunctional nanoparticle. The multifunctional nanoparticles are widely applied in cancer treatment due to their high potential to overcome the barriers in various extracellular and intracellular conditions [8] [9].

Chitosan is the second most abundant polymer after Glucose and one of the most popular biological nanocarriers in the drug delivery [10]. The properties of polymeric carrier chitosan are the natural positive charge, ability to absorb selectively, and the effect of neutralizing the surface charge in tumor cells. The charge on the plasma membrane's surface leads to the nanocarrier's absorption and high adhesion strength to the cells which makes it a suitable option in the drug delivery for solid tumor tissues [11] [12]. The lower toxicity effect of chitosan than other cationic polymers is another benefits [13]. The most crucial chitosan issue is the poor solubility at physiological PH due to minor proton presence in the acetyl amine group of this compound's structure.

One of the major strategies to eliminate the weak solubility of chitosan is the use of water-soluble derivatives such as PEG groups [11]. The benefits of PEG-containing medicinal compounds include high blood retention, reduced rate of drug degradation by metabolic enzymes, and reduced immunogenicity [12]. The chitosan-containing PEG, later to be digested by proteolytic enzymes and gastric intestinal fluid [14].

The use of magnetic particles and the penetration of magnetic fields into cell tissues, and their ability to diagnose and treat diseases have always been of interest to researchers. The constituent molecules of these particles and atoms have a magnetic property and a size of less than 100 nm in magnetic materials, directed to the target area by applying an external magnetic field. It can play an important part in diagnosing Magnetic Resonance Imaging (MRI) and as carriers for some anticancer drugs. The simplest structure of these nanoparticles consists of a magnetic core (such as iron oxide, nickel, and cobalt) with a modified surface of several layers of organic polymer, inorganic metals (such as gold), or oxide surfaces (such as silica and alumina) to be prepared for activation through the binding of bioactive molecules [15]. The efficiency of mediator metals (iron, cobalt, nickel) as magnetic carriers can be enhanced using their compounds and alloys instead of their pure form (e.g. FeCo nanoparticles). These metal nanoparticles tend to retain magnetic torque and absorb magnetic fields than iron oxide; and FeCo magnetic saturation is significantly high. The use of same mass of these carriers compared to other carriers can create a strong propulsive force and increase the drug delivery process efficiency. Simultaneously, in order to have the same effect of a specific magnetic field, lower concentrations, or smaller particles of these carriers can be used [16].

Researchers are uncertain about trial elements like Co for practical applications since they are less abundant in the body than iron and concerned about testing elements such as Co for practical applications. According to Nina Matoussevitch, carrying out a research on producing biocompatible Fe, Co, and FeCo nanoparticles at the Institute of Chemistry of the Karlsruhe Research Center in Germany, the toxicity of elements such as Cobalt is one of the deterrents for scientific research in this area and various proposed theories have not been widely accepted. Small amounts of cobalt are good for human health. For example, this compound is needed to form vitamin B12 and used to treat anemia. Cobalt compounds are generally excreted in the body and do not accumulate. There is no evidence that cobalt nanoparticles are toxic to the body, but more research need to be carried out. Although tens of thousands of millions of magnetic particles can be used in the targeted drug delivery, their actual weight will be deficient (approximately a few tens of milligrams) [17]. Over the past decades, nanoparticles have been used to optimize drugs and genes, reduce their side effects, and deliver drugs in a targeted

method for effective treatment [18]. Folic acid (FA) is an essential nutrient for the human body that can enter the cell through folate receptors (FRs) [19]. In the human body, folic acid is used for DNA synthesis. Thus, the effects of folate receptors on cancer cells is higher than normal cells due to their need for high folic acid levels. The endocytosis pathway targeted nanoparticles based on the interaction between cell surface receptors and ligands [20] [21].

2. Material and Methods

2.1 Synthesis of PLA-PEG-FA copolymer

Preparation of PLA-PEG-FA copolymer was started with the synthesis of OH-PLA-PEG-COOH according to the method described by Hami et al [18]. An appropriate amount of lactide monomers added to HO-PEG-COOH under dry argon, then the reaction was continued has for 24 hours at 140 ° C in the presence of (Sn(Oct)2) as a catalyst. The product has been precipitated by a mixture of methanol and ether of equal volume. Then, the HO-PLA-PEG-COOH copolymer was dried under vacuum and dissolved in DCM solution containing DCC (1.2 mmol) and NHS (0.6 mmol). The product was stirred at 0 °C and 25°C for 1 h and 24 h respectively. After that, Triethylamine (TEA) and propargylamine (0.6 mmol) were added to the product. Then mixture was stirred for 24 h at 25 ° C. The HO-PLA-PEG-alkyne copolymer was precipitated in cold ether, filtered and dried under vacuum at 30 ° C. Then, the HO-PLA-PEG-alkyne copolymer (0.1 mmol) was conjugated with acryloyl chloride (C3H3ClO) (0.2 mmol) in dry toluene containing triethylamine (C6H15N) (0.2 mmol). The sample stirred for 10 hours at 80°. After filtration and washing by N-Hexane, it was dried at 25 ° C under a vacuum. In order to bind folic acid to acrylate-PLA-PEG-alkyne copolymer, the acrylate-PLA-PEG-alkyne copolymer (0.1 mmol) and Azido-functionalized folate and Azido-functionalized glucose dissolved in 30 ml of NH4HCO3 (10 Mm). Then, sodium ascorbic acid (50 mmol) and cuSO4 (20 mmol) were added to the acrylate-PLA-PEG-alkyne copolymer and stirred with a rotator, and the product was filtered using a 0.2 µm filter. After adding the certain amount of NaCl, it was precipitated several times by dichloromethane.

2.2 Synthesis of FeCO-Chitosan-PLA-PEG-FA nano-particles

Synthesis of FeCO-Chitosan-PLA-PEG-FA nano-particles has been performed by conjugating the amine group in FeCO-Chitosan nano-particles with alkyne group in the acrylate-PLA-PEG-alkyne copolymer. For this purpose, FeCO-Chitosan nano-particles and acrylate-PLA-PEG-alkyne copolymer were dissolved separately in 6 ml of chloroform and gently mixed under shaking conditions. The produced suspension was stirred at 45 ° C for 24 h. Finally, FeCO-Chitosan-PLA-PEG-FA nanoparticles were collected using a magnet, and after washing with a mixture of water and methanol, they were dried by the freeze dryer machine.

2.3 Investigation of properties of FeCO-Chitosan-PLA-PEG-FA nano-particles

Transfer electron microscopy (TEM) has been used to evaluate the morphological properties of nanoparticles. For this purpose, a certain amount of various nanoparticles was sonicated by a sonicator for one

minute, then observed and examined by the transmission electron microscope. DLS device was used to evaluate the size and zeta potential of nanoparticles. FTIR and NMR were used to confirm the synthesis of nanoparticles.

3. Results and Discussions

The results of NMR spectroscopy of PLA-PEG-FA copolymer confirmed the correct synthesis of this copolymer. As shown in Figure 1, the peak observed in the range of 3.6 corresponds to (-CH2CH2O-) in the PLA-PEG structure, and the peaks observed in the range of 2.5 and 1.5 correspond to the CH and CH3 protons in the PLA, respectively. In addition, the peaks observed in the range of 4.5 to 8.6 are related to folic acid protons, and the peak in the range of 8.1 is related to the triazole ring in the PLA-PEG-FA copolymer composition.

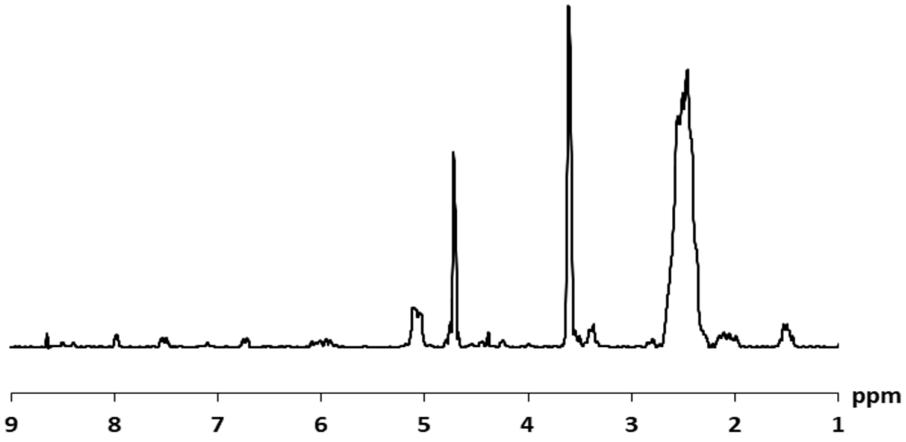

Figure 1. H NMR spectra of PLA-PEG-FA

The FTIR spectroscopy results of PEG, PLA-PEG, PLA-PEG-FA polymers, FeCO, FeCO-chitosan, and FeCO-Chitosan-PLA-PEG-FA nanoparticles are shown in Figure 2. The findings showed that the peak observed in the range of 1712 in PEG are related to the carboxylic group of PEG and also the peak observed in the range of 1762, 1647, and 1100 in the PLA-PEG copolymer are related to the groups C = O, C-O-C, and COOH in the PLA-PEG copolymer. The existing of weak peaks in the range of 1580 to 1650 indicates that the successful binding of folic acid to the PLA-PEG copolymer.

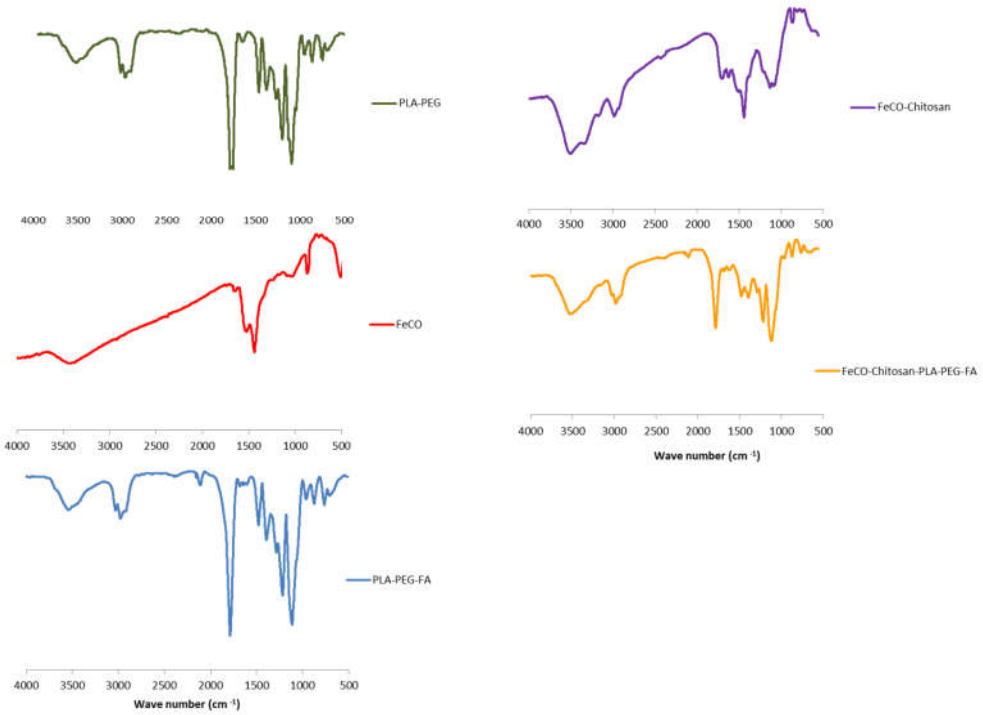

Figure 2. FT-IR spectrum of various copolymers and FeCo-Chitosan-PLA-PEG-FA nanoparticles

The electron microscopy image results of FeCO-Chitosan-PLA-PEG-FA nanoparticles showed that these nanoparticles have a spherical structure and a size 20-40 nm. These results were consistent with the results of the DLS. The results of DLS showed that the nanoparticles have about 28 nm and a cationic surface charge (2.5 mV) (Figures 3 and 4).

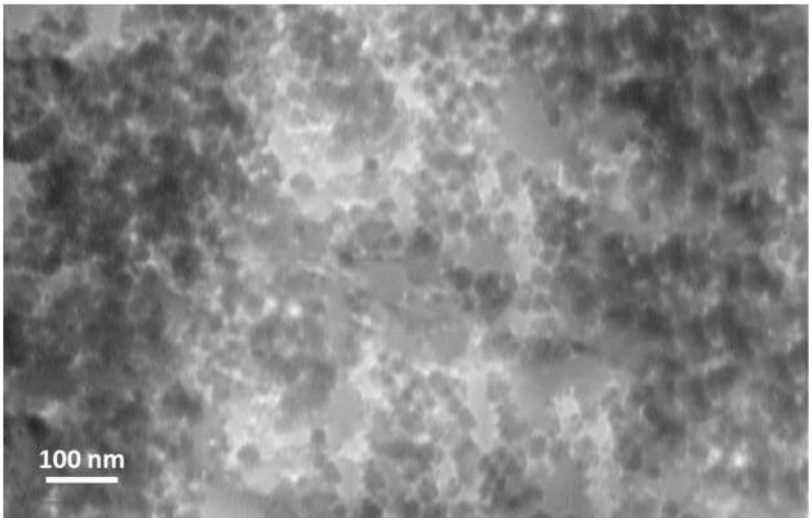

Figure 3. TEM image of FeCO-Chitosan-PLA-PEG-FA nanoparticles

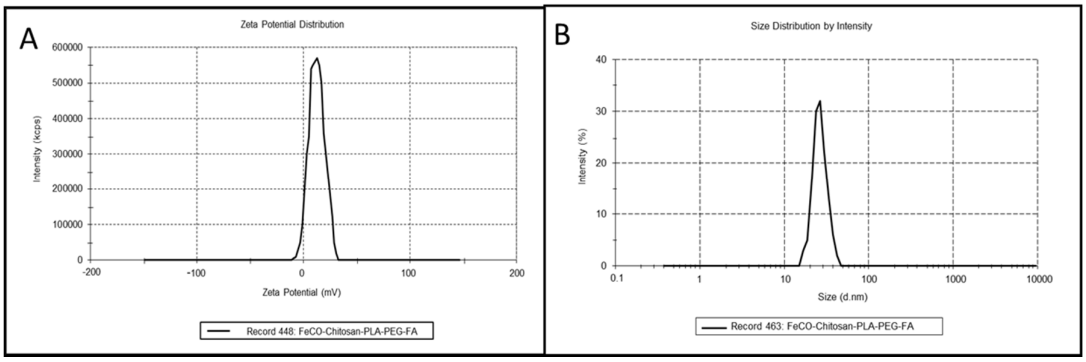

Figure 4. Size and surface charge of FeCO-Chitosan-PLA-PEG-FA nanoparticles measured by DLS

Acknowledgements

This study has been supported by the Biology Department, University of Mohaghegh Ardabili

References

[1] Gfeller, D., et al., SwissTargetPrediction: a web server for target prediction of bioactive small molecules. Nucleic acids research, (32-38) (2014) doi:10.1093/nar/gku293

[2] Akhtar, M.J., et al., Nanotoxicity of cobalt induced by oxidant generation and glutathione depletion in MCF-7 cells. Toxicology in Vitro, (94-101) (2017) doi:10.1016/j.tiv.2016.12.012

[3] Hardainiyan, S. and B. Chandra Nandy, Nakuleshwar Dut Jasuja, Vyas, Pramod K Ragha v. Recent Trends in Dermal and Transdermal Drug Delivery Systems. The Pharma Innovation, (1-6) (2013)

[4] Li, S. and M. Vert, Biodegradable polymers: polyesters. (1999)

[5] Perez, C., et al., Poly (lactic acid)-poly (ethylene glycol) nanoparticles as new carriers for the delivery of plasmid DNA. Journal of controlled Release, (211-224) (2001) doi:10.1016/S0168-3659(01)00397-2

[6] Wang, J., Delivery of siRNA with nanoparticles based on PEG–PLA block polymer for cancer therapy. Nanomedicine: Nanotechnology, Biology and Medicine, (464) (2016) doi:10.1016/j.nano.2015.12.052

[7] Abebe, D.G., et al., Three-layered biodegradable micelles prepared by two-step self-assembly of PLA-PEI-PLA and PLA-PEG-PLA triblock copolymers as efficient gene delivery system. Macromolecular bioscience, (698-711) (2015) doi:10.1002/mabi.201400488

[8] Yan, K., et al., Self-assembled magnetic fluorescent polymeric micelles for magnetic resonance and optical imaging. Biomaterials, (344-355) (2014) doi:10.1016/j.biomaterials.2013.09.035

[9] Liu, J., et al., Multifunctional aptamer-based nanoparticles for targeted drug delivery to circumvent cancer resistance. Biomaterials, (44-56) (2016) doi:10.1016/j.biomaterials.2016.03.013

[10] Khakrizi, E., M. BikhofTorbati, and M. Shaabanzadeh, The Study of Anticancer Effect of Magnetic Chitosan-Hydroxyurea Nanodrug on HeLa Cell line: A Laboratory Study. Journal of Rafsanjan University of Medical Sciences, (715-730) (2018)

[11] Abd Elgadir, M., et al., Impact of chitosan composites and chitosan nanoparticle composites on various drug delivery systems: A review. Journal of food and drug analysis, (619-629) (2015) doi:10.1016/j.jfda.2014.10.008

[12] Aruna, U., et al., Role of chitosan nanoparticles in cancer therapy. Int J Innov Pharm Res, (318-324) (2013)

[13] Zhong, H., et al., Augmentation of adenovirus 5 vector-mediated gene transduction under physiological pH conditions by a chitosan/NaHCO 3 solution. Gene therapy, (232-239) (2011) doi:10.1038/gt.2010.129

[14] Chopra, S., et al., Advances and potential applications of chitosan derivatives as mucoadhesive biomaterials in modern drug delivery. Journal of Pharmacy and Pharmacology, (1021-1032) (2006) doi:10.1211/jpp.58.8.0002

[15] Sun, C., J.S. Lee, and M. Zhang, Magnetic nanoparticles in MR imaging and drug delivery. Advanced drug delivery reviews, (1252-1265) (2008) doi:10.1016/j.addr.2008.03.018

[16] Sahoo, S., et al., Characterization of a novel polymeric scaffold for potential application in tendon/ligament tissue engineering. Tissue engineering, (91-99) (2006) doi:10.1089/ten.2006.12.91

[17] Thanh, N.T., Magnetic nanoparticles: from fabrication to clinical applications. 2012: CRC press.

[18] Hami, Z., et al., Doxorubicin-conjugated PLA-PEG-Folate based polymeric micelle for tumor-targeted delivery: Synthesis and in vitro evaluation. DARU Journal of Pharmaceutical Sciences, (30) (2014) doi:10.1186/2008-2231-22-30

[19] Zwicke, G.L., G. Ali Mansoori, and C.J. Jeffery, Utilizing the folate receptor for active targeting of cancer nanotherapeutics. Nano reviews, (18496) (2012) doi:10.3402/nano.v3i0.18496

[20] Kim, Y.-I., Folate and carcinogenesis: evidence, mechanisms, and implications. The Journal of nutritional biochemistry, (66-88) (1999)

[21] Mason, J.B., Folate: effects on carcinogenesis and the potential for cancer chemoprevention. (1996)

A review on the application of metal nanoparticles in biodegradable films: The effects on antimicrobial, physicochemical and mechanical properties

Sina Ardebilchi Marand[1*] and Hadi Almasi[2]

1. Master's student, Department of Food Science and Technology, Urmia university, Urmia, Iran

2. Associate professor, Department of Food Science and Technology, Urmia University, Urmia, Iran

*Email: sinaardebilchimarand@gmail.com

Abstract

One of the global issues in packaging technology is environmental problems caused by the non-biodegradablity of synthetic petroleum-based plastics. Therefore, in recent decades, so many researches have been done on the alternatives of these plastics such as bioplastics. The bioplastics have various problems to be used in food packaging. Thereupon, some methods have been used for overcoming to these problems like incorporation of nanoparticles and addition of functional materials to the polymers. Metal oxides are important nanoparticles which can be incorporated in biodegradable films for addressing their problems. The main purpose of this study is to review the characteristics of nanocomposites containing several metal oxides such as ZnO, TiO_2, silver and copper derived chemicals.

Keywords: Nanobiotechnology, Nanocomposites, Biopolymers, Active packaging, Metal oxides.

1. Introduction

The destructive effects on the environment due to the accumulation of non-degradable synthetic plastics is one of the most important concerns in the world. According to the large amount of plastics used in food packaging, food science and technology scientists have been looking for alternatives to synthetic polymers. One of the suitable alternatives to these polymers is biodegradable films based on biopolymers (carbohydrates, proteins, and lipids). In the production of biodegradable films, raw materials are mainly obtained from renewable agricultural raw materials or waste products of the seafood processing industry, so the usage of this kind of films can be an investment in preservation of natural resources. Furthermore, biodegradability and composting are the other advantages of biodegradable packaging, which can act as fertilizer and soil material and improve crop yields [[1]-[3]]. Many materials have been researched in the manufacture of biodegradable packaging. Carbohydrates (such as starch, chitosan, pectin, and cellulose derivatives) and proteins (such as proteins derived from milk, soy, and fish) are among the most widely studied substances in food packaging [[4]- [9]].

Despite the biocompatible and environmentally-friendly properties of biopolymers, these polymers have various disadvantages for packaging applications. Poor mechanical and low gas and moisture barrier properties

are some problems of these biopolymer-based films. The most frequently used methods to enhance performance of bioplastics are the use of polymer blends, multilayered films, chemically modification of natural biopolymers and nano-reinforcements. Several composites have been developed by adding reinforcing compounds (fillers) to polymers to enhance their properties. However, many reinforced materials present poor adhesion at the interface of their components. The application of nanoscale fillers is leading to the development of new composite crop which called "nanocomposites". Polymer nanocomposites are the materials aimed at solving the problems [10].

In respect to the inorganic agents, some of the oxidized nanoparticles including TiO_2, ZnO, MgO, and CuO have attracted so much attention as they resist the harsh processing conditions and impose robust biocidal effects against foodborne pathogens. **Fig. 1** shows the different proposed biocidal mechanisms induced by nanoparticles [11]. Furthermore, application of the metal oxides in food packaging can improve the barrier, mechanical and thermal properties of the films [12].

The main purpose of this study is to review the application and effects of common metal oxide nanoparticles in biodegradable films.

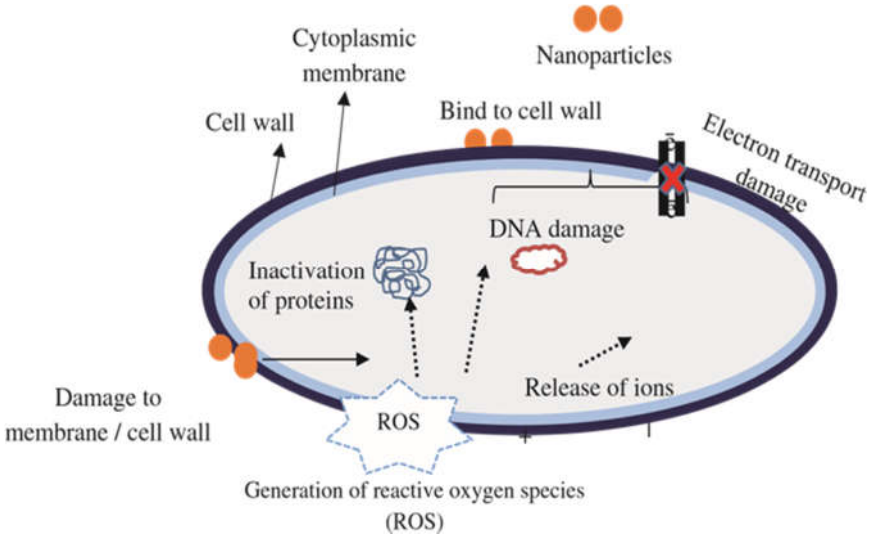

Fig. 11 Antibacterial effects of the nanoparticles (biocidal mechanisms) [11].

2. Zinc oxide (ZnO) nanoparticles

ZnO is described as a functional, strategic material with an attractive chemical sensing, semiconducting, electric conductivity and optical properties that has wide range of applications. Reduction in the particle size of ZnO to the nanometer range gives ZnO high antibacterial effect, then nano-sized ZnO can interact with bacterial surface and/or with the bacterial core where it enters inside the cell, and subsequently exhibits distinct bactericidal mechanisms. Furthermore, it has high photocatalytic activity which shows its potential applications in wastewater treatments [13].

The various effects of ZnO nanoparticles on biodegradable active films have been studied. Sani et al. (2020) reported that the incorporation of ZnO nanoparticles improved the performance of sodium caseinate films. According to the results of this research, with the incorporation of low amounts of ZnO nanoparticles into the protein network matrix, the physical and mechanical properties of the film samples improved significantly. Water barrier and mechanical properties of the films improved which was related to the proper interactions between the protein matrix and ZnO nanoparticles. The antibacterial activity of the active films was increased by addition of ZnO to the films [14]. Tang et al. (2019) also characterized soybean protein isolate films incorporated with ZnO nanoparticles for Food Packaging. The effects of different contents of ZnO nanoparticles in the films on the oxygen barrier, antibacterial activity, and thermal and mechanical properties were evaluated. A ZnO nanoparticles content of 0.2% in the films improved the tensile strength and microbial inhibition by 231% and 16%, respectively. The thermal stability and oxygen barrier properties of film samples were also improved with incorporation of ZnO nanoparticles. The ZnO nanoparticles dispersed uniformly in the soy protein isolate films enhanced the interactions between soy protein isolate molecules via hydrogen bonding, and the results suggest potential applications of ZnO nanoparticles in food packaging [15].

3. Titanium dioxide (TiO_2) Nanoparticles

TiO_2 is a white colour found in all kinds of paints, printing ink, plastics, paper, synthetic fibers, rubber, condensers, painting colours and crayons, ceramics, electronic components along with food and cosmetics. These nanoparticles have unique properties and can be used as fillers in biodegradable packaging. One of the most important properties of TiO_2 is their photochemical and photocatalytic properties. **Fig. 2** illustrates the scheme principal photocatalytic process in the TiO_2 particles [16].

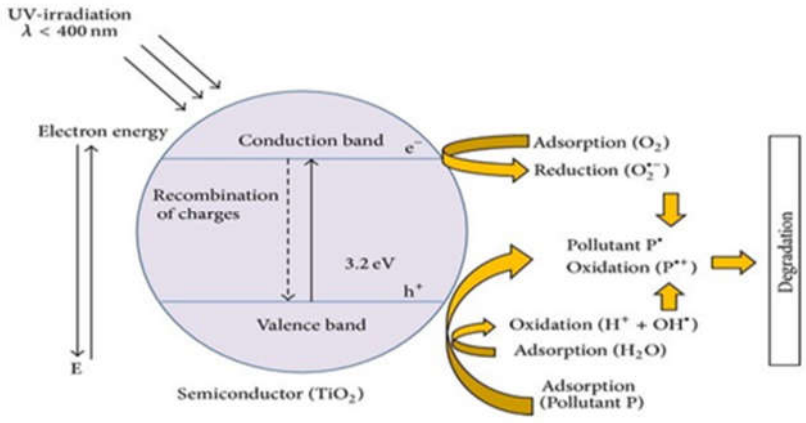

Fig. 2 Principal photocatalytic process in the TiO_2 particles [16].

There are many fields of applications for TiO_2 nanoparticles due to perfect properties included air purification, water purification, antibacterial, tooth paste, UV protection, photocatalysis, sensing and paint application [16].

TiO_2 is widely used in biodegradable films. El-Wakil et al. (2015) characterized wheat gluten/nanocellulose/titanium dioxide nanocomposites. The mechanical and barrier properties of nanocomposites were significantly improved when 7.5% nanocellulose and 0.6% TiO_2 added to wheat gluten. A significant reduction in CFU was observed against the organisms compared to TiO_2-free coated paper [17]. In another research, Fathi et al. (2019) investigated physicochemical and photocatalytic properties of sesame protein isolate films containing TiO_2 nanoparticles. The nanoparticles were added in 3 levels (1, 3 and 5%w/w) and the uniform dispersion of nanoparticles was at the concentrations lower than 3%. Water barrier properties, tensile strength and opacity of nanocomposites were enhanced up to 3% addition of nanoparticles to the films, but the higher concentrations had negatively affected the film properties [18].

4. Silver nanoparticles (AgNPs)

Silver is a transition metal with high electrical and thermal conductivity. Silver nanoparticles have attracted considerable attention and their applications has increased in recent years because of the important antimicrobial activities of these nanomaterials, allowing their use in several industrial sectors. AgNPs play a great role in the study of biology and medicine because of their unique properties. In medicine, silver and AgNPs used as ointments to prevent infection against burn and open wounds [[19], [20]].

One of the important applications of this nanoparticle is in biodegradable active packaging and so many researches have been done on this subject. Kanmani and Rhim (2014) investigated the properties of gelatin based nanocomposites incorporated with AgNPs and nanoclay. The results showed that the transparency of films was decreased with addition of nanoparticles, but UV barrier properties was improved, which was more pronounced with AgNPs included. Mechanical properties were enhanced with addition of both nanomaterials. The antimicrobial tests demonstrated a significant improvement in nanocomposite films in comparison with pure gelatin films [21]. Furthermore, Jafari et al. (2016) investigated inhibitory, structural and physicochemical characteristics of chitosan nanocomposite films containing AgNPs and chitin nanofiber. The results demonstrated that the addition of AgNPs at concentration of 1% had negative effects on mechanical and colour properties of chitosan films. But incorporation of CHNF improved their mechanical and barrier properties significantly [22].

5. Copper oxide (CuO) nanoparticles

Copper has been used as a biocide for centuries. Copper nanoparticles are being used in so many fields such as medicine and food packaging because of their high antimicrobial and antifungal activity. Synthesis of copper nanoparticles can be cost effective due to copper availability. **Fig. 3** demonstrates antimicrobial activity of copper nanoparticles against bacteria, fungi, and viruses [23].

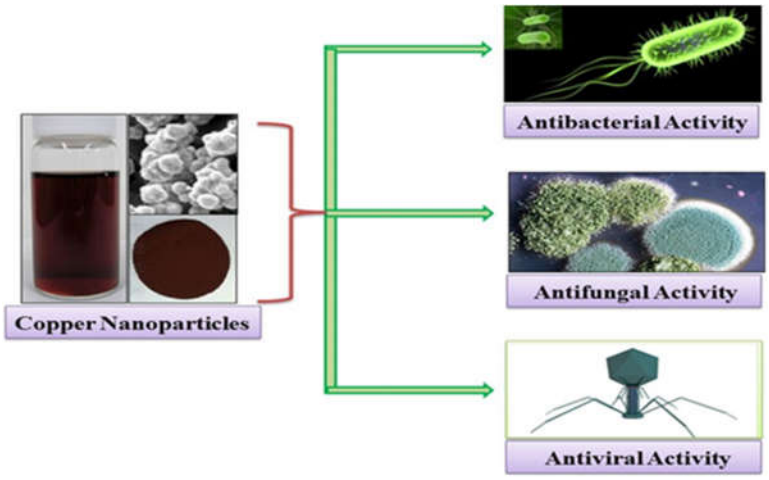

Fig. 3 Schematic representation of antimicrobial activity of copper nanoparticles against bacteria, fungi, and viruses [23].

Shankar et al. (2017) evaluated the carbohydrate based nanocomposite films incorporated with CuO nanoparticles. According to the results, the thickness, tensile strength, UV barrier property, relative humidity, and water vapor barrier property increased with the addition of CuONPs. The CuONPs incorporated composite films exhibited strong antibacterial activity against *Escherichia coli* and *Listeria monocytogenes*. It could be concluded that the developed composite films could be used as a UV-light barrier antibacterial films for active food packaging [24].

6. Magnesium oxide (MgO) nanoparticles

MgO is an important inorganic material which has been used in many applications such as catalysis, toxic waste remediation, refractory materials and adsorbents, reflecting and anti-reflecting coatings, superconducting and ferroelectric thin films as the substrate. In medicine, MgO is used for the relief of heartburn, sore stomach, and for bone regeneration. Recently, MgO nanoparticles have shown promise for application in tumor treatment. MgO nanoparticles also have considerable potential as an antibacterial agent [25]. Jin and He (2011) have investigated the antibacterial activities of MgO nanoparticles against *Escherichia coli* and *Salmonella Stanley*. The results showed that MgO nanoparticles have strong antibacterial activity against the pathogens [26].

Swaroop and Shukla (2019) fabricated and characterized blown polylactic acid/MgO nanocomposites for food packaging applications. The results showed that MgO reinforcement improved the tensile strength and plasticity of nanocomposite films. The oxygen and water vapour barrier properties improved by nearly 65% and 57%, respectively for the 1% formulation. The nanocomposites showed high antibacterial effects against *E. coli*. Finally, this research establishes the successful production of large scale, sustainable, blown PLA/MgO food packaging films [27].

7. Conclusions

Nanotechnology plays a vital role in the developments of biodegradable packaging. Metal oxide nanoparticles are very important additives in the production of biodegradable films. The results of this review showed the effects and importance of metal oxide nanoparticles such as TiO_2, ZnO, CuO, MgO in biodegradable active packaging. Incorporation of the nanoparticles into the films can enhance the properties of nanocomposites. Furthermore, having antimicrobial activity of these nanoparticles is a great advantage for active packaging applications.

References

[1] C. A. Romero-Bastida, L. A. Bello-Pérez, M. A. García, M. N. Martino, J. Solorza-Feria, & N. E. Zaritzky, Physicochemical and microstructural characterization of films prepared by thermal and cold gelatinization from non-conventional sources of starches, Carbohydrate Polymers, 60(2) (2005) 235-244. doi: 10.1016/j.carbpol.2005.01.004.

[2] R. N. Tharanathan, & N. Saroja, Hydrocolloid-based packaging films—alternate to synthetic plastics, (2001).

[3] E. Jahed, M. A. Khaledabad, M. R. Bari, & H. Almasi, Effect of cellulose and lignocellulose nanofibers on the properties of Origanum vulgare ssp. gracile essential oil-loaded chitosan films, Reactive and Functional Polymers, 117 (2017) 70-80. doi: 10.1016/j.reactfunctpolym.2017.06.008.

[4] M. Z. Elsabee, E. S. Abdou, K. S. Nagy, & M. Eweis, Surface modification of polypropylene films by chitosan and chitosan/pectin multilayer, Carbohydrate Polymers, 71(2) (2008) 187-195. doi: 10.1016/j.carbpol.2007.05.022.

[5] Y. X. Xu, K. M. Kim, M. A. Hanna, & D. Nag, Chitosan–starch composite film: preparation and characterization, Industrial crops and Products, 21(2) (2005) 185-192. doi: 10.1016/j.indcrop.2004.03.002.

[6] B. Ghanbarzadeh, H. Almasi, & A. A. Entezami, Physical properties of edible modified starch/carboxymethyl cellulose films, Innovative food science & emerging technologies, 11(4) (2010) 697-702. doi: 10.1016/j.ifset.2010.06.001.

[7] M. Oussalah, S. Caillet, S. Salmiéri, L. Saucier, & M. Lacroix, Antimicrobial and antioxidant effects of milk protein-based film containing essential oils for the preservation of whole beef muscle, Journal of agricultural and food chemistry, 52(18) (2004) 5598-5605. doi: 10.1021/jf049389q.

[8] P. Guerrero, A. Retegi, N. Gabilondo, & K. De la Caba, Mechanical and thermal properties of soy protein films processed by casting and compression, Journal of Food Engineering, 100(1) (2010) 145-151. doi: 10.1016/j.jfoodeng.2010.03.039.

[9] Y. A. Arfat, S. Benjakul, T. Prodpran, P. Sumpavapol, & P. Songtipya, Properties and antimicrobial activity of fish protein isolate/fish skin gelatin film containing basil leaf essential oil and zinc oxide nanoparticles, Food Hydrocolloids, 41 (2014) 265-273. doi: 10.1016/j.foodhyd.2014.04.023.

[10] B. Ghanbarzadeh, S. A. Oleyaei, & H. Almasi, Nanostructured materials utilized in biopolymer-based plastics for food packaging applications, Critical reviews in food science and nutrition, 55(12) (2015) 1699-1723. doi: 10.1080/10408398.2012.731023.

[11] M. Hoseinnejad, S. M. Jafari, & I. Katouzian, Inorganic and metal nanoparticles and their antimicrobial activity in food packaging applications, Critical reviews in microbiology, 44(2) (2018) 161-181. doi: 10.1080/1040841X.2017.1332001.

[12] S. Jafarzadeh, & S. M. Jafari, Impact of metal nanoparticles on the mechanical, barrier, optical and thermal properties of biodegradable food packaging materials, Critical reviews in food science and nutrition, (2020) 1-19. doi: 10.1080/10408398.2020.1783200.

[13] A. Sirelkhatim, S. Mahmud, A. Seeni, N. H. M. Kaus, L. C. Ann, S. K. M. Bakhori, ... & D. Mohamad, Review on zinc oxide nanoparticles: antibacterial activity and toxicity mechanism, Nano-micro letters, 7(3) (2015) 219-242. doi: 10.1007/s40820-015-0040-x.

[14] I. K. Sani, S. A. Marand, M. Alizadeh, S. Amiri, & A. Asdagh, Thermal, Mechanical, Microstructural and Inhibitory Characteristics of Sodium Caseinate Based Bioactive Films Reinforced by ZnONPs/Encapsulated Melissa officinalis Essential Oil, Journal of Inorganic and Organometallic Polymers and Materials, (2020) 1-11. doi: 10.1007/s10904-020-01777-2.

[15] S. Tang, Z. Wang, W. Li, M. Li, Q. Deng, Y. Wang, ... & P. K. Chu, Ecofriendly and biodegradable soybean protein isolate films incorporated with ZnO nanoparticles for food packaging, ACS Applied Bio Materials, 2(5) (2019) 2202-2207. doi: 10.1021/acsabm.9b00170.

[16] A. J. Haider, Z. N. Jameel, & I. H. Al-Hussaini, Review on: titanium dioxide applications, Energy Procedia, 157 (2019) 17-29. doi: 10.1016/j.egypro.2018.11.159.

[17] N. A. El-Wakil, E. A. Hassan, R. E. Abou-Zeid, & A. Dufresne, Development of wheat gluten/nanocellulose/titanium dioxide nanocomposites for active food packaging, Carbohydrate polymers, 124 (2015) 337-346. doi: 10.1016/j.carbpol.2015.01.076.

[18] N. Fathi, H. Almasi, & M. K. Pirouzifard, Sesame protein isolate based bionanocomposite films incorporated with TiO2 nanoparticles: Study on morphological, physical and photocatalytic properties, Polymer Testing, 77 (2019) 105919. doi: 10.1016/j.polymertesting.2019.105919.

[19] R. de Lima, A. B. Seabra, & N. Durán, Silver nanoparticles: a brief review of cytotoxicity and genotoxicity of chemically and biogenically synthesized nanoparticles, Journal of Applied Toxicology, 32(11) (2012) 867-879. doi: 10.1002/jat.2780.

[20] H. D. Beyene, A. A. Werkneh, H. K. Bezabh, & T. G. Ambaye, Synthesis paradigm and applications of silver nanoparticles (AgNPs), a review, Sustainable materials and technologies, 13 (2017) 18-23. doi: 10.1016/j.susmat.2017.08.001.

[21] P. Kanmani, & J. W. Rhim, Physical, mechanical and antimicrobial properties of gelatin based active nanocomposite films containing AgNPs and nanoclay, Food Hydrocolloids, 35 (2014) 644-652. doi: 10.1016/j.foodhyd.2013.08.011.

[22] H. Jafari, M. Pirouzifard, M. A. Khaledabad, & H. Almasi, Effect of chitin nanofiber on the morphological and physical properties of chitosan/silver nanoparticle bionanocomposite films, International journal of biological macromolecules, 92 (2016) 461-466. doi: 10.1016/j.ijbiomac.2016.07.051.

[23] T. Ameh, & C. M. Sayes, The potential exposure and hazards of copper nanoparticles: a review, Environmental toxicology and pharmacology, 71 (2019) 103220. doi: 10.1016/j.etap.2019.103220.

[24] S. Shankar, L. F. Wang, & J. W. Rhim, Preparation and properties of carbohydrate-based composite films incorporated with CuO nanoparticles, Carbohydrate Polymers, 169 (2017) 264-271. doi: 10.1016/j.carbpol.2017.04.025.

[25] Z. X. Tang, & B. F. Lv, MgO nanoparticles as antibacterial agent: preparation and activity, Brazilian Journal of Chemical Engineering, 31(3) (2014) 591-601. doi: http://dx.doi.org/10.1590/0104-6632.20140313s00002813.

[26] T. Jin, & Y. He, Antibacterial activities of magnesium oxide (MgO) nanoparticles against foodborne pathogens, Journal of Nanoparticle Research, 13(12) (2011) 6877-6885. doi: 10.1007/s11051-011-0595-5.

[27] C. Swaroop, & M. Shukla, Development of blown polylactic acid-MgO nanocomposite films for food packaging, Composites Part A: Applied Science and Manufacturing, 124 (2019) 105482. doi: 10.1016/j.compositesa.2019.105482.

Pharmacokinetic and Pharmacodynamic Evaluation of Quercetin for Targeting Inflammation: an in silico study

Farshad Qalekhani[1, 2] and Mahnaz Ghowsi[3*]

[1] Pharmaceutical Sciences Research Center, Health Institute, Kermanshah University of Medical Sciences (KUMS), Kermanshah, Iran.

[2] Medical Biology Research Center, Health Technologies Institute, Kermanshah University of Medical Sciences (KUMS), Kermanshah, Iran.

[3] Department of Biology, Faculty of Sciences, Razi University, Kermanshah, Iran.

*Email: Ghaousi.mahnaz@razi.ac.ir; Ghowsi.mahnaz@gmail.com

Abstract

This in-silico study was performed to predict the pharmacodynamics, toxicity profiles and biological anti-inflammatory activities of quercetin. Online pharmacokinetic tools, the pkCSM, and Vienna LiverTox SwissADME web servers were used to predict potential of quercetin as a specific anti-inflammatory drug and the prediction of potential targets of this compound were examined by using Swiss-PdbViewer 1.1.0 and AutoDockTools (ADT) softwares. In order to investigate the different interactions of quercetin with the targets IKK, cyclooxygenase (COX), and TANK-binding kinase-1 (TBK-1**)** as key targets of the inflammatory pathway, the AutoDock Vina software was used. This study demonstrates that quercetin can bind to amino acid residues in the active sites of TBK-1, IKK, and COX-II with significant binding energies that imply it may have inhibitory effects on the TBK-1, IKK, and COX-II. Also, these results suggest that it has anti-inflammatory activities which are comparable to the inhibitory effects of amlexanox, XNM, and SC-558 as three inhibitors of the targets mentioned above. According to the results of our study, the inhibition of IKK, COX-II, and TBK-1 were predicted as some mechanisms for the anti-inflammatory effects of quercetin. This compound is proposed to have activities against a variety of human chronic inflammatory systemic diseases. Also, quercetin was non-toxic and may be a valuable therapeutic choice in the development of novel anti-inflammation drugs.

Keywords: Quercetin, Anti-inflammation, In-silico study, Pharmacodynamics, Pharmacokinetic.

1. Introduction

Inflammation is the immune system's response to various factors such as pathogens, damaged cells and toxic compounds in the heart, pancreas, liver, kidney, lung, brain, intestinal tract, reproductive system, and may result in the tissue damage or a verity of diseases including arthritis, cancer and stroke, neurodegenerative and cardiovascular diseases. While inflammation is an intrinsically beneficial process that helps the elimination of offending factors and the restoration of normal cell structure and function [[1], [2]], an inflammatory response

that lasting for a long period of time may lead to the development of various chronic diseases, such as cancer and inflammation [3].

In the body, the blood monocytes differentiate into tissue resident macrophages that through release of proinflammatory mediators such as nitric oxide (NO), interleukin-6 (IL-6), tumor necrosis factor-α (TNF-α), as well as induction of inducible cyclooxygenase (COX-II) for production of prostaglandins, play axial roles in the promotion and propagation of inflammatory responses [4].

Nuclear factorkB (NF-κB) is a protein transcription factor that regulates the transcription of numerous genes including cytokines and growth factors, adhesion molecules, immunoreceptors, and acute-phase proteins that are involved in immunity, inflammation and protection from programmed cell death (apoptosis). Various studies show that maximal transcription of many cytokines that are involved in the generation of acute inflammatory responses such as TNF-α, IL-1, IL-6, and IL-8 is mediated by NF-κB [[5], [6]]. The transcription factors NF-κB are usually kept inactive in the cytoplasm through interaction with inhibitory molecules of the IκB family. But, various stimuli including inflammatory cytokines, bacterial or viral products, or various types of stress causes the IκB molecules become phosphorylated on two serine residues and as a consequence, they are polyubiquitinated and destructed by the proteasome. Therefore, free NF-κB can enter in the nucleus and activate the transcription of different genes that are involved in the immune and inflammatory response, and cell adhesion. The kinases responsible for the phosphorylation of the IκB inhibitors are known as Ser/Thr-specific IKK and they contain two related catalytic subunits, IKKα and IKKβ [7]. The activated IKK causes phosphorylation of the IκB like domain in a member of NF-kB family which called NF-kB2 (p49/p100) (NFKB2 in humans) [8].

The members of the Toll-like receptors (TLRs) family function as pattern recognition receptors (PRRs), and identify the conserved microbial motifs in molecules such as bacterial lipopolysaccharide (LPS), peptidoglycan, flagellin, unmethylated CpG DNA, double and single stranded RNA an so on and activation of TLRs by each of these molecules promote an inflammatory response in the hosts and made them to initiate an immune response [9]. The activation of the TLR4 by the harmful stimuli activates NF-κB and Interferon Regulatory Factor 3 (IRF3) as two distinct transcription factors. Therefore, both activated NF-κB and IRF3 dimers translocate in the nucleus and promote the transcription of the proinflammatory cytokines [9].

In addition, NF-kB signaling pathways are associated with various human diseases such as inflammatory disorders and cancer. So, NF-kB signaling pathways are potentially important therapeutic targets for human chronic inflammatory systemic diseases [8].

The TANK-binding kinase-1 (TBK-1**)** is a serine/threonine protein kinase that plays axial roles in the innate immunity antiviral response. It has been shown that the activation of TBK-1 causes phosphorylation of IRF3 that results in the formation of IRF3 dimer complex which in turn, up-regulates the transcription of proinflammatory cytokines. Therefore, TBK-1 is a potentially target for the finding of lead anti-inflammatory compounds [10].

Cyclooxygenase is a protein that catalyzes the conversion of arachidonic acid to prostaglandin (PG) H2, the immediate precursor to prostaglandins, thromboxane, and prostacyclin. There are two isoforms of COX that are known as COX-I and COX-II. While many tissues express COX-I constitutively for that production of prostaglandins needed to regulate normal “housekeeping” functions such as renal water retention, gastric acid secretion, parturition, and hemostasis, the expression of COX-II is induced by inflammatory stimuli that activate the immune response. This immune response is associated with production of prostaglandins that results in the

development of pain, fever, and inflammation [11]. In addition, it has been shown that NF-κB can up-regulate COX-II expression [12].

Quercetin is a unique bioflavonoid that is found in abundance in various types of vegetables and fruits [13]. It exhibits numerous beneficial effects on the human health, and acts as a potent antioxidant, anti-carcinogenic, anti-inflammatory, anti-infective, neuroprotective, and psychostimulant agent [14].

Various in vitro and in vivo studies have suggested that quercetin exhibit anti-inflammatory efficacy [15]. Therefore, in the present study, in order to find the mechanisms of the anti-inflammatory effects of quercetin, we investigated the pharmacokinetics and pharmacodynamics of quercetin in the inhibition of the key targets of inflammatory pathway using bioinformatics techniques. For this purpose, PDB files of COX-II, IKK, and TBK-1 target were downloaded and the inhibitors in the crystallographic file of each target i.e. amlexanox, XNM, and SC-558 was used as positive controls.

Material and Methods

1.1 Molecules Preparation and Docking

Three dimensional structures of COX-II (PDB Id: 6COX), IKK (PDB Id: 3RZF) and TBK-1 (PDB Id: 5W5V) were downloaded in PDB format from protein data bank (www.rcsb.org). Then, the proteins were processed and structure refinement performed utilizing the Swiss-PdbViewer 1.1.0 software. All the waters and cocrystal ligands were deleted from the molecules by Discovery Studio4.5 software. Grid box center were calculated using AutoDockTools (ADT) software. After adding polar hydrogens to the 3D- structure of proteins, PDBQT files were created using ADT software. The 3D conformations of SC-558 (PubChem CID: 1396), XNM (PubChem CID: 52914873), amlexanox (PubChem CID: 2161), quercetin (PubChem CID: 5280343) were downloaded from PubChem (https://www.pubchem.ncbi.nlm.nih.gov/). PDBQT files were created using ADT software. AutoDock Vina software was used for docking. PDBQT files were used as input for AutoDock Vina software. After docking, the Log and out-pdbqt files were saved for further analysis [[16], [17], [18]].

1.2 Druglikeness

The molecular structures of every ligand were analyzed using SwissADME server (http://www.swissadme.ch/) in order to confirm whether the ligands follow druglikeness or not [19].

1.3 Toxicity

pkCSM server was used to check for toxicity. General toxicity parameters such as carcinogenicity, hepatotoxicity, cardiotoxicity, etc were investigated. The possibility of inhibition of hERG enzyme was assessed

through the Pred- hERG 4.2 server. Vienna LiverTox server was used to evaluate the inhibition of liver enzymes [[20], [21], [22]].

1.4 Pharmacokinetics

Pharmacokinetics, derived from the Greek words pharmakon (drug) and kinetikos (movement), is used to describe the absorption, distribution, metabolism, and excretion of a compound. The ADME for each of the ligand molecules was carried out using an online based server pkCSM (http://biosig.unimelb.edu.au/pkcsm/) to predict their various pharmacokinetic properties including blood brain barrier permeability, human abdominal adsorption, AMES toxicity, cytochrome P (CYP) inhibitory capability, carcinogenicity, mutagenicity, Caco-2 permeability etc. [20].

2. Results and Discussions

2.1 Molecules Preparation and Docking

In the present study, the PDB files of the targets were downloaded and a receptor inhibitor in the crystallographic file of each target was used as a positive control. The structure of the used ligands was downloaded in SDF format. Table 1 contains the full name of each ligand. The structure of each of the ligands can be seen in the Figure 1. Also, the three-dimensional structure of each target is shown in Figure 2.

Table 1: the IUPAC names of the ligands.

Name	IUPAC Name	PubChem CID
SC-558	4-[5-(4-bromophenyl)-3-(trifluoromethyl)pyrazol-1-yl]benzenesulfonamide	1396
XNM	[4-[[4-(4-chlorophenyl)pyrimidin-2-yl]amino]phenyl]-[4-(2-hydroxyethyl)piperazin-1-yl]methanone	52914873
Amlexanox	2-amino-5-oxo-7-propan-2-ylchromeno[2,3-b]pyridine-3-carboxylic acid	2161
Quercetin	2-(3,4-dihydroxyphenyl)-3,5,7-trihydroxychromen-4-one	5280343

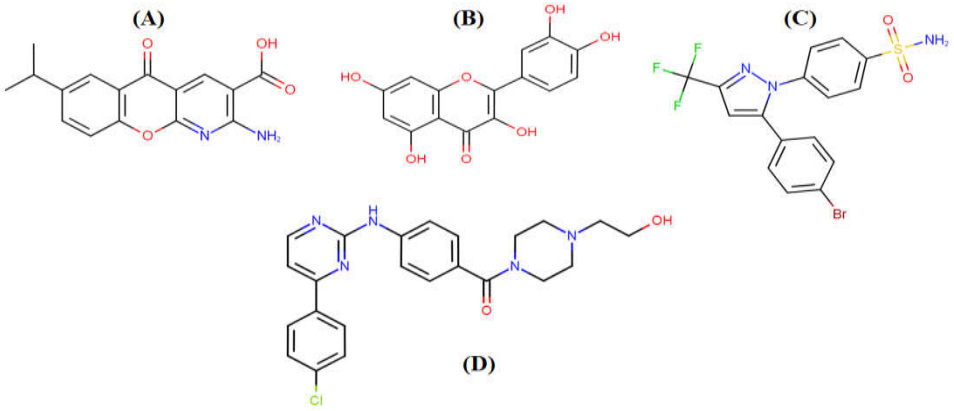

Figure 1. Chemical structures of (A) Amlexanox (PubChem CID: 2161), (B) Quercetin (PubChem CID: 5280343), (C) SC-558 (PubChem CID: 1396), and (D) XNM (PubChem CID: 52914873).

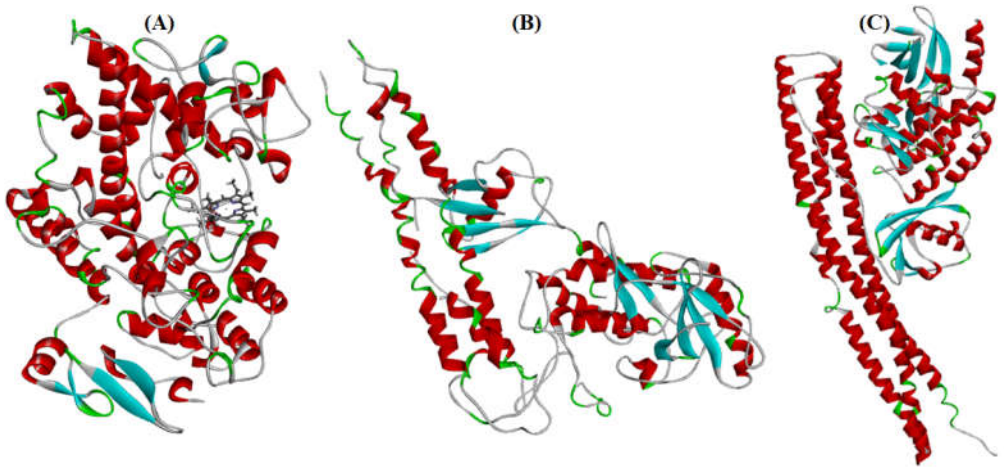

Figure 2. The 3D crystallographic conformation of target molecules (A) COX-II (PDB Id: 6COX), (B) IKK (PDB Id: 3RZF) and (C) TBK-1 (PDB Id: 5W5V).

After docking calculations, the energy value of each complex was determined and the results of these calculations are given in table 2. Also, these values are compared with each other in the figure 3. The figure 4 shows the interactions between of quercetin and each receptor in compare to the positive control (Table 2, Figure 3 and 4).

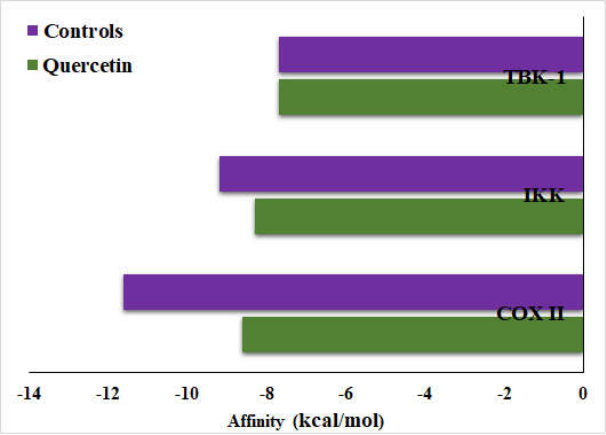

Figure 3. The energy diagram of molecular docking between quercetin and receptors COX-II, IKK, and TBK-1.

Table 2. The energy of interactions between quercetin and receptors COX-II, IKK, and TBK-1.

Complex Name	Affinity (kcal/mol)	Complex Name	Affinity (kcal/mol)
COX II & Quercetin	-8.6	COX II & SC-558	-11.6
IKK & Quercetin	-8.3	IKK & XNM	-9.2
TBK-1 & Quercetin	-7.7	TBK-1 & Amlexanox	-7.7

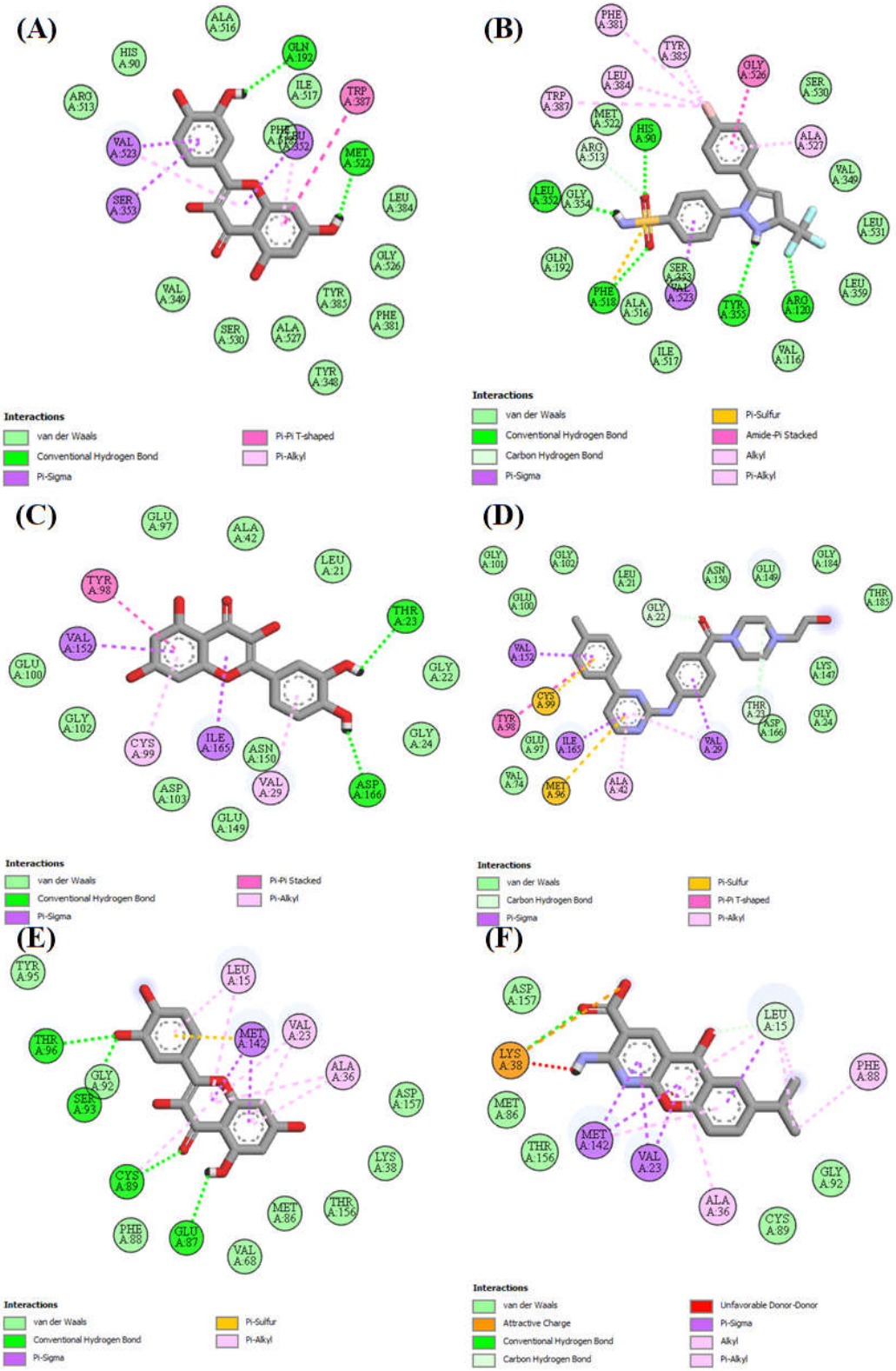

Figure 4. 2D representation of interactions between ligand molecules (A) COX II & quercetin, (B) COX II & SC-558, (C) IKK & quercetin, (D) IKK & XNM (E) TBK-1 & quercetin (F) TBK-1 & amlexanox.

2.2 Drug-likeness

The results of evaluation the drug-likeness for each ligand are summarized in the Table 3.

Table 3: The summary of drug likeness property analysis results.

Row	Name	MW	Rotatable bonds	H-bond acceptors	H-bond donors	TPSA	MLOGP
1	SC-558	446.24	4	7	1	86.36	3.03
2	XNM	437.92	7	5	2	81.59	2.15
3	Amlexanox	298.29	2	5	2	106.42	0.43
4	Quercetin	302.24	1	7	5	131.36	-0.56

2.3 Toxicity

The results of the general toxicity and cardiac toxicity evaluations for each ligand are summarized in Table 4. Also, the results of hepatotoxicity test are summarized in Table 5.

Table 4: The summarry of general toxicity and cardiotoxicity property analysis results.

Property	Model Name	SC-558	XNM	Amlexanox	Quercetin	Unit
Toxicity	AMES toxicity	No	Yes	No	No	Categorical
Toxicity	Max. tolerated dose (human)	0.144	0.322	1.175	0.499	(log mg/kg/day)
Toxicity	hERG I inhibitor	No	No	No	No	Categorical
Toxicity	hERG II inhibitor	No	Yes	No	No	Categorical
Toxicity	Oral Rat Acute Toxicity (LD50)	2.06	3.002	2.023	2.471	(mol/kg)
Toxicity	Oral Rat Chronic Toxicity (LOAEL)	1.039	0.925	2.228	2.612	(log mg/kg_bw/day)
Toxicity	Hepatotoxicity	Yes	Yes	No	No	Categorical
Toxicity	Skin Sensitisation	No	No	No	No	Categorical

Table 5: The summary of hepatotoxicity property analysis results.

Model	SC-558	XNM	Amlexanox	Quercetin
BSEP Inhibition	negative	positive	negative	negative
BSEP Transport	negative	negative	negative	positive
P-glycoprotein Inhibition	negative	positive	negative	negative
P-glycoprotein Transport	negative	negative	negative	positive
MRP4 Inhibition	positive	positive	negative	positive
MRP2 Transport	negative	negative	positive	negative
MRP3 Inhibition	positive	positive	negative	negative
MRP3 Transport	negative	negative	negative	positive
BCRP Inhibition	negative	negative	negative	negative
BCRP Transport	negative	positive	negative	positive
OATP1B1 Inhibition	negative	positive	negative	negative
OATP1B3 Inhibition	negative	positive	negative	negative
Drug-induced liver injury	positive	positive	positive	positive
Hyperbilirubinemia	negative	positive	negative	negative
Cholestasis	positive	positive	negative	positive

2.4 Pharmacokinetics

Absorption, distribution, metabolism, and excretion were examined for each ligand and the results are shown in Table 6.

Table 6: The results of ADME property analysis.

Property	Model Name	SC-558	XNM	Amlexanox	Quercetin	Unit
Absorption	Water solubility	-4.699	-3.676	-3.015	-2.925	(log mol/L)
Absorption	Caco2 permeability	0.801	0.964	0.98	-0.229	(log Papp in 10-6 cm/s)
Absorption	Intestinal absorption (human)	91.026	95.847	68.642	77.207	(% Absorbed)
Absorption	Skin Permeability	-2.706	-2.742	-2.735	-2.735	(log Kp)
Distribution	VDss (human)	-0.336	1.045	-1.297	1.559	(log L/kg)
Distribution	Fraction unbound (human)	0.111	0.118	0.288	0.206	(Fu)
Distribution	BBB permeability	-1.097	-1.319	-0.209	-1.098	(log BB)
Distribution	CNS permeability	-1.971	-2.571	-2.243	-3.065	(log PS)
Metabolism	CYP2D6 substrate	No	No	No	No	Categorical
Metabolism	CYP3A4 substrate	Yes	Yes	No	No	Categorical
Metabolism	CYP1A2 inhibitior	Yes	Yes	No	Yes	Categorical
Metabolism	CYP2C19 inhibitior	Yes	Yes	No	No	Categorical
Metabolism	CYP2C9 inhibitior	Yes	No	No	No	Categorical
Metabolism	CYP2D6 inhibitior	No	No	No	No	Categorical
Metabolism	CYP3A4 inhibitior	Yes	Yes	No	No	Categorical
Excretion	Total Clearance	-0.081	0.52	0.276	0.407	(log ml/min/kg)
Excretion	Renal OCT2 substrate	No	Yes	No	No	Categorical

3. Discussions

In this study, we attempted to explore the anti-inflammatory property of the quercetin, in silico. The AutoDock vina has been proven as an effective tool in predicting bound orientation and binding energy of the small molecule ligands with macromolecular targets, in a quick and precise way. Quercetin was utilized to explore anti-inflammatory activities against three signaling proteins in the TLR4 pathway. Molecular docking analysis of the quercetin showed that it was able to bind to the amino acid residues in the active site of TBK-1, IKK, and COX II. Quercetin showed interesting interactions and satisfactory binding energies when docked into these targets. Quercetin may have inhibitory effects on the TBK-1, IKK, and COX-II. In silico pharmacokinetics and ADME analysis indicated that quercetin may be a potent inhibitory compound for inflammation and potentially is safe to be incorporated into active pharmaceutical drugs against inflammation. However, more studies are needed to identify the precise mechanisms in the anti-inflammatory properties of quercetin.

References

[1] E. Ricciotti, G.A. FitzGerald, Prostaglandins and inflammation, Arteriosclerosis thrombosis, and vascular biology 31(2011) 986-1000. doi:10.1161/ATVBAHA.110.207449.

[2] L. Chen, H. Deng, H. Cui, J. Fang , Z. Zuo, J. Deng, Y. Li, X.Wang, L. Zhao, Inflammatory responses and inflammation-associated diseases in organs, Oncotarget 9 (2018)7204-7218. doi: 10.18632/oncotarget.23208.

[3] C. H. Liu, N. D. Abrams, D. M. Carrick, P. Chander, J. Dwyer, M. R. Hamlet, et al., Imaging inflammation and its resolution in health and disease: current status, clinical needs, challenges, and opportunities, The FASEB Journal 33 (2019) 13085-13097. doi: 10.1096/fj.201902024.

[4] S-I. Kanno, A. Shouji, A. Tomizawa, T. Hiura, Y. Osanai, M. Ujibe, et al., Inhibitory effect of naringin on lipopolysaccharide (LPS)-induced endotoxin shock in mice and nitric oxide production in RAW 264.7 macrophages, Life Sciences 78 (2006) 673-681. doi: 10.1016/j.lfs.2005.04.051.

[5] T. S. Blackwell, J. W. Christman, The role of nuclear factor-κ B in cytokine gene regulation. American journal of respiratory, cell and molecular biology 17 (1977) 3-9. doi: 10.1165/ajrcmb.17.1.f132.

[6] H.N. Lee, .S. A. Shin, G. S. Choo, H. J. Kim, Y. S. Park, B. S. Kim, et al., Anti‐inflammatory effect of quercetin and galangin in LPS‐stimulated RAW264. 7 macrophages and DNCB‐induced atopic dermatitis animal models, International journal of molecular medicine 41 (2018) 888-898. doi: 10.3892/ijmm.2017.3296.

[7] A. Israël, The IKK complex, a central regulator of NF-κB activation. Cold Spring Harbor perspectives in biology. 2010;2:a000158. doi: 10.1101/cshperspect.a000158.

[8] D. J. Kaczorowski, A Nakao, R. Vallabhaneni, K. P. Mollen, R. Sugimoto, J Kohmoto, et al., Mechanisms of Toll-like receptor 4 (TLR4)-mediated inflammation after cold ischemia/reperfusion in the heart, Transplantation 87 (2009) 1455-1463. doi:10.1097/TP.0b013e3181a36e5e.

[9] G. Xu, Y-C Lo , Q. Li , G. Napolitano , X. Wu , X. Jiang, et al., Crystal structure of inhibitor of κB kinase β, Nature 472 (2011) 325-330. doi:10.1038/nature09853.

[10] T. S. Beyett, X. Gan, S. M. Reilly, L. Chang, A. V. Gomez, A. R. Saltiel, et al. Carboxylic acid derivatives of amlexanox display enhanced potency toward TBK1 and IKKε and reveal mechanisms for selective inhibition. Molecular pharmacology. 94 (2018)1210-1219. doi: 10.1124/mol.118.112185.

[11] C. A. Harman, M. V. Turman, K. R. Kozak, L. J. Marnett, W. L. Smith, R. M. Garavito, Structural basis of enantioselective inhibition of cyclooxygenase-1 by S-α-substituted indomethacin ethanolamides, Journal of Biological Chemistry 282 (2007) 28096-28105. doi: 10.1074/jbc.M701335200.

[12] B. Poligone , A. S. Baldwin, Positive and negative regulation of NF-κB by cOX-2 roles of different prostaglandins, Journal of Biological Chemistry 276 (2001) 38658-38664. doi: 10.1074/jbc.M106599200.

[13] H. Khan, H. Ullah, M. Aschner, W. S. Cheang, E.K. Akkol, Neuroprotective effects of quercetin in Alzheimer's disease, Biomolecules 10 (2020) 59. doi:10.3390/biom10010059.

[14] E. Tavana, H. Mollazadeh, E. Mohtashami, SMS Modaresi, A. Hosseini, H. Sabri, et al., Quercetin: a promising phytochemical for the treatment of glioblastoma multiforme, BioFactors 46 (2020)356-366. doi: 10.1002/biof.1605.

[15] R. Kleemann, L. Verschuren, M. Morrison, S. Zadelaar, M. J. van Erk, P. Y. Wielinga, et al. Anti-inflammatory, anti-proliferative and anti-atherosclerotic effects of quercetin in human in vitro and in vivo models, Atherosclerosis 218 (2011) 44-52. doi: 10.1016/j.atherosclerosis.2011.04.023.

[16] Studio, Discovery. Discovery Studio. Accelrys [2.1] (2008).

[10]

[17] R. Huey, Morris G. M., Using AutoDock 4 with AutoDocktools: a tutorial, The Scripps Research Institute, USA 8 (2008) 54-56.

[18] O. Trott, and A. J. Olson, AutoDock Vina: improving the speed and accuracy of docking with a new scoring function, efficient optimization, and multithreading, Journal of computational chemistry 31 (2010) 455-461. doi:10.1002/jcc.21334.

[19] A Daina, O Michielin, V, Zoete, SwissADME: a free web tool to evaluate pharmacokinetics, drug-likeness and medicinal chemistry friendliness of small molecules, Scientific reports 7 (2017) 42717. doi:10.1038/srep42717.

[20] D. E. V. Pires, T. L. Blundell, D. B. Ascher, pkCSM: predicting small-molecule pharmacokinetic and toxicity properties using graph-based signatures, Journal of medicinal chemistry 58 (2015) 4066-4072. doi: 10.1021/acs.jmedchem.5b00104.

[21] R. C. Braga, V. M. Alves, M. F.B. Silva, E. Muratov, D. Fourches, L. M. Lião, A. Tropsha, C.H. Andrade, Pred-hERG: A novel web-accessible computational tool for predicting cardiac toxicity, Molecular informatics 34 (2015): 698-701. doi: 10.1002/minf.201500040.

[22] F. Montanari, B. Knasmüller, S. Kohlbacher, C. Hillisch, C. Baierová, M. Grandits, G. F. Ecker, Vienna LiverTox Workspace—A Set of Machine Learning Models for Prediction of Interactions Profiles of Small Molecules With Transporters Relevant for Regulatory Agencies, Frontiers in Chemistry 7 (2020) 899. doi.org/10.3389/fchem.2019.00899.

Evaluation of hybridization techniques and PCR-ELISA diagnosis method as a precise technique in clinical identification and diagnosis

Seyed mohamad amin mousavi rad [1], Jafar Amani 2*, AliMirhosseini[2], Shohreh Zare Karizi[3]

[1] MSc in Genetics, Department of Biology, Science and Research Branch, Islamic Azad University, Tehran.

[2] Associate Professor, Applied Microbiology Research Center, Systems Biology and Poisonings Institute, Baqiyatallah University of Medical Sciences, Tehran, Iran.

[3] Department of Genetics, Faculty of Life Sciences, Islamic Azad University, Varamin Branch - Pishva, Varamin, Iran.

*Email: Jafar.amani@gmail.com

Abstract

Today, with the increasing prevalence of infectious and viral diseases worldwide and with the advancement of knowledge in the field of diagnosis and identification of infectious agents, this has led to many medical researches to design and launch simple and effective methods in diagnosis and treatment. These types of diseases are managed. Setting up and using more accurate, sensitive, easier and cheaper diagnostic methods that can be implemented in all medical diagnostic laboratories and in all regions of the country, is an undeniable necessity in this regard. Because this will play a very important and effective role in the process of rapid diagnosis and selection of the correct treatment for infectious and viral diseases, including in critical situations such as military crises and in epidemic situations.

PCR-ELISA has been able to overcome many of the disadvantages and limitations of other methods, including conventional PCR. Therefore, PCR-ELISA is more sensitive than conventional PCR methods that are not based on ethidium bromide staining and states that PCR-ELISA is a suitable and reliable laboratory method for diagnosing diseases.

Keywords: PCR-ELISA, diseases, diagnosis, hybridization.

1. Introduction

So far, several methods have been proposed for clinical diagnosis and diagnosis, each of which has advantages and disadvantages. In the following, we will examine these methods[1, 2].

1.1 Multiplex PCR :1

Multiplex PCR is an extensive method in cell biology for amplifying multiple targets in a simple PCR experiment[3]. Multiplex PCR can use several pairs of primers in a reaction mixture and amplify more than one sequence[4]. To increase the practical use of PCR, this technique has significant potential in saving time[5].

1.2 Real-time PCR: 1

The real-time technique is similar to conventional PCR in many ways. The reaction program consists of an initial cycle of 30 to 40 chain cycles, including DNA stranding, primer binding, and polymerization of the new strand or DNA expansion[6]. The materials used to perform the reaction have the same composition as a conventional PCR reaction. The reaction mechanism is similar to PCR in that the number of copies copied per cycle is doubled. The difference between the two is that in the real-time system, by using fluorescent dyes and following them during the reaction and observing the changes in fluorescent absorption, the reaction progress can be tracked moment by moment and at the end of the program, the results of the reactions can be observed. If in a normal PCR reaction, after the reaction is complete, the results can be seen by transferring the samples to the gel[7, 8]. The real-time detection system, in addition to eliminating the steps that take place after the PCR reaction to confirm the accuracy of the test, makes it possible to measure the amount of amplified DNA[9, 10]. For this purpose, real-time devices, in addition to having a heat generating part, also have a light production and measuring part. In general, the real-time device consists of two different parts, including a heat rotating part and a fluorimeter part[11]. The rotating part is designed to perform the PCR reaction quickly, and unlike conventional PCR machines in which the reaction takes several hours, in the real-time system, the PCR reaction takes place within 45 to 60 minutes. The fluorimeter comprises a light source, optical filters, and light sensing equipment that first irradiates the solution in which the PCR reaction is taking place, excites the fluorescent material, and then measures the amount of fluorescent emitted. These two parts are placed next to each other in such a way that they are able to perform special functions such as product detection, quantitative detection of mutations[12]. The real-time device is able to detect the exponentially increasing state of PCR reaction progress, and use it to quantify DNA. Fluorescent colors give this unique power to the real-time device. In this way, by detecting DNA through fluorescent radiation that they emit and convert the exponential increase of DNA to increase fluorescent radiation in each PCR reaction cycle, this increase is measured and recorded by the device's fluorimetry system and with the help of computer software Is analyzed[13].

1.2.1 The most important advantages and disadvantages of the Real time method are as follows:1.2

- The amount of product in each cycle can be traced, while the product of traditional methods is determined after the end of the reaction and electrophoresis[14].
- It is possible to check and analyze several different transcripts in one tube[15].

- With the help of this technique, a small valuation can be done and the amount of the initial pattern can be accurately estimated[16].
- This technique also has a high resolution power so that it can detect changes of less than two folds. While the solubility of agarose gel is very poor[17].
- This method is used to evaluate accurate amounts of DNA and RNA, while not having the difficulties of the conventional method. But in addition to these advantages, we can also point out the inability of this technique to estimate the size of the reproduced product and its high cost[18].

1.3 PCR-ELISA:1

In this method, after DNA extraction, the PCR reaction is performed in such a way that in addition to amplification of the gene region, the products are labeled with the molecule of hapten digoxin. Azdigoxin gene has developed a suitable and non-radioactive diagnostic method for PCR products in the form of microtiter containers[19].

In this method, a primer with digoxin gene is used in the PCR reaction, which leads to the entry of these compounds into the structure of PCR products. The products are poured into containers covered with streptavidin, strepto-ovidin is coated in the bottom of the plate and the probe at the end of 5 biotins. It is attached to it with a strong covalent bond that is finally attached to the amplified fragment containing digoxin gene with the help of anti-digoxin gene antibody to the enzyme peroxidase at a wavelength of 490 nm using an ELISA reader. Metering is determined by the minimum level (cut off)[20, 21]. Figure 1-1 shows a schematic example of all PCR-ELISA steps.

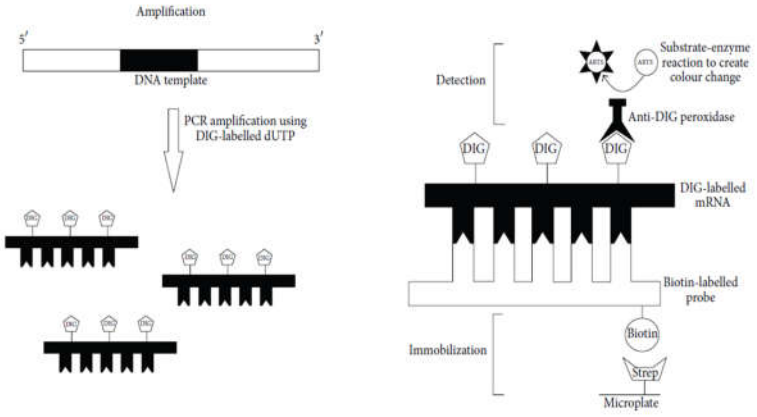

Figure 1-1 - A schematic view of the steps and factors involved in this method is shown. Involvement factors and steps on PCR-ELISA

1.3.1 The most important advantages of using PCR-ELISA method compared to the described methods include:1.3

- The ELISA method, due to the simplicity of the work steps, includes several stages of increasing incubation[21].
- Enhance the specificity of the technique by using a dedicated probe[22].
- No need for UV illuminator and dark room[23].
- Ability to analyze samples on a large scale[24].
- Do not use radioactive and carcinogenic substances such as ethidium bromide, which is harmful to humans in terms of safety and health[23].
- This technique eliminates the need for expensive equipment and probes used in methods such as real-time, and instead uses the basic and common tools available in every medical diagnostic laboratory[25].
- This method determines the lowest level of genomic DNA and contamination that can be detected in pure culture medium by PCR ELISA[26].
- Using this method, an experimental limit on the number of specimens typically occurs when the disease appears in the form of a pandemic and epidemic if it resolves, and it is possible to typically detect 96 to 384 specimens at a time[19].

1.4 Overview of PCR-ELISA applications:1

Susan Rezavand et al. In a study entitled Determining the diagnostic value of PCR-ELISA compared to classical methods and PCR to identify methicillin-resistant strains of Staphylococcus aureus using specific primers, the mecA gene of Staphylococcus aureus was amplified to a fragment It was 310 pairs open. The results of PCR-ELISA showed that this technique did not have any cross-reactivity with Klebsiella pneumoniae, Bacillus subtilis and Escherichia coli as controls and its sensitivity was evaluated as 0.5 ng. The prevalence of methicillin-resistant clinical isolates by disk diffusion, agar dilution and PCR-ELISA were 60, 58.5 and 60%, respectively. Obtained[27].

Samira Rami et al. In a study entitled Detection of specific gene of Escherichia coli enteropathogenic bacterium using the new PCR-ELISA method, the results of which were amplified using specific primers of enteropathogenic Escherichia coli eae gene, resulting in a 999 bp fragment. The results of PCR-ELISA showed that this technique did not have any cross-reactivity with the bacteria of the same family and also its sensitivity was evaluated as 11 picograms. Presented[28].

Fatemeh Ghaffarifar et al. The clock was detected with high sensitivity. In addition, experiments were performed to evaluate the sensitivity of the method used, and a standard curve related to the sensitivity of the method was drawn. Toxoplasma DNA can be detected after 4 hours and no other factors are involved in this method; Therefore, only this parasite is reproduced and identified[29].

2. Material and Methods

It includes the collection of related articles that were done by electronic search of academic databases and the Internet.

3. Results and Discussions

In recent years, various PCR methods to improve the speed and sensitivity of clinical diagnosis in different samples have been provided. In addition to being time consuming, toxic substances such as ethidium bromide are also used in this method. PCR-ELISA method is a suitable alternative method for the above mentioned materials and provides acceptable speed and sensitivity in detecting small amounts of specific sequences of pathogenic genes. In the meantime, however, the PCR technique is widely used for clinical identification and diagnosis. However, it increases the risk of contamination of laboratory personnel and the environment due to the use of agarose gel to observe the reaction result and the continuous use of ethidium bromide for gel staining in PCR-based methods. Although researchers have tried one after another to eliminate the defects of the previous methods, but they are constantly trying to find new techniques in which some of the shortcomings of the previous methods have been eliminated or have better performance and sensitivity than previous methods. It is intended by researchers.Therefore, PCR-ELISA (PCR Enzyme-Linked Immunosorbent Assay) is a very good alternative to these cases because it provides acceptable speed and sensitivity in detecting small amounts of specific gene sequences of the patient and the need to use carcinogenic dyes. The use of biotin and streptavidin provides an appropriate and non-radioactive detection method for the detection of PCR products, in which specific primers in region 5 are labeled with biotin and a specific probe of the target gene is then designed with The PCR reaction and the use of streptavidin, which is labeled with HRP, are detected and finalized to identify the interaction between the probe and the PCR product using the ELISA method.PCR-ELISA is almost 100 times more sensitive than conventional PCR and can be a good alternative to older methods due to the lack of agarose gel and electrophoresis.References.

References

[1] Laskar, P., M.M. Yallapu, and S.C. Chauhan, *"Tomorrow Never Dies": Recent Advances in Diagnosis, Treatment, and Prevention Modalities against Coronavirus (COVID-19) amid Controversies.* Diseases, 2020. **8**(3): p. 30.

[2] Primiceri, E., et al., *Key enabling technologies for point-of-care diagnostics.* Sensors, 2018. **18**(11): p. 3607.

[3] Feng, Y., et al., *Rapid detection of hypervirulent serovar 4h Listeria monocytogenes by multiplex PCR.* Frontiers in microbiology, 2020. **11**: p. 1309.

[4] Tsai, C.-L., et al., *Rapid identification of the invasive fall armyworm Spodoptera frugiperda (Lepidoptera, Noctuidae) using species-specific primers in multiplex PCR.* Scientific Reports, 2020. **10**(1): p. 1-8.

[5] Baveja, A., et al., *Development and validation of multiplex-PCR assay to simultaneously detect favourable alleles of shrunken2, opaque2, crtRB1 and lcyE genes in marker-assisted selection for maize biofortification.* Journal of Plant Biochemistry and Biotechnology, 2020: p. 1-10.

[6] Kralik, P. and M. Ricchi, *A basic guide to real time PCR in microbial diagnostics: definitions, paramters, and everything.* Frontiers in microbiology, 2017. **8**: p. 108.

[7] Leach, L., Y. Zhu, and S. Chaturvedi, *Development and validation of a real-time PCR assay for rapid detection of Candida auris from surveillance samples.* Journal of clinical microbiology, 2018. **56**(2).

[8] Park, M., et al., *Optimization of primer sets and detection protocols for SARS-CoV-2 of coronavirus disease 2019 (COVID-19) using PCR and real-time PCR.* Experimental & molecular medicine, 2020. **52**(6): p. 963-977.

[9] Pichon, M., et al., *Diagnostic accuracy of a noninvasive test for detection of Helicobacter pylori and resistance to clarithromycin in stool by the Amplidiag H. pylori+ ClariR real-time PCR assay.* Journal of Clinical Microbiology, 2020. **58**(4).

[10] Floriano, I., et al., *Accuracy of the Polymerase Chain Reaction (PCR) test in the diagnosis of acute respiratory syndrome due to coronavirus: a systematic review and meta-analysis.* Revista da Associação Médica Brasileira, 2020. **66**(7): p. 880-888.

[11] Shirato, K., et al., *An ultra-rapid real-time RT-PCR method for detecting Middle East respiratory syndrome coronavirus using a mobile PCR device, PCR1100.* Japanese Journal of Infectious Diseases, 2019: p. JJID. 2019.400.

[12] Hatch, A.C., et al., *Continuous flow real-time PCR device using multi-channel fluorescence excitation and detection.* Lab on a Chip, 2014. **14**(3): p. 562-568.

[13] Gudnason, H., et al., *Comparison of multiple DNA dyes for real-time PCR: effects of dye concentration and sequence composition on DNA amplification and melting temperature.* Nucleic acids research, 2007. **35**(19): p. e127.

[14] Larionov, A., A. Krause, and W. Miller, *A standard curve based method for relative real time PCR data processing.* BMC bioinformatics, 2005. **6**(1): p. 62.

[15] Kang, K., et al., *A novel real-time PCR assay of microRNAs using S-Poly (T), a specific oligo (dT) reverse transcription primer with excellent sensitivity and specificity.* PloS one, 2012. **7**(11): p. e48536.

[16] Liu, J., et al., *Identification of appropriate reference genes for gene expression studies by quantitative real-time PCR in Tribolium castaneum after exposure to phosphine.* Journal of Agricultural Biotechnology, 2014. **22**(2): p. 257-264.

[17] Wolff, B.J., et al., *Detection of macrolide resistance in Mycoplasma pneumoniae by real-time PCR and high-resolution melt analysis.* Antimicrobial agents and chemotherapy, 2008. **52**(10): p. 3542-3549.

[18] McCabe, E.M., et al., *Development and evaluation of DNA and RNA real-time assays for food analysis using the hilA gene of Salmonella enterica subspecies enterica.* Food microbiology, 2011. **28**(3): p. 447-456.

[19] Zhou, Y.-C., et al., *A Rapid and Accurate Detection Approach for Multidrug-Resistant Tuberculosis Based on PCR-ELISA Microplate Hybridization Assay.* Laboratory Medicine, 2020.

[20] Munch, M., et al., *Detection and subtyping (H5 and H7) of avian type A influenza virus by reverse transcription-PCR and PCR-ELISA.* Archives of virology, 2001. **146**(1): p. 87-97.

[21] Perelle, S., et al., *Comparison of PCR-ELISA and LightCycler real-time PCR assays for detecting Salmonella spp. in milk and meat samples.* Molecular and cellular probes, 2004. **18**(6): p. 409-420.

[22] Gilligan, K., et al., *Identification of Staphylococcus aureus enterotoxins A and B genes by PCR-ELISA.* Molecular and cellular probes, 2000. **14**(2): p. 71-78.

[23] Andersen, U.V., et al., *Recent advances in diagnosing pathogenic equine gastrointestinal helminths: the challenge of prepatent detection.* Veterinary Parasitology, 2013. **192**(1-3): p. 1-9.

[24] Laitinen, R., E. Malinen, and A. Palva, *PCR-ELISA: I: Application to simultaneous analysis of mixed bacterial samples composed of intestinal species.* Systematic and applied microbiology, 2002. **25**(2): p. 241-248.

[25] Adler, M., *Immuno-PCR as a clinical laboratory tool.* Advances in clinical chemistry, 2005. **39**: p. 239-292.

[26] Beifuss, B., et al., *Direct detection of five common dermatophyte species in clinical samples using a rapid and sensitive 24-h PCR–ELISA technique open to protocol transfer.* Mycoses, 2011. **54**(2): p. 137-145.

[27] Rezavand, S., et al., *Determination of PCR-ELISA Diagnostic Value in Comparison With Classical Methods and PCR to Detect Resistance to Methacillin.* Iranian Journal of Medical Microbiology, 2019. **13**(1): p. 22-31.

[28] Rami, S., J. Amani, and T. Saleh, *Detection of Specific eae Gene from Enteropathogenic Escherichia coli by PCR-ELISA.* Journal of Mazandaran University of Medical Sciences, 2019. **28**(170): p. 43-55.

[29] Norouzi, R., et al., *Application of PCR-ELISA method based on RE domain for diagnosis of toxoplasmosis in experimentally infected rat (Rattus norvegicus).* Pathobiology Reaearch, 2008. **11**(1): p. 99-107.

Prognostic role of SMAD4 and KRAS expression in overall survival of gastric cancer patients

Mehrdad Nasrollahzadeh Sabet[1], Mohammad Foad Heidari[2] and Javad Behroozi[1*]

[1] Department of Genetics and Biotechnology, School of Medicine, AJA University of Medical Sciences, Tehran, Iran.

[2] Department of Medical Laboratory Sciences, School of Allied Health Medicine, AJA University of Medical Sciences, Tehran, Iran.

*Email: jvdbehroozi@gmail.com

Abstract

Gastric cancer (GS) is evolved from a series of changes in the gastric mucosa. This cancer is currently the third leading cause of global cancer-related death and more than 930,000 new cases of gastric cancer are being diagnosed each year with more than 723,000 deaths annually. SMAD4 is initially isolated as a tumor suppressor gene on chromosome 18q21 and acts as a signal transducer for the members of the TGF-β superfamily. KRAS is one of the most frequently mutated oncogenes in human cancer and its gain of function mutations occur in approximately 30 percent of all human cancers. Here we aim to elucidate the prognostic role of SMAD4 and KRAS expression in the overall survival of gastric cancer patients. To investigate the relationship between SMAD4 and KRAS expression and prognosis of gastric cancer, survival data associated with GC patients were obtained from Kaplan-Meier Plotter. Overall survival data for 876 patients were divided into two groups according to the median expression of genes and Kaplan-Meier plots were created. We used a database with 876 GC patients from six independent datasets. Kaplan–Meier analysis of this dataset indicated that increased SMAD4 and KRAS expression was correlated with the overall survival of patients. Patients in the high expression group of KRAS had a significantly shorter OS than patients in the low expression group. In contrast, patients in the high expression group of SMAD4 had a significantly longer OS than patients in the low expression group. SMAD4 and KRAS expression was significantly associated with GC overall survival. However further studies are needed to validate these results and paving a way for the clinical application of KRAS in practice.

Keywords: Overall survival, SMAD4, KRAS, gastric cancer.

1. Introduction

Gastric cancer (GS) is a heterogeneous malignant disease that evolves from a series of changes in the gastric mucosa which progress from normal gastric mucosa to non atrophic gastritis, multifocal gastric atrophy, intestinal metaplasia, dysplasia, and finally to cancer [1]. This cancer is currently the third leading cause of global cancer-

related death and more than 930,000 new cases of gastric cancer are being diagnosed each year with more than 723,000 deaths annually [2]. Metastatic GC mortality is associated with peritoneal dissemination, hematogenous spread, and lymph node invasion. Investigation of the molecular mechanism of gastric cancer progression such as proliferation, growth, migration, invasion, and apoptosis in the goal of many studies [3].

SMAD4 is initially isolated as a tumor suppressor gene on chromosome 18q21 and acts as a signal transducer for the members of the TGF-β superfamily. This signaling leads to tumor development and progression [4]. Inactivation of SMAD4 at the gene or protein level has been shown to be essential for the progression of several tumors, resulting in decreased gene expression [5]. KRAS is one of the most frequently mutated oncogenes in human cancer and its gain of function mutations occur in approximately 30 percent of all human cancers [6]. Although many previous studies have determined the impact of the overexpression of KRAS on several cancers, little is known about the prognostic role of its expression in GS. Here we aim to elucidate the prognostic role of SMAD4 and KRAS expression in the overall survival of gastric cancer patients.

2. Material and Methods

To investigate the relationship between SMAD4 and KRAS expression and prognosis of gastric cancer, survival data associated with GC patients were obtained from Kaplan-Meier Plotter [7]. Overall survival (OS) data for 876 patients were divided into two groups according to the median expression of genes and Kaplan-Meier plots were created. These patients were related to GSE14210, GSE15459, GSE22377, GSE29272, GSE51105, and GSE62254 datasets.

3. Results and Discussions

We used a database with 876 GC patients from six independent datasets. Kaplan–Meier analysis of this dataset indicated that increased SMAD4 and KRAS expression was clearly correlated with the overall survival of patients (Figure 1). Patients in the high expression group of KRAS had a significantly shorter OS than patients in the low expression group (log-rank P <0.0001). The median survival of the high and low expression group was 25.5 and 42 months, respectively. These results indicate a pivotal role for KRAS overexpression in GC. KRAS overexpression gastric cancers are being considered incurable. However, there are a chance of inhibiting signaling cascades downstream of KRAS, in particular, the MAPK and PI3K pathways [8].

Our results showed that the expression level of SMAD4 has a positive correlation with the overall survival of GC patients and patients with the high expression level of SMAD4 live longer than patients with low expression (log-rank P <0.0001). The median survival in the high and low expression group was 44.07 and 23.6 months, respectively.

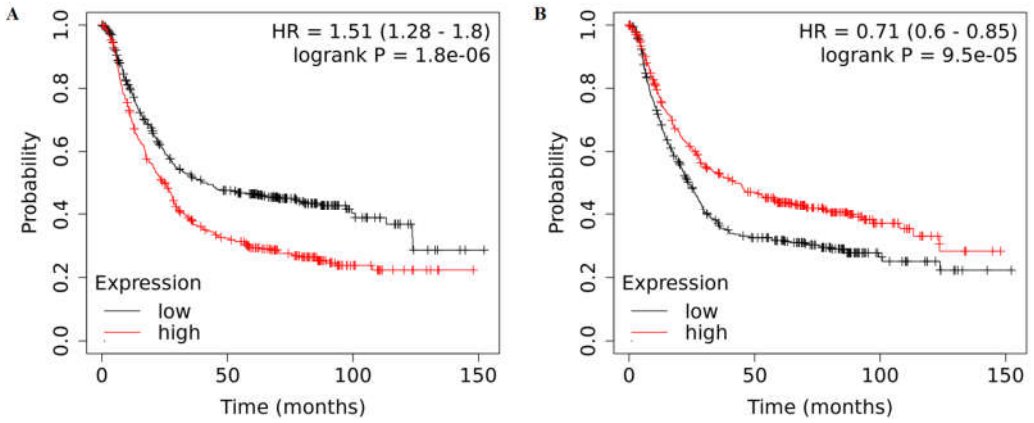

Figure 1. Overall survival of gastric cancer patients in high and low expression groups. A) KRAS and B) SMAD4 Kaplan-Meier plots

Currently, the prognosis of GC patients is primarily determined using depth of wall invasion, lymph node or distant metastasis status, and age; however, these prognostic factors are limited in clinical practice, and may not result in an accurate prognosis [9]. Our results introduce the expression level of SMAD4 and KRAS as a new tool for the prognosis of GC patients. Regardless of the tremendous attempts in the past decades that covered the multiple aspects of KRAS activation, the KRAS mutant remains being considered undruggable. As a result, much focus has been put on alternative approaches instead, such as inhibiting signaling cascades downstream of RAS, in particular, the MAPK and PI3K pathways. SMAD4 and KRAS expression was significantly associated with GC overall survival. However larger well-designed studies with more ethnic groups and larger population studies are required to validate these results and paving a way for the clinical application of KRAS and SMAD4 in practice.

References

[1] Cueva, P., et al., Etiology of stomach cancer (C16) in Central and South America. Cancer in Central and South America. Lyon: International Agency for Research on Cancer, 2016.

[2] Tan, P. and K.-G. Yeoh, Genetics and molecular pathogenesis of gastric adenocarcinoma. Gastroenterology, 2015. 149(5): p. 1153-1162. e3.

[3] Hao, N.-B., et al., The role of miRNA and lncRNA in gastric cancer. Oncotarget, 2017. 8(46): p. 81572.

[4] Jiang, Y.-L., et al., Prognostic role of Smad4 expression in gastric cancer: a meta-analysis. Int J Clin Exp Med, 2016. 9(12): p. 23134-23143.

[5] Wang, L.-H., et al., Inactivation of SMAD4 tumor suppressor gene during gastric carcinoma progression. Clinical cancer research, 2007. 13(1): p. 102-110.

[6] Liu, P., Y. Wang, and X. Li, Targeting the untargetable KRAS in cancer therapy. Acta Pharmaceutica Sinica B, 2019. 9(5): p. 871-879.

[7] Szász, A.M., et al., Cross-validation of survival associated biomarkers in gastric cancer using transcriptomic data of 1,065 patients. Oncotarget, 2016. 7(31): p. 49322.

[8] Hwang, K.-T., et al., Prognostic Role of KRAS mRNA Expression in Breast Cancer. Journal of Breast Cancer, 2019. 22(4): p. 548-561.

[9] Han, J., et al., Clinicopathological Characteristics and Prognosis of cT1N0M1 Gastric Cancer: A Population-Based Study. Disease markers, 2019. 2019.

Comparison of common versus blockchain based health systems: advantages and challenges

Elnaz Nazari zare[1*], Narges Tabatabai mashhadi[2,] and Ebrahim Daneshi far[2]

[1] M.Sc. Student, Biomedical Engineering, Imam Reza International University, Mashhad, Iran.

[2] Professor Assistant, Imam Reza International University, Mashhad, Iran.

*Email: elnaznazari93@gmail.com

Abstract

The exchange of medical information includes maintenance, care, diagnosis, counseling, and treatment. Recently, attention to medical data transfer and educational issues has also become important. To achieve the desired result in a system requires the right decisions based on having high-quality information, and it is necessary to use new information technology. Using information systems and technology in health can be used in education, medical and paramedical sciences, improving the quality of treatment, and reducing the center's costs. A large amount of medical information is recorded and transmitted daily. This large database of medical information needs to be managed in privacy, security, and availability. Blockchain technology can provide a solution that helps record and share medical records. The transition to blockchain technology in healthcare processes also poses problems. Sufficient training is needed for health care providers and patients. Users need to coordinate on distributing and managing distributed controllers and network performance to ensure network security and services among software. However, in this study, an attempt has been made to compare existing health systems and blockchain-based health systems so that this new science can be used in health.

Keywords: Blockchain, Distribution of medical information, Secure transfer of medical data, security Medical data, Telehealth, Validation of medical data.

1. Introduction

With the advancement of communication technologies and the abundance of health devices and programs over time, a branch of medicine was formed. A patient could benefit from medical services and information without having a physical presence with his doctor. Telemedicine techniques in primary care have proven that better access to clinical care is possible using telecommunications technologies to connect multiple medical centers and exchange information over long distances. Proper and correct communication between physicians and patient is the cornerstone of good activity and medical constructiveness. It plays a pivotal and essential role in creating and continuing an optimal treatment process. This type of relationship, due to its virtual form and nature, needs to be

identified. Its ethical considerations to pave the way to achieve the goals and benefits by considering these points [1]. Therefore, identifying its ethical challenges in various areas such as satisfaction, confidentiality, privacy, and medical professional commitments and anticipating the necessary arrangements in this field is very important and needs attention. One of the major benefits of the digital health system is better access to health care records for professionals, researchers, and patients, which indicates an improvement in the quality and efficiency of health care.

Also, much medical information is recorded and transmitted every day, so this large medical information database needs to be managed in privacy, security, and availability. Hospitals and physicians should have access to patient medical information throughout the treatment process while ensuring patient safety and privacy and sharing their clinical information. As data is widely shared and stored in different places, securing it becomes an important issue [2]. Increasing the volume and complexity of good prospects in developing treatment offers new security and privacy challenges. At present, medical information is not limited to clinical records and includes a significant amount of biomedical imaging, tests, etc. The daily produced significant amounts of clinical information that includes information that can be considered private. Many efforts have been made to ensure the proper use of data and appropriate standards for privacy [3]. Uncertainty about a patient record has financial and legal consequences for patient care. Privacy includes ensuring that only authorized parties can access a patient's medical record. This affects the health care system. Because privacy has both ethical and legal implications, the need for proper data comprehension and processing is well understood. One of the main concerns in the production and use of data is privacy issues. This is especially important in healthcare because a high percentage of health data can be private. To ensure data management competence, some rules govern processes such as the production, use, transmission, access, and exchange of information [4].

Therefore, in most of the ethical codes of medical professional associations and organizations, privacy and confidentiality have been emphasized. Even in some countries, laws have been enacted in this regard, such as the HIPAA law in the United States.

One of the main concerns in the production and use of data is privacy issues. Privacy is important in healthcare because a high percentage of health data can be private. To ensure data management competency, some rules govern processes such as the production, use, transmission, access, and exchange of information [5]. Proper communication between physician and patient plays an essential role in the treatment process. The use of information technology in the health sector due to its virtual infrastructure requires different standards in different areas such as patient satisfaction, privacy, personal data, and clinical and medical expertise [1]. The use of information technology in medicine has several advantages, including better access to clinical information, better service to the patient, and better research work. It should always be borne in mind that the volume of information and the number of people who join or share this huge health information network is increasing day by day, so in the meantime, information security is considered an important issue [3].

However, the complexities and problems we have addressed require the development of systems and procedures that ensure proper data use. We significantly enable data to use to make significant progress in facilitating health outcomes—taken, felt. The main purpose of this work is to describe a correct and reliable approach to sharing health information. In a network, patient records must be consistent everywhere, and data boundaries and access conditions must be specified. In other words, this data must not only be shared but must be

shared in such a way that all interested parties can benefit from it. It should be noted that the blockchain in the health field that is a very new topic in recent years has been investigated.

2. Common systems using information technology in the medical field

HIS system is a comprehensive and integrated information system designed for the hospital's executive and clinical management [6]. This system's advantages can be to create a logical order in different units, increase speed, accuracy, and quality in providing services, increase the possibility of management control over daily hospital activities, reduce medical violations, prevent wastage of consumables and drugs access to the latest department information. Various and direct supervision of hospital affairs etc. noted. One of the most important challenges in using HIS systems is protecting patient information and documents confidentially, which must be ensured by reliable methods. Standards for this subject are not yet well developed, and easy access to information has reduced data security, especially after patient discharge. It is necessary to ensure the confidentiality of information for many years after discharge without the slightest damage. Other challenges include the lack of cooperation between different parts of the organization in automation between them. For example, some insurance companies do not trust hospital information, which reduces these system's efficiency.

Electronic Health Record (EHR) shows information about a person referring to health centers. It also includes social care, home care, support systems [7]. Features of the health record include the security and confidentiality of information, accessibility for authorized persons at any time and place, and the fact that all of a person's health information is focused on it. Problems related to health records include lack of integrated health information, misuse of health support services due to lack of concentration of information, incomplete implementation of laws related to medical affairs, reproduction of health information in parallel during visits to different medical centers, and lack of Support for correct information noted.

In 1394, according to Article 13 of the Law on Combating Commodity and Currency Smuggling, the activity of systems with the acronym T-Tack began. In this system, the authenticity of all health-oriented products, including drugs, medical equipment, food and medicine, cosmetics, was considered. Measures such as "registration, order registration, clearance, identification, and authenticity of goods" were also considered [8]. Among the problems that existed during the implementation of the T-Tack system are the lack of cooperation between the distribution companies and the management changes of the Food and Drug Administration, which slowed down the process of completing the T-Tack, the lack of up-to-date servers, and the lack of budget forecasting in this area. The organization's important data should be kept with low-security conditions, transfer of this system to the private sector due to inability, technical knowledge, and specialized forces in government systems where information security can pose a risk and lack proper identification of individuals allocating government currency to import drugs. He pointed out that people who do not have the authority and act like a mafia in medicine and import drugs whose import has been banned..

3. Blockchain-based health system

One of the most important goals of using blockchain in medicine is a safer and more efficient way to exchange data. All patient's treatment records can be recorded together due to the use of blockchain. Each patient can have a unique blockchain fingerprint to ensure that their identity and medical records are authentic. Other goals of blockchain include medical research, counterfeiting, data security, and health care monitoring. Because all blockchain transactions are sealed and unchangeable, health offenders are easily identifiable

3.1 blockchain

Blockchain is a public database like an e-book that can be openly shared among different users and creates an unchangeable record of their transactions; each block is sealed and linked once with the previous block [9]. Blockchains are commonly used to store information. The digital record or transaction at issue is called to set a block or certain periods of allowing users to participate in the Digital Forum. The blockchain can only be updated by agreement between the participants in the network. Once new data has been entered, it can never be changed or deleted, thus ensuring data integrity in the blockchain. The blockchain contains a verifiable record of each transaction ever made in the system.

A blockchain distributes a file system where participants maintain a copy of the file and agree to coordinate changes from a network perspective. This file is made up of blocks. Each block contains a set of transactions and the original data, including the scheduling and encryption signature (hash) of the previous block, the current block hash, and some other information. The previous block hash connects the current block to the previous block, and the next blocks also need the current hash block, so these blocks are chained together. If something in the block is modified, its hash is calculated, and another value will be declared as the new hash, and the block will not accept it. Each blockchain block is cryptically linked to the previous block, making it difficult to change historical records or make it easier to identify when invading [9]. Key features of blockchain technology are decentralization, immutability, anonymity, stability, and reliability. Blockchain technology is an integrated infrastructure that includes cryptography, mathematics, algorithms, and economic models, network partner networks, and the use of distributed agreement algorithms to solve the problem of traditional database synchronization [9].

The Bitcoin blockchain can be thought of as a very large Excel spreadsheet that contains information on all the transactions that have taken place in its history, along with the exact location of each bitcoin. Every 10 minutes, this Excel page is updated, and new blocks of new transfers are added to it. Anyone can have a copy of this information, and it is completely transparent to everyone. Each of these blocks has its hash. A hash is a string of characters that is created with specific functions. In a blockchain, subsequent hashes also contain previous hashes. The hash is obtained in each blockchain with a specific mathematical function that the developers specify. The slightest change in a block of information changes its hash altogether. A hash is obtained by placing basic information in a strong mathematical formula called a hash operator[10]. The blockchain operation is shown in Figure 1.

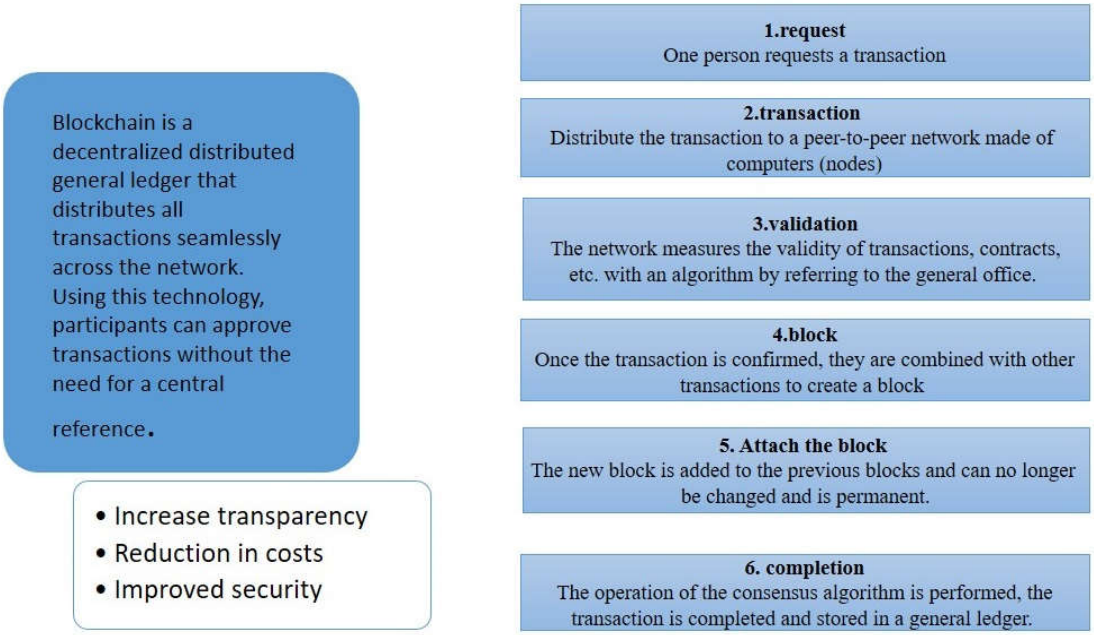

Figure 1- Blockchain performance

3.2 blockchain architecture

A blockchain is a sequence of blocks containing a complete list of transaction records or entries of all transactions, such as a regular public library. Figure 2 shows an example of a blockchain. Each block includes a block header, a parent block hash (previous block hash), and a transaction logs list. The blockchain's first block is called the genesis block, which has no parent blocks [10]. Transaction data is permanently stored in files called blocks. Each block contains the block header and the history of some or all recent transactions and refers to the previous block.

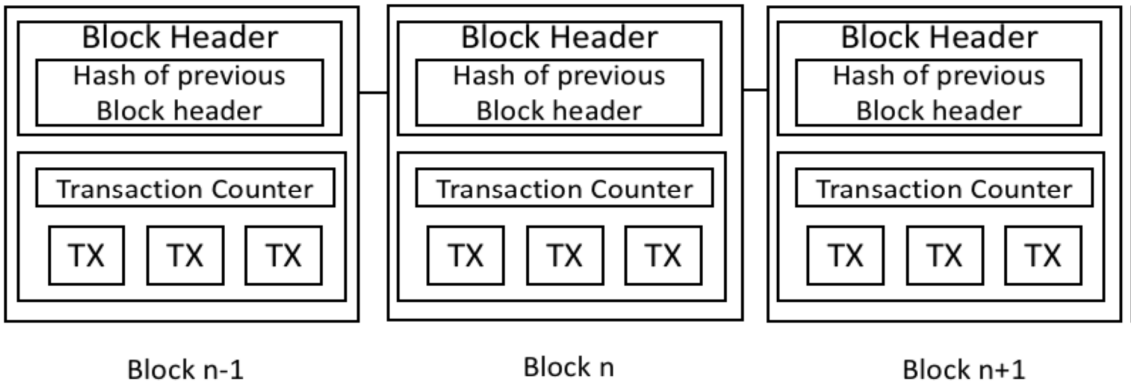

Figure 2- Blockchain Architecture [10]

3.3 Infrastructure and implementation platforms

The infrastructure and implementation platform include a description of installation steps, preparation of services, and facilities that ultimately lead to a specific operation and purpose. There are various infrastructures to implement projects with blockchain, the most common of Bitcoin and Ethereum infrastructure.

Comparable cases between the two include the following:

1. Bitcoin manages about 7 trades per second, Ethereum trades about 20 trades per second[11].

2. It currently takes about 10 minutes on the network for Ethereum and about 14 seconds for Bitcoin to create blocks that contain the transaction[12].

3- The blockchain bitcoin's current size is equal to 190.65 GB, and the size of the blockchain Ethereum is equal to 330.61 GB[12].

4. The Bitcoin blockchain is currently distributed worldwide in 11,877 complete nodes, and the Ethereum blockchain is distributed worldwide in 17,263 complete nodes[12].

3.4 Implemented health systems based on blockchain

With the advancement of technology and the abundance of health devices and health programs, much medical information is recorded and transmitted every day. This large database of medical information needs to be managed in privacy, security, and availability. Hospitals and physicians should have access to patient medical information during the treatment process while ensuring patient safety, privacy, and sharing their clinical information. As data is widely shared and stored in different places, securing it becomes an important issue.

Blockchain technology can provide a solution that not only helps to record and share medical records but also protects the privacy of each patient's data by giving their patients their personal medical information [12]

It is reasonable to assume that every event impacts patient care under one or more events. For example, a copy may be obtained after positive laboratory tests. This concept can be well described in the blockchain model, where a current event's identity depends on all past events. Blockchain technology will provide more efficient and secure tools in this area. This technology's unchangeable nature could be dramatic changes brought to the health sector and, therefore, seem quite appropriate for this section[13].

The main goals of using blockchain in the medical field are safer and more efficient data exchange. Using the blockchain can be recorded in one place, all the records of patients. Each patient can have a unique blockchain fingerprint to ensure that their identity and medical records are authentic. Other goals of blockchain include medical research, counterfeiting, data security, and health care monitoring.

Table 1- Sample of blockchain generated systems in the field of medical information distribution

System name	link	Country	Implementation platform	field of activity
Guardtime	https://guardtime.com/health	Estonia	Blockchain	EMR management using blockchain
Healthbank	https://www.healthbank.coop	Switzerland	Blockchain	Full control of patient's information by themselves
Dermonet	https://www.dermonet.com	Italy	Blockchain	Telemedicine - Establishing the ability to visit several physicians and compare their prescriptions

4. Comparison of blockchain-based health systems

The blockchain information encryption feature can be used in the field of health. Organizations or individuals themselves can include information about a person (such as the time of admission and discharge, as well as a photograph of him or her and all medical records) in a dedicated blockchain so that when the doctor and patient need it, they can look at their medical records. The blockchain has access to all of his information, but there is a very serious challenge in this, and that is the dispersion of data. Doctors, nurses, and other health care providers use a variety of electronic systems to record patient records. Due to this system's diversity, there is not much transparency, and it is not easy to access records from one system to another, but blockchain can solve this problem[14].

In general, both the patient and the provider are provided with the opportunity to benefit from a robust exchange infrastructure. It can be concluded that the significant benefits gained by providers and organizations bring greater convenience and better outcomes in patient care [10].

For a better summary, the advantages - disadvantages, and challenges of using blockchain-based systems in the field of health are listed in Table 2.

Table2 Summary of blockchain-based health systems

group	disadvantages	advantages	challenges
people	The possibility of the physician using the patient's clinical information for research work after the first access to information and without the patient's consent	Maintaining patient clinical information in a unified manner	The difficulty of working with these systems for ordinary people
		Clinical information is always available	The issue of commitment, ethics, and adherence to it by both the physician and the patient
		More patient control over their clinical information	
Processing	To make changes to this technology's current infrastructure, the access management level must first be legally approved.	High resistance of these systems to invasion	Barriers to comply with legal requirements and technical barriers related to storage and distribution, as determined by agreements to share information
		High accuracy, transparency, and efficiency	
		Reduce the production of counterfeit drugs and clinical trials by reducing the current amount spent on third-party verification	The amount of data that can be stored
			Open source blockchain

5. Conclusion

With the advent of blockchain technology and its capabilities, we can hope for blockchain applications in everyday life and make them tangible. The technology acts as a digital signature and is a distributed platform that allows information to be transferred from one place to another with high security. The key factor in blockchain technology is its enormous power for automatic tuning. Blockchain is an open-source technology that no one owns, it does not have a central executor to verify transactions, and it automatically sets up the network. This

technology can be a database, protocol, or software. Once the information is stored, it will no longer be possible to overwrite or change it. This design allows the blockchain to create a lasting historical record.

Because blockchain is a public data structure, it can be applied to domains other than digital money. It also makes sense to assume that each patient care event is affected by one or more previous incidents. For example, a prescription may be positive after a laboratory test. This concept can be well described in the blockchain model, where a current event's identity depends on all past events [10]. Blockchain technology will provide more efficient and secure tools in this area. This technology's unchanging nature can bring about dramatic changes in the healthcare sector, and for this reason, it seems perfectly appropriate for this sector.

As we have said about the benefits of using blockchain in health, it is necessary to note that in the meantime, information security is considered an important issue [3]. What certain is that important issues such as confidentiality, which has an important effect on maintaining patient's trust in the medical community, and maintaining the confidentiality of patient's electronic information, which is a necessary process, must be ensured, and effective protection of information during storage, transmission, and receipt Take place. Therefore, the privacy and effective communication goals mentioned in this article should not be sacrificed to the benefits of these blockchain-based methods. As security needs become more acute, scales of data use and data integration are increasing rapidly. Blockchain technology offers a scalable solution to many of the common security issues faced by large data sets. Therefore, it can be boldly said that distributed general ledger technology (like the same technology found in digital currencies such as Bitcoin) is not necessarily related to finance and digital money. These technologies decentralize information while maintaining information security, encryption, and accuracy and can be addressed with a medical engineering approach.

References

[1] M. Zali, "New Principles of Physician-Patient Relationship," Iranian Academy of Medical Sciences, Summer 2001. ISBN: 978-964-7277-59-4

[2] M. Parsa, "Privacy and Confidentiality in Medicine and Its Different Aspects," Journal of Medical Ethics and History, Year 14, Number 9, Summer 2017, Pages 1-14.

[3] P. Mamoshina, L. Ojomoko, "Converging blockchain and next-generation artificial intelligence technologies to decentralize and accelerate biomedical research and healthcare" Oncotarget, vol. 9, no. 5, pp. 5665–5690, 2018.Atluri, S.N., and Shen, S. (2002), "The Meshless Local Petrov–Galerkin (MLPG) Method," Tech Science Press, USA. doi: 10.18632/oncotarget.22345

[4] W .Stallings, "Cryptography and network security: principles and practices." Pearson Education, India, 2006. ISBN: 978-0134444284

[5] M. Mettler, "Blockchain Technology in Healthcare" IEEE 18th International Conference on e-Health Networking, Application and Services, 2016. doi: 10.1109/HealthCom.2016.7749510

[6] R. Krishnamurthy, D. Novillo. World Health Organization and Pan American Health Organization, Handbook for Electronic Health Records Implementation, no. June 2017.

[7] L. Ismail, H. Materwala, "Blockchain paradigm for healthcare: Performance evaluation," Symmetry (Basel)., vol. 12, no. 8, 2020. doi: 10.3390/sym12081200

[8] Fars News Agency, the reason for the disruption in the Ministry of Health / the case of transferring the system servers abroad. Retrieved September 12, 1998, from https://www.farsnews.com/news/

[9] Z.Zheng, S.Xie, H.Dai, X, Chen, H.Wang (2017). "An overview of Blockchain technology: Architecture, consensus, and future trends"(pp. 557-564). IEEE. doi: 10.1109/BigDataCongress.2017.85

[10] J. H. Mosakheil, Master Thesis, "Security Threats Classification in Blockchains," Culminating Proj. Inf. Assur., p. 141, 2018.

[11] T. Dinh, A. Wang, J. Chen, G., Liu, R., Ooi, B. C., & Tan, K.-L. (, 2017). Blockbench: A framework for analyzing private blockchains. In Proceedings of the 2017 ACM International Conference on Management of Data (pp. 1085-1100).doi: 10.1145/3035918.3064033

[12] A.Ellervee, (2017).Master Thesis, "A reference model for Blockchain-based distributed ledger technology, " The University of Tartu.

[13] K. Mannarino, G. Barilla, A. Pinna, and S. Ibba, "A blockchain approach applied to a teledermatology platform in the Sardinian Region (Italy)," Inf. vol. 9, no. 2, 2018.doi: 10.3390/info9020044

[14] M. N. Almunawar and M. Ansari, "Health Information Systems (HIS): Concept and Technology," no. March 2012.

Advancements in Isothermal Nucleic Acid Sequence-based Amplification (NASBA) and its Applications in Point-of-care Diagnostics

Rozi Asadi [1], Hamidreza Mollasalehi*[2], Zahra Kianmehr[1]

[1] Department of Biochemistry, Faculty of Biological Science, North Tehran Branch, Islamic Azad University, Tehran, Iran

[2] Department of Microbiology and Microbial Biotechnology, Faculty of Life Sciences and Biotechnology, Shahid Beheshti University, Tehran, Iran. Postal Code: 1983969411

*Corresponding Author: *Dr. Hamidreza Mollasalehi*

Department of Microbiology and Microbial Biotechnology, Faculty of life Sciences and Biotechnology, Shahid Beheshti University, Velenjak, Tehran, Iran.

Tel: +98-21-29905942

Fax: +98-21-22431664

E-mail: H_mollasalehi@sbu.ac.ir

Abstract

Isothermal amplification methods are designed to overcome the main shortcomings of conventional amplification methods. Nucleic acid sequence-based amplification (NASBA) is specifically for the detection of ribonucleic acid (RNA) molecules using a system of three enzymes and two primers. Further improvements to the conventional NASBA resulted in a higher efficiency of the method in diagnostic applications. It could also undergo miniaturization which will make the approach well-suited for point of care tests (POCT). The mechanism of the method, some advancements to the main drawbacks and applications will be discussed.

Keywords: Diagnostic assay, Isothermal amplification, NASBA, POCT, RNA.

1. Introduction

Before the advent of polymerase chain reaction (PCR), diagnostic processes were based on cell culture that was time-consuming, laborious, low sensitivity, and drawbacks in the cultivation of many viruses and bacteria [[1],[2]]. PCR, as a direct in-the-field nucleic acid test in molecular biology, gradually crossed the borders and became the most dominant method for diagnostic purposes [2]. However, PCR-based methods have several drawbacks such as high contamination risk, expensive instruments, false-positive results, and time-consuming process. Disadvantageous of PCR led the researchers to devise other methods that not only address the limitations of PCR but also have advantages over it. In the other hand, with the increasing prevalence of infectious diseases with the bacterial and viral origin, the need for a fast, accurate, and sensitive method with high specificity that is

not limited to the lab but can be exploited in POCTs, has introduced a new criterion. Hence, these led the researchers to develop the isothermal amplification technologies to become an alternative for PCR and a promising technology for "in-field" diagnosis[3],[4]. In contrast to PCR counterpart, isothermal amplification techniques are carried out at a constant temperature without a need for expensive and power-hunger thermal cycler instruments. This feature makes them capable of miniaturization for POCT purposes [5],[6]. Various isothermal techniques have been developed in the last two decades. Some methods such as LAMP, NASBA, MDA, SDA, RCA, and HDA are the most well-known among them. Although each exhibit unique capabilities, all still needs to undergo further improvements and optimization to fulfill the requirements [3].

Mechanism of NASBA, advancement, and applications

NASBA or self-sustained sequence replication (3SR) is an isothermal nucleic acid amplification technique developed by J.Compton in 1991 [7]. The technique was designed to detect RNA sequences, although it is also feasible on DNA molecules by applying two denaturation steps[[8],[9]]. NASBA is similar to another isothermal amplification method so-called transcription-mediated amplification (TMA) [10], as both utilize a reverse transcriptase to generate cDNA from RNA targets [11].

The amplification reaction is conducted at 41^{o}C by utilizing two primers and three enzymes including reverse transcriptase adopted from avian myeloblastosis virus (AMV-RT), T7 DNA-dependent RNA polymerase (DdRp), and RNase H[[7],[12]]. One primer (P1) is a forward anti-sense with a non-complementary region with target RNA at 5`end. It includes a promoter sequence for the corresponding T7 RNA polymerase [13]. The other primer (P2) is a shorter reverse one designed to hybridize with cDNA generating from P1. The target sequence is a single strand sense RNA (+) with 100-150 bp length [11]. The amplification of the target takes place in two cyclic and non-cyclic stages (Figure 1) [14].

Following the hybridization of P1 with the target RNA, AVM-RT generates a complementary cDNA. The resulting DNA/RNA hybrid undergoes the first denaturation step by RNase H in order to further priming of single-stranded cDNA with P2 primer and formation of subsequent dsDNA. At the end of the non-cyclic stage, RNA polymerase recognizes the T7 promoter and transcripts the corresponding RNA strands. Each RNA product could serve as a template in a cyclic stage of the reaction results in exponential amplification and accumulation of long anti-sense single strands of RNAs as NASBA amplicon.

Typical NASBA assay could achieve 10^{9}-fold amplification within 1.5– 2h at a constant temperature [10]. Since the NASBA amplicons are single-stranded in the absence of two-step denaturation, they may readily undergo hybridization-based detection [8].

NASBA amplicons could be detected by a variety of detection methods such as gel electrophoresis, ELISA, enzyme-linked gel assay (ELGA) [15] electrochemiluminescent (ECL), and more suitably and specifically a real-time detection with molecular beacons (MBs). However, the selection of an appropriate detection method also depends on the assay configuration [5].

Multiplex-NASBA is also developed to detect multiple targets simultaneously in a single reaction, although it is less sensitive compared to the single-plex assay [6].

The counterpart of NASBA method is RT-PCR which is widely used for amplification of RNA molecules. NASBA exhibits some advantages over the RT-PCR that is expensive, complicated, laborious [16]. Furthermore,

NASBA is less time-consuming and more sensitive [14]. These make NASBA an ideal alternate for RT-PCR [[9],[8]].

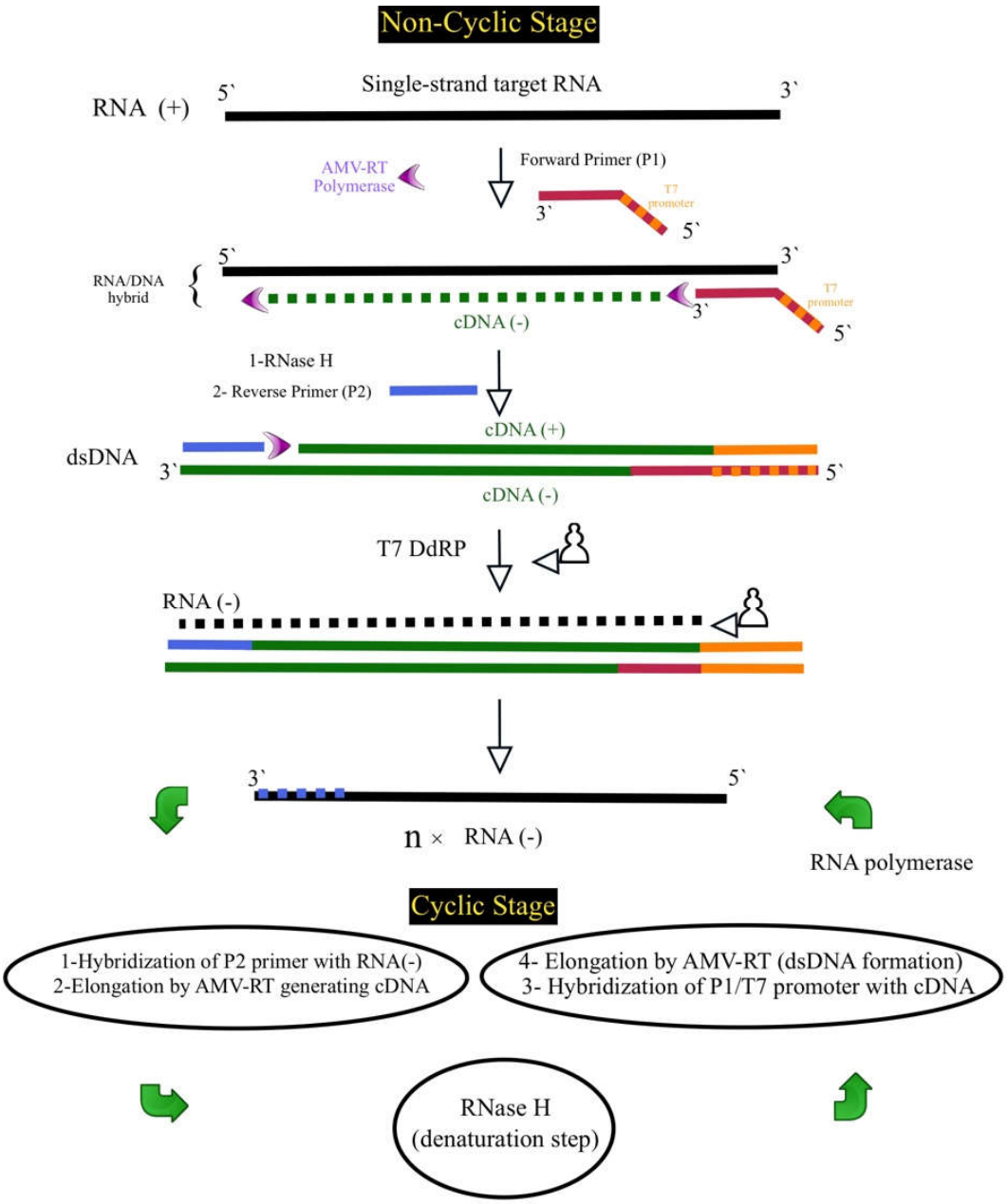

Figure 1. *NASBA reaction scheme.*

Many improvements have been applied to the NASBA reaction itself and the detection methods of the amplification products.

NASBA-ELISA system offers more sensitivity and specificity for the detection of viable *M. tb* with no affection from non-specific contaminant DNA/RNA in the reaction background. The amplification of template RNAs and labeling the amplicons with DIG (digoxigenin) is simultaneously occurring. Following the hybridization of DIG-labeled amplicons with biotin-labeled ssDNA probes, the resulting DNA/RNA hybrid capture by streptavidin-coated surface. Upon the addition of anti-DIG and HRP (horseradish peroxidase), a readable output signal can be achieved through this in-solution hybridization ELISA [1].

A rapid and sensitive detection method based on PPi (pyrophosphate) byproduct of NASBA reaction can be achieved by using hypoxanthine phosphoribosyl transferase (HPT) and 2-nitroso-5-(N-propyl-N-sulfopropylamino) phenol (Nitroso-PSAP). The selective chelation of nitroso-PSAP with fe^{2+} ions give rise to the intense color output. This colorimetric detection has advantages over the other visual-based detection methods. Fluorometric assay with expensive fluorescence detector as well as enzyme-based colorimetric assay using tetrazolium salt, to generate formazan that is a water-insoluble dye and thus, require extra steps [17].

Recently, a diagnostic platform termed specific high-sensitivity enzymatic reporter unlocking (SHERLOCK) achieved an attomolar sensitivity by using nucleases from CRISPR–Cas system in the NASBA assay to detect both RNA and DNA targets [18]. The cause of the current COVID-19 outbreak "SARS-CoV-2" (a single-stranded RNA virus) successfully detected by the CRISPER-Cas13 variant of this system with high accuracy. Furthermore, the SHERLOCK system is sensitive enough to detect single nucleotide polymorphism (SNP) as well as pathogen detection [19].

Although this system can overcome the non-specific artifacts of isothermal amplification, there are also some limitations. Complicated reaction scheme and much time-consuming compared to the typical assay and more expenses owing to employing six different enzymes.

Further studies that can detect attomolar amounts of RNA molecules based on NASBA amplification proposed nested mango NASBA (NMN) in which, fluorogenic aptamer coding sequence embedded into the NASBA inner primers. By employing three enzymes, 2.5 aM (1.5 RNA/μL) of *P. fluorescent ClpB* target is detected successfully by this system [2].

Detection of *B1 rRNA* gene of *Toxoplasma gondii parasite* based on real-time NASBA successfully achieved in a shorter time with a limit of detection (LOD) of one parasite/ml of blood compared to ten parasites/ml in an RT-PCR assay[20].

Multiple copies of 16S rRNA genes in cells candidates it as a suitable target to detect particularly, in RNA-based assays. However, the high homology between rRNA genes led to the development of improved single specific primer-NASBA. SSP-NASBA system employing highly- specific anti-sense primers, along with degenerate ones for hybridization with rRNA template. Anti-sense primers alone are sufficient to provide specificity of NASBA reaction. Besides the high specificity that can discriminate endemic agents e.g. *S. Enteritidis and S. Typhimurium*, the detection of common pathogenic *Salmonella* serovars with LOD less than 10 CFUs mL−1 has been achieved. [21]

Furthermore, the combination of SSP-NASBA with non-cross linking gold nano-probes detection of *Salmonella* genus was proposed as a rapid, specific, and highly sensitive assay with LOD of about 5 CFUs *Salmonella* per amplification tube. Successful integration of a simple, rapid detection method of NASBA amplicon based on non-crosslinking gold nanoprobe with RNA amplification was reported before on *dnak* mRNA of *Salmonella Typhimurium*. [16] Improved NASBA nano-detection system is feasible to quick response-demanded affairs and outbreaks [12].

The addition of reagents such as DMSO, DTT would decrease the risk of non-specific interactions of primers that generates due to a constant low-temperature hybridization [7].

NASBA is exploited in a wide variety of applications. Detection of infectious and non-infectious agents, bloodborne and respiratory pathogens, viability studies has been done with different configurations in NASBA assay [7]. Some examples of NASBA application includes the detection of *Mycoplasma pneumoniae*[22][23], parasites like *Trypanosoma brucei* [24] *Toxoplasma gondii* [1] human *bocavirus (HBoV)* [25], and more recently *SARS-CoV2* (COVID-19 disease) [19].

2. Conclusion

Due to the need for in-hand diagnostic tools in today's world, the use of point-of-care-testing (POCTs) in healthcare systems is increasing. Therefore, the integration and automation of nucleic acid amplification techniques in portable platforms has become a challenge in the field of molecular biology methods. An efficient system that can be used for this purpose should be rapid, accurate, simple, low-cost, and require few reagents. Without needing sophisticated laboratory equipment, isothermal nucleic acid amplification systems are good candidates for exploiting in POCTs. However, in order to fulfill all the criteria, more studies for further improvements and optimizations of the assays are required. Although NASBA has advantages over its counterparts, to achieve the most efficient yet simple and cost-effective conditions efforts are still being made.

References

[1] R. Ramezani, M. Forouzandeh Moghadam, and M. J. Rasaee, "Development of Sensitive and Rapid RNA Transcription-based Isothermal Amplification Method for Detection of Mycobacterium tuberculosis.," *Avicenna J. Med. Biotechnol.*, vol. 11, no. 2, pp. 169–175, 2019, [Online]. Available: http://www.ncbi.nlm.nih.gov/pubmed/31057719%0Ahttp://www.pubmedcentral.nih.gov/articlerender.fcgi?artid=PMC6490409.

[2] A. Abdolahzadeh, E. V. Dolgosheina, and P. J. Unrau, "RNA detection with high specificity and sensitivity using nested fluorogenic Mango NASBA," *Rna*, vol. 25, no. 12, pp. 1806–1813, 2019, doi: 10.1261/rna.072629.119.

[3] H. Deng and Z. Gao, "Bioanalytical applications of isothermal nucleic acid amplification techniques," *Anal. Chim. Acta*, vol. 853, no. 1, pp. 30–45, 2015, doi: 10.1016/j.aca.2014.09.037.

[4] V. Doseeva *et al.*, "Multiplex isothermal helicase-dependent amplification assay for detection of Chlamydia trachomatis and Neisseria gonorrhoeae," *Diagn. Microbiol. Infect. Dis.*, vol. 71, no. 4, pp. 354–365, 2011, doi: 10.1016/j.diagmicrobio.2011.08.021.

[5] J. Li and J. Macdonald, "Advances in isothermal amplification: Novel strategies inspired by biological processes," *Biosens. Bioelectron.*, vol. 64, pp. 196–211, 2015, doi: 10.1016/j.bios.2014.08.069.

[6] P. Craw and W. Balachandran, "Isothermal nucleic acid amplification technologies for point-of-care diagnostics: A critical review," *Lab Chip*, vol. 12, no. 14, pp. 2469–2486, 2012, doi: 10.1039/c2lc40100b.

[7] M. Fakruddin, R. Mazumdar, A. Chowdhury, and K. Mannan, "Nucleic acid sequence based amplification (NASBA)-prospects and applications," *Int J Life Sci Pharma Res*, vol. 2, no. 1, p. 106, 2012.

[8] J. W. Romano, K. G. Williams, R. N. Shurtliff, C. Ginocchio, and M. Kaplan, "NASBA technology: Isothermal RNA amplification in qualitative and quantitative diagnostics," *Immunol. Invest.*, vol. 26, no. 1–2, pp. 15–28, 1997, doi: 10.3109/08820139709048912.

[9] G. A. Obande and K. K. B. Singh, "Current and future perspectives on isothermal nucleic acid amplification technologies for diagnosing infections," *Infect. Drug Resist.*, vol. 13, pp. 455–483, 2020, doi: 10.2147/IDR.S217571.

[10] Y. Zhao, F. Chen, Q. Li, L. Wang, and C. Fan, "Isothermal Amplification of Nucleic Acids," *Chem. Rev.*, vol. 115, no. 22, pp. 12491–12545, 2015, doi: 10.1021/acs.chemrev.5b00428.

[11] P. Gill and A. Ghaemi, "Nucleic acid isothermal amplification technologies - A review," *Nucleosides, Nucleotides and Nucleic Acids*, vol. 27, no. 3, pp. 224–243, 2008, doi: 10.1080/15257770701845204.

[12] H. Mollasalehi and R. Yazdanparast, "An improved non-crosslinking gold nanoprobe-NASBA based on 16S rRNA for rapid discriminative bio-sensing of major salmonellosis pathogens," *Biosens. Bioelectron.*, vol. 47, pp. 231–236, 2013, doi: 10.1016/j.bios.2013.03.012.

[13] B. Deiman, P. Van Aarle, and P. Sillekens, "Characteristics and applications of Nucleic Acid Sequence-Based Amplification (NASBA)," *Appl. Biochem. Biotechnol. - Part B Mol. Biotechnol.*, vol. 20, no. 2, pp. 163–179, 2002, doi: 10.1385/MB:20:2:163.

[14] O. L. Bodulev and I. Y. Sakharov, "Isothermal Nucleic Acid Amplification Techniques and Their Use in Bioanalysis," *Biochem.*, vol. 85, no. 2, pp. 147–166, 2020, doi: 10.1134/S0006297920020030.

[15] M. Fakruddin *et al.*, "Nucleic acid amplification: Alternative methods of polymerase chain reaction," *J. Pharm. Bioallied Sci.*, vol. 5, no. 4, pp. 245–252, 2013, doi: 10.4103/0975-7406.120066.

[16] H. Mollasalehi and R. Yazdanparast, "Non-crosslinking gold nanoprobes for detection of nucleic acid sequence-based amplification products," *Anal. Biochem.*, vol. 425, no. 2, pp. 91–95, 2012, doi: 10.1016/j.ab.2012.03.008.

[17] A. Isobe *et al.*, "A highly sensitive and rapid enzymatic method using a biochemical automated analyzer to detect inorganic pyrophosphate generated by nucleic acid sequence-based amplification," *Clin. Chim. Acta*, vol. 511, pp. 298–305, 2020, doi: 10.1016/j.cca.2020.10.026.

[18] M. J. Kellner, J. G. Koob, J. S. Gootenberg, O. O. Abudayyeh, and F. Zhang, "SHERLOCK: nucleic acid detection with CRISPR nucleases," *Nat. Protoc.*, vol. 14, no. 10, pp. 2986–3012, 2019, doi: 10.1038/s41596-019-0210-2.

[19] X. Xiang *et al.*, "CRISPR-cas systems based molecular diagnostic tool for infectious diseases and emerging 2019 novel coronavirus (COVID-19) pneumonia," *J. Drug Target.*, vol. 28, no. 7–8, pp. 727–731, 2020, doi: 10.1080/1061186X.2020.1769637.

[20] R. Norouzi, A. Dalimi, and M. F. Moghadam, "Comparison of a Nucleic Acid Sequence-based Amplification (NASBA) and real-time reverse transcriptase PCR methods for detection of Toxoplasma gondii in rat blood samples," vol. 1, no. 1, pp. 15–23, 2016.

[21] H. Mollasalehi and R. Yazdanparast, "Development and evaluation of a novel nucleic acid sequence-based amplification method using one specific primer and one degenerate primer for simultaneous detection of Salmonella Enteritidis and Salmonella Typhimurium," *Anal. Chim. Acta*, vol. 770, pp. 169–174, 2013, doi: 10.1016/j.aca.2013.01.053.

[22] C. Huang, P. T. Huang, J. Y. Yao, Z. W. Li, L. B. Weng, and X. G. Guo, "Pooled analysis of nuclear acid sequence-based amplification for rapid diagnosis of Mycoplasma pneumoniae infection," *J. Clin. Lab. Anal.*, vol. 33, no. 5, pp. 1–8, 2019, doi: 10.1002/jcla.22879.

[23] R. A. Collins, L. S. Ko, K. L. So, T. Ellis, L. T. Lau, and A. C. H. Yu, "Detection of highly pathogenic and low pathogenic avian influenza subtype H5 (Eurasian lineage) using NASBA," *J. Virol. Methods*, vol. 103, no. 2, pp. 213–225, 2002, doi: 10.1016/S0166-0934(02)00034-4.

[24] C. M. Mugasa, T. Laurent, G. J. Schoone, P. A. Kager, G. W. Lubega, and H. D. F. H. Schallig, "Nucleic acid sequence-based amplification with oligochromatography for detection of Trypanosoma brucei in

clinical samples," *J. Clin. Microbiol.*, vol. 47, no. 3, pp. 630–635, 2009, doi: 10.1128/JCM.01430-08.

[25] A. Böhmer *et al.*, "Novel application for isothermal nucleic acid sequence-based amplification (NASBA)," *J. Virol. Methods*, vol. 158, no. 1–2, pp. 199–201, 2009, doi: 10.1016/j.jviromet.2009.02.010.

Study of neurofeedback effects in acute depressive disorder

Mozhgan shahbazi

Master of Medical Rehabilitation Engineering, Tehran University of Science and Research

mozhgaanshahbazi@gmail.com

Abstract

Depression is a physical and mental illness. People who are depressed, They can feel uneasy, anxious, empty, hopeless, helpless, worthless, ashamed, or restless. They may eat less of the activities they used to enjoy, lose focus, have difficulty remembering details and making decisions, and have problems in their relationships. And think of suicide and even commit suicide. Depressive disorder can also cause insomnia, excessive sleep, fatigue, digestive problems or low energy. Depression is one of the most important neurological disorders, The probability of contracting it during life is about 17%, About 10% of people worldwide need serious treatment.

One way to treat depression is to use neurofeedback. Neurofeedback is a method for learning to consciously control different brain states. The neurofeedback device, with the information it receives from the brain waves, helps the brain to regulate its activities in a desirable way. Neurofeedback therapy is non-invasive and is a fun and stimulating state for the brain. The aim of this article was to evaluate the effectiveness of neurofeedback therapy in reducing the severity of acute depressive symptoms.

key words: Neurofeedback, depression, brain waves, non-drug treatment

1. Introduction

Depression is a disturbing thought that is on the conscious side of the mind. Today, more than 300 million people around the world suffer from depression [1]. The prevalence of depression in women is 10 to 25 percent and in men it is 5 to 12 percent. Depression is a mood disorder that affects a person's thoughts, feelings and performance and ultimately leads to disability, low self-esteem and loneliness [2].

Depression tends to become chronic and patients experience worsening symptoms. Each stage of acute depression recurrence increases it by 16%, and the more the patient can pass without depression, the lower the risk of recurrent depression.

Depression can be treated with a variety of methods, including psychotherapy and biotherapy in psychotherapy, the trained person establishes a professional relationship with the patient in order to eliminate or reduce the patient's symptoms and destructive patterns of behavior

In Neurofeedback treatment method, Neurofeedback measures the neural activity of the brain and informs the person at the same time through visual or auditory feedback of the nervous activity of their brain. This process facilitates the regulation of neural mechanisms that underlie a particular behavior or pathology. The use of neurofeedback in the treatment of many disorders such as ADHD, hyperactivity disorder, bipolar disorder, anxiety, attention deficit, sleep disorders, brain damage and obsession has been confirmed.

The importance of depression has increased in the last decade due to the harassment of patients. Also, depressive disorder is a serious risk with high individual and social costs, risk of suicide and the damage it causes

every year. In recent years, the cost of psychiatric care in different countries has grown significantly. Therefore, researchers are researching to choose the most effective and least expensive treatment. In various studies on the treatment of depression with neurofeedback, this treatment has been proven to be very effective.

2-Causes of depression

2-1 Biological causes

Genetic: Having a family history of depression increases a person's risk of developing depression. Of course, depression is a complex disorder, and a combination of genetic conditions can cause depression.

Medicines: Long-term use of some medications, such as medications used to control blood pressure, sleeping pills or birth control pills, can cause depressive symptoms in some people.

Serotonin and other neurotransmitters: Neurotransmitter abnormalities at the synaptic level have been observed in depressed patients. Impaired secretion of norepinephrine and dopamine is also seen in depressed patients.

Diseases: Sometimes depression occurs at the same time as an important physical illness. Having a chronic illness, such as cardiovascular disease, stroke, diabetes, cancer, and Alzheimer's or migraine, puts one at greater risk for depression. Studies show that depression is more common in people who have had a heart attack.

2-2 Psychological causes

Stress: Stressful life events, especially the loss or threat of losing a loved one or a job, can trigger depression.

social factors: Dissatisfaction with society and community-related psychological factors can also play a role in depression.

Character: Some personality traits, such as low self-esteem and extreme dependence, sensitivity and pessimism to stress, increase the likelihood of depression. Having an obsessive, regular, serious, perfectionist or highly dependent personality also predisposes a person to depression.

failure in life: Lack of work, marriage or relationship can lead to depression, death or loss of a loved one, loss of something important (job, home, capital), change of job or relocation can lead to depression.

Surgery: Performing some surgeries such as breast removal due to cancer, transition from one stage to another such as menopause or retirement.

mental illnesses: Anxiety, mental retardation, forgetfulness, eating disorders and drug abuse.

3-Brain waves

The term brain waves refers to the electrical activity of the brain that can be recorded by the Electroencephalogram(EEG).This electrical pattern is characterized by frequency, amplitude and shape.

Brain waves are divided into several categories based on frequency: alpha, beta, theta, delta and gamma. Each of the brain waves is responsible for controlling and influencing a part of human mental, emotional and behavioral

functions. The higher the activity of the cerebral cortex, the higher the frequency of brain waves. The highest frequency of the brain is seen when waking up and the lowest frequency is seen in coma and anesthesia. Based on the speed of the brain waves, the frequencies are each divided into three categories per hertz: slow, medium and fast waves. The lowest frequency wave is the delta wave, followed by theta, alpha, beta and gamma waves, respectively.

Brainwaves, Frequency Bands and Functions

Unconscious	Conscious				
Delta	Theta	Alpha	SMR	Beta	Gamma
Instinct	Emotion	Consciousness	Focused	Thought	Will
Survival, deep sleep, coma, repair, complex problem solving	Drives, feelings, dreams, creativity, insight, deep states	Aware of the body, integration of feelings, alert and peaceful, reading, meditation	Mental alertness, physical relaxation	Perception, mental activity, thinking, focusing, sustained attention	Extreme focus, energy, ecstasy, learning, cognitive processing

4-Biofeedback

Biofeedback is a type of exercise therapy that uses electronic devices to measure and process information about nerves, muscles, and body activity, and to show it as feedback to the patient and their therapist. Biofeedback helps patients become more aware of the body's autonomic functions and increase their voluntary control over them [3].

In this way, people can control body functions, including heart rate, with the help of the mind. Biofeedback is used in a wide range of disorders, including anxiety disorders. It is also a safe treatment and seems to be a useful supplement to other treatments.

Biofeedback means the treatment of the mind and body that helps people use electronic tools to control and be aware of their psychological and biological processes. Biofeedback therapists guide the person to learn to control the body and mind more easily.

5-neurofeedback

Neurofeedback is actually the biological feedback of brain waves[4]. This is a safe and non-invasive method that affects various indicators such as attention, concentration, anxiety, learning, etc [5]. Neurofeedback, or neural feedback, attempts to self-regulate by recording electrical waves in the brain and giving feedback. Feedback is usually provided by audio or video, and the person finds out if he or she has made a proper change in the activity of his or her brain waves. Neurofeedback is used to increase brain function.

When the waves go out of their defined frequency and function, neurofeedback exercises during various brain sessions train the brain to function properly in the right pattern. This condition involves increasing or decreasing the activity of certain waves in certain areas of the brain [6]. Today, even professional football and chess athletes use neurofeedback to increase the accuracy and organization of their thoughts, so neurofeedback training affects the balance of different athletes [7]. This method strengthens decision-making, planning and emotion control.

Neurofeedback is a treatment method because it normalizes the brain waves that are disrupted due to depression, anxiety, obsession, migraine, etc., and treats these disorders. Neurofeedback is one of the short-term treatments [8]. Neurofeedback is effective in treating ADHD, learning disabilities and ADHD and increases concentration. Accuracy and concentration increase and the organization of thoughts and actions is created. Sudden and impulsive work is reduced and excessive mobility is reduced.

5.1 How the neurofeedback device works

In this method, the person sits in front of the monitor and the electrode placed on the head receives his brain waves and sends them to the computer. By seeing your brain waves on the monitor screen, you can adjust and control them, for example, move a boat and gradually learn how to do it faster and more consistently.You are actually learning how to create useful waves in a part of the brain.

In fact, neurofeedback enables a person to see the world inside their brain, For example, you see a simulated shape of a brain wave playing on a monitor screen, and you start playing by looking at the monitor screen without using your hands. The machine processes your brainwave patterns, and if these patterns are appropriate, you will move forward in the game, otherwise you will fail, In this way, you will learn, for example, how you can adjust your brain to anxiety so that calm can replace anxiety.

5-2 treatment with neurofeedback and how to do it

With neurofeedback therapy, the patient learns how to correct the electrical activity of a disturbed area of the brain and return it to normal, and because he learns in a few sessions, he will never forget it.

Neurofeedback is approved by the FDA for the treatment of stress, depression, anxiety, hyperactivity, inattention, headache (migraine), chronic pain, sleep disorders, drug use, obsessive-compulsive disorder, epilepsy, and stroke rehabilitation.

5-3 Therapeutic benefits of neurofeedback compared to drug therapy

- The drug only temporarily relieves the symptoms, such as the treatment of diseases such as ADHD or hyperactivity and OCD or obsession, etc., which recur as soon as the drug is stopped.But neurofeedback therapy is more stable.
- It does not have the side effects of many medications
- Regulation of brain activity in neurofeedback

6- Therapeutic protocol in neurofeedback training

First, a record is taken from the client. Then they sit on a special chair. The electrodes are placed on the patient's scalp, Electrodes record the electrical activity of a person's brain and show it in the form of brain waves (often in the form of a simulation in the form of a computer game or movie). The patient is asked to relax completely and look at the computer screen in front of him.

In this case, playing movies or computer games is done without the use of hands and only with the brain waves of the person. In this way, by seeing the progress or stopping of the game and receiving rewards or losing points or changes that occur in the sound or play of the film, the person realizes the favorable or unfavorable conditions of his brain waves and tries to guide the game. Or film to improve the state of your brain wave production. During training, brain activity is controlled using conscious and unconscious attention, and in the face of new and out-of-order problems, it does not need foreign drugs because it can achieve its new order through a self-regulatory process. After several sessions of practice and repetition, the brain learns tasks and adapts to them. At the end of the session, the electrodes are removed from the patient and homework is given.

A treatment protocol or Instructions for neurofeedback has six parts:

- Location of electrodes on the scalp
- Which of the following brain wave frequencies should we work on?
- Training should be with the eyes open or closed or training should be done with or without a specific task.
- What type of assembly should be used in the training: unipolar or bipolar
- What kind of feedback should be provided to the reference: touch, audio, video or combination
- Duration of protocol implementation

The type of feedback provided as well as the duration of the protocol vary according to factors such as the purpose of treatment, the type of response to treatment, the individual profile and the standards defined for each protocol.

Conclusion:

1- The recovery rate of real neurofeedback was more effective in regulating brain waves and reducing depressive symptoms than unreal neurofeedback(Research results of Eskandari et al(2014))[9]
2- Drug failure for depression imposes long delays in relieving and reducing depression and The alpha wave on the electroencephalogram is a non-invasive and cost-effective indicator and is a fun and boosting mode for the brain(Thin et al(2011)).
3- The human brain is able to heal itself, that is, it has the ability to re-learn the self-regulating mechanisms of brain waves(Rosenfeld1997).
4- Neurofeedback is effective in improving brain function and improving various disorders such as major depression.; Thus, neurofeedback training strengthens self-regulatory mechanisms for effective brain function.
5- Neurofeedback is more effective in reducing depressive symptoms in women.

Reference:

[1] Marefti, Zahra, 1399, Ways to treat depression, 8th National Conference on Sustainable Development in Educational Sciences and Psychology, Social and Cultural Studies, Tehran

[2] Zandi, Alireza and Adeli, Mohammad, 1397, Using Biofeedback Systems to Improve and Treat Patients with Depression: A Systematic Review, National Conference on Rehabilitation Based Care and Rehabilitation, Dezful

[3] Dadarkhah, Afsaneh va Eslami, Ehsan, 1396, Design and construction of compression biofeedback machine based on new quantities for muscle rehabilitation, 2nd International Conference on Applied Research in Physical Education, Sports and Championship Sciences, Tehran

[4]Hammond DC. What is neurofeedback? Journal of Neurotherapy. 2007; 10(4):25-36. Doi

[5] Nan W, Qu X, Yang L, Wan F, Hu Y, Mou P, et al. Beta/theta neurofeedback training effects in physical balance of healthy people. Paper Presnted at: The World Congress on Medical Physics and Biomedical Engineering. 7-12 June, 2015; Toronto, Canada

[6] Hammond DC. Neurofeedback for the enhancement of athletic performance and physical balance. The Journal of the American Board of Sport Psychology. 2007; 1(1):1-9

[7] Hammond DC. Neurofeedback for the enhancement of athletic performance and physical balance. The Journal of the American Board of Sport Psychology. 2007; 1(1):1-9.

[8] Yadalahi, Sara, 1397, The effectiveness of neurofeedback therapy in the treatment of anxiety and depression, Third International Conference on New Research in the field of educational sciences and psychology and social studies in Iran, Tehran

[9] Eskandari,Z taremian,F nazari,M A bakhtiari,M momtazi,S V rezai(2014), The effectiveness of neurofeedback therapy in reducing the severity of symptoms of major depressive disorder, Scientific Research Journal of Zanjan University of Medical Sciences95-86-92

Structure-Based Drug Design, Virtual Screening and High-Throughput Screening in Order to Identify Lead Compounds for Inhibition Acetylcholinesterase

Farshad Qalekhani[1, 2] and Mahnaz Ghowsi[3*]

[1] Pharmaceutical Sciences Research Center, Health Institute, Kermanshah University of Medical Sciences (KUMS), Kermanshah, Iran.

[2] Medical Biology Research Center, Health Technologies Institute, Kermanshah University of Medical Sciences (KUMS), Kermanshah, Iran.

[3] Department of Biology, Faculty of Sciences, Razi University, Kermanshah, Iran.

*Email: Ghaousi.mahnaz@razi.ac.ir; Ghowsi.mahnaz@gmail.com

Abstract

Alzheimer's disease (AD) is a neurodegenerative disorder that causes cognitive problems such as learning and memory deficits and some evidence shows that its pathogenesis is linked to the decreased acetylcholine levels in the brain. Currently some acetylcholinesterase inhibitors are widely used to symptomatic treatment of AD patients. However, the duration of their therapeutic efficacy is limited and they may have adverse side effects. Therefore, there is a need to identify natural lead compounds to develop novel new drugs. The computational drug designing methods can provide a huge chance to both discover and predict the efficacy of novel acetylcholinesterase inhibitors from food sources. Here, we identified a lead compound for inhibition of acetylcholinesterase and evaluated its drug-likeness, ADME and toxicity properties by using several advanced computational methods. Our results showed that neogitogenin compound is the lead compound with a good drug-likeness, and an appropriate absorption, distribution, metabolism, excretion properties, and low toxicity properties on the liver and heart that is comparable to donepezil as a FDA approved drug. This study informs the future laboratory attempts to develop a novel drug with using neogitogenin compound for treating AD patients.

Keywords: Alzheimer's disease, Acetylcholinesterase, Drug design, Virtual screening, Lead compound, Neogitogenin.

1. Introduction

Alzheimer's disease (AD), the most common form of dementia, is a neurodegenerative disease which causes cognitive problems such as progressive deficits in decision making and language, learning, memory, judgment, loss of mental function, and the prevalence of amnesia [[1], [2]]. AD accounts for 60-70% of cases of dementia worldwide and its universal incidence is approximately 24.3 million cases [1]. In AD, the volume of hippocampus

and entorhinal cortex is smaller than those of controls and neurodegeneration in the different areas of cortex such as tempotoparietal and hypocampus is seen [[3], [4]]. Various studies show that β-amyloid deposition, oxidative stress, and inflammation are important aspects in the aetiology of AD [[5], [1]]. Also, it has been shown that tauopathy play an important role in the development of AD, and tau protein hyperphosphorylation results in the formation of intracellular neurofibrillary tangles of the microtubule and neurodegeneration [[1], [6], [7]]. Specially, the pathogenesis of AD has been linked to a loss of function of neurotransmitter acetylcholine in the brain [[8]], [5]]. The cholinergic neurons are distributed almost all regions of the central nervous system such as the spinal cord, hindbrain, medial habenula, mesopontine region, basal forebrain, striatum, olfactory tubercle and islands of Cajella complex [8]. The cholinergic neurotransmission is involved in the critical physiological processes, including attention, learning, memory, stress response, wakefulness, sleep, and sensory information [8]. The brains of Alzheimer's patients have been reported to be deficient in acetylcholine, and it is believed that behavioral and functional deficits in Alzheimer's disease are due to the inability to transmit nerve impulses during cholinergic synapses that are involved in the process of memory [9].

Various researches have shown that the reduction in the acetylcholine in the synaptic cleft results in the neurodegeneration of the cholinergic neurons. Some evidence shows that the increase in the brain acetylcholine levels by using acetylcholinesterase inhibitors may help prevention of AD [10]. Different studies show that the agonists of the M1 acetylcholine receptor be significant therapeutic tool to management of AD because, different AD major hallmarks of AD such as cholinergic deficit, cognitive dysfunction, and tau and Aβ pathologies are influenced by M1 receptor signaling pathway [8]. Also, the inhibitors of acetylcholinesterase are used to care for AD patients and currently four FDA-approved drug donepezil, galantamine and rivastigmine that are among available drugs for treatment of AD patients are cholinesterase inhibitor [2]. These drugs have positive influences for an approximately 1 to 3 years-period of time that is a short time in this progressive disease [8].

High-throughput virtual screening (HTVS) methods play axial role in the fast identification active natural compounds with impressive effects on the special bimolecular mechanism or pathway at cellular level that can help to development preliminary ideas for drug design [11]. Rapid advances in the medicinal chemistry and high throughput screening (HTS) can accelerate the drug discovery process by development of a large library of chemical compounds via a short-term synthesis and screening [[12], [13]]. In medicine, a chemical compound with potential actions on the specific genes or proteins involved in a certain disease that shows promise as a treatment for a disease and may lead to the development of a new drug is called a lead compound. Currently, by using high throughput screening methods, it is possible that large libraries of chemical compounds on a specific drug target be investigated in the shortest time. Therefore, through limiting laboratory tests to the lead compounds, in addition to reduction in the research costs, the efficiency of experimental methods can be increased. In this study, we applied a large library containing various compounds in foods, to find a strong inhibitor of acetylcholinesterase enzyme with low toxicity and its pharmacokinetic properties (such as absorption, distribution, metabolism and excretion) was evaluated and compared to the existing drugs.

2. Material and Methods

2.1 Preparation of Ligand and Receptor

At the first stage, the acetylcholinesterase enzyme PDB file was downloaded from the Protein Data Bank ((PDB ID: 1EVE) https://www.rcsb.org/). The library used in this study is called FOOD-lib which contains 10,997 chemical compounds in foods. The Discovery Studio and AutoDockTools (ADT) softwares were applied to prepare the molecules used in docking. The ligand and water molecules that were present with the acetylcholinesterase protein in the PDB file were removed using Discovery Studio software [[14], [15]].

The ADT software was used to create PDBQT files. The grid box center was determined by using ADT software. Donepezil is an FDA approved drug is utilized to inhibit the acetylcholinesterase enzyme in the treatment of Alzheimer's patients. Donepezil, which was present as a co-crystalline ligand in the acetylcholinesterase protein PDB file, was used as a positive control.

2.2 Molecular docking

For virtual screening using AutoDock Vina software, MTiOpenScreen computing server was used. The input files were uploaded to the server and after determining the docking settings, including dimensions and center of the Grid box, the run was performed. After the docking process, the outputs were received in mol2 and csv file formats. In order to ensure the accuracy of the docking results, the top 20 ligands were re-docked on the personal computer using AutoDock Vina software [[16], [17]].

2.3 Drug-likeness

The Swiss computing server (http://www.swissadme.ch/) was used to check for 2.3 drug-likeness. For this purpose, 6 basic properties of medicinal chemistry, including: molecular weight (MW), lipophilicity, number of hydrogen bond donors, number of hydrogen bond acceptors, the number of rotatable bonds and topological polar surface area (TPSA) were investigated.

The top 20 ligands of the previous step that had the lowest binding energy to the acetylcholinesterase enzyme were evaluated for drug-likeness at this stage. Candidate compounds that were not optimal at this stage in terms of the 6 specific items mentioned above were removed from subsequent evaluations. (The cut-offs used for these properties are: Molecular weight less≤ 500, hydrogen bond acceptor ≤10, hydrogen bond donors≤5 and MlogP ≤ 4.30, polar surface area less than 140, and rotatable bonds≤10) [18].

2.4 General Toxicity

The pkCSM computing server was used to evaluate the general toxicity. After entering the SMILES formula of the candidate compounds into the pkCSM server, properties such as mutagenicity, hepatotoxicity, cardiotoxicity, skin sensitivity and maximum food tolerance that are tolerable for humans were evaluated, and finally the compounds that are non-toxic in each of the mentioned features were selected for further analysis [19].

2.5 Hepatotoxicity and Cardiotoxicity

The compounds approved for general toxicity in the previous step, were evaluated for specific hepatotoxic and cardiotoxic effects with dedicated servers. We used the Pred-hERG server to investigate the effect of the lead compound on hEGR I and II transporter enzymes in the heart, and the Vienna LiverTox server to evaluate the effect of the lead compound on the inhibition of hepatocyte membranes transmitters [[20], [21]].

2.6 Pharmacokinetics

In this step, the compounds that were recognized as permissible in terms of toxicity in the previous steps were subjected to ADME pharmacokinetic studies.

ADME, sometimes described as what the body does to a drug, ADME is an abbreviation in pharmacokinetics and pharmacology for "absorption, distribution, metabolism, and excretion". pkCSM computing server was employed to study of ADME. The pkCSM Server uses the SMILES formula as input and its outputs include various ADME parameters [19].

2.7 Cytochromes P450 Metabolism site

After determining the lead compound in the acetylcholinesterase enzyme inhibition, the metabolic status of this compound on the cytochrome P450 were evaluated. Cytochromes P450 (CYPs) are a superfamily of enzymes with heme as a cofactor that function as monooxygenases. In the mammals, these proteins oxidize steroids, fatty acids, and xenobiotics, and play axial roles in the clearance of various compounds and hormone synthesis and breakdown. Also, due to important roles of the cytochrome P450 (CYP) family enzymes in the metabolism of various xenobiotics including drugs, a special attention is paid to these enzymes for the discovery of drugs. In the present study, the RS-Web Predictor computing server was applied to determine the CYP-P450 mediated sites of metabolism [[22], [23]].

2.8 The two dimensional diagram of interaction between ligand and receptor

Finally, the Discovery Studio software was employed to illustrate the interactions between the lead compound and receptor, as well as the interactions between positive the control with receptor [14].

3. Results and Discussions

3.1 Docking

After completing the docking process and receiving the outputs from the server, 20 top ligands (in terms of energy) were selected for the next stages of drug design and screening. The results obtained from the computing server were consistent with the results obtained from the redocking in the personal computer, which indicates the repeatability of the calculations and the accuracy of the operation on the server (Table 1).

3.2 Drug-likeness

At this stage, the 20 ligands that had the greatest affinity were examined for drug-likeness. The results for the evaluation of the mentioned parameters are present in Table 1. In this table, the ligands that had drug-likeness based on the mentioned parameters are marked in blue and the compounds that did not have drug-likeness in terms of the mentioned parameters are marked in green. The docking energy is also listed in the table for each ligand.

Table 1. The results of Drug-likeness examination.

Compound	AutoDock E	MW	Rotatable bonds	H-bond acceptors	H-bond donors	TPSA	MLOGP
Neogitogenin_ZINC000118916627	-10.9	432.64	0	4	2	58.92	4.23
Yuccagenin_ZINC000038140885	-10.8	430.62	0	4	2	58.92	4.09
Amentoflavone_ZINC000003984030	-14.9	538.46	3	10	6	181.8	0.25
Ginkgetin_ZINC000001531664	-14.1	566.51	5	10	4	159.8	0.63
Sapogenins_ZINC000257348757	-13.6	400.64	0	2	0	18.46	5.96
Solasodiene_ZINC000004081783	-13.2	395.62	0	2	1	21.26	5.71
Smilagenone_ZINC000118936408	-12.9	414.62	0	3	0	35.53	4.94
Bilobetin_ZINC000003979028	-12.5	552.48	4	10	5	170.8	0.44
Collettiside_I_ZINC000253558558	-12.5	576.76	3	8	4	117.84	2.41
ZINC000003824120	-12.3	412.69	4	1	1	20.23	6.62
ZINC000030725521	-12.2	398.66	4	1	1	20.23	6.43
Solanidine_ZINC000118917270	-12	397.64	0	2	1	23.47	5.41
ZINC000078817078	-11.1	413.64	0	3	2	41.49	4.94
ZINC000032050928	-11.1	468.71	2	3	0	43.37	5.92
Yamogenin_ZINC000242701899	-10.8	414.62	0	3	1	38.69	4.94
ZINC000028524746	-10.8	454.68	1	3	1	54.37	5.73
ZINC000003881982	-10.7	456.7	1	3	2	57.53	5.82
ZINC000013919089	-10.7	470.73	2	3	1	46.53	6.01
ZINC000008952015	-9.3	472.7	1	4	3	77.76	4.97
ZINC000118919208	-8.7	399.65	0	2	1	23.47	5.56

3.3 General Toxicity

In addition to the inhibitory properties of a chemical compound on the target receptor, its non-toxicity is also important. In this regard, the compounds that were approved in the previous step in terms of drug-likeness were examined for toxicity, too. The results of the toxicity analysis compared to the positive control are present in Table 2.

Table 2. The results of the toxicity analysis compared to the positive control.

Name	Neogitogenin	Yuccagenin	Donepezil (+Control)	Unit
AMES toxicity	No	No	No	Categorical
Max. tolerated dose (human)	-0.878	-0.621	-0.036	(log mg/kg/day)
hERG I inhibitor	No	No	No	Categorical
hERG II inhibitor	No	Yes	Yes	Categorical
Oral Rat Acute Toxicity (LD50)	2.881	2.775	2.999	(mol/kg)
Oral Rat Chronic Toxicity (LOAEL)	1.42	1.366	1.514	(log mg/kg_bw/day)
Hepatotoxicity	No	No	No	Categorical
Skin Sensitisation	No	No	No	Categorical

3.4 Hepatotoxicity and Cardiotoxicity

Following previous steps, it was finally determined that neogitogenin ligand could be a precursor to inhibit the enzyme acetylcholinesterase.

In order to investigate the toxic effects of this compound, we specifically examined its hepatotoxicity in comparison to donepezil. The results showed that this compound was acceptable in terms of hepatotoxicity parameters and was comparable to donepezil as an FDA approved drug. The results hepatotoxicity & cardiotoxicity tests are shown in the Table 3 and Figure 1, respectively.

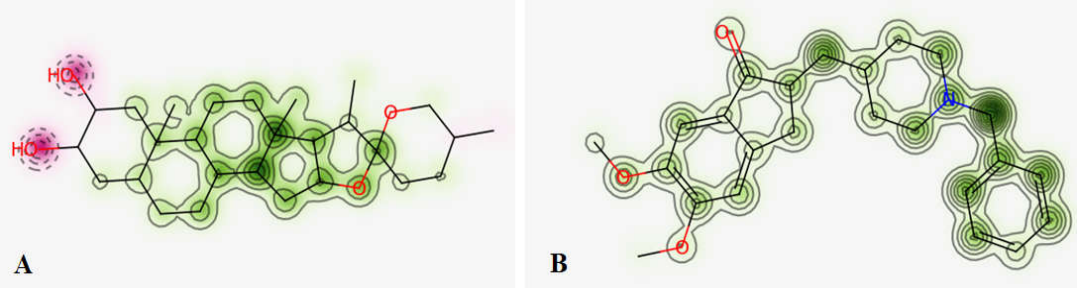

Figure 1. The results of potential cardiotoxici effects of neogitogenin (A) and donepezil (B) for cardiac hERG I and II enzymes. Negative contribution to the hERG blockage (Pink). More contour lines and intense green color denotes a higher positive contribution of an atom or a fragment to the hEGR blockage (Green).

As is shown in the Figure 1, considering the results of cardiotoxicity analysis for hERG I II enzymes, it can be concluded that the composition of neogitogenin has no role in the block of hERG I and II enzymes. However, the compound donepezil as an accepted drug has a high ability to inhibit the enzyme hERG I II and cause cardiac

complications. Cardiotoxicity analysis results for cardiac hERG I II enzymes were consistent with general toxicity analysis results.

Table 3. The effect of neogitogenin and donepezil on hepatic transporter enzymes.

Model	Neogitogenin	Donepezil (Control)
BSEP Inhibition	positive	positive
BSEP Transport	negative	negative
P-glycoprotein Inhibition	negative	positive
P-glycoprotein Transport	positive	negative
MRP4 Inhibition	negative	positive
MRP2 Transport	positive	positive
MRP3 Inhibition	positive	positive
MRP3 Transport	negative	negative
BCRP Inhibition	positive	positive
BCRP Transport	negative	negative
OATP1B1 Inhibition	positive	negative
OATP1B3 Inhibition	positive	negative
Drug-induced liver injury	negative	negative
Hyperbilirubinemia	negative	positive
Cholestasis	positive	negative

According to Table 3, the effects of neogitogenin ligand on hepatic transporter enzymes is similar to those of donepezil. The blue areas in Table 3 show that the effects of neogitogenin are similar to the donepezil effects. The orange areas represent different parts in terms of their effect on the liver enzymes. As is seen in the table 3, the neogitogenin has acceptable hepatic effects.

3.5 Pharmacokinetics

At this stage, we examined the pharmacokinetic properties of neogitogenin as a lead compound in the inhibition of AChE and this compound was analyzed for the potential ADME profiles. The results are shown in the Table 4.

Table 4. The results of ADME studies for neogitogenin.

Property	Model Name	Predicted Value	Unit
Absorption	Water solubility	-5.452	(log mol/L)
Absorption	Caco2 permeability	1.305	(log Papp in 10-6 cm/s)
Absorption	Intestinal absorption (human)	98.865	(% Absorbed)
Absorption	Skin Permeability	-3.392	(log Kp)
Distribution	VDss (human)	-0.219	(log L/kg)
Distribution	Fraction unbound (human)	0	(Fu)
Distribution	BBB permeability	-0.242	(log BB)
Distribution	CNS permeability	-1.629	(log PS)
Metabolism	CYP2D6 substrate	No	Categorical
Metabolism	CYP3A4 substrate	Yes	Categorical
Metabolism	CYP1A2 inhibitior	No	Categorical
Metabolism	CYP2C19 inhibitior	No	Categorical
Metabolism	CYP2C9 inhibitior	No	Categorical
Metabolism	CYP2D6 inhibitior	No	Categorical
Metabolism	CYP3A4 inhibitior	No	Categorical
Excretion	Total Clearance	0.338	(log ml/min/kg)
Excretion	Renal OCT2 substrate	No	Categorical

3.6 *Cytochromes P450 Metabolism sites*

The metabolic sites of neogitogenin on the enzyme cytochromes P450 are shown in Figure 2. The potential sites for metabolism of neogitogenin against CYP3A4 of cytochrome P450 family were checked. neogitogenin had multiple atoms which are vulnerable to a specific enzyme of CYP450 family (Figure 2).

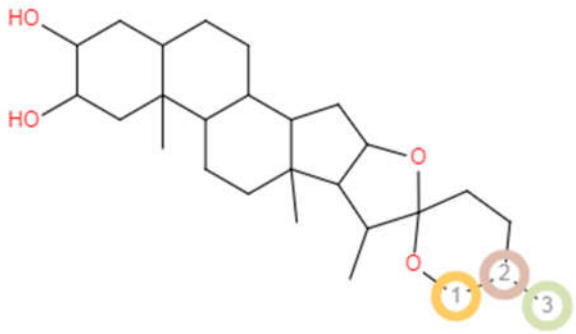

Figure 2. The potential sites for metabolism of neogitogenin against CYP3A4 of cytochrome P450 family.

3.7 *The two dimensional diagram of interaction between ligand and receptor*

The interactions between the ligands and the receptor were illustrated by Discovery Studio software. The results of the interactions between neogitogenin compound and the acetylcholinesterase enzyme are shown in Figure 3.

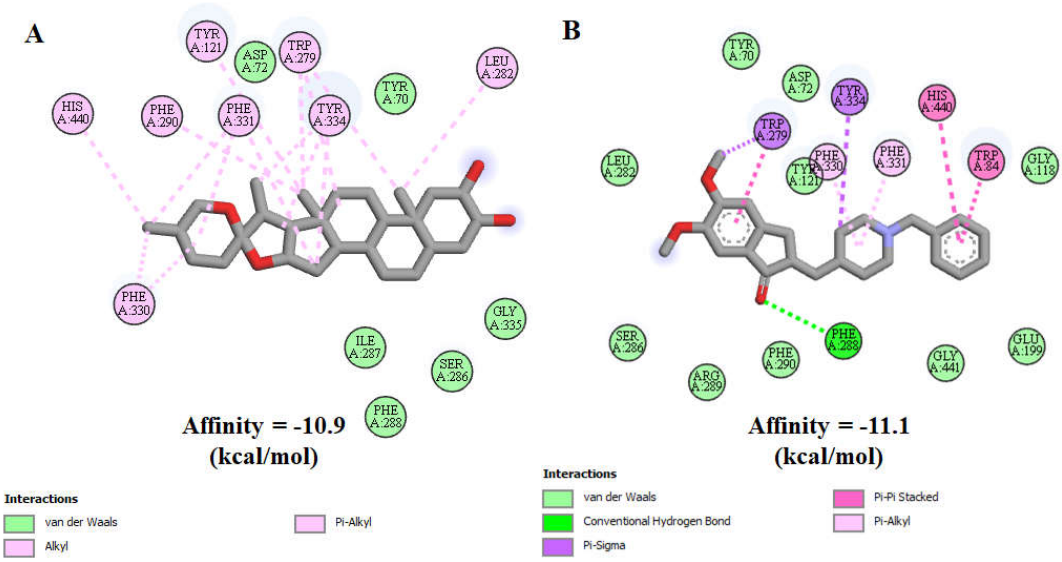

Figure 3. The interactions between neogitogenin and the acetylcholinesterase enzyme (A) & the interactions between donepezil and the acetylcholinesterase enzyme (B).

3.8 Discussions

In the present study, we found a suitable compound to inhibit the acetylcholinesterase by using virtual screening methods and machine learning algorithms.

Recent studies have suggested that the increase in the synaptic levels of AChE in the brain by inhibiting the AChE may be the most promising approach for the symptomatic treatment of AD and hence, recently, the AChE inhibitors such as galanthamine, donepezil, rivastigmine, and tacrine are consumed as the main drugs in the clinical management of AD.

In the present study, after virtual screening of 10997 food combinations, we reached the top 20 combinations. After numerous pharmacological chemistry studies the number of combinations were decreased, and finally, after toxicological studies, a lead chemical compound neogitogenin was identified to inhibit the AChE. Finally, the pharmacokinetic properties of neogitogenin were fully determined and its metabolic locus on the cytochrome P450 was determined.

The information obtained from this study informs the future laboratory attempts to develop a novel drug with using neogitogenin compound for treating AD patients. We can emphasize that neogitogenin can be considered as a potential lead structure in the drug design. However, more research and experiments are necessary to approve and recognize the neogitogenin in the inhibition of AChE and its direct effects on the pathophysiology of AD should be evaluated.

Acknowledgements

The authors wish to thank Pharmaceutical Sciences Research Center, Health Institute, Kermanshah University of Medical Sciences (KUMS), Kermanshah, Iran and Razi University, Kermanshah, Iran for their supports and assistance.

References

[1] K. Sharma, Cholinesterase inhibitors as Alzheimer's therapeutics, Molecular medicine reports 20 (2019) 1479-1487. doi: 10.3892/mmr.2019.10374.

[2] S. Agatonovic-Kustrin, C. Kettle, D. W. Morton, A molecular approach in drug development for Alzheimer's disease, Biomedicine & Pharmacotherapy 106 (2018) 553-565. doi: 10.1016/j.biopha.2018.06.147.

[3] D. P. Devanand, G. Pradhaban, X. Liu, A. Khandji, S. De Santi, S. Segal, H. Rusinek, G.H. Pelton, L. S. Honig, R. Mayeux, Y. Stern, M. H. Tabert, M. J. De Leon, Hippocampal and entorhinal atrophy in mild cognitive impairment: prediction of Alzheimer disease, Neurology 68 (2007) 828-836. doi: 10.1212/01.wnl.0000256697.20968.d7.

[4] N. Parsa, Alzheimer's disease: A medical challenge of 21st century, Journal of Arak University of Medical Sciences 14 (2011) 100-108.

[5] N. Tabet, Acetylcholinesterase inhibitors for Alzheimer's disease: anti-inflammatories in acetylcholine clothing, Age and ageing 35 (2006) 336-338. doi: 10.1093/ageing/afl027.

[6] D. P. Perl, Neuropathology of Alzheimer's disease, Mount Sinai Journal of Medicine 77 (2010) 32-42. doi:10.1002/msj.20157.

[7] A. Takashima, Tau aggregation is a therapeutic target for Alzheimer's disease, Current Alzheimer Research 7 (2010) 665-669. doi: 10.2174/156720510793611600.

[8] T. H. Ferreira-Vieira, I. M. Guimaraes, F. R. Silva, F. M. Ribeiro, Alzheimer's disease: targeting the cholinergic system, Current neuropharmacology 14 (2016) 101-115. doi: 10.2174/1570159X13666150716165726.

[9] P. B. Dowom, M. Darvishi, K. Heidarbeigi, neurological alterations in cognitive impairment, The Neuroscience Journal of Shefaye Khatam, 4 (2016) 99-115. doi: 10.18869/acadpub.shefa.4.4.99.

[10] P. Anad, B. Singh, N. Singh, A review on coumarins as acetylcholinesterase inhibitors for Alzheimer's disease, Bioorganic & medicinal chemistry 20 (2012) 1175-1180. doi: 10.1016/j.bmc.2011.12.042.

[11] D. Anupam, S. Raza, R. Jahan, M. Lohani, J. M. Arif, High-Throughput Virtual Screening (HTVS) of natural compounds and exploration of their biomolecular mechanisms: an in silico approach, New look to phytomedicine (2019) 523-548. doi.org/10.1016/B978-0-12-814619-4.00020-3.

[12] L. Roger, How many leads from HTS?, Drug discovery today 4(1999) 447-448. doi: 10.1016/s1359-6446(99)01393-8.

[13] V. Lobanov, Using artificial neural networks to drive virtual screening of combinatorial libraries, Drug Discovery Today: BIOSILICO 2 (2004)149-156. doi: 10.1016/S1741-8364(04)02402-3.

[14] Studio, Discovery. "Discovery Studio." Accelrys [2.1] (2008).

[15] R. Huey, G. M. Morris, Using AutoDock 4 with AutoDocktools: a tutorial, The Scripps Research Institute, USA 8 (2008) 54-56.

[16] L. Céline M., J. Rey, D. Lagorce, M. Vavruša, J. Becot, O. Sperandio, B. O. Villoutreix, P. Tufféry, M. A. Miteva, MTiOpenScreen: a web server for structure-based virtual screening, Nucleic acids research 43.W1 (2015) W448-W454. doi: 10.1093/nar/gkv306.

[17] G. M. Morris, R. Huey, A. J. Olson, Using autodock for ligand□receptor docking, Current protocols in bioinformatics 24 (2008) 8-14. doi: 10.1002/0471250953.bi0814s24.

[18] A. Daina, M. Olivier, V. Zoete, SwissADME: a free web tool to evaluate pharmacokinetics, drug-likeness and medicinal chemistry friendliness of small molecules, Scientific reports 7 (2017) 42717. dio: 10.1038/srep42717.

[19] D. E.V. Pires, T. L. Blundell, D. B. Ascher, pkCSM: predicting small-molecule pharmacokinetic and toxicity properties using graph-based signatures, Journal of medicinal chemistry 58 (2015) 4066-4072. doi:10.1021/acs.jmedchem.5b00104.

[20] R. C. Braga, V. M. Alves, M. F. B. Silva, E. Muratov, D. Fourches, L. M. Lião, A. Tropsha, C. H. Andrade, Pred□hERG: A novel web□accessible computational tool for predicting cardiac toxicity, Molecular informatics 34 (2015) 698-701. doi:10.1002/minf.201500040.

[21] F. Montanari, B. Knasmüller, S. Kohlbacher, C. Hillisch, C. Baierová, M. Grandits, GF. Ecker, Vienna LiverTox Workspace—a set of machine learning models for prediction of interactions profiles of small

molecules with transporters relevant for regulatory agencies, Frontiers in Chemistry 7 (2020) 899. doi: 10.3389/fchem.2019.00899.

[22] P. áB. Danielson, The cytochrome P450 superfamily: biochemistry, evolution and drug metabolism in humans, Current drug metabolism 3 (2002) 561-597. doi: 10.2174/1389200023337054.

[23] O. Tarasova, A. Rudik, A. Dmitriev, A. Lagunin, D. Filimonov, V. Poroikov, QNA-based prediction of sites of metabolism, Molecules 22 (2017) 2123. doi: 10.3390/molecules22122123.

Study of exon 12 polymorphisms of *PRODH* gene in schizophrenic patients

Sohrab Boozarpour*, Sakineh Alijanpour and Mina Lashkarboloki

Department of Biology, Faculty of Basic Sciences, Gonbad kavous University, Gonbad kavous, Golestan, Iran.

*E-mail: so.boozarpour@gmail.com

Abstract

Schizophrenia is a strong and very severe mental illness that is affected by a combination of environmental and genetic factors. One of the most important genes involved in this disease is the proline dehydrogenase gene. , Create. Exon 12 of the proline dehydrogenase gene has been identified as one of the high risk areas for various polymorphisms. Therefore, in this study, we investigated the occurrence of polymorphisms introduced for exon 12 as well as new polymorphisms. The method was as follows: after collecting blood samples from 10 patients, their DNA was extracted. Then, the sequence of 681 bp of exon 12 of PRODH gene was amplified by two reciprocating primers, by PCR. The resulting product was sequenced. Our results showed that among the three polymorphisms observed in patients, the occurrence of two polymorphisms, rs2904551 and rs2870983, alters the amino acid sequence of the protein proline dehydrogenase, and as a result, the structure or function of the enzyme proline oxidase may change. Schizophrenia may be involved.

Keywords: Schizophrenia, proline dehydrogenase, exon 12, polymorphism

1. Introduction

According to the World Health Organization, one of the most important diseases in this century is mental illness, especially schizophrenia. Schizophrenia is a severe mental disorder that affects a person's performance and affects his or her personality [1]. Schizophrenia is a multifactorial disease and a combination of environmental and genetic factors are involved in its occurrence. Environmental factors include date, place of birth and seasonal effects, infectious diseases, pregnancy and difficult births such as Rh factor problems, influenza and prenatal viral infections, fetal malnutrition, drug use, Stress and geographical differences affect the incidence of the disease [2]. However, studies conducted in different population show that 82-84% of the causes of schizophrenia are genetic and the remaining low percentage are influenced by environmental factors [3]. The mode of transmission of the disease is polygenic or oligogenic, in which case a single gene will be able to develop the disease [4].

To date, more than 30 different genes associated with schizophrenia have been identified in different populations. One of the most important loci containing genes associated with this disease is the long arm of chromosome 22, which contains genes such as *PRODH*, *COMT*, *ZDHHC8* [5].

The enzyme proline dehydrogenase (proline oxidase) is a product of the proline dehydrogenase (*PRODH*) gene, which catalyzes the breakdown of proline into delta-1-proline-5-carboxylate in the mitochondria. Which play a major role in the physiology of schizophrenia [6].

Proline dehydrogenase also plays a role in regulating the function of acetylcholine, a metabolic precursor to glutamate in neurons [7]. Numerous studies have shown a link between changes in the proline dehydrogenase gene and mental disorders, most of which are caused by mutations in the gene. Dehydrogenase decreases enzyme activity, and proline breaks down incompletely, and proline accumulates in the blood plasma. Researchers believe that increased levels of proline affect the function of certain chemicals that transmit nerve signals between neurons in the brain (neurotransmitters) and cause epileptic seizures, mental retardation, or other neurological problems. Psychology includes schizophrenia [[8],[9]].

Due to the fact that schizophrenia has a large population in the world and on the other hand has many negative social consequences and also due to the fact that so far no suitable molecular diagnostic and therapeutic methods have been identified for this disease. Due to the role of proline dehydrogenase enzyme in the development of schizophrenia in this study, we examine the exon 12 sequence of this gene, which has been reported as one of the regions of occurrence of multiple polymorphisms.

2. Material and Methods

In this study, in order to investigate the polymorphisms in exon 12 of proline dehydrogenase gene and its association with the incidence of schizophrenia, 10 patients admitted to a schizophrenia care center were sampled with 9 ml of blood. Patients' environment was taken for genetic tests. DNA extraction from the samples was done by salt method and precipitation with ethanol. After measuring the quantity and quality of the extracted DNA using spectrophotometer and agarose gel electrophoresis, in order to amplify the proline dehydrogenase gene, Forward primer (F5'-GGGAGTCTGGAGCACATGAT-3') and Reverse primer (R 5'-AGGGAACTGTGGCCAATTTTG-3') was used to amplify the 681 bp fragment, with the exon 12 sequence located in the middle of the amplified fragment. The PCR program consisted of a cycle of 95 ° C for 3 minutes, 40 cycles with a program of 45 seconds at 94 ° C, 45 seconds at 59 ° C, 35 seconds at 72 ° C, and a cycle of 72 ° C for 5 minutes. To ensure the accuracy of the reaction and the thermal cycler, we used a genomic DNA that was previously used as a positive control of the reaction. After PCR reaction, all samples were sent to Dena Zist Company in 1.5 ml microtubes packed separately for sequencing, and the results of product sequencing were received via email.

3. Results and Discussions

DNA extracted from blood was observed as a clear band after agarose gel electrophoresis (Figure 1).

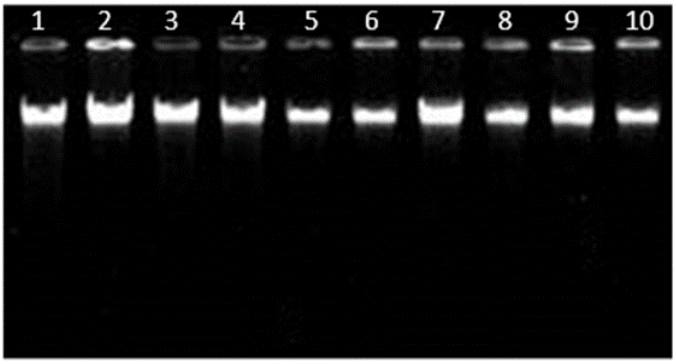

Figure 1: Image of genomic DNA electrophoresis extracted on 0.8% agarose gel. 1-10: Genomic DNA

After determining the appropriate protocol with *PRODH* gene primer and binding temperature of 59 ° C and concentration of 1.5 mM, PCR reaction was performed on all samples and its 681 bp band was observed on 1.5% agarose gel (Figure 2).

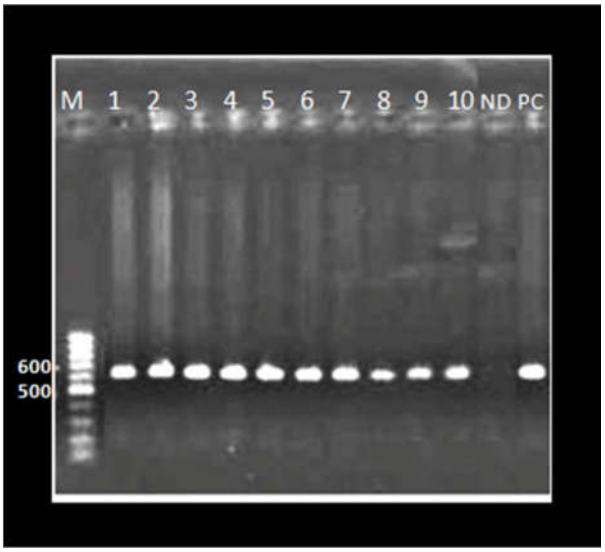

Figure 2: PCR products of exon 12 of proline dehydrogenase gene on 1.5% agarose gel, M: DNA marker, 1 to 10) PCR product of schizophrenia samples, ND: negative control, PC: positive control

Sequencing of exon 12 of proline dehydrogenase gene in the studied samples showed that out of 10 samples, 7 samples had no polymorphisms in this exon. The point to consider in our studies was that no mutations were observed in the women studied. However, rs16983466 polymorphism was observed in three samples as heterozygous and rs2904551 polymorphism as heterozygous and rs2870983 as homozygous were observed in only one sample (Table 1).

Table 1: Sequencing results of exon 12 of *PRODH* gene in 10 samples of schizophrenia patients in Golestan province

Sample No.	sex	Polymorphism	Ancestral allele	Alteration of mRNA Seq (amino acid)
1	male	-	-	-
2	male	-	-	-
3	male	rs16983466	G	GAC ⇒ GAT [Asp] ⇒ [Asp]
4	male			
5	male	rs16983466	G	GAC ⇒ GAT [Asp] ⇒ [Asp]
		rs2904551	A	CTG ⇒ CCG [Leu] ⇒ [Pro]
		rs2870983	C	GCC ⇒ ACC [Ala] ⇒ [Thr]
6	male	rs16983466	G	GAC ⇒ GAT [Asp] ⇒ [Asp]
7	female	-	-	-
8	female	-	-	-
9	female	-	-	-
10	male	-	-	-

3.1 Discussion

Schizophrenia is a strong and very severe mental illness that usually occurs in late adolescence and early adulthood. In this case, the psychological symptoms and features of the disease appear and lead to a hard life, with suffering for the person. The patient and his family return. According to a report by the World Health Organization on the extent of the disease's damage to developed countries, schizophrenia is ranked fifth in terms of severity of the disease and its consequences on society [[8],[10]]. One of the most important genes involved in this disease is proline dehydrogenase gene. Studies have shown that the occurrence of polymorphisms in different exons of proline dehydrogenase gene leads to a change in the function of this enzyme. Exon 12 of the proline dehydrogenase gene has been identified as a hot spot for polymorphisms [11]. Therefore, in this study, we aimed to investigate the occurrence of polymorphisms introduced for exon 12 as well as new polymorphisms in this region of the proline dehydrogenase gene in patients.

Rs16983466 polymorphism normally has G allele. If a single nucleotide polymorphism G to A occurs at this site, the GAC codon is converted to GAT, which both are encoded aspartic acid codons. The results obtained by Glasser *et al*. In 2006 from experiments on *PRODH* gene variants showed that the incidence of rs16983466 polymorphism was not significantly associated with the occurrence of schizophrenia. Because this polymorphism is a kind of silent mutation and does not cause a change in the amino acid aspartic acid [12]. Ota et al. showed

that the occurrence of rs2904551 polymorphism in exon 12 of the *PRODH* gene is associated not only with schizophrenia but also with hyperprolinemia. In fact, rs2904551 polymorphism is a missense mutation which altered CTG to CCG. Normally, the CTG codon encodes the amino acid leucine, but the occurrence of this polymorphism causes to encode proline. So, the occurrence of rs2904551 polymorphism is considered as a risk factor for schizophrenia [11].

In 2008, a study of proline dehydrogenase gene polymorphisms, concluded that the occurrence of rs2870983 polymorphism in the proline dehydrogenase gene reduces the function of this enzyme [13]. This polymorphism by changing the nucleotide of cytosine to thymine causes replacement of threonine instead of alanine in PRODH protein, which is effective in altering the structure and function of proline dehydrogenase gene, given the importance of this gene in the development of schizophrenia [6], this provides the basis for the development of this disease.

Our results showed that there are only 3 polymorphisms rs16983466, rs2904551, and rs2870983 in exon 12 of PRODH gene in the study population. As seen in other studies, the occurrence of rs2904551 and rs2870983 polymorphisms alters the amino acid sequence of proline dehydrogenase protein and may alter the structure or function of this enzyme, thus confirming the results of other studies performed on these polymorphisms and their association with the incidence of schizophrenia. However, to confirm that the occurrence of rs2904551 and rs2870983 polymorphisms in the study population is directly related to the incidence of schizophrenia, it is necessary to study a larger number of samples from this population. Since none of the polymorphisms observed in men were seen in women and the frequency of male patients is higher than female patients in this population, this could be due to association of sex with the incidence of this disease. There are differing views on risk factors for the development of schizophrenia, one of which is genetic changes such as polymorphisms. Identifying these factors can go a long way in predicting and thus preventing schizophrenia.

References

[1] J.B. Fan, J. Ma, C.S. Zhang, J.X. Tang, N.F. Gu, G.Y. Feng, D. St Clair, L. He., A family-based association study of T1945C polymorphism in the proline dehydrogenase gene and schizophrenia in the Chinese population, Neuroscience letters 338 (2003) 252-254. doi:10.1016/S0304-3940(02)01362-9.

[2] J. Janoutova, P. Janackova, O. Sery, T. Zeman, P. Ambroz, M. Kovalova, K. Varechova, L. Hosak, V. Jirik, V. Janout., Epidemiology and risk factors of schizophrenia, Neuroendocrinology Letters 37 (2016) 1-8.

[3] F. Thibaut., Why schizophrenia genetics needs epigenetics: a review, Psychiatria Danubina 24 (2012) 25-27.

[4] J.A. Gogos., Schizophrenia susceptibility genes: in search of a molecular logic and novel drug targets for a devastating disorder, International review of neurobiology 78 (2007) 397-422. doi: 10.1016/S0074-7742(06)78013-8.

[5] C.M. O'Tuathaigh, D. Babovic, G. O'Meara, J.J. Clifford, D.T. Croke, J.L. Waddington., Susceptibility genes for schizophrenia: characterisation of mutant mouse models at the level of phenotypic behavior, Neuroscience and biobehavioral reviews 31 (2007) 60-78. doi: 10.1016/j.neubiorev.2006.04.002.

[6] H.E. McDermid, B.E. Morrow., Genomic disorders on 22q11, American journal of human genetics 70 (2002) 1077-1088. doi: 10.1086/340363.

[7] N. Braverman, G. Steel, C. Obie, A. Moser, H. Moser, S.J. Gould, D. Valle., Human PEX7 encodes the peroxisomal PTS2 receptor and is responsible for rhizomelic chondrodysplasia punctata. Nature genetics 15 (1997) 369-376. doi: 10.1038/ng0497-369.

[8] H. Jacquet, G. Raux, F. Thibaut, B. Hecketsweiler, E. Houy, C. Demilly, S. Haouzir, G. Allio, G. Fouldrin, V. Drouin, B. Jacqueline, P. Michel, C.C. Dominique, F. Thierry., PRODH mutations and hyperprolinemia in a subset of schizophrenic patients, Human molecular genetics 11 (2002) 2243-2249. doi: 10.1093/hmg/11.19.2243.

[9] P. Roussos, S.G. Giakoumaki, P. Bitsios., A risk PRODH haplotype affects sensorimotor gating, memory, schizotypy, and anxiety in healthy male subjects, Biological psychiatry 65 (2009) 1063-1070. doi: 10.1016/j.biopsych.2009.01.003.

[10] J.A. Gogos, D.J. Gerber., Schizophrenia susceptibility genes: emergence of positional candidates and future directions, Trends in pharmacological sciences 27 (2006) 226-233. doi: 10.1016/j.tips.2006.02.005.

[11] V.K. Ota, F.T. Bellucco, A. Gadelha, M.L. Santoro, C. Noto, D.M. Christofolini, I.B. Assuncao, , K.M Yamada, A.K. Ribeiro-dos-Santos, S.Santos, J.J. Mari, M.A.C. Smith, M.I. Melaragno, R.A. Bressan, J.R. Sato, A.P. Jackowski, S.I. Belangero., PRODH polymorphisms, cortical volumes and thickness in schizophrenia, PloS one 9 (2014) e87686. doi: 10.6084/m9.figshare.1230185.

[12] B. Glaser, V. Moskvina, G. Kirov, K.C. Murphy, H. Williams, N. Williams, M.J. Owen, M.C. O'Donovan., Analysis of ProDH, COMT and ZDHHC8 risk variants does not support individual or interactive effects on schizophrenia susceptibility, Schizophrenia research 87 (2006) 21-27. doi: 10.1016/j.schres.2006.05.024.

[13] L. Kempf, K.K. Nicodemus, B. Kolachana, , R. Vakkalanka, , B.A. Verchinski, , M.F. Egan, , R.E. Straub, , V.A. Mattay, J.H. Callicott, D.R. Weinberger, M.L. Andreas., Functional polymorphisms in PRODH are associated with risk and protection for schizophrenia and fronto-striatal structure and function, PLoS genetics 4 (2008) e1000252. doi: 10.1371/journal.pgen.1000252.

Preparation of decellularized scaffold of nerve tissue and its applications

Hadi Atashkar[1], Asadollah Asadi [1*] , Saber Zahri[1] and Arash Abdolmaleki[2,3]

[1] Department of Biology, Faculty of Sciences, University of Mohaghegh Ardabili, Ardabil, Iran.

[2] Department of Engineering Sciences, Faculty of Advanced Technologies, University of Mohaghegh Ardabili, Namin, Iran.

[3] Bio Science and Biotechnology Researchcenter (BBRC), Sabalan University of Advanced Technologies (SUAT), Namin, Iran.

*Email: asady@uma.ac.ir

Abstract

Decellularized tissues are widely used clinically for tissue repair and regeneration. The purpose of the present study was to prepare and evaluate the decellularized scaffolds in comparison with fresh nerves. After cessation of the sciatic nerve of the rats, by surgery, nerves enter the decellularization stage. The sciatic nerve was decellularized using solutions such as trytion X 100 and sodium deoxycholate.

Scaffolds from extracellular matrix can be a good platform for studying cellular behaviors by preserving the main components of the tissue. It seems that the preparation of such scaffolds will be an important part of future bioscience studies that can have wide applications in the science of regenerative medicine and tissue engineering.

Keywords: decellularized scaffolds, extracellular matrix, regeneration, sciatic nerve, tissue engineering.

1. Introduction

Decellularized tissues are widely used clinically for tissue repair and regeneration. In basic research and preclinical studies, numerous tissues and organs have now been decellularized and used in various regenerative medicine applications [1]. The extracellular matrix (ECM), which remains after decellularization, plays a crucial role as a structural support for tissue as well as a source of biochemical and biophysical cues for the cells that reside within it. Through these two roles the ECM directs cell proliferation, migration, differentiation, and behavior [2]. The ECM of each tissue provides a unique tissue specific microenvironment for resident cells. This cell niche has been adapted by nature to provide the cells with the structure and biochemical cues that are required for their function [3]. It has therefore been hypothesized that decellularized tissue materials should have distinct effects on cell differentiation based on which tissue the material was sourced. Using nature's tailored cell niches to direct cells to differentiate towards specific cell lineages has become a popular avenue for tissue engineering studies. By understanding decellularized tissues' effects on cell differentiation more thoroughly, this technology could provide a useful platform for controlling cell fate and generating regenerative therapies.

2. Material and Methods

Preparation of Decellularized Scaffold:

In this study, 20 adult male rats weighing 270-230 g were used to prepare the scaffold. The mice were anesthetized with ketamine 60 mg/kg, Then sciatic nerve fragments of the rats were removed above the nerve branching site and after cleansing of the tissues were decellularized by Sondell method, briefly nerves were treated with a series of detergent baths consisting of distilled water for 7 h, Triton X-100 for 12 h, and sodium deoxycholate for 24 hours according to the Sondell protocol. All acellularization steps were performed at room temperature. After repeating the above steps, the sciatic nerves were stored in PBS.

3. Results and Discussions

3.1 Results:

Scaffolds from extracellular matrix can be a good platform for studying cellular behaviors by preserving the main components. It seems that the preparation of such scaffolds will be an important part of future bioscience studies that can have wide applications in the science of regenerative medicine and tissue engineering. The results of examining the appearance of the decellularized nerve in comparison with the non-decellularized nerve showed that the appearance of the decellularized nerve was clearer and brighter than that of the non-decellularized nerve. This may indicate the destruction of cells in the decellularized nerve. (Figure 1 and 2)

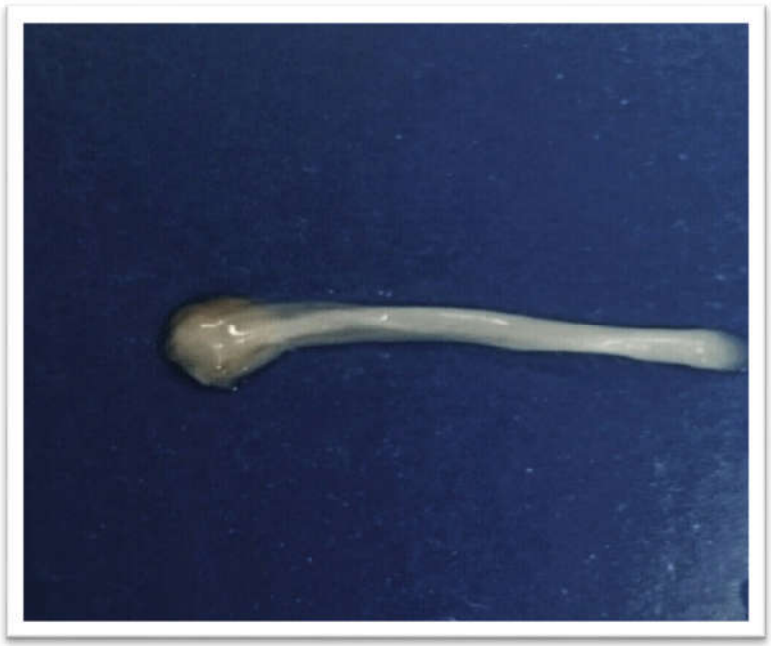

Figure 12: Non-decellularized nerve

Figure 13: Decellularized nerve

3.2 Discussions:

In recent years, remarkable progresses have been reached in the use of biomaterials for promoting neuronal regeneration. Regardless that further studies are required to understand the role of tissue-specific decellularized matrices in neuronal regeneration, decellularized scaffolds still represent promising biomaterials for the development of alternative regenerative strategies [4]

Scaffold materials of tissue engineering mainly include natural polymers,[5] Synthetic polymers,[6] compound polymers and decellularized scaffold [7–10]. Natural polymer is characterized by low immunogenicity and favorable biocompatibility. However, there are significant mechanical differences compared with normal nerves and the natural polymers do not possess the three-dimensional meshwork structure for cell growth [11,12]. Synthetic polymers make up the mechanical defects of natural polymer and establish the three-dimensional meshwork structure similar to normal nerves. However, the synthetic polymer has a low affinity for cell and poor biocompatibility. In addition, the material of synthetic polymers can easily lead to inflammatory response,[13] which greatly limit the application of synthetic polymers [14]. Compound polymers have good mechanical properties and biocompatibility, as well as improve the affinity with cells, but it is difficult to set up three dimensional meshwork structure similar to normal nerves [15,16]. Decellularized scaffold possess the three-dimensional meshwork structure and retain the mechanical character of normal nerves which can apply function of guiding and protection for cell growth. In addition, the cellular constituent of decellularized scaffold has been removed so that it has no immunogenicity but good biocompatibility [17–19]. In this context, how to prepare decellularized scaffold has become a hot spot.

The use of decellularized tissue materials had success in many different applications. The current designs of these materials include different types of entire organ matrices, sections, blocks, hydrogels and coatings. There is room to expand on the materials and methods for creating decellularized ECM in order to maintain the native architecture and incorporate all of the cues that are beneficial for cell differentiation [2, 3, 20]. Each tissue has its own obstacles when decellularizing and processing the material, and as new tissues are used for decellularization experiments there will be new challenges that will have to be overcome. Each material category also has its own benefits for specific applications. Entire organ matrices can be used for larger transplants and organ replacements. Hydrogels are best for creating 3D environments and can be used as injectable therapies. Sections and coatings are useful for discovering the effects of the matrix components on cell differentiation directly. [21]

Overall, there are clear effects of decellularized materials on cell differentiation. To date, lung, liver, kidney, heart, central nervous system, adipose, tendon, muscle, cartilage, and other decellularized tissues have shown signs of positive impact on cell differentiation in laboratory settings. However, the extent to which each tissue can direct cell lineage differs. [21]

It is important to remember this variation among tissue and material types when designing decellularized tissue materials. Though it is generally understood that the ECM contains necessary cues for directing tissue specific gene expression, there are many factors that are needed for differentiation and the ECM alone may not be sufficient for every tissue engineering purpose. However, the papers reviewed demonstrate that decellularized tissue materials can be a powerful tool by harnessing what nature has already designed. With future research and

development, this field has excellent potential to provide a greater impact in both basic and translational tissue engineering studies. [21]

Acknowledgements

The authors would like to thank the Research Council of University of Mohaghegh Ardabili for the financial support of this study.

References

[1] Keane TJ, Swinehart IT, Badylak SF. Methods of tissue decellularization used for preparation of biologic scaffolds and in vivo relevance. Methods. 2015; 84:25–34. [PubMed: 25791470]

[2] Hoshiba T, Lu H, Kawazoe N, Chen G. Decellularized matrices for tissue engineering. Expert Opin Biol Ther. 2010; 10:1717–28. [PubMed: 21058932]

[3] Badylak SF. The extracellular matrix as a scaffold for tissue reconstruction. Semin Cell Dev Biol. 2002; 13:377–83. [PubMed: 12324220]

[4] . Wang H, et al. (2015) Decellularization technology in CNS tissue repair. Expert Rev. Neurother 15: 493-500.

[5] Jain A, Kim YT, McKeon RJ, Bellamkonda RV. In situ gellinghydrogels for conformal repair of spinal cord defects, and local delivery of BDNF after spinal cord injury. Biomaterials 2006;27: 497–504.

[6] Moore MJ, Friedman JA, Lewellyn EB, Mantila SM, Krych AJ,Ameenuddin S, Knight AM, Lu L, Currier BL, Spinner RJ, Marsh RW, Windebank AJ, Yaszemski MJ. Multiple-channel scaffolds to promote spinal cord axon regeneration. Biomaterials 2006;27:419–429.

[7] Burk J, Erbe I, Berner D, Kacza J, Kasper C, Pfeiffer B, Winter K,Brehm W. Freeze-thaw cycles enhance decellularization of large tendons. Tissue Eng Part C Methods 2013.

[8] Naderi S, Zadeh JK, Shahri NM, Abady KNS, Cheravi M, BahararaJ, Rad SAB, Bahrami AR. Three-dimensional scaffold from decellularized human gingiva for cell cultures: Glycoconjugates and cell behavior. Cell J (Yakhteh) 2013;15:166.

[9] Yin Z, Chen X, Zhu T, Hu JJ, Song HX, Shen WL, Jiang LY, HengBC, Ji JF, Ouyang HW. The effect of decellularized matrices on human tendon stem/progenitor cells differentiation and tendon repair. Acta Biomater 2013;9:9317–9329.

[10] Zang M, Zhang Q, Chang EI, Mathur AB, Yu P. Decellularized trachealmatrix scaffold for tissue engineering. Plast Reconstr Surg 2012;130: 532–540.

[11] Petrigliano FA, McAllister DR, Wu BM. Tissue engineering foranterior cruciate ligament reconstruction: A review of current strategies. Arthroscopy 2006;22:441–451.

[12] Willerth SM, Sakiyama-Elbert SE. Approaches to neural tissueengineering using scaffolds for drug delivery. Adv Drug Deliv Rev 2007;59:325–338.

[13] Kainer MA, Linden JV, Whaley DN, Holmes H, Jarvis W, JerniganD, Archibald L. Clostridium infections associated with musculoskeletal-tissue allografts. New Engl J Med 2004;350:2564– 2571.

[14] Seyrek M, Vural IM, Tunca YM, Aydin C, Ulku C, Demirkaya K,Inal A, Yildiz O. The vasodilatory effect of a synthetic polymerbased root canal material on thoracic aorta. Int Endod J 2010;43: 590–599.

[15] Elder BD, Eleswarapu SV, Athanasiou KA. Extraction techniquesfor the decellularization of tissue engineered articular cartilage constructs. Biomaterials 2009;30:3749–3756.

[16] Nisbet DR, Pattanawong S, Ritchie NE, Shen W, Finkelstein DI,Horne MK, Forsythe JS. Interaction of embryonic cortical neurons on nanofibrous scaffolds for neural tissue engineering. J Neural Eng 2007;4:35.

[17] Barnes CA, Brison J, Michel R, Brown BN, Castner DG, BadylakSF, Ratner BD. The surface molecular functionality of decellularized extracellular matrices. Biomaterials 2011;32:137–143.

[18] Guo SZ, Ren XJ, Wu B, Jiang T. Preparation of the acellular scaffold of the spinal cord and the study of biocompatibility. Spinal cord 2010;48:576–581.

[19] Nowocin AK, Southgate A, Gabe SM, Ansari T. Biocompatibilityand potential of decellularized porcine small intestine to support cellular attachment and growth. J Tissue Eng Regen Med 2013.

[20] Faulk DM, Johnson SA, Zhang L, Badylak SF. Role of the extracellular matrix in whole organ engineering. J Cell Physiol. 2014; 229:984–9

[21] Curr Opin Solid State Mater Sci. 2016 August ; 20(4): 193–201. doi:10.1016/j.cossms.2016.02.001.

Preparation of decellularized scaffold of pancreas tissue and its application

Neda Farazi [1]، Asadollah Asadi*[1]، Arash Abdolmaleki[2, 3]، Saber Zahri[1]

[1] Department of Biology, Faculty of Sciences, University of Mohaghegh Ardabili, Ardabili, Iran.

[2] Department of Engineering Sciences, Faculty of Advanced Technologies, University of Mohaghegh Ardabili, Namin, Iran.

[3] Bio Science and Biotechnology Research center (BBRC), Sabalan University of Advanced Technologies (SUAT), Namin, Iran.

*Email: asady@uma.ac.ir

Abstract

Recent advances in tissue engineering make it possible to use decellularized organs as scaffolds for cell therapy. The decellularized pancreas can be a good scaffold because it can maintain the native extracellular matrix (ECM) and arteries. The main purpose of this study was to prepare and evaluate models of decellularized scaffold tissue of rat pancreas and compare it with fresh pancreas.

Materials and Methods: After separation of the rats' pancreas, by surgery, the pancreas enters the decellularization stage. In order to remove cells from the target tissue chemical decellularization was performed using SDS and Triton x100 at concentrations of 0.5 and 1% at 12 and 24 hour intervals.

Discussion and Conclusion: The results of this study show that the scaffold prepared in this study can be a suitable model for further studies in the field of tissue engineering and regenerative medicine.

Keywords: Decellulrized scaffold , Extracellular matrix, Pancreas, Tissue Engineering , Regeneration

1. Introduction

Tissue engineering plays a key role in repairing, maintaining or strengthening tissues and organs by creating a bridge between biology and engineering [1]. Scaffolding is a temporary structure to support cells, connect, proliferate and differentiate cells into expected tissues and organs [2]. Today, these scaffolds are used in various fields such as drug delivery, gene therapy and cell therapy. Their main application is in tissue engineering and regenerative medicine [3].Using various decellularization methods such as repeated thawing and freezing cycles, irradiation and lyophilization, researchers have been able to remove tissue cells to some extent, but these methods alone are not able to remove cell debris from scaffolds, which is an obstacle in the process of repair [4] Researchers intend to use scaffolding to produce scaffolds that have the most compatibility with the natural extracellular matrix while removing the maximum number of cells and antigenic compounds [5،6].The use of de-cellular scaffolds

has advantages such as reduced post-transplant immune response [7].In the field of regenerative medicine, organs are decellularized to remove cellular components to produce acellular extracellular matrix (ECM) or as known as decellularized scaffolds. These scaffolds, since they lack cellular components and maintain ECMs, are "rejectless" when implanted, and able to act as an inductive template for recellularization [8،9].Decellularized scaffolds have become an emerging approach for treatment[10،11]. Scaffolds obtained from tissue decellularization can be transplanted directly to the damaged tissue or by implanting the patient's cells on it, strengthen the repair ability of these scaffolds [12،13،14].Purpose of the present study was to find a fast and reproducible protocol for decellularization the complete pancreas of rat.

2. Material and Methods

Preparation of Decellularized rat pancreas Scaffold:

To prepare the de-cellular scaffold of rat pancreas, 20 adult male Wister rat weighing 230-270 gr were purchased.Rats were killed by CO2. After separation of pancreatic tissue, chemical decellularization steps of mouse pancreas were started. The sample was first placed in PBS solution. Then was transferred to 0.5% SDS solution and after 12 hours the sample was washed with distilled water for 15 minutes. Immediately the sample was transferred to Triton x100 (1%). After 24 hours, the tissue was washed with distilled water and transferred to PBS and stored in 4 °C. All acellularization steps were performed at room temperature.

3. Results and Discussions

3.1 Results:

The decellularization and recellularization of parenchymal organs has in recent years emerged in the field of tissue engineering. The preparation of decellularized scaffolds will be an important part of future bioscience studies that can have wide applications in the science of tissue engineering and regenerative medicine.The results of examining the appearance of the decellularized pancreas in comparison with the non-decellularized pancreas showed that the appearance of the decellularized pancreas was clearer and brighter than that of the non-decellularized pancreas. This may indicate the destruction of cells in the decellularized pancreas. (Figure 1 and 2)

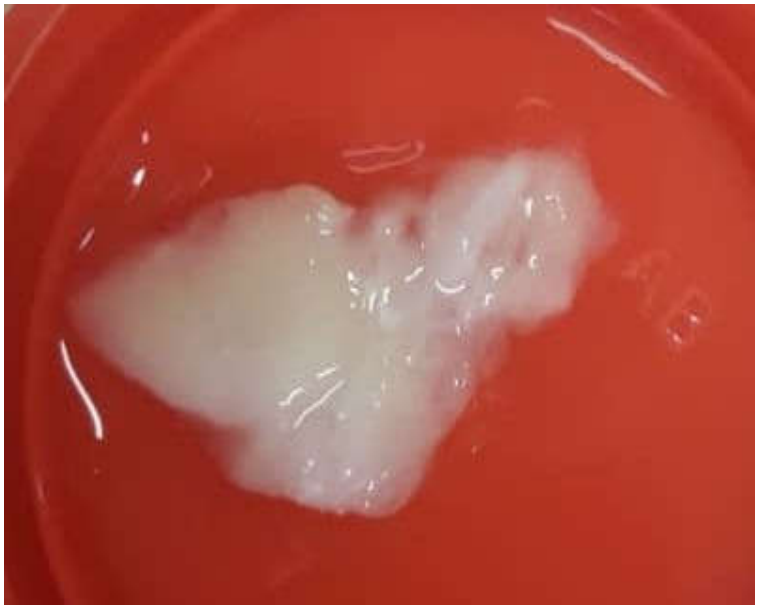

Figure 14: Non-decellularized scaffold of rat pancreas.

Figure 15: Decellularized scaffolding of rat pancreas.

3.2 Discussions:

Tissue engineering (TE) and regenerative medicine have arisen as new biomedical fields that bring advanced approaches for damaged tissue regeneration and healing [15]. Recently, in connection with the unprecedented development of biotech, regenerative medicine has acquired independent significance. The pancreas historically became one of the first objects of regenerative medicine, apparently in connection with notable inconsistency of other approaches in relation to this organ [16]. While great advancements are being made in regenerative medicine through decellularization, it is essential that protocols be further developed to optimize the process. Current decellularization methods are beneficial in some regards but oftentimes lack in others. Ideal methods will produce cell- and genetic material-free ECM that retains important structural, biochemical, and biomechanical properties crucial to its inherent function [17]. Scaffolds can be obtained by following the decellularization of organs and tissues [18]. Decellularization methods have been used on different types of tissues either to examine the treatment on a less complex tissue or to create a scaffold for simpler applications [19].

The objectives for successful decellularization are 1) complete or near complete removal of cellular material, and 2) preservation of ECM composition [20]. Commonly reported decellularization protocols require mechanical agitation or freezing and thawing which may take up to days or weeks to remove all cellular materials [21].Such protocols do not guarantee preservation of the ECM micro-structure, which has been shown to be instrumental for the generation of functional tissue engineered constructs [22].Decellularized pancreata can serve as a biocompatible scaffold to subsequently infuse pancreatic islets and are non-toxic and free of cellular components. They retain ECM and preserve inner vasculature structures. This study provided new insights on pancreas decellularization and its applications [23].

The decellularization and recellularization of parenchymal organs has in recent years emerged in the field of tissue engineering. This interesting new technique could provide several improvements: by removing all cellular material from an allogeneic or even xenogeneic organ, a less immunogenic three-dimensional scaffold can be generated that can be repopulated [24]. The production of an intact acellular organ such as the pancreas by perfusion-decellularization offers a promising alternate approach for pancreatic tissue engineering and functional organ replacement. Herein, we demonstrate that perfusion-decellularization of whole pancreas results in the generation of a natural pancreas ECM scaffold with a perfusable vascular tree, ductal network and intact 3D architecture, which acts as a suitable template for pancreatic tissue engineering and whole organ regeneration [25].

The main goal of any attempt to stimulate pancreatic repair is to restore the number of functionally active β-cells to ensure the maintenance of sufficient insulin production. This goal can be achieved in two ways: The reduction in the death rates of β-cells or the production of new β-cells. The methods of regenerative medicine relevant to these tasks can be listed as follows: (1) The use of biologically active substances, especially peptide or protein growth and differentiation factors, that regulate cell cycle, apoptosis, inflammation and repair; (2) Transplantation of donor β-cells or progenitor cells to replace the damaged islets; (3) Transplantation of the tissue-engineered bioartificial pancreatic constructs; and (4) Reprogramming of cells into insulin-producing phenotypes [26]. Another important consideration for organ decellularization is minimizing the undesirable alteration and loss of biologically active ECM components.

The ultimate goal, which is to provide an acceptable level of functional activity of the insulin-secreting β-cells, is pursued by two prospective broad strategies of regenerative medicine: β-cell replacement and β-cell regeneration [27].

Development of methods and tools to stimulate regeneration of damaged tissues and organs has always been a prominent theme in medical science. However, only recently, in connection with the unprecedented development of biotech, regenerative medicine has acquired independent significance. Our ideas about reparative regeneration (restoration of the structure and function of tissues and organs damaged by pathology or trauma) are constantly expanding and replenishing the existing clinical strategies [28].

In contrast, our approach of whole organ perfusion-decellularization reduces the diffusion distance required for decellularization agents to reach the cells and facilitates removal of the cellular material from the tissue by convective transport [29]. This technique allowed the efficient generation of acellular scaffold with preserved ECM, 3D architecture and perfusable network resembling a native organ.

Acknowledgements

The authors would like to thank the Research Council of University of Mohaghegh Ardabili for the financial support of this study.

References

[1] . Barre`re F, Mahmood TA, de Groot K. Blitterswijk, CA. Advanced biomaterials for skeletal tissue regeneration: Instructive and smart functions.Materials Science and Engineering. 2008; 59(5): 38–71

[2] . Runyan CM, Taylor JA. Clinical Applications of Stem Cells in Craniofacial Surgery. Facial Plast Surg 2010; 26(5): 385-95.

[3] Preparation of biological scaffolds derived from bladder sheep and evaluation of Bio compatibility and mechanical properties of the scaffold R Najafi Zangir, A Asadi, S Zahri - Journal of Cell & Tissue, 2019 - jct.araku.ac.ir

[4] . Johnson AP, Wood MD, Moore AM, Mackinnon SE. Tissue engineered constructs for peripheral nerve surgery. European Surgery, 45(3), 122-135.

[5] Johnson PJ, Wood MD, Moore AM,. Mackinnon SE. Tissue engineered constructs for peripheral nerve Surgery. Eur Surg, 2013. 45:122–135

[6] *Gilbert* TW, *Sellaro* TL, *Badylak* SF. *Decellularizationoftissuesandorgans*,*s*, 2006. 19: 3675–3683

[7] Furth ME, Atala A, Van Dyke ME. Smart biomaterials design for tissue engineering and regenerative medicine. Biomaterials, 2007. 28(34): 5068-5073

[8] Burk J, Erbe I, Berner D, Kacza J, Kasper C, Pfeiffer B, Winter K,Brehm W. Freeze-thaw cycles enhance decellularization of large tendons. Tissue Eng Part C Methods 2013.

[9] Decellularized pancreas matrix scaffolds for tissue engineering using ductal or arterial catheterization J Hashemi, P Pasalar, M Soleimani, E Arefian… - Cells Tissues …, 2018 - karger.com

[10] Decellularized and solubilized pancreatic stroma promotes the in vitro proliferation, migration and differentiation of BMSCs into IPCs

[11] Extracellular matrix scaffold technology for bioartificial pancreas engineering: state of the art and future challenges

[12] M Salvatori, R Katari, T Patel, A Peloso… - Journal of diabetes …, 2014 - journals.sagepub.com Yin Z, Chen X, Zhu T, Hu JJ, Song HX, Shen WL, Jiang LY, HengBC, Ji JF, Ouyang HW. The effect of decellularized matrices on human tendon stem/progenitor cells differentiation and tendon repair. Acta Biomater 2013;9:9317–9329.

[13] Zang M, Zhang Q, Chang EI, Mathur AB, Yu P. Decellularized trachealmatrix scaffold for tissue engineering. Plast Reconstr Surg 2012;130: 532–540.

[14] Kumari A, Yadav SK, Yadav SC. Biodegradable polymeric nanoparticles based drug delivery systems. Colloids Surf B Biointerfaces. 2010; 75(1): 1-18

[15] Methods to generate tissue-derived constructs for regenerative medicine applications JP Zambon, A Atala, JJ Yoo - Methods, 2020 - Elsevier

[16] [HTML] Regenerative medicine of pancreatic islets IV Arutyunyan, TK Fatkhudinov… - World Journal of …, 2020 - ncbi.nlm.nih.gov

[17] Perfusion-decellularized skeletal muscle as a three-dimensional scaffold with a vascular network template J Zhang, ZQ Hu, NJ Turner, SF Teng, WY Cheng… - Biomaterials, 2016 - Elsevier

[18] Bio-scaffolds in organ-regeneration: Clinical potential and current challenges S Yesmin, MB Paget, HE Murray, R Downing - … in translational medicine, 2017 - Elsevier

[19] Strategies based on organ decellularization and recellularization KH Hillebrandt, H Everwien, N Haep… - Transplant …, 2019 - Wiley Online Library

[20] Tissue-specific decellularization methods: rationale and strategies to achieve regenerative compounds U Mendibil, R Ruiz-Hernandez… - International Journal of …, 2020 - mdpi.com

[21] Decellularization and cell seeding of whole liver biologic scaffolds composed of extracellular matrix DM Faulk, JD Wildemann, SF Badylak - Journal of clinical and experimental …, 2015 - Elsevier

[22] Bioengineering the Pancreas: Cell-on-Scaffold Technology A Peloso, A Citro, G Oldani, S Brambilla… - Scaffolds in Tissue …, 2017 - books.google.com

[23] The Research of Acellular pancreatic bioscaffoldas a natural 3D platform In Vitro X Wang, Z Li - MS&E, 2018 - iopscience.iop.org

[24] Crapo PM, Gilbert TW, Badylak SF. An overview of tissue and whole organ decellularization processes. Biomaterials, 2011. 32:3233–3243

[25] Kainer MA, Linden JV, Whaley DN, Holmes H, Jarvis W, JerniganD, Archibald L. Clostridium infections associated with musculoskeletal-tissue allografts. New Engl J Med 2004;350:2564– 2571.

[26] Engineering an endocrine Neo-Pancreas by repopulation of a decellularized rat pancreas with islets of Langerhans H Napierala, KH Hillebrandt, N Haep, P Tang… - Scientific reports, 2017 - nature.com

[27] Perfusion-decellularized pancreas as a natural 3D scaffold for pancreatic tissue and whole organ engineering SK Goh, S Bertera, P Olsen, JE Candiello, W Halfter… - Biomaterials, 2013 – Elsevier

[28] Decellularized pancreas as a native extracellular matrix scaffold for pancreatic islet seeding and culture R Guruswamy Damodaran… - Journal of tissue …, 2018 - Wiley Online Library

[29] Decellularization T Kwon, KH Moon - Clinical Regenerative Medicine in Urology, 2018 - Springer

Investigation of the Effect of Silibinin on Apoptosis in Two Human Breast Cancer Cell Lines

Sanaz Ranapour[1], Nasrin Motamed[2*]

[1]Department of Cellular and Molecular Biology, School of Biology, College of Science, University of Tehran, Tehran, Iran

[2]Department of Cellular and Molecular Biology, School of Biology, College of Science, University of Tehran, Tehran, Iran

*Email: motamed2@khayam.ut.ac.ir

Abstract

Breast cancer is a heterogeneous disease and the second most common cause of cancer-related deaths among women worldwide. Silymarin is a mixture of flavonolignans extracted from Silybum marianum (milk thistle), as well as the most active ingredient of this extract, silybin. The flavonolignan silibinin represents a hepatoprotective, natural antioxidant, and anticancer activity. This study aims to evaluate the cytotoxicity of silibinin on the MCF-7 and T47D cell lines. The human MCF-7 and T47D breast cancer cell lines was cultured in Mediums (RPMI, DMEM respectively) and treated with different concentrations of silibinin (50-250 µg/mL) for 24, 48 and 72 hours. The cytotoxic effect of silibinin on MCF-7 and T47D viability was determined using Methyl-Thiazolyl-Tetrazolium (MTT) assay by IC50 determination. Apoptosis was evaluated by Annexin V/propidium iodide staining. The IC50 values for silibinin in MCF-7 and T47D Cell Lines at 48 hours were obtained 221.3 µg/mL and 144.6 µg/mL, respectively. Silibinin induced cytotoxic and apoptotic effects in T47D cells more than the MCF-7 cells.

Keywords: Breast cancer, Silibinin, Apoptosis.

1. Introduction

Today, cancer is the second leading cause of death, and breast cancer is the most common cancer, among women. The present study investigated the cytotoxic effect of SB on MCF-7 and T47D cell lines was tested by assessing cell viability at different concentrations and period times. Then apoptosis induction were evaluated in treated cells.

2. Material and Methods

2.1 Cell lines and culture

The human MCF-7 and T47D breast cancer cell lines was cultured in Mediums (RPMI, DMEM respectively).

2.2 MTT cell viability assay in T47D and MCF-7

The human MCF-7 and T47D breast cancer cell lines was treated with different concentrations of silibinin (50-250 µg/mL) for 24, 48 and 72 hours. The cytotoxic effect of silibinin on MCF-7 and T47D viability was determined using Methyl-Thiazolyl-Tetrazolium (MTT) assay by IC50 determination

2.3 Flow cytometric analysis for apoptotic

Apoptosis was evaluated by Annexin V/propidium iodide staining.

3. Results and Discussions

3.1 IC_{50} concentrations of SB

IC_{50} concentrations of SB were 144.6 % ± 9.41 and 221.3 ± 10.32 for T47D and MCF-7 cells after 48h treatment respectively which demonstrated that SB cytotoxic activity on T47D was stronger than MCF-7 cells.

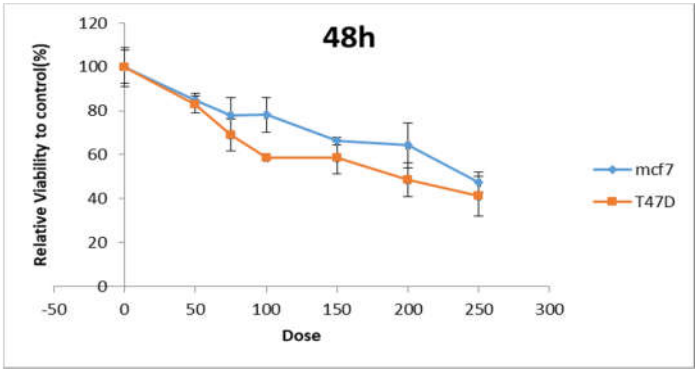

3.2 Flow cytometry results

Flow cytometry results illustrated that SB induced significant apoptosis cell death in MCF-7 and T47D cells in comparison to untreated ones.

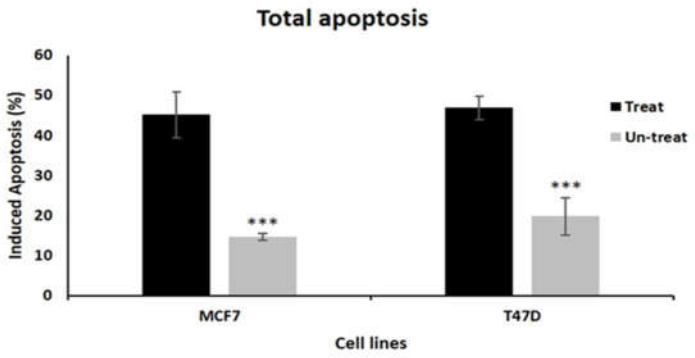

References

[1] Si, L., et al., In Mol Cell Biochem, 2020; Vol. 463, pp. 189-201.

[2] El-Masry, OS., et al., In Asian Pac J Cancer Prev, 2019; Vol. 20, pp. 3763-3770.

[3] Torre, L.A., et al., Global cancer statistics, 2012. CA: a cancer journal for clinicians, 2015. 65(2): p. 87-108.

[4] Morgan, D.M., Tetrazolium (MTT) assay for cellular viability and activity, in Polyamine protocols. 1998, Springer. p. 179-184.

[5] Sharma, G., et al., Silibinin induces growth inhibition and apoptotic cell death in human lung carcinoma cells. Anticancer research, 2003. 23(3B): p. 2649-2655.

Does cellular glycation in diabetic patients interfere with the N-glycosylation of the transmembrane proteins?

Maryam Azimzadeh Irani[1*]

[1]Faculty of Life Sciences and Biotechnology, Shahid Beheshti University, Tehran, Iran.

*Email: m_azimzadeh@sbu.ac.ir

Abstract

Glycation is a non-enzymatic modification of proteins with carbohydrates. High rate of cellular glycation has been observed in diabetic patients that could alter several cellular machineries such as transmembrane receptors. All transmembrane receptors are post-translationally modified in an enzymatic activity known as N-glycosylation. Here Interleukine-1 Receptor Type I that is a critical signalling receptor in regulating the immune response was used as a case study to investigate the potential interfering roles of these two processes. Molecular docking results shows that due to the small size of the carbohydrate units in glycation, they cannot reside on the protein surface and their favourable binging poses are mainly located at the buried parts of the protein and distant from the N-glycosylation sites. Thus, it is unlikely that they could interact with the covalently attached glycans.

Keywords: Glycation, N-glycosylation, Interleukine-1 Receptor Type I, Molecular docking.

1. Introduction

Glycation is a non-enzymatic modification of proteins with carbohydrates [1]. High rate of cellular glycation has been observed in diabetic patients that could alter several cellular machineries such as transmembrane receptors [1]. All transmembrane receptors are also post-translationally modified in an enzymatic activity known as N-glycosylation [2]. Structural role of N-glycosylation in activation, ligand binding and dimerization of proteins is proven to be critical [3]. Here, the interfering effect of these two processes was studied on the transmembrane Interleukine-1 Receptor Type I as a case study. Interleukine-1 Receptor Type I is the signaling key receptor of the Interleukine-1 family that regulate the immune response upon injury, stress and infections [4].

2. Material and Methods

2.1 Model building of the glycosylated Interleukine-1 Receptor Type I

PDB ID 4DEP [4] was selected as the initial model of the Interleukine-1 Receptor Type I extracellular domain. N-glycan models where attached to Asn83, Asn176, Asn216, Asn232, Asn246 and Asn280 of the protein using the GLYCAM online builder [3].

2.2 Molecular Docking of glucose to the Interleukine-1 Receptor Type I

Docking was performed with HADDOCK server [5]. The first five binding poses were energetically analyzed and the complex structures were visualized with PyMOL [6].

3. Results and Discussions

3.1 Interfering structural effect of the glycation/N-glycosylation on Interleukine-1 Receptor Type I

Molecular docking results shows that due to the small size of the glucose units in glycation, they cannot reside on the protein surface and their favourable binging poses are mainly located at the buried parts of the protein and distant from the N-glycosylation sites. Thus, it is unlikely that they could interact with the covalently attached glycans. However, under a higher concentration of blood sugar depending on the stage of the diabetic patient, aggregation of the sugar moieties could occur. Resulting in conformational change of the protein structure and potential malfunctioning of the receptor.

References

[1] F. e. a. Sun, Comprehensive Analysis of Protein Glycation Reveals Its Potential Impacts on Protein Degradation and Gene Expression in Human Cells, 2019.

[2] A. a. W. J. L. Yan, Unraveling the mechanism of protein N-glycosylation, 2005.

[3] M. S. K. a. C. V. Azimzadeh Irani, Role of N□glycosylation in EGFR ectodomain ligand binding, 2017.

[4] C. J. F. B. a. K. C. G. Thomas, Structure of the activating IL-1 receptor signaling complex, 2012.

[5] S. J. e. a. De Vries, HADDOCK versus HADDOCK: new features and performance of HADDOCK2. 0 on the CAPRI targets, 2007.

[6] W. L. DeLano, PyMOL, 2002.

Effect of oleic acid on ovine fresh semen under normal and oxidative stress conditions

Leila Soltani[1]*

[1] Department of Animal Sciences, College of Agriculture and Natural Resources, Razi University, Kermanshah, Iran

*Corresponding Author email: l.soltani@razi.ac.ir; Tel: (+98)9372725987)

Abstract

The effects of oxidative stress on motility and viability lead to decreased sperm quality and fertility. Oleic acid is a fatty acid with antioxidant effect. The aim of this study was to investigate the addition of oleic acid to fresh ovine semen diluent to reduce oxidative stress induced by hydrogen peroxide. For this purpose, semen samples were prepared from three mature and fertile sheep. After diluting the semen with Tris-base extender, different concentrations of oleic acid (0.3, 0.6 and 0.9 mM) were added to it under normal and induced oxidative stress conditions with the using hydrogen peroxide. 50 mM of hydrogen peroxide was used to induce oxidative stress. The group that did not receive any supplement was considered as the control group. MTT solution was added to each group and incubated in the incubator for 2 hours at 37 °C. After the incubation period, the reading was performed with the help of ELISA reader. Addition of oleic acid at a concentration of 0.9 mM improved the viability of ram sperm in normal conditions compared to other treatments and control group. Addition of oleic acid under induced oxidative stress conditions reduced the mortality rate of treated cells compared to the oxidative stress group. It seems that oleic acid reduces the destructive effects of induced oxidative stress.

Key words: Oleic acid, Oxidative stress, Sheep, Semen.

1. Introduction

Reactive oxygen species (ROS) is produced by spermatozoa in the male reproductive system [1]. Under physiological conditions, spermatozoa produce small amounts of ROS [2]. Small amounts of ROS are required for normal sperm functioning. However, ROS are toxic in normal cells with high concentrations [3]. Oxidative stress is an imbalance between the production of ROS and the scavenging capacity of the antioxidants in a particular milieu [4]. When the production of ROS exceeds the antioxidant defense system, this substantial ROS results in the oxidative damage of membrane lipids, proteins and DNA in the sperm which leads to an impairment of sperm plasma membrane (loss of function), reduced viability and motility [5,6]. Although the antioxidant capacity of sperm is low, the intracellular antioxidant systems consists of enzymatic antioxidants (superoxidase dismutase, catalase and glutathione peroxidase) and non-enzymatic (alpha-tocopherol, beta-carotene, ascorbate, and glutathione) [7,8]. In most studies, the role of antioxidants in natural conditions is examined and their exact role in oxidative stress conditions is unclear. Numerous reports have examined the role of oleic acid during the storage and cryopreservation of semen from many of the species [9,10]. The specific objectives of the study were to comparison the optimal anti-oxidative effects of oleic acid supplementation in Tris-based extender during normal and induced oxidative stress with peroxide hydrogen on fresh diluted semen.

2. Material and Methods

2.1 Materials

All the chemicals used in this study were obtained from Sigma-Aldrich Company (Sigma) unless otherwise was stated.

2.2 Animals and semen collection

Ejaculates from three rams (2 and 3 years of age) were applied in the study. The rams, belonging to sheep facility located in the Faculty of Agriculture, Razi University and Kermanshah, Iran, were maintained under uniform feeding and housing conditions. Ejaculates were collected from the rams with the aid of an artificial vagina twice a week, according to AI standard procedures. To overcome any individual variation, semen samples were pooled. Fresh semen parameters including semen concentration, pH, volume, and progressive motility were investigated. Only ejaculates with progressive motility and normal morphology, more than 80%, were used for evaluation.

2.3 Semen processing

A Tris-based extender (tris 297.58 mM, fructose 82.59 mM, citric acid 105.35 mM, glycerol 6% and egg yolk 20% (v/v), pH 6.8) was applied as the base extender [11]. Each pooled ejaculate was split into eight equal aliquots and diluted with the tris-based extender. This experiment was performed using 8 treatments:

1- Control group (did not receive any supplement)

2- Control group + 0.3 mM of oleic acid

3- Control group + 0.6 mM of oleic acid

4- Control group + 0.9 mM of oleic acid

5- Induced oxidative stress group (received 50 mM hydrogen peroxide)

6- Induced oxidative stress group + 0.3 mM of oleic acid

7- Induced oxidative stress group + 0.6 mM of oleic acid

8- Induced oxidative stress group + 0.9 mM of oleic acid.

MTT solution (with a concentration of 5 mg/ml DPBS) was prepared and passed through a 0.22 µm pore size filter to remove undissolved particulates. To evaluate the toxicity, 20 µl of MTT solution was added to 200 µl of diluted semen in 1.5 ml Eppendorf, and was incubated in humidity, 2 hrs at 37°C in 5% CO2 incubator. After the incubation period, 200 microliters of DMSO solution was added to each tube and mixed completely dissolve to dissolve the violet formazan crystals. Then, tubes were centrifuged and the adsorption of the supernatant into a 96- 96 well plate at 570 nm was measured using microplate reader. The number of viable cells was calculated using the standard curve and the absorption of the each sample.

2.4 Statistical analysis

Statistical analysis in this study was performed using SPSS software. Results are reported as means ± standard error of the mean. The comparison of sperm parameters among treatment groups were performed by Duncan's new multiple range test. $P < 0.05$ was considered to be significantly different.

3. Results and Discussions

Results from this study show that the addition of oleic acid (at a concentration of 0.9 mM) to ram semen diluent was improved viability compared with the control group and other treatment groups ($p<0.05$, Figure 1). In addition, induced oxidative stress reduced sperm viability following MTT assay, which showed a significant difference with other treatment groups. Also, oleic acid, especially at a higher concentration (0.9 mmol), was improved cell viability after induced oxidative stress, which showed an improvement in viability compared to the oxidative stress group (Figure 1). Other concentrations of oleic acid (0.3 and 0.6 mM) under induced oxidative stress showed a relative improvement in viable cells compared to the induced oxidative stress group, but the values were lower than 0.9 mM of oleic acid.

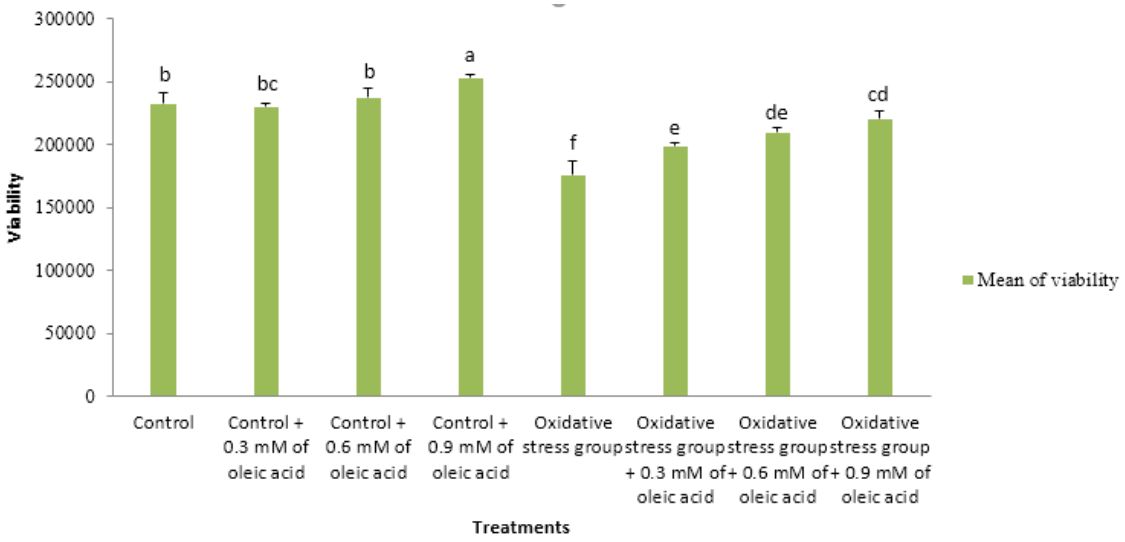

Figure 1: Mean ± SD survival rate of fresh ram semen supplemented with different concentrations of oleic acid under normal and induced oxidative stress conditions.

Oxidative stress is one of the factors affecting sperm viability. Over-production of ROS in spermatozoa can lead to male infertility [12]. In the present study, the antioxidant effects of oleic acid under natural and oxidative stress conditions on fresh ram semen were evaluated. In this study, it was found that higher concentration of oleic acid (0.9mM) improved sperm viability under normal conditions, which showed a significant difference compared to other treatment groups. Also, oleic acid lead to a relative preservation of viability in induced oxidative stress condition, which showed a significant difference compared to the oxidative stress group. A study investigating the addition of oleic acid under induced oxidative stress condition did not available on fresh semen storage, cold storage and cryopreservation conditions. For this objective, this study compared with other observational studies under normal conditions. Addition of palmitic acid and oleic acid to fresh boar semen diluent and stored for 3 h at 37 °C showed increased activities of malate dehydrogenase, and succinate dehydrogenase enzymes as well as motility parameters compared to control [10]. Addition of oleic/linoleic acids improved the viability and motility of ram semen after freezing and thawing [13]. Low concentrations of oleate on rooster semen had beneficial effects on semen quality during the cold storage. Also, Lipid peroxidation levels decrease and antioxidant capacity increased [9]. In another study conducted by Kiernan et al. [14], it was observed that viability and motility were increased following supplementation of bull semen with 50 and 100µM oleic acid. In contrast, De Graaf et al. [15] reported that dietary supplementation of rams with oleic acid or linoleic acid did not improve the cryo-survival of ram spermatozoa. In the present study, following the addition of higher concentration of oleic acid, improved viability under normal condition and reduced the detrimental effects of induced oxidative stress after MTT assay (which shows the activity of oxidordioctase enzymes in the mitochondria of living cells) were observed.

In the present study, it appears that oleic acid at a higher concentration in fresh ram semen dilute could improve sperm viability and reduce the harmful effects of oxidative stress induced by hydrogen peroxide. Further studies are needed to determine the beneficial effects of this compound under natural and oxidative stress conditions during short-term and long-term semen storage.

References

[1] J.G. Alvarez, J.C. Touchstone, L. Blasco, B.T. Storey, Spontaneous lipid peroxidation and production of hydrogen peroxide and superoxide in human spermatozoa. Superoxide dismutase as major enzyme protectant against oxygen toxicity. Journal of Andrology. 8 (1987) 338–348.

[2] E. Gomez, D.S. Irvine, R.J. Aitken, Evaluation of a spectrophotometric assay for the measurement of malondialdehyde and 4-hydroxyalkenals in human spermatozoa: relationships with semen quality and sperm function. International Journal of Andrology. 21 (1998) 81–94.

[3] M.R. Moein, V.O. Dehghani, N. Tabibnejad, S. Vahidi., Reactive Oxygen Species (ROS) level in seminal plasma of infertile men and healthy donors. Journal Iranian Journal of Reproductive. 5 (2007) 51–55.

[4] M.N. Bucak, N. Başpınar, P.B. Tuncer, K. Coyan, S. Sarıözkan, P.P. Akalın, S. Büyükleblebici, S. Küçükgünay, Effects of curcumin and dithioerythritol on frozen-thawed bovine semen. Andrologia 44 (2012) 102–109.

[5] M. Hernandez, J. Roca, J.J. Calvete, L. Sanz, T. Muino-Blanco, J.A. Cebrian-Perez, J.M. Vázquez, E.A. Martínez, Cryosurvival and in vitro fertilizing capacity postthaw is improved when boar spermatozoa are frozen in the presence of seminal plasma from good freezer boars. Journal of Andrology. 28 (2007) 689–697.

[6] H.Y. Jang, Y.H. Kim, H.T. Cheong, J.T. Kim, I.C. Park, C.K. Park, B.K. Yang., Curcumin attenuates hydrogen peroxide induced oxidative stress on semen characteristics during in vitro storage of boar semen. Reproduction, Fertility and Development 33 (2009) 99–105.

[7] SA. Sheweita, AT. Tilmisany, H. Al-Sawaf., Mechanisms of male infertility: role of antioxidants. Current Drug Metabolism. 6 (2005) 495-501

[8] W.S. Oo, H. Chen, P.H. Chow., Male genital tract antioxidant enzymes—their ability to preserve sperm DNA integrity. Molecular and Cellular Endocrinology 250 (2006) 80–3.

[9] M. Eslami, A. Ghaniei, H. Mirzaei Rad., Effect of the rooster semen enrichment with oleic acid on the quality of semen during chilled storage. Poultry Science 0 (2016) 1–7.

[10] S. Salamon, W. Maxwell., Storage of ram semen. Animal Reproduction Science, 62 (2000) 77–111.

[11] E. Marti, J.I. Marti, T. Muiño-Blanco, J.A. Cebrián-Pérez., Effect of the cryopreservation process on the activity and immunolocalization of antioxidant enzymes in ram spermatozoa. Journal of Andrology, 29(2008) 459-467.

[12] B.A. Ball, Oxidative stress osmotic stress and apoptosis: impacts on sperm function and preservation in the horse. Animal Reproduction Science. 107 (2008) 257-267.

[13] Z. Zhu, R. Li, C. Feng, R. Liu, Y. Zheng, S.A.M. Hoque, D. Wu, H. Lu, T. Zhang, W. Zeng., Exogenous Oleic Acid and Palmitic Acid Improve Boar Sperm Motility via Enhancing Mitochondrial B-Oxidation for ATP Generation. Animals (Basel). 10 (2020) 591.

[14] M. Kiernan, A. Fahey, S. Fair., The effect of the in vitro supplementation of exogenous long-chain fatty acids on bovine sperm cell function. Reproduction, fertility and development, 25 (2013) 947–954.

[15] S.P. de Graaf, K. Peake, W.M.C. Maxwell, J.K. O'Brien, G. Evans., Influence of supplementing diet with Oleic and Linoleic acid on the freezing ability and sex-sorting parameters of ram semen. Livestock Science 110 (2007) 166–173.

Evaluation of calcium deposits and Alkaline Phosphatase activity of human adipose tissue-derived stem cells in vitro

Tabatabai Tayebeh Sadat[1], Haji Ghasem Kashani Maryam[1]*

1: Department of Cellular and Molecular Biology, School of Biology and Institute of Biological Sciences , Damghan University, Damghan , Iran

***Corresponding Author:** Haji Ghasem Kashani Maryam, Department of Cellular and Molecular Biology, School of Biology, Damghan University, Damghan, Iran

Abstract

Electromagnetic fields and betaine are among the biophysical and biochemical stimuli that have been considered as an alternative option for the treatment of bone disorders. Therefore, the aim of this study was to investigate the effects of these two stimuli on the osteogenic differentiation of human adipose tissue-derived stem cells (hASCs). hASCs were extracted from abdominal adipose tissue of cesarean women after obtaining written informed consent and cultured in vitro until the third passage. Stem cells were confirmed by flow cytometry and differentiation into osteocytes and adipocytes. The experimental groups were: negative control (cultured cells in α-MEM and 10% FBS), positive control (cultured cells in osteogenesis differentiation medium), BET (cultured cells in osteogenesis differentiation medium containing 10 mM betaine), EMF (cultured cells in osteogenesis differentiation medium and waves). After 7 and 14 days of incubation, cells exposed to waves (8 h daily) with a frequency of 50 Hz and intensity 1mT with sinusoidal waveform. Then osteogenic differentiation by evaluating the morphology of cells, the qualitative and quantitative Alizarin red staining and alkaline phosphatase activity was evaluated. There were significant increase of the calcium deposits formation (at the end of day 14) and alkaline phosphatase activity in the positive control group compared to the negative control. In addition, significant increase of the calcium deposits formation and Alkaline phosphatase activity were observed in BET group compared to the positive control, while a significant decrease of the calcium deposits formation (at the end of day 14) and alkaline phosphatase activity (at the end of day 7) were observed in the EMF group compared to the positive control. The EMF group showed a significant decrease in the formation of calcium deposits and alkaline phosphatase activity, compared to the BET group. The combination of betaine and osteogenesis differentiation medium leads to increased calcium matrix deposits and alkaline phosphatase activity and finally increased osteogenic differentiation of hADSCs, while the combination of electromagnetic field and osteogenesis differentiation medium decreased of the calcium deposits formation and alkaline phosphatase activity and finally decreased osteogenic differentiation of hADSCs. As a result, the synergy of osteogenesis differentiation medium and betaine can be used to treat bone disorders.

Keywords: Human adipose stem cells, Electromagnetic field, Betaine, Osteogenic differentiation

1. Introduction

Human adipose tissue- derived mesenchymal stem cells (hADSCs) due to easy extraction, relative abundance, in vitro expansion and differentiation potential, frozen storage capability, and ability to secrete cytokines, compared to other stem cells are appropriate candidate in regenerative medicine. Adult stem cells are affected by many biochemical and biophysical stimuli, such as hormones, growth factors (VEGF, IGF, BMP2, TGF-b1), hydrostatic pressure, trophic factors, stress ,and electromagnetic field, so that pathological conditions result from disruption of these factors (1). Electromagnetic fields and betaine could stimulate the proliferation and differentiation of hADSCs into osteoblasts or other stem cells. Pulsed electromagnetic field (PEMF) has been used since 1979 with the approval of the United States for the treatment of osteoporosis, osteoarthritis, etc. (3-7). Exposure to PEMF has been reported to increase the proliferation and differentiation rate of osteoblasts. They increase the rate of extracellular matrix formation, bone mineralization and reduce matrix degradation (8-10). EMF can affect biochemical reactions and behavior such as gene expression and cell fate determination. EMF can cause changes in membrane permeability to ions, which in turn change the membrane potential (2-4). Intracellular calcium is one of the main determinants of cell destiny, and the concentration of free intracellular calcium can trigger cell signaling pathways. Evidence suggests a vital role in the movement of calcium into the osteoblast through the L-type VGCC channel along with membrane depolarization. In the 1860s, Scheibler extracted Beta vulgaris from sugar beet and called Betaine. (5). Betaine is widely found in animals, plants, and microorganisms. Betaine is found in seafood (1%), wheat or bran germination (1%), and spinach (0.7%). Betaine could be a promising therapeutic agent for sarcopenia and osteoporosis (6). Evidence suggests that betaine, as a derivative of trimethylglycine, regulates several vital biological processes such as oxidative stress, inflammatory, osteoblast differentiation, and cellular apoptosis (7-9) Betaine stimulates three signaling pathways in human osteoblasts, including cytosolic calcium influx, ERK activation, and IGF-I production that leading to enhanced bone formation. IGF-I stimulates the *RUNX2* gene during the osteogenesis process, which leads to the activation of other specific osteogenic transcription factors, such as osterix. These factors regulate type 1 collagen, bone sialoprotein (*BSP*), and osteopontin (*OPN*), thereby stimulating osteogenesis. ERK pathway can regulate bone development in vivo by *RUNX2*. In fact, the differentiation of human BMSCs into osteoblasts is associated with phosphorylation of the ERK1/2 signaling pathway. Betaine induced calcium influx through L-type channels and caused membrane depolarization and Ca^{2+}/calmodulindependent kinase II (CaMKII) signal activation (6). EMF-ELF and Betaine are used as two safe factors to repair bone fractures, and since research has shown that EMF and Betaine are both through common pathways such as the impact on calcium infiltration causes the differentiation of BMSCs and ADSCs into osteoblasts. Therefore, the aim of this study was to investigate the effects of these two stimuli on the osteogenic differentiation of hASCs.

2. Material and Methods

Construction and calibration of the magnetic field generator:

In this project, we intended to study the effect of the 50 Hz magnetic field with an intensity of 1 mT on cell samples. the magnetic field over the sample volume must be uniform and the magnetic flux lines remain parallel. To produce this uniform magnetic field, a coil with dimensions of 68 by 100 square millimeters, corresponding to the dimensions of the cell flask, was used. The coil was made of 2200 turns of 0.4 mm diameter enameled wire wound around a plastic spool. A magnetic silicon alloy core was placed into the spool. To prevent heat from the Eddy-current, this magnetic core was made of a large number of very thin EI-shaped sheets. Finally, the whole coil was sealed with an air-during varnish. As the cell flask holder, a 24-well plate cover with dimensions of 85 × 128 mm^2 was placed on the coil. Alternating variable power supply was used to generate the variable magnetic field in the coil. The intensity of the magnetic field was measured using a Teslameter (PHYWE, 13610-93). By adjusting the output voltage of the power supply, the intensity of the magnetic field in the sample position was adjusted to 1 mm Tesla. To evaluate the stability of the magnetic field, the coil was placed in an incubator for 48 hours and the intensity of the magnetic field was measured alternately. The stability of the magnetic field strength and the lack of heating of the coil were confirmed.

Isolation and culture of human ADSCs:

To isolate hADSCs, adipose tissue samples were collected from women (mean age 40±5) undergoing liposuction. Informed consent was obtained from the participants and approval of the local Ethics Committee at Velayat Hospital (Damghan, Iran). The study was carried out following the guidelines of the Medical Ethics Committee, Ministry of Health of Iran. Firstly, the sample was cut to the very small pieces and then 0.2% collagenase (Gibco, 17100-017) was added and incubated at 37°C for 2 h. To stop digestion, DMEM (Invitrogen, USA) containing 10% FBS was added to the suspension and centrifuged at 1200 rpm for 5 min at 37°C. Finally, the isolated cells were transferred and cultured in a 25 cm^2 flask and incubated at 37°C in 5% CO2 for 72 h. hADSCs adhered to the bottom of the flask, while floating blood cells washed away by replacing the medium with a fresh one. Cells were subcultured and used for experiments at passage 3 (10).

Experimental groups:

The hADSCs were treated as follows:

Negative control: cultured P4- cells in α-MEM (α-Minimal Essential Medium, Invitrogen USA) containing 10% FBS.

Positive control: cultured P4- cells in Osteogenesis Differentiation Medium (OD).

BET: cultured P4- cells in OD containing 10 mM of Betaine.

EMF: cultured P4- cells in OD and exposed to EMF with 50 Hz frequency, 1 mT intensity (8 h, daily).

Alizarin Red staining and calcium deposit quantification:

To identify the mineralized matrix of differentiated cells, Alizarin Red (069K1639, Sigma-Aldrich) staining was used on day 21. After removing the medium, the samples were washed with cold PBS and fixed in cold 4% paraformaldehyde (Merck, Germany) for 20 min at 4˚C. Fixative was removed and cells were washed twice with PBS. The fixed cells were stained with 400µl Alizarin Red at pH 7.2 for 5-10 min. Finally, the cells were washed again with PBS for three times and observed by inverted microscope (4).

For calcium quantification, 300 µl of 10% acetic acid was added to the cells stained with Alizarin Red and incubated for 30 min at RT with agitation. Cells were scraped off, transferred to microtubes, vortexed ,and incubated. Samples were centrifuged for 30 min at 2000 rpm and then 200 µl of the supernatant was transferred to another microtube, 22.5 µl of 10% ammonium hydroxide was added to neutralize the acid and mixed. Finally, the absorbance was measured at 405 nm by the BioTek device (11).

Alkaline Phosphatase activity:

To measure alkaline phosphatase (ALP) activity, the total protein of the cells at days 7, 14 post- induction, were lysed with 30 µl of Triton X-100 lysis buffer. The lysate was centrifuged at 2000 rpm at 4°C for 10 min and the ALP activity of supernatant was measured using paranitrophenylphosphate (pNPP) as a phosphatase substrate (ALP Kit, Iran) at 405 nm by a microplate reader (BioTek Instruments, USA). Finally, the enzyme activity level (IU) was normalized against the total protein (12).

3. Results:

Morphological study

Human adipose-derived stem cells are seen in different forms in early culture. In primary culture, a set of stem and hematopoietic cells is observed, but following repeated passages, the number of blood cells is reduced and stromal cells are increased. These cells have a spindle-shaped, fibroblast-like appearance that attach to the bottom of the culture flask with the help of their appendages. Figure 1:A shows this. Figure 1: B shows that the morphology of hADSCs changed from a spindle-shaped state to a triangular or polygonal state after treatment by the Osteogenesis Differentiation Medium. Also in the cells of this group we see the formation of mineral deposits. The morphology of the cells of the BET group (1: C) became triangular and polygonal like the morphology of the cells of the positive control group; However, the levels of cytosolic granulosa and matrix synthesis in this group increased significantly compared to the positive control group. The following images of EMF group cells (1: D) do not show a significant difference in terms of mineral deposits formation with positive control group cells.

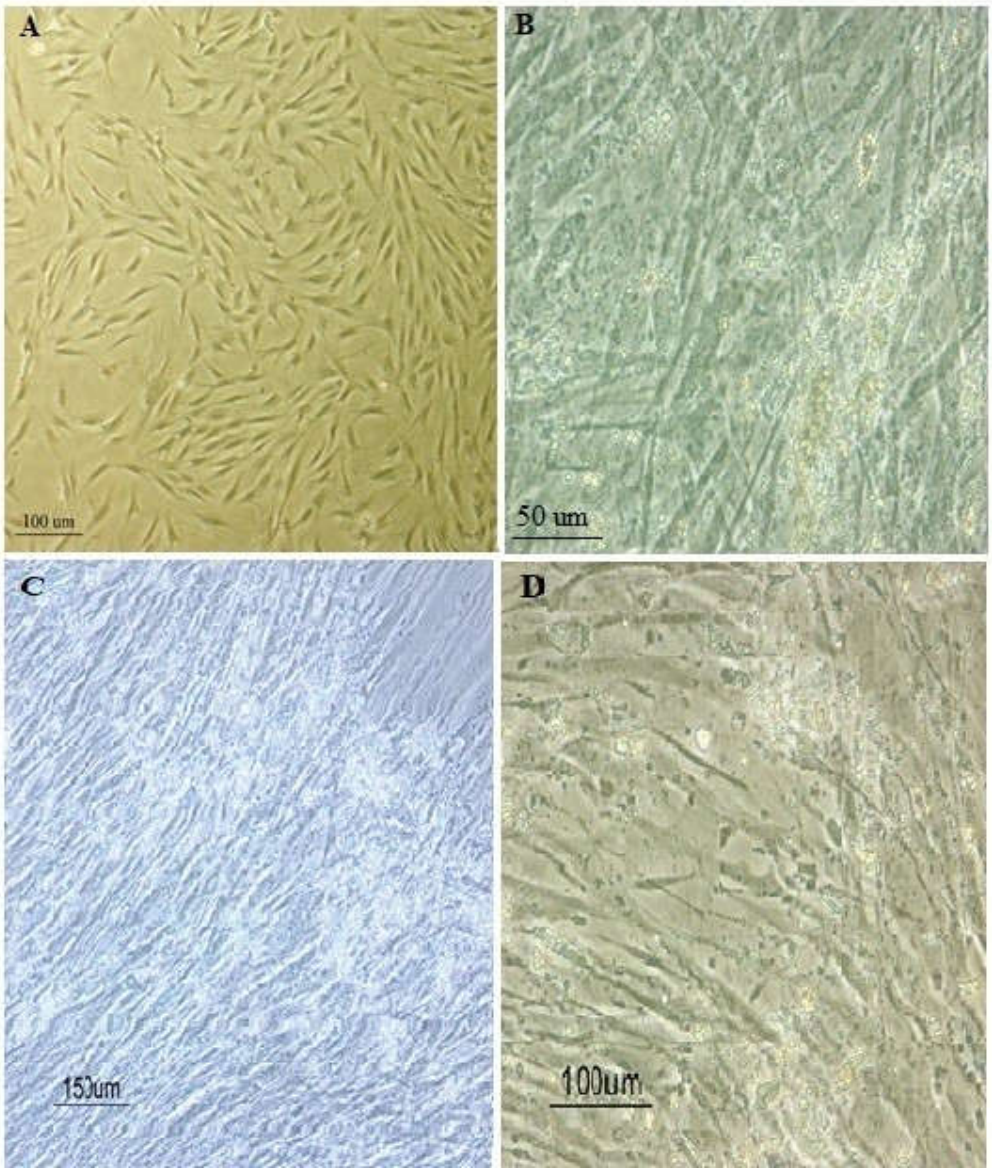

Figure 1: Phase contrast images of hADSCs: The cells of passage 3 with spindle fibroblast-like morphology were observed (A). The triangular or polygonal cells in Positive control group with mineralized extracellular matrix (B). BET group (C). EMF group (D)

Alizarin Red quality staining

The amount of calcium phosphate production of the studied groups in this study was evaluated after 7 and 14 days by Alizarin Red staining. Examination of the images shows that the amount of stained mineral deposits in the BET group has increased significantly compared to other groups. While the amount of stained mineral deposits in the other groups did not differ significantly.

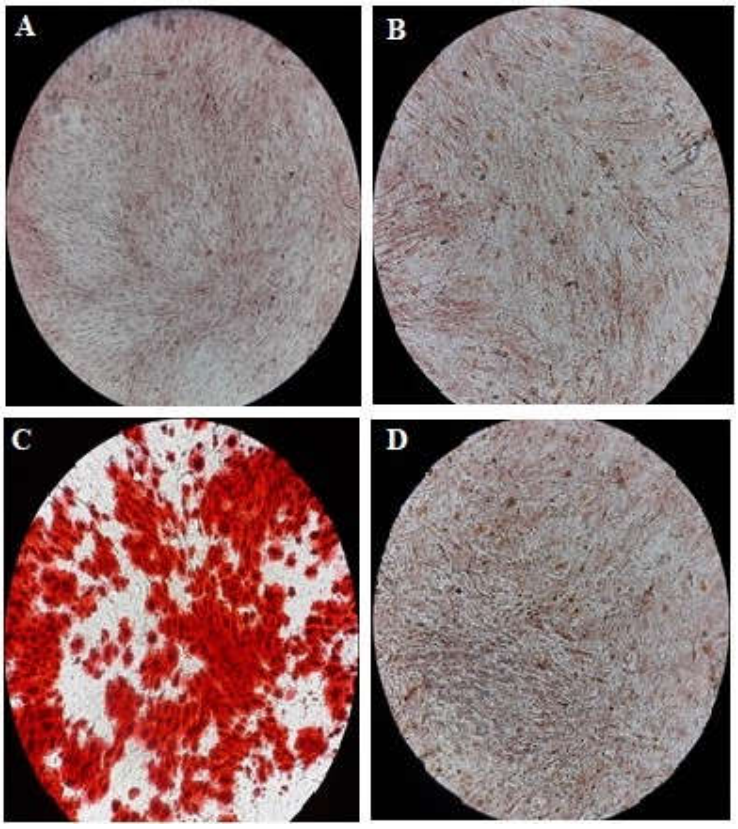

Figure 2: Calcified matrix depositions were visualized with Alizarin Red staining. A:Negative control. B: Positive control. C: BET. D: EMF. Magnification 100×

Detection and quantification of mineralization:

The results of quantitative staining of the studied groups were measured after 7 and 14 days, the results are shown in Figure 3. At the end of day 7, the amount of calcium phosphate production in the positive control group (0.313 ± 0.012) was not significantly different from the negative control group (0.2653± 0.013) P 0.05. Also, the amount of calcium phosphate production In BET group (0.4513 ± 0.003) compared to the positive control group showed a significant increase. P 0.05. While a significant decrease in calcium phosphate formation was observed in the EMF group (0.2333 ± 0.0205) compared to the positive control and BET groups (P 0.05).

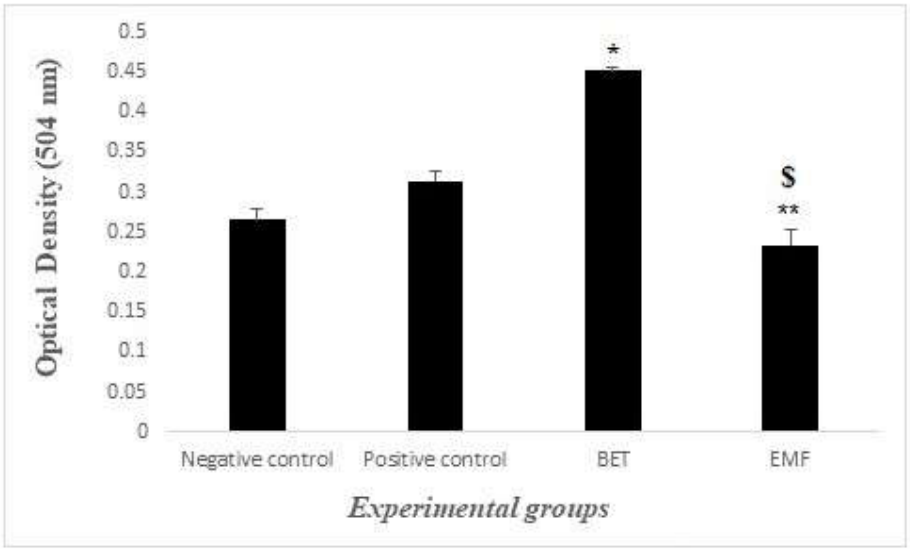

Figure 3: Diagram of the amount of production of calcium phosphate hADSCs through quantitative staining of Alizarin Red on day 7. Negative control (cultured cells in α-MEM containing 10% FBS); Positive control (cultured cells in Osteogenesis Differentiation Medium); BET (cultured cells in Osteogenesis Differentiation Medium containing Betaine); EMF (cultured cells in Osteogenesis Differentiation Medium exposed to EMF), (* significant increase versus positive control, ** significant decrease versus positive control, $ significant decrease versus BET group (P <0.05).

At the end of day 14, the amount of calcium phosphate production in the positive control group (0.2507 ± 0.0012) was significantly increased compared to the negative control group (0.0957 ± 0.002). P 0.05. Also the amount of calcium phosphate production in the BET group (0.368 ± 0.017) compared to the positive control group showed a significant increase of P 0.05. While the amount of calcium phosphate formation in the EMF group (0.111 ± 0.00058) compared to the positive control and BET groups showed a significant decrease of P 0.05.

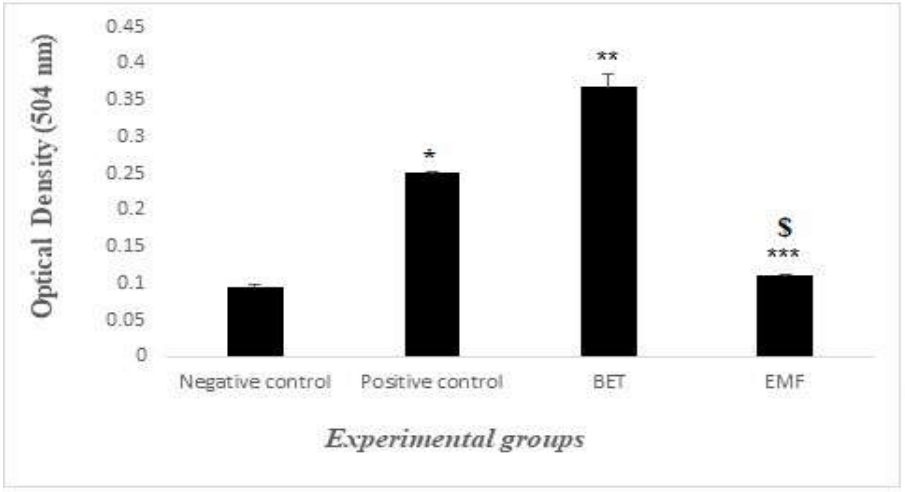

Figure 4: Diagram of the amount of production of calcium phosphate hADSCs through quantitative staining of Alizarin Red on day 14. * significant increase versus negative control, ** significant increase versus positive control, *** significant decrease versus positive control, $ significant decrease versus BET group (P <0.05).

Alkaline Phosphatase activity

The ALP enzyme expression of the studied groups was measured after 7 and 14 days. The results are shown in Figures 5 and 6. After 7 days, ALP expression in the positive control group (1.24 ± 0.007) compared to the negative control group (0.575± 0.022) showed a significant increase $P < 0.05$. Also ALP expression in BET group (1.871 ± 0.003) compared to the positive control group showed a significant increase $P < 0.05$. While ALP expression in the EMF group (0.54 ± 0.0003) compared to the positive control and BET groups showed a significant decrease $P < 0.05$.

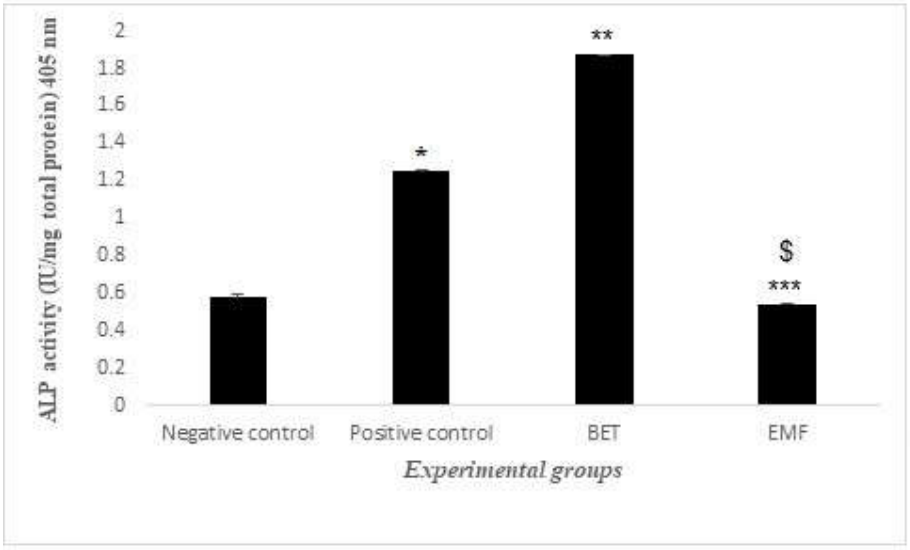

Figure 5: ALP expression rate of the experimental groups on day7. * significant increase versus negative control, ** significant increase versus positive control, *** significant decrease versus positive control, $ significant decrease versus BET group ($P < 0.05$).

After 14 days, ALP expression in the positive control group (0.3837 ± 0.00186) compared to the negative control group (0.293±0.01) showed a significant increase $P < 0.05$. ALP expression in BET group (0.57 ± 0.0061) showed a significant increase compared to the positive control group $P < 0.05$. While there was no significant difference in ALP expression in the EMF group (0.37 ± 0.00289) compared to the positive control group P 0.05. Also, ALP expression in the EMF group compared to the BET group showed a significant decrease $P < 0.05$.

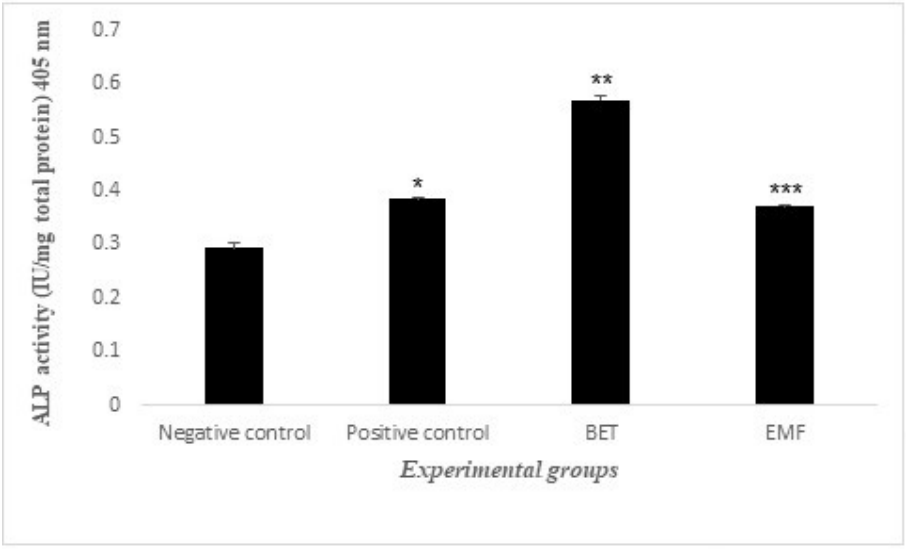

Figure 6: ALP expression rate of the experimental groups on day14. * significant increase versus negative control, ** significant increase versus positive control, *** significant decrease versus BET group (P <0.05).

4. Discussions

The electromagnetic field is one of the physical factors that has been considered as an alternative option for the treatment of bone disorders such as fractures and osteoporosis (13, 14). PEMF exposure reduces inflammatory processes and also has anti-inflammatory effects in several cell lines and laboratory models. Therefore, PEMF can be an appropriate and non-invasive treatment to stimulate bone formation, fractures healing, pain reduction, and also neutralize the inflammatory pathways caused by osteoporosis (15, 16). Despite the clinical success of PEMF in the treatment of a wide range of bone disorders, there have been negative reports of the effects of PEMF on bone proliferation, differentiation and formation in vitro. In fact, the effect of biophysical and biochemical stimuli on bone formation may be stimulatory or inhibitory and depends on the stage of maturation of the stimulated cells (17). Also Betaine has been reported as a promising therapeutic agent against sarcopenia and osteoporosis (a major cause of bone weakness and mortality)(6). Betaine has been reported to have stimulatory effects on human osteoblasts by activating synergistic pathways (through the production of IGF-1) that lead to the expression of bone related genes and ultimately the production of matrix proteins. Therefore, according to the above reports and the osteogenic effects of electromagnetic field and betaine, the purpose of this study was to investigate the effects of these two stimuli on osteogenic differentiation of hADSCs. According to the images of this study, we observed that hADSCs, like other stem cells, appear to be spindle-shaped with the ability to adhere to the culture flask and form a fibroblast colony, and after the second or third passage onwards, a broad morphology was appeared. The morphology of the cells in the positive control changed from spindle-shaped to triangular. The osteogenesis differentiation medium also induced the formation of mineral deposits. Comparison of EMF and positive control groups did not show significant difference in morphology and mineral deposits formation. In fact, it was concluded that the electromagnetic field have no effect on the differentiation of hADSCs. The results of our study were similar to those of Sun et al. They BMSCs exposed to PEMF (15 Hz frequency and

1.8 mT intensity) and observed an increase in cell proliferation, cell density, as well as changes in cell cycle. But they did not observe any effect on the surface phenotype or their differentiation potential of these cells (18). While the results of this study were different from those reported by Luo et al. After exposure to BMSCs, Luo et al. Observed changes in cell morphology as well as an increase in the expression of ALP and bone markers (19). Of course, the reason for these conflicting results may be related to the type of cell used. Also, the comparison of the images of the BET group with the positive control showed an extremely large increase in the amount of calcium deposits and mineralized extracellular matrix, thus we can understand the stimulant role of betaine in the osteogenic differentiation of hADSCs. Similar to this study, Villa observed changes in the morphology of these cells when he treated hOBs with betaine. He also suggested that betaine increase osteogenic differentiation of hOBs (6). quality staining of Alizarin Red showed that the amount of stained calcium deposits in the BET group increased significantly compared to the other groups, while there was no significant difference in the amount of stained calcium deposits between the other groups. From these observations, it can be concluded that the electromagnetic field had no effect on the osteogenic differentiation of hADSCs, which is contrary to the results of Chen reports. Chen did not observe any effect of PEMF on the survival of the exposed cells for 8 hours, but matrix mineral deposits increased after PEMF induction (20). In this study, It was determined the stimulatory effect of betaine on the calcified matrix deposits level. Similar to this study, Villa reported that betaine, through the Runx2-OSX axis, activates bone marker proteins such as collagen type 1, BSP, and OPN. Expression and activation of these proteins lead to bone formation, matrix mineralization, and bone regeneration. In this way, the role of betaine in the mineralization of the matrix is determined. The results of quantitative staining of this study showed a significant increase of calcium phosphate production in the BET group compared to the positive control. Thus, the stimulatory effect of betaine on calcium phosphate production and induction of osteogenic differentiation of hADSCs was determined. These results were consistent with the results of the Villa report (6). Also the amount of calcium phosphate production in the EMF group decreased significantly as compared to the positive control. Therefore the inhibitory role of the electromagnetic field in the osteogenesis of hADSCs was determined. Fu et al. Observed a significant increase in calcium phosphate production after exposure of BMSC to PEMF (frequency 15 Hz and intensity 2 mT) (21). When Ongaro exposed BMSCs and ASCs to PEMF (frequency 75 Hz and intensity 1.5 mT) for 28 days, osteogenic differentiation of ASCs and an increase in the amount of matrix calcium were observed (22). Ceccarelli et al. also revealed a significant increase of extracellular matrix calcium deposition after exposure of BMSC to PEMF (75 Hz frequency and 2 mT intensity) (23). It was assumed that the cause of the contradictory results of the electromagnetic field effect of this study with previous studies may be related to the different frequency and waveform of PEMF. Alkaline phosphatase is an enzyme that hydrolyzes organic phosphate during the bone formation process. Through this process, the phosphonic acid required for the formation of hydroxyapatite ceramic deposits is provided and bone formation is enhanced. The expression of the alkaline phosphatase marker is the beginning of bone formation and differentiation. When calcium is present, type 1 osteocalcin (a non-collagenous protein secreted by osteoblasts) combines with hydroxyapatite to stabilize ossification. Thus alkaline phosphatase and osteocalcin are two important indicators that reflect the differentiation of osteoblasts into osteocytes and the onset of calcification of the matrix. PEMF Increases the activity of alkaline phosphatase and consequently the secretion of osteonectin and collagen (24). Tasi et al. Observed that when they exposed hBMSCs for 28 days (2 hours daily) to PEMF (frequency 7.5 Hz and

intensity 0.13 mT), ALP expression increased significantly at day 7. It reached its highest level on day 28 (13). Esposito also made changes in cell cycle, proliferation and ALP activity of MSC when exposed to waves (frequency 75 Hz and intensity 1.8 to 3 mT) for 21 days (8 hours daily) (25). Jansen after exposure of BMSCs to PEMF (frequency 15 Hz and intensity 0.1mT), observed no effect of PEMF on ALP activity. Different results may be due to frequency, intensity, waveform, different amplitude, or different duration of PEMF exposure.Our study results showed that after the end of days 7 and 14, ALP activity of cultured hADSCs exposed to EMF was significantly reduced compared to the positive control. In this way, it can be claimed that the electromagnetic field had an inhibitory effect on ALP expression. The results of this study contradict the results of the Tasi and Esposito reports and are similar to Jansen's study. Comparison of BET group with positive control group and EMF group shows the stimulatory effect of betaine which is similar to Villa study.

Villa reported that after treatment of hOBS with betaine (10 mM) there was a significant increase in the expression of ALP and Osteocalcin (6).

5. Conclusion:

The combination of betaine and osteogenesis differentiation medium leads to increased calcium matrix deposits, alkaline phosphatase activity and finally osteogenic differentiation of hADSCs. While the combination of electromagnetic field and osteogenesis differentiation medium decreased calcium matrix deposits and alkaline phosphatase activity and finally increased osteogenic differentiation of hADSCs. As a result, the synergy of osteogenesis differentiation medium and betaine can be used to treat bone disorders.

Acknowledgements

This study was financially supported by Biological School of Damghan University. There is no conflict of interest in this article

References

[1] Maziarz A, Kocan B, Bester M, Budzik S, Cholewa M, Ochiya T, et al. How electromagnetic fields can influence adult stem cells: positive and negative impacts. Stem Cell Research & Therapy. 2016;7(1):54.

[2] Petecchia L, Sbrana F, Utzeri R, Vercellino M, Usai C, Visai L, et al. Electro-magnetic field promotes osteogenic differentiation of BM-hMSCs through a selective action on Ca2+-related mechanisms. Scientific Reports. 2015;5:13856.

[3] Diniz P, Soejima K, Ito GJNO. Nitric oxide mediates the effects of pulsed electromagnetic field stimulation on the osteoblast proliferation and differentiation. *BIO ELECTRO MAGNETICS,* 2002;7(1):18-23.

[4] Wen L, Wang Y, Wang H, Kong L, Zhang L, Chen X, et al. L-type calcium channels play a crucial role in the proliferation and osteogenic differentiation of bone marrow mesenchymal stem cells. Biochemical and biophysical research communications. 2012;424(3):439-45.

[5] Day CR, Kempson SA. Betaine chemistry, roles, and potential use in liver disease. Biochimica et biophysica acta. *Biochim Biophys Acta.* 2016;1860(6):1098-106.

[6] Villa I, Senesi P, Montesano A, Ferraretto A, Vacante F, Spinello A, et al. Betaine promotes cell differentiation of human osteoblasts in primary culture. Journal of translational medicine. 2017;15(1):132.

[7] Yang Q, Yin W, Chen Y, Zhu D, Yin J, Zhang C, et al. Betaine alleviates alcohol-induced osteonecrosis of the femoral head via mTOR signaling pathway regulation. ELSEVIER. 2019;120:109486.

[8] Veskovic M, Mladenovic D, Milenkovic M, Tosic J, Borozan S, Gopcevic K, et al. Betaine modulates oxidative stress, inflammation, apoptosis, autophagy, and Akt/mTOR signaling in methionine-choline deficiency-induced fatty liver disease. ELSEVIER. 2019;848:39-48.

[9] Li C, Wang Y, Li L, Han Z, Mao S, Wang GJCS, et al. Betaine protects against heat exposure–induced oxidative stress and apoptosis in bovine mammary epithelial cells via regulation of ROS production. *Cell Stress and Chaperones* **volume** 2019;24(2):453-60.

[10] Locke M, Windsor J, Dunbar PRJAjos. Human adipose□derived stem cells: isolation, characterization and applications in surgery. Journal compilation. 2009;79(4):235-44.

[11] Gregory CA, Gunn WG, Peister A, Prockop DJJAb. An Alizarin red-based assay of mineralization by adherent cells in culture: comparison with cetylpyridinium chloride extraction. ELSEVIER. 2004;329(1):77-84.

[12] Seyedjafari E, Soleimani M, Ghaemi N, Shabani IJB. Nanohydroxyapatite-coated electrospun poly (l-lactide) nanofibers enhance osteogenic differentiation of stem cells and induce ectopic bone formation. *Biomacromolecules.* 2010;11(11):3118-25.

[13] Tsai MT, Li WJ, Tuan RS, Chang WH. Modulation of osteogenesis in human mesenchymal stem cells by specific pulsed electromagnetic field stimulation. Journal of orthopaedic research : official publication of the Orthopaedic Research Society. 2009;27(9):1169-74.

[14] Lohmann C, Schwartz Z, Liu Y, Guerkov H, Dean DD, Simon B, et al. Pulsed electromagnetic field stimulation of MG63 osteoblast□like cells affects differentiation and local factor production. Orthopaedic Research.2000;18(4):637-46.

[15] Matsumoto H, Ochi M, Abiko Y, Hirose Y, Kaku T, Sakaguchi KJCoir. Pulsed electromagnetic fields promote bone formation around dental implants inserted into the femur of rabbits.CLINICAL ORAL IMPLANTS RESEARCH. 2000;11(4):354-60.

[16] Canè V, Botti P, Soana SJJoOR. Pulsed magnetic fields improve osteoblast activity during the repair of an experimental osseous defect. Orthopaedic Research Society. 1993;11(5):664-70.

[17] Diniz P, Shomura K, Soejima K, Ito GJBJotBS, The Society for Physical Regulation in Biology, Medicine TEBA. Effects of pulsed electromagnetic field (PEMF) stimulation on bone tissue like formation

are dependent on the maturation stages of the osteoblasts. BIO ELECTRO MAGNETICS. 2002;23(5):398-405.

[18] Sun LY, Hsieh DK, Yu TC, Chiu HT, Lu SF, Luo GH, et al. Effect of pulsed electromagnetic field on the proliferation and differentiation potential of human bone marrow mesenchymal stem cells. BIO ELECTRO MAGNETICS. 2009;30(4):251-60.

[19] Luo F, Hou T, Zhang Z, Xie Z, Wu X, Xu JJO. Effects of pulsed electromagnetic field frequencies on the osteogenic differentiation of human mesenchymal stem cells. **Orthopedics.** 2012;35(4):e526-e31.

[20] Kaivosoja E, Sariola V, Chen Y, Konttinen YTJJote, medicine r. The effect of pulsed electromagnetic fields and dehydroepiandrosterone on viability and osteo□induction of human mesenchymal stem cells. Journal of Tissue Engineering and Regenerative Medicine. 2015;9(1):31-40.

[21] Fu YC, Lin CC, Chang JK, Chen CH, Tai IC, Wang GJ, et al. A novel single pulsed electromagnetic field stimulates osteogenesis of bone marrow mesenchymal stem cells and bone repair. PloS one. 2014;9(3):e91581.

[22] Ongaro A, Pellati A, Bagheri L, Fortini C, Setti S, De Mattei M. Pulsed electromagnetic fields stimulate osteogenic differentiation in human bone marrow and adipose tissue derived mesenchymal stem cells. Bioelectromagnetics. 2014;35(6):426-36.

[23] Ceccarelli G, Bloise N, Mantelli M, Gastaldi G, Fassina L, De Angelis MG, et al. A comparative analysis of the in vitro effects of pulsed electromagnetic field treatment on osteogenic differentiation of two different mesenchymal cell lineages. BioResearch open access. 2013;2(4):283-94.

[24] Luo F, Hou T, Zhang Z, Xie Z, Wu X, Xu J. Effects of pulsed electromagnetic field frequencies on the osteogenic differentiation of human mesenchymal stem cells. Orthopedics. 2012;35(4):e526-31.

[25] Esposito M, Lucariello A, Riccio I, Riccio V, Esposito V, Riccardi GJIv. Differentiation of human osteoprogenitor cells increases after treatment with pulsed electromagnetic fields. International Institute of Anticancer Research. 2012;26(2):299-304.

The study of *Cdx2* gene expression in mouse blastocysts influenced by embryo splitting

Mohaddeseh Rahbaran [1], Farid Heidari [1]*, Aydin Tayefe [1]

[1] Animal Biotechnology Department, National Institute of Genetic Engineering and Biotechnology (NIGEB), Tehran, Iran

*Email: heidari@nigeb.ac.ir

Abstract

Embryo splitting is widely used as a novel technique in reproduction biotechnology. After splitting the embryo at the two-, four- or eight-cell stages, every single blastomere can be developed into a separate embryo that is similar to another blastomere genetically. In the present study, the effects of the mouse embryo splitting on the Cdx2, as a pluripotent gene, expression were evaluated. After stimulating ovulation in female mice and isolating two-cell embryos, they were grouped as split and non-split, then washed and transferred in M16 medium. When zona pellucida was removed, the blastomeres of the split group were dispersed then transferred into embryonic fibroblasts to develop. Cdx2 gene expression was analyzed by real-time PCR. The results demonstrated that pluripotent gene expression was similar between split and non-split groups.

Keywords: Embryo Splitting, Mouse Blastocyst, Two-cell Embryo, *Cdx2*.

1. Introduction

Embryo splitting actually resembles to a natural process to create identical twins. Split two-cell-stage embryo into blastomeres which are allowed to develop to fetus then adults, can produce monozygotic twins [1]. These twins can be extremely efficient to understand how human twins could be different in phenotype very much, although they are near [2]. Particularly, twin animal can be employed to investigate how much and which phenotypic discordance is related to epigenetic changes including DNA methylation caused by environmental and other effects, during the time [3].

In this field of study on mouse embryo splitting, the developmental ability of the single blastomere, isolated from two-cell-stage embryo, has been examined and also their totipotency growing to adult has been reported [4]. Moreover, isolating two-cell blastomeres could promote the development and growth of the blastomeres to full-term live fetus and consequently adult mice [5]. During the last decades, there can be found several reported methods that can be used in embryo splitting. Depending on the growth stage of the embryo, blastomere biopsy and bisection can be employed for splitting embryo in cleavage stage and morulae or blastocysts, respectively. Mechanical division of the mouse embryos can predominantly causes cellular damage and consequently decrease the chance of the effective embryo splitting [6]. Bisection of the mouse morulae could successfully create twin

embryos to transfer into the surrogate females. 25 percent of these cases could grow and develop to full-term live fetus [7]. Besides, half-embryos of mouse developed from eight-cell-stage blastomeres which were isolated by biopsy, indicated non-significant results, after transferring the embryos to surrogate females [4]. Molecular analysis of the gene expression could be an efficient approach to select embryo. During evolution of the mouse embryo, dividing cell lines is actually controlled by some gene regulation networks containing transcriptional factors which are specifically expressed in each cell type [8]. The influence of the mouse embryo splitting on *Cdx2*, as a pluripotent gene, expression were evaluated in the present study.

2. Material and Methods

2.1 Collecting two-cell mouse embryos

In the study, 120 female NMRI mice, average 23-21 g, were utilized, respecting the guidelines of the Animal Ethics and Biosafety Committee of the National Institute of Genetic Engineering and Biotechnology (NIGEB), Tehran, Iran. IU8 Pregnant Mare Serum Gonadotropin was injected intraperitoneally for supravolution on the first day, as well as IU8 Human Chorionic Gonadotropin after 48 hours. Female mice were mated with matured male mice. 1.5-day pregnant mice were used for extracting embryos. After surgery and isolating the fallopian tubes, the embryos were obtained by the washing of the fallopian tubes with M2 media. Finally, the embryos were divided into the split and non-split groups, then transferred to the M16 medium containing mineral oil and incubated in 5% CO2 at 37° C [9].

2.2 Isolating and culturing blastomeres

Zona pellucida (ZP) of Two-cell embryos eliminated by acid Tyrode's solution. The embryos were split and washed by repeatedly pipetting with trypsin 25% for a minute and M2 medium, respectively, then incubated in M16 medium under mineral oil at 37ºC. Single blastomeres without ZP, as split group, which was morphology normal, and two-cell embryos, as non-split group, were incubated to differentiate into blastocyst within separate plates containing TCM-199 culture medium and inactivated embryonic fibroblast cells at 37ºC. Single blastomeres and two-cell embryos were differentiated after 68-72 and 40-48 hours, respectively.

2.3 Gene expression assay

RNA was extracted for RT-PCR, along with a random hexamer sequences in reaction solution of a kit. The reaction solution was incubated at 42ºC for 60 min then at 70ºC for 5 min. Primers were designed for *Cdx2* gene by using SnapGene and Primer Blast software (Table 1). Primer length, product length, cytosine and guanine percentage, the presence of the repetitive sequences, palindrome, and hairpin-end were analyzed. CT comparative method of Real time-PCR was utilized to analyze *Cdx2* gene expression by using a kit (Intron, 25344) containing

SYBER Green I dye in a thermo cycler. 40 cycles were completed at 64ºC as the annealing temperature, with 3 repetitions for each treatment. The data were analyzed by Rest 2009 software.

Table 1. Primers' features used in RC-PCR

Gene	Sequence (5' to 3')	Melting point (C)	Length (bp)	Product (bp)
Cdx2	F: CTGCAGACGCTCAACCTCG	62	19	170
	R: GTACACCACCCGGTATTTGTC	62	21	

3. Results and Discussions

Changes in the expression of *Cdx2* gene in split, non-split, and blastocyst in vivo groups were analyzed by Rest 2009 software. There was no significant difference among relative the expression of *Cdx2* gene in the studied groups ($p<0.05$; Table 2), although slight and insignificant differences was observed (Figure 1).

Table 2. The comparison *Cdx2* gene expression in the study groups

Gene	S-B	S-N	B-N
Cdx2	0.10	0.075	0.368

Splitting = S groups, Non-Splitting = N, and Blastocyst *in vivo* = B. Data normalization was performed with the *GAPDH* gene as the Housekeeping gene.

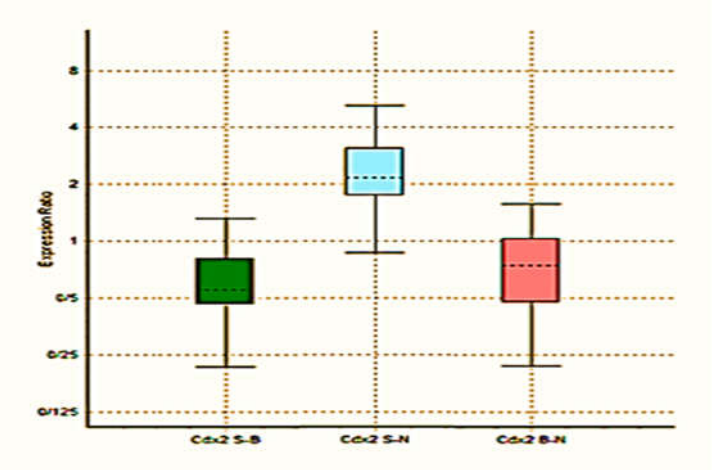

Figure 3: Relative expression of *Cdx2* gene in groups (Splitting = S), (Non Splitting = N) and (Blastocyst *in vivo* = B)

In this study, it is shown that there is no effect of the embryo splitting on *Cdx2* gene expression; because no significant difference was reported between three groups, split, non-split, and blastocyst *in vivo*. Besides, *Oct4* and *Cdx2* gene expression has previously been observed in mouse embryo splitting [4]. *Cdx2* gene is a key regulatory factor of the trophectoderm cell line and the first identified marker for differentiation between

trophectoderm and ICM. This gene expression is initiated at the eight-cell stage, then restricted to external cells before blastocyst formation. *Cdx2* knockout embryos are able to form blastocyst, but lose all external epithelial cells and stop developing ICM to trophectoderm, then die consequently about implanting duration [10].

According to the results of the study, there is no unpleasant and harmful effect on the growth capacity of mouse twin embryos. It finally seems that sister blastomeres, derived from split mouse embryo at two-cell stage, equally resemble together in term of the growth and developmental potential. Thus, it is required to test live-born offspring molecularly for achieving to the more understanding about using embryo splitting for clinical aims.

References

[1] Nissen, S. B., Perera, M., Gonzalez, J. M., Morgani, S. M., Jensen, M. H., Sneppen, K., ... & Trusina, A.. Four simple rules that are sufficient to generate the mammalian blastocyst. *PLoS biology,* (2017), *15*(7), e2000737.

[2] Casser, E., Israel, S., & Boiani, M.. Multiplying embryos: experimental monozygotic polyembryony in mammals and its uses. *International Journal of Developmental Biology,* (2019), *63*(3-4-5), 143-155.

[3] Kim, K., Lee, K., Bang, H., Kim, J. Y., & Choi, J. K. Intersection of genetics and epigenetics in monozygotic twin genomes. *Methods,* (2016) *102*, 50-56.

[4] Casser, E., Israel, S., Witten, A., Schulte, K., Schlatt, S., Nordhoff, V., & Boiani, M. Totipotency segregates between the sister blastomeres of two-cell stage mouse embryos. *Scientific reports,* (2017), *7*(1), 1-15.

[5] Klimczewska, K., Kasperczuk, A., & Suwińska, A. The regulative nature of mammalian embryos. In *Current topics in developmental biology*, (2018). Vol. 128, pp. 105-149, Academic Press.

[6] Noli, L. Comparative Analyses of Twin Blastocysts. *Reproduction,* (2017) *23*, 156-65.

[7] Taşkin, A. C., Akkoc, T., Sağirkaya, H., Bağiş, H., & Arat, S. Comparison of the development of mouse embryos manipulatedwith different biopsy techniques. *Turkish Journal of Veterinary and Animal Sciences,* (2016), *40*(2), 157-162.

[8] Gleicher, N., & Orvieto, R. Is the hypothesis of preimplantation genetic screening (PGS) still supportable? A review. *Journal of ovarian research,* (2017), *10*(1), 21.

[9] Tang, H. H., Tsai, Y. C., & Kuo, C. T. Embryo splitting can increase the quantity but not the quality of blastocysts. *Taiwanese Journal of Obstetrics and Gynecology,* (2012), *51*(2), 236-239.

[10] Menchero, S., de Aja, J. S., & Manzanares, M. Our first choice: cellular and genetic underpinnings of trophectoderm identity and differentiation in the mammalian embryo. In *Current Topics in Developmental Biology,* (2018),Vol. 128, pp. 59-80. Academic Press.

Evaluation of subacute toxicity of *Lactobacillus rhamnosus (ATCC: 7469)* with haematological and biochemical parameters in male Wistar rats

Seyed Ali Alavi[1*], Amir Abbas Barzegari[1], Seyed Babak Khalifeh Zadeh Kaleybar[2]

[1]Department of Biology, University of Maragheh, Maragheh, East Azerbaijan, Iran.

[2]Department of Pathology, Islamic Azad University, Tabriz Branch, Tabriz, Iran

*Email: seyedalialavi.ac@gmail.com

Abstract

One of the main criteria of probiotics is their safety. The purpose of present research was to evaluate the safety of *Lactobacillus rhamnosus (ATCC: 7469)* in male Wistar rats. A subacute 28-day toxicity study was conducted. Two groups of male rats (n=6/group) were used. Control group received saline and the experimental group received 1 × 109 CFU/rat of *L. rhamnosus (ATCC: 7469)* for 28 consecutive days. Analysis of weigh changes, general observations, hematological factor, and serum parameters showed no toxicity of the bacterium in male Wistar rats.

Keywords: Subacute toxicity, Wistar rat, serum parameter, haematological parameters.

1. Introduction

Lactobacillus is one of the bacterial genera belonging to the group of lactic acid bacteria (LAB). Because of their important properties in fermenting sugars and producing lactic acid, humans have used LABs in preparing fermented foods for thousands of years [1]. These bacteria can produce secondary metabolites such as bacteriocins and organic acids such as propionic acid and butyric acid; the products that increase the shelf life of fermented foods [2]. Lactic acid bacteria are the most important bacterial species of probiotics. Probiotics are living microorganisms that, if consumed in sufficient quantities, have beneficial health effects on human or animal hosts [3]. In recent years, there are many reports on the beneficial health effects of probiotics in alleviating or preventing several disorders. *Lactobacillus rhamnosus* is a species of Lactobacilli that is widely used in the pharmaceutical industry and in the production of dairy foods [12]. For example, Lactobacillus rhamnosus GG have been used for over 30 years in the treatment of gastrointestinal infections and diarrhoea, and other diseases in which the dysbiosis of gut microbiota occurs [13]. Although Lactobacilli are generally recognized as safe (GRAS) organisms [14], some of them may have pathogenicity in the host [15]. Since the safety aspect is very important for every probiotic strain, different methods, including in vitro studies, animal studies, and human clinical studies, have been used for assessing the safety of probiotic bacteria. In preclinical toxicity studies, OECD guideline suggest the laboratory rats as appropriate species. To the best of our knowledge, no study has been performed on the evaluation of subacute toxicity of *Lactobacillus rhamnosus (ATCC: 7469)* on Wistar rats. Therefore, the present

study was undertaken to investigate the safety of this strain of *lactobacillus rhamnosus* with a 28-day subacute toxicity test in Wistar rats.

2. Material and Methods

2.1 Lactobacillus culture

The Lactobacillus strain *L. rhamnosus (ATCC: 7469)*, were cultured in MRS broth medium (Ibresco, Iran) and incubated for 16-18 h at 37°C. After incubation, the culture of strain was centrifuged (Eppendorf 5810r) at 4000 rpm for 20 min at 4°C. Supernatants were discarded and cell pellets were immediately transferred to sterile normal saline. For cell suspension preparation, normal saline was used as a diluent. Every day, the cell suspensions were freshly prepared from the overnight culture just before administration to the animals.

2.2 Animals

A total of 12 male Wistar rats were used. The weight of animals was between 240-270g at the beginning of the experiments. They were prepared from animal house at the University of Maragheh. They housed in wire-topped plastic cages (47 cm l × 35 cm w × 20 cm h) with appropriate space and had free access to tap water and standard rodent diet. The subacute oral toxicity study was carried out in conformity with international guidelines for the care and use of laboratory animals and was approved by a local ethic committee.

2.3 Experimental design

The animals were randomly assigned into two groups of six rats in each: one control group and one experimental group. The experiments were begun after a 7-day acclimatization period. The duration of the subacute toxicity study was 28 days. In these days, the animals in the control group received 0.5 ml of normal saline, and the experimental rats were given 1 × 109 CFU/rat of *L. rhamnosus (ATCC: 7469)*. All the animals received just one daily treatment in the same time of the day.

2.4 General observations and body weigh

General observations for finding any changes in skin and fur, eyes, mucous membranes, respiration, tremors, convulsions, salivation, diarrhea, lethargy, sleep, gait and posture were performed. Body weight was recorded once a day, at the same time of the day, on days 1, 7, 14, 21, and 28 of the experimental period

2.5 Hematological and serum biochemistry analyses

At the end of the experiment, animals were anesthetized with a ketamine and xylazine solution. Sampling of blood was conducted through cardiac puncture under deep anesthesia. For hematological study, blood was collected in tubes containing K2EDTA, and for harvesting the serum samples the coagulated blood samples were centrifuged for 15 minutes at 3000 g. The hematology test was performed using an automated analyzer (BT 1500, Italy). The following parameters were analyzed: red blood cell count, hemoglobin, mean corpuscular volume, mean corpuscular hemoglobin concentration, thrombocytes, white blood cell count, and lymphocyte count. For serum biochemistry analysis, an automatic clinical chemistry analyzer (Biolis i50, Japan) was used. The following parameters: urea, creatinine, alkaline phosphatase total (ALP), alanine transaminase (ALT), and aspartate transaminase (AST) were analyzed to evaluate the liver and kidney toxicity.

2.6 Statistical analysis

SPSS Software and independent samples T-test were used to analyze data. The data were expressed as mean ± SEM. In the present research, $P<0.05$ considered as significant.

3. **Results and Discussions**

3.1 Effects of L. rhamnosus (ATCC 7469) on general health status and body weight:

Administration of the bacterium to the rats (for 28 days) had no significant effects on general health status, and changes of body weight in the experimental group compared to the saline-treated group (Figure 1). Reduction in weight gain is a good indicator of toxicity of substances. Therefore, weight change data show that the bacterium is nontoxic.

3.2 Effects of L. rhamnosus (ATCC 7469) on haematology parameters:

Analysis of haematological parameters showed no significant difference between the experiential and control groups (table 1). Change in haematological parameters are good indicators of toxicity of substances. Moreover, the presence of an inflammation or infection in the body may change some of these parameters. Therefore, these data show that the bacterium had no adverse effects on blood parameters.

3.3 Effects of L. rhamnosus (ATCC 7469) on serum parameters:

Comparison of serum parameters between the experimental and control groups showed no significant difference in any of the parameters (table 2). Changes in the liver enzyme, as well as urea and creatinine, may indicate liver and kidney toxicity. Hence, the lack of difference between the serum parameters in the rats that received the bacterium, and the control groups shows that in the present experiment the bacterium had no toxic effect on the liver and kidney.

3.4 Conclusion

In this research analyzing the haematological and serum parameters showed that administration of *L. rhamnosus (ATCC 7469)* in a single dose (for 28 consecutive days) had no toxicity in male Wistar rats.

Table 1: Influence of *Lactobacillus rhamnosus* (ATCC 7469) on blood parameters. Values are mean ± S.D. of six Wistar rats. * $P < 0.05$ compared with the control group.

group	*WBC* (×10³/µL)	*Lym* (%)	*RBC* (×10⁶/µL)	*HGB* (g/dL)	*HCT* (%)	*MCV* (fL)	*MCH* (pg)	*MCHC* (g/dL)	*PLT* (×10³/µL)
control	5.09±1.2	65.3±5.8	8.74±0.16	15.5±0.4	48.1±0.71	55±0.46	17.7±0.19	32.2±0.33	844±48.1
experimental	4.81±09	66.8±3.9	8.36±0.3	15.3±0.36	48.7±1.2	58.7±0.85	18.4±0.23	31.4±0.53	861±68.3

Table 2: Influence of *Lactobacillus rhamnosus (ATCC 7469)* on biochemical parameters. Values are mean ± S.D. of six Wistar rats. * $P < 0.05$ compared with the control group.

Group	*ALP* (U/L)	*ALT* (U/L)	*AST* (U/L)	*Urea* (mg/dl)	*Creatinine* (mg/dl)
Control	729±*77*	61±*18.3*	179±*158*	40±*3.7*	0.52±0.16
experimental	792±*46*	76±*15.2*	205±*9.6*	42± 2.2	0.58±*0.8*

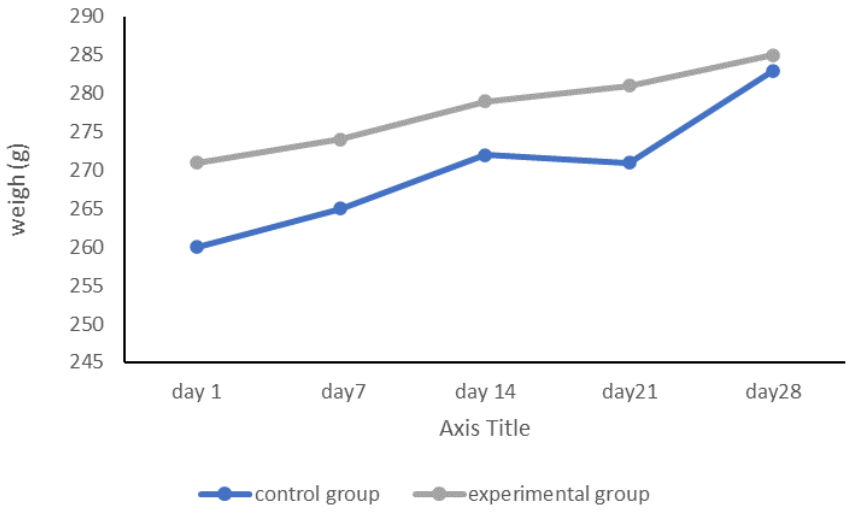

Figure1: Effects of *Lactobacillus rhamnosus (ATCC 7469)* on weight changes in male Wistar rats.

Acknowledgements

This research was performed in the animal house at the University of Maragheh, and we thank those who sped up the establishment of the animal house.

References

[1] M. Adams, Safety of industrial lactic acid bacteria., Journal of Biotechnology 68 (2-3) (1999) 171-178. doi:10.1016/S0168-1656(98)00198-9.

[2] J. Šušković, et al., Antimicrobial activity–the most important property of probiotic and starter lactic acid bacteria., Food Technology and Biotechnology 48 (3) (2010) 296-307.

[3] L. Morelli, L.Capurso., FAO/WHO guidelines on probiotics: 10 years later., Journal of clinical gastroenterology, 46 (2012) S1-S2. doi:10.1097/MCG.0b013e318269fdd5.

[4] D. Cameron, et al., Probiotics for gastrointestinal disorders: proposed recommendations for children of the Asia-Pacific region., World journal of gastroenterology 23 (45) (2017) 7952. doi:10.3748/wjg.v23.i45.7952.

[5] Q. Guo, et al., Probiotics for the prevention of pediatric antibiotic□associated diarrhea., Cochrane Database of Systematic Reviews, (4) (2019). doi:10.1002/14651858.CD004827.pub5.

[6] S.J Oak, R. Jha., The effects of probiotics in lactose intolerance: a systematic review., Critical reviews in food science and nutrition, 59 (11) (2019) 1675-1683. doi:10.1080/10408398.2018.1425977.

[7] D. Jakubczyk, K. Leszczyńska, S. Górska., The Effectiveness of Probiotics in the Treatment of Inflammatory Bowel Disease (IBD)—A Critical Review., Nutrients, 12 (7) (2020) 1973. doi:10.3390/nu12071973.

[8] M. Molska, J. Reguła., Potential mechanisms of probiotics action in the prevention and treatment of colorectal cancer., Nutrients, 11 (10) (2019) 2453. doi:10.3390/nu11102453.

[9] J. Zhang, et al., Preventive effect of *Lactobacillus plantarum CQPC10* on activated carbon induced constipation in Institute of Cancer Research (ICR) mice., Applied Sciences, 8 (9) (2018) 1498. doi:10.3390/app8091498.

[10] M. Mennini, et al., Probiotics in asthma and allergy prevention., Frontiers in pediatrics, 5 (2017) 165. doi:10.3389/fped.2017.00165.

[11] A. Rø, et al., Reduced Th22 cell proportion and prevention of atopic dermatitis in infants following maternal probiotic supplementation., Clinical & Experimental Allergy, 47 (8) (2017) 1014-1021. doi:10.1111/cea.12930.

[12] Y. Hooshyar, et al., Effects of *Lactobacillus rhamnosus ATCC 7469* on Different Parameters Related to Health Status of Rainbow Trout (Oncorhynchus mykiss) and the Protection Against Yersinia ruckeri., Probiotics and Antimicrobial Proteins, (2020) 1-15. doi:10.1007/s12602-020-09645-8.

[13] L. Capurso, Thirty years of *Lactobacillus rhamnosus GG*: a review., Journal of clinical gastroenterology., 53 (2019) S1-S41. doi:10.1097/MCG.0000000000001170

[14] E. Salvetti, S. Torriani, G.E. Felis., The genus Lactobacillus: a taxonomic update., Probiotics and antimicrobial proteins, 4 (4) (2012) 217-226. doi:10.1007/s12602-012-9117-8

[15] P. Shokryazdan, et al., Safety assessment of two new Lactobacillus strains as probiotic for human using a rat model., PLoS One, 11 (7) (2016) e0159851. doi:10.1371/journal.pone.0159851

Design and characterization of multifunctional magnetic nanoparticles for targeted siRNA delivery to AGS cells

Fatemeh Abedi Sarvestani[1] , Asadollah Asadi[1*], Saeid Latifi-Navid[1] , Saber Zahri[1]

[1]Department of Biology, Faculty of Science, University of Mohaghegh Ardabili, Ardabil, Iran

*Email: asad.asadi@gmail.com

Abstract

The properties of drug nanocarriers have been optimized to facilitate penetration into the cells and increase the drug's effectiveness and protect from drug damage and enzymatic agents, and reduce the side effects of drugs by targeting cancerous cells drug delivery. The chitosan has many medicinal capabilities due to its unique properties such as cationic properties, solubility in the aqueous medium, biocompatibility, and biodegradability. It is possible to produce the nanoscale chitosan particles used as the nanocarriers to transfer proteins, enzymes, drugs, and genes to cancerous cells. The chitosan can also react with siRNA in such a way that the high cationic charge of amine groups in chitosan can electrostatically interact with the negative charge of the siRNA phosphate group neutralizing the negative charge. Furthermore, the chitosan coating in nanocarriers enhances siRNA cellular uptake. In this regard, the transition metal compounds such as FeCo, which have magnetic properties and are absorbed by the magnetic field, can increase the efficiency of nanocarriers and their targeting characteristics. In this research, FeCO @ SiO2-SS-Chitosan nanoparticles have been designed, prepared and investigated the interaction effects of these new nanoparticle with siRNA-FAM and AGS cell transfection using FeCO @ SiO2-SS-Chitosan / siRNA-FAM nanoparticles which has resulted in a new type of nanoparticles to improve the delivery of diagnostic and therapeutic agents to cancer cells.

Keywords: siRNA, AGS, Magnetic Nanoparticles

1. Introduction

The characteristics of drug nanocarriers have enhanced to make the penetration into the cells facilitated, increase the efficiency of drug, make a protection for the drug against enzymatic agents, and decrease the side effects of drugs by targeting drug delivery to cancerous cells [1]. The main aim in making nanoparticles as a drug delivery system is to control the particle size, surface properties, and release of a specific and efficient drug in a specific area and period in order to make the drug as effective as possible. The nanoparticles used for drug release needs to have biocompatibility, biodegradability properties, capability to be released in proportion to time, desirable mechanical properties and an easy manufacturing process .The polymer-based nanoparticles are good tools for conducting biomolecules, drugs, genes, and vaccines. The solubility and shelf life of the drugs can be improved by encapsulating these drugs in these nanoparticles. The main purpose is to target the drug in a specific concentration and, ultimately patient satisfaction within the treatment window [2]. The simultaneous targeting of cancer cells using two or more drugs can be a new effective approach to overcome the current issues of drug resistance [3, 4]. In recent years, the use of siRNA to suppress oncogene's expression has been considered a

promising solution for cancer treatment [5, 6]. Although this method are useful, due to the complexity of human cancer, additional treatments may be needed to improve the effectiveness of siRNA cancer treatment [7, 8]. The combination of siRNA and chemotherapy drugs has been considered a useful strategy to increase cancer treatment effectiveness [9] .The chitosan is an abundant natural polysaccharide that has been extensively studied to prepare nanoparticles for drug delivery [10, 11]. The biocompatibility, biodegradability, easy injection, high surface to volume ratio, and reduced embolus risk are among the valuable properties of the polymer making it suitable for drug delivery purposes in the body are (Embolus) [12].

The chitosan is a natural polycationic distilled polymer composed of N-acetyl D-glucosamine and D-glucosamine units [13, 14]. In chitosan structure, due to the presence of the amine group at the carbon position 2 in D- units, polysaccharide is converted to polycation in an acidic environment [12, 15]. Therefore, microparticles and nanoparticles can be easily prepared by the electrostatic reaction between the existence of amine groups in chitosan and a large group of biocompatible polyanionic materials [12, 16, 17]. The chitosan can also interact with siRNA in that the amine groups in chitosan with high cationic charge electrostatically interacting with the negative charge of the phosphate group in siRNA and neutralizing its negative charge. The chitosan coating in nanocarriers also increases siRNA cell uptake. In one study, the chitosan nanoparticles and catalytic nucleic acids (DNAzym) were studied to treat cancer. This study aimed to investigate gene therapy including encapsulation of DNAzym and siRNA (small interfering RNA) and small interference of RNA inside the chitosan nanoparticles. The results showed that these therapeutic agents improve the treatment process along with chitosan nanocarriers [18]. In another study, the albumin nanoparticles with a coating of chitosan showed an increased siRNA cell uptake. In vivo administration of siRNA, using chitosan-based nanoparticles has reduced the expression of the target gene's expression resulting in cancer cell death [19]. The use of magnetic properties of particles and the penetration of magnetic fields into cellular tissues, and its ability to diagnose and treat diseases in humans have long been studied, and the magnetic nanoparticles are of great interest for drug delivery and practical applications. In addition to moving towards a magnet, these nanoparticles also have higher efficiency in cell adsorption than other nanocarriers. The essential modifications on these compounds' surface makes it possible to bind drugs, proteins, and genetic materials. In this way, the targeted transference of these compounds is possible by the effect of an external magnetic field [20]. The transition metal nanoparticles including pure iron, cobalt, or their compounds such as FeCo can be used for this purpose. These metal nanoparticles have a high tendency to maintain the magnetic torque and absorb magnetic fields. The toxicity of cobalt elements is one of the setbacks for its application, but cobalt in small quantities are useful for the body. This compound is necessary for the formation of vitamin B12 and is used to treat anemia. The cobalt compounds are excreted with no accumulation in the body, therefore certain quantities of cobalt particles are not toxic [21].

2. Material and Methods

2.1 Synthesis of FeCO nanoparticles

For this purpose, first, an appropriate amount of FeO (OH) and Co3O4 were separately dissolved in trioctylamine, then reacted for 3 hours at 170 ° C under argon gas. Following that, the product was stirred and the temperature was rise rapidly to 370 ° C. Finally, the resulting nanoparticles were collected at room temperature by centrifugation and washed with hexane and ethanol [22].

2.2 Synthesis of FeCO @ SiO2-SS-Chitosan nanoparticles

In order to synthesize FeCO @ SiO2-SH nano-particles, 200 mg of FeCO nanoparticles were sonicated in ethanol for 15 minutes. Then, one ml of each of NH3.H2O, MPTMS, and TEOS was added to FeCO nanoparticles under sonication conditions. The resulting mixture was washed several times with ethanol and water and dried under a vacuum. In order to bind the COOH group to surface of FeCO @ SiO2-SH nanoparticles, 200 mg of FeCO @ SiO2-SH nanoparticles were dissolved in methanol (2 ml) and then reacted with an equal amount of 2-carboxyethyl 2-pyridyl for 36 hours. The resulting nanoparticles were washed and dried based on the above method process. The activation of the carboxyl terminus in FeCO @ SiO2-SS-COOH nanoparticles for chitosan binding was performed by adding 200 mg of FeCO @ SiO2-SS-COOH nanoparticles 16 ml of phosphate buffer containing NHS (10 mg) and EDC (20 mg). The resulting mixture was kept at room temperature for 24 hours, then 200 mg of chitosan was added to the above product and stirred at room temperature for 48 hours. Finally, the resulting nanoparticles were dried by freeze-drying after washing with water and ethanol. XRD and TGA spectroscopy was used to confirm the synthesis of FeCO and FeCO @ SiO2-SS-Chitosan nanoparticles.

2.3 Investigation of the ability of FeCO @ SiO2-SS-Chitosan nanoparticles to interact with siRNA-FAM

In order to load siRNA-FAM by FeCO @ SiO2-SS-Chitosan nanoparticles, 5 µg of siRNA-FAM with different FeCO @ SiO2-SS-Chitosan nanoparticles (0.5, 1, 2.5, 5, and 10 mg) were mixed. The agarose gel electrophoresis was then used to achieve the interaction of nanoparticles with siRNA-FAM. For this purpose, FeCO @ SiO2-SS-Chitosan / siRNA-FAM nanoparticles were electrophoresed with 4% agarose gel at a voltage of 80 V for 30 minutes. Finally, agarose gel was observed by ethidium bromide after UV staining.

2.4 Transfection of AGS cells using FeCO @ SiO2-SS-Chitosan nanoparticles

The different ratios of FCO @ SiO2-SS-Chitosan / siRNA-FAM nanoparticles were used to transfect AGS cells. For this aim, AGS cells with the same cell density in RPMI-1640 culture medium containing 10% FBS were

transferred to each of the 24-plate wells and kept for 24 hours at 37 ° C and 5% CO2. After 24 hours, FeCO @ SiO2-SS-Chitosan / siRNA-FAM nanoparticles were added to each well separately in three replications. In this study, the uncoated siRNA-FAM was used as a negative control. After storing the cells for 24 hours at 37 ° C and 5% CO2, fluorescence microscopy was used to evaluate the transfection of FeCO @ SiO2-SS-Chitosan / siRNA-FAM nanoparticles.

3. Results and Discussions

The results of XRD spectroscopy showed that FeCO nanoparticles in the range of 30 to 45 and 55 to 65 θ had good crystallization. These results also showed that the highest degree of crystallization was observed for the chitosan range of 5 to 35 θ. However, crystallization for FeCO @ SiO2-SS-Chitosan nanoparticles was observed in the crystallization range for FeCO and chitosan nanoparticles. However, the coating of FeCO nanoparticles reduced the degree of crystallization. These results were consistent with the research findings by Hong et al [22]. (Figure 1). The results of TGA spectroscopy showed that FeCO nanoparticles have higher heat resistance compared to chitosan. These results also showed that the highest percentage of weight loss of FeCO nanoparticles was observed in the range of 550 to 650 ° C, while chitosan weight loss was observed in more than two stages. The comparison of weight loss diagrams of FeCO @ SiO2-SS-Chitosan nanoparticles with FeCO and chitosan nanoparticles showed. Overall, the weight loss of FeCO @ SiO2-SS-Chitosan nanoparticle is achieved in the weight ranges of FeCO and chitosan weight loss. The results indicate chitosan and FeCO compounds in FeCO @ SiO2-SS-Chitosan nanoparticles (Figure 1).

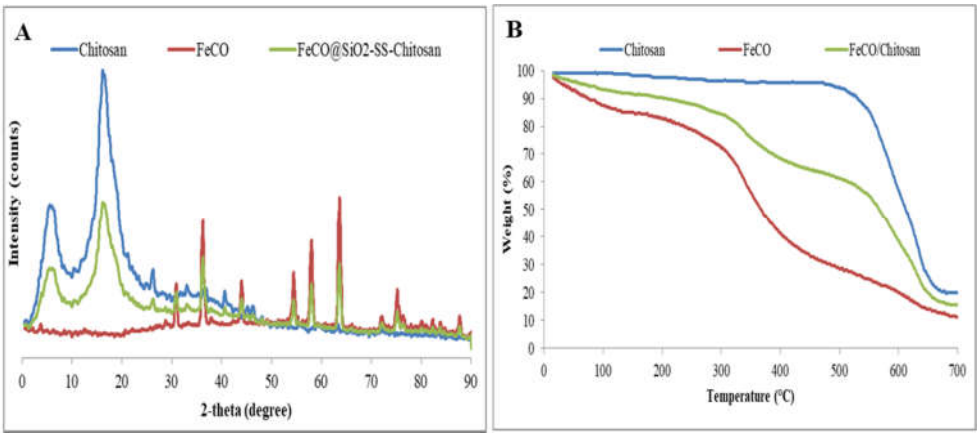

Figure 1. XRD Spectroscopy (A) and TGA (B) of FeCO, Chitosan, FeCO@SiO2-SS-Chitosan

3.1 Investigation of FeCO @ SiO2-SS-Chitosan nanoparticle properties

The transmission electron microscopy (TEM) showed that FeCO @ SiO2-SS-Chitosan nanoparticles were spherical and about 20 nm in size. In addition, the DLS device results showed that these nanoparticles had a positive surface charge and an average size of 26 nm which were consistent with the results of the transmission electron microscopy (Figure 2).

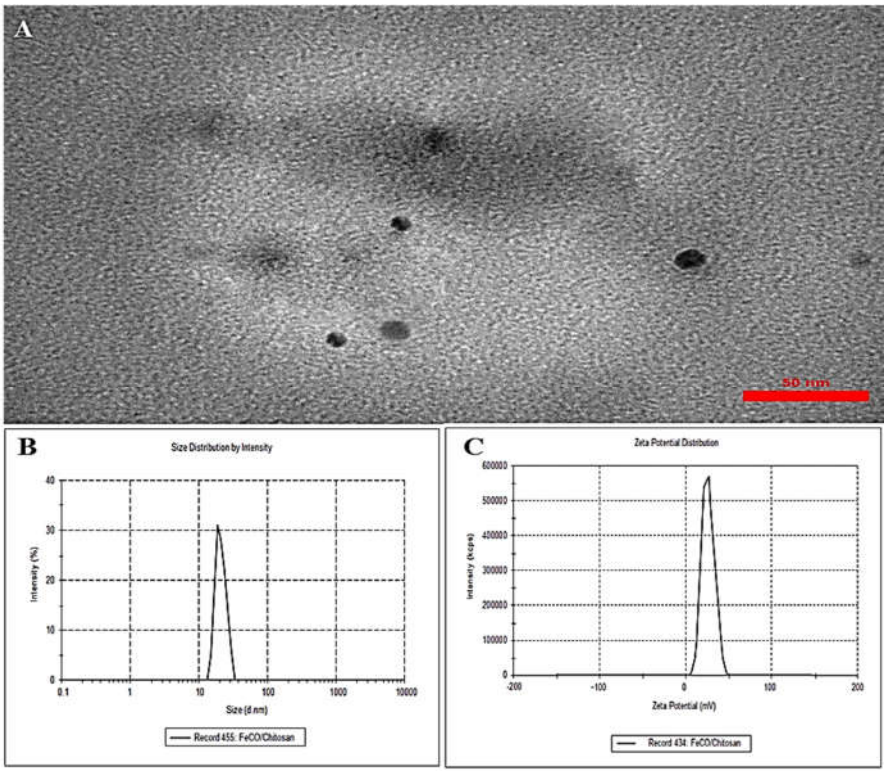

Figure 2. TEM image (A) and DLS (B and C) of FeCO@SiO2-SS-Chitosan nanoparticles

3.2 Investigation of the ability of FeCO @ SiO2-SS-Chitosan nanoparticles to interact with siRNA-FAM

The amine groups in this chitosan have a high cationic charge that can electrostatically interact with the negative charge of phosphate group in siRNA and neutralize its negative charge. By increasing the ratio of FeCO @ SiO2-SS-Chitosan to RNA, the negative charge of RNA gradually reduced, and its movement in the agarose gel towards the positive pole of the device was reduced; therefore, the RNA movement stopped and remained completely the same at high ratios of FeCO @ SiO2-SS-Chitosan to RNA. The agarose gel results showed that FeCO @ SiO2-SS-Chitosan / siRNA-FAM nanoparticles in a ratio higher than 5 mg of FeCO @ SiO2-SS-Chitosan nanoparticles completely neutralizes the negative charge of RNA (Figure 3).

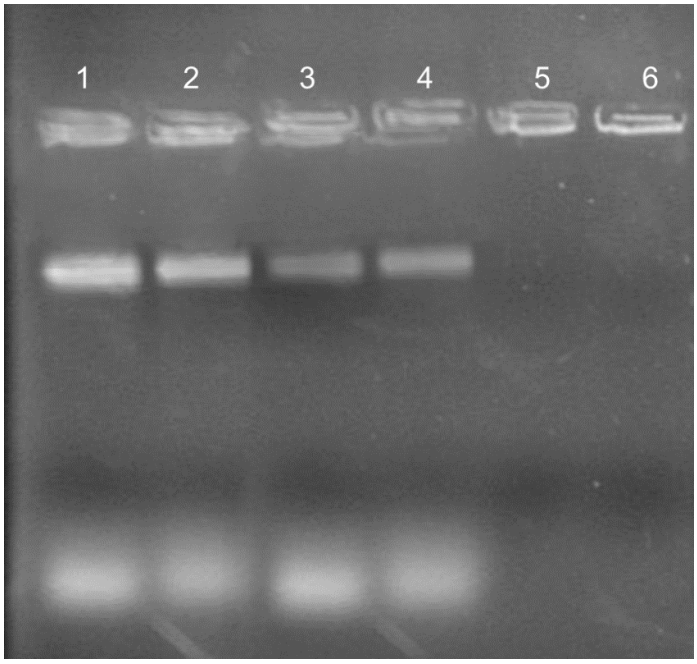

Figure 3. Investigation of the ability of FeCO @ SiO2-SS-Chitosan / siRNA-FAM nanoparticles containing different ratios of FeCO @ SiO2-SS-Chitosan in interaction with siRNA-FAM. Wells 1 to 6 were controlled siRNA and siRNA loaded with 0.5, 1, 2.5, 5 and 10 mg of FeCO @ SiO2-SS-Chitosan nanoparticles, respectively.

3.3 Transfection of AGS cells using FeCO @ SiO2-SS-Chitosan / siRNA-FAM nanoparticles

The uncoated RNA is difficult to transfer into the cell due to the inadequate surface size and potential, early digestion of RNA by the cell defense mechanism during intracellular and cellular transfer, etc. (Harvie et al., 1998). The ability of FeCO @ SiO2-SS-Chitosan / siRNA-FAM nanoparticle to deliver RNA to AGS cells was demonstrated by fluorescence microscopy (Figure 4). The fluorescence microscopy image showed in some AGS cells were treated with FeCO @ SiO2 nanoparticles SS-Chitosan / siRNA-FAM. The observed green emission indicates the ability of these nanoparticle to transmit and release RNA within these cells. In contrast, the uncoated RNA could not transmit to AGS cells. These results also showed that the highest RNA transfer efficiency was observed in FeCO @ SiO2-SS-Chitosan / siRNA-FAM nanoparticles with a ratio of 5 mg of FeCO @ SiO2-SS-Chitosan nanoparticles. The lowest RNA transfer efficiency was observed in FeCO @ SiO2-SS-Chitosan / siRNA-FAM nanoparticles prepared in the ratio of 0.5 mg of FeCO @ SiO2-SS-Chitosan nanoparticles.

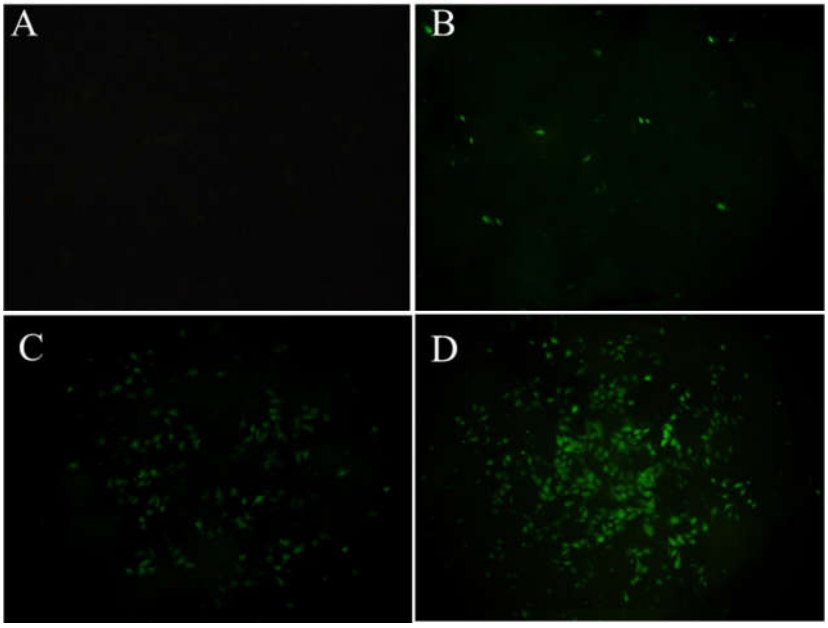

Figure 4. Fluorescence microscopy of AGS cells treated with siRNA-FAM (A), and FeCO @ SiO2-SS-Chitosan / siRNA-FAM nanoparticles prepared by 1, 2.5 and 5 mg of FeCO @ SiO2- nanoparticles SS-Chitosan

Acknowledgements

This study has been supported by the Biology Department, University of Mohaghegh Ardabili

References

[1] Mu, L. and S. Feng, A novel controlled release formulation for the anticancer drug paclitaxel (Taxol®): PLGA nanoparticles containing vitamin E TPGS. Journal of controlled release, (33-48) (2003) doi:10.1016/S0168-3659(02)00320-6

[2] Dinarvand, R., et al., Polylactide-co-glycolide nanoparticles for controlled delivery of anticancer agents. International journal of nanomedicine, (877) (2011) doi: 10.2147/IJN.S18905

[3] He, Q., et al., Preparation and characteristics of DNA-nanoparticles targeting to hepatocarcinoma cells. World Journal of Gastroenterology, (660) (2004) doi: 10.3748/wjg.v10.i5.660

[4] Mancini, M., et al., Co-targeting the IGF system and HIF-1 inhibits migration and invasion by (triple-negative) breast cancer cells. British journal of cancer, (2865-2873) (2014) doi: 10.1038/bjc.2014.269

[5] Kumar, M., et al., Image-guided breast tumor therapy using a small interfering RNA nanodrug. Cancer research, (7553-7561) (2010) doi: 10.1158/0008-5472.CAN-10-2070

[6] Patil, Y. and J. Panyam, Polymeric nanoparticles for siRNA delivery and gene silencing. International journal of pharmaceutics, (195-203) (2009) doi:10.1016/j.ijpharm.2008.09.039

[7] Peng, S.-F., et al., Novel PEI/Poly-γ-gutamic acid nanoparticles for high efficient siRNA and plasmid DNA co-delivery. Molecules, (86) (2017) doi:10.3390/molecules22010086

[8] Yang, X.-Z., et al., Systemic delivery of siRNA with cationic lipid assisted PEG-PLA nanoparticles for cancer therapy. Journal of controlled release, (203-211) (2011) doi:10.1016/j.jconrel.2011.07.035

[9] Kapse-Mistry, S., et al., Nanodrug delivery in reversing multidrug resistance in cancer cells. Frontiers in pharmacology, (159) (2014) doi:10.3389/fphar.2014.00159

[10] Morris, G.A., et al., Polysaccharide drug delivery systems based on pectin and chitosan. Biotechnology and Genetic Engineering Reviews, (257-284) (2010) doi:10.1080/02648725.2010.10648153

[11] Aranaz, I., R. Harris, and A. Heras, Chitosan amphiphilic derivatives. Chemistry and applications. Current Organic Chemistry, (308-330) (2010)

[12] Yang, X., et al., High-efficiency loading and controlled release of doxorubicin hydrochloride on graphene oxide. The Journal of Physical Chemistry C, (17554-17558) (2008) doi:10.1021/jp806751k

[13] Bulmer, C., A. Margaritis, and A. Xenocostas, Production and characterization of novel chitosan nanoparticles for controlled release of rHu-Erythropoietin. Biochemical engineering journal, (61-69) (2012) doi:10.1016/j.bej.2012.07.007

[14] Patel, J. and N. Jivani, Chitosan based nanoparticles in drug delivery. International journal of pharmaceutical sciences and Nanotechnology, (517-522) (2009) doi:10.37285/ijpsn.2009.2.2.4

[15] Kim, Y.T., et al., Dithiocarbamate chitosan as a potential polymeric matrix for controlled drug release. Drug Development and Industrial Pharmacy, (192-200) (2014) doi:10.3109/03639045.2012.753900

[16] Hauser-Kawaguchi, A.M. and L.G. Luyt, Nanomedicine—nanoparticles in cancer imaging and therapy, in Genomic Instability and Cancer Metastasis. Springer, (205-244) (2015) doi:10.1007/978-3-319-12136-9_10

[17] Taranejoo, S., et al., Chitosan microparticles loaded with exotoxin A subunit antigen for intranasal vaccination against Pseudomonas aeruginosa: An in vitro study. Carbohydrate Polymers, (1854-1861) (2011) doi:10.1016/j.carbpol.2010.10.051

[18] Tan, M.L., P.F. Choong, and C.R. Dass, Cancer, chitosan nanoparticles and catalytic nucleic acids. Journal of Pharmacy and Pharmacology, (3-12) (2009) doi:10.1211/jpp.61.01.0002

[19] Omrani, M.M., M. Ansari, and N. Kiaie, Therapeutic effect of stem cells and nano-biomaterials on Alzheimer's disease. Biointerface Research in Applied Chemistry, (2016)

[20] Zhong, H., et al., Augmentation of adenovirus 5 vector-mediated gene transduction under physiological pH conditions by a chitosan/NaHCO 3 solution. Gene therapy, (232-239) (2011) doi:10.1038/gt.2010.129

[21] Thanh, N.T., Magnetic nanoparticles: from fabrication to clinical applications. CRC press, (2012)

[22] Pearson, R.M., et al., Understanding nano-bio interactions to improve nanocarriers for drug delivery, (2014)

Inhibitory activity of FDA approved Iron oxide nanoparticles on COVID-19 main protease: A computational study

Nahid Shahabadi[1,2*], Saba Zendehcheshm[1,2] & Mohammad Mahdavi[1,2]

[1] Department of Chemistry, Faculty of Chemistry, Razi University, Kermanshah, Iran

[2] Center of Medical Biology Research (MBRC) Kermanshah University of Medical Sciences, Kermanshah, Iran

*Email: nahidshahabadi@yahoo.com

Abstract

The pandemic caused by novel coronavirus disease 2019 (COVID-19) infecting millions of populations worldwide and counting, has demanded quick and potential therapeutic strategies. Current approved drugs or molecules under clinical trials can be a good pool for repurposing through *in-silico* techniques to quickly identify promising drug candidates. In this work, we investigated the potential antiviral activity of Iron oxide nanoparticles (Fe_2O_3 and Fe_3O_4) on SARS-CoV-2 by molecular docking studies. Iron oxide nanoparticles were previously approved by the US food and drug administration (FDA) for anemia treatment and studies have also demonstrated its antiviral activity *in vitro*. Our models revealed that both Fe_2O_3 and Fe_3O_4 interacted efficiently with main protease of SARS-CoV-2. We found that Fe_3O_4 formed a more stable complex with main protease of SARS-CoV-2. We hope the present study should help workers in the field to develop potential vaccines and therapeutics against the novel coronavirus.

Keywords: Fe_2O_3 ; Fe_3O_4; COVID-19 main protease; Molecular Docking.

1. Introduction

The coronavirus (COVID-19) is a newly emerged human-infectious coronavirus (CoV), pandemic and a global health emergency. Unfortunately, at present there is no well-defined treatment or therapeutics against COVID-19 is available but the preventive measures are being recommended worldwide. A new occurred human coronavirus (COVID-19) is informed in December 2019 in Wuhan, China. Rapidly, it has become a global pandemic and spread to other countries such as Republic of Korea, Thailand, Iran, Italy, United States of America, India, etc. Recently, the total number of cases around the world was recorded to be **81**,**743**,**26**2 confirmed cases with more than 1,**783**,**411** deaths (https://www.worldometers.info/coronavirus/). Main protease (Mpro) is the one of the greatest-characterized drug targets among coronaviruses. SARS-CoV-2 uses the viral surface spike glycoprotein to bind to the host cell. After infecting the host cell with its RNA, it forces the host cell to bend and leave free copies of the virus created within the cell (a process known as "budding"). So the virus specific

molecular interaction with the host cell represents a promising therapeutic target for identifying SARS-CoV-2 antiviral drugs. With the available experimental techniques, such selection is a difficult task as they offer lower solution data to study the necessary interactions. In this regard potential in silico methods can be applied to select promising drug molecules with fewer trials and errors effectively reducing time and cost of researchers. [1]. Although there are many efficient antiviral agents in use, they still have drawbacks due to the development of viral resistance and the accumulation within off-target organs leading to adverse effects. Therefore, there is a high demand for discovery of novel strategies to improve the antiviral therapies to control or limit the spread of viral infections. Abo-zeid *et al.*[2] reported the interaction of Iron oxide nanoparticles (Fe_2O_3 and Fe_3O_4) with the spike protein receptor binding domain (S1-RBD) of SARS-CoV-2 that is required for virus attachment to the host cell receptors by molecular docking studies. Iron oxide nanoparticles were previously approved by the US food and drug administration (FDA) for anemia treatment [3] and studies have also demonstrated its antiviral activity *in vitro*. In this study, we tried to understand the mechanism of Iron oxide nanoparticles (Fe_2O_3 and Fe_3O_4) against main protease of SARS-CoV-2 by molecular docking simulation.

2. Material and Methods

2.1 Molecular docking

To perform blind docking calculations AutoDock Vina [۶] with MGL tools 1.5.4 were used. It has been reported that AutoDock Vina 4.2 program performs more accurate docking calculations and also performs faster that AutoDock software [٦]. The SARS-CoV-2 main protease was used as the receptor and downloaded from Protein Data Bank (PDB ID: 6LU7). Coordinate of Fe_3O_4 and Fe_2O_3 was obtained from the American Mineralogist Crystal Structure Database and was selected as a model of NPs. We put the receptor in a 64×66×64 box directions and grid spacing of 1.00 Å with grid set centers of -26.28**,** 12.61 and 58.96. We used the BIOVIA Discovery Studio software to do the visualization of docked.

3. Results and Discussions

3.1 Docking of Fe_2O_3 and Fe_3O_4 against SARS-CoV-2 protease

Molecular docking of Fe_2O_3 and Fe_3O_4, with the SARS-CoV-2 protease was performed and, Iron oxide nanoparticles showed a binding energy of -8.4 kcal/mol and -9.1 kcal/mol, respectively. The docked ligand molecules with the protease are shown in Figures 1 and 2. The hydrogen bonding and electrostatic interactions between SARS-CoV-2 protease and Iron oxide nanoparticles are presented in Table 1 and 2. The binding free energy of Fe_3O_4 (-9.1 Kcal/mol) is lower than Fe_2O_3 (-8.4 Kcal/mol) indicating the higher stability of the Fe_3O_4 protease complex. Thus, protease of SARS-CoV-2 favors interaction with Fe_3O_4 over Fe_2O_3. The interaction of

Fe_3O_4 with protease of SARS-CoV-2 involved the formation of thirteen hydrogen bonds, with a total intermolecular energy of -9.1 Kcal/mol. In addition, electrostatic interaction of Fe_3O_4 was detected with HIS41 (Table 2). In contrast, Fe_2O_3 interactions involved the formation of twenty four hydrogen bonds with a total intermolecular energy of -8.4 Kcal/mol. The docked structures (Figures 1 and 2) show the binding region of the protease of SARS-CoV-2 - Iron oxide nanoparticles complex is surrounded by amino acid residues HIS164, GLU166, GLN189, MET165, GLU166, THR190, GLN192, GLN189, HIS41, SER46, CYS44, THR24, THR25, THR45, and GLY143. Our results reveal that Iron oxide nanoparticles could be a promising candidate to be considered either for antiviral therapy or for infection prevention and control. To be used in antiviral therapy a major challenge is their large-scale manufacture and their safety profile *in vivo*. Fortunately, Iron oxide nanoparticles manufacturing at industrial scale has been established and these have been FDA approved. We hope our recent study should help workers in the field to develop potential vaccines and therapeutics against SARS-CoV- 2 virus.

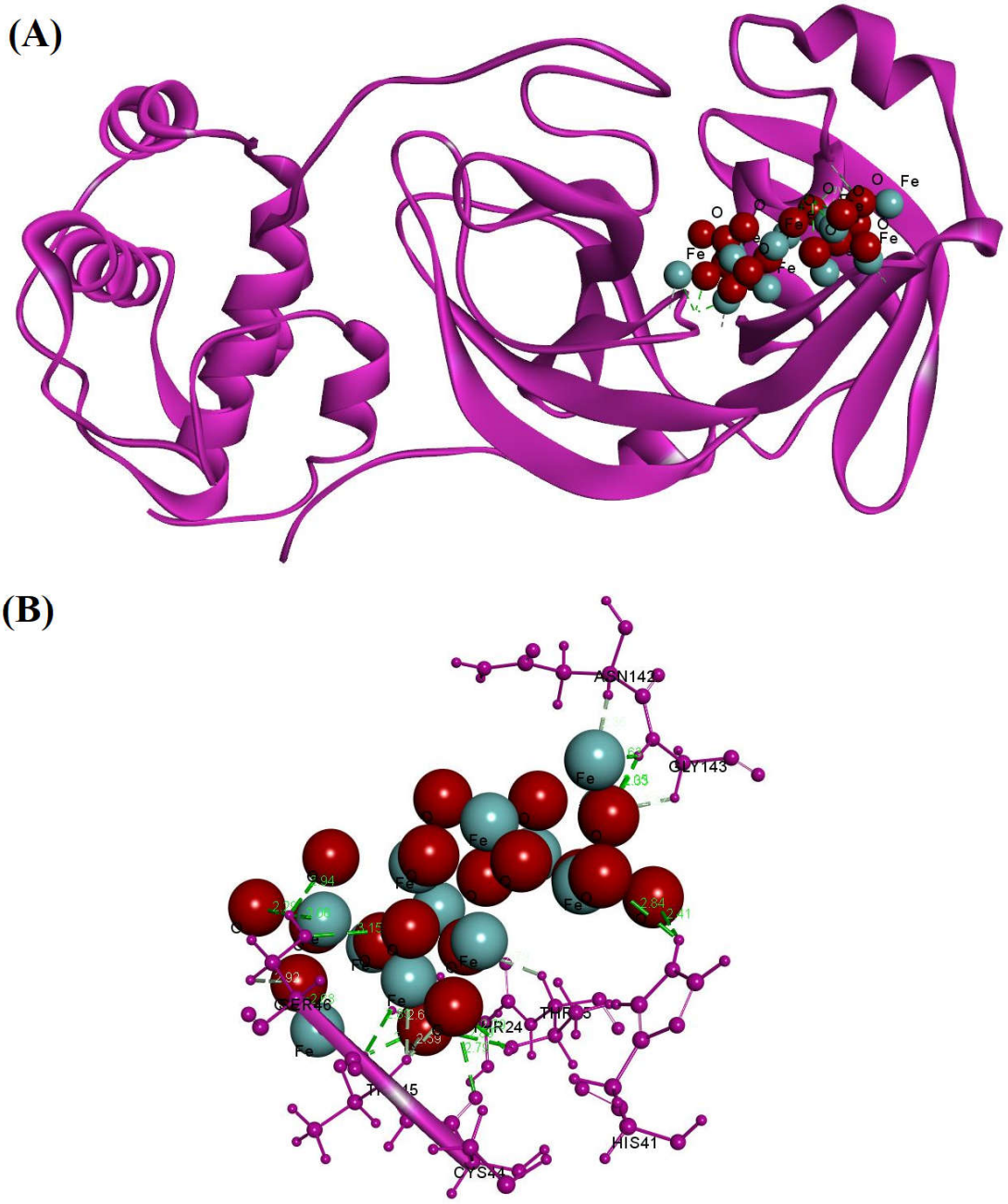

Fig. 1 Molecular docking perspective of Fe_2O_3 – SARS-CoV-2 main protease.

Table 1. Predicted bonds between interacting atoms of Fe_2O_3 – SARS-CoV-2 main protease.

S. No.	Amino acid	Amino acid atom	Fe_2O_3 atom	Distance	Nature of interaction
١	THR25	H-Acceptor	O (H-Donor)	2.89	Hydrogen Bond
٢	SER46	H-Acceptor	O (H-Donor)	٣,١٥	Hydrogen Bond
٣	CYS44	H-Acceptor	O (H-Donor)	٢,٧٩	Hydrogen Bond
٤	THR24	H-Donor	O(H-Acceptor)	١,٨٦	Hydrogen Bond
٥	THR25	H-Donor	O(H-Acceptor)	٢,٢٨	Hydrogen Bond
٦	HIS41	H-Donor	O(H-Acceptor)	٢,٤١	Hydrogen Bond
٧	HIS41	H-Donor	O(H-Acceptor)	٢,٨٤	Hydrogen Bond
٨	THR45	H-Donor	Fe(H-Acceptor)	٢,٨٩	Hydrogen Bond
٩	THR45	H-Donor	O(H-Acceptor)	٢,١٢	Hydrogen Bond
١٠	SER46	H-Donor	O(H-Acceptor)	٢,٦٨	Hydrogen Bond
١١	SER46	H-Donor	O(H-Acceptor)	٢,٩٤	Hydrogen Bond
١٢	SER46	H-Donor	Fe(H-Acceptor)	٢,٠٦	Hydrogen Bond
١٣	SER46	H-Donor	O(H-Acceptor)	٢,٢٩	Hydrogen Bond
١٤	GLY143	H-Donor	Fe(H-Acceptor)	٢,٠٥	Hydrogen Bond
١٥	GLY143	H-Donor	Fe(H-Acceptor)	٢,٦٣	Hydrogen Bond
١٦	GLY143	H-Donor	O(H-Acceptor)	٢,٣٣	Hydrogen Bond

١٧	THR24	H-Donor	Fe(H-Acceptor)	٢,٨٤	Hydrogen Bond
١٨	THR25	H-Donor	O(H-Acceptor)	٢,٧٩	Hydrogen Bond
١٩	THR45	H-Donor	Fe(H-Acceptor)	٢,٦٩	Hydrogen Bond
٢٠	THR45	H-Donor	O(H-Acceptor)	٢,٥٩	Hydrogen Bond
٢١	THR45	H-Donor	O(H-Acceptor)	٢,١٣	Hydrogen Bond
٢٢	SER46	H-Donor	O(H-Acceptor)	٢,٩٢	Hydrogen Bond
٢٣	ASN142	H-Donor	Fe(H-Acceptor)	٢,٣٦	Hydrogen Bond
٢٤	GLY143	H-Donor	Fe(H-Acceptor)	٢,٣١	Hydrogen Bond

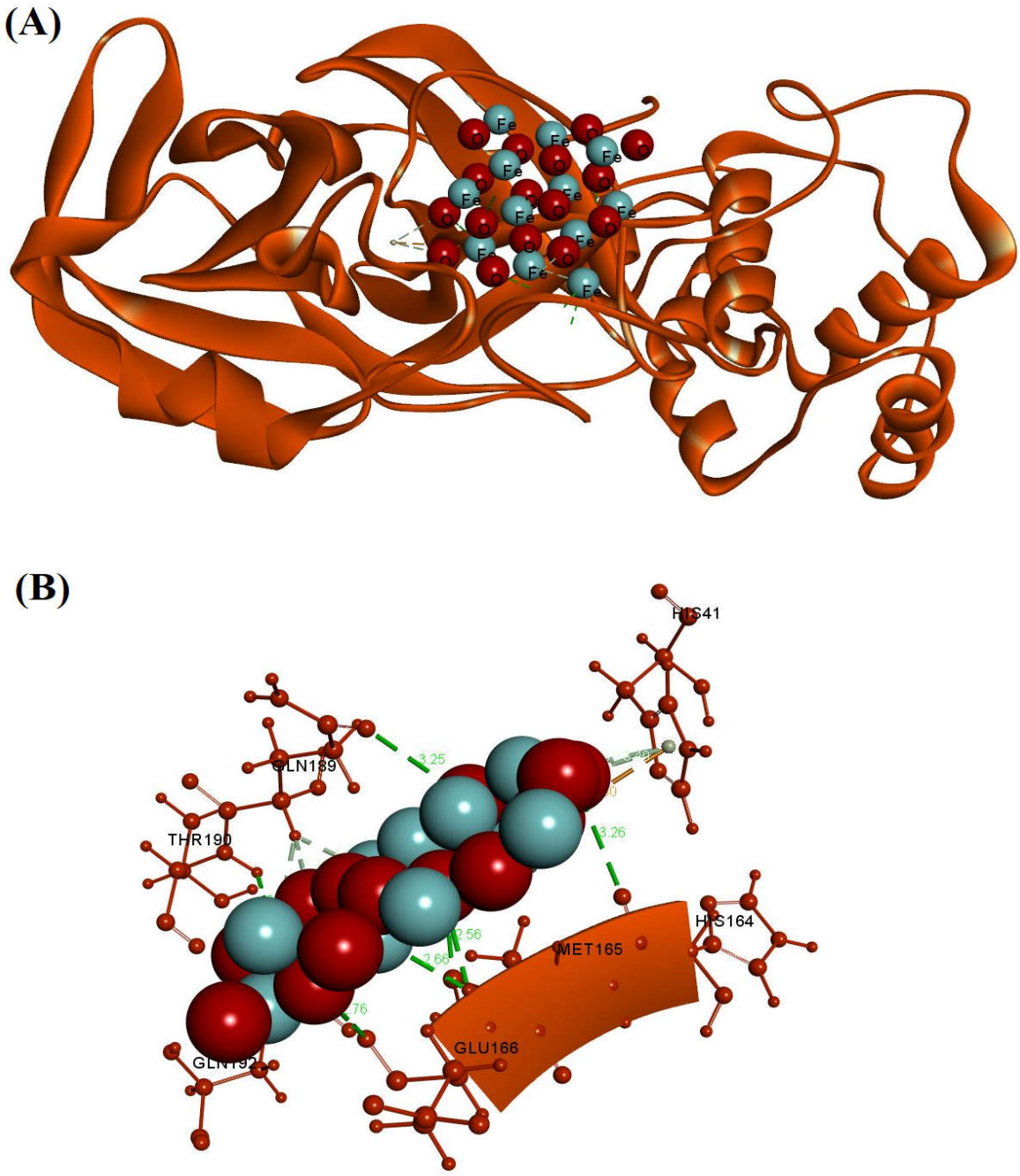

Fig. 2 Molecular docking perspective of Fe_3O_4 – SARS-CoV-2 main protease.

Table 2. Predicted bonds between interacting atoms of Fe_3O_4 and SARS-CoV-2 main protease.

S. No.	Amino acid	Amino acid atom	Fe_3O_4 atom	Distance	Nature of interaction
١	HIS164	H-Acceptor	O (H-Donor)	3.26	Hydrogen Bond
٢	GLU166	H-Acceptor	O (H-Donor)	2.76	Hydrogen Bond
٣	GLN189	H-Acceptor	O (H-Donor)	3.25	Hydrogen Bond
٤	MET165	H-Acceptor	O (H-Donor)	٣,٧٥	Hydrogen Bond
٥	GLU166	H-Donor	Fe(H-Acceptor)	٢,٦٦	Hydrogen Bond
٦	GLU166	H-Donor	O(H-Acceptor)	٢,٥٦	Hydrogen Bond
٧	THR190	H-Donor	Fe(H-Acceptor)	٢,٥٤	Hydrogen Bond
٨	GLN192	H-Donor	Fe(H-Acceptor)	٢,٥٧	Hydrogen Bond
٩	GLN189	H-Donor	Fe(H-Acceptor)	٢,٢٧	Hydrogen Bond
١٠	GLN189	H-Donor	Fe(H-Acceptor)	٢,٧٤	Hydrogen Bond
١١	GLN189	H-Donor	O(H-Acceptor)	٢,٢٩	Hydrogen Bond
١٢	HIS41	Pi-Orbital	Fe(Negative)	٤,٨٠	Electrostatic
١٣	HIS41	Pi-Orbital	O (H-Donor)	٣,٤٠	Hydrogen Bond
١٤	HIS41	Pi-Orbital	O (H-Donor)	٣,٤٢	Hydrogen Bond

Conclusion

In this study, we investigated the potential antiviral activity of Iron oxide nanoparticles (Fe_2O_3 and Fe_3O_4) on SARS-CoV-2 by molecular docking studies. Our models revealed that both Fe_2O_3 and Fe_3O_4 interacted efficiently with SARS-CoV-2 protease. We found that Fe_3O_4 formed a more stable complex with SARS-CoV-2 protease. The present molecular docking simulation studies suggest that the Iron oxide nanoparticles may have considerable

effect on structure protease of SARS-COV-2, which may lead to significant inhibitory effect.Therefore, these nanoparticles might be tested *in vivo* as a potent and promising drug against COVID-19.

Acknowledgements

The authors thank the Razi University Research Council for support of this work.

References

[1] N. Baildya, N.N. Ghosh, A.P. Chattopadhyay., Inhibitory activity of hydroxychloroquine on COVID-19 main protease: An insight from MD-simulation studies, Journal of Molecular Structure 2 (2020) 128595. doi:10.1016/j.molstruc.2020.128595.

[2] Y. Abo-Zeid, N.S. Ismail, G.R. McLean, N.M. Hamdy., A molecular docking study repurposes FDA approved iron oxide nanoparticles to treat and control COVID-19 infection, European Journal of Pharmaceutical Sciences 153 (2020) 105465. doi:10.1016/j.ejps.2020.105465

[3] D.W. Coyne., Ferumoxytol for treatment of iron deficiency anemia in patients with chronic kidney disease□, Expert opinion pharmacotherapy 15(2009) 2563–2568. doi:10.1517/14656560903224998

[4] N. Muralidharan, R. Sakthivel, D. Velmurugan, M.M. Gromiha., Computational studies of drug repurposing and synergism of lopinavir, oseltamivir and ritonavir binding with SARS-CoV-2 Protease against COVID-19, Journal of Biomolecular Structure and Dynamics 14(2020) 1-6. doi:10.1080/07391102.2020.1752802

[5] O. Trott, A.J. Olson., AutoDock Vina: improving the speed and accuracy of docking with a new scoring function, efficient optimization, and multithreading, Journal of Computational Chemistry 31 (2010) 455-461. doi:10.1002/jcc.21334

[6] S. Shahraki, F. Shiri, H. Mansouri-Torshizi, J. Shahraki., Characterization of the interaction between a platinum(II) complex and human serum albumin: spectroscopic analysis and molecular docking, Journal of the Iranian Chemical Society 13 (2016) 723–731. doi:10.1007/s13738-015-0784-8

The effects of Lactobacillus casei ATCC: 39392 on acetaminophen-induced hepatorenal toxicity in male Wistar rats

Seyed Ali Alavi[1], Amir Abbas Barzegari[1*] Seyed Babak Khalifeh Zadeh Kaleybar[2], Maryam Naseri[1]

[1]Department of Biology, University of Maragheh, Maragheh, East Azerbaijan, Iran.

[2]Department of Pathology, Islamic Azad University, Tabriz Branch, Tabriz, Iran.

* Email: barzegaridoctora@gmail.com

Abstract

Acetaminophen is one of the most widely used drugs in pain treatment. However, high dose of this drug may cause hepatorenal toxicity. The purpose of present research was to investigate the effects of pre-treatment with *Lactobacillus casei (ATCC: 39392)* on acetaminophen-induced toxicity in male rats. We randomly allocated twenty male Wistar rats to four groups of five. One control group that received saline, one acetaminophen group that received single high dose of this drug, one probiotic group that received *L. casei* for 21 days, and one experimental group that after 21 days treatment with the bacterium received a single high-dose acetaminophen. Twenty-four hours after the acetaminophen injection (day 22), all the animals were deeply anesthetised, and their serum were harvested for later analysis. The results showed that single high-dose acetaminophen could induce hepatorenal toxicity. This was showed with high levels of aminotransferases, urea, and creatinine in the serum of the rats. Moreover, pre-treatment with this strain of *L. casei* could prevent of renal but not liver toxicity in Wistar rats. The reason was the significantly lower levels of urea and creatinine in the rats that received pre-treatment of the bacterium before receiving the high-dose acetaminophen compared to the acetaminophen group. The bacterium by itself had no significant effect on liver enzymes, urea and creatinine. In conclusion, this bacterium may be useful to prevent renal toxicity by high doses of acetaminophen.

Keywords: Acetaminophen, liver, Kidney, toxicity, *Lactobacillus casei*, rats

1. Introduction

Acetaminophen, also called Paracetamol or N-acetyl-para-aminophenol (APAP), as a non-steroidal anti-inflammatory drug (NSAID), was first used clinically by von Mering in 1887 [1]. APAP commonly is prescribed as an analgesic and antipyretic drug [2]. APAP is available by prescription or over the counter (OTC). Millions of people use this over the counter pain reliever every day to treat minor aches and pains. APAP produces analgesic effects by inhibiting cyclooxygenase (COX) enzymes that catalyse the conversion of arachidonic acid (a fatty acid in cell membranes) to prostaglandins that produce pain, inflammation, and fever [3]. Examination of APAP metabolism shows that, glucuronyl transferases/sulfotransferases directly conjugate a large portion of the therapeutic dose of APAP. The remaining part is converted to a reactive metabolite, N-acetyl-p-benzoquinone

imine (NAPQI), by cytochrome P450 2E1 (CYP2E1) [6]. NAPQI forms a glutathione (GSH) adduct that is excreted in bile leading to depletion of hepatocellular GSH. After exhaustion of GSH, the remaining NAPQI reacts with other cellular proteins. Binding of NAPQI to mitochondrial proteins is the key initiator of APAP-induced cell death, leading to liver toxicity [7]. Therefore, oxidative stress plays a key role in APAP-induced oxidative stress. APAP is generally safe at recommended doses, but if taken in larger dosages or frequency, it can cause serious and even fatal liver damage [3]. High doses of APAP can also induce life-threatening kidney lesions [2]. As oxidative stress plays a key role in acetaminophen toxicity, dietary antioxidants may have a protective role against the acetaminophen-induced toxicity [8]. Previous research has shown that some strains of probiotic bacteria may have antioxidant properties [[4],[5]]. The World Health Organization defines probiotics as live microorganisms which, when administered in adequate amounts, confer a health benefit on the host [10, 11]. Lactic acid bacteria (LAB) are one of the most important groups of probiotics. These bacteria produce lactic acid by fermenting sugars. LABs are believed to play a leading role in preservation of the health benefit of the host. Several genera and species such as Lactobacillus and Bifidobacteria spp. showed various nutritional and therapeutic benefits [12]. The effects of probiotics depend on the strain that is used [14]. Thus, the aim of the present study was to study the preventive effect of *Lactobacillus casei (ATCC: 39392)* against APAP-induced hepatorenal toxicity in male Wistar rats.

2. Material and Methods

2.1 Animals

Twenty male Wistar rats weighing 220–250 g were purchased from pasture institutes and were transported to the animal house of the University of Maragheh. The rats were housed, four per cage. Animals were maintained under a 12/12 h light/dark cycle at an optimum temperature (22 ± 2 °C) and had free access to food and water. Rats were adapted for one week before the treatments. All experiments were carried out in conformity with international guidelines for the care and use of laboratory animals that were approved by a local ethical committee at the University of Maragheh.

2.2 Preparation of Bacterial strain

The Lactic acid bacterial strain, *Lactobacillus casei ATCC:39392* was purchased from Iranian Research Organization for Science and Technology (IROST). The strain was cultured in de Man Rogosa Sharpe (MRS) broth (Ibresco, Iran), incubated at 37 °C for 16-18 h in anaerobic jars and centrifuged (Eppendorf 5810r) at 4000 rpm for 20 min at 4 °C. Then the cultured supernatant was removed, and the live bacterial sediment immediately moved to sterile normal saline. In continue the tubes containing a dose of 1×10^9 colony forming units [CFU] per 0.5 ml were prepared under sterile conditions. For preparing those number of bacteria, we prepared different

dilution of bacterial suspensions using standard growth curve using light absorption at OD_{600} by spectrophotometer (Shimadzu Uv 1800).

2.3 Experimental design

The animals randomly were divided into four groups of five. The first group comprises control animals that received normal saline in all days of treatment. The rats in the second group received Lactobacillus casei ATCC: 39392 suspension, 1×10^9 colony forming units [CFU]/ rats for 21 days. The animals in the third group received a single overdose of APAP (Sigma-Aldrich ®) (1 g/kg b.w) on the twenty-first day. Finally, the rats in the fourth group received the *Lactobacillus casei ATCC: 39392* suspension, 1×10^9 colony forming units [CFU]/ rats for 21 days and a single overdose of APAP (1 g/kg b.w) in the last day of trial [12]. Both drug and bacterial suspension was administered orally by gavage through an intragastric tube. After 24 h of APAP administration, all the rats were sacrificed, and sampling of serum were conducted.

2.4 Collection and analysis of serum

On the last day of the experiment, all the animals were anesthetized with administration ketamine (80 mg/kg b.w) and xylazine (20 mg/kg b.w). Blood samples were obtained by cardiac puncture and were collected into tubes. After coagulation of the blood samples, at room temperature, the samples were centrifuged at 2000 rpm for 15 min and serum collected for later analysis. The serum samples were analyzed using an auto-analyzer (BT 1500, Italy and Biolis 50i, Japan). The following parameters were tested: urea, creatinine, alkaline phosphatase total (ALP), alanine transaminase (ALT), aspartate transaminase (AST).

2.5 Statistical analysis

Data were analyzed using SPSS software. One-way ANOVA and LSD post hoc tests were used to determine any significant difference between the groups. The results showed as mean±SEM, and $P<0.05$ considered as significant.

3. **Results and Discussions**

3.1 Effects of Lactobacillus casei ATCC: 39392 on liver enzymes

SPSS analysis showed that the liver enzyme in the group that received acetaminophen were significantly higher than these factors in the control group. Moreover, pre-treatment of the rats with the probiotic bacterium had nonsignificant reducing effects on AST and ALT (table 1).

3.2 Effects of Lactobacillus casei ATCC: 39392 on urea and creatinine

Analysis of urea and creatinine showed that, compared to the control group, these factors were significantly higher in the acetaminophen group. Moreover, pre-treatment with *Lactobacillus casei ATCC: 39392* could prevent of the elevation of urea and creatinine in the serums of the rats, significantly (table 1).

3.3 Conclusion

These data show that *Lactobacillus casei ATCC: 39392* may have preventive effects on acetaminophen-induced renal but not hepatic toxicity in male Wistar rats. Acetaminophen exerts its toxic effects through oxidative stress [[9],[13]]. Therefore, the preventive effects of this bacterium on the renal toxicity by high-dose acetaminophen may because of antioxidant effects of *Lactobacillus casei ATCC: 39392*. However, this theory needs more investigations in the future.

Table 1. Effects of L. casei on serum parameters of rats. ** shows P<0.01 compared to acetaminophen group. + and ++ show the P<0.05 and P<0.01 compared to control group, respectively.

Group	**ALP (U/L)**	**ALT (U/L)**	**AST (U/L)**	**Urea (mg/dl)**	**Creatinine (mg/dl)**
control	664±59	41,5±4.7	130.5±21.6	21.6±2	**0.65±0.2**
probiotic (1×10^9 CFU/rat)	671±147	72.5±10.40	188.5± 18	37.5±1.9	**0.52±0.16**
acetaminophen	+ 724±86	++ 353±14.8	++ 309.4±65	++ 60.6±2.2	++ **0.90±0.4**
Probiotic + acetaminophen	++ 736±54	166±16.6	228.4±70	** 45.6.5±2	** **0.74±0. 5**

Acknowledgements

We thank the University of Maragheh for establishment of the animal house for animal research.

References

[1] X. Wang., et al., Paracetamol: overdose-induced oxidative stress toxicity, metabolism, and protective effects of various compounds in vivo and in vitro., Drug metabolism reviews 49 (4) (2017) **49**(4) 395-437. doi:10.1080/03602532.2017.1354014

[2] M.S. Reshi, et al., Acetaminophen-induced renal toxicity: preventive effect of silver nanoparticles., Toxicology Research 9 (4) (2020) 406-412. doi:10.1093/toxres/tfaa040

[3] T. Long, M. Nichols, and J. O'Toole., Acetaminophen: When It Becomes Dangerous.

[4] S. De Marco., et al., Probiotic cell-free supernatants exhibited anti-inflammatory and antioxidant activity on human gut epithelial cells and macrophages stimulated with LPS., Evidence-Based Complementary and Alternative Medicine (2018). doi: 10.1155/2018/1756308

[5] Y. Xu., et al., Preparation of a probiotic rice tablet: Sensory evaluation and antioxidant activity during gastrointestinal digestion., LWT 124 (2020) 108911. doi: 10.1016/j.lwt.2019.108911.

[6] F.J Gonzalez, Role of cytochromes P450 in chemical toxicity and oxidative stress: studies with CYP2E1., Mutation Research/Fundamental and Molecular Mechanisms of Mutagenesis 569 (1-2) (2005) 101-110. doi:10.1016/j.mrfmmm.2004.04.021

[7] H. Jaeschke, C. Cover, and M.L. Bajt., Role of caspases in acetaminophen-induced liver injury., Life sciences 78 (15) (2006) 1670-1676. doi:10.1016/j.lfs.2005.07.003

[8] S. Segawa, et al., Oral administration of heat-killed Lactobacillus brevis SBC8803 ameliorates alcoholic liver disease in ethanol-containing diet-fed C57BL/6N mice., International journal of food microbiology., 128 (2) (2008). **128**(2) 371-377. doi:10.1016/j.ijfoodmicro.2008.09.023

[9] M. I. Yousef, et al., Potential protective effects of quercetin and curcumin on paracetamol-induced histological changes, oxidative stress, impaired liver and kidney functions and haematotoxicity in rat., Food and Chemical Toxicology 48 (11) (2010) 3246-3261. Doi: 10.1016/j.fct.2010.08.034

[10] D. Gawkowski, M. Chikindas., Non-dairy probiotic beverages: the next step into human health., Beneficial microbes 4 (2) (2013) 127-142. doi: 10.3920/BM2012.0030

[11] A.C.P Hotel, A. Cordoba., Health and nutritional properties of probiotics in food including powder milk with live lactic acid bacteria., Prevention 5 (1) (2001) 1-10.

[12] M. Song, et al., Characterization of selected Lactobacillus strains for use as probiotics., Korean journal for food science of animal resources 35 (4) (2015) 551. doi:10.5851/kosfa.2015.35.4.551

[13] F. Almeida, B. Nunes., Effects of acetaminophen in oxidative stress and neurotoxicity biomarkers of the gastropod Phorcus lineatus., Environmental Science and Pollution Research 26 (10) (2019) 9823-9831. doi:10.1007/s11356-019-04349-1

[14] Y. Ohashi, K. Ushida., Health□beneficial effects of probiotics: Its mode of action., Animal Science Journal 80 (4) (2009) 361-371. doi:10.1111/j.1740-0929.2009.00645.x

RNA Mutations in Gastric Cancer

Mehrdad Nasrollahzadeh Sabet[1], Arezoo Farhadi[2] and Javad Behroozi[1*]

[1] Department of Genetics and Biotechnology, School of Medicine, AJA University of Medical Sciences, Tehran, Iran.

[2] Department of Genetics and Biotechnology, Faculty of Life Science, Varamin- Pishva Branch, Islamic Azad University, Varamin, Iran.

*Email: jvdbehroozi@gmail.com

Abstract

Gastric cancer (GC) is the second most common cancer worldwide and it is responsible for approximately 700,000 deaths annually. GC is biologically and genetically heterogeneous and its pathogenesis is carried out by cumulative effects of genetic and environmental factors. RNA editing is a widespread modification mechanism that allows specific nucleic changes at the RNA level without affecting the corresponding DNA sequence. The edited nucleotide acts like guanosine and confers characteristics of A to G mutation. RNA-seq raw data of eight primary gastric adenocarcinomas and their adjacent normal tissue were retrieved from the Gene Expression Omnibus (GEO) database. After pre-processing of raw reads, several stringent filtering steps were employed to increase the accuracy of identifying true A to G editing sites. Among the 12362 editing sites, 4868 sites were found within both normal and cancer samples. From the remaining sites, 3985 and 3509 editing sites were specific to normal and cancer tissues, respectively. The 3´UTR was the most edited region, with 5870 editing sites, followed by the upstream regions. Editome of gastric cancer vastly differs from adjacent normal tissue. Depending on genomic location and level of editing, these editing events could lead to cancer initiation and development.

Keywords: Editome, ADARs, Gastric Cancer, RNA editing.

1. Introduction

GC is the second most common cancer worldwide, with a variable frequency in different countries [1] and it is responsible for approximately 700,000 deaths annually. This means the case-fatality ratio of this cancer is much higher than other common cancers like colorectal, prostate, and breast cancer [2]. This cancer is biologically and genetically heterogeneous with an unclear molecular mechanism [3]. Both genetic and environmental factors have important causal roles in GC pathogenesis. Diagnosis of GC is frequently made when the disease is at an advanced stage because disease-related symptoms often appear late or are atypical during cancer progression. Because of late diagnosis most patients are symptomatic at the time of diagnosis [4].

RNA editing is a widespread post-transcriptional and/or co-transcriptional modification mechanism that allows specific nucleic changes at the RNA level without affecting the corresponding DNA sequence [5]. Deamination of A to I is the most common type of RNA editing. The reaction catalyzed by a family of enzymes named ADARs (Adenosine Deaminases Acting on RNA) and the result is an RNA mutation. The edited nucleotide acts like guanosine and confers characteristics of A to G mutation [6]. In this study, we aimed to explore editome of patients with gastric cancer.

2. Material and Methods

2.1 Pre-processing of RNA-seq data

RNA-seq raw data of eight primary gastric adenocarcinomas and their adjacent normal tissue were retrieved from the Gene Expression Omnibus (GEO) database. These data are publicly available with accession number GSE85465. The original data and sample details are described by Ooi et al. [7]. We used FastQC and Trimmomatic tools for quality control and quality trimming of raw reads [8, 9]. Hisat2 software was employed to the alignment of raw reads to the human reference genome [10]. To exclude PCR duplicates MarkDuplicates tool from the Picard package was used. The GATK tool was employed to improve the quality of reads and the alignment of the indel flanking regions.

2.2 Systematic detection of RNA editing sites

RNA-DNA differences (RDDs) were called using the HaplotypeCaller [11]. The identified RDDs were removed from further analysis if they corresponded to known SNPs found in Ensembl human SNP database version 151. Several stringent filtering steps were employed to increase the accuracy of identifying true RNA editing sites. A to G and editing sites were kept for further analysis and other non-canonical editing sites were excluded.

3. Results and Discussions

3.1 Distribution of editing sites

Next-generation sequencing technology has facilitated the identification of RNA editing sites across genomic regions, however, the main obstruction is the identification of true RNA editing sites from rare SNPs and sequencing or alignment errors. To accurately detect the RNA editing sites at the genome-wide level in gastric cancer, we developed a computational approach by using a precise strategy. We found 12362 RNA editing sites across the genome. The location of editing sites was annotated according to the Ensembl database. Investigation

of the genomic distribution of editing sites showed that the number of RNA editing sites were greatly varied across genomic regions. Overall, the 3´UTR was the most edited region, with 5870 editing sites, followed by the upstream. The number of editing events in different genomic regions has been shown in Figure 1.

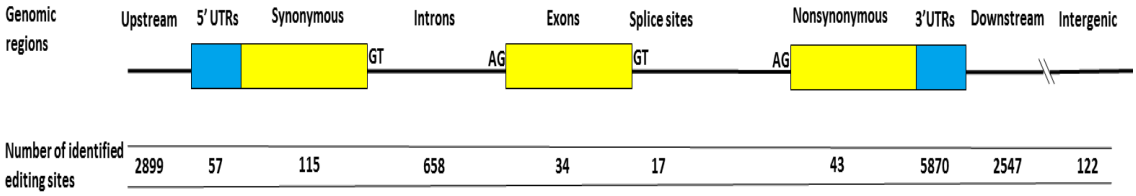

Figure 16. Distribution of RNA editing sites in different genomic sequences

3.2 Tissue-specific editing sites

Among the 12362 editing sites, 4868 sites were found within both normal and cancer samples. From the remaining sites, 3985 and 3509 editing sites were specific to normal and cancer tissues, respectively. Statistical analysis revealed 285 differentially edited events among common editing sites. Notably, 129 cancer-specific and 173 normal-specific editing sites were found to be differentially edited (Figure 2).

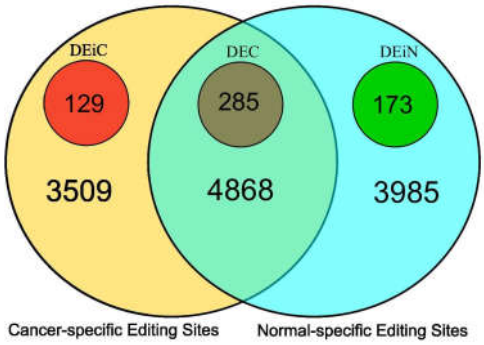

Figure 17. Number of tissue-specific and common editing sites

Gastric cancer initiation and progression caused by different molecular alterations, RNA editing is a widespread post-transcriptional mechanism and could be part of these disruptions. Editome of gastric cancer vastly differs from adjacent normal tissue in terms of the number of editing sites. Depending on genomic location and level of editing, these editing events could lead to cancer initiation and development.

References

[1] Dicken, B.J., et al., Gastric adenocarcinoma: review and considerations for future directions. Annals of surgery, 2005. 241(1): p. 27.

[2] Power, D.G., D.P. Kelsen, and M.A. Shah, Advanced gastric cancer–slow but steady progress. Cancer treatment reviews, 2010. 36(5): p. 384-392.

[3] Matsuoka, T. and M. Yashiro, Biomarkers of gastric cancer: Current topics and future perspective. World journal of gastroenterology, 2018. 24(26): p. 2818.

[4] Ren, W., et al., A tumor-specific prognostic long non-coding RNA signature in gastric cancer. Medical Science Monitor: International Medical Journal of Experimental and Clinical Research, 2016. 22: p. 3647.

[5] Wang, Y., et al., Systematic characterization of A-to-I RNA editing hotspots in microRNAs across human cancers. Genome research, 2017. 27(7): p. 1112-1125.

[6] Chan, T.H.M., et al., A disrupted RNA editing balance mediated by ADARs (Adenosine DeAminases that act on RNA) in human hepatocellular carcinoma. Gut, 2014. 63(5): p. 832-843.

[7] Ooi, W.F., et al., Epigenomic profiling of primary gastric adenocarcinoma reveals super-enhancer heterogeneity. Nature communications, 2016. 7: p. 12983.

[8] Shafiei, H., M. Bakhtiarizadeh, and A. Salehi, Large-scale potential RNA editing profiling in different adult chicken tissues. Animal genetics, 2019. 50(5): p. 460-474.

[9] Bolger, A.M., M. Lohse, and B. Usadel, Trimmomatic: a flexible trimmer for Illumina sequence data. Bioinformatics, 2014. 30(15): p. 2114-2120.

[10] Kim, D., B. Langmead, and S.L. Salzberg, HISAT: a fast spliced aligner with low memory requirements. Nature methods, 2015. 12(4): p. 357.

[11] DePristo, M.A., et al., A framework for variation discovery and genotyping using next-generation DNA sequencing data. Nature genetics, 2011. 43(5): p. 491.

Correlation of CDH1 mutation status with gene expression in gastric cancer

Mehrdad Nasrollahzadeh Sabet[1], Arezoo Farhadi[2] and Javad Behroozi[1*]

[1] Department of Genetics and Biotechnology, School of Medicine, AJA University of Medical Sciences, Tehran, Iran.

[2] Department of Genetics and Biotechnology, Faculty of Life Science, Varamin- Pishva Branch, Islamic Azad University, Varamin, Iran.

*Email: jvdbehroozi@gmail.com

Abstract

Gastric cancer (GC) is the fourth most common cancer and the third leading cause of cancer mortality worldwide with obscure etiology and pathogenesis. Both genetic and environmental factors are associated with GC pathogenesis. Gene mutations in stomach epithelial cells are major genetic causes for gastric cancer. CDH1 is the most mutated gene in GC, which encodes the E-cadherin protein. E-cadherin is a calcium-dependent cell-cell adhesion protein playing a crucial role in maintaining the structure and function of epithelial tissues. Disruption in gene expression regulation is another characteristic of GC. However, the relation between CDH1 mutation status and gene expression in GS is mainly unknown. This study aims to investigate the correlation of CDH1 mutation status and gene expression profile in GS. The muTarget platform was used to explore the relation of CDH1 mutation status and its expression level, which is an online portal to identify genes with altered expression in relation to a given mutation. In the second step, we investigated the gene expression profile of 372 GC patients to identify altered expression in samples harboring CDH1 mutated genes. Our results showed 10 genes with significant alteration of expression level in CDH1 mutated patients. Nine of these genes were upregulated. TMEM119 was the most upregulated gene in GC patients followed by COL16A1, OMD, PRRX1, PCOLCE, EMILIN1, CYP1B1, S1PR2, and GAS1. Interestingly, C5orf34 showed downregulation in CDH1 mutated GC patients. We also found that mutation in the CDH1 gene leads to its downregulation. In conclusion, our bioinformatics analysis provides a list of 10 genes that are significantly dysregulated in GC patients with mutated CDH1. These genes may be potentially involved in the invasion, metastasis, and carcinogenesis of GC.

Keywords: Gastric cancer, CDH1, gene expression, mutation.

1. Introduction

Gastric cancer (GC) is the fourth most common cancer and the third leading cause of cancer mortality worldwide with obscure etiology and pathogenesis. GC is also the most commonly diagnosed cancer in the world

[1]. Recent studies show a significant reduction in 5-year mortality of GC, thanks to the development of gastrointestinal endoscopy and surgical technique. However, in advanced gastric cancer, the 5-year mortality is 30 to 50 percent [2]. Both genetic and environmental factors are associated with GC pathogenesis [3]. Helicobacter pylori infection is one of the main environmental risk factors for the development of gastric cancer. On the other hand gene mutations in the stomach, epithelial cells are major genetic causes for gastric cancer [4]. CDH1 is the most mutated gene in GC, which encodes the E-cadherin protein. E-cadherin is a calcium-dependent cell-cell adhesion protein playing a crucial role in maintaining the structure and function of epithelial tissues [5]. Down-regulation of CDH1 reduces cell-cell adhesions, making it possible for tumor cells to dissociate from primary tissue, invade surrounding tissues, and metastasis to other sites [6].

Gene expression profiling of gastric cancer has increased our understanding of the heterogeneous biology of this disease and promises to impact clinical care. Disruption in gene expression regulation is characteristic of GC and other cancers [7]. However, the relation between CDH1 mutation status and gene expression in GS is mainly unknown. This study aims to investigate the correlation of CDH1 mutation status and gene expression profile in GS.

2. Material and Methods

We used muTarget platform in order to explore the relation of CDH1 mutation status and its expression level, which is an online portal to identify genes with altered expression in relation to a given mutation [8]. In the second step, we investigated the gene expression profile of 372 GC patients to identify altered expression in samples harboring CDH1 mutated genes.

3. Results and Discussions

Our results showed 10 genes with significant alteration of expression level in CDH1 mutated patients. Nine of these genes were upregulated. TMEM119 was the most upregulated gene in GC patients followed by COL16A1, OMD, PRRX1, PCOLCE, EMILIN1, CYP1B1, S1PR2, and GAS1. Interestingly, C5orf34 showed downregulation in CDH1 mutated GC patients. We also found that a mutation in the CDH1 gene leads to its downregulation (Figure 1).

Corso et al. reported CDH1 mutation frequency of 4.5%, LOH frequency of 4.5%, and methylation frequency of 25.4% in diffuse and mixed gastric tumors [9]. The essential role of CDH1 and its associated protein E-Cadherin in cell-cell cohesion has been confirmed in various experimental data and tumor cell systems. Handschuh et al. showed that E-cadherin mutations alter cellular morphology, decrease cellular adhesion, and increase cellular motility [10]. Loss of function mutations in the CDH1 gene lead to the process of epithelial-mesenchymal transition and subsequently, the cell loses its cell-cell adhesion capabilities and apical polarity [11]. Altogether these data indicate CDH1 can be considered a tumor suppressor gene which may be linked with human cancer susceptibility and its mutation and expression is associated with GC.

Expression fold change of OMD in patients with mutant CDH1 was 3.45 fold higher than patients with wild type CDH1. We also found that the expression level of C5orf34 in CDH1 mutated patients is 1.85 fold lower than patients with wild type CDH1.

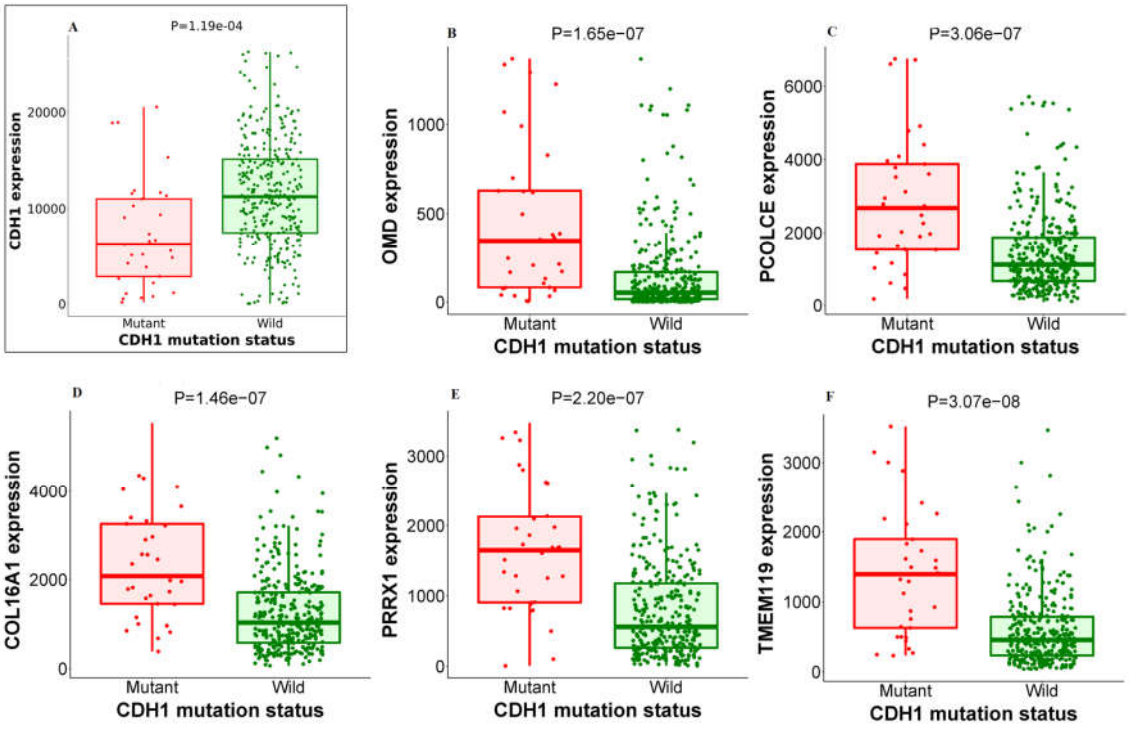

Figure 1. Correlation of expression profile and CDH1 mutation status. A) Correlation of CDH1 mutation status and its expression in gastric cancer patients. B-F) Correlation of CDH1 gene mutation status with five significant genes.

CDH1 pathway plays an important physiological role in maintaining cell-cell adhesions, architecture, motility, and cell homeostasis. Mutation of the CDH1 gene has been linked to dysregulation of several other genes which may lead to gastric carcinogenesis. In conclusion, our bioinformatics analysis provides a list of 10 genes that are significantly dysregulated in GC patients with mutated CDH1. These genes may be potentially involved in the invasion, metastasis, and carcinogenesis of GC.

References

[1] Rawla, P. and A. Barsouk, Epidemiology of gastric cancer: global trends, risk factors and prevention. Przeglad gastroenterologiczny, 2019. 14(1): p. 26.

[2] Hao, N.-B., et al., The role of miRNA and lncRNA in gastric cancer. Oncotarget, 2017. 8(46): p. 81572.

[3] Piazuelo, M.B. and P. Correa, Gastric cancer: overview. Colombia Medica, 2013. 44(3): p. 192-201.

[4] Cheng, X.J., J.C. Lin, and S.P. Tu, Etiology and prevention of gastric cancer. Gastrointestinal tumors, 2016. 3(1): p. 25-36.

[5] Liu, X. and K.-M. Chu, E-cadherin and gastric cancer: cause, consequence, and applications. BioMed research international, 2014. 2014.

[6] Rossi, T., et al., E-cadherin Downregulation and microRNAs in sporadic intestinal-type gastric Cancer. International journal of molecular sciences, 2019. 20(18): p. 4452.

[7] Jiang, H., et al., Gene expression profiling of gastric cancer. Eur Rev Med Pharmacol Sci, 2014. 18(15): p. 2109-2115.

[8] Nagy, Á. and B. Győrffy, muTarget: A platform linking gene expression changes and mutation status in solid tumors. International Journal of Cancer, 2020. 148(2): p. 502-511.

[9] Corso, G., et al., Somatic mutations and deletions of the E-cadherin gene predict poor survival of patients with gastric cancer. Journal of Clinical Oncology, vol. 31 (7) p. 868-75, 2013.

[10] Handschuh, G., et al., Tumour-associated E-cadherin mutations alter cellular morphology, decrease cellular adhesion and increase cellular motility. Oncogene, 1999. 18(30): p. 4301-4312.

[11] Shenoy, S., CDH1 (E-cadherin) mutation and gastric cancer: genetics, molecular mechanisms and guidelines for management. Cancer Management and Research, 2019. 11: p. 10477.

Smart drug delivery systems: Concepts and clinical applications

Saeideh Hosseini[1]

[1]Independent Researcher

*Email: hsaeideh@gmail.com

Abstract

Given that the production of a new drug molecule is time consuming and costly, pharmaceutical scientists seek to create a drug delivery system that is safe, effective, stable, and has good patient compliance. Targeted drug delivery is an advanced method of drug delivery that involves the controlled release of drugs at the target site (organs / tissues / cells) over a period of time. Targeted drug delivery is also known as smart or Intelligent drug delivery. In this method, the prescribed dose is reduced, which in turn improves the treatment by reducing the side effects of the drug. In designing such systems, important factors that should be considered are: Chemical and physical properties of drugs, Side effects or cytotoxicity for healthy cells, the route to be taken to deliver the medicine, the desired location, disease, Specific properties of target cells, the nature of markers or transport carriers or vehicles, which carry drugs to specific receptors and ligands and physically modulated components. The various drug carriers that can be used in this advanced delivery system include: Polymer-drug conjugates and nanoparticle systems such as Inorganic nanoparticles (e.g., magnetic nanoparticles, quantum dots), Dendrimers, liposomes and lipoproteins are monoclonal antibodies, microspheres, microemulsions and neutrophils, fibroblasts, artificial cells, micelles and immune micelles. These drug delivery systems are used in stem cell therapy, regeneration methods and cancer treatments. In this review article, the drug delivery system and the importance of targeting strategies as well as the basic aspects of targeted drug delivery were studied. Current approaches and future perspectives on clinical applications are also presented.

Keywords: Targeted drug delivery, Magic bullet, Smart drug delivery systems, stimulant-sensitive materials

1. Introduction

Conventional drug delivery systems (DDS) often have systematic side effects Due to nonspecific biological distribution and uncontrolled drug release characteristics. Since drug delivery technology can have commercial and therapeutic value for health products, there has been rapid growth in drug delivery over the past three decades. [1] Controlled drug delivery is an essential tool in controlling the release of the required amount of drug, increasing the effectiveness of the drug in the body, protecting it from physiological degradation, the ability to control the actual drug delivery site, and thus improving patient comfort [2-5]. The first generation of controlled drug delivery systems is a type of controlled release system that uses a polymer matrix or pump as a speed control device to deliver the drug in a fixed and predetermined pattern for an arbitrary period of time [6] These systems have the

following advantages over other prescription methods: (1) the possibility of maintaining the plasma drug levels, which is therapeutically desirable, (2) The possibility of eliminating or reducing side effects from systemic administration (3) The possibility of improving and facilitating drug administration in areas with poor medical (4) The possibility of prescribing drugs with a short half-life in the body, (5) Reduction of pain caused by high doses, (6) the possibility of increasing in patient compliance, and (7) The possibility of producing a relatively low cost product and less drug.

The design of drug delivery systems is difficult due to the existence of different mechanisms in drug secretion processes. [7] Various factors such as drug uptake or limitations of drug release into the environment, drug properties, method of administration, nature of vehicle, drug release mechanism, targeting ability, and biocompatibility should be considered for effective treatment. these cases briefly Shown in Figure 1. In addition, the reliability and reproducibility are the key points in the design of such a system. Achieving a system that includes all of these is not easy due to the widespread independence of these factors.

Figure 1: Design requirement for a drug delivery system. [8]

2. Different Approaches (Systems) for Controlled Drug Delivery

Sustained Drug Delivery (Zero Order Release Profile)

Injectable or ingestible drugs have first-order kinetics, so that after administration, the initial level of the drug in the body is at the highest possible value and then decreases in concentration, thus reducing the effect of the drug. Therefore, it is considered an undesirable kinetics. Especially in cases where the distance between the toxicity and the required level of therapeutic concentration is small. The graph of concentration changes is shown in Figure 2.

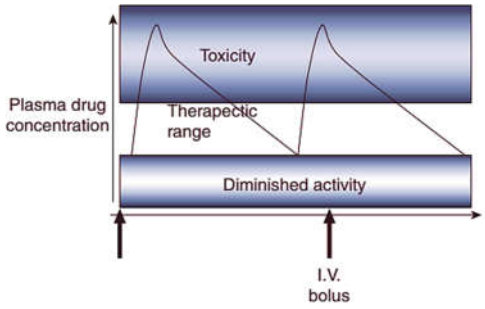

Figure 2: Plasma concentration versus time curve for intravenous (IV) drug administration showing first-order kinetic [8]

Drug delivery systems with controlled release are characterized by a continuous drug release profile that corresponds to zero-order kinetics. In this case, the blood level of the drugs remains constant during the delivery period. Therefore, drug delivery systems with continuous release have significant therapeutic benefits and include the following: Possibility of predicting in vivo release based on in vitro data; Decreased plasma peak levels and the risk of toxic effects; Predictability of operation time and increased durability; Reduce discomfort by administering repeated doses and thus improving patient compliance [9,10]. The constant plasma concentration, which is desirable for many therapeutic agents, is shown in Figure 3.

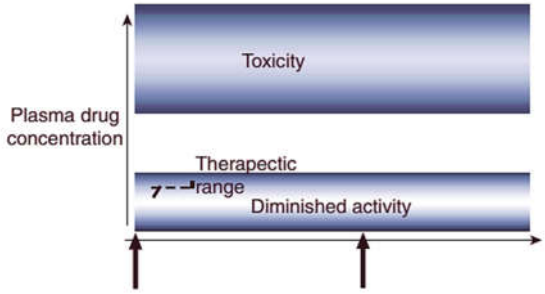

Figure 3: Plasma concentration versus time curve for sustained release profile of zero-order kinetics and pulsatile release profile. [8]

Modulated Drug Delivery (Nonzero-Order Release Profile)

Creating a delivery system that has the ability to achieve a manipulable nonzero-order release profile is a significant challenge in drug delivery. The drug release profile (curve) can take many forms, such as pulsatile or ramp or some other pattern. Figure 2 shows pulsatile release profile within the therapeutic window. [8]

Feedback Controlled Drug Delivery.

The drug delivery system with feedback-controlled drug delivery that releases the drug in response to a therapeutic marker is an ideal drug delivery system. modulated and triggered device are two classes of this system.

A modulated device is characterized by the ability to monitor the chemical environment and the constant change of drug delivery rate in response to a specific external marker, whereas in a triggered device the drug is released only by stimulation by a marker. These different drug delivery approaches can be administered via oral, pulmonary, pulmonary inhalation, transmucosal mucosa, and implantable systems. [8]

Implantable Controlled Drug Delivery Devices.

Ideally, Implantable devices is electronically controlled with a long-life power source and follows a feedback-controlled diffusion mechanism. Implantable devices are placed completely under the skin (usually in a convenient but unspecified location) and are replaced by repeated IV catheters. These systems can be used in the following cases: For the treatment of some diseases that require chronic medication. For a number of drugs that cannot be delivered orally or are absorbed irregularly through the gastrointestinal tract (GI). (9). [11] These systems are especially suitable for the pharmaceutical needs of insulin, steroids, chemotherapy, antibiotics, painkillers, birth control pills and heparin.

Localized Drug Delivery.

In many cases, medications can be delivered to a specific location (tissue or organ). In this type of regional treatment mechanism, systematic toxicity is reduced and the amount of drug in the desired location reaches the highest possible level. Medications such as anti-cancer drugs, anti-fertility drugs and anti-inflammatory steroids need this type of treatment due to their many unwanted side effects. [8]

Targeted Drug Delivery

Ehrlich first introduced the concept of target drug delivery system based on the term "magic bullet" in 1906. **[12]** The main idea of a targeted drug delivery system was based on three basic factors: namely finding the particular target for the disease, finding the drug which will effectively treat the disease, and selecting appropriate target vehicles to carry the drug in stable form while preventing other interactions and damage to the healthy tissues. Targeted drug delivery is an intelligent drug delivery system in which a specific amount of a therapeutic substance is delivered to a target area in the patient's body over a long period of time. [13,14] [15]**.** Cancers [16], autoimmune diseases, neurological disorders, pulmonary diseases, cardiovascular diseases and most other conditions require effective, safe, specific targeting of drugs to certain receptors or direct delivery into the organ [17] and TDD is expected to serve to these needs.

Ideally, TDD systems should have the following features: TDD systems should be biochemically inert (non-toxic), non-immunogenic, physically and chemically stable in vivo and in vitro conditions. Additionally, they should have restricted drug distribution to target cells or tissues or organs and should have uniform capillary distribution. TDD should have controllable and predictable rate of drug release and drug action should not depend on the release kinetics. It should have therapeutic amount of drug release and minimal drug leakage during transit.

Carriers used should be bio-degradable or readily eliminated from the body without any problem. The preparation of the delivery system should be easy or reasonably simple, reproductive and cost effective. [18-20]

3. Targeted Drug Delivery Carriers

Targeted delivery requires special carrier systems. A TDD carrier is a special molecule, particle, composite, or system that has the ability to hold the drug in or on them, either by encapsulation and / or by means of a separator. [21, 22,19].

Drug Delivery Vehicles must meet several requirements: They must be able to pass through hard-to-reach places, such as the blood-brain barrier, which can be easily identified by target cells, and in the case of tumor chemotherapy, tumor vessels. The drug ligand complex must be stable in biological fluids, plasma, interstitial and other materials. It must be specifically and selectively identified by target cells and must retain the character of surface ligands. Once detected, the carrier system must release the drug into target organs, tissues, or cells. [21, 23, 24, 19].

The drug vehicle used must be non-toxic and non-immunogenic. high loading / encapsulation amount of the drug, [25] zero premature release of drug molecules, [26] cell type or tissue specificity and site directing ability, and [27] proper controlled release rate of drug molecules to achieve an effective local concentration [25] are other features of drug carriers.

At present, nanotechnology-based drug delivery systems have been studied due to the development and fabrication of various nanostructures. [16, 28]. These particles or structures can easily penetrate tissues (absorption of nanoparticles is about 15-250 times higher than that of microparticles) and be absorbed by cells. They also protect drugs from being destroyed by various gastrointestinal enzymes, so they can transport the drug to the target as safely as possible. [29-31].

Nano-carrier-based TDDs have advantages such as higher surface-to-volume ratio, higher and more reactive activity centers, stronger adsorption capacity, and other properties such as morphological preferences. The mode of control and secretion of drugs by these carriers at the target sites is relatively unique and special, in that initially an outbreak occurs and eventually leads to continuous release for a long time. Therefore, nanocarriers significantly increase the efficacy of drugs in limited concentrations and also reduce the side effects of drugs and reduce the suffering of patients from various diseases. [32]

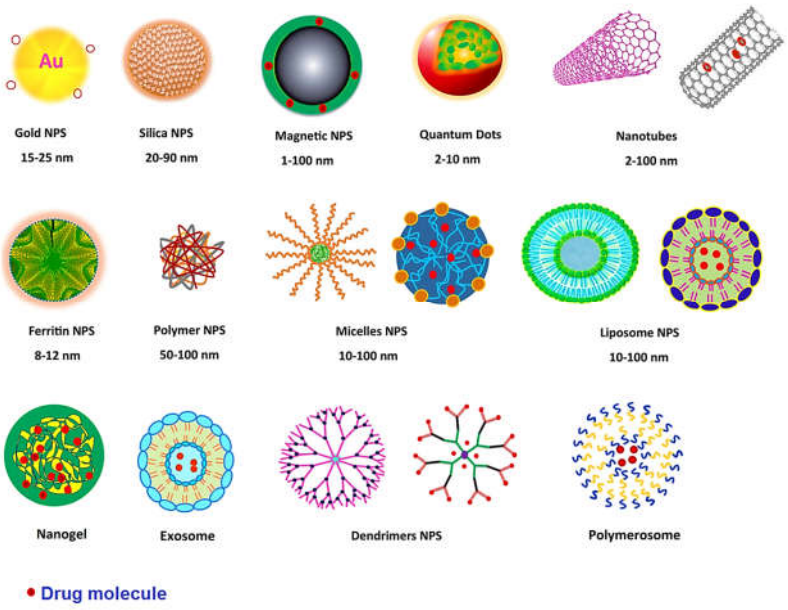

Figure 4: Targeted Drug Delivery Carriers [33,34]

4. Types of Targeted Drug Delivery

Increasing the therapeutic effectiveness and reducing the toxicity of the drug are among the benefits of targeting the drug to an area of interest in the body. There are basically six strategies for drug targeting to the desired organ/tissue of interest: Passive Targeting, Active Targeting, Inverse Targeting, Physical Targeting, Dual Targeting and Double Targeting. [35]

4.1 Inverse Targeting

Reverse targeting of drugs means preventing inactive absorption of colloidal carriers by the Reticulo Endothelial Systems (RES). This can be achieved by suppressing the regular function of RES by injecting large amounts of empty colloidal carriers or macromolecules such as dextran sulfate. This method facilitates RES saturation and suppresses the defense mechanism. This type is usually used as an effective way to target the drug (s) to non-RES organs in the body. [36]

4.2 Physical Targeting

This approach can be achieved by changing some characteristics of environmental conditional changes such as pH, system temperature, light intensity, magnetic field, electric field or ionic strength and other small and even specific stimuli such as glucose concentration or gas concentration to localize the drug carrier at a predetermined

location. This method is used to target nanoparticles for tumors as well as in the cytosolic delivery of entrapped drug or genetic materials. [37]

4.3 Dual Targeting

In this system, the carrier molecule has therapeutic activity and therefore increases the therapeutic effect and activity of the drug. For instance, the net synergistic effect of drug conjugate or the composite can be seen when a carrier molecule with antibacterial or antifungal activity is loaded with an antibacterial or antifungal drug (e.g., loading antibacterial drugs on porous ZnO nanoparticles). [38]

4.4 Double Targeting

The combination of temporal and spatial methodologies to target a carrier system is called dual targeting. Here, it is possible to control the rate of drug delivery to the desired location by spatial placement targets drugs to specific organs, tissues, cells or even subcellular containers and temporal delivery. [39]

4.5 Active Targeting

Active targeting is the specific interaction between the drug / drug carrier and target cells through specific ligand-receptor interactions for intracellular localization that occurs only after blood circulation and extravasations. In this method, special modified nanosystems are used to identify and interact with specific cells. Vitamins, carbohydrates, lipids, peptides and surface proteins, Antibodies and nucleic acids are among the various targeting agents that are used in active targeting. [40-42]. The main reason for active targeting is the selectively increase in the amount and size of drug delivery to target tumor cells due to the avid and specific interaction between nanocarriers and target cells. [43,42,44, 45]**.** This approach can be classified into three different levels of targeting. 1) First order targeting, refers to the distribution of the drug in the capillaries of general target sites such as compartmental targeting in lymphatics, peritoneal cavity, plural cavity, cerebral ventricles and eyes, joints. 2) Second order targeting, selective drug delivery to specific cell types, such as tumor cells, rather than to normal cells, for example, selective drug delivery to Kupffer cells in the liver. [46]**.** 3) Third order targeting is a specific type of drug delivery in which the drug is targeted intracellularly through endocytosis or through receptor-based ligand interactions at the site. [22]

4.6 Passive targeting

Passive targeting is one of the natural phenomena that exists in the human body. Hormones, neurotransmitters, growth factors, etc. have a natural tendency to target receptors at their site of action, such as insulin and insulin

receptors. This concept also applies to drugs. Some tissues in disease conditions physiologically offer opportunities that can be exploited by passively targeting nanocarriers. This is called the enhanced permeability and retention (EPR) effect, in which nanocarriers accumulate in diseased tissues due to loosen fenestrations and / or poorly formed lymphatic drainage (Figure 5). [47-49] [47,50-53,45]

Accrual of drugs / drug-carrier systems at the site of operation leads to targeted drug secretion over a period of time**.** [54,14,55]**.** Due to the clearance of nanocarriers by the reticulo-endothelial system (RES) consisting of macrophages and mononuclear phagocytes, it can be used to passively target macrophages and even the lymph nodes and spleen to treat infections that affect RES (e.g., Leishmaniasis and malaria). [56-59]**.** In order to create features such as long-circulating, RES avoidance, and granting them time to accumulate at target sites in high amounts (long-circulating nanocarriers), Modifications (e.g., binding of polyethylene glycol; PEG) are often performed on nanocarriers. [60]

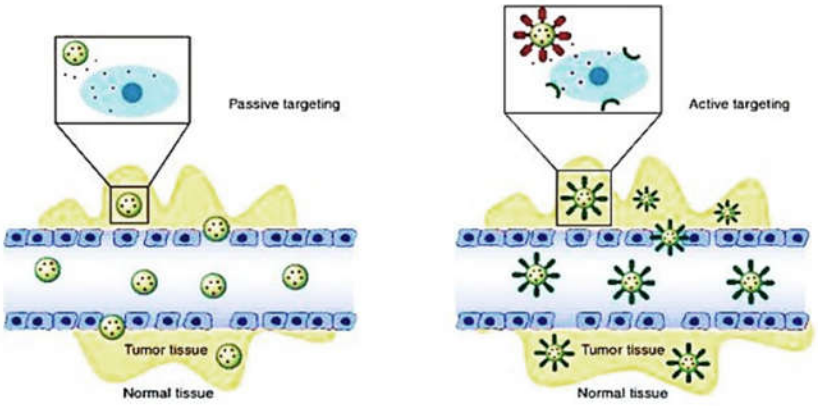

Figure 5: A schematic representation of Passive targeting and Active Targeting [61]

internal stimuli, such as pH difference (e.g., low pH in tumor microenvironment [62]), redox systems (e.g., exploiting high glutathione in cancer [63]), etc. are used in passive targeting. such stimuli provoke the Stimuli-sensitive drug targeting systems and cause the drug to be released at the site. These systems have been widely studied. [64-68]

5. Stimuli and suitable smart DDSs

In controlled release systems, the activated drug can be released at the site in response to certain physical, chemical, or biochemical processes, some of which are induced internally and some externally. Therefore, they can be classified into two main classes of responsive DDS: (1) Those that modulate or activate the release rate by detecting changes in the biological environment (e.g., pH, temperature, or concentration of certain substances) are termed closed-loop or self-regulating systems and (2) DDSs that release the drug (switch drug release on/off) as a function of specific external stimuli (e.g., light, or electric or magnetic field) operate in open circuit and, if activated by an external agent, provide the drug pulse emission. [69,70]. Research into advanced excipients, which can lead to responsive formulations, has provided an additional incentive to find suitable stimulant-sensitive materials and increased the publication of articles on "smart" delivery systems.

Sensitivity to internal or external signals can be created in these systems by using synthetic or semi-synthetic materials (mainly polymers) that have functional groups that change their properties as a function of signal strength. [71-73].

There may be various complications to these changes. For example, (i) the ability to change shape, solubility, aggregation mode of individual components (e.g., assembly–disassembly of micelle unimers or sol–gel transition); (ii) possible modifications in the conformation of chemically cross-linked networks that lead to the volume phase transition in affinity towards other chemical or molecular species. (III) the Possibility to perform reversible stretching– shrinking of surface-immobilized chains or networks on inert substrates (Fig. 6). [70,74-76]**.** These possible structural changes can be considered "intelligent" DDS behavior when they act reversibly and in proportion to the intensity of the stimulus.

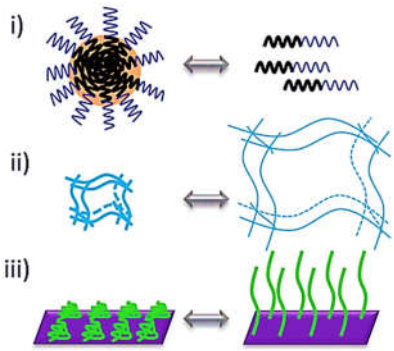

Figure 6: Some transitions associated with the responsiveness to a stimulus: (i) de-aggregation of amphiphilic polymers; (ii) volume phase transition; and (iii) helix to random coiling [77]

In many intelligent (smart) DDS, drug release requires structural changes throughout the carrier or in specific layers or channels caused by the stimulus. [78-80]. These are designed to physically trap drugs. carriers made of labile bonds or having the drug molecules conjugated through cleavable bonds, which are broken under the action of the stimulus are affected by stimuli such as pH or enzymes [81].

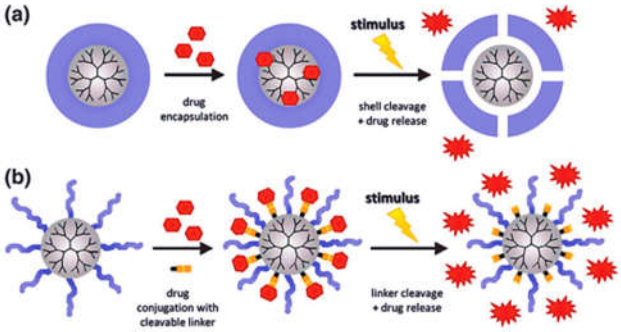

Figure 7: Release of active agents from (a) supramolecular complexes like dendritic core–shell particles with a cleavable shell and (b) dendritic scaffolds with attached solubilizing/stealth groups using cleavable linkers for the drug conjugation. [81].

5.1 pH

Because there are a variety of pH fluctuations in various organs and tissues of the body, such as the stomach (pH≈ 2) and intestines (pH≈ 7), pH is one of the most widely used stimuli in smart DDS. [82-85]. Also, due to the significant pH difference found at the cellular level between the cytosol (7.4), the Golgi apparatus (6.40), the endosome (5.5-6.0) and the lysosome (4.5-5.5), They are especially suitable for design intracellular-specific delivery. [86]. In addition, there is a difference between the extracellular pH of blood and healthy tissues (7.4) and damaged tissues such as tumor tissues (6.5-7.0) and inflammatory tissues (pH drop to 6.5). [87, 88]. Also, healing progress index, is another application of pH-changes. [89] Although the pH stimulant is the most widely used stimulant for drug secretion, but to achieve a very accurate and specific diffusion in the required places, it must be combined with other stimuli such as temperature, oxidation. [90,67,91].

The use of polymers with weak acid (e.g., carboxylic acid) or base (e.g., primary and tertiary amines) groups that cause sharp changes in ionization at the desired pH is the basis for the development of pH-responsive systems. In this way, changes in the conformation and affinity of the chains for the solvent, as well as the interactions among them and resulting in either the disassembly of components or the swelling– shrinking of covalent networks can be caused by increasing the degree of ionization. Changes in the nature of the co-monomers used to prepare the polymer is a way to adjust the pH-responsiveness. [92]

5.2 Redox conditions.

In nature, molecules containing sulfur (II) such as cysteine and cysteine-derived compounds (eg, glutathione, GSH, etc.) are known as defense compounds. [93]. GSH – glutathione disulfide is the most important redox pair in animal cells. Reduction of GSH by NADPH and glutathione reductase is a known redox system in cancer cells. Also, since GSH is an intracellular substance present in different parts of the body and its amount in tumor tissues is higher than healthy tissues (4 to 7 times more), therefore the role of GSH as a stimulus to stimulate drug release in tumor cells Strengthens [94]. Thus, the design and fabrication of redox-responsive stimuli can be a promising approach to the design of smart DDSs [95] and have received much attention for the treatment of diseases. [96,97]

5.3 Molecule-responsiveness and imprinted systems

Stimulants such as pathological markers (e.g., enzymes and antibodies) that have the ability to precisely control and feed-back regulation of drug release have been extensively studied. Impaired regulation of enzyme function causes many types of diseases, so it can be used to diagnose diseases. [98].

For example, overexpression of Capthesins, plasmin, urokinase-type plasminogen activator, prostate-specific antigen, matrix metalloproteases, b-glucuronase, b-glucuronase carboxylesterases are a symptom of a tumor. [81]. The use of enzymes with distinctive features such as substrate specificity and high selectivity under mild conditions has emerged as a stimulus in the design of smart DDS in recent years. [99-101].

Carriers prone to degradation by the relevant enzyme, drug–polymer conjugates with linkers as enzyme substrates and Capped nanoparticles removable by enzyme function are considered as the basis for designing enzymatically triggered DDSs. [103-106]

In addition, in another method, the internal (inner) pH of the network was changed by integrating the enzyme into the pH-responsive networks and the enzyme-substrate reaction. That is, in the absence of substrate, there is no change in the conformation of the network, but at a certain concentration of the substrate, the reaction takes place and the product causes a change in the local pH, and as a result will change the degree of swelling of the network.

5.4 Temperature

Temperature is one of the easiest and most effective stimulants to control drug secretion. [107-109]. In general, thermo-sensitive nanocarriers are designed to store their payloads at a physiological temperature of 37° C and when the temperature rises above 40-45 ° C, release the cargo quickly. Typically, pathophysiological conditions such as inflammation, infarction or tumor, as well as infections caused by microorganisms cause a local increase in temperature in the affected tissues [110,111]. Another temperature-responsive strategy is the concentrated increase in temperature using external stimuli (e.g., ultrasound, magnetic field, etc.) that can be applied to the skin or can be done by irradiating metals in DDS that heat energy. Converts, remotely created. [94].

5.5 Light

One way to stimulate drug release at the target by external light illumination are light-responsive systems. Stimulation of formulations placed on the skin or that circulate through blood vessels close to the body surface (e.g., eye structures) by ultraviolet (UV) rays and visible light causes the drug to be released. In Photo sensitive carriers, excitation by one-time or repeatable light irradiation is accompanied by the opening or closing of the nanostructure, resulting in the release of the drug. [95]. Knowledge related to Previously commercialized photodynamic therapy-based treatments can be used to develop these responsive DDSs. However, limitation of light wavelength is one of the drawbacks of practical treatment, which means that it inhibits non-invasive programs for deep tissues. [112].

5.6 Electrical field

Electrically sensitive networks can be created using polyelectrolytes with a high density in ionizable groups. [113]. injectable drug-loaded microparticles or implants for subcutaneous insertion can be used to prescribe these networks. In this way, by placing an electro-conducting patch on the skin through the implantation site and turning on the battery, the protons move towards the cathode and by changing the pH near the electrodes, it causes the network to shrink, thus the drug is released by squeezing. As the battery shuts off and the electric field is removed,

the hydrogel swells again. Therefore, it is possible to adjust drug release rate and duration by adjusting the intensity of the electrical field and current application time.

5.7 Magnetic field

Magnetite- and magmite-based nanoparticles are the most commonly used magnetic nanoparticles as contrast agents for magnetic resonance imaging (MRI) [114]. Using magnetic stimuli, a non-invasive approach is possible to temporally and spatially control of the carriers to the targets and Release of the drug is performed under programmable exposure of external magnetic field. [115-117]. [94, 118-121] [122-128]. Compared to other responsive systems that do not allow tissue guidance on their own, it is possible to guide and concentrate drug carriers with magnetic particles in a specific area using high-gradient magnetic fields. [114]. As a result, even at low injectable doses, high local concentration occurs and when the alternating magnetic field is on, the drug is released, resulting in site-specific treatment [129].

5.8 Ultrasound

Because ultrasound has high immunity and the ability to penetrate body tissues with low frequency and very low scattering, it is widely used in clinics for diagnosis and treatment. Ultrasound can be applied to the body using common physiotherapy equipment by adjusting the frequency, duty cycles and time of exposure to capture drug carriers and trigger drug release. As a result, it can be used as a unique technique in the development of intelligent nanocarriers (ultrasonic sensitive nanocarriers). [130-132]. In addition to identifying the effects of ultrasound on cell apoptosis and genotoxicity, [133]. there are other barriers to the clinical use of ultrasound-responsive DDSs and theranostic systems that are being investigated. [134, 135]. For example, overcoming ultrasound attenuation by bone is possible by combining modern imaging techniques, as a result, it is possible to deliver the drug through the healthy skull to the target areas in the brain. [136].

5.9 Other responsive systems

Glucose and other Saccharide Sensitive Systems [137-139]. electro-responsive systems [113, 140-142] and Autonomous responsiveness are other stimuli used to control the release of payloads within nanocarriers. In addition, the use of a hybrid stimulus can further improve the accuracy of drug delivery. Among these systems, Dual stimuli-responsive DDSs have been extensively studied, such as thermo- and pH responsive systems [143,144], thermo- and light responsive systems [145, 146], redox- and pH-responsive systems [67,91]. ultrasonic and magnetic responsive systems [147-151], In order to develop and use intelligent systems, a wide range of stimuli with the ability to trigger the drug release at target place and expected time are included in nanostructures (various nano-architectures). To ensure the sustainability and bioavailability of these strategies, it is necessary to consider adjust the response to each stimulus both in vitro and in vivo.

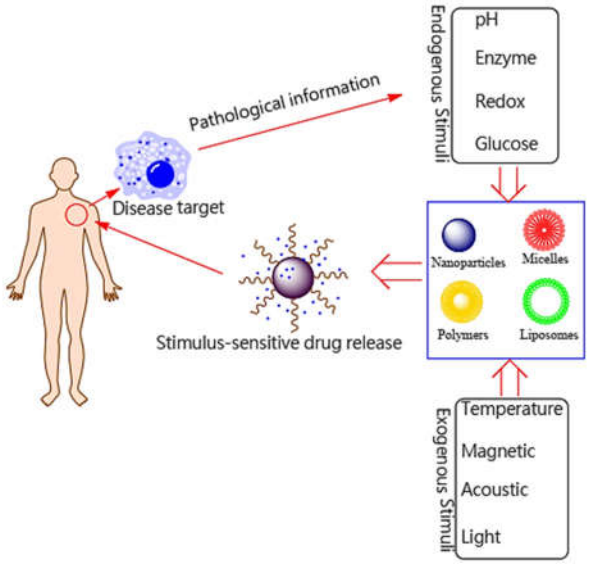

Figure 8: Schematic illustration for stimuli-responsive DDSs. [152]

Table1: Some medicines based on stimuli-responsive components that are in clinical trials or already commercialized. [77, 152]

Product	Stimuli (Stimulus) / Drug formulation	Structure	Clinical status
Opaxiot	Tumor enzyme	Paclitaxel poligumex	Approved orphan drug for glioblastoma multiforme
Trastuzumab-DM1	GSH concentration	Antibody–drug conjugate	Phase II/III in breast cancer
Maytansine	GSH concentration	Antibody–drug conjugate	Phase II/III in multiple myeloma
Nanocapsule prototype	Dually responsive to GSH and ROS	Camptothecin-based topoisomerase I inhibitor conjugated to nanocapsules	In vivo tests with breast tumor xenograft models and autochthonous colon cancer models
Implant prototype for antinflammatory release	OH radicals	Lipoidal-chitosan-poly(ecaprolactone) nanoparticles coated with hyaluronic acid, alginate and poly (acrylic acid)	Intraocular tests in the rabbit model of uveitis
Nanocarrier prototype for tissue	Thrombin in the clot	tPA camouflaged with human serum albumin via a thrombin cleavable peptide, and coated with a homing	Rat thrombosis model

plasminogen activator (tPA)		peptide that binds with GPIIb/IIIa expressed on activated platelets	
Glucose biosensors Guardian Real-Times, Sevens, Dexcoms G4t Platinum, or Enlitet, FreeStyle Navigators	Glucose concentration	Glucose oxidase enzyme coupled to other enzymes and transducers for continuous monitoring of glucose levels and regulation of insulin release from pumps	Approved, commercially available implantable biosensors

Table1: continued

Product	Stimuli (Stimulus) / Drug formulation	Structure	Clinical status
Nanoparticles as traps of bee venom	Melittin	Imprinted nanocarrier that selectively captures melittin in the bloodstream	Mice models
ThermoDoxs	Thermosensitive (external source)	DPPC-based liposomes for tumorspecific release of doxorubicin	Phase III in liver cancer, Phase II in chest wall recurrence of cancer, colorectal liver metastases, lung cancer and bone metastases Phase II/III Breast cancer, primary liver cancer
Visudynes	UV light	NonPEGylated liposome formulation of photosensitizer verteporfin	Approved, commercially available injectable solution
Rotaxane-functionalized mesoporous silica nanoparticles	UV light	Nanoparticles with pores capped with chains of triazole/ethylene glycol and an azobenzene unit that interact with a-cyclodextrin	Wild-type zebrafish larvae
Cornell dots (C dots)	Near infrared radiation	Fluorescent core–shell silicabased nanoparticles	Approved for human stage I molecular imaging of cancer
AuroShell	Near infrared radiation	Gold nanoparticles for solid tumor hyperthermia	Phase I solid tumors

	Thermosensitive	gold nanoshell	Nanospectra Biosciences Phase I/ Intracranial tumors
NanoXray products	X-rays	Hafnium crystals that amplify the dose of radiation delivered to the tumor	Phase I
Cochlear implants coated with ICPs	Electrical stimulus	Coatings of intrinsically conducting polymers that switch neurotrophin release on and off	Animal models
NanoTherms	Magnetic sensitive (Magnetic field)	Water-dispersable iron oxide nanoparticles coated with aminosaline	Approved for thermoablation of glioblastoma; Phase I prostate and pancreatic carcinoma, Phase I/II www.magforce.de Glioblastoma, prostata cancer,eosphageal cancer, pancreatic cancer
Nanocarrier prototype for tissue plasminogen activator (tPA)	Ultrasound	tPA encapsulated in gelatin-PEG nanoparticles for localized thrombolysis	Rat thrombosis model
Opaxio	Enzyme-activated	polymeric NP	Cell Therapeutics, Inc. Phase III/Ovarian cancer

6. Applications

Targeted drug delivery systems in various diseases such as the treatment of various tumors (brain tumors, breast cancer, ...), [153-155], cardiovascular diseases, [156, 157], neurological diseases such as depression, [158] oral diseases (caries, oral cancer and gingivitis) [159] and also in the treatment of diseases Infectious diseases (tuberculosis, malaria and immunodeficiency syndrome (AIDS)) have been used. [160]

7. Conclusion

Targeted drug delivery (TDD) is being developed as one of the most advanced medical science techniques in the diagnosis and treatment of diseases. As the name implies, it means that the drug is delivered to the target cells

and tissues. This results in a lower dose as well as a significant reduction in side effects with maximum bioavailability and high efficacy of the drugs. Nanoparticles are used as drug delivery systems due to their chemical, physical and biocompatibility properties, which can improve the pharmacological and therapeutic properties of drugs. There are countless nanoparticles that have been approved for clinical use. The inherent advantage of this method has caused it to be considered as a highly preferred and facilitating field in the pharmaceutical world.

Targeted drug delivery systems are faced with problems. For example, in most cases, drugs are synthesized in poorly reproducible conditions and by non-standard methods. In addition, cytotoxicity, genotoxicity, antigenicity and purification are the main topics to be clarified. The bioavailability of drugs embedded in smart DDS must be measured in the target tissue or cell. Therefore, to do this, it is necessary to develop appropriate analytical techniques. In this regard, guidance for the preparation and evaluation of materials by regulatory agencies is still ongoing. Another problem attributed to targeting is the extrapolation of behavior from animal to human models. Because small animals have pathologies, physiologies, anatomies, immune systems and host responses to substances are significantly different compared to humans. [109]. This may include immune responses to antibody-guided therapies and the inability to achieve consistent pharmacokinetics during the transition from preclinical animal studies to clinical trials. There is also limited information on in vivo function. Evaluating the cost-effectiveness of smart products is another important point in this regard. [161]. Despite the relevant concerns mentioned above, TDDS is still an appropriate approach to achieving optimized design, easily translatable production and evaluation in humans of more efficient formulations, and continued exploration will lead to the development of successful treatments. Among the new plans for the future are the creation of multifunctional devices that are able to meet different biological and therapeutic needs, as well as scaling processes that rapidly bring innovative medical institutions to market.

References

[1] S.W. Song, K, Hidajat, S. Kawi., Functionalized SBA-15 materials as carriers for controlled drug delivery: influence of surface properties on matrix-drug interactions, Langmuir 21 (2005) 9568–9575. doi:10.1021/la051167e.

[2] V.P. Torchilin., Recent advances with liposomes as pharmaceutical carriers, Nat Rev, 4 (2005) 145-160, doi: 10.1038/nrd1632

[3] J.W. Yoo, CH. Lee., Drug delivery systems for hormone therapy, J Control Release;112 (2006)1-14. doi: 10.1016/j.jconrel.2006.01.021.

[4] M. Malmsten., Soft drug delivery systems, Soft Mater 2 (2006) 760-769. doi.org/10.1039/B608348J

[5] M. Hrubý, SK. Filippov, P. Štěpánek Smart polymers in drug delivery systems on crossroads: Which way deserves following? European Polymer Journal. 65 (2015) 82-97, DOI: 10.1016/j.eurpolymj.2015.01.016

[6] R. Langer Implantable controlled release systems. Pharmacol Ther , 21 (1983)35–51. doi.org/10.1016/0163-7258(83)90066-9

[7] C. Barbé, J. Bartlett, L. Kong, K. Finnie, H.□Q. Lin, M. Larkin, S. Calleja, A. Bush, G. Calleja., Silica particles: a novel drug-delivery system, Adv. Mater. 16 (2004) 1959–1966. doi:10.1002/adma.200400771

[8] D. Paolino, M. Fresta, P. Sinha, M. Ferrari, DRUG DELIVERY SYSTEMS, Encyclopedia of Medical Devices and Instrumentation, Second Edition, edited by John G. Webster Copyright # John Wiley & Sons, Inc. (2006) 437-495

[9] DD. Breimer, Future challenges for drug delivery. J Control Rel, 62 (1999) 3–6

[10] EA, Klausner et al. Novel levodopa gastroretentive dosage form: in-vivo evaluation in dogs. J Control Rel; 88 (2003) 117–126.

[11] VV. Ranade, MA, Hollinger., Drug Delivery Systems. CRC Press; 1996, ISBN 9781439806180

[12] TM. Fahmey, PM. Fong, A. Goyal, WM. Saltzman., Targeted for drug delivery. Nanotoday; 8 (2005) 18-26. doi:10.1016/S1369-7021(05)71033-6.

[13] RH. Muller, CM. Keck., Challenges and solutions for the delivery of biotech drugs-a review of drug nanocrystal technology and lipid nanoparticles. Journal of Biotechnology, 113 (2004) 151-170. doi: 10.1016/j.jbiotec.2004.06.007.

[14] TM. Allen, PR. Cullis, Drug Delivery Systems: Entering the Mainstream. Science, 303 (2004) 1818-1822. doi: 10.1126/science.1095833.

[15] Bertrand, N.; Leroux, J. The journey of a drug-carrier in the body: An anatomophysiological perspective. J. Control. Release, 161 (2012), 152-163. doi: 10.1016/j.jconrel.2011.09.098.

[16] Cho, K.; Wang, X.; Nie, S.; Chen, Z.; Shin, D. Therapeutic nanoparticles for drug delivery in cancer. Clin. Cancer Res., 14 (2008) 1310-1316. doi: 10.1158/1078-0432.CCR-07-1441.

[17] Jong, W.H.D.; Borm, P.J.A. Drug delivery and nanoparticles: Applications and hazards. Int. J. Nanomedicine, 3 (2008) 133-149. doi: 10.2147/ijn. s596

[18] E. Mastrobattista, GA. Koning, G. Storm; Immunoliposomes for the targeted delivery of antitumor drugs. Advance Drug Delivery Reviews, 40 (1999) 103-127. doi: 10.1016/s0169-409x(99)00043-5.

[19] SP. Vyas, RK. Khar; Basis of targeted Drug Delivery. In Targeted and controlled Drug Delivery, CBS Publishers and Distributor Reprint, 2008: 42-46, 74.

[20] R. Won; Method for delivering an active ingredient by controlled time release utilizing a novel delivery vehicle which can be prepared by a process utilizing the active ingredient as a porogen, Patent No 4690825 US: 1987.

[21] R. Duncan; Book Review: Drug Targeting. Organ-Specific Strategies. Grietje Molema and Dirk K. F. Meijer. Angewandte Chemie International Edition, 41 (2002) 1245.

[22] 11. R. Kannagi, M. Izawa, T. Koike, K. Miyazaki, N. Kimura., Carbohydrate-mediated cell adhesion in cancer metastasis and angiogenesis. Cancer Science, 2004; 95: 377– 384. doi: 10.1111/j.1349-7006. 2004.tb03219. x.

[23] G. Köhler, C. Milstein; Continuous cultures of fused cells secreting antibody of predefined specificity. Nature, 256 (1975) 495-497. doi: 10.1038/256495a0

[24] Gujral SS, Khatri S; A Review on Basic Concept of Drug Targeting and Drug Carrier System. International Journal of Advances In Pharmacy, Biology and Chemistry, 2013; 2(1): 134-136.

[25] Slowing II, Vivero-Escoto JL, Wu CW, Lin VSY. Mesoporous silica nanoparticles as controlled release drug delivery and gene transfection carriers. Adv Drug Delivery Rev 60 (2008)1278–1288. doi: 10.1016/j.addr.2008.03.012.

[26] Vallet-Regi M, Ramila A., Del Real RP, Pe´rez-Pariente J. A new property of MCM-41: drug delivery system. Chem Mater 13 (2001) 308–11. doi:10.1021/cm0011559.

[27] Gonzalez B, Colilla M, Lopez de Laorden C, Vallet-Regi M. A novel synthetic strategy for covalently bonding dendrimers to ordered mesoporous silica: potential drug delivery applications. Mater Chem 19 (2009) 9012–24. doi:10.1039/B915331D.

[28] R. Singh, J.W. Lillard, Nanoparticle-based targeted drug delivery. Exp. Mol. Pathol., 2009 86(3), 215-223. doi: 10.1016/j.yexmp.2008.12.004.

[29] K.Y. Win, S. Feng, Effects of particle size and surface coating on cellular uptake of polymeric nanoparticles for oral delivery of anticancer drugs. Biomaterials, 2005, 26(15), 2713- 2722. doi: 10.1016/j.biomaterials.2004.07.050.

[30] S. Patil, A. Sandberg, E. Heckert, W. Self, S. Seal, Protein adsorption and cellular uptake of cerium oxide nanoparticles as a function of zeta potential. Biomaterials, 2007, 28(31), 4600- 4607. doi: 10.1016/j.biomaterials.2007.07.029.

[31] A.K. Gupta, M.Gupta, Cytotoxicity suppression and cellular uptake enhancement of surface modified magnetic nanoparticles. Biomaterials, 2005, 26(13), 1565-1573. doi: 10.1016/j.biomaterials.2004.05.022.

[32] B.J. Bruno, G.D. Miller, C.S. Lim, Basics and recent advances in peptide and protein drug delivery. Ther. Deliv., 2013, 4(11), 1443-1467. doi: 10.4155/tde.13.104.

[33] U. A. Ashfaq, M. Riaz, E. Yasmeen, M. Z. Yousaf, Recent Advances in Nanoparticle Based Targeted Drug-Delivery Systems Against Cancer and Role of Tumor Microenvironment, Crit Rev Ther Drug Carrier Syst.;34 (2017) 317-353. doi: 10.1615/CritRevTherDrugCarrierSyst.2017017845.

[34] J. Meng., V. Agrahari and I. Youm., Advances in Targeted Drug Delivery Approaches for the Central Nervous System Tumors: The Inspiration of Nanobiotechnology, J Neuroimmune Pharmacol. Mar;12 (2017) 84-98. doi: 10.1007/s11481-016-9698-1.

[35] S. Dunuweera, S. Rajapakse, M. G. G. S. N. Thilakarathna, R.M G. Rajapakse., Review on Targeted Drug Delivery Carriers Used in Nano Biomedical Applications, Current Nanoscience 15 (2019) 382-397. doi: 10.2174/1573413714666181106114247.

[36] J.P. Balthasar, H.L. Fung, Inverse targeting of peritoneal tumors: Selective alteration of the disposition of methotrexate through the use of anti-methotrexate antibodies and antibody fragments. J. Pharm. Sci., 1996, 85, 1035-1043. doi: 10.1021/js960135w.

[37] J.M. Morachis, E.A. Mahmoud, A. Almutairi, Physical and chemical strategies for therapeutic delivery by using polymeric nanoparticles. Pharmacol. Rev., 2012, 64(3), 505-519. doi: 10.1124/pr.111.005363.

[38] S. Noimark, J. Weiner, N. Noor, E. Allan, C.K. Williams, M.S.P. Shaffer, I.P. Parkin, Dual-mechanism antimicrobial polymer–ZnO Nanoparticle and crystal violet-encapsulated silicone. Adv. Funct. Mater., 2015, 25, 1367-1373. doi:10.1002/adfm.201402980.

[39] Z. Sun, X. Yan, Y. Liu, L. Huang, C. Kong, X. Qu, H. Qin, Application of dual targeting drug delivery system for the improvement of anti-glioma efficacy of doxorubicin. Oncotarget, 8 (2017)58823-58834. doi: 10.18632/oncotarget.19221.

[40] R.S. Reddy, S. Dathar, Nano drug delivery in oral cancer therapy: An emerging avenue to unveil. J Med Radiol Pathol Surg 1 (2015) 17-22. doi: 10.15713/ins.jmrps.31.

[41] MS. Muthu, L. Mei, SS. Feng., Nanotheranostics: Advanced nanomedicine for the integration of diagnosis and therapy. Nanomedicine (Lond) 9 (2014) 1277-1280.

[42] L. van Vlerken, T. Vyas, M. Amiji, Poly (ethylene glycol)-modified Nanocarriers for Tumor-targeted and Intracellular Delivery. Pharmaceutical research 24(2007)1405–1414. doi: 10.1007/s11095-007-9284-6.

[43] M. Yokoyama, Drug targeting with nano-sized carrier systems. J Artif Organs 8 (2005) 77–84. doi: 10.1007/s10047-005-0285-0.

[44] D. Peer, JM. Karp, S. Hong, OC. Farokhzad, R. Margalit, R. Langer, Nanocarriers as an emerging platform for cancer therapy. Nat Nano 2 (2007) 751–760. doi:10.1038/nnano.2007.387.

[45] A.A. Gabizon, H. Shmeeda, S. Zalipsky, Pros and cons of the liposome platform in cancer drug targeting. Journal of Liposome Research 16 (2006) 175–183. doi: 10.1080/08982100600848769.

[46] B.N. Melgert, P. Olinga, J.M.S.Van Der Laan, B. Weert, J. Cho, Targeting dexamethasone to Kupffer cells: effects on liver inflammation and fibrosis in rats. Hepatology, 34 (2001) 719-728. doi: 10.1053/jhep.2001.27805.

[47] Y. Matsumura, H. Maeda, A new concept for macromolecular therapeutics in cancer chemotherapy: mechanism of tumoritropic accumulation of proteins and the antitumor agent smancs. Cancer Res 46 (1986) 6387–6392.

[48] T. Stylianopoulos, EPR-effect: utilizing size-dependent nanoparticle delivery to solid tumors. Ther Deliv 4 (2013) 421–423. doi: 10.4155/tde.13.8.

[49] V. Torchilin, Tumor delivery of macromolecular drugs based on the EPR effect. Adv Drug Deliv Rev 63 (2011) 131–135. doi: 10.1016/j.addr.2010.03.011

[50] H. Maeda, Advances in Enzyme Regulation, Oxford: Pergamon-Elsevier Science Ltd; The enhanced permeability and retention (EPR) effect in tumor vasculature: The key role of tumor-selective macromolecular drug targeting; 41 (2001) 189-207.

[51] K. Greish, Enhanced permeability and retention of macromolecular drugs in solid tumors: a royal gate for targeted anticancer nanomedicines. J Drug Target 15 (2007) 457–464. doi: 10.1080/10611860701539584.

[52] F. Yuan, M. Dellian, D. Fukumura, M. Leunig, DA. Berk, VP. Torchilin, RK. Jain, Vascular permeability in a human tumor xenograft: molecular size dependence and cutoff size. Cancer Research 55 (1995) 3752–3756.

[53] I. Brigger, C. Dubernet, P. Couvreur, Nanoparticles in cancer therapy and diagnosis. Advanced Drug Delivery Reviews 54 (2002) 631–651. doi: 10.1016/s0169-409x(02)00044-3.

[54] MC. Garnett, Targeted drug conjugates: principles and progress. Adv Drug Deliv Rev 53 (2001)171–216. doi: 10.1016/s0169-409x(01)00227-7.

[55] ES. Lee, KT. Oh, D. Kim, YS. Youn, YH. Bae., Tumor pH-responsive flower-like micelles of poly (Llactic acid)-b-poly (ethylene glycol)-b-poly(L-histidine). Journal of Controlled Release 123 (2007) 19–26. doi: 10.1016/j.jconrel.2007.08.006.

[56] NS. Santos-Magalhaes, VC. Mosqueira., Nanotechnology applied to the treatment of malaria. Adv Drug Deliv Rev 62 (2010) 560–575. doi: 10.1016/j.addr.2009.11.024.

[57] K. Rani and S. Paliwal, "A review on targeted drug delivery: Its entire focus on advanced therapeutics and diagnostics," Scholars Journals of Applied Medical Sciences, (2014).

[58] Y.H. Bae and K. Park, "Targeted drug delivery to tumors: Myths, reality and possibility," Journal of Controlled Release, 153, 2011. doi: 10.1016/j.jconrel.2011.06.001.

[59] R. Gref, Y. Minamitake, MT. Peracchia, V. Trubetskoy, V. Torchilin, R. Langer., Biodegradable long-circulating polymeric nanospheres. Science, 1994; 263(5153):1600– 1603. doi: 10.1126/science.8128245

[60] V.P. Torchilin, Targeted pharmaceutical nanocarriers for cancer therapy and imaging. AAPS J 9 (2007) E128–E147. doi: 10.1208/aapsj0902015.

[61] Link: http://www.medscape.com/viewarticle/770397_3.

[62] X. Zhang, Y. Lin, RJ. Gillies, Tumor pH and its measurement. J Nucl Med 51(2010):1167–1170. doi: 10.2967/jnumed.109.068981.

[63] S. Singh, AR. Khan, AK. Gupta, Role of glutathione in cancer pathophysiology and therapeutic interventions. J Exp Ther Oncol 9 (2012) 303–316.

[64] RR. Sawant, et al., Polyethyleneimine-lipid conjugate-based pH-sensitive micellar carrier for gene delivery. Biomaterials 33 (2012) 3942–39511. doi: 10.1016/j.biomaterials.2011.11.088

[65] H. Wu, L. Zhu, V.P. Torchilin., pH-sensitive poly(histidine)-PEG/DSPE-PEG co- polymer micelles for cytosolic drug delivery. Biomaterials 34(2013)1213–1222. doi: 10.1016/j.biomaterials.2012.08.072

[66] J. Liu, et al., Redox-responsive polyphosphate nanosized assemblies: a smart drug delivery platform for cancer therapy. Biomacromolecules 12 (2011) 2407–2415. doi:10.1021/bm2005164

[67] YJ. Pan, et al., Redox/pH dual stimuli-responsive biodegradable nanohydrogels with varying responses to dithiothreitol and glutathione for controlled drug release. Biomaterials 33 (2012)6570–6579. doi: 10.1016/j.biomaterials.2012.05.062.

[68] ES. Lee, K. Na, YH. Bae., Doxorubicin loaded pH-sensitive polymeric micelles for reversal of resistant MCF-7 tumor. J Control Release 103 (2005) 405–418. doi: 10.1016/j.jconrel.2004.12.018

[69] S. Sershen and J. West, Adv. Implantable, polymeric systems for modulated drug delivery, Drug Delivery Rev., 54 (2002) 1225. doi: 10.1016/s0169-409x(02)00090-x.

[70] C. Alvarez-Lorenzo and A. Concheiro, Intelligent drug delivery systems: polymeric micelles and hydrogels, Mini-Rev. Med. Chem., 2008, 8, 1065-74. doi: 10.2174/138955708785909952

[71] D. Schmaljohann, Adv. Thermo- and pH-responsive polymers in drug delivery, Drug Delivery Rev., 58 (2006) 1655-70. doi: 10.1016/j.addr.2006.09.020.

[72] M. Motornov, Y. Roiter, I. Tokarev and S. Minko, Stimuli-responsive nanoparticles, nanogels and capsules for integrated multifunctional intelligent systems, Prog. Polym. Sci., 35 (2010) 174. doi: 10.1016/j.progpolymsci.2009.10.004

[73] G. Pasparakis and M. Vamvakaki, Multiresponsive polymers: nano-sized assemblies, stimuli-sensitive gels and smart surfaces, Polym. Chem., 2 (2011) 1234-1248. doi:10.1039/C0PY00424C

[74] S. Grund, M. Bauer and D. Fischer, Polymers in Drug Delivery-State of the Art and Future Trends, Adv. Eng. Mater., 13 (2011) B61. doi. 10.1002/adem.201080088

[75] C. Alexander and K. M. Shakesheff, Responsive Polymers at the Biology/Materials Science Interface, Adv. Mater., 18 (2006) 3321-28. doi: 10.1002/adma.200502640

[76] C. Alvarez-Lorenzo, E. Bucio, G. Burillo and A. Concheiro, Medical Devices Modified at the Surface by γ-Ray Grafting for Drug Loading and Delivery, Expert Opin. Drug Delivery, 7 (2010) 173-85. doi:10.1517/17425240903483174.

[77] C. A. Lorenzo and A. Concheiro, Smart drug delivery systems: from fundamentals to the clinic, Chem. Commun., 2014, 50, 7743, doi: 10.1039/c4cc01429d.

[78] R. Lehner, X. Wang, M. Wolf and P. Hunziker, Designing switchable nanosystems for medical application. J. Controlled Release, 161 (2012) 307-16. doi: 10.1016/j.jconrel.2012.04.040.

[79] S. Pavlukhina and S. Sukhishvili, in Smart Materials for Drug Delivery, ed. C. Alvarez-Lorenzo and A. Concheiro, Royal Society of Chemistry, London, 2 (2013) 117.

[80] H. Zhang, Y. Tian and L. Jiang, From symmetric to asymmetric design of bio-inspired smart single nanochannels, Chem. Commun., 2013, 49, 10048-10063. doi:10.1039/C3CC45526B.

[81] E. Fleige, M. A. Quadir and R. Haag, Stimuli-responsive polymeric nanocarriers for the controlled transport of active compounds: concepts and applications, Adv. Drug Delivery Rev., 2012, 64, 866-84. doi: 10.1016/j.addr.2012.01.020.

[82] 21. J. Liu, Y. Huang, A. Kumar, A. Tan, S. Jin, A. Mozhi, et al. pH-Sensitive nano-systems for drug delivery in cancer therapy. Biotechnology Advances. 2014; 32:693-710. doi: 10.1016/j.biotechadv.2013.11.009

[83] VA. Ganesh, A. Baji, S. Ramakrishna, Smart functional polymers–a new route towards creating a sustainable environment. RSC Advances. 2014; 4:53352-64. doi.org/10.1039/C4RA10631H

[84] W. Gao, JM. Chan, OC. Farokhzad, pH-responsive nanoparticles for drug delivery. Molecular Pharmaceutics. 2010; 7:1913-20.

[85] P. Yu, H. Yu, C. Guo, Z. Cui, X. Chen, Q. Yin, et al. Reversal of doxorubicin resistance in breast cancer by mitochondria-targeted pH-responsive micelles. Acta Biomaterialia. 2015; 14:115-24. doi: 10.1016/j.actbio.2014.12.001.

[86] N. Nishiyama, Y. Bae, K. Miyata, S. Fukushima and K. Kataoka, Smart polymeric micelles for gene and drug delivery, Drug Discovery Today: Technol., 2005, 2, 21-26. doi: 10.1016/j.ddtec.2005.05.007.

[87] B. A. Webb, M. Chimenti, M. P. Jacobson and D. L. Barber, Dysregulated pH: a perfect storm for cancer progression, Nat. Rev. Cancer, 2011, 11, 671-7. doi: 10.1038/nrc3110.

[88] S. Ganta, A. Iyer and M. Amiji, in Targeted Delivery of Small and Macromolecular Drugs, ed. R. I. Mahato and A. S. Narang, Taylor & Francis, CRC Press, Boca Raton, FL, (2010) 555

[89] L. A. Schneider, A. Korber, S. Grabbe and J. Dissemond, Influence of pH on wound-healing: a new perspective for wound therapy? Arch. Dermatol. Res., 298 (2007) 413 -20. doi: 10.1007/s00403-006-0713x.

[90] R. Cheng, F. Meng, C. Deng, H-A. Klok, Z. Zhong, Dual and multi-stimuli responsive polymeric nanoparticles for programmed site-specific drug delivery. Biomaterials. 34 (2013)3647-57. doi: 10.1016/j.biomaterials.2013.01.084.

[91] W. Chen, P. Zhong, F. Meng, R. Cheng, C. Deng, J. Feijen, et al. Redox and pH-responsive degradable micelles for dually activated intracellular anticancer drug release. Journal of Controlled Release. 2013; 169:171-9. doi: 10.1016/j.jconrel.2013.01.001.

[92] R. Siegel and B. A. Firestone, pH-dependent equilibrium swelling properties of hydrophobic polyelectrolyte copolymer gels Macromolecules, 1988, 21, 3254-59. doi: 10.1021/ma00189a021.

[93] T. Rausch and A. Wachter, Sulfur metabolism: a versatile platform for launching defense operations, Trends Plant Sci., 2005, 10, 503 -9. doi: 10.1016/j.tplants.2005.08.006.

[94] Torchilin V.P. Multifunctional, stimuli-sensitive nanoparticulate systems for drug delivery. Nature Reviews Drug Discovery. 2014; 13:813-27, doi:10.1038/nrd4333

[95] S. Mura, J. Nicolas, P. Couvreur, Stimuli-responsive nanocarriers for drug delivery. Nature Materials. 2013; 12:991-1003. doi:10.1038/nmat3776

[96] M. Huo, J. Yuan, L. Tao, Y. Wei, Redox-responsive polymers for drug delivery: from molecular design to applications. Polymer Chemistry. 2014; 5:1519-28. doi:10.1039/C3PY01192E.

[97] J. Wang, X. Sun, W. Mao, W. Sun, J. Tang, M. Sui, et al. Tumor Redox Heterogeneity□Responsive Prodrug-Nanocapsules for Cancer Chemotherapy. Advanced Materials. 2013; 25:3670-6. doi:10.1002/adma.201300929

[98] P. F. Caponi and R. V. Ulijn, in Smart Materials for Drug Delivery, ed. C. Alvarez-Lorenzo and A. Concheiro, Royal Society of Chemistry, London, 1 (2013) 232.

[99] MM. Nguyen, AS. Carlini, MP. Chien, S. Sonnenberg, C. Luo, RL. Braden, et al. Enzyme□Responsive Nanoparticles for Targeted Accumulation and Prolonged Retention in Heart Tissue after Myocardial Infarction. Advanced Materials. 2015; 27:5547-52. doi: 10.1002/adma.201502003.

[100] CE. Callmann, CV. Barback, MP. Thompson, DJ. Hall, RF. Mattrey, NC. Gianneschi, Therapeutic Enzyme□Responsive Nanoparticles for Targeted Delivery and Accumulation in Tumors. Advanced Materials. 2015; 27:4611-5. doi:10.1002/adma.201501803

[101] R. De La Rica, D. Aili, MM. Stevens, Enzyme-responsive nanoparticles for drug release and diagnostics. Advanced Drug Delivery Reviews. 2012; 64:967-78. doi: 10.1016/j.addr.2012.01.002

[102] LL. Lock, Z. Tang, D. Keith, C. Reyes, H. Cui, Enzyme-Specific Doxorubicin Drug Beacon as Drug-Resistant Theranostic Molecular Probes. ACS Macro Letters. 2015; 4:552-5. doi:10.1021/acsmacrolett.5b00170

[103] W. Fischer, M. Calderon, A. Schulz, I. Andreou, M. Weber and R. Haag, Bioconjugate Dendritic Polyglycerols with Oligoamine Shells Show Low Toxicity and High siRNA Transfection Efficiency in Vitro, Chem., 2010, 21, 1744-52. doi. 10.1021/bc900459n

[104] M. R. Clark, H. A. Aliyar, C. won Lee, J. I. Jay, K. M. Gupta, K. M. Watson, R. J. Stewart, R. W. Buckheit and P. F. Kiser, Enzymatic triggered release of an HIV-1 entry inhibitor from prostate specific antigen degradable microparticles. Int. J. Pharm., 2011, 413, 10. doi: 10.1016/j.ijpharm.2011.04.004.

[105] A. Bernardos, L. Mondragon, E. Aznar, M. D. Marcos, R. MartinezMan˜ez, F. Sancenon, J. Soto, J. M. Barat, E. P. Paya and C. Guillem, Enzyme-responsive intracellular controlled release using nanometric silica mesoporous supports capped with "saccharides", ACS Nano, 2010, 4, 6353-68. doi: 10.1021/nn101499d.

[106] N. Singh, A. Karambelkar, L. Gu, K. Lin, J. S. Miller, C. S. Chen, M. J. Sailor and S. N. Bhatia, Bioresponsive mesoporous silica nanoparticles for triggered drug release, J. Am. Chem. Soc., 2011, 133, 19582-5. doi: 10.1021/ja206998x.

[107] Y. Shi, ET. van den Dungen, B. Klumperman, CF. van Nostrum, WE. Hennink, Reversible Addition–Fragmentation Chain Transfer Synthesis of a Micelle-Forming, Structure Reversible Thermosensitive Diblock Copolymer Based on the N-(2-Hydroxy propyl) Methacrylamide Backbone. ACS Macro Letters. 2 (2013) 403-8. doi:10.1021/mz300662b.

[108] Y. Shi, MJ. van Steenbergen, EA. Teunissen, Ls. Novo, S. Gradmann, M. Baldus, et al. Π–Π stacking increases the stability and loading capacity of thermosensitive polymeric micelles for chemotherapeutic drugs. Biomacromolecules. 2013; 14:1826-37. doi:10.1021/bm400234c.

[109] Y. Shi, RM. Cardoso, CF. Van Nostrum, WE. Hennink, Anthracene functionalized thermosensitive and UV-crosslinkable polymeric micelles. Polymer Chemistry. 2015; 6:2048-53. doi:10.1039/C4PY01759E.

[110] F. Danhier, O. Feron, V. Préat, To exploit the tumor microenvironment: passive and active tumor targeting of nanocarriers for anti-cancer drug delivery. Journal of Controlled Release. 2010; 148:135-46. doi: 10.1016/j.jconrel.2010.08.027.

[111] M. D. White, C. M. Bosio, B. N. Duplantis and F. E. Nano, Human body temperature and new approaches to constructing temperature-sensitive bacterial vaccines, Cell. Mol. Life Sci., 2011, 68, 3019-31. doi: 10.1007/s00018-011-0734-2.

[112] S. Lal, SE. Clare, NJ. Halas, Nanoshell-enabled photothermal cancer therapy: impending clinical impact. Accounts of Chemical Research. 2008; 41:1842-51. doi:10.1021/ar800150g.

[113] S. Murdan, Electro-responsive drug delivery from hydrogels. J. Controlled Release, 92 (2003) 1-17. doi:10.1016/S0168-3659(03)00303-1

[114] E. Kim, K. Lee, Y. M. Huh and S. Ham, Magnetic nanocomplexes and the physiological challenges associated with their use for cancer imaging and therapy, J. Mater. Chem. B, 2013, 1, 729-39. doi:10.1039/C2TB00294A

[115] J. Sun, Y. Zhang, Z. Chen, J. Zhou, N. Gu, Fibrous Aggregation of Magnetite Nanoparticles Induced by a Time□Varied Magnetic Field. Angewandte Chemie International Edition. 2007; 46:4767-70. doi;10.1002/ange.200604474

[116] J. Liu, Y. Zhang, C. Wang, R. Xu, Z. Chen, N. Gu, Magnetically sensitive alginate-templated polyelectrolyte multilayer microcapsules for controlled release of doxorubicin. The Journal of Physical Chemistry C. 2010; 114:7673-9. doi;10.1021/jp911933b.

[117] Z. Chen, J-J. Yin, Y-T. Zhou, Y. Zhang, L. Song, M. Song, et al. Dual enzyme-like activities of iron oxide nanoparticles and their implication for diminishing cytotoxicity. Acs Nano. 2012; 6:4001-12. doi:10.1021/nn300291r

[118] K. Fang, L. Song, Z. Gu, F. Yang, Y. Zhang, N. Gu, Magnetic field activated drug release system based on magnetic PLGA microspheres for chemo-thermal therapy. Colloids and Surfaces B: Biointerfaces. 2015; 136:712-20. doi: 10.1016/j.colsurfb.2015.10.014.

[119] F. Yang, X. Zhang, L. Song, H. Cui, JN. Myers, T. Bai, et al. Controlled Drug Release and Hydrolysis Mechanism of Polymer–Magnetic Nanoparticle Composite. ACS Applied Materials & Interfaces. 2015; 7:9410-9. doi:10.1021/acsami.5b02210.

[120] K. Hu, J. Sun, Z. Guo, P. Wang, Q. Chen, M. Ma, et al. A novel magnetic hydrogel with aligned magnetic colloidal assemblies showing controllable enhancement of magnetothermal effect in the presence of alternating magnetic field. Advanced Materials. 2015; 27:2507-14. doi:10.1002/adma.201405757.

[121] F. Wang, D-K. Kim, T. Yoshitake, S. Johansson, B. Bjelke, M. Muhammed, et al. Diffusion and clearance of superparamagnetic iron oxide nanoparticles infused into the rat striatum studied by MRI and histochemical techniques. Nanotechnology. 2010; 22:015103. doi: 10.1088/0957-4484/22/1/015103.

[122] C. Yue-Jian, T. Juan, X. Fei, Z. Jia-Bi, G. Ning, Z. Yi-Hua, et al. Synthesis, self-assembly, and characterization of PEG-coated iron oxide nanoparticles as potential MRI contrast agent. Drug Development and Industrial Pharmacy. 2010; 36:1235-44. doi: 10.3109/03639041003710151.

[123] J. Xie, Y. Zhang, C. Yan, L. Song, S. Wen, F. Zang, et al. High-performance PEGylated Mn–Zn ferrite nanocrystals as a passive-targeted agent for magnetically induced cancer theranostics. Biomaterials. 2014; 35:9126-36. doi: 10.1016/j.biomaterials.2014.07.019.

[124] F. Xiong, Y. Chen, J. Chen, B. Yang, Y. Zhang, H. Gao, et al. Rubik-like magnetic nanoassemblies as an efficient drug multifunctional carrier for cancer theranostics. Journal of Controlled Release. 2013; 172:993-1001. doi: 10.1016/j.jconrel.2013.09.023.

[125] L. Song, F. Zang, M. Song, G. Chen, Y. Zhang, Effective PEGylation of Fe3O4 nanomicelles for in vivo MR imaging. Journal of Nanoscience and Nanotechnology. 2015; 15:4111-8. doi:10.1166/JNN.2015.9803.

[126] Liu D, Wu W, Chen X, Wen S, Zhang X, Ding Q, et al. Conjugation of paclitaxel to iron oxide nanoparticles for tumor imaging and therapy. Nanoscale. 2012; 4:2306-10. doi:10.1039/C2NR11918H.

[127] H-W. Yang, M-Y. Hua, H-L. Liu, C-Y. Huang, R-Y. Tsai, Y-J. Lu, et al. Self-protecting core-shell magnetic nanoparticles for targeted, traceable, long half-life delivery of BCNU to gliomas. Biomaterials. 2011; 32:6523-32. doi: 10.1016/j.biomaterials.2011.05.047.

[128] K. Hayashi, M. Nakamura, W. Sakamoto, T. Yogo, H. Miki, S. Ozaki, et al. Superparamagnetic nanoparticle clusters for cancer theranostics combining magnetic resonance imaging and hyperthermia treatment. Theranostics. 2013; 3:366-76. doi: 10.7150/thno.5860.

[129] S. Y. Chen, S. H. Hu and T. Y. Liu, in Smart Materials for Drug Delivery, ed. C. Alvarez-Lorenzo and A. Concheiro, Royal Society of Chemistry, London, 2 (2013) 32.

[130] T. J. Mason, Therapeutic ultrasound an overview, Ultrason. Sonochem., 2011, 18, 847-52. doi: 10.1016/j.ultsonch.2011.01.004.

[131] R. Deckers and C. T. W. Moonen, Ultrasound triggered, image guided, local drug delivery, J. Controlled Release, 2010, 148, 25-33. doi: 10.1016/j.jconrel.2010.07.117.

[132] JL. Paris, MV. Cabañas, M. Manzano, M. Vallet-Regí., Polymer-Grafted Mesoporous Silica Nanoparticles as Ultrasound-Responsive Drug Carriers. ACS Nano. 2015; 9:11023-33. doi:10.1021/acsnano.5b04378.

[133] Y. Furusawa, Y. Fujiwara, P. Campbell, Q. L. Zhao, R. Ogawa, M. A. Hassan, Y. Tabuchi, I. Takasaki, A. Takahashi and T. Kondo, DNA double-strand breaks induced by cavitational mechanical effects of ultrasound in cancer cell lines, PLoS One, 2012, 7, e29012. doi: 10.1371/journal.pone.0029012.

[134] Y. Z. Zao, L. N. Du, C. T. Lu, Y. G. Jin and S. P. Ge, Potential and problems in ultrasound-responsive drug delivery systems, Int. J. Nanomed., 2013, 8, 1621-33. doi: 10.2147/IJN.S43589.

[135] X. Wang, H. Chen, K. Zhang, M. Ma, F. Li, D. Zeng, S. Zheng, Y. Chen, L. Jiang, H. Xu and J. Shi, Small, 2013, 8, 1621.

[136] M. A. O'Reilly and K. Hynynen, Ultrasound Enhanced Drug Delivery to the Brain and Central Nervous System, Int. J. Hyperthermia, 2012, 28, 386–396. doi: 10.3109/02656736.2012.666709

[137] Q. Guo, T. Zhang, J. A, Wu Z, Zhao Y, Dai X, et al. Block versus Random Amphiphilic Glycopolymer Nanopaticles as Glucose-Responsive Vehicles. Biomacromolecules. 2015; 16:3345-56. doi: 10.1021/acs.biomac.5b01020

[138] Q. Wu, L. Wang, H. Yu, J. Wang, Z. Chen., Organization of glucose-responsive systems and their properties. Chemical Reviews. 2011; 111:7855-75. doi:10.1021/cr200027j.

[139] Z. Gu, AA. Aimetti, Q. Wang, TT. Dang, Y. Zhang, O. Veiseh, et al. Injectable nano-network for glucose-mediated insulin delivery. ACS Nano. 2013; 7:4194-201. doi:10.1021/nn400630x

[140] J. Yun, JS. Im, Y-S. Lee, Kim H-I. Electro-responsive transdermal drug delivery behavior of PVA/PAA/MWCNT nanofibers. European Polymer, Journal. 2011; 47:1893-902. doi: 10.1016/j.eurpolymj.2011.07.024

[141] X. Ying, Y. Wang, J. Liang, J. Yue, Xu C, L. Lu, et al. Angiopep□Conjugated Electro□Responsive Hydrogel Nanoparticles: Therapeutic Potential for Epilepsy. Angewandte Chemie International Edition. 2014; 53:12436-40. doi: 10.1002/anie.201403846.

[142] M. Curcio, UG. Spizzirri, G. Cirillo, O. Vittorio, N. Picci, FP. Nicoletta, et al. On demand delivery of ionic drugs from electro-responsive CNT hybrid films. RSC Advances. 2015; 5:44902-11. doi:10.1039/C5RA05484B.

[143] D. Schmaljohann, Thermo-and pH-responsive polymers in drug delivery. Advanced Drug Delivery Reviews. 2006; 58:1655-70. doi: 10.1016/j.addr.2006.09.020.

[144] L. Zhang, R. Guo, M. Yang, X. Jiang, B. Liu., Thermo and pH Dual□Responsive Nanoparticles for Anti□Cancer Drug Delivery. Advanced Materials. 2007; 19:2988-92. doi:10.1002/adma.200601817.

[145] Z. Zhang, J. Wang, C. Chen Near□Infrared Light□Mediated Nanoplatforms for Cancer Thermo□Chemotherapy and Optical Imaging. Advanced Materials. 2013; 25:3869-80. doi: 10.1002/adma.201301890.

[146] FD. Jochum, P. Theato, Thermo-and light responsive micellation of azobenzene containing block copolymers. Chemical Communications. 2010; 46:6717-9. doi:10.1039/C0CC01288B

[147] F. Yang, P. Chen, W. He, N. Gu, X. Zhang, K. Fang, et al. Bubble microreactors triggered by an alternating magnetic field as diagnostic and therapeutic delivery devices. Small. 2010; 6:1300-5. doi:10.1002/smll.201000173.

[148] F. Yang, S. Hu, Zhang Y, X. Cai, Y. Huang, F. Wang, et al. A Hydrogen Peroxide□Responsive O2 Nanogenerator for Ultrasound and Magnetic□Resonance Dual Modality Imaging. Advanced Materials. 2012; 24:5205-11. doi: 10.1002/adma.201202367.

[149] F. Yang, M. Zhang, W. He, P. Chen, X. Cai, L. Yang, et al. Controlled release of Fe3O4 nanoparticles in encapsulated microbubbles to tumor cells via sonoporation and associated cellular bioeffects. Small. 2011; 7:902-10. doi: 10.1002/smll.201002185.

[150] Yang F, Li M, Cui H, Wang T, Chen Z, Song L, et al. Altering the response of intracellular reactive oxygen to magnetic nanoparticles using ultrasound and microbubbles. Science China Materials. 2015; 58:467-80. doi:10.1007/s40843-015-0059-9.

[151] X. Cai, F. Yang, N. Gu, Applications of magnetic microbubbles for theranostics. Theranostics. 2012; 2:103-12. doi: 10.7150/thno.3464.

[152] D. Liu, F. Yang, F. Xiong, and N. Gu., The Smart Drug Delivery System and Its Clinical Potential, Theranostics. 2016;6(9):1306-23. doi: 10.7150/thno.14858.

[153] Cobleigh MA, Langmuir VK, Sledge GW, Miller KD, Haney L, Novotny WF, Reimann JD, Vassel A. A Phase I/II Dose-Escalation Trial of Bevacizumab in Previously Treated Metastatic Breast Cancer, Semin Oncol. Oct; 30 (2003)117-24. doi: 10.1053/j.seminoncol.2003.08.013.

[154] S. Bashyal, TARGETED DRUG DELIVERY TO CANCER CELLS: ADVANCES IN NANOTECHNOLOGY, Innovare Journal of Life Sciences, 6 (2018) 1-4.

[155] N. Sanadgol, J.mWackerlig, Developments of Smart Drug-Delivery Systems Based on Magnetic Molecularly Imprinted Polymers for Targeted Cancer Therapy: A Short Review, Pharmaceutics. 12 (2020) 831. doi: 10.3390/pharmaceutics12090831.

[156] P.Galvin, D. Thompson, K. B Ryan, A. McCarthy, A. C Moore, C.S Burke, M.Dyson, B. D Maccraith, Y. K. Gun'ko, M.T. Byrne, Y. Volkov, C. Keely, E. Keehan, M. Howe, C. Duffy, R. MacLoughlin,

Nanoparticle-based drug delivery: case studies for cancer and cardiovascular applications, doi: 10.1007/s00018-011-0856-6.

[157] Aiming for the heart: targeted delivery of drugs to diseased cardiac tissue, Cell Mol Life Sci. 69 (2012) 389-404. doi: 10.1007/s00018-011-0856-6.

[158] S. Deore, S. R. Shahi, and P. Dabir. NANOPARTICLE: AS TARGETED DRUG DELIVERY SYSTEM FOR DEPRESSION, International Journal of Current Pharmaceutical Review and Research 8 (2016) 7-11.

[159] J. Lakshmi Prabha, A. Roy, T. Lakshmi, Targeted drug delivery systems used in dentistry - A short review, Drug Invention Today, 10 (2018) 2747-51.

[160] P. V. Devarajan, S. Jain, Chapter 1- Targeted Drug Delivery Systems: Strategies and Challenges, Targeted Drug Delivery: Concepts and D.esign, Controlled Release Society, (2015) doi:10.1007/978-3-319-11355-5.

[161] J. Wang, X. Sun, W. Mao, W. Sun, J. Tang, M. Sui, et al. Tumor Redox Heterogeneity□Responsive Prodrug Nanocapsules for Cancer Chemotherapy. Advanced Materials. 25 (2013) 3670-6. doi: 10.1002/adma.201300929.

Immunopathogenesis of Covid-19: A Molecular approach

Ahmad Ali Badr

Department of Biology, Faculty of Basic Sciences, Behbahan Khatam Al-Anbia University of Technology

Badr713@gmail.com

Abstract

Background: The COVID-19 pandemic as a highly contagious disease is caused by a new strain of coronaviruses family named SARS-CoV-2. In this article we aim to review the latest findings about immunopathogenesis of Covid-19 with a molecular approach.

Methods: Literatures were searched by following keywords: SARS-CoV-2, immune response, molecular mechanism, cytokine storm. Electronic databases (PubMed/Medline, Scopus and Web of Science) were screened.

Results: The results of various studies have shown that in human, SARS-CoV-2 virus causes sever respiratory tract infection. It has recently been shown that this virus enters to the human respiratory epithelial cells through interaction between angiotensin converting enzyme 2 (ACE2) cell receptor and viral spike protein (S protein). ACE2 gene is highly expressed in epithelial cells of respiratory airway. In viral-host receptor interaction , proteolytic cleavage of S protein determines the disease severity. Various studies emphasize in this disease, the host's immune response is impaired and overexpression of inflammatory factors especially cytokines against virus leads to infection. The exact mechanis ms of virus induced lung injury are still undefined; However,it has recently been determined that "Cytokine storm" to be invoved in virus-induced damage. High levels of these inflammatory mediators cause damage to host lung cells. It seems, the proinflammatory cytokine interleukin 6 (IL-6) is the key mediator in the early stage of virus-receptor interaction.

Conclusion: In summary, understanding the cellular and molecular mechanisms involved in immune system irregulation and high virulence potential of SARS-CoV-2 will help to efficient targeted therapy against it.

Keywords: Covid-19, Immune Response, Molecular mechanism, Cytokine storm.

1. Introduction

Coronaviruses (CoVs) can cause diseases in humans leading to the common cold, mild infections, or in some cases more serious lower respiratory system distress and death, targeting mainly In older people [1]. CoVs are named for the spike proteins that are shaped like crowns on the surface of the virus [2]. human CoVs (HCoVs) were first identified in the 1960s [3]. CoVs belong to the very large Coronaviridae family of viruses, which are classified into four groups according to their genetic information as follows: Alphacoronavirus (α-CoV), Betacoronavirus (β-CoV),Gammacoronavirus (γ-CoV), and Deltacoronavirus (δ-CoV) [4]. The α-CoVs include HCoV-229E and HCoV-NL63, whereas the β-CoVs include HCoVOC43, HCoV-Hong Kong University 1 (HCoV-HKU1), Middle East respiratory syndrome (MERS-CoV), severe acute respiratory syndrome (SARS-

CoV), and SARS-CoV-2. Generally, α-CoVs and β-CoVs are limited to only mammals, whereas γ- CoVs and δ-CoVs can infect mostly birds but are capable to infect mammals in some cases [5]. To date, seven types of CoVs have been discovered that have the ability to infect humans: HCoV-229E, HCoV-NL63, HCoV-OC43, HCoV-HKU1, MERS-CoV, SARS-CoV, and most recently SARS-CoV-2. The novel SARS-CoV-2 started from Wuhan, China, with a subsequent international outbreak leading to the current global pandemic [6]. Exploring the molecular mechanisms of how SARS-CoV-2 interacts with host cells and stimulates the immune system may constitute an great strategy for developing new COVID-19 therapies. In this article we aim to review the latest findings about immunopathogenesis of Covid-19 with a molecular approach.

2. Genome structure of SARS-CoV-2

Discovering the suitable drug to cure COVID-19 is crucial; comprehension the genome and pathophysiology of the virus can only help in this effort. CoVs are the largest RNA viruses with a genome size approximately 27–31 kb [7]. When CoVs enter a host cell, the viral genomic RNA (gRNA) operates as a transcript for gene 1, which contains of a pair of large open reading frames (ORFs), ORF1a and ORF1ab (Fig. 1). ORF1a [8] is translated generating polypeptide1a (pp1a; 440– 500 kDa); ORF1ab is translated generating polypeptide1ab (pp1ab; 740–810 kDa). These ORFs proteolytically are then cleaved into 16 nonstructural proteins (nsps) [9,10]. Viral proteases simplify the proteolytic cleavage function. One of the nsps generated in this process is the viral enzyme RNAdependent RNA polymerase (RdRp), which is an essential part of the replication/transcription machinery of CoVs [11]. The 30 CoV gRNA encodes four fundamental structural proteins (sps): spike glycoprotein (S), integral membrane protein (M), envelope protein (E), and nucleocapsid protein (N), along with many accessory proteins [12].

3. Molecular Pathogenesis of COVID-19

3.1. Characteristics of spike proteins

Recently, SARS-CoV-2 showed an open reading frame 3a protein; coded by one of the specific genes, and revealed no sequence similarity to other known structural coronavirus proteins. It interacts with the S and E proteins while the M protein is glycosylated in all coronaviruses. Therefore, the close homology of the M protein glycosylation and its similarity to 3a protein could result to survey the glycosylation of these two membrane proteins [13]. Viral spike (S) glycoprotein is a trimeric class I fusion protein stimulates the SARS-CoV-2 entry into the host cell and the main goal of neutralizing antibodies upon infection. Previous investigations have shown that the action of spike protein depends on its cleavage by host proteolytic enzyme into the S1 and S2 subunit. Attachment of virus to the host cell was facilitated by the S1 subunit whereas the S2 subunit assists in the fusion of viral and human cell membrane. Additionally, both the C-terminal domain (CTD) and the N-terminal domain (NTD) of the S1 subunit are able in function as a receptor-binding entity [14]. However, the S1 CTD region is utilized by both SARS-CoV and MERS-CoV to identify the receptor, the region responsible for SARS-CoV-2 S-protein-hACE2 interaction remains unknown. Studies conducted with Cryo-electron microscopy (Cryo-EM) have revealed that 14-16 N-glycans are present on 22 potential sites in S-protein which are responsible for suitable protein folding and priming of the protein by host proteases.

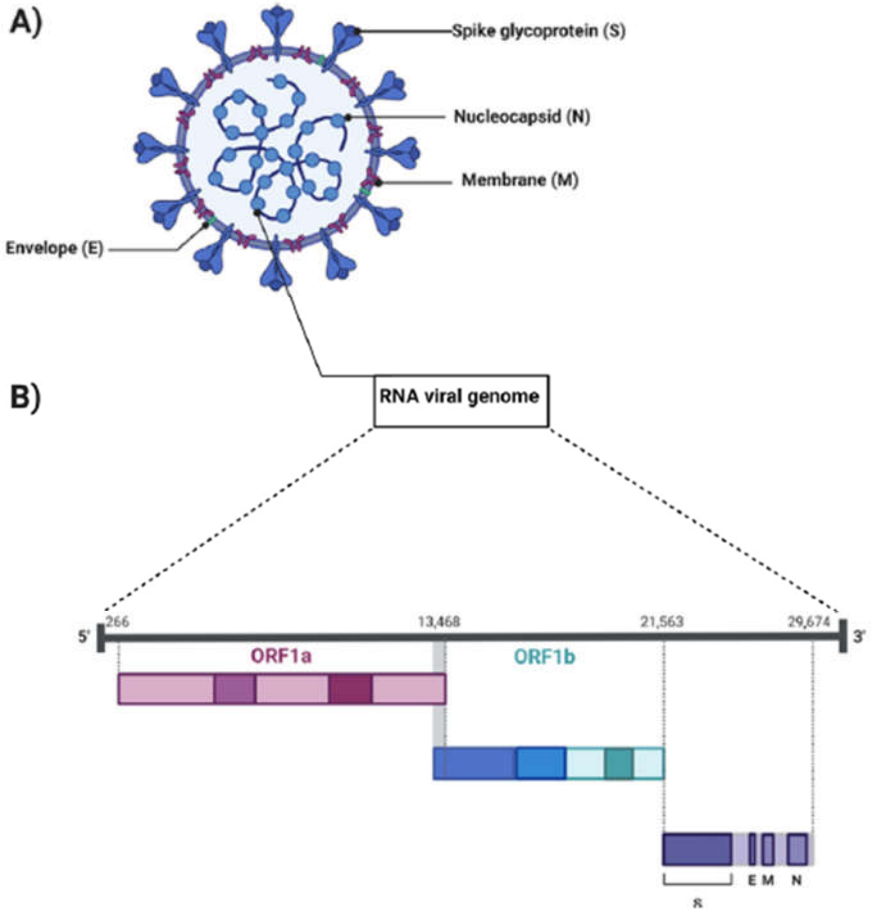

Fig 1: Schematic of SARS-CoV-2 virion and genomic structure. A) The SARS-CoV-2 virion includes four major structural proteins: spike glycoprotein (S), membrane protein (M), envelope protein (E), and nucleocapsid protein (N). B) The genomic single-stranded RNA can be considered in thirds: the first third encodes ORF1a, the second third encodes ORF1ab, and the last third encodes the four essential structural proteins and other accessory proteins [15].

The glycosylation pattern of the S-protein is one of the major features as it operates as a possible site for mutation and also facilitates the coronavirus to avoid both adaptive as well as innate immune responses [13]. A recent investigation suggests that prediction of SARS-CoV-2 spike glycoprotein structure, glycan shield pattern and pattern of glycosylation has excellent inference on understanding the viral cover as well as the outline of cell entry, and also facilitate the progress of new small-molecule drugs, vaccines and screening the human host targets [13].

3.2. ACE2 Receptor – Main Entry Site for SARS-CoV-2

Receptor diagnosis is one of the main steps in viral infection of host cells and viral infection and pathogenesis. SARS-CoV-2 depends upon ACE2 (angiotensin-converting enzyme 2) receptor which is highly expressed in human epithelial, endothelial, cardiovascular, renal tissue, and lung parenchyma [16]. Human ACE2 is a type I integral metallocarboxypeptidase function as a key player in the Renin-Angiotensin system. ACE2

exhibits protective action in the cardiovascular system, and other organs and operate as a major target site for the cure of hypertension. ACE2 protein is more abundantly expressed on the apical surface of polarized epithelial cells as well as well-differentiated cells and specified progenitor cells in the bronchi [17]. Expression of ACE2 receptor in progenitor cells of respiratory system cells with hair-like projections called cilia helps for the coronavirus entrance site in the human body. Well differentiated epithelial cells expressing ACE2 are easily infected by coronavirus. The viral infection so correlates with the cell differentiation condition, ACE2 receptors expression, and localization of membrane attachment. Neverthless, to date, there are still unanswered questions remain about ACE2 expression in human epithelial cells and its modulatory role in coronavirus. Questions include the type of epithelial cells involved in disease, the polarity of ACE2 expression on epithelial cells, and if the coronavirus infection is ACE2 dependent.

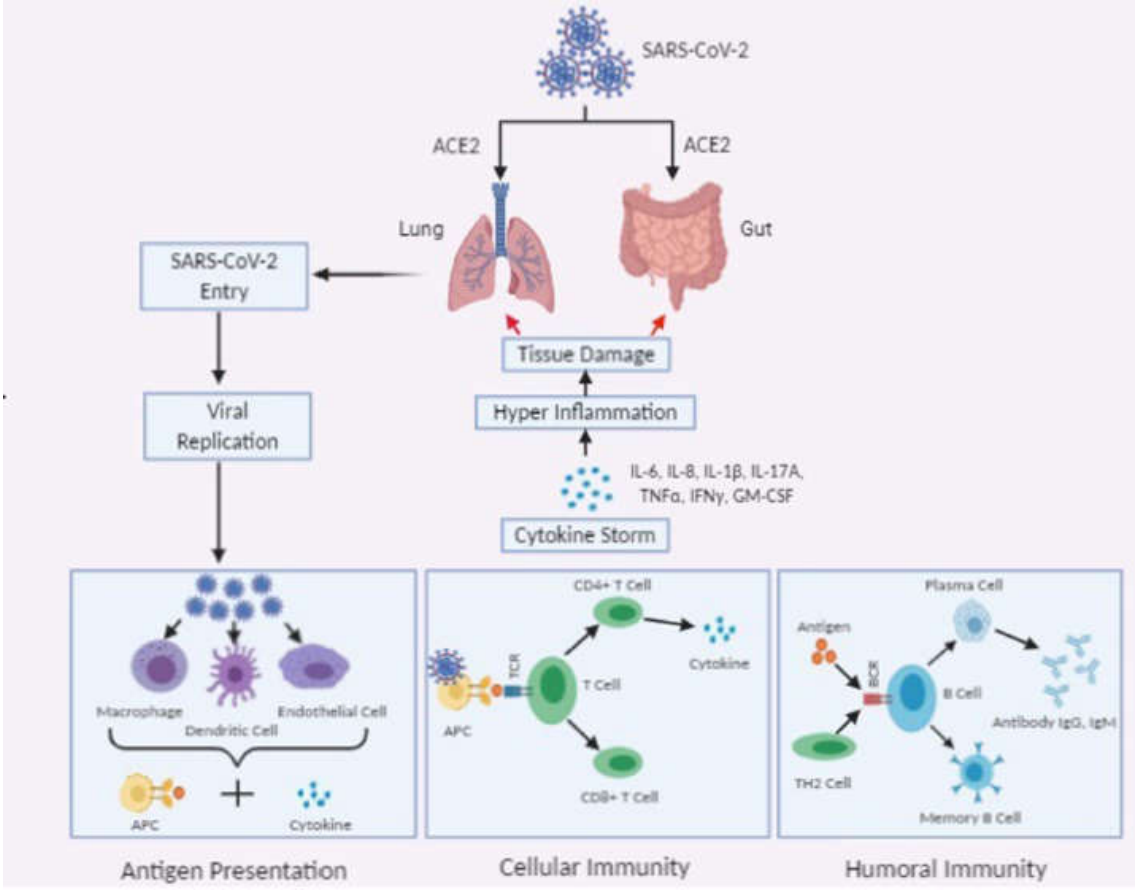

Fig 2: Schematic representation of immunopathogenesis of SARS-CoV-2 infection [18].

Interestingly, emersion of ACE2 receptor density on the progenitor cell surface enhanced with age and are usually present higher in men than in women [19]. An investigation by Wu et al. [20], using computer modeling has demonstrated the presence of identical 3-D structures in the receptor-binding domain of the spike proteins of both SARS-CoV-2 as well as SARS-CoV. Biochemical interaction survey and crystal structure analysis by Wan

et al. have confirm that SARS-CoV-2 receptor-binding domain (RBD) contain residue 394, which has sequence similarity with SARS-CoV residue 479, and both can be accepted by the human ACE2 receptor on the critical lysine 31 [21].

Angiotensin converting enzyme 2 is an entrance receptor for SARS-CoV-2 and shows 76% amino acid sequence similarity with the SARS-CoV-S. Structural configuration investigation shows that, ACE2 include 17 amino acid N-terminal signal sequences and a 22 amino acid hydrophobic transmembrane sequence near the C-terminus. ACE2 also contains 43 amino acid cytoplasmic domain, a potential phosphorylation sites, eight cysteine amino acids, and seven potential Af-linked glycosylation sites [22]. The viral spike (S) protein of SARS-CoV-2 attaches to cellular receptor ACE2 in a homological way to SARS-CoV-1 but with a 10- to 20-fold higher binding affinity. These results suggest that elevated ACE2 expression might confer easier transmissibility and also enhances the susceptibility of SARS-CoV-2 into the host cell [23].

investigations using angiotensin-II receptor blockers (ARB) and ACE-inhibitors (ACE-i) propose that the upregulation of cellular ACE2 expression facilitates the attachment of SARS-CoV-2 and associated with severe disease manifestation. This receptor cognition by viral cell leads to host cell entry of the virus in combination with S-protein priming by the host cell protease TMPRSS2. Downregulation of ACE2 expression by SARS-CoV-2 could decrease the angiotensin-II permission and lead to deteriorate of tissue damage. Recognition of interaction site and the downstream signaling cascade of SARS-CoV-2 and ACE2 receptor in the human cells will aid to design the antibody-based therapeutic strategy [24].

4. Overview of the innate, adaptive and complement immune systems

The human immune system is consists of cells, molecules that work together to prepare protection to skin, respiratory passages, the gastrointestinal tract, and other sections of the body against Threatening factors such as bacteria, parasites, viruses, fungi, toxins, and cancer cells. The immune system can be simply divided as two lines of defense: innate (non-specific) and adaptive (specific) immunity [25]. For the host immune system to contain viral spread and weaken infection, it needs to employ both immune defenses; innate immunity can perform its effects through inflammatory cytokines and innate immune cells, whereas adaptive immunity removes the infection using T-helper cells CD4+, CD8+ cells to clear the infected cells, and B cells to produce antibodies to neutralize and exterminate free virus [26]. The innate immune system includes phagocytic cells (macrophages and neutrophils), mast cells, eosinophils, basophils, natural killer cells (NKs), dendritic cells (DCs), and lymphoid cells [25,27]. The innate immune system operates rapidly, within minutes of pathogen agent exposure. It is programmed to find invariant microbial components shared by the majority of pathogen groups; moreover, it helps as the central player in activating next responses of adaptive immunity [27,28]. Within innate immunity, macrophages and DCs both constitute phagocytic and antigen presenting cells (APCs), whereas mast cells and basophils are responsible for cytokine release and the beginning of acute inflammatory responses such as in asthma and allergies. In turn, eosinophils remove parasites and NKs are responsible for the destruction of virus-infected cells and tumor cells by releasing granzymes and perforins, causing cell lysis.

4.1. Cytokines targeted in immunomodulation

Cytokines are a group of small molecules generated by several cells to create communication and intercellular signaling. Cytokines target specific cells in an endocrine, autocrine and paracrine manner. Moreover, they might have unrelated actions depending on the presence or absence of specific cytokines or the targeted cell [29]. By attaching to certain receptors, specific cytokines trigger versatile responses such as proliferation, cell differentiation, angiogenesis, inflammation, and immune responses. These different responses contain an overlapping network with varying degrees of abundance involved in different and important modulations. Consideration should so be given to defining key stages of cytokine responses during an infection to mark specific cytokines as therapeutic intervention targets [29].

4.2. The cytokine storm

The term cytokine storm has gained consideration since it was first introduced in the 1990s to illustrate the start of events aimed at modulating graft-versus-host disease (GVHD) [30]. Cytokine storm illustrate the role of the immune system in generating a public and uncontrolled inflammatory response [29] and can be used in parallel with the other term, cytokine release syndrome (CRS). Both terms mirror processes in which the same biomarker signatures and clinical phenotypes are presented; however, they possess separately different characteristics. CRS describes a perspective of reactions observed post targeted therapy administration leading to significant immune system activation; these therapies include chimeric antigen receptor (CAR) T-cell therapy and bispecific T-cell-engaging antibodies. Reciprocally, cytokine storm is an overwhelming activation of the immune system leading to systemic inflammation, which occurs independently from tumor targeting therapies [31]. Some infectious and non-infectious diseases are related with presentation of the cytokine storm; a drawback of some therapeutic interposition attempts is that this type of action is promoted [32]. Cytokine storm has been related with avian influenza virus (H5N1) infection [33]; clinical findings showed that most infected patients presented with fever, dyspnea, dry cough, and lung bilateral ground-glass opacities on chest computed tomography (CT) scans [34]. Early reports of COVID-19 indicated that one of the clinical aftereffects of SARS-CoV-2 infection appeared to be ARDS, which accounts for significant deaths among infected patients. Therefore, the process of cytokine storm should be considered as an immune-mediated hallmark of SARS-CoV-2 infection, as previously described for MERS-CoV and SARS-CoV [35]. ARDS is defined by the presence of severe hypoxemia and bilateral lung infiltrates; it accounts for nearly 40% of mortality incidents and can be an unfortunate result of several clinical situations including pneumonia, sepsis, and pancreatitis. The pathogenesis of ARDS results in alveolocapillary membrane permeability owing to inflammatory injury, leading to protein-rich pulmonary fluid perfusion into the airspaces causing edema, which eventually leads to insufficient respiration [36]. Increased levels of circulating proinflammatory cytokines (e.g., INFc, IL-B1, IL-6, and IL-12) and chemokines (e.g., CXCL10 and CCL2) are features of pulmonary inflammation in patients with SARS and similar to MERS-CoV infection [37].

5. Discussion and Conclusion

Since, the world, COVID-19 infection causes intense public health concern, analysis of the characteristics particularities of SARS-CoV-2, its interaction with the host cell receptor and immune responses, the phylogenetic and genomic similarity with other viruses will provide a clearer picture of diseases onset in individuals. Several groups of scientists have postulated that just like SARS-CoV, SARS-CoV-2 also depends upon the ACE2 as a

receptor for host cell entry. The interaction of the virus transmembrane spike (S) glycoprotein with host cell receptors operate as the determinant of the pathogenesis. A higher grade of disease violence is associated with viral load and sex and age of the patients. In old patients, the high viral bar is associated with low immunity as well as higher expression of the ACE2 cell receptor in some hematopoietic cells and macrophages and monocytes. At the same time, male patients are more sensitive to the SARS-CoV-2 infection than their female counterparts. "Lymphopenia" (low blood lymphocyte count) is correlated with the clinical severity of COVID-19 related infection. This study also, suggests that in one or more host species SARS-CoV-2 bined with integrins as cell receptors, through a conserved sequence RGD (403–405:Arg-Gly-Asp) with the RBD domain of the spike proteins.

In this review article, we summaries the various aspect of the therapeutic potential of the several anti-viral derivative. Finally, most advisable options must be evaluated better in clinical trials against the COVID-19 pandemic. It might contain of either mono-therapy or combinational therapies include of interferon beta-1b, lopinavir-ritonavir, and/ormAbs and antiviral peptides. Complete analyses of glycans are necessary for the expansion of glycoprotein-based vaccine which might near to correlate the immunogenicity with structural variations. In various expression systems, glycosylation operate as a measure to evaluate antigen quality. Fundamental understanding correlated with RBD domain of the spike protein of SARS-CoV-2 contain of complex sialylated N-glycans and sialylated mucin type O-glycans will be beneficial to design suitable immunity for vaccine extension. MBL is a serum C-type lectin, which can attach SARS-CoV per se or infected cell and also capable to prevent the infectivity of the virus. Investigations have shown that "MBLdeficient" individuals are at more risk to SARS infection. We support, MBL as a strong therapeutic and prophylactic strategy in the inhibition of SARS-CoV-2 pandemics. Shortly, it will be feasible to develop broad-spectrum, new, antiviral drugs active against a larger arrangement of coronavirus, and also will be the final treatment strategy for circulating and appearing COVID infections.

References

[1] Saif, L. J., Wang, Q., Vlasova, A. N., Jung, K., & Xiao, S. (2019). Coronaviruses. Diseases of swine, 488-523.

[2] Chen, J., Hu, C., Chen, L., Tang, L., Zhu, Y., Xu, X., ... & Li, L. (2020). Clinical study of mesenchymal stem cell treatment for acute respiratory distress syndrome induced by epidemic influenza A (H7N9) infection: a hint for COVID-19 treatment. Engineering, 6(10), 1153-1161.

[3] Hamre, D., & Procknow, J. J. (1966). A new virus isolated from the human respiratory tract. Proceedings of the Society for Experimental Biology and Medicine, 121(1), 190-193.

[4] Frieman, M., Yount, B., Heise, M., Kopecky-Bromberg, S. A., Palese, P., & Baric, R. S. (2007). Severe acute respiratory syndrome coronavirus ORF6 antagonizes STAT1 function by sequestering nuclear import factors on the rough endoplasmic reticulum/Golgi membrane. Journal of virology, 81(18), 9812-9824.

[5] Woo, P. C., Lau, S. K., Lam, C. S., Lau, C. C., Tsang, A. K., Lau, J. H., ... & Yuen, K. Y. (2012). Discovery of seven novel Mammalian and avian coronaviruses in the genus deltacoronavirus supports bat

coronaviruses as the gene source of alphacoronavirus and betacoronavirus and avian coronaviruses as the gene source of gammacoronavirus and deltacoronavirus. Journal of virology, 86(7), 3995-4008.

[6] Pillaiyar, T., Meenakshisundaram, S., & Manickam, M. (2020). Recent discovery and development of inhibitors targeting coronaviruses. Drug discovery today, 25(4), 668-688.

[7] Smith, E. C., & Denison, M. R. (2013). Coronaviruses as DNA wannabes: a new model for the regulation of RNA virus replication fidelity. PLoS Pathog, 9(12), e1003760.

[8] Cowley, J. A., Dimmock, C. M., Spann, K. M., & Walker, P. J. (2000). Gill-associated virus of Penaeus monodon prawns: an invertebrate virus with ORF1a and ORF1b genes related to arteri-and coronaviruses. Microbiology, 81(6), 1473-1484.

[9] Cong, Y. Y. (2019). Molecular insights into viral respiratory infections (Vol. 212). Groningen: University of Groningen.

[10] Kim, D., Lee, J. Y., Yang, J. S., Kim, J. W., Kim, V. N., & Chang, H. (2020). The architecture of SARS-CoV-2 transcriptome. Cell, 181(4), 914-921.

[11] Gao, Y., Yan, L., Huang, Y., Liu, F., Zhao, Y., Cao, L., ... & Rao, Z. (2020). Structure of the RNA-dependent RNA polymerase from COVID-19 virus. Science, 368(6492), 779-782.

[12] Dhama, K., Khan, S., Tiwari, R., Sircar, S., Bhat, S., Malik, Y. S., ... & Rodriguez-Morales, A. J. (2020). Coronavirus disease 2019–COVID-19. Clinical microbiology reviews, 33(4).

[13] Song, W., Gui, M., Wang, X., & Xiang, Y. (2018). Cryo-EM structure of the SARS coronavirus spike glycoprotein in complex with its host cell receptor ACE2. PLoSPathog 14: e1007236.

[14] Millet, J. K., Kien, F., Cheung, C. Y., Siu, Y. L., Chan, W. L., Li, H., ... & Nal, B. (2012). Ezrin interacts with the SARS coronavirus Spike protein and restrains infection at the entry stage. PLoS One, 7(11), e49566.

[15] Alnefaie, A., & Albogami, S. (2020). Current approaches used in treating COVID-19 from a molecular mechanisms and immune response perspective. Saudi Pharmaceutical Journal.

[16] Tikellis, C., & Thomas, M. C. (2012). Angiotensin-converting enzyme 2 (ACE2) is a key modulator of the renin angiotensin system in health and disease. International journal of peptides, 2012.

[17] Li, W., Moore, M. J., Vasilieva, N., Sui, J., Wong, S. K., Berne, M. A., ... & Farzan, M. (2003). Angiotensin-converting enzyme 2 is a functional receptor for the SARS coronavirus. Nature, 426(6965), 450-454.

[18] Chatterjee, S. K., Saha, S., & Munoz, M. N. M. (2020). Molecular pathogenesis, immunopathogenesis and novel therapeutic strategy against COVID-19. Frontiers in molecular biosciences, 7, 196.

[19] Xie, X., Chen, J., Wang, X., Zhang, F., & Liu, Y. (2006). Erratum to "Age-and gender-related difference of ACE2 expression in rat lung". Life Sciences, 26(79), 2499.

[20] Wu, C., Liu, Y., Yang, Y., Zhang, P., Zhong, W., Wang, Y., ... & Li, H. (2020). Analysis of therapeutic targets for SARS-CoV-2 and discovery of potential drugs by computational methods. Acta Pharmaceutica Sinica B, 10(5), 766-788.

[21] Wan, Y., Shang, J., Graham, R., Baric, R. S., & Li, F. (2020). Receptor recognition by the novel coronavirus from Wuhan: an analysis based on decade-long structural studies of SARS coronavirus. Journal of virology, 94(7).

[22] Jia, H. (2016). Pulmonary angiotensin-converting enzyme 2 (ACE2) and inflammatory lung disease. Shock, 46(3), 239-248.

[23] Bourgonje, A. R., Abdulle, A. E., Timens, W., Hillebrands, J. L., Navis, G. J., Gordijn, S. J., ... & van Goor, H. (2020). Angiotensin-converting enzyme 2 (ACE2), SARS-CoV-2 and the pathophysiology of coronavirus disease 2019 (COVID-19). The Journal of pathology, 251(3), 228-248.

[24] Gue, Y. X., Kanji, R., Markides, V., & Gorog, D. A. (2020). Angiotensin Converting Enzyme 2 may mediate disease severity in COVID-19. American Journal of Cardiology, 130, 161-162.

[25] Marshall, J. S., Warrington, R., Watson, W., & Kim, H. L. (2018). An introduction to immunology and immunopathology. Allergy, Asthma & Clinical Immunology, 14(2), 1-10.

[26] Christiaansen, A., Varga, S. M., & Spencer, J. V. (2015). Viral manipulation of the host immune response. Current opinion in immunology, 36, 54-60.

[27] Iwasaki, A., & Medzhitov, R. (2010). Regulation of adaptive immunity by the innate immune system. science, 327(5963), 291-295.

[28] Turvey, S. E., & Broide, D. H. (2010). Innate immunity. Journal of Allergy and Clinical Immunology, 125(2), S24-S32.

[29] Tisoncik, J. R., Korth, M. J., Simmons, C. P., Farrar, J., Martin, T. R., & Katze, M. G. (2012). Into the eye of the cytokine storm. Microbiology and Molecular Biology Reviews, 76(1), 16-32.

[30] FERRARA, J. M., Abhyankar, S., & Gilliland, D. G. (1993). Cytokine storm of graft-versus-host disease: a critical effector role for interleukin-1. In Transplantation proceedings (Vol. 25, No. 1, pp. 1216-1217).

[31] Porter, D., Frey, N., Wood, P. A., Weng, Y., & Grupp, S. A. (2018). Grading of cytokine release syndrome associated with the CAR T cell therapy tisagenlecleucel. Journal of hematology & oncology, 11(1), 1-12.

[32] Suntharalingam, G., Perry, M. R., Ward, S., Brett, S. J., Castello-Cortes, A., Brunner, M. D., & Panoskaltsis, N. (2006). Cytokine storm in a phase 1 trial of the anti-CD28 monoclonal antibody TGN1412. New England Journal of Medicine, 355(10), 1018-1028.

[33] Yuen, K. Y., & Wong, S. S. Y. (2005). Human infection by avian influenza A H5N1. Hong Kong Medical Journal.

[34] Guan, Y., Zheng, B. J., He, Y. Q., Liu, X. L., Zhuang, Z. X., Cheung, C. L., ... & Poon, L. L. M. (2003). Isolation and characterization of viruses related to the SARS coronavirus from animals in southern China. Science, 302(5643), 276-278.

[35] Xu, Z., Shi, L., Wang, Y., Zhang, J., Huang, L., Zhang, C., ... & Wang, F. S. (2020). Pathological findings of COVID-19 associated with acute respiratory distress syndrome. The Lancet respiratory medicine, 8(4), 420-422.

[36] Bhatia, M., Zemans, R. L., & Jeyaseelan, S. (2012). Role of chemokines in the pathogenesis of acute lung injury. American journal of respiratory cell and molecular biology, 46(5), 566-572.

[37] Channappanavar, R., & Perlman, S. (2017, July). Pathogenic human coronavirus infections: causes and consequences of cytokine storm and immunopathology. In Seminars in immunopathology (Vol. 39, No. 5, pp. 529-539). Springer Berlin Heidelberg.

Enhancement of stability and acaricidal potential of the monoterpenoid 1,8-cineole through nanoencapsulation in zeolite A3

Asgar Ebadollahi[1]* and Jalal Jalali-Sendi[2]

[1] Moghan College of Agriculture and Natural Resources, University of Mohaghegh Ardabili, Ardabil, Iran

[2] Department of Plant Protection, Faculty of Agricultural Sciences, University of Guilan, Rasht, Iran

Email: ebadollahi@uma.ac.ir

Abstract

Plant-derived agents have announced as environmentally safe and efficient alternatives to synthetic pesticides. Monoterpenoids such as 1,8-cineole, well-known secondary metabolites in many aromatic plants, exhibited great potential in the pest management strategies. But due to the effect of light, oxygen, high temperatures, and ultraviolet rays, they have short environmentally persistent. In the current study, fumigant toxicity of pure and nanoencapsulated 1,8-cineole was evaluated against a cosmopolitan and damaging mite in the greenhouses, fields, and orchards; *Tetranychus urticae* Koch (Acari: Tetranychidae). The encapsulation efficiency of 1,8-cineole in zeolite A3 was 92.26 ± 0.60%, and the size of the encapsulated monoterpenoid was measured less than 100 nm by SEM. The durability of toxicity expanded from 4 days for 1,8-cineole to 24 days for 1,8-cineole–zeolite A3 nanoparticles. In general, encapsulation of 1,8-cineole in zeolite A3 improved its stability, and the toxicity significantly increased. According to the current results, the nanoencapsulation of 1,8-cineole by zeolite A3 is a suitable method for overcoming its low stability and maybe resulted in the applicable control of *T. urticae*.

Keywords: Augmentation, 1,8-Cineole, Fumigant toxicity, Zeolite A3.

1. Introduction

Indiscriminate utilization of synthetic pesticides has resulted in serious environmental consequences such as pest resistant and resurgence, bioaccumulation, and harmful effects on non-target organisms [1, 2]. Thus, the deployment of safe and efficient alternatives for pest management is necessary.

The two-spotted spider mite, *Tetranychus urticae* Koch (Tetranychidae), is one of the most detrimental pest of up to 150 host plant species in orchards, greenhouses, and field crops [3]. Along with direct and indirect losses in host plants, the importance of two-spotted spider mite in medicinal aspect was also approved [4].

Mesoporous materials such as zeolites have many applications in the biological, chemical, environmental, and medicinal fields [5]. It was confirmed that the encapsulation of bio-rational agents in the controlled-release techniques is one of the new applications of these materials [6]. Zeolites are aluminum silicates that form crystal or frame structures with adjacent sides via sharing oxygen molecules and have large empty spaces which may be

filled with cations such as sodium and potassium, and cationic groups such as water and ammonia, and even larger molecules [7].

Monoterpenoids such as 1,8-cineole, thymol, γ-terpinene, p-cymene, α-pinene, and limonene presented high potential in the control of several pests [8]. 1,8-Cineole extracted from many plant essential oils exhibited diverse biological effects, including antibacterial, antiviral, antifungal and antioxidant activities along with pesticidal efficiency [9].

The present study aims to compare the fumigant toxicity of pure and zeolite A3-nanoencapsulated 1,8-cineole against two-spotted spider mite, assuming that the nanoencapsulation of this monoterpenoid will increase its durability and toxicity.

2. Material and Methods

2.1 Synthesis of mesoporous material

All required materials were obtained from Merck (Germany). For the synthesis of zeolite A3, aluminum oxide, silicate, sodium oxide, and water used at a ratio of 1, 2, 0.55, and 0.45 (0.55Na2O. Al2O3. 2SiO2. 0.45H2O). The resulting mixture poured into water, and after adding potassium chloride (35% zeolite weight), stirred for 2 hours. The mixture was passed through the filter and dried after washing.

2.2 Two-spotted spider mite rearing

A two-spotted spider mite colony was reared on navy bean (*Vigna unguiculata* Walp) plants. Then the plants were kept in cages (120 × 300 × 100 cm) which were covered with mesh cloth. Fifty adult-females were transferred to the bean leaves and allowed to lay eggs within 24 h. The females removed, and leaves were detained to eggs hatching and the larvae to develop into synchronized adults. The synchronized female-adults were used for bioassays. All experiments were carried out at 25 ± 2 °C, 60 ± 5% RH, and a photoperiod of 16: 8 (L : D).

2.3 Nanoencapsulation of 1,8-cineole

Twenty mg zeolite A3 dissolved in 100 µl acetone added to 6.067 µl 1,8-cineole dissolved in 100 µl acetone in another container . For achieving the initially weight of mesoporous material (20 mg) in the control groups, the solution stirred for 20 minutes. Using this time, the final 1,8-cineole-loaded mesoporous materials were prepared with same approach. The size distributions of the mesoporous particles were determined by SEM (Hitachi su8040). The encapsulation efficiency percentage and loading percentage were determined as follows;

$$\text{Encapsulation Efficiency Percentage} = \frac{\text{weight of encapsulated essential oil}}{\text{weight of essential oil used initially}} \times 100$$

2.4 Fumigant persistence of pure and encapsulated 1,8-cineole

The persistence of pure and nanoencapsulated 1,8-cineole was measured as follow; 750 ml containers with tight caps were used as the fumigant chambers. Filter papers (2 × 2 cm strip) impregnated with 6.067 µl 1,8-cineole were used beside leaf discs (3 cm in diameter punched from leaves of bean plants). Unloaded nanoparticles, as a control group, and nanoencapsulated 1,8-cinele were also poured beside leaf discs in the fumigant chamber. The mortality was counted for each 24 h of exposure time and 10 mites were introduced to fumigant chamber per each time step. Four replications were considered for each treatment and control groups.

3. Results and Discussions

The encapsulation efficiency percentage of 1,8-cineole loaded in zeolite A3 was 92.26 ± 0.60%. According to figure 1, although the size of some particles were larger than 100 nm, their common size was approximately 50 nm.

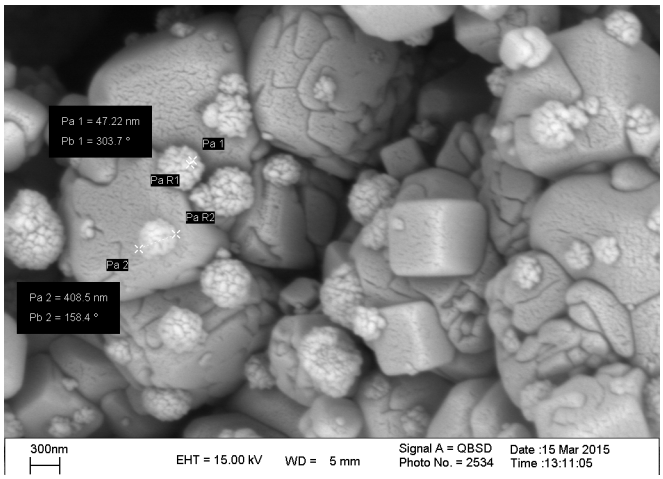

Figure 1. SEM micrograph of 1,8-cineole loaded in zeolite A3.

Persistency of 1,8-cineole was ended after 4 days exposure time. Encapsulation 1,8-cineole in zeolite A3 was improved its durability so that the fumigant toxicity persistent of zeolite A3 based nanoencapsulated agents were extended to 24 days. Further, mortality was increased from 54 mites for pure monoterpenoid to 141 mites for capsulated one (Figure 2).

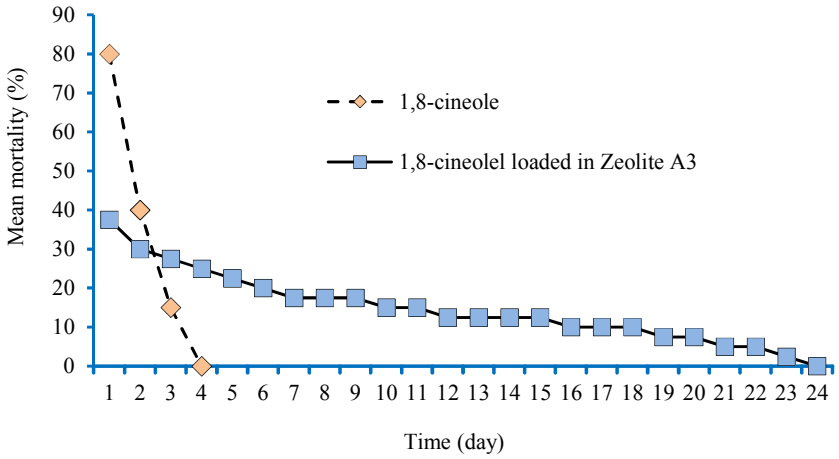

Figure 2. Comparison of the fumigant persistency of pure and zeolite A3 nanoencapsulated 1,8-cineole against *Tetranychus urticae*.

The possibility of using monoterpenoid compounds such as 1,8-cineole in pest control was confirmed in many studies. For example, significant toxicity of 1,8-cineole on Southern house mosquito (*Culex quinquefasciatus* Say, Diptera: Culicidae), Rice weevil (*Sitophilus oryzae* L., Coleoptera: Circulionidae), and German cockroach (*Blattella germanica* L., Blattodea: Blattellidae) has been approved in previous works [10-12]. According to outcomes of present study, 1,8-cineole has also high potential in the management of two spotted spider mite. Despite the positive effects of 1,8-cineole on pest control, its durability in the environment is low, so that in the present study, the lethality of this compound was last on the fourth day. According to recent studies, mesoporous materials may be considered as a useful agents in the stability improvement of bio-agents in the frame of the controlled-release technique [13-14]. For example, nanoencapsulation of *Thymus eriocalyx* and *Thymus kotschyanus* essential oils by MCM-41, (one of the well-known mesoporous materials) improved their fumigant-toxicity persistent against two spotted spider mite from 6 and 5 days to 20 and 18 days, respectively [15]. In the current study, the persistence of the fumigant toxicity of 1,8-cineole improved from 4 to 24 days by loading in zeolite A3.

Plant-derived secondary metabolites such as essential oils and their main components, including monoterpenes, are considered as efficient bio-rational pesticides. Along with all advantages of these bio-rational agents, such as low or less toxicity to mammals and availability, low persistent is the main problem for their application and commercialization. In the present study, the persistence of fumigant-toxicity of 1,8-cineole before two-spotted spider mite significantly increased by loading in zeolite A3. On the other hand, nanoencapsulation of 1,8-cineole by zeolite A3 augmented its toxicity and durability.

References

[1] R. J. Gill, O. Ramos-Rodriguez, N. E. Raine, Combined pesticide exposure severely affects individual- and colony-level traits in bees, Nature 491 (2012) 105-108.

[2] S. Mostafalou, M. Abdollahi, Pesticides and human chronic diseases: evidences, mechanisms, and perspectives, Toxicology and Applied Pharmacology 268 (2013) 157-177.

[3] Z. Q. Zhang, Mites of Greenhouses; Identification, Biology and Control, CABI Publishing, Wallingford, UK, 2003, 244 p.

[4] Y. K. Kim, Y. Y. Kim, Spider-mite allergy and asthma in fruit growers, Curr. Opin. Allergy. Clin. Immunol. 2 (2002) 103–107.

[5] R. Xu, W. Pang, J. Yu, Q. Huo, J. Chen, Chemistry of zeolites and related porous materials: synthesis and structure, John Wiley & Sons, Singapore, (2007).

[6] S. Giri, B.G. Trewyn, M.P. Stellmaker, V.S.Y. Lin, Stimuli-responsive controlled-release delivery system based on mesoporous silica nanorods capped with magnetic nanoparticles. Angew. Chem. Int. Ed. 44 (2005) 5038–5044.

[7] A. D. Elliot, D. K. Zhang, Controlled Release Zeolite Fertilizers: A Value Added Product Produced from Fly Ash, World of Coal Ash, Lexington, Kentucky, USA. (2005).

[8] A. Ebadollahi, M. Ziaee, F. Palla, Essential oils extracted from deferent species of the Lamiaceae plant family as prospective bioagents against several detrimental pests, Molecule 25 (2020) 1556.

[9] D. R. Batish, H. P. Singh, R. K. Kohli, S. Kaur, Eucalyptus essential as natural pesticide, For. Ecol. Manage. 256 (2008) 2166–2174.

[10] H. J. Yeom, J. S. Kang, G. H. Kim, I. K. Park, Insecticidal and acetylcholine esterase inhibition activity of Apiaceae plant essential oils and their constituents against adults of German cockroach (*Blattella germanica*), J. Agric. Food Chem. 60(2012) 7194-7203.

[11] S. Andrade-Ochoa, J. Correa-Basurto, L. M. Rodriguez-Valdez, L. E. Sanchez-Torres, B. Nogueda-Torres, GV.Nevarez-Moorillon, In vitro and in silico studies of terpenes, terpenoids and related compounds with larvicidal and pupaecidal activity against *Culex quinquefasciatus* say (Diptera: Culicidae), Chem. Cent. J. 12 (2018): 53 doi: 10. 1186/ s13065- 018- 0425-2

[12] T. T. Liu, L. K. P. Chao, K. S. Hong, Y. J. Huang, T. S. Yang, Composition and insecticidal activity of essential oil of *Bacopa caroliniana* and interactive effects of individual compounds on the activity, Insects 11(2020) 23. doi: 10. 3390/ inse cts1 1010023

[13] J. Chen, W. Wang, Y. Xu, X. Zhang, Slow-release formulation of a new biological pesticide, pyoluteorin, with mesoporous silica, J. Agr. Food Chem. 59 (2011) 307-311.

[14] A. Bernardos, T. Marina, P. Žáček, É. Pérez-Esteve, R. Martínez-Mañez, M. Lhotka, L. Kouřimská, J. Pulkrábek, P. Klouček, Antifungal effect of essential oil components against *aspergillus niger* when loaded in silica mesoporous supports, *J. Sci. Food Agric.* 95 (2015) 2824-2831.

[15] A. Ebadollahi, J. Jalali Sendi, A. Aliakbar, Efficacy of nanoencapsulated *Thymus eriocalyx* and *Thymus kotschyanus* essential oils by a mesoporous material MCM-41 against *Tetranychus urticae* (acari: tetranychidae), Journal of Economic Entomology 110 (2017) 2413-2420.

Controlled-release of thymol through nanoencapsulation in zeolite A3 and acaricidal efficiency

Asgar Ebadollahi[1]* and Jalal Jalali-Sendi[2]

[1] Moghan College of Agriculture and Natural Resources, University of Mohaghegh Ardabili, Ardabil, Iran

[2] Department of Plant Protection, Faculty of Agricultural Sciences, University of Guilan, Rasht, Iran

Email: ebadollahi@uma.ac.ir

Abstract

Although pesticidal effects of plant secondary metabolites such as monoterpenes have been reported in several recent researches, due to the adverse effect of environmental factors, including light, oxygen, high temperatures, and ultraviolet rays, they have short persistent. In the present study, a well-known monoterpene thymol was nanoencapsulated in the mesoporous material zeolite A3 to overcome its low fumigant persistence, and the toxicity of synthesized nanocapsule was assessed against one of the important pests of greenhouse, orchard, and filed crops; two spotted spider mite (*Tetranychus urticae* Koch). The encapsulation efficiency of thymol in zeolite A3 was 95.00 ± 0.96%. The size of the encapsulated monoterpenoid was measured by SEM, in which its nano size (less than 100 nm) was confirmed. Nanoencapsulation of thymol by zeolite A3 improved its persistence so that the fumigant toxicity persistency from 6 days for pure thymol reached to 29 days for capsulated formulation. On the other hand, loading of in zeolite A3 prolonged the acaricidal activity and persistence of thymol. According to the results of present study, the nanoencapsulation by zeolite A3 is an appropriate technique to overcome low stability of thymol, and can be considered for management of *T. urticae*.

Keywords: Acaricidal activity, Nanoencapsulation, Thymol, Zeolite A3.

1. Introduction

The application of synthetic chemicals is the main tool in the management of arthropod pests. However, there is a world-wide concern about several side-effects of such chemicals, including environmental pollution, toxicity to non-target organisms ranging from soil microorganisms to pollinator, fish, and even humans, pest resistance, and resurgence of secondary pests [1-3]. Therefore, the introduction of eco-friendly and efficient alternatives for pest management is crucial.

The two-spotted spider mite [*Tetranychus urticae* Koch (Tetranychidae)] is one of the most damaging pest on up to 150 host plants from orchards, greenhouses, and field crops. Along with direct and indirect losses in host plants, such as defoliation, leaf burning, decreases in plant photosynthesis and plant death, the importance of two-spotted spider mite in medicinal aspect was also approved [4, 5].

Monoterpenes as well-known secondary metabolites showed great potential in the management of different groups of pests [6]. Monoterpenoid thymol extracted from many aromatic plants especially the *Thymus* genus and displayed several biological effects such as antibacterial, antifungal, and antioxidant activities [7]. However, due to the low persistence, the application and commercialization of these materials are restricted. The use of mesoporous materials for capsulation of biological agents in the controlled-release techniques is a novel approach to overcome the low persistent problem [8,9]. Zeolites are crystal aluminium silicates with large empty spaces that may be filled with cations such as sodium and potassium, and cationic groups such as water and even larger molecules [10].

The present study conducted to compare the toxicity of pure and zeolite A3-nanoencapsulated formulations of thymol against two-spotted spider mite. The present study hypothesized that the encapsulation by zeolite A3 would increase the toxicity and persistence of thymol.

2. Material and Methods

2.1 Two-spotted spider mite rearing

The colony of two-spotted spider mite was reared on *Vigna unguiculata* Walp (navy bean). The plants were held in 120 × 300 × 100 cm cages which were covered with mesh cloth. Fifty adult-females of mite were relocated on the bean leaves and allowed to lay eggs within 24 h. The adult females removed, eggs hatched and the larvae developed into synchronized adults. The synchronized female-adults of mite were used for bioassays.

2.2 Synthesis of zeolite A3

All required materials were obtained from Merck (Germany). For the synthesis of zeolite A3, aluminum oxide, silicate, sodium oxide, and water used at a ratio of 1, 2, 0.55, and 0.45 (0.55Na2O. Al2O3. 2SiO2. 0.45H2O). The

resulting mixture poured into water, and after adding potassium chloride (35% zeolite weight), stirred for 2 hours. The mixture was passed through the filter and dried after washing.

2.3 Nanoencapsulation of thymol

Twenty mg zeolite A3 dissolved in 100 µl acetone and added to a solution of 4.281 mg/l thymol in 100 µl acetone. After 20 minute shaking at room temperature, initially weight of mesoporous material (20 mg) was attained in the control groups. Considering this time, the final thymol-loaded mesoporous materials were prepared with same approach.). The size distributions of the mesoporous particles were determined by SEM (Hitachi su8040). The encapsulation efficiency percentage and loading percentage were determined as follows;

$$\text{Encapsulation Efficiency Percentage} = \frac{\text{weight of encapsulated essential oil}}{\text{weight of essential oil used initially}} \times 100$$

2.4 Fumigant persistence of pure and encapsulated formulations of thymol

The persistence of pure and nanoencapsulated formulations of thymol was evaluated in 750 ml containers with tight caps as the fumigant chambers. Filter papers (2 × 2 cm strip) impregnated with 4.281 mg/l thymol were used beside leaf discs (3 cm in diameter punched from leaves of bean plants). Unloaded nanoparticles considered as a control group, and nanoencapsulated thymol were also poured beside leaf discs in the fumigant chamber. The mortality was documented for each 24 h- time interval, and 10 mites were introduced to fumigant chamber per each time step. Four replications were considered for each treatment and control groups. All experiments were carried out at 25 ± 2 °C, 60 ± 5% RH, and a photoperiod of 16: 8 (L : D).

3. **Results and Discussions**

The encapsulation efficiency percentage of zeolite A3 nanoencapsulated formulation of thymol was 95.00 ± 0.96%. The common size of nanocapsules was approximately 50 nm. However, according to figure 1, the size of some particles were larger than 100 nm.

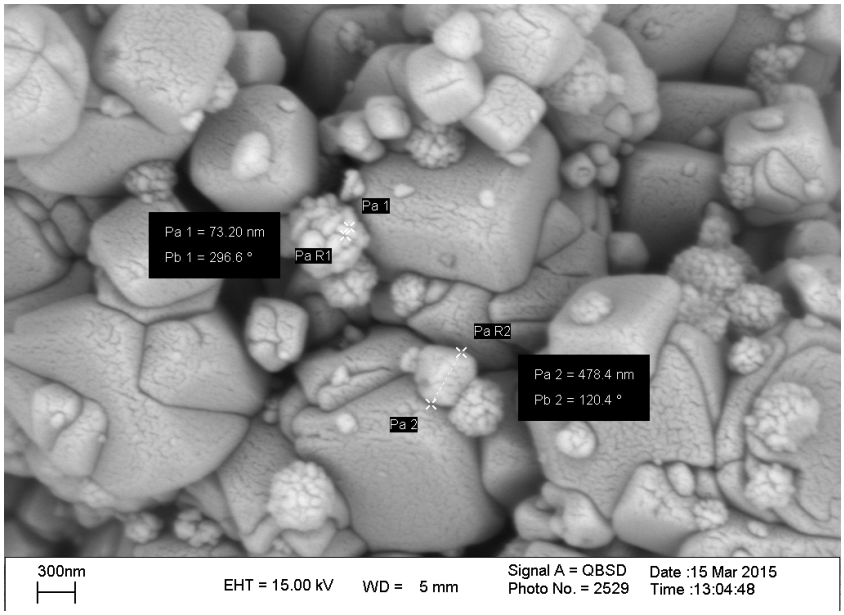

Figure 1. SEM micrograph of zeolite A3 nanoencapsulated formulation of thymol.

Persistency of thymol was broken up after 6 days exposure time. Encapsulation of thymol in zeolite A3 was improved its stability so as to the persistent of nanocapsules fumigant toxicity were stretched to 29 days. Further, mortality was augmented from 71 mites for pure monoterpenoid to 168 mites for capsulated formulation (Figure 2).

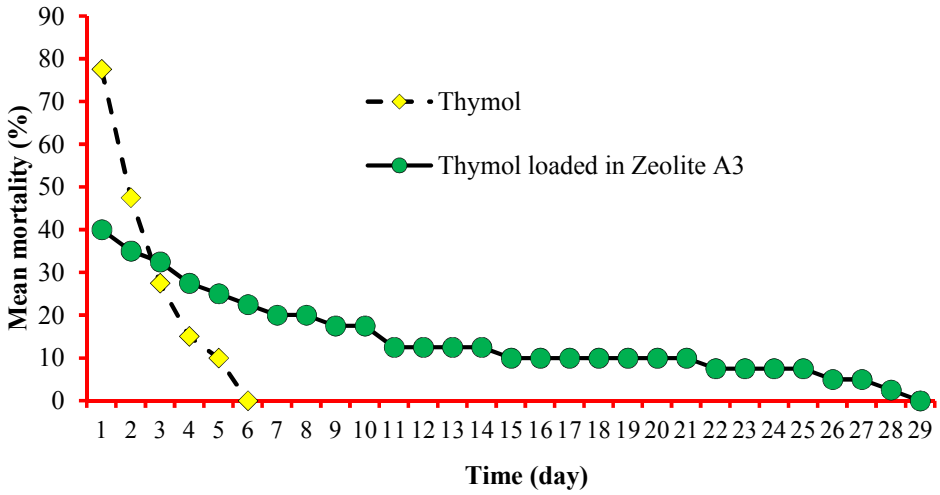

Figure 2. Comparison of the fumigant persistency of pure and zeolite A3 nanoencapsulated formulations of thymol against *Tetranychus urticae*.

High potential of monoterpenoid thymol in pest management reported in previous studies. For example, significant pesticidal effects of thymol on wheat grain weevil (*Sitophilus granaries* L., Coleoptera: Circulionidae), Rice weevil (*Sitophilus oryzae* L., Coleoptera: Circulionidae), Southern house mosquito (*Culex quinquefasciatus*

Say, Diptera: Culicidae), and German cockroach (*Blattella germanica* L., Blattodea: Blattellidae) has been approved in previous works [11-14]. According to resutls of present study, thymol has great potential in the management of two spotted spider mite. However, despite the constructive effects of thymol on pest control, its environmental stability is low so that its toxicity was last after 6 days.

Some previous studies revealed that mesoporous materials can be considered as useful agents in the controlled-released of bio-agents [15-16]. For example, nanoencapsulation of *Thymus eriocalyx* and *Thymus kotschyanus* essential oils by a another well-known mesoporous MCM-41 improved their fumigant persistent before two spotted spider mite from 6 and 5 days to 20 and 18 days, respectively [7]. In the present study, the toxicity persistence of thymol enhanced from 6 to 29 days through encapsulation in zeolite A3.

Secondary metabolites extracted from aromatic plants, such as essential oils and their main components, are considered as effective pesticides. As bio-rational pesticides, they have several advantages, including low or less toxicity to mammals, availability, and low pest-resistant chance before them. The main problem for the commercialization of these bio-agents is their low persistence. In the present study, the acaricidal persistence of thymol was significantly extended by loading in zeolite A3. On the other hand, zeolite A3-based nanocapsules can be introduced as a suitable formulation for improving the acaricidal efficiency of thymol.

References

[1] C. A. Damalas, I. G. Eleftherohorinos, Pesticide exposure, safety issues, and risk assessment indicators, Int. J. Environ. Res. Public Health 8 (2011) 1402–1419.

[2] R. Mulé, G. Sabella, L. Robba, B. Manachini, Systematic review of the effects of chemical insecticides on four common butterfly families, Front. Environ. Sci. 5 (2017) 32.

[3] V. L. Zikankuba, G. Mwanyika, J. E. Ntwenya, A. James, Pesticide regulations and their malpractice implications on food and environment safety, Cogent Food Agric. 5 (2019) 1601544.

[4] Z. Q. Zhang, Mites of Greenhouses; Identification, Biology and Control, CABI Publishing, Wallingford, UK, 2003, 244 p.

[5] Y. K. Kim, Y. Y. Kim, Spider-mite allergy and asthma in fruit growers, Curr. Opin. Allergy. Clin. Immunol. 2 (2002) 103–107.

[6] A. Ebadollahi, M. Ziaee, F. Palla, Essential oils extracted from deferent species of the Lamiaceae plant family as prospective bioagents against several detrimental pests, Molecule 25 (2020) 1556.

[7] A. Ebadollahi, J. Jalali Sendi, A. Aliakbar, Efficacy of nanoencapsulated Thymus eriocalyx and Thymus kotschyanus essential oils by a mesoporous material MCM-41 against Tetranychus urticae (acari: tetranychidae), Journal of Economic Entomology 110 (2017) 2413-2420.

[8] S. Giri, B. G. Trewyn, M. P. Stellmaker, V. S. Y. Lin, Stimuli-responsive controlled-release delivery system based on mesoporous silica nanorods capped with magnetic nanoparticles, Angew. Chem. Int. Ed. 44 (2005) 5038–5044.

[9] R. Xu, W. Pang, J. Yu, Q. Huo, J. Chen, Chemistry of zeolites and related porous materials: synthesis and structure, John Wiley & Sons, Singapore, (2007).

[10] A. D. Elliot, D. K. Zhang, Controlled Release Zeolite Fertilizers: A Value Added Product Produced from Fly Ash, World of Coal Ash, Lexington, Kentucky, USA. (2005).

[11] H. J. Yeom, J. S. Kang, G. H. Kim, I. K. Park, Insecticidal and acetylcholine esterase inhibition activity of Apiaceae plant essential oils and their constituents against adults of German cockroach (Blattella germanica), J. Agric. Food Chem. 60 (2012) 7194-7203.

[12] S. Andrade-Ochoa, J. Correa-Basurto, L. M. Rodriguez-Valdez, L. E. Sanchez-Torres, B. Nogueda-Torres, GV.Nevarez-Moorillon, In vitro and in silico studies of terpenes, terpenoids and related compounds with larvicidal and pupaecidal activity against Culex quinquefasciatus say (Diptera: Culicidae), Chem. Cent. J. 12 (2018): 53 doi: 10. 1186/ s13065- 018- 0425-2

[13] T. T. Liu, L. K. P. Chao, K. S. Hong, Y. J. Huang, T. S. Yang, Composition and insecticidal activity of essential oil of Bacopa caroliniana and interactive effects of individual compounds on the activity, Insects 11 (2020) 23. doi: 10. 3390/ inse cts1 1010023

[14] S.Kordali, A. Usanmaz, N. Bayrak, A. Çakır, Fumigation of volatile monoterpenes and aromatic compounds against adults of Sitophilus granarius (L.) (Coleoptera: Curculionidae), Rec. Nat. Prod. 11 (2017) 362-373.

[15] J. Chen, W. Wang, Y. Xu, X. Zhang, Slow-release formulation of a new biological pesticide, pyoluteorin, with mesoporous silica, J. Agr. Food Chem. 59 (2011) 307-311.

[16] A. Bernardos, T. Marina, P. Žáček, É. Pérez-Esteve, R. Martínez-Mañez, M. Lhotka, L. Kouřimská, J. Pulkrábek, P. Klouček, Antifungal effect of essential oil components against Aspergillus niger when loaded in silica mesoporous supports, J. Sci. Food Agric. 95 (2015) 2824-2831.

Antimicrobial activities of alcoholic extract in Asteraceae family in shabestar area of Esat Azarbaijan in Iran

Leila joudi[1]*

Department of agriculture, shabestar branch, Islamic Azad University, shabestar, Iran

Corresponding Auteur: Joudi.leila@yahoo.com

Abstract

The extracts or essential oils or extracts of some medicinal plants show strong antimicrobial effects, and could be used as antimicrobial drugs or food preservation. Many spices of Asteraceae family have large amounts of effective materials and frequently show antimicrobial properties. In this research antimicrobial activity of alcoholic extract of species of Asteraceae family, were studied on 2 spices of bacteria, Bacillus subtilis and Esherichia Coli. Disk Diffusion method used for determine inhibitory caused by effect of plant extracts. All the tests were compared with inhibitory effect of proper antibiotic commonly used against these bacteria (Tetracycline). The results of experiments demonstrated that alcoholic extract showed significant antibacterial effects. The results indicated that B. subtilis has been affected by Onopordon leptoedis, frequently, C.aggregate , C.virgata, A.vermicularis and C.oxyacantha. all plants can't inhibit on E. coli. We matched the effect of extract and antibiotic (TE) on bacteria. The results were as follow, the extract of some plants on B. subtilis were almost as strong as tetracycline and can use as alternative chemical drugs.

Keywords: antimicrobial activity, Asteraceae, disc diffusion.

Introduction

Medicinal plants that have already been used as traditional drugs, have been entered new pharmaceutical systems, in recent years and are used in drugs compositions as volatile oils, extracts and pure forms. In many parts of the world, these products found an important role in providing health care services. Nowadays, chemical preservatives that are added to the food for long term storage, cause undesirable side roles and failure of vital body system. Therefore, in order to protect the food and pharmaceutical microbial corruption, various additives that are of natural origin are recommended. For this reason, species of Compositae that are rich in effective material is used to prevent and inhibit the growth of pathogenic microorganisms. Resistance to antimicrobial agents has become an increasingly important and pressing global problem. Of the 2 million people who acquire bacterial infections in lots of hospitals each year, 70% of cases now involve strains that are resistant to at least one drug (Mabberley, 1997). Several species of compositae, with nearly 500 species, is mainly distributed around the Mediterranean area and in western Asian (Mabberley, 1997). It has been the subject of many chemical investigations, which led to the isolation of various types of compounds, such as sesquiterpene lactones, being the most abundant group, flavonoids, lignans, nor-isoprenoids and volatile constituents. Antimicrobial activity of secondary metabolites isolated from compositae species. In 1988 Singh et al worked on antibacterial activities of etteral extract of Sphaeranthus indicus that inhibited activity of Staphyloccus aureus،S.albus و E.coli (Singh,

1988). In 2000 antimicrobial activity of Aspilla africana was reported on 4 gram positive and 4gram negative bacteria (Adeniyi, 2000).

Materials and Methods:

Plant material

Compositae family species consist of(Lactoca seriola, Centaurea cheirantifolia, Centaurea aggregate, Carthamus oxyacantha, Tragopogon marginatus, Cousinia Calcitrapa, Achillea vermicularis, Crepis sancta, Cardus pycnocephalus, Acroptilon repens, Achillea millefollium, Centaurea virgate, Arctium lappa, Senecio mollis, Lactuca glaucifolia, Chicoriun intybus, Taraxacum syriacum, Tragopogon pratensis, Achillea tenuifolia, Onopordon leptolepis) at flowering stage were collected from shabestar area, which is located in East Azerbaijan province (Iran). Shabestar is located in the north-west of Tabriz and the geographic coordinates 37 degrees and 42 minutes of north latitude and 45 degrees and 5 minutes and 46 degree and 9 minutes East longitude. Collected plant materials were dried in shadow, and all areal parts of plant were separated from the root, and ground in a grinder with a 2 mm diameter mesh. The voucher specimen has been deposited at the Herbarium of Medicinal Plants Institute, shabestar, Iran. Isolation of the extract of plant materials were prepared by using solvents. About 100 g of dry powdered plant materials were extracted with Ethanol for 24 h. solvents were purchased from Merck. The extracts were evaporated under reduced pressure and dried using rotary evaporator. Dried extracts were stored in labelled sterile screw capped bottles at -20°C (Kivrak et al., 2009).

Table1. Scientific classification of Asteraceae

Scientific classification	
Kingdom	Plantae
unranked	Angiosperms
unranked	Eudicots
unranked	Asterids
Order	Asterales
Family	Asteraceae

Microbial strains

Esherichia Coli (PTCC 1535)and Listeria monocytogenes (PTCC1301) were used to evaluate the antimicrobial activities of the selected extracts. Bacteria were prepared from the center of collection of bacteria and fungi of Iran (PTCC). Inhibitory effect by the disc diffusion method the antimicrobial activity of the alcoholic extracts of all species were assayed by the standard disc diffusion method (Mercan et al., 2006). In this method, the microorganisms were sub-cultured into 5 ml of MHA, followed by incubation at 37 °C for 24 h. During this period, microorganisms grew. Disks were located in areas that in case of being anti-microbial to inhibit the growth of microbes and a halo were created around the disks that is called inhibition halo and its diameter can be measured with a caliper. Diameter of inhibition caused by samples were compared with each other. MHA was poured into each sterile Petri dish (10 x 100 mm diameter) after injecting cultures (0/1 ml) of bacteria and distributing medium in Petri dishes homogeneously. Sterile discs (6 mm; Schleicher and Schuell, No. 2668, Germany) were

impregnated with 20 / l of a solution prepared with 100 mg of extract in 1 ml Ethanol and allowed to dry at room temperature. The discs injected with extracts were placed on the inoculated agar by pressing slightly. The bacteria were incubated at 37°C for 24 h. At the end of the period, inhibition zones formed on the medium were evaluated in mm. Ethanol which was used as a negative control did not show any antimicrobial activity. Tetracycline was used as positive control for bacteria.

Results

Results of inhibition zones in the disc diffusion method for extracts and antibiotic were shown in Table 2 and figure1.

Figure1. Effect of extract on microorganisms

	O. leptolepis	C.aggregate	C.Calcitrapa	A.repens	C.oxyacantha	A.vermicularis	C.virgata	C.sancta
B. subtillis	16	15	15	13	12	12	12	0
L.monocytogenes	0	0	0	0	0	0	0	0

	L.seriola	A.tenuifolia	A. millefollium	A. lappa	S. mollis	T.marginatus	L.glaucifolia
B. subtillis	9	7	8	0	0	0	0
L.monocytogenes	0	0	0	0	0	0	0

	Ch. intybus	T. syriacum	T. pratensis	C.cheirantifolia	C. pycnocephalus	Tetracycline
B. subtillis	0	0	0	0	0	24
L.monocytogenes	0	0	0	0	0	22

Table2. Effect of extract and antibiotic on microorganisms

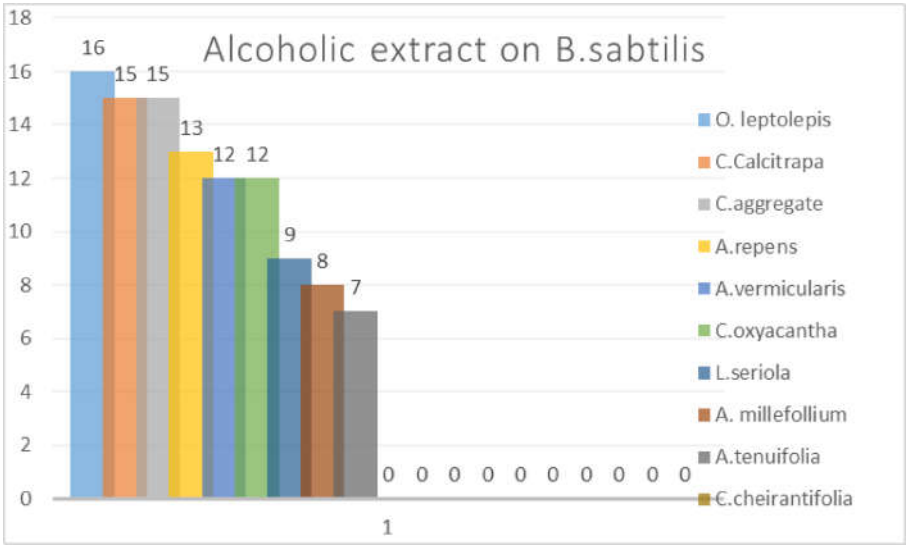

Discussion

In general, antibacterial activities of extracts showed significant effect against tested strains, as seen in Table 2, while alcoholic extract from Onopordon leptolepis shows the most effect on B. subtilis, consequently, C.aggregate , C.virgata, A.vermicularis and C.oxyacantha introduced as good species in antibacterial characteristic. some of extracts like don't have any antimicrobial activities. None of alcoholic extracts of plants show medicinal effect on E. coli.

Similar result was also reported by Masika and Afolayan (2002). As known, S. aureus, L. monocytogenes and Bacillus species especially B. cereus are agents of food poisoning. The most interesting area of application for plant extracts is the inhibition of growth and reduction in numbers of the more serious foodborne pathogens such as Salmonella spp., Escherichia coli O157:H7 and L. monocytogenes (Burt, 2004). The highest level of antibacterial activity was found in the ethyl acetate fraction of C.cankiriense. When comparing the antimicrobial activity of the tested samples to that of reference antibiotics, the inhibitory potency of tested extracts could mostly be considered as important. This is due to the fact that medicinal plants are of natural origin, which means more safety for consumers, and are considered to have low risk for resistance development by pathogenic microorganisms. (Cansaran, 2010). It was found to inhibit the growth of microorganisms that cause infectious diseases and C.aggregata can be used as a natural preservative in food against food-born disease. Future investigations will focus the research on the antioxidant activity and on chemical compositions of the antimicrobial ingredients in the screened efficacious extracts. In summary, it might be said that C. aggregata, especially the ethanolic extract of areal parts, could be used for protection against bacteria in ethno-medicine.

Recommends

1. Further Search for effective compounds of these medicinal plants, isolation and investigation on their antimicrobial effects.

2. In vivo study with these plants for identification of their mechanism on bacteria in live animal.

3. Study on cultivation of these plants with modern agronomic technology for obtains of effective medicinal products for possible pharmacological and nutritional application and marketing, also for prevention of genocide of these plants in the nature and continuous efficiency.

ACKNOWLEDGEMENT

This study was supported by Islamic Azad University **(IRI)**, Shabestar Branch, Shabestar, Iran.

References

[1] Burt S (2014). Essential oils: Their antibacterial properties and potential applications in foods-a review. Int. J. Food. Microbiol. 94: 223-253.

[2] Ciric A, Karioti A, Glamoclija J, Sokovic M and Skaltsa H (2011). Antimicrobial activity of secondary metabolites isolated from Centaurea spruneri Boiss. & Heldr. J. Serb. Chem. Soc. 76 (0) 1–8.

[3] Davis PH (1975). Flora of Turkey and the East Aegean Islands Edinburgh University Press. 5: 465-585.

[4] CansaranA, Mercan Do_anN, Öztekin M and AcarG (2010). Antimicrobial activity of various extracts of Centaurea cankiriense A. Duran and H. Duman. African Journal of Microbiology Research Vol. 4 (8), pp. 608-612, 18 April.

[5] Adeniyi BA and Odufowora RO (2000). Invitro antimicrobial properties of Aspilla africana (compositae).Afr.J.Biomed.Red.Vol 3:167-170.

[6] Kivrak I, Duru ME, Öztürk M, Mercan N, Harmandar M, Topçu G (2009). Antioxidant, anticholinesterase and antimicrobial constituents from the essential oil and ethanol extract of Salvia potentillifolia. Food Chemistry, 116: 470-479.

[7] Masika PJ, Afolayan AJ (2002). Antimicrobial activity of some plants used for the treatment of livestock disease in Eastern Cape, South Africa. J. Ethnopharmacol. 83: 129-134.

[8] Mercan N, Kivrak _, Duru ME, Katircioglu H, Gulcan S, Malci S, Acar G, Salih B (2006). Chemical composition effects onto antimicrobial and Antioxidant activities of propolis collected from different regions of Turkey. Ann. Microbiol. 56: 373-378.

[9] Singh SK, Saroj KM, Tripathi VJ, Singh AK, Singh RH (1988). An Antimicrobial principle from Sphaeranthus indicus l. (Family Compositae). Pharmaceutical Biology,V(26):235-239.

[10] Mabberley J (1997). The Plant Book, 2nd ed., Cambridge University Press, Cambridge, p.138.

Effect of Environment Impact of Ethinylestradiol and Progestin Hormones on Germination and Emergence of Grass Pea (Lathyrus Sativus L.)

Seyed Saeid Hojjat*

Research Center for Plant Sciences, Ferdowsi University of Mashhad, Mashhad, Iran.

*Email: seyedsaeidhojjat@gmail.com

Abstract

The aim of this study was to assess the effects of combined Oral Contraceptive pill, on morphological characteristics and parameters of biomass production, which includes fresh and dry matter weight (FMW and DMW, g/plant), root and shoot length of Grass pea seeds (*Lathyrus sativus* L.). The combined oral contraceptive pill (COCP), is a type of birth control that is designed to be taken orally by women. It consists of a combination of an estrogen [generally Ethinylestradiol ($C_{20}H_{22}O_2$)] and a progestogen (specifically a progestin). They're currently utilized by extra than one hundred million women worldwide. This review checked out studies that as compared pills with 20 µg Ethinylestradiol. Plants were grown hydroponically and three different doses of Ethinylestradiol, 0.0 mgL^{-1} (control), 0.1mgL^{-1}, and 0.2 mg L^{-1} had been imposed on 2 days after sowing for 28 days' duration. Experimental plots have been set up in a randomized block design with three replications. Seed germination, The Root Length (RL); Shoot Length (SL); Fresh Matter Of Roots (FMR); Fresh Matter Of The Shoot (FMS); Dry Matter Of The Roots (DMR); Dry Matter Of The Shoot (DMS) have been decided. Morphometric parameters of roots have estimated the usage of an image analysis software program. Root length (RL) and specific root length (SRL) have been calculated. The growth and biomass response of Grass pea have been more suitable due to adding on Ethinylestradiol. Results showed that Ethinylestradiol in concentrations discovered in sewage water can affect the vegetative boom of Grass pea.

Keywords: Ethinylestradiol, natural environment, Grass Pea, COCP, Water pollution.

1. Introduction

Pollution of essential water sources has become extreme trouble across a great deal of the world [1]. The specific contaminants main to pollution in water consist of a wide spectrum of chemicals, pathogens, and physical changes including elevated temperature and discolouration. Whilst most of the chemical substances and physical changes which might be regulated can be naturally occurring (calcium, sodium, iron, manganese, and so on.) the attention is regularly the key in determining what a natural aspect of water is and what a contaminant is. High concentrations of naturally going on materials will have negative effects on aquatic flora and fauna [2]. Depending at the degree of eutrophication, subsequent negative environmental outcomes which include anoxia (oxygen depletion) and extreme reductions in water quality can also occur, affecting fish and other animal populations [2]. One example of water pollution due to human beings is dumping waste merchandise as effluent into most

important rivers and waterways. Thus far, the greatest quantity of waste that finally ends up in marine ecosystems is sewage [3].

Sometimes naturally happening chemical substances, including hormones, also can increase in these aquatic environments because of waste effluent. One of the most not unusual estrogenic resources in wastewater effluent comes from the urine of women who take birth control pills. one of contraception, consisting of the contraceptive patch, use the synthetic estrogen (EE2) that is located in COCPs and might add to the hormonal concentration within the water while flushed down the restroom [4]. Some birth control tablets incorporate hormones estrogen and progestin. Those hormone treatments incorporate artificial ethynylestradiol in addition to significant quantities of 17β-estradiol [5]. Ethinylestradiol (EE) is an estrogen medication which is used extensively in birth control tablets in mixture with progestins. It's also every now and then used as a component of menopausal hormone remedy for the remedy of menopausal signs and symptoms in combination with progestins [6]. In mammals, the steroid intercourse hormones play a key role in controlling the methods of improvement and reproduction and they're additionally engaged inside the control of mineral and protein metabolism [7]. Mammalian sex hormones together with estrogens, androgens, and progesterone belong to steroids, a collection of compounds which have a simple sterane carbon skeleton. The different steroids in residing organisms are decided by the location and styles of useful groups connected to the sterane (Fig. 1). Steroid sex hormones implemented exogenously (e.g. progesterone, estrone, β-estradiol, testosterone) stimulate growth and improvement (callus proliferation, cell division, root and shoot elongation, pollen germination flowering) [8] [9] [10] [11] [12]. The impact of exogenous mammalian sex hormones on plant increase at the beginning of the twentieth century, it turned into shown that estrone inspired the growth of an isolated pea embryo in-vitro [13][14]. Estrone, at the awareness of 0.1 µg per plant, additionally stimulated the growth of *Pisum sativum* L. seedlings by approximately forty% [15]. In sunflower seedlings, 17β-estradiol and progesterone (0.25 µg in step with plant) extended shoot increase but inhibited root growth, however, root elongation became promoted through progesterone on the attention 0.1 µg per plant. Testosterone promoted cotyledon axillary bud formation at concentrations of 0.1 and 0.25 µg per plant [9]. In tomato seedlings, estrone and 17β-estradiol (as sulfate derivatives, on the attention of 1 µM in nutrient solution), decreased root growth in addition to root number in shoot cuttings [16]. Research carried out on varying species of plants established that β-estradiol reduced the germination percent of lettuce, carrot, and tomato seeds (*Lactuca sativa* L., *Daucus carota* L., and *Lycopersicon esculentum* Mill. respectively). Germination turned into decreased by 57% in L. Sativa, 6% in D. carota, and 18% in L. esculentum when in comparison to the controls [17]. The examine carried out on chickpea seeds (Cicer arietinum L.) ended in a dramatically extraordinary set of results. Each β-estradiol and progesterone improved seed germination. After forty-eight hours seed germination extended from 85% inside the control to 100% within the β-estradiol handled group [18].

Grass pea (*Lathyrus sativus* L.) is an annual crop and associated with the Fabaceae (Leguminosae) genus. In archeological unearthings in Turkey and Iraq, seeds of Lathyrus species had been found as collected or developed things. So also, seeds from 2500 bc were recognized within the most seasoned excavations in India [19] and as of now within the Balkan in 8000 bc. Agreeing to the legend, grass pea was brought to Ethiopia (Abyssinia) by the queen of Sheba after going by Lord Salomon within the tenth century bc [20]. Grass pea presents a fascinating paradox, it's far both a lifesaver and a destroyer. It's far without difficulty cultivated and might face up to extreme

environments from drought to flooding because of this hardiness, grass pea is regularly the only alternative to starvation while other crops fail [21]. With the massive environmental motion that ushered within the millennium, scientists started to take any other look at the role that contaminants play in the environment and specifically started out to study their consequences on plant life. Cutting-edge research has focused on the consequences of these contaminants on vegetative plant growth [1]. The purpose of this research was to investigate the effects of a major pollutant, Ethinylestradiol, at the vegetative growth of grass pea.

2. Material and Methods

This study was carried out at the research centre for Plant Sciences, Ferdowsi University of Mashhad, Mashhad, Iran. It was carried out in a laboratory under the hydroponic situations on the ambient temperature. Seeds of grass pea have been from the seed bank of research centre for Plant Sciences, the Ferdowsi University of Mashhad (Fig. 1). All of the seeds have been first checked for their viability with the aid of suspending them in deionized water. The seeds which settled to the bottom have been decided on for in addition study. Seeds were sterilized in a 5% sodium hypochlorite solution for 10 mins [22], rinsed via with deionized water several times. The birth combined oral contraceptive pill (COCP) became dissolved first in a small quantity of Distilled water after which diluted in water that allows you to obtain the subsequent concentrations: 10 and 15 M. plants had been transferred to plastic containers (20 L) with a nutrient solution Nutrient solutions (Hoagland solution) have been constantly aerated with the aid of an air-pump to maintain it oxygenate and to preserve homogeneous the solution. The Hoagland solution is a hydroponic nutrient solution (table 1.) that changed into developed by using Hoagland and Arnon in 1950 and is one of the most famous solution compositions for growing plants. The Hoagland solution provides every nutrient vital for plant growth and is appropriate for the increase of a huge variety of plant species [23].

Table 1. Concentration ranges of essential mineral elements Hoagland & Arnon (1938)

Nutrient	Mg L^{-1}
N	210
P	31
K	234
Ca	160
Mg	34
S	64
Fe	2.5
Cu	0.02
Zn	0.05
Mn	0.5
B	0.5
Mo	0.01

Every treatment became replicated three times. The nutrient solution turned into renewed weekly and the containers have been watered if necessary. Plants have been sampled after 28 days of treatment. For the germination tests, Semipermeable paper (Whatman No. 2) was put in standard scale Petri dishes (100 mm × 15 mm). Eight seeds were set equally over each paper and secured with another layer of Whatman No.2-channel paper forming a sandwich. Five mL of the proper birth combined oral contraceptive pill (COCP) arrangement was added to each Petri dish utilizing Air displacement micropipettes. Following the situation of the seeds on the filter paper, the filter papers were soaked with the appropriate test saline solutions. The temperature during germination was held at 25 ±1 °C [24]. Three reproduces of each testing condition have been accommodated investigation.

Fig. 1. Grass pea (*Lathyrus sativus* L.)

Roots and shoots were separated and weighed. Roots were thoroughly rinsed in the faucet and distilled water. Then both shoots and roots have been rinsed in distilled water for two min. determination of Root Morphology At day 28, root length (cm) and root surface vicinity (cm2) of Grass pea were determined using a root scanner, Delta-T test (model D55/151). Plant material changed into dried at 60 ºC for seventy-two h. Parameters Measurer/ Shoot length (mm), shoot dry weight (mg), root dry weight (mg), total dry weight (mg), (all dried at 80 ºC for forty-eighth). The following relationships have been derived: the ratio of shoot dry weight/root dry weight, ratio of stem dry weight to stem length. Leaf proline substance was evaluated according to the strategy of [25] from completely extended leaf tests collected from to begin with shaped essential branches on particular collect dates. SPSS Ver.16 was used for comparing the means the use of the Duncan test at P<0/05, level of significance [26].

3. Results and Discussions

The goal of this experiment was to determine if Water major pollutants, combined Oral Contraceptive, had an effect at the growth of grass pea (*Lathyrus sativus* L.) seedlings. Grass Pea plants have been grown in the absence or presence of the Combined Oral Contraceptive (Ethinylestradiol), under various conditions. analysis of the effect of various amounts of Ethinylestradiol at the Grass Pea attention showed a significant difference between experimental groups, control, and case groups P<0/05. Data presented in Table 2 indicated that seed germination was significantly affected by lower and highest Ethinylestradiol and progestin concentration in the culture medium (0.1 and 0.2). At smaller concentrations, it appears that Ethinylestradiol causes a slight escalation in overall germination, 97% in 0.1 mg when compared to the control at 92%. Germination is a key phase in the initiation of

plant growth. At the highest concentration of the hormone, 0.2 mg/L, the overall germination was reduced to 73%. This indicates that at some level Ethinylestradiol is toxic to the kernels at high concentrations.

If germination is being inhibited by high concentrations of the hormone, this could indicate that seed sown in fields that are exposed to contaminated water or soil, may have reduced germination rates and therefore reduced overall yield. These results seem to fall in line with the plant species *Lactuca sativa* L. (lettuce) and *Lycopersicon esculentum* Mill. (Tomato) which also exhibited a reduction in the overall rate of germination when exposed to β-estradiol [17]. The growth of shoots and roots was also negatively affected by Ethinylestradiol in studied Grass pea (0.2 mg L^{-1}). The average increase for the Grass Pea plants that received combined oral contraceptive pill (COCP) was 51 cm as compared to 28 cm for Grass Pea plants that did not receive estrogen. After 42 days of cultivation in medium containing 0.2 mg L^{-1} Ethinylestradiol, the reduction of shoot length ranged from 3.8% to 34.4% compared to the non-treated control. In mammals, β-estradiol plays a key role in controlling the processes revolving round improvement and reproduction in addition to being worried about the control of both mineral and protein metabolism [1]. Numerous research was carried out on different plant species to be able to determine this.

Table 2. Effect of Ethinylestradiol application on biomass accumulation and growth parameter of Grass pea

Treatment	**Control**	**0.1mgL^{-1}**	**0.2 mg L^{-1}**
Seed germination	86.3a	93.3a	42.9b
Primary branches/plant	13.52a± 0.16	16.14b± 0.11	5.67c± 0.15
Root length (mm)	18a±24.7	27.3a±12.1	8.7c±7.4
Shoot length (mm)	45.8a±11.4	55.2b±3.3	17.7c±8.6
Root DW (gr/plant)	0.21a± 0.33	0.25a± 0.17	0.06b± 0.04
Shoot DW (gr/plant)	1.16a ±0.28	1.85a ±0.12	0.75b± 0.14
Leaf Proline Content μmol/(gr FW)	2.64a± 0.53	2.75b± 0.61	3.55c ±0.85

Data are means ± standard error of a least three replicates, Means followed by common letters are not significantly different ($P < 0.05$, ANOVA); FW= Fresh weight; DW= Dry weight

In sunflower seedlings (*Helianthus annuus* L.), β-estradiol concentrations of 1 µg according to plant increased overall shoot growth however had been shown to inhibit general root growth [7]. In chickpeas (*Cicer arietinum* L.), the hormone considerably enhanced the root and shoot growth of the seedlings at concentrations of 10-4, 10-9, 10-12, and 10-15 M [27]. Among the growth traits, plant height, the number of primary branches, and leaves per plant reduced markedly in Grass Pea seedlings subjected to 0.2mgL-1 but increased markedly in Grass Pea seedlings subjected to 0.1mgL-1. According to the one factor ANOVA analysis, there's a distinction in effect that Ethinylestradiol concentration and the controls had on the Grass Pea plants. Treatment with Ethinylestradiol in, 0.1 mg-1 (increases both shoot and root dry weight). Plants exposed to higher concentrations of Ethinylestradiol had significantly lower root growth, Increasing the Ethinylestradiol concentrations in a medium led to a decrease

of root growth between 68.8% in Grass pea, The highest level of Ethinylestradiol (0.2 mg L^{-1}) decreased the root length between 88.3% and 97.8% compared to the control treatment (0.2 mg L^{-1}), indicating a toxic effect of Ethinylestradiol. Increasing Ethinylestradiol concentration in the media the weight of the plants significantly decreased from 16.5% at 0.1 mg L^{-1} Ethinylestradiol to 89.5% in 0.2 mg L^{-1} Ethinylestradiol. It can be concluded that Ethinylestradiol in concentrations discovered in sewage water can have an effect on the vegetative growth of Grass Pea plants Ethinylestradiol application had significant effects on shoot diameter and number of leaves. Mean shoot and root lengths numerous significantly according to Ethinylestradiol application (table 2). Ethinylestradiol inoculation additionally resulted in a higher mean number of leaves per plant (Table 2). Among the parameters responding to Ethinylestradiol treatment, rapid accumulation of free proline content is one of the significant events in plants. In grass pea, leaf proline content increased with increasing exposure to Ethinylestradiol (Table 2).

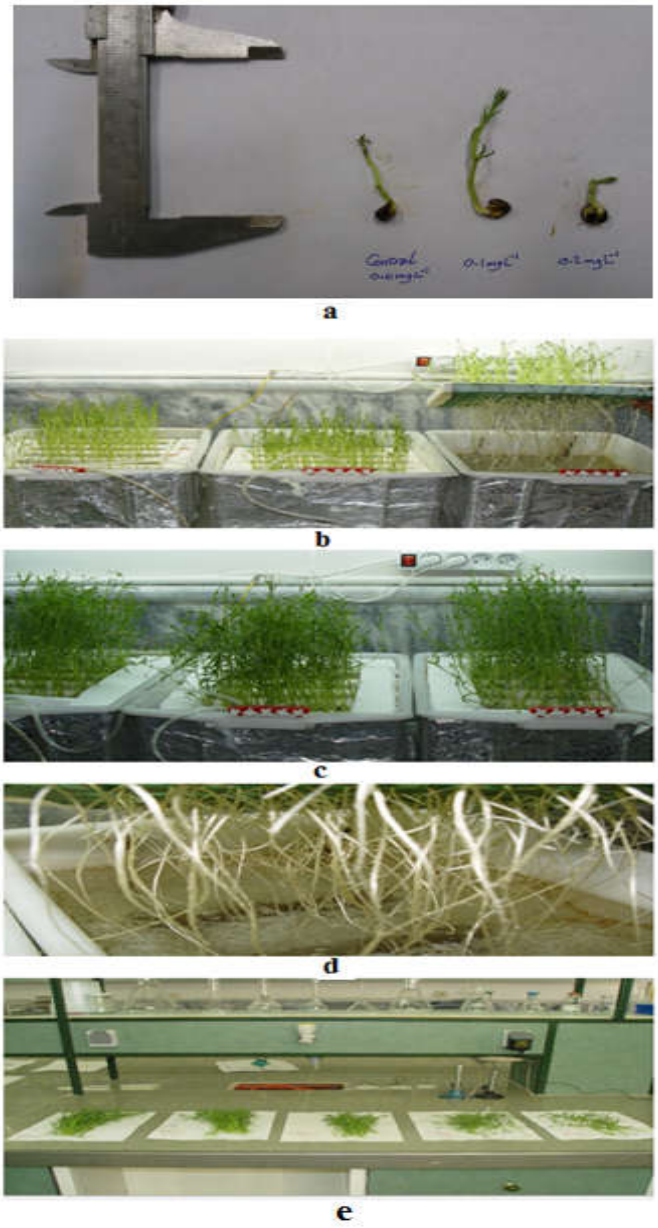

Fig. 2. Effect of Ethinylestradiol applications on Grass Pea root growth. Seedling day 7 (a)Root and Shoot length of 28-day old control (b) and Ethinylestradiol (c) treated. Number of lateral roots in 28-day old, Ethinylestradiol (d). Representative image of the Shoot in 28-day old, control and Ethinylestradiol treated (e)

4. Conclusion

worldwide, steroid estrogens including estrone, estradiol, and estriol, pose severe threats to soil, plants, water resources, people and have gained outstanding interest in current years, because of their rapidly increasing concentrations in soil and water all over the world, and the problem has been expressed concerning the access of estrogens into the human food chain which, in turn, relates to how plants absorb metabolism estrogens [27]. Estrogens and estrogen-like compounds (xenoestrogens) from livestock manure, animal waste, and human waste (especially pharmaceutical waste), are being disposed of and excreted at high charges into the agricultural soil and groundwater all around the international [28]. Hence, in the gift study, we aimed to search the effect of the combined oral contraceptive pill (COCP) on morphologic (roots and stem length) parameters in Grass Pea. To the excellent of our knowledge, there has not been any report at the effect of mammalian sex hormones on morphologic (roots and stem length) in Grass Pea seeds, one of the most critical legume crops of the world. Due to the fact, there isn't always sufficient research and knowledge on the effects of combined Oral Contraceptive pill in plant life, its miles necessary to achieve advanced researchers on biochemical parameters.

Acknowledgements

I would like to gratefully acknowledge The Research Center for Plant Sciences, Ferdowsi University of Mashhad, for providing laboratory equipment.

References

[1] K.M. Bowlin., Effects of β-Estradiol on Germination and Growth in Zea mays L (Doctoral dissertation, M. Sc. thesis Northwest Missouri State University, Maryville, Missouri, USA) (2014) 90.

[2] M. Upadhyay, B.L. Sahu and O.P, Pardhi., Degradation of water quality due to heavy pollution in industrial area of Korba, Chhattisgarh. Recent Research in Science and Technology 27(2013) 37-39.

[3] M.S. Islam, M. Tanaka., Impacts of pollution on coastal and marine ecosystems including coastal and marine fisheries and approach for management: a review and synthesis. Marine pollution bulletin 48(2004) 624-649. doi: 10.1016/j.marpolbul.2003.12.004.

[4] S. Batt., Pouring Drugs Down the Drain. Herizons 18 (2005) 12–3.

[5] J, Batty. R, Lim., Morphological and reproductive characteristics of male mosquitofish (*Gambusia affinis holbrooki*) inhabiting sewage-contaminated waters in New South Wales, Australia. Archives of Environmental Contamination and Toxicology 36(1999) 301-307. doi.org/10.1007/s002449900475.

[6] H. Kuhl., Pharmacology of estrogens and progestogens: influence of different routes of administration. Climacteric, 8(2005) 3-63. DOI: 10.1080/13697130500148875.

[7] A. Janeczko, A. Skoczowski., Mammalian sex hormones in plants. Folia Histochemica et cytobiologica 43(2005)71-79. doi.org/10.5603/4616.

[8] J.M. Geuns., Steroid hormones and plant growth and development. Phytochemistry, 17(1978)1-14.

[9] doi.org/10.1016/S0031-9422(00)89671-5.

[10] B. Bhattacharya, K. Gupta., Steroid hormone effects on growth and apical dominance of sunflower. Phytochemistry 20(1981) 989-91. doi.org/10.1016/0031-9422(81)83014-2.

[11] J. Kopcewicz., Estrogens in developing bean (*Phaseolus vulgaris*) plants. Phytochemistry, 10(1971)1423-1427. doi.org/10.1016/0031-9422(71)85003-3.

[12] L.S. Shore, Y. Kapulnik,, B. Ben-Dor, Y. Fridman, S. Wininger, M. Shemesh., Effects of estrone and 17 β-estradiol on vegetative growth of Medicago sativa. Physiologia Plantarum 84(1992)217-222.

[13] doi.org/10.1111/j.1399-3054. 1992.tb04656. x.

[14] B. Ylstra, A.Touraev R.M.B. Moreno, E. Stöger, A.J. van Tunen, O.Vicente, J.N. Mol, E. Heberle-Bors., Flavonols stimulate development, germination, and tube growth of tobacco pollen. Plant physiology 100 (1992) 902-907. doi.org/10.1104/pp.100.2.902.

[15] J. Bonner, G. Axtman., The growth of plant embryos in vitro. Preliminary experiments on the role of accessory substances. Proceedings of the National Academy of Sciences of the United States of America 23 (1937) 453. doi.org/10.1073/pnas.23.8.453.

[16] F. Kogl, A.J. A.J. Haagen-Smit., Biotin und aneurin als phytohormone. Zeit. physiol. Chem 243 (1936) 2.

[17] J. Kopcewicz., Influence of estrone on growth and endogenous gibberellins content in dwarf pea. Bulletin de l'Academie polonaise des sciences. Serie des sciences biologiques 17(1966)727-731.

[18] M. Guan, J.G. Roddick., Epibrassinolide-inhibition of development of excised, adventitious and intact roots of tomato (Lycopersicon esculentum): comparison with the effects of steroidal estrogens. Physiologia Plantarum 74(1988)720-726. doi.org/10.1111/j.1399-3054. 1988.tb02043.x

[19] B. D'Abrosca, A. Fiorentino, A. Izzo, G. Cefarelli, M.T. Pascarella, P. Uzzo, P. Monaco, Phytotoxicity evaluation of five pharmaceutical pollutants detected in surface water on germination and growth of cultivated and spontaneous plants. Journal of Environmental Science and Health 43(2008)285-294.

[20] S. Erdal, R. Dumlupinar. Progesterone and β-estradiol stimulate seed germination in chickpea by causing important changes in biochemical parameters. Zeitschrift für Naturforschung C 65 (2010) 239-244. doi.org/10.1515/znc-2010-3-412.

[21] M.E. Kislev., Origins of the cultivation of *Lathyrus sativus* and L. cicera (fabaceae). Economic botany 43(1989) 262-270.

[22] EA. Budge, A. Wallis., A History of Ethiopia, Nubia and Abyssinia 1(1928). doi.org/ 10.4324 /97813 15762722.

[23] C.G. Campbell., Grass pea, *Lathyrus sativus* L Bioversity International Plant Genetic Resources Institute, Rome, Italy 18(1997).

[24] EPAU. Ecological effects test guidelines. Gammarid acute toxicity test OPPTS (1996) 850.

[25] D.R. Hoagland, D.I Arnon., The water-culture method for growing plants without soil. Circular. California agricultural experiment station 347(1950) 1-32.

[26] R. Marlia, D.G.S. Santana, W R, Ferreira C. Mendes-Rodrigues., Calculating germination measurements and organizing spreadsheets. Brazilian Journal of Botany 32(4) (2009)849-855. doi.org/10.1590/S0100-84042009000400022 .

[27] L.S Bates, R.P. Waldren, I.D. Teare., Rapid determination of free proline for water-stress studies. Plant and soil 139 (1973) 205-207. doi.org/10.1007/bf00018060.

[28] DB. Duncan., Multiple Ranges and Multiple F. test Biometrics. Biometrics 11(1955) 1- 42. doi.org/10.2307/3001478.

[29] M. Adeel, X. Song Y. Wang, D. Francis. Y, Yang., Environmental impact of estrogens on human, animal and plant life: a critical review. Environment International 99 (2017) 107-19. doi.org /10.1016 /j.envint. 2016.12.010.

[30] LS. Shore, M. Shemesh., Naturally produced steroid hormones and their release into the environment. Pure and Applied Chemistry 75 (2003)1859-71. doi.org/10.1351/pac200375111859

Modeling and optimization of the fumigant toxicity of *Lippia citriodora* essential oil against red flour beetle

Asgar Ebadollahi * and Ebrahim Taghinezhad

Moghan College of Agriculture and Natural Resources, University of Mohaghegh Ardabili, Ardabil, Iran

Email: ebadollahi@uma.ac.ir

Abstract

The use of synthetic chemicals is the chief strategy in the management of damaging agricultural pests. However, their overuses resulted in several side-effects, including environmental contamination, dangerous residues on crops and foods, the threat to mammals and other non-target organisms, and pest resistance. Accordingly, introducing novel, safe, and efficient agents in requisite amounts to alternate with detrimental chemicals is crucial. Plant essential oils considered as healthy and available bio-rational pesticides in recent years. In the present study, modeling and optimization of fumigant toxicity of *Lippia citriodora* Kunth essential oil were performed using Response Surface Methodology (RSM) before a cosmopolitan economic pest; the red flour beetle, *Tribolium castaneum* Herbst. The coefficients of independent variables the essential oil concentration (five concentrations) and time (three times) were positive, indicating their increase resulted in direct augmentation in the mortality of red flour beetle. On the other hand, the fumigant toxicity of essential oil against pest was concentration-time dependent. A quadratic polynomial equation was achieved for the toxicity of essential oil using multiple regression analysis; 10.73482 - 0.31673 A + 0.28454 B + 4.10264E-003 AB + 4.55729E-003 A^2 + 0.011721 B^2. Analysis of variance was used to approve the accuracy of announced model. Result also indicated that 61.76 µl/l of essential oil and 72.00 h-exposure time would be sufficient to realize 92.08% mortality of pest. According to the present outcomes, response Surface Methodology (RSM) is a suitable method to the modeling and optimization of fumigant toxicity of *L. citriodora* essential oil against *T. castaneum*.

Keywords: essential oil, *lippia citriodora*, modeling, optimization, toxicity.

1. Introduction

Overuse of synthetic chemicals in the management of insect pests associated with serious concerns such as environmental contamination, pest resistance and resurgence, dangerous residues on crops and foods, and harmful effects on non-target organisms [1-3]. Therefore, the introduction of safe, available, and efficient alternatives in the pest management strategies is necessary.

The red flour beetle (*Tribolium castaneum* Herbst, Coleoptera: Tenebrionidae) is one of the most worldwide damaging stored-product insect pests. The quantity and quality of several stored-products with animal and plant origins, including beans, cereal grains and flour, and the leather was affected directly by feeding and indirectly by

insect skin and benzoquinone compounds excreted from its abdominal glands. Further, its medicinal importance has also been recognized in recent studies, based on the ability of this pest in the transmission of pathogenic microbes [4-6].

Essential oils, as well-known secondary metabolites and responsible for plant aroma, have a principal role in the aromatic plant defines before phytophagous and pathogenic agents [7]. Along with low or less toxicity to the mammals and environmentally biodegradation capability, the essential oils have been considered as prospective fumigants against diverse groups of stored-product insect pests [8-10].

Response surface methodology (RSM) can set a polynomial model for experimental outcomes by combining mathematical and statistical techniques. It can also explain the best conditions to optimize response under several variables and evaluate the more potent factor between affecting variables. So, RSM has used in several agricultural and pharmacological fields in recent studies [11-13].

Therefore, present study was conducted to evaluate the best model and optimized conditions for fumigant toxicity of essential oil extracted from lemon verbena (*Lippia citriodora* Kunth, Verbenaceae), as one of the most cultivated medicinal plants throughout the world [14], against red flour beetle under different exposure time.

2. Material and Methods

2.1 Plant samples and essential oil

The leaves of *L. citriodora* were collected from the 10 cm end of young stems, and the samples were dried at room temperature. After grinding, fifty grams of powders were poured into a 1000 ml balloon of a Clevenger apparatus. Extracted essential oils were stored in a refrigerator at 4 °C.

2.2 Tested insect

The adult of *T. castaneum* were collected from contaminated wheat grains in Moghan region, Ardabil province, Iran, and the colony was reared on wheat grains in an incubator at 25 ± 2°C and 65 ± 5% relative humidity in the dark. One to seven old-days adults were selected for experiment.

2.3 Fumigant toxicity

Twenty adult insects were placed into fumigant chamber (340 ml container). Obtained considerations based on the preliminary experiment were poured on filter papers (2 × 2 cm) which were sealed to the inside of container lids, and the lids were closed using parafilm. Insect mortality was documented after 24, 48 and 72 h exposure times. All experiments were carried out for control groups without adding any essential oil concentration, and each treatment was repeated four times.

2.4 Analysis using Response Surface Methodology

The historical data design used to evaluate the effects of essential oil concentrations and exposure times (independent variables) on the insect-pest mortality (dependent variable) by selecting the polynomial equation in RSM through Design Expert 8.0.6 (Stat-Ease, Inc. USA). The essential oil concentrations (µl/l) and exposure times (h) had five and three levels, respectively, and three replications. Analysis of variance (ANOVA) was also done to find the interactions between independent variables and responses. Correlation coefficients of determination (R^2), adjusted R^2, and predicted R^2 were used to evaluate the association between the independent and dependent variables.

3. Results and Discussions

The interaction between essential oil concentrations and exposure times on the mortality of red flour beetle is displayed in Figure 1; the mortality was decreased by increasing the essential oil concentration and time.

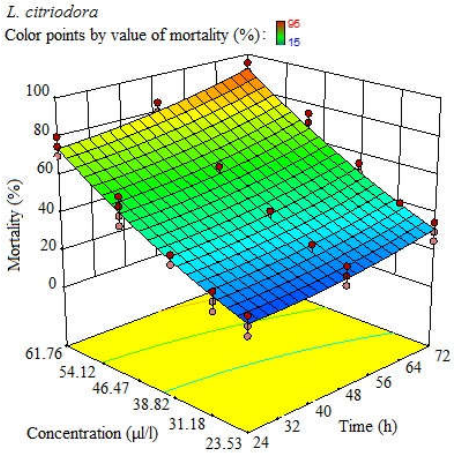

Figure 1. Three-dimensional diagrams of the mortality of red flour beetle caused by the fumigation of *L. citriodora* essential oil.

The plot of residuals against predicted response is shown in Figure 2, indicating the introduced mortality model is proper for predicting the mortality of red flour beetle.

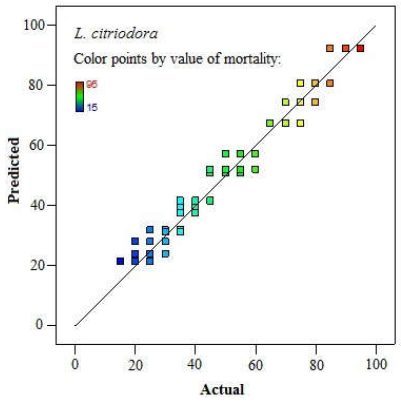

Figure 2. Plots of residual against predicted mortality of *T. castaneum* caused by the fumigation of *L. citriodora* essential oil.

According to table 1, the lack of fit test was non-significant, representative the validation of treatment. Analysis of variance designated A (exposure time), B (concentration), AB, A^2, and B^2 significantly affected the mortality. Also, it can be found that the greatest mortality was gained by the essential oil concentration in comparison with the exposure time (Table 1).

Table 1. Results of analysis of variance for prediction of the fumigant toxicity of *L. citriodora* essential oil against red flour beetle.

Source	Sum of Squares	df	Mean Square	F value	p-value
Model	26559.92	5	5311.98	300.34	< 0.0001
A	1960.57	1	1960.57	110.85	< 0.0001
B	24210.90	1	24210.90	1368.88	< 0.0001
AB	71.37	1	71.37	4.04	0.0496
A^2	91.88	1	91.88	5.19	0.0266
B^2	190.04	1	190.04	10.74	0.0018
Residual	955.08	54	17.69		
Lack of Fit	117.58	9	13.06	0.70	0.7036 ^{NS}
Pure Error	837.50	45	18.61		
Cor Total	27515.00	59			

A and B are the exposure time (h) and essential oil concentrations (µl/l), respectively. NS: Non-Significant.

The calculated model for fumigant toxicity of *L. citriodora* essential oil against red flour beetle is indicated in Table 2. The R^2 values are more than 80%, indicate a well-adjusted regression model. Further, based on that the coefficients of independent variables are positive, an increase in the essential oil concentration and exposure time results in an extension of pest mortality.

Table 2. Estimated regression model for the fumigant toxicity of *L. citriodora* essential oil against *T. castaneum*.

Equation	R^2 value	Adj R^2	Pred R^2	C.V. (%)
10.73482 - 0.31673 A + 0.28454 B + 4.10264E-003 AB + 4.55729E-003 A^2 + 0.011721 B^2	0.9653	0.9621	0.9568	8.67

A and B are exposure time (h) and essential oil concentrations (µl/l), respectively, and response variable is mortality percentage.

The optimized conditions for fumigant toxicity of *L. citriodora* essential oil against red flour beetle is designated in Table 3. To achieve 92.08% mortality of insect pest, the 72 h-exposure times, and 61.76 µl/l essential oil concentration would be adequate (Table 3).

Table 3. Optimization of the mortality of *T. castaneum* caused by the fumigation of *L. citriodora* essential oil.

Mortality (%)	Time (h)	Concentration (µl/l)	Desirability
50.000	29.170	46.825	1.000
92.078*	72.000	61.760	0.963

*The maximum significant mortality percentage based on high desriability calculated by Desighn Expert Sofftware.

The insecticidal effects of *L. citriodora* essential oil has been reported in some recent studies. For example, two Argentinian *Lippia* essential oils, including *L. citriodora* and *L. polystachya* were toxic against the soybean pest (*Nezara viridula*) [15]. In the other study, *L. citriodora* and *L. polystachya* essential oils also exhibited significant fumigant toxicity against the confused flour beetle (*Tribilium confosum* Du Val) [16]. Khani et al. [17] found that *L. citriodora* essential oil had significant fumigant toxicity on the adults of cowpea weevil (*Callosobruchus maculatus* (F.)) and the confused flour beetle. Results of the mentioned above studies are in parallel with our outcomes in view of the toxicity of *L. citriodora* essential oil on insect-pests.

The use of RSM for modeling and optimization of pesticidal effects of essential oils was reported in some recent studies; for toxicity of *Thymus kotschyanus* Boiss. & Hohen essential oil against the lesser grain borer (*Rhyzopertha dominica* F.) [17], a high coefficient of variation value (8.02%) and an exponential model (52.08 + 3.49B + 22.84A - 1.72AB - 2.06A^2 + 3.73AB^2 - 5.60A^3, concentration (A) and time (B)) were estimated. Also, they indicated that 24.62 µl/l of essential oil and 57.98 h-exposure time was adequate to kill 50% of insect population. In the other work on red flour beetle and essential oil of *Teucrium polium* L., "+0.71- 0.047A - 8.84E-3B + 3.89E-4AB + 3.27E-3A^2 + 8.38E-5B^2" was presented as the best model, and the optimal conditions to 97.97% mortality was 20 µl/l essential oil concentration and 72 h-exposure time [18].

In the present study, the probability of *T. castanem* control by *L. citriodora* essential oil was approved. Because of the necessity to determine the accurate amount of applied pesticides and to predict pest death, optimization and modeling of this bio-effect was also performed using RSM.

References

[1] R. J. Gill, O. Ramos-Rodriguez, N. E. Raine, Combined pesticide exposure severely affects individual- and colony-level traits in bees, Nature 491 (2012) 105-108.

[2] S. Mostafalou, M. Abdollahi, Pesticides and human chronic diseases: evidences, mechanisms, and perspectives, Toxicology and Applied Pharmacology 268 (2013) 157-177.

[3] D. Goulson, Ecology: pesticides linked to bird declines, Nature 511 (2014) 295-296.

[4] J. Li, S. Lehmann, B. Weißbecker, I. O. Naharros, S.Schütz, G. Joop, E. A. Wimmer, Odoriferous defensive stink gland transcriptome to identify novel genes necessary for quinone synthesis in the red flour beetle, Tribolium castaneum, PLoS Genet 9 (2013) 1003596.

[5] C.Prabha Kumari, R. Sivadasan, A. Jose, Microflora associated with the red flour beetle, Tribolium castaneum (Coleoptera: Tenebrionidae), J Agr Technol 7 (2011) 1625-1631.

[6] H. A. Q. Bosly, M. A. Kawanna, Fungi species and red flour beetle in stored wheat flour under Jazan region conditions, Toxicol Ind Health 30 (2014) 304-310.

[7] S. Rajendran, V. Sriranjini, Plant products as fumigants for stored product insect control, J Stored Prod Res 44 (2008) 126-135.

[8] D. R. Batish, H. P. Singh, R. K. Kohli, S. Kaur, Eucalyptus essential as natural pesticide, For Ecol Manage 256 (2008) 2166-2174.

[9] A. Ebadollahi, M. Ziaee, F. Palla, Essential oils extracted from deferent species of the Lamiaceae plant family as prospective bioagents against several detrimental pests, Molecule 25 (2020) 1556.

[10] M. B. Isman, Commercial development of plant essential oils and their constituents as active ingredients in bioinsecticides, Phytochem Rev 19 (2020) 235-241.

[11] G. Kaur, V. Kumar, A. Goyal, B. Tanwar, J. Kaur, Optimization of nutritional beverage developed from radish, sugarcane and herbal extract using response surface methodology, Nutr Food Sci 48 (2018) 733-743.

[12] J. Ning, S. Yue, Optimization of preparation conditions of eucalyptus essential oil microcapsules by response surface methodology, J Food Process Preserv 43 (2019) 14188.

[13] F. D. O. Riswanto, A. Rohman, S. Pramono, S. Martono, Application of response surface methodology as mathematical and statistical tools in natural product research, J Appl Pharm Sci 9 (2019) 125-133.

[14] S. Kizil, H. Dinc, E. Diraz, O. Toncer, M. Kizil, S. Karaman, Effects of different harvest periods on essential oil components of Lippia citriodora Kunth under semi-arid climatic conditions and biological activities of its essential oil, Acta Scientiarum Polonorum, Hortorum Cultus 17 (2018) 39-48.

[15] J. O. W. González, M. M. Gutiérrez, A. P. Murray, A. A. Ferrero, Biological activity of essential oils from Aloysia polystachya and Aloysia citriodora (Verbenaceae) against the soybean pest Nezara viridula (Hemiptera: Pentatomidae), Natural Product Communications 5 (2010) 301-306.

[16] V. Benzi, N. Stefanazzi, A. P. Murray, J. O. W. González, A. Ferrero, Composition, repellent, and insecticidal activities of two South American plants against the stored grain pests Tribolium castaneum and Tribolium confusum (Coleoptera: Tenebrionidae), ISRN Entomologym (2014) http://dx.doi.org/10.1155/2014/175827.

[17] Ebadollahi, A. The essential oil extracted from Thymus kotschyanus Boiss. & Hohen as a natural substance for management of the lesser grain borer, Rhyzopertha dominica F, Agric For 64 (2018) 490-495.

[18] A. Ebadollahi, E. Taghinezhad, Modeling and optimization of the insecticidal effects of Teucrium polium L. essential oil against red flour beetle (Tribolium castaneum Herbst) using response surface methodology, Inf Process Agric 7 (2020) 286-293.

Nasturtium officinale, a plant with a wide range of important medicinal properties

Zahra Mohebi[1*]

[1]Department of Natural Resources, Faculty of Agricultural Sciences & Natural Resources, Razi University, Kermanshah, Iran.

Email: z.mohebi@razi.ac.ir

Abstract

Nasturtium officinale (Watercress) is a medicinal plant that used in traditional medicine for many disorders. Several studies have been conducted to detect its herbal components and therapeutic characteristics. Increasing cruciferous vegetable intake has been associated with reduced risk of diseases. This review article has introduced *N. officinale* morphological, biosystematics properties, and herbal components, and assessed its valuable therapeutic properties. Experimental and epidemiological studies suggest that the watercress it is a cruciferous vegetable with high concentration of compounds with recognized preventive and curative activities such as antibacterial**,** antioxidant, anticancer, antidiabets, hypothyroidism etc. Traditional applications of *N. officinale* in treatment of many diseases and its valuable medicinal and herbal components could provide a context for scientists to develop plant-derived medications such as antibiotics, cancer and diabetes treating drugs, and key to conducting clinical trials.

Keywords: Compounds**,** *Nasturtium officinale*, anticancer, antidiabets, hypothyroidism

1. Introduction

Nasturtium has been known as aquatic genera of the family Cruciferae in Iran [1]. This genera is recognized as a distinct genus with five species in the world [2]. The most common and widespread species of the genus Nasturtium is *Nasturtium. officinale* that is native to Eurasia and northern Africa and widely naturalized elsewhere [2]. *Nasturtium nasturtium-aquaticum* (nomenclaturally invalid) and *nasturtium-aquaticum L.* are synonyms of *N. officinale*. This species is considered as watercress of commerce and grows on the wet habitats in most parts of Iran.

Fig. 1. Watercress, *Nasturtium officinale*. Clockwise from top left: flowers; leaves; fruit pods and a patch of *N. officinale*

Documentary evidence for the use of Watercress as a medicinal plant extends from the first century A. D. to the nineteenth. It is known for its spicy, peppery taste [3]. It is highly nutritious, with plenty of vitamins, proteins, and minerals [4]. Additionally, watercress has historically been widely used for medicinal purposes, dating back to Roman times [3]. Among its medicinal uses are as a potential anti-carcinogen [5], a diuretic, expectorant, purgative, stimulant, stomachic, and tonic. It has been used as a treatment for anemia, eczema, kidney and liver disorders, tuberculosis, boils, warts, and tumors [4].

Watercress (*Nasturtium officinale*) contains one of the highest concentrations of glucosinolates of any vegetable, together with high concentrations of carotenoids such as lutein and b-carotene [[6],[7]]. Glucosinolates are sulphur-containing glycosides with aliphatic, aromatic, or indole side-chains found in brassicaceous plants. These plants include the economically important salad crops such as garden cress (*Lepidium sativum*) and watercress (*Nasturtium officinale*) as well as many brassica vegetables, e.g. broccoli (*Brassica oleracea var. italica*). Glucosinolate content in these brassicas is about 1% of dry weight in some tissues although the level is highly variable. The content can approach 10% in the seeds of some brassicas where glucosinolates may represent one half of the sulphur content [8].

From a human health perspective, isothiocyanates are the most important of the products formed from glucosinolate degradation. There is convincing evidence that benzyl isothiocyanate (BITC), phenylethyl isothiocyanate (PEITC), and sulphoraphane (4-methylsulphinylbutyl isothiocyanate) are effective inhibitors of chemically induced tumours in one or more organ sites of rodents [[9[,[10],[11]].

2. Evaluation of chemical compounds

The compounds of the essential oil of *N. officinale* were identified according to data and information available in the GC-MS library. The conditions of the compounds identified from the essential oil of *N. officinale* using GC/MS method are shown in Table 1 [12].

From the essential oil of flowers of *N. officinale*, 15 constituents were identified, representing 94.7% of the total oil, among which limonene (43.6%), α - terpineol (19.7%), p-cymene-8-ol (7.6%) and caryophyllene oxide (6.7%) were the major components. In the oil prepared from leaves, nine components were identified (97% of the total oil), myristicin (57.6%), α - terpineol (8.9%) and limonene (6.7%) being the main components. The oil of stems yielded eight compounds, which represented 100% of the total oil, with caryophyllene oxide (37.2%), p-cymene-8-ol (17.6%), α - terpineol (15.2%) and limonene (11.8%) being the most abundant.

Table 1. Compositions (%) of essential oil from leaves, stems and flowers of *N. officinale* (Amiri, 2012)

Compounds	RI	Composition (%)		
		Flowers	Stems	Leaves
α - Pinene	935	0.4	-	-
β - Pinene	974	2.6	-	0.3
β - Myrcene	988	0.9	-	0.4
Octana	997	-	1.3	-
Limonene	1025	43.6	11.8	16.7
Trans-β-ociemen	1045	0.7	-	-
α - Terpinolene	1087	19.7	15.2	8.9
ρ-Cymene-8-ol	1182	7.6	17.6	3.1
α - Terpineol	1192	2.3	-	-
α-Copaen	1372	0.9	2.2	-
β-Caryophyllene	1414	6.6	13.1	4.3
α-Humulene	1449	0.4	-	-
Myristicin	1522	-	-	57.6
β-Sesquiphellandrene	1523	0.8	-	-
Caryophyllene oxide	1596	6.7	37.2	4.2
δ-Cadinol	1651	0.7		
Neophytadienen	1690	0.8	1.6	1.5

3. Antibacterial and antioxidant activities of extraction

The chemical compounds extracted of *N. officinale* using GC/MS method are shown in Table 2 [13].

Table 2. The obtained compounds of *N. officinale* ethanolic extract using GC/MS (Mahdavi et al., 2019).

No	Compound	Composition (%)	No	Compound	Composition (%)
1	Hexanal	1.06	17	2-methoxy-4-vinyl phenol	3.12
2	Normal hexanol	0.42	18	3-carene-10-acethyl-methyl	9.41
3	2-pentyl furan	1.32	19	Neryl asetone	1.53
4	Normal nontanal	0.91	20	Megastigma Trianon	0.49
5	Decanal normal	0.54	21	Anthracene	0.49
6	Trimethyl	0.55	22	Eucusan	1.44
7	Beta-Dumas Senon	7.42	23	2-E hexanal	0.96
8	3-carene-10-acethyl-methyl	9.41	24	Benzaldehyde	0.25
9	E-beta-lavonone	7.15	25	Normal Octanol	0.55
10	Megastigmatrienone	20.18	26	Safranal	0.74

11	Phytol	30.20	27	1-cyclohexene-1-acetaldoyde	0.55
12	2-E hexanal	0.96	28	Cyclohexane	1.41
13	2-heptane	0.28	29	2-Butanone	4.10
14	Bnz- E- acetaldehyde	0.74	30	Alpha Humolin	0.48
15	2-Nonnal	0.34	31	Hexadekan	0.25
16	Naphthalene-2,1-dihydro-6,1,1-trimethyl	1.25	32	2-Pentadecanone-14,10,6-trimethyl-25/1% -15,12,9-octo-deca tri-acetic acid	1.20

The results of MIC and MBC analysis in this study show that *N. officinale* ethanolic extraction has a bacteriostatic effect on *S. aureus*, *E. coli*, *B. cereus* and *S. enterica* [13]. The presence of normal hexanol in medicinal plant phytochemicals is one of the inhibitory factors for the *S. aureus* and *E. coli* bacteria, which is compatible with this study [14]. Also, the presence of 1-cyclohexan acetaldehyde in the extract of this medicinal plant indicates its antimicrobial ability, which has an inhibitory effect on *S. aureus*, *E. coli* and *K. pneumonia*.

Aqueous and ethanolic extracts of watercress exhibited remarkable DPPH radical scavenging activity [15]. This research show that the percentage of inhibition on lipid peroxidation of linoleic acid system from 500 mg ethanolic extract (96.34%) showed higher antioxidant activity than 500 mg of aqueous extract (92.21%).

4. The anticancer effects

The major active compounds of *Nasturtium officinale* are found to be phenolic compounds and glucosinolates. Main phenolic compounds were reported to be chlorogenic acid and isorhamnetin. Gluconasturtiin, a precursor of 2-phenylethyl isothiocyanate is reported as a glucosinolate compound with anticarcinogenic and antimicrobial activity.

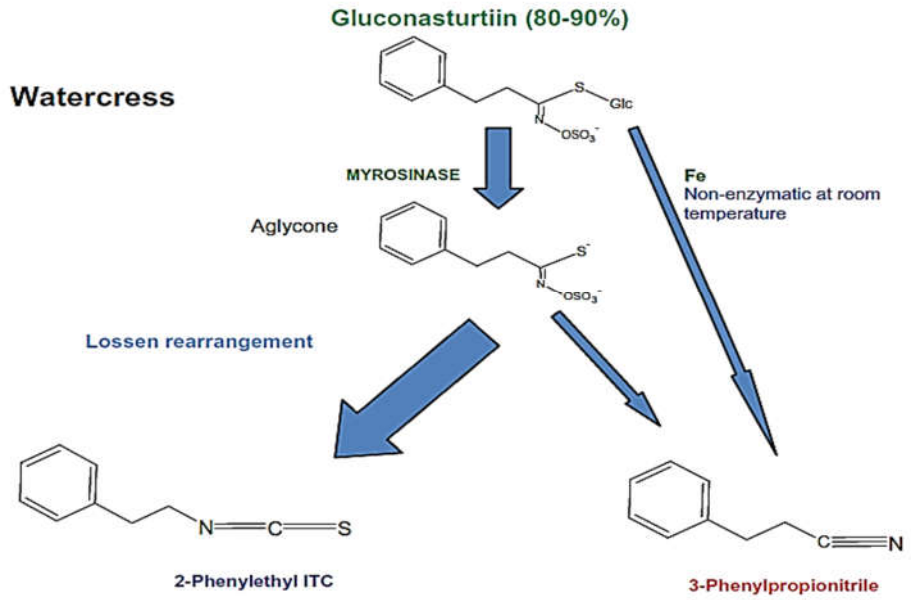

Fig. 2. Model of glucosinolate degradation of gluconasturtiin in watercress seeds at room temperature. Widths of arrows are proportional to the amounts of degradation product formed [16].

In addition to these secondary metabolites, having high amounts of minerals and with high antioxidant activity, it is worth for searching *Nasturtium officinale* for cancer protective effects [[17],[18],[19]]. Watercress is rich in the glucosinolate compound gluconasturtiin (2-phenethylglucosinolate). Also, 2-phenethyl isothiocyanate (ITC) can effectively inhibit tumorigenesis by increasing metabolism and enhancing excretion of the lung carcinogen 4-(methylnitrosamino)-1-(3-pyridyl)-1-butanone, as demonstrated in both animal and human studies [[20],[21],[22]]. When human subjects consumed 30 g of raw watercress containing 21.6 mg gluconasturtiin, in vivo urinary excretion studies revealed the potential conversion to 2.3–5.0 mg of 2-phenethyl isothiocyanate [23].

Since apoptosis in a cell does not lead to death in adjacent cells, inflammation or tissue damage is not caused. So today, one of the interesting strategies that has been considered in chemotherapy for cancer is medication that can mediate the death of malignant cells by inducing apoptosis.

According to new researches, eating a portion of watercress every day could help prevent breast cancer. Phenylethyl isothiocyanate was found to have an activity to inhibit the migration and invasion of human colorectal carcinoma cells and stop the proliferation of cancer cells. In the cell lines of human breast cancer, phenylethyl isothiocyanate was shown to decrease matrixmetalloprotease-9 and ALDH1 marker and also inhibit tumor invasion [[24],[25]].

As well as, the other study demonstrate that the daily intake of aqueous solution of watercress, both before and after the inoculation of the experimental Ehrlich tumor cells, was able to cause suppression of tumor growth [26]. This solution is likely to have chemopreventive and chemoprotective effects, and may be related to the main compounds present in watercress with antitumor properties.

5. Anti-diabetic properties

Oral administration of *Nasturtium officinale* has a significant hypoglycemic effect. in other words, treated diabetic group in a study showed significant lower level of serum glucose as compared to untreated diabetic group ($p<0.05$) [27]. Another research was evaluated *N. officinale* extracts on the blood glucose level in diabetic rats. Only 800 and 1000 mg/kg of the methanol extract of *N. officinale* caused a significant decrease in the blood glucose level after one week treatment. At the end of two months treatment with ethyl acetate extract, the blood glucose level reduced and this reduction was significant statistically in the group, received 100 mg/kg of the extract. The decreasing of blood glucose was comparable with glybenclamide as an anti-diabetic drug [28].

6. Hypothyroidism

The problems related to the thyroid include throat itch, tachycardia, arm pain, chokings, dizziness and fainting. The most extreme side effects symptoms are associated with the T4 hormone replacement for patients whose thyroid was partially or completely removed. The doses used vary from 50 to 200mcg/day of sodic levotiroxine. Some compounds of natural origin have shown to affect the thyroid hormone feedback system by interfering with different components of this homeostatically regulated system: biosynthesis, secretion and metabolism, transport, distribution, and action of thyroid hormones, including the feedback mechanism.

In addition to the plants cited for treatment of thyroid problems, watercress (*Nasturtium officinale*, R.Br.) is a rich source of iodine, the amount it contains probably depending on the amount of iodine available to it during growth [29].

7. Conclusion

Due to the tendency of people to consume food with natural preservatives, plant sources are not only used as flavoring, but are also used as antimicrobial compounds. Therefore, many plant species have been used in the food industry due to their antimicrobial and anti-oxidant properties. As a traditional culinary plant with vitamins, minerals and phytonutrients such as isothiosionates and gluconasturtiin, *Nasturtium officinale* L. may be considered as potential source for anticancer, anti-diabetic and hypothyroidism compounds of natural origin. Further *in vitro* and *in vivo* studies and clinical researches are needed to be conducted on *Nasturtium officinale* L. and we suggest continuing the phytochemical study to find out its pharmacologically active component(s).

References

[1] I. C. Hedge, Nasturtium in K. H. Rechinger (ed.) Flora Iranica, 57 (Cruciferae) (1968). Akademische Druck- U. Verlagsanstalt, Graz.

[2] I.A . Al-Shehbaz, Price RA. Delimitation of the genus Nasturtium (Brassicaceae), Novon. (1998) Jul 1:124-6.

[3] Washington Department of Ecology, Working for Washington's future: healthy watersheds, healthy people, (2008). Retrieved from http://www.ecy.wa.gov/pubs/0801018.pdf

[4] University of Purdue – Department of Horticulture and Landscape Architecture, NewCROP Factsheets watercress (2009). Retrieved from http://www.hort.purdue.edu/newcrop/medaro/ factsheets/WATERCRESS.html

[5] Wisconsin Department of Natural Resources, Nasturtium officinale Invasive Species Classification, (2009). Retrieved from http://dnr.wi.gov/invasives/classification/pdfs/L R_Nasturtium_officinale.pdf

[6] P. Rose, K. Faulkner, G. Williamson, R. Mithen., 7-Methylsulfinylheptyl and 8-methylsulfinyloctyl isothiocyanates from watercress are potent inducers of phase II enzymes, Carcinogenesis 21 (2000) 1983–1988.

[7] ME. O'Neill, Y. Carroll, B. Corridan, B. Olmedilla, F. Granado, I. Blanco, HV. Berg, I . Hininger, AM. Rousell, M. Chopra, S. Southon, DI. Thurnham., A European carotenoid database to assess carotenoid intakes and its use in a five-country comparative study, Br J Nutr (2001) 499-507.

[8] J. W. Fahey, Y. Zhang, P. Talalay., Broccoli sprouts: An excellent rich source of inducers of enzymes that protect against chemical carcinogens. Proc. Natl. Acad. Sci. U.S.A. 94, (1997) 10367–10372.

[9] P. Talalay, Y. Zhang., Chemoprotection against cancer by isothiocyanates and glucosinolates, Biochemical Society Transactions 24 (1996) 806–810.

[10] S.S. Hect., Inhibition of carcinogenesis by isothiocyanates, Drug Metabolism Reviews 32 (2000) 395–411.

[11] Y. Zhang., Cancer-preventative isothiocyanates: measurement of human exposure and mechanism of action. Mutation Research 555 (2004) 173–190.

[12] H. Amiri., Volatile constituents and antioxidant activity of flowers, stems and leaves of *Nasturtium officinale* R. Br. Natural product research 26(2) (2012) 109-115.

[13] S. Mahdavi, M. Kheyrollahi, H. Sheikhloei, A. Isazadeh., Antibacterial and Antioxidant Activities of Essential Oil on Food Borne Bacteria. The Open Microbiology Journal 13(1) (2019) 81-85.

[14] JD. Cha, MR. Jeong, SI. Jeong., Chemical composition and antimicrobial activity of the essential oils of *Artemisia scoparia* and *A. capillaris*, Planta Med 71(2) (2005) 186-90.

[15] T. Ozen., Investigation of antioxidant properties of *Nasturtium officinale* (watercress) leaf extracts, Acta Poloniae Pharmaceutica – Drug Research 66 (2009) 187–913.

[16] DJ. Williams, C. Critchley, S. Pun, M. Chaliha, TJ. O'Hare., Differing mechanisms of simple nitrile formation on glucosinolate degradation in *Lepidium sativum* and *Nasturtium officinale* seeds, Phytochemistry 70(11-12) (2009) 1401-1409.

[17] CR. Balistreri, C. Caruso, G. Candore, The role of adipose tissue and adipokines in obesity-related inflammatory diseases, Mediators of inflammation 2010 (2010) 1-19.

[18] M. Libra, F. Nicoletti., inflammation and cancer: a journey from prevention to treatment. In Updates in pathobiology: causality and chance in ageing, age-related diseases and longevity, University Press (2017) (145-162).

[19] G. Accardi, C. Caruso., Immune-inflammatory responses in the elderly: an update, Immun Ageing 15 (2018) 1-11.

[20] S. S. Hecht, S. G. Carmaella., Murphy, S. E. Effects of watercress consumption on urinary metabolites of nicotine in smokers, Cancer Epidemiol Biomarkers PreVention 8 (1999) 907–913.

[21] G. Boysen, P. M. J. Kenney, P. Upadhyaya, M. Wang, S. S. Hecht., Effects of benzyl isothiocyanate and 2-phenethyl isothiocyanate on benzo[a]pyrene and 4-(methylnitrosamino)-1-(3-pryridyl)-1-butanone metabolism in F-344 rats, Carcinogenesis 24 (2003) 517–525.

[22] L. B. von Weymarn, J. A. Chun, P. F. Hollenberg., Effects of benzyl and phenethyl isothiocyanate on P450s 2A6 and 2A13: Potential for chemoprevention in smokers, Carcinogenesis 27 (2006) 782–790.

[23] F.L. Chung, M. A. Morse, K. I. Eklind, J. Lewis., Quantitation of human uptake of the anticarcinogen phenethyl isothiocyanate after a watercress meal, Cancer Epidemiol Biomarkers PreVention 1 (1992) 383–388.

[24] P. Rose, Q. Huang, C. N. Ong, M. Whiteman., Broccoli and watercress suppress matrix metalloproteinase-9 activity and invasiveness of human MDA-MB-231 breast cancer cells, Toxicology and applied pharmacology (209) 2 (2005): 105-113.

[25] B. E. Cavell, S. S. S. Alwi, A. Donlevy, G. Packham., Anti-angiogenic effects of dietary isothiocyanates: mechanisms of action and implications for human health, Biochemical pharmacology (81) 3 (2011) 327-336.

[26] D. A. de Souza, P. M. Costa, R. I. M. Ribeiro, P. V. Vidigal, F. C. Pinto., Daily intake of watercress causes inhibition of experimental Ehrlich tumor growth, Jornal Brasileiro de Patologia e Medicina Laboratorial (52)6 (2016) 393-399.

[27] MH. Qeini, ME. Roghani, AH. Alagha., The effect of *Nasturtium officinale* feeding on serum glucose and lipid levels and reorganization of beta cells in diabetic rats. Razi Journal of Medical Sciences 17(73) (2010) 53-61.

[28] HF. Hoseini, AR. Gohari, S. Saeidnia, NS. Majd, A. Hadjiakhoondi., The effect of *Nasturtium officinale* on blood glucose level in diabetic rats. Pharmacologyonline 3 (2009) 866-71.

[29] Chilean Iodine Educational Bureau, Iodine Content of Foods 90 Shenval Press (1952).

Sequence of ITS1 gene is a new biomarker to classify Aspargillus fungi

Zohreh Hassanzadeh[1], Reza Yari[1] Farzad Parsa[*1]

[1]Department of Biology, Faculty of Sciences, Boroujerd branch, Islamic Azad University, Boroujerd, Iran.

*Email: zohrehasanzadeh6823@gmail.com

Abstract

Introduction: Aspergillusis a diverse genus of filamentous fungi including numerous groups and species. The aim of the present study was to determine the sequence of the ITS1 gene along with morphological data to identifying Aspergillus species isolated from food.

Materials and Methods: In this study, 25 isolates of Aspergillus were isolated from different foods. All isolates were cultured on Sabouro dextrose agar medium and their genomic DNA was extracted after cultivation. Subsequently, the ITS1 gene of each sample was amplified by polymerase chain reaction (PCR) and the nucleotide sequence of 25 isolates was determined and the resultant data were sequenced.

Results: Out of 25 sequenced Aspergillus isolates, the total genetic variation among all calculated isolates and standard strains was 0.15.The highest genetic variation was reported to be 0.730 units. The results of the phylogenic tree with NJ method showed that the standard strain of A.flavus was selected as an internal control because it had the highest number among isolates.

Discussion and Conclusion: The results of this study showed that sequencing the ITS1 gene for identification of Aspergillus species at species level was very valuable. The use of molecular methods is recommended for further study on Aspergillus species.

Keywords: Aspergillus, ITS1, PCR-Sequencing,Blast.

1. Introduction

The genus Aspergillus is one of the most important filamentous fungal genera. Aspergillus species are used in the fermentation industry, but they are also responsible of various plant and food secondary rot, with the consequence of possible accumulation of mycotoxins. The aflatoxin producing A. flavus and A. parasiticus, and ochratoxinogenic A. niger, A. ochraceus and A. carbonarius species are frequently encountered in agricultural products. Studies on the biodiversity of toxigenic Aspergillus species is useful to clarify molecular, ecological and biochemical characteristics of the different species in relation to their different adaptation to environmental and geographical conditions, and to their potential toxigenicity[1]. Here we analysed sequence diversity of *Internal transcribed spacer1(ITS1)* gene of Aspargillus that was extracted from 25 different food source.

2. Material and Methods

2.1 Sample extraction

We are extracting Aspargillus mold from 25 different food sources like ten of them are listed below like Tea, Organge, Flowers, Pistachino, Carrots, Marmalade, Wafer, Soya, Rice and Tarkhine (that name of traditional food of Borujerd city).

Tarkhine (traditional food)

TEA

Flower

Pistachio

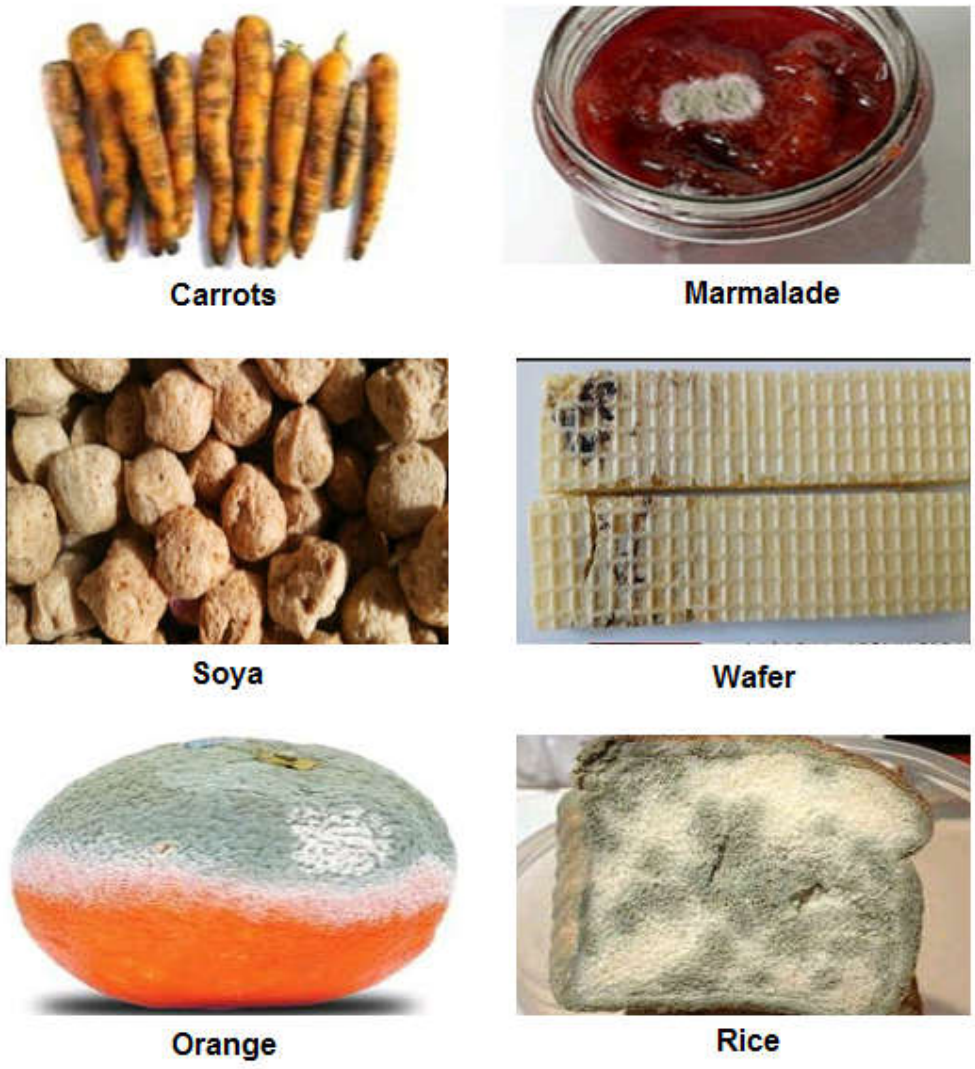

Fiqure 1: Food source that Aspargillus was extracted.

2.2 Cell Culture

We are utilizing three culture medium:

Sabouraud Dextros Agar (SDA)

Malt Extract Agar (MEA)

Czapek Yeast extract Agar (CYA)

2.3 DNA Extraction

To this end we used Extraction Kit of DNA and also select SDA products as a template to Aspargillus DNA extraction.

2.4 PCR to proliferation of ITS1 gene

Which are primers designed for revers and forward sequence of ITS1 gene are showed in below table.

Table 1: Primer Design of ITS1 gene

Primer name	ITS1 sequence order 5' to 3'
Reverse primer	5' - TCC TCC GCT TAT TGA TAT GC -3'
Forward primer	5' - TCC GTA GGT GAA CCT GCG G -3'

PCR program

Table 2: PCR program

PCR program	Temprature °C	Time	Cycle
Initial denaturation	95	5 minute	1
Denaturation	95	45 second	
Annealing	55	45 second	36
Extension	72	1 minute	
Final Extension	72	6 minute	1

2.5 DNA Sequencing

PCR production was sequenced by PISHGAM Company and that results were analysed with MEGA7 software[2]. Also the sequences were compared with NCBI database to check and found species are similar (>= 99%) with Asparagillus fungi by BLAST method[3].

2.6 Phylogeny

Our results of sequencing were performed with BLAST analysis to found and check similar sequences from NCBI database. Also we tried to draw phylogeny tree with MEGA7 software.

3. Results and Discussions

3.1 Resutls of SDA culture medium

After identification of samples of Aspergillus, all strain was extracted and cultured in the SDA medium with 25 °C, after that many of them are showed with below fig:

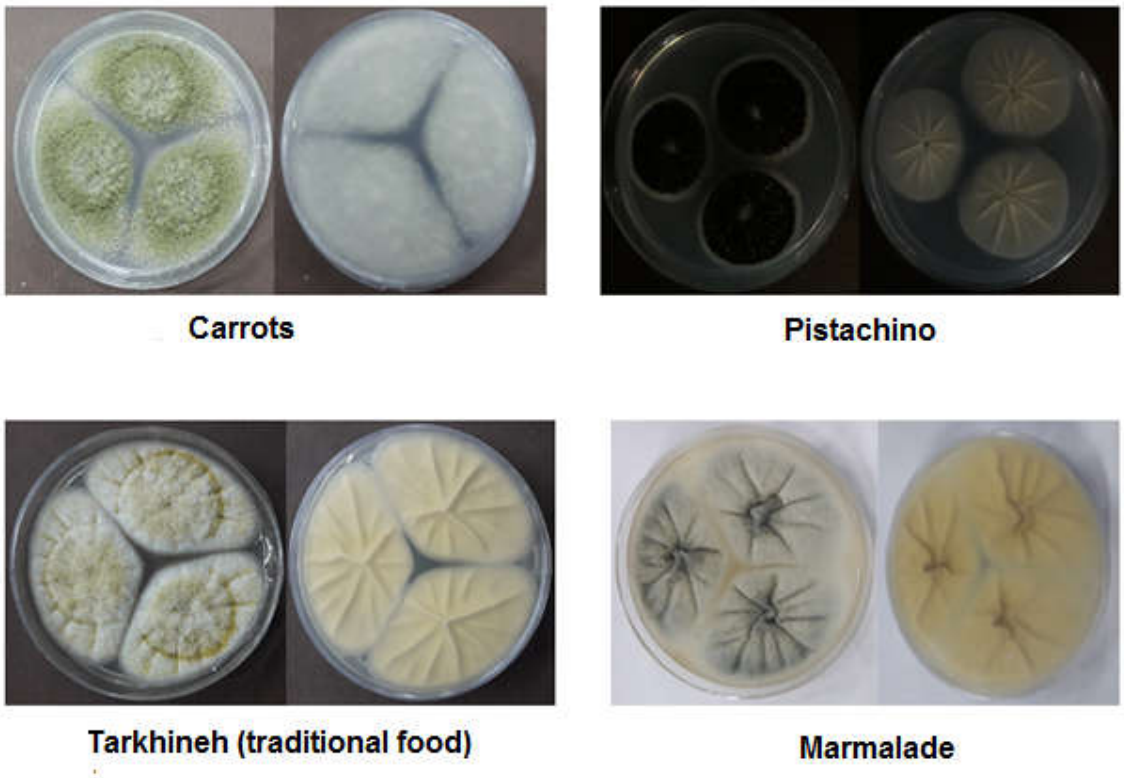

Figure 2: Front and Back of the Aspargillus colony in SDA medium.

3.2 PCR results

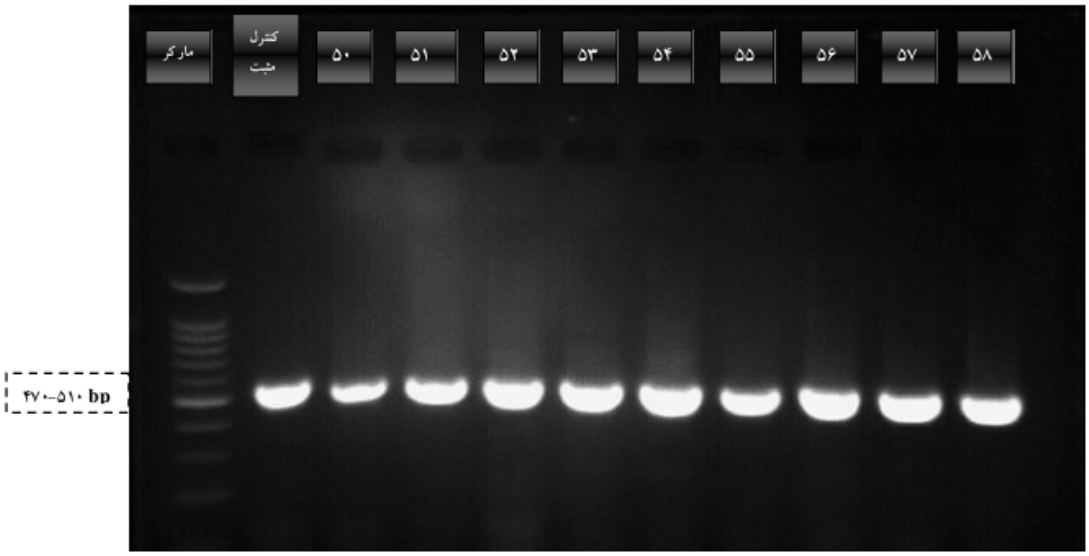

Figure 3: PCR product was run to the gel electrophoresis and some many of samples was showed in figure 3. In the level of 470 – 510 bp ITS1 is represented strongly bonds.

3.3 Phylogenetic tree analysis

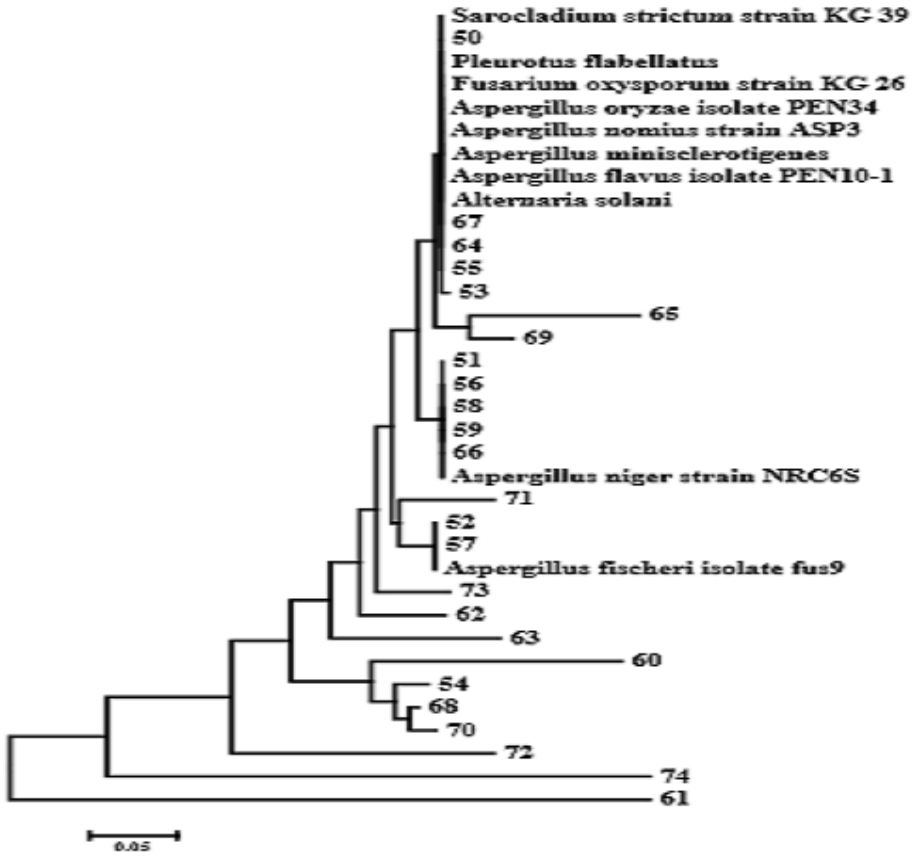

Figure 4: Phylogenetic results of different Aspargillus with NJ procedures

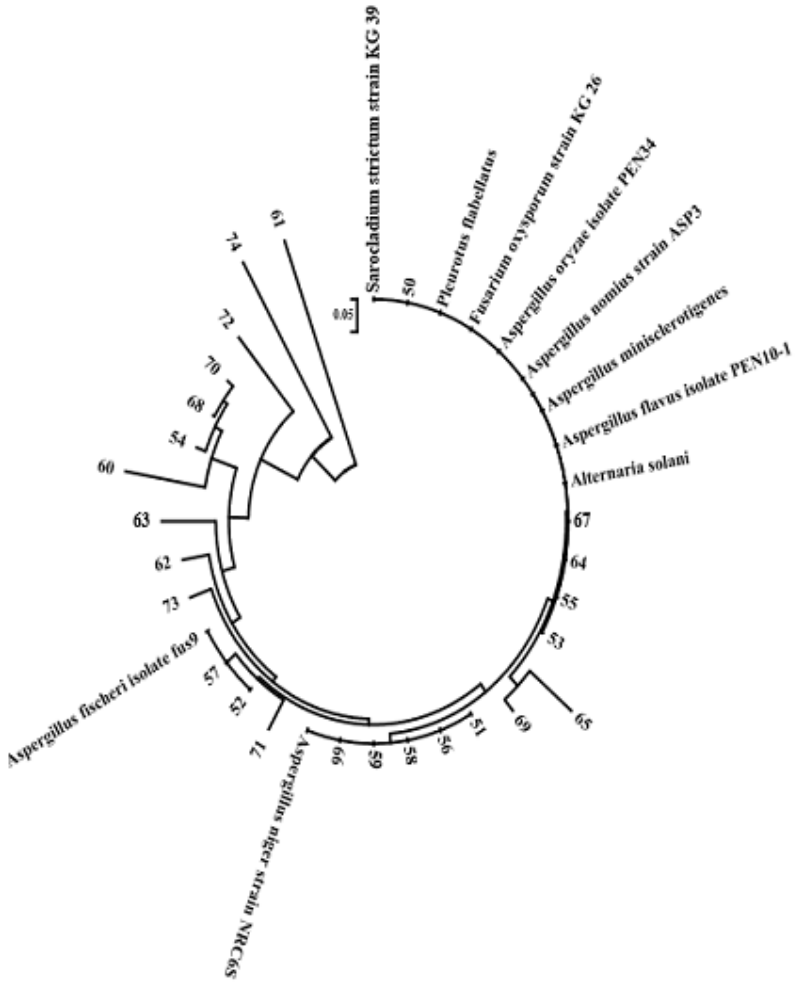

Figure 5: Phylogenetic results of different Aspargillus with NJ procedures

Results of phylogenetic analysis indicate that most genetic differences between 25 samples were showed between two 61 and 74 samples with 0/730 value. Also *A.Flavus* was selected as standard strain. Samples 50, 53, 55, 64, 67 and also *Pleurotus flabellatus, Fusarium oxysporum, Aspergillus oryzae, Aspergillus nomius, Aspergillus minisclerotigenes, Aspergillus flavus, Alternaria solani* are showed distance less than 0.10 that mean indicated they are very closely from genetic variation.Based on nowadays insight that represented a species of fungi should have one name. Our results indicated new marker to better classify Aspargillus with ITS1 gene sequence.

Acknowledgements

This study supported by Islamic Azad University of Borujerd branch.

References

[1] Perrone G, Susca A, Cozzi G, Ehrlich K, Varga J, Frisvad JC, Meijer M, Noonim P, Mahakarnchanakul W, Samson RA. Biodiversity of Aspergillus species in some important agricultural products. Studies in mycology. 2007 Jan 1;59:53-66.

[2] Kumar S, Stecher G, Tamura K. MEGA7: molecular evolutionary genetics analysis version 7.0 for bigger datasets. Molecular biology and evolution. 2016 Mar 22;33(7):1870-4.

[3] Johnson M, Zaretskaya I, Raytselis Y, Merezhuk Y, McGinnis S, Madden TL. NCBI BLAST: a better web interface. Nucleic acids research. 2008 Apr 24;36(suppl_2):W5-9.

Antibacterial effect of Silver and Iron Oxide Nanoparticles on Pathogenic and Non-Pathogenic Bacteria

Foozieh Moghadami

Department of Biology, Payame Noor University, Tehran, Iran

*Email: fouziehm@yahoo.com

Abstract

Many research studies have investigated the antimicrobial activity of nanoparticles on pathogenic bacteria. Nevertheless, there are a few studies on antimicrobial activity of nanoparticles on non-pathogenic bacteria. The aim of this study was to evaluate the differences of the antimicrobial activity of silver and iron oxide nanoparticles, against pathogenic and non-pathogenic bacteria. To determine of the antibacterial activity of silver and iron oxide nanoparticles, the minimum inhibitory concentration (MIC), minimum bactericidal concentration (MBC) and agar well diffusion methods on *P.aeruginosa*, *E.coli*, *S.aureus*, *B.subtilis*, *G.oxydans* and *G.japonicus* were performed. The results of this study showed that MIC and MBC of silver and iron oxide nanoparticles for non-pathogenic bacteria (*G.oxydans* and *G.japonicus*) was lower than the others were. The highest inhibition zones (15.5 and 14.9 mm) were also belonging to non-pathogenic bacteria for silver nanoparticles against *G.oxydans* and *G.japonicus*, respectively. The findings suggest that the antibacterial activity of silver and iron oxide nanoparticles can be vary against pathogenic and non-pathogenic bacteria.

Keywords: Nanoparticle, Silver, Iron oxide, Antibacterial, Pathogenic, Non-pathogenic

1. Introduction

Application of antibiotics is the most common approach to treat bacterial infection. However, the rise of resistant bacteria has made routine antibiotic ineffective. Thus, it is urgent to find an antibacterial agent that can kill drug-resistant bacteria. One of the suitable candidates is nanoparticles [1]. Nanoparticles are materials that having dimensions in the order of 1–100 nm [2]. Silver has been demonstrated to possess effective antibacterial effect and has been vastly used in medicine. Moreover, silver can be manufactured into silver nanoparticles through nanotechnology to have improved physical, chemical, and biological properties. The nanoparticles, such as nano-metal materials, have appeared to be promising candidates, since they have wide cytotoxicity activity against the broad- spectrum of microorganisms such as bacteria, fungi and even viruses [3]. Many investigations have performed on the antimicrobial activity of nanoparticles, and recent research achievements revealed that it is possible to produce new types of nanoparticles for achieving more antibacterial activity [4]. The metallic nanoparticles such as Ag, Au, Fe_2O_3, Fe_3O_4, ZnO, CuO, and TiO_2 have been studied [5]. However, various findings have been known in this regard, the possible antibacterial mechanisms of nanoparticles are still unclear.

It seems that comparing the antimicrobial properties of nanoparticles against different bacterial strains can be effective in better understanding their possible mechanisms [6].

The present study was carried out to evaluate the differences of the antimicrobial activity of the silver and iron oxide nanoparticles, against pathogenic and non-pathogenic bacteria. For this purpose, six bacterial strains were used. The Gram-negative pathogenic bacteria: *Pseudomonas aeruginosa* and *Escherichia coli,* the Gram-positive pathogenic bacteria: *Staphylococcus aureus* and *Bacillus subtilis* and the Gram-negative non-pathogenic bacteria: *Gluconobacter oxydans* and *Gluconobacter japonicus*.

2. Material and Methods

2.1 Chemicals, Microorganisms and Media

The silver (Ag) and iron oxide (Fe_3O_4) nanoparticles with dimensions of 20 and 20-30 nm respectively were purchased from US Research Nanomaterials Co (USA). All other chemicals were of analytical grade from standard suppliers. Antibacterial activities of silver and iron oxide nanoparticles were performed on 4 bacteria obtained from clinical specimens including *Pseudomonas aeruginosa* and *Escherichia coli* (Gram-negative pathogenic bacteria), *Staphylococcus aureus* and *Bacillus subtilis* (Gram-positive pathogenic bacteria), and 2 Gram-negative non-pathogenic bacteria *Gluconobacter oxydans* H621 (was purchased from Persian Type Culture Collection) and *Gluconobacter japonicus*. The last ones were isolated and identified previously [7]. These strains were maintained on Nutrient Agar at 4°C for subsequent studies.

2.2 Determination of minimum inhibitory concentration (MIC) and minimum bactericidal concentration (MBC) of silver and iron oxide nanoparticles

The microtiter plate assay was used to determine the MIC of silver and iron oxide nanoparticles. The iron oxide and silver nanoparticles were used separately with concentrations of 0.02, 0.05, 0.1, 0.2, 0.3, 0.4, 0.5 and 0.6 mg/ml for each bacterial strain. The bacterial strain suspensions were prepared in the sterile normal saline to a concentration of 0.5 McFarland standard solutions. To determination of MBC of silver and iron oxide nanoparticles 10 µL from all wells of MIC assay that had no visible bacterial growth was removed and cultured on the NA media. The plates were incubated at 37°C for 24 h. MBC is defined as the lowest concentration of antimicrobial agent that apparently kills 99.9% of the initial bacterial population and therefore it is not observed any significant growth in the NA medium.

2.3 *Antibacterial activity of silver and iron oxide nanoparticle*

Antibacterial activity of the silver and iron oxide nanoparticles was studied using the agar well diffusion method. The petri dishes including semi solid Mueller Hinton agar (MHA) were cultured with 1.5×10^8 CFU/mL suspensions of test bacteria. Different concentration of silver and iron oxide nanoparticles (ranging from 0.02 to 0.6 mg/mL) was inoculated into the wells (6 mm diameter). The plates were incubated at 37°C for 24 h. Antimicrobial activity was measured based on the diameter of inhibition zone in mm.

3. **Results and Discussions**

3.1 *MIC and MBC of silver and iron oxide nanoparticles*

The results of the MIC and MBC of silver and iron oxide nanoparticles on the *P.aeruginosa*, *E.coli*, *S.aureus*, *B.subtilis*, *G.oxydans* and *G.japonicus* bacteria are shown in Table 1 and 2. The main aim of this study was the investigation of differences of the antibacterial effect of iron oxide and silver nanoparticles on pathogenic and non- pathogenic bacteria. The results of this study showed that MIC and MBC of silver and iron oxide nanoparticles for non-pathogenic bacteria (*G.oxydans* and *G.japonicus*) was lower than the others were. The antibacterial effects of nanoparticles on the various bacteria have been investigated so far [8]. The investigations have shown that most nanoparticles have antibacterial activity [9, 10]. The antibacterial effects of nanoparticles have been studied mostly on pathogenic bacteria [11, 12]. There are a few studies performed on the antibacterial effect of nanoparticles on the non-pathogenic bacteria. Garcia-Ruiz *et al*. showed that the concentrations higher than 45 µg / ml of various silver nanoparticles (silver-polyethylene glycol nanoparticles and silver-glutathione nanoparticles) inhibited the growth of *G. oxydans* [13].

Table 1. The MIC and MBC of silver nanoparticles against pathogenic and non- pathogenic bacteria.

	AgNPs(mg/ml)	0.02	0.05	0.1	0.2	0.3	0.4	0.5	0.6
Gram-negative pathogenic bacteria	*P.aeruginosa*	+	+	+	+	+	MIC	MBC	-
	E.coli	+	+	+	+	MIC	MBC	-	-
Gram-positive pathogenic bacteria	*S.aureus*	+	+	+	+	+	MIC	MBC	-
	B.subtilis	+	+	+	MIC	MBC	-	-	-
Gram-negative non-pathogenic bacteria	*G.oxydans*	+	MIC	MBC	-	-	-	-	-
	G.japonicus	+	MIC	MBC	-	-	-	-	-

Table 2. The MIC and MBC of iron oxide nanoparticles against pathogenic and non- pathogenic bacteria.

	Fe_3O_4NPs(mg/ml)	0.02	0.05	0.1	0.2	0.3	0.4	0.5	0.6
Gram-negative pathogenic bacteria	*P.aeruginosa*	+	+	+	+	+	+	MIC	MBC
	E.coli	+	+	+	+	+	+	MIC	MBC
Gram-positive pathogenic bacteria	*S.aureus*	+	+	+	+	+	+	MIC	MBC
	B.subtilis	+	+	+	+	+	MIC	MBC	-
Gram-negative non-pathogenic bacteria	*G.oxydans*	+	+	+	MIC	MBC	-	-	-
	G.japonicus	+	+	MIC	MBC	-	-	-	-

3.2 Antibacterial activity of silver and iron oxide nanoparticles

In this study, the antimicrobial activities of silver and iron oxide nanoparticles were also investigated by growing *P.aeruginosa*, *E.coli*, *S.aureus*, *B.subtilis*, *G.oxydans* and *G.japonicus* colonies on MHA plates, supplemented with different concentrations of silver and iron oxide nanoparticles. The results of inhibition zone diameter (mm) of silver and iron oxide nanoparticles for *P.aeruginosa*, *E.coli*, *S.aureus*, *B.subtilis*, *G.oxydans* and *G.japonicus* are shown in Table 3 and 4. The inhibition zones of bacterial inhibition by silver and iron oxide nanoparticles showed that the maximum inhibition zones were belonging to *G.japonicus*, with 14.9 mm and *G.oxydans* with 15.5 mm in the presence of 0.6 mg/mL silver nanoparticle. The findings suggest that the antibacterial activity of silver and iron oxide nanoparticles can be vary against pathogenic and non-pathogenic bacteria.

Table 3. Inhibition zone diameter (mm) of silver nanoparticle for *P.aeruginosa*, *E.coli*, *S.aureus*, *B.subtilis*, *G.oxydans*, *G.japonicus*. The related MIC values are shown in bold.

AgNPs(mg/ml)	*P.aeruginosa*	*E.coli*	*S.aureus*	*B.subtilis*	*G.oxydans*	*G.japonicus*
0.02	7.1 ± 0.2	7.9 ± 0.5	6.4 ± 0.2	7.6 ± 0.4	9.4 ± 0.4	9.1 ± 0.1
0.05	7.5 ± 0.8	8.1 ± 0.3	6.9 ± 0.3	8.1 ± 0.4	**12.0 ± 0.3**	**12.3 ± 0.4**
0.1	7.9 ± 0.3	8.7 ± 0.9	7.2 ± 0.6	8.9 ± 0.8	12.7 ± 0.5	12.6 ± 1.1
0.2	8.1 ± 0.5	9.1 ± 0.7	7.8 ± 0.5	**11.1 ± 0.9**	13.2 ± 0.9	13.5 ± 0.2
0.3	8.7 ± 0.1	**11.5 ± 0.1**	8.0 ± 0.5	11.8 ± 0.4	13.9 ± 0.2	13.6 ± 0.9

0.4	**10.8 ± 0.7**	12 ± 0.5	**11.8 ± 0.5**	12.5 ± 0.3	14.5 ± 0.5	13.9 ± 0.6
0.5	11.4 ± 0.4	12.7 ± 0.2	12.4 ± 0.4	13.0 ± 0.2	14.8 ± 0.6	14.4 ± 0.5
0.6	12.0 ± 0.4	13.5 ± 0.6	13.1 ± 0.4	13.8 ± 0.4	15.5 ± 0.7	14.9 ± 0.5

Table 4. Inhibition zone diameter (mm) of iron oxide nanoparticle for *P.aeruginosa*, *E.coli*, *S.aureus*, *B.subtilis*, *G.oxydans*, *G.japonicus.* The related MIC values are shown in bold.

Fe_3O_4NPs(mg/ml)	*P.aeruginosa*	*E.coli*	*S.aureus*	*B.subtilis*	*G.oxydans*	*G.japonicus*
0.02	6.8 ± 0.3	6.0 ± 1.0	6.7 ± 0.7	7.0 ± 1.1	9.1 ± 0.3	9.2 ± 0.2
0.05	7.1 ± 0.5	7.8 ± 0.7	7.0 ± 0.8	8.2 ± 0.5	9.6 ± 0.6	9.6 ± 0.4
0.1	7.4 ± 1.1	8.3 ± 0.5	7.6 ± 0.5	8.9 ± 0.7	10.2 ± 0.7	**12.2 ± 0.6**
0.2	7.7 ± 0.4	9.1 ± 0.4	7.9 ± 0.4	9.6 ± 0.5	**13.1 ± 0.3**	12.5 ± 0.4
0.3	7.9 ± 0.9	9.6 ± 0.1	8.3 ± 0.7	10.1 ± 0.5	13.3 ± 1.0	13.1 ± 0.8
0.4	8.2 ± 0.8	10.1 ± 0.7	11.8 ± 0.4	**12.0 ± 0.3**	13.5 ± 0.9	13.8 ± 0.3
0.5	**10.9 ± 0.3**	**12.3 ± 0.4**	**11.9 ± 0.7**	12.6 ± 0.2	14.1 ± 0.9	14.5 ± 0.4
0.6	11.6 ± 0.4	13.3 ± 0.4	12.5 ± 0.7	12.8 ± 0.3	15.0 ± 0.5	14.8 ± 0.5

The results also showed that the effect of the silver nanoparticles had a stronger antibacterial activity than the iron oxide nanoparticle had. The similar result was obtained in other studies e.g. the antimicrobial effect of silver nanoparticles was shown to be greater than other nanoparticles such as iron, zinc and gold [14]. It has been mentioned that the dimensions of nanoparticles are effective on their antimicrobial effects [15]. In this study the dimensions of the silver nanoparticles (20 nm) was slightly smaller than the iron oxide nanoparticles (20-30 nm). Therefore, this could be a reason for higher antibacterial activity of the silver nanoparticles. Hajipour revealed that the antibacterial activities of nanoparticles depend on two main factors. One of them is physicochemical properties of nanoparticles and the other is the type of bacteria. Although there are good correlations in the results of nanoparticles antibacterial activities, it is difficult to generalize individual studies [8].

In conclusion, it has been demonstrated that silver and iron oxide nanoparticles display excellent antibacterial potential for the Gram-positive and Gram-negative bacteria. However, it was revealed that the antibacterial activities of silver and iron oxide nanoparticles could be varying against pathogenic and non-pathogenic bacteria. This investigation suggests that further studies should be performed on the differences in the antibacterial activity of nanoparticles against pathogenic and non-pathogenic bacteria to reveal possible differences in existing mechanisms.

Acknowledgements

The author wish to thank Payam-noor University for the financial support.

References

[1] M. Zarei, A. Jamnejad, E. Khajehali. Antibacterial Effect of Silver Nanoparticles Against Four Foodborne Pathogens. Jundishapur Journal of Microbiology. 7(1): 2014 e8720

[2] A. Nagy, A. Harrison, S. Sabbani, RS. Munson , PK. Dutta, WJ. Waldman. Silver nanoparticles embedded in zeolite membranes: release of silver ions and mechanism of antibacterial action. International Journal of Nanomedicine.6: 2011.1833–1852.

[3] N. Sanchooli, S. Saidi, H. Khandan, E. Sanchooli. In vitro antibacterial effects of silver nanoparticles synthesized using *Verbena officinalis* leaf extract on *Yersinia ruckeri, Vibrio cholera* and *Listeria monocytogenes*. Iranian Journal of Microbiology 10(6):2018. 400–408

[4] S. Stankic, S. Suman, F. Haque, J. Vidic. Pure and multi metal oxide nanoparticles: synthesis, antibacterial and cytotoxic properties. Journal of Nanobiotechnology.14(1):2016.73. doi:10.1186/s12951-016-0225-6

[5] E. Nazoori, A. Kariminik. In Vitro Evaluation of Antibacterial Properties of Zinc Oxide Nanoparticles on Pathogenic Prokaryotes. Journal of Applied Biotechnology Reports. 5(4):2018.162-165. Doi:10.29252/JABR.05.04.05

[6] Yn. Slavin, J. Asnis, UO. Hafeli, H. Bach. Metal nanoparticles: understanding the mechanisms behind antibacterial activity. Journal of Nanobiotechnology.15(1):2017.65. doi:10.1186/s12951-017-0308-z.

[7] F. Moghadami, J. Fooladi, R. Hosseini. Introducing a thermotolerant *Gluconobacter japonicus* strain, potentially useful for coenzyme Q_{10} production. Folia Microbiology 64(4):2019 471-479. doi: 10.1007/s12223-018-0666-4.

[8] M. Hajipour, K. Fromm, A. Ashkarran, D. Aberasturi, I. Larramendi, T. Rojo, V. Serpooshan. Antibacterial properties of nanoparticles. Trends in Microbiology. 30(10):2012.499-511

[9] B. Ramalingam, T. Parandhaman , SK. Das. Antibacterial effects of biosynthesized silver nanoparticles on surface ultrastructure and nanomechanical properties of gram-negative bacteria viz. Escherichia coli and Pseudomonas aeruginosa. ACS Applied Material Interfaces.8(7):2016. 4963–4976

[10] JR. Morones. The bactericidal effect of silver nanoparticles. Nanotechnology.16: 2005. 2346–2353

[11] M. Arakha, S. Pal , D. Samantarrai. Antimicrobial activity of iron oxide nanoparticle upon modulation of nanoparticle-bacteria interface. Science Reports 5, 14813 .2015. doi./10.1038/srep14813

[12] L. WangL, C. Hu , L. Shao . The antimicrobial activity of nanoparticles: present situation and prospects for the future. International Journal of Nanomedicine. 12: 2017.1227–1249. doi: 10.2147/IJN.S121956

[13] N. Garsia-Ruiz, J. Crespo , J. Lopez-de-Luzuriaga , M. Olmos, M. Monge. Novel biocompatible silver nanoparticles for controlling the growth of lactic acid bacteria and acetic acid bacteria in wines. Food Control.50: 2015. 613-619

[14] I. Sondi , B. Salopek-Sondi . Silver nanoparticles as antimicrobial agent: a case study on *E. coli* as a model for Gram negative bacteria. Journal of Colloid Interface Science .275: 2004.177–182

[15] A. Simon-Deckers , S. Loo, M. Mayne-Lhermite. Size, composition and shape-dependent toxicological impact of metal oxide nanoparticles and carbon nanotubes toward bacteria. Environmental Science Technology.43(21):2009.8423-8429. doi:10.1021/es9016975

Mitigating the effects of aflatoxin producing fungus (Aspergillus flavus) by means of RNAi

Saeede Ansari[1], Amir Mousavi[1*], MohammadReza Safarnejad[2], Naser Farrokhi[3*], Seyed Mehdi Alavi[1]

[1] National Institute of Genetic Engineering and Biotechnology, Tehran, Iran

[2]Plant Protection Research Institute of Iran, Tehran, Iran

[3]Faculty of Life Sciences and Biotechnology, Shahid Beheshti University, Tehran, Iran

*Email: m-amir@nigeb.ac.ir, n_farrokhi@sbu.ac.ir

Abstract

Aspergillus flavus is a major fungal phytopathogen and an opportunistic pathogen to humans. The fungus produces immunosuppressive and carcinogenic aflatoxins. The biological function of a highly immunogenic cell wall antigen *A. flavus* mannoprotein 1 (AFLMP1) was investigated by RNA interference (RNAi). Phylogenetic analysis indicated that AFLMP1 is exclusively present in Aspergillus section Flavi such as *A. flavus* and *A. parasiticus*, making it an excellent candidate for the RNAi-based control of aflatoxigenic fungi in the field and fungal therapy. For this, a chemically synthesized AFLMP1-specific 27-mer RNA duplex was used. The incubation of the substrate with *A. flavus* and *A. parasiticus* conidia resulted in growth inhibition at low concentrations and germination failure at higher concentrations.

Keywords: Aspergillus, Aflatoxin, siRNA, Opera system.

1. Introduction

Aspergillus belongs to group of ascomycetes that includes more than 180 species. Members of the genus are mainly saprophyte, especially in oily nuts (pistachios, hazelnuts, walnuts and peanuts), oilseeds (corn, rapeseed, cotton), pepper and coffee [2]. Many of which are capable of heightening health risk for all organisms via producing mycotoxins such as aflatoxins [3]. In agricultural production, Aspergillus species have devastating effect (more than 20%) on final produce. Corresponding damage becomes even more sever once accompanied by the production of aflatoxins. In humans, Aspergillus spores cause varieties of diseases including raging allergies to aspergillosis [4,5]. It is estimated that more than 4.5 billion people in developing countries are exposed to aflatoxins from contaminated food [6]. Here, inhibitory effect of siRNA against antigenic manoprotein (AFLMP1), which is specific to the cell wall of *Aspergillus flaus*, as a highly immunogenic target was monitored via Opera® High Content Screening system. Use of specific antibodies against a fungal pathogen, targeting its

extracellular domains, is being considered as a pivotal mean to describe the morphology of the fungus and to demonstrate localization and function of the immunogenic target protein.

2. Material and Methods

The biological function of AFLMP1 was investigated by a specific 27-mer RNA duplex as an RNA interference (RNAi). Fungal cell walls were stained with Calcofluor White (20 µl of 1:20 dilution in H_2O) (Sigma, # 18909) for 10 min at 22 °C. For the visualization and quantitative representation of the inhibitory effect of the siRNA, the Opera® High Content Screening System (Emission440nm/ Absorption355nm) was used.

3. Results and Discussions

The synthetic inhibitory effect of specific RNAi on the growth inhibition of pathogenic fungi was investigated microscopically [7]. The sharp decline of *Aspergillus flavus* growth was noted and quantified due to the RNAi gene silencing of the transcript to AFLMP1. The microscopic images highlighted that the manoprotein (AFLMP1) plays a very important role in the germination and growth of *Aspergillus flavus*.

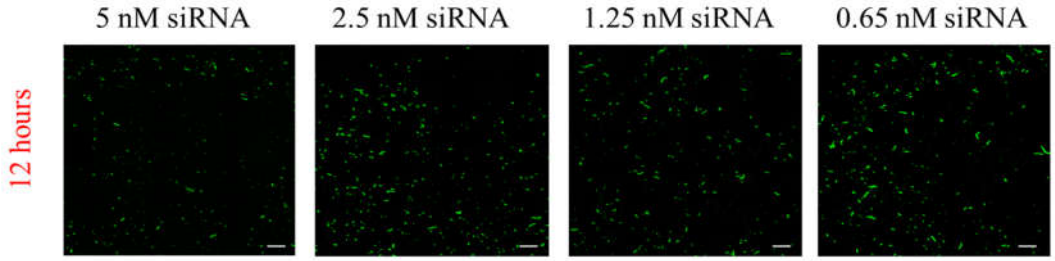

Figure 1: Effect of siRNAs inhibition on the growth of *A. flavus*. Micro titer plates were incubated with spores of *A. flavus* (200 spores/cavity) with siRNA (0.065 to 5 nM) for 12-36 h at 37 °C in dark (here present only the result related to 12 h incubation). After adding Calcofluor White (1:20) the visualization of stained hyphae by confocal microscopy with Opera® High Content Screening System took place.

Acknowledgements

The authors would like to thank Dr. Stefano di Fiore (Fraunhofer IME, Aachen) for his help with the Opera® High Content Screening System. This work was supported by DAAD (Germany), grant number:
FKZ50739422.

References

[1] Woo PC, Chong KT, Leung AS, Wong SS, Lau SK, Yuen KY. *Aflmp1* encodes an antigenic cel wall
[2] protein in *Aspergillus flavus*. J Clin Microbiol, 2003;41(2):845-50. doi: 10.1128/jcm.41.2.845-

[3] 850.2003

[4] Shivaprakash M. Rudramurthy, Raees A. Paul, Arunaloke Chakrabarti, Johan W. Mouton Jacques F. Meis, Invasive Aspergillosis by *Aspergillus flavus*: epidemiology, diagnosis, antifungal resistance, and management, J. Fungi, 2019; 5(3):55. doi: 10.3390/jof5030055.

[5] Ahmad F.Alshannaq, JohnG.Gibbons, Mi-Kyung Lee, Kap-Hoon Han, Seung-Beom Hong, Jae-HyukYu, Controlling aflatoxin contamination and propagation of *Aspergillus favus* by a soy-fermenting

[6] *Aspergillus oryzae* strain, J Scientific Reports, 2018; 8(1). doi: 10.1038/s41598-018-35246-1.

[7] Hedayati MT, Pasqualotto AC, Warn PA, Bowyer P, Denning DW. *Aspergillus flavus*: human pathogen, allergen and mycotoxin producer. Microbiology, 2007; 153(Pt6):1677-92. doi: 10.1099/mic.0.2007/007641-0.

[8] Yu J, Cleveland TE, Nierman WC, Bennett JW. *Aspergillus flavus* genomics: gateway to human and

[9] animal health, food safety, and crop resistance to diseases. Rev Iberoam Micol 2005;22(4):194-202.

[10] doi: 10.1016/s1130-1406(05)70043-7.

[11] Md-Sajedul Islam, Kenneth A. Callicott, Charity Mutegi, Ranajit Bandyopadhyay, Peter J. Cotty, *Aspergillus flavus* resident in Kenya: High genetic diversity in an ancient population primarily shaped by clonal reproduction and mutation-driven evolution, J Fungal Ecology, 2018. 35: 20-33.

[12] A. Fire, S. Xu, M. Montgomery, S. Kostas, S. Driver, C. Mello, Potent and specific genetic interference by double-stranded RNA in *Caenorhabditis elegans*, Nature, 391 (1998), pp. 806-811.

Optimization of the carbon and nitrogen sources for coenzyme Q10 production by Gluconobacter oxydans H621

Foozieh Moghadami

Department of Biology, Payame Noor University, Tehran, Iran

*Email: fouziehm@yahoo.com

Abstract

Coenzyme Q_{10} (CoQ_{10}) is used in some industries such as food, pharmaceutical and cosmetics due to its antioxidant properties. Its production has been considered through fermentation methods. In this study, the production of CoQ_{10} was investigated by *Gluconobacter oxydans* 621H in the presence of various carbon sources (glucose, sucrose, fructose, sorbitol, mannitol, glycerol, ethanol, molasses, whey and malt extract) and nitrogen sources (yeast extract, ammonium sulfate, peptone, casein, urea, corn steep liquid). The HPLC instrument was used to analysis of the CoQ_{10} production. The results of this study showed that the strain of 621H produced the highest amount of CoQ_{10} in the presence of sorbitol and yeast extract as the carbon and nitrogen sources (2 and 2.3 mg/L respectively). When two sources of nitrogen were used in combination, CoQ_{10} production increased so that in the presence of yeast extract and ammonium sulfate, CoQ_{10} production reached 3.4 mg/L. According to the results of this study, it can be concluded that sorbitol and yeast extract-ammonium sulfate were the most effective carbon and nitrogen sources for CoQ_{10} production by *Gluconobacter oxydans* H621, respectively.

Keywords: Coenzyme Q_{10}, *Gluconobacter*, HPLC, Carbon, Nitrogen

1. Introduction

Coenzyme Q_{10}, which is chemically called 2, 3-dimethoxy 5-methyl-6-multiprenyl 1, 4-benzoquinone, contains 10 isoprene units in the isoprenoid chain. The molecule was discovered in 1957 by two research groups at the same time and was named Coenzyme Q_{10} and ubiquinone [1]. The production of coenzyme Q_{10} is currently mainly performed by three methods of chemical synthesis, semi-chemical synthesis (extraction from plants and structural modification) and microbial fermentation process. This molecule has a certain structural complexity and its biosynthesis pathway is complex [2]. The cost of chemical and semi-chemical synthesis is high and optical isomers are produced. Therefore, the microbial fermentation process is more important . It is revealed that bacteria can also be good sources of coenzyme Q_{10} [3]. Many studies have been performed on a wide range of coenzyme Q_{10}-producing bacteria for further production, some of which have been promising for industrial production [4]. Coenzyme Q_{10}has been shown to play a key role in the cell. The main function of coenzyme Q_{10} is to transfer electrons through the respiration chain and ultimately cause energy production [5]. Due to the high affinity of this molecule, it absorbs additional electrons of harmful oxygen molecules (ROS) and thus shows its antioxidant effect on oxygen free radicals. It also prevents the oxidation of lipids, proteins and DNA [6].

It is indicated that CoQ_{10} is the part of the *Gluconobacter* respiratory chain [7]. *Gluconobacter* is a gram-negetive bacterium belonging to the family *Acetobacteraceae* has been shown to be well adapted for industrial uses [8]. The main industrial important applications of *Gluconobacter* are the production of vitamin C, dihydroxyacetone, 6-amino-L-sorbose, shikimate and 3-dehydroshikimate. These products are the results of incomplete oxidation performing by this genus [9].

In this study, the production of coenzyme $Q_{10}$was investigated by *Gluconobacter oxydans* 621H in the presence of various carbon sources.

2. Material and Methods

2.1 Microorganisms and Media

The microorganism used in this study, *Gluconobacter oxydans* H621 was purchased from Persian Type Culture Collection. This strain was maintained on the GYC medium (glucose 50 g/L, yeast extract 10 g/L, $CaCO_3$ 30 g/L, Agar 25 g/L) for 2-3 months, in a frozen state at -70° C as stock. The seed culture contained 20 g/L glucose, 3 g/L yeast extract and 3 g/L peptone. The production culture containing 70 g/L glucose, 20 g/L yeast extract, 1.5 g/L NH_4SO_4, 1.5 g/L KH_2PO_4 and 0.5 g/L $MgSO_4$. All experiments were performed in 250-mL flasks containing 100 mL of the medium with pH 6.5, agitation speed of 180 rpm and incubation temperature of 30 °C. Extraction of coenzyme Q_{10} and measurement of dry cell weight was performed after 40 h of incubation.

2.2 Optimization of carbon and nitrogen sources

The various carbon and nitrogen sources used in this study for coenzyme Q_{10} production. The carbon sources included glucose, sucrose, fructose, sorbitol, mannitol, glycerol, ethanol, molasses, whey and malt extract. After finding the best carbon source, the effect of different concentrations of sorbitol (70-120 g/L) were investigated on increasing DCW and coenzyme Q_{10} production. The nitrogen sources also included yeast extract, ammonium sulfate, peptone, casein, urea, corn steep liquid. The effect of combined nitrogen sources was investigated on increasing cell biomass and coenzyme Q_{10} production. In all experiments, the concentration of nitrogen source was considered 20 g/L.

2.3 Extraction and measurement of CoQ_{10}

The cells in 1 mL of *Gluconobacter oxydans H621* cultures were harvested at 9000 × g for 15 min. The pellets were washed with 1 mL of distilled water and suspended in 0.5 mL of the Cell Lytic B (Sigma- Aldrich). After 30 min incubation at 30 °C and shaking well, 1 mL of hexane: 2-propanol (5:3) was added to the solution and mixed well. The upper phase was transferred into the new tube and after adding 0.5 mL of hexane and mixing vigorously, the upper phase was re-transferred into the tube. After evaporation, 0.5 mL of ethanol was added to

the dried residue. Analysis of CoQ_{10} was performed by high-performance liquid chromatography (Agilent 1120, USA) with a Thermo scientist C18 column (250 mm× 4.5 mm× 5 µm) coupled to a UV detector with ethanol: methanol (70:30) as the mobile phase at a flow rate of 1 mL/min. CoQ_{10} was detected at 275 nm.

2.4 Measurement of dry cell Weight

For the Dry Cell Weight (DCW) determination, 1 mL of the cultures was centrifuged at 9000×g for 15 min, washed twice and dried at 60 °C overnight to reach a constant weight.

3. Results and Discussions

3.1 Production of coenzyme Q_{10} by H621 strain

The Coenzyme Q_{10} was analyzed by HPLC at a wavelength of 275 nm. Figure 1 shows the chromatogram of the HPLC analysis of coenzyme Q_{10} standard purchased from Sigma-Aldrich. As can be seen in the figure 1, the standard coenzyme Q_{10} peak is plotted at an retention time of 5.8 minutes.

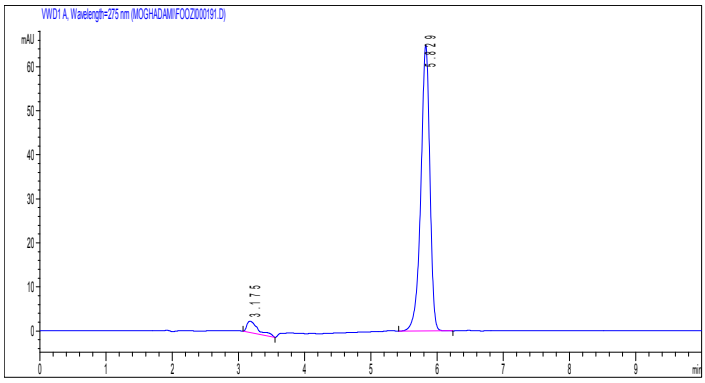

Fig. 1. The chromatogram of the HPLC analysis of CoQ_{10} standard. The peak in the retention time of 5.8 represents CoQ_{10}. Coenzyme Q_{10} standard was purchased from Sigma-Aldrich CAS number: 303-98-0 (≥98%-HPLC).

3.2 The effect of carbon sources on CoQ_{10} production

The effect of carbon sources was evaluated on DCW and CoQ_{10} production. The results showed that sorbitol was the desirable carbon source for cell growth and CoQ_{10} production by the H621 strain. Mannitol and glycerol were the second and third desirable carbon sources for cell growth, respectively while the specific CoQ_{10} content in the presence of glycerol was higher than that of mannitol (Table 1). The effect of different sorbitol

concentrations on DCW and CoQ_{10} production is shown in Table 2. Among the various carbon sources, sorbitol was the most effective for DCW and CoQ_{10} production. The specific contents of CoQ_{10} produced by the H621 strain in the presence of sugar alcohols were higher than those of other sugars. Ha et al. reported a constant enhancement of specific content of CoQ_{10} in *Agrobacterium tumfaciens*, independent of specific carbon source [10]. Nevertheless, in this study, in addition to the DCW and CoQ_{10} level, specific content also varied in the presence of different kinds of carbon sources. For example, the cell dry weight produced in the presence of sorbitol and mannitol was the same, while the production of coenzyme Q_{10} in the presence of sorbitol was almost twice that of mannitol, which made the specific production capacity constant. On the other hand, it was observed that the specific production capacity in the presence of sugars was more than sugar alcohols. This means that sugars are more involved in the production of coenzyme Q_{10} and sugar alcohols are more involved in the production of DCW.

Table 1. Effect of various carbon sources on DCW and CoQ_{10} production

Carbon Source (g/L)	DCW (g/L)	Co Q_{10} (mg/L)	□ SC Co Q_{10} (mg/gDCW)
Sorbitol	4.2 ± 0.04	1.8 ± 0.03	0.42
Mannitol	3.9± 0.04	1.3 ± 0.04	0.33
Glycerol	3.6 ± 0.04	1.1 ± 0.03	0.30
Ethanol	2.6 ± 0.02	0.40	0.15
Sucrose	4.1 ± 0.06	0.67± 0.02	0.16
Fructose	2.8 ± 0.05	0.65± 0.02	0.23
Glucose	2.0 ± 0.04	0.5 ± 0.03	0.25

□ Specific Content of CoQ_{10}

Table 2. Effect of different sorbitol concentrations on DCW and CoQ_{10} production

Sorbitol (g/L)	DCW (g/L)	CoQ_{10} (mg/L)	□ SC CoQ_{10} (mg/g DCW)
70	4.2 ± 0.04	1.8 ± 0.03	0.42
80	4.5 ± 0.14	2.1 ± 0.04	0.46
90	4.5 ± 0.23	2.3 ± 0.03	0.51
100	4.6 ± 0.02	2.2 ± 0.12	0.47
110	4.7 ± 0.12	2.1± 0.02	0.44
120	4.6 ± 0.04	2.2 ± 0.03	0.47

3.3 The effect of nitrogen sources on CoQ_{10} production

The effect of nitrogen sources including yeast extract, peptone, ammonium sulfate, corn steep liquid (CSL), casein and urea was also studied on DCW and CoQ_{10}. Among the different nitrogen sources, yeast extract singularly displayed the highest effect on cell growth and CoQ_{10}. In the next step, yeast extract was used along with other nitrogen sources such as peptone, CSL, ammonium sulfate and casein. Results showed that the highest DCW and CoQ_{10} were achieved in the medium containing yeast extract and ammonium sulfate together (Table 2).

Table 3. Effect of various nitrogen sources singly and in combination, on DCW and CoQ_{10} production

Nitrogen Source (g/L)	DCW (g/L)	CoQ_{10} (mg/L)	□ SC of CoQ_{10} (mg/g DCW)
Yeast extract	4.5 ± 0.09	2.7 ± 0.08	0.60
Peptone	4.2 ± 0.06	2.5 ± 0.05	0.59
Corn steep liquid	3.9 ± 0.03	2.4 ± 0.06	0.61
Ammonium sulfate	3.7 ± 0.12	0.3 ± 0.19	0.08
Casein	3.2 ± 0.19	0.5 ± 0.09	0.15
Urea	2.9 ± 0.01	0.2 ± 0.12	0.06
Yeast extract + peptone	4.5 ± 0.05	3.1± 0.11	0.68
Yeast extract + CSL	4.6 ± 0.07	3.0 ± 0.13	0.65
Yeast extract + ammonium sulfate	4.5 ± 0.06	3.4 ± 0.06	0.75

□ Specific Content of CoQ_{10}

The results of this study also showed that the H621 strain in the presence of yeast extract as the nitrogen source produced the highest amount of CoQ_{10}. When two sources of nitrogen were used in combination, CoQ_{10} production increased. In the presence of yeast extract and ammonium sulfate, CoQ_{10} production reached 3.4 mg/L. According to the results of this study, the combination use of two sources of nitrogen can increase the amount of CoQ_{10} in the H621 strain. So far, many studies have been conducted on the effect of different sources on the growth and production of different products in acetic acid bacteria [11-13]. It has been found that 90% of the glucose absorbed for energy production by *G.oxydans* is oxidized by membrane-bound dehydrogenases and only 10% is used in metabolic cycles [14]. This could indicate the importance of membrane-bound dehydrogenases in this bacterium in energy production. On the other hand, the activity of dehydrogenases is directly related to the quinone pool or coenzyme Q_{10}. Therefore, it is not far from the mind that increasing the activity of these dehydrogenases can increase the production of coenzyme Q_{10}.

In the present study, we investigated *Gluconobacter oxydans* H621 for CoQ_{10} production in the presence of various carbon and nitrogen sources. The results of the present study indicate that the carbon and nitrogen sources played an important role in cell growth and production of coenzyme Q_{10}. According to the results of this study, it

can be concluded that sorbitol and yeast extract-ammonium sulfate were the most effective carbon and nitrogen sources for CoQ_{10} production by *Gluconobacter oxydans* H621, respectively.

References

[1] Choi JH, Ryu YW, Seo JH. Biotechnological production and applications of coenzyme Q_{10}. Appl Microbiol Biotechnol. 2005. 68:9-15. Doi: 10.1007/s00253-005-1946-x

[2] Ndikubwimana JD, Lee BH. Enhanced Production Techniques, Properties and Uses of Coenzyme Q10. *Biotechnol Let*. 2014; Vol. 36: pp. 1917-1926. DOI: 10.1007/s10529-014-1587-1

[3] Cluis CP, Pinel D, Martin VJJ. The Production of Coenzyme Q_{10} in Microorganisms. Dordrecht: Springer. 2012. Reprogramming microbial metabolic pathways, Wang X, Chen J, Quinn P. 2012. pp. 303-326.

[4] Jeya M, Moon HJ, Lee JL, Kim IW, Lee JK. Current State of Coenzyme Q_{10} Production and its Application. *Appl Microbiol Biotechnol*. 2010; Vol. 85: pp. 1653-1663. Doi: 10.1007/s00253-009-2380-2.

[5] Turunen M, Olsson J, Dallner G. Metabolism and Function of Coenzyme Q10. *Biochem Bioph Acta*. 2004; Vol. 1660: pp. 171-199.

[6] Bentinger M, Tekle M, Dallner G. Coenzyme Q10 Biosynthesis and Functions. *Biochem Bioph Research Com.* 2010*;* Vol. 396: pp. 74-79.

[7] Bringer S, Bott M. Central Carbon Metabolism and Respiration in *Gluconobacter oxydans*. Tokyo: Springer. 2016. Acetic Acid Bacteria: Ecology & Physiology, Matsushita K, Toyama H, Tonouchi N, Okamoto-Kainuma A. pp. 235-249.

[8] Gupta A, Singh VK, Qazi GN, Kumar A. *Gluconobacter oxydans*: Its Biotechnological Applications. *J Molecul Microbiol* Biotechnol. 2001; Vol. 3: pp. 445-456.

[9] Deppenmier U, and Ehrenreich A. 2002. Physiology of acetic acid bacteria in light of the genome sequence of *Gluconobacter oxydans*. J Mol Microbiol Biotechnol 16:69–80. Doi: 10.1159/000142895

[10] Ha SJ, Kim SY, Seo JH, Moon DK, Lee JK. Optimization of Culture Conditions and Scale-up to Pilot and Plant Scales for Coenzyme Q10 Production by *Agrobacterium tumefaciens*. *Appl Microbiol Biotechnol.* 2007; Vol. 74: pp. 974-980. https://doi.org/10.1007/s00253-007-0995-8.

[11] Poyrazoglu Copan E, Biyik H (2011) Effect of various carbon and nitrogen sources on cellulose synthesis by *Acetobacter lovaniensis* HBB5. Afric J Biotechnol 10(27): 5346-5354

[12] Santos S, Carbajo JM, Villar JC (2013) The Effect of Carbon and Nitrogen Sources on Bacterial Cellulose Production and Properties from *Gluconacetobacter sucrofermentans* CECT 7291 Focused on its use in Degraded Paper Restoration. Bioresources 8(3): 3630-3645

[13] Lee SA, Choi Y, Jung, Kim S (2002) Effect of initial carbon sources on the electrochemical detection of glucose by *Gluconobacter oxydans*. Bioelectrochemistry 57: 173– 178

[14] Adachi O, Yakushi T. Membrane-bound Dehydrogenases of Acetic Acid Bacteria. Tokyo: Springer. 2016. Acetic Acid Bacteria: Ecology & Physiology, Matsushita K, Toyama H, Tonouchi N, Okamoto-Kainuma A. pp. 273-294

Fungal decolorization of Disperse Acid yellow 121 dye

Samira Eshghi[1] , Fereshteh Jookar Kashi[2*]

1, 2 Department of Cell and Molecular Biology, Faculty of Chemistry, University of Kashan, Kashan, Islamic Republic of Iran

Email address: samiraeshghi@yahoo.com, Telephone number: 00989130928875

Corresponding author: jookar@kashanu.ac.ir

Abstract

The textile industry discharges large volumes of wastewater intense in various types of pollutants. The textile industrial wastewaters contain multiple pollutants. So, among various industries, the textile dyeing industries produce a large volume of wastewater.

Some pigments, in particular, anthraquinone and azo groups, have toxicity for animals and humans as well as co-carcinogenic, carcinogenic, and mutagenic activities.

This study aimed to isolate and identify Disperse Acid yellow 121 degrading fungi, which appeared as a mould on persimmon fruit. This fungal strain showed a great ability to decolorize at pH 7 and 30°C after 10 days. The results of UV–Vis analyses indicated that decolorization was due to biodegradation.

Keywords: Microorganism, Disperse Acid yellow 121, Decolorization, Textile industry

1. Introduction

Various microorganisms, including fungi, aerobic bacteria, facultative anaerobic, and some yeasts, can decolorize various azo dyes. Organic synthetic dyes (such as azo dyes) are used in various industries, including the food industry, the textile industry, the printing industry, and the pharmaceutical industry [1]. Some azo dyes or their decomposition compounds are toxic, carcinogenic, and mutagenic [2]. However, microbial decontamination is also valuable in helping the health of the environment [3]. Dye-decolorizing microorganisms include bacteria, fungi and yeasts [1]. Microbial decolorization has been studied in the textile industry as an effective and powerful way to remove dyes. The type of dyes and decomposing factors determine the efficiency of the process. Biological agents such as fungi, yeasts and bacteria are among the most cost-effective and environmentally friendly decomposers used for decolorization. Biodegradation of dyes is a method environmentally friendly, low-cost and safe [4,5]. This study investigates the decolorization ability of one fungal strain isolated from persimmon mould for Disperse Acid yellow 121dye.

2. Material and Methods

The fruits were sliced into small segments (3 mm in diameter) by a sterilized blade. Then surface-sterilized in 1% hypochlorite for 2 min. Afterward, the samples were cultured on Sabouraud dextrose agar (SDA) aseptically and then incubated at 28°C for 5 days. A pure culture was taken by sub-culturing each of the different colonies that grow on the SDA plates and incubating at 28°C for 5 days. A pure culture was taken by sub-culturing each of the different colonies that grow on the SDA plates and incubating at 28°C for 5 days. First, 10 g/l glucose and 50 mg/ml of Acid Violet 7 were added to a tube containing SD broth, then the mould was inoculated into the tube and incubated at 30 ^{0}C. After 10 days, Acid Violet 7 dye was decomposed by a fungal strain isolated from persimmon mould. The dye analysis was investigated using UV-Vis spectroscopy. Then, to identify the fungal strain, the isolate was stained, and the sample was observed under a microscope.

3. Results and Discussions

This study was conducted to determine the ability of fungi to decolorization of dyes. A fungal strain with a high ability to decolorize Disperse Acid yellow 121 dye was separated from persimmon fruit. The decolorization analysis was determined after 10 days of incubation. The dye analysis was investigated by UV-Vis spectroscopy. Fungi staining was done, and its morphology was observed under a microscope. Fungi are identified by their colony shape, division, and morphology. Fig .1 exhibited the UV–Vis spectrum of Disperse Acid yellow 121 dye decomposition by fungal strain. The λmax of Disperse Acid yellow 121 was 553 nm. However, clear disappearance of peaks at 553nm for treated samples suggested biodegradation of the dye. The fungal strain decolorized Acid Violet 7 (92%) at 10 days (Fig.2).

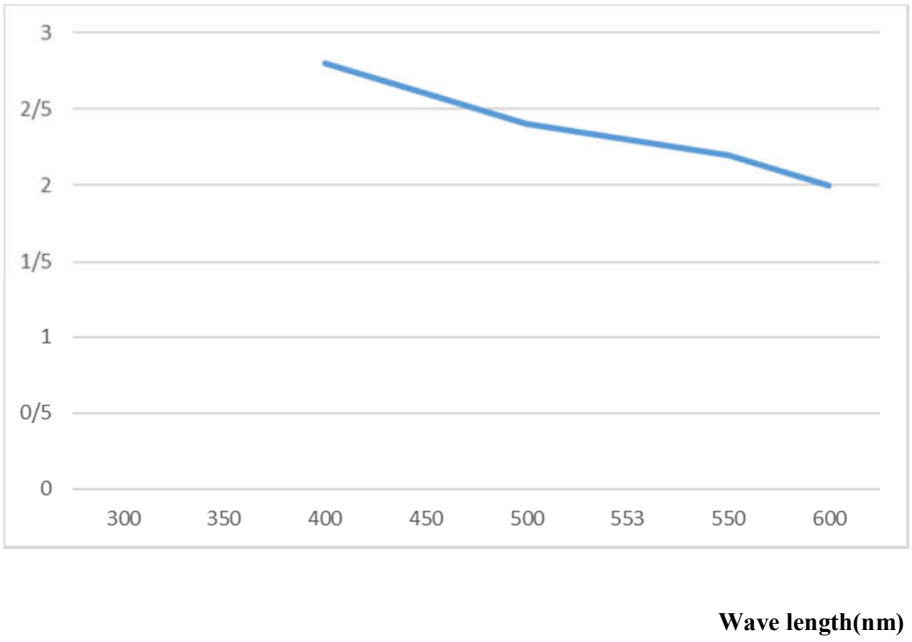

Fig.1. UV–Vis spectral analysis of Disperse Acid yellow 121 after biodecolorization by fungal strain after 10 days

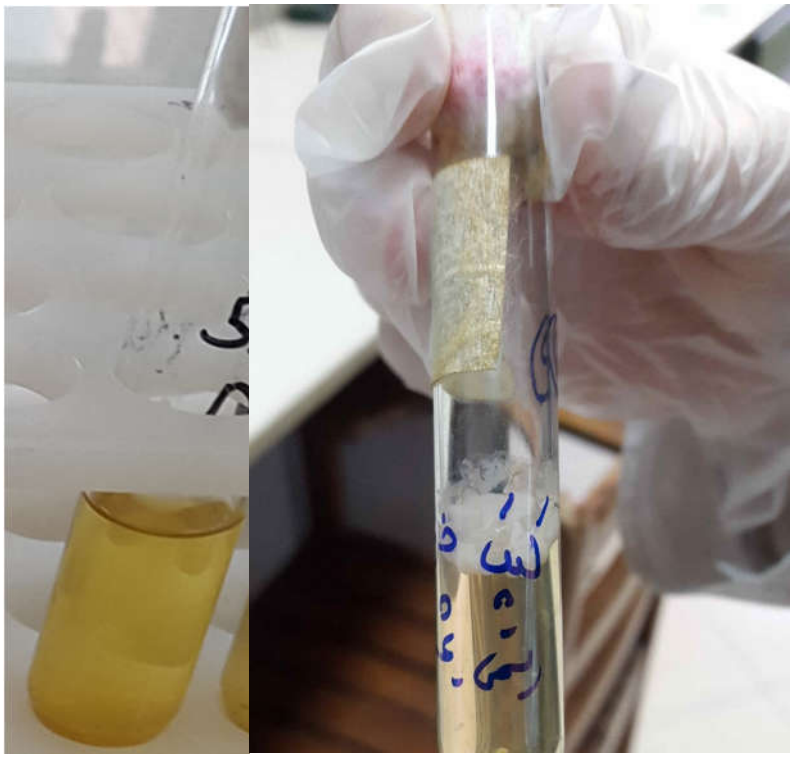

Fig.2. Decolorization of Disperse Acid yellow 121 dye by a fungal strain. Control culture (right) and the fungal decolorization (left) after 10 days.

References

[1] Ramalho, P. A., H. Scholze, M. H. Cardoso, M. T. Ramalho, and A.M. Oliveira- Campos. 2002. Improved conditions for the aerobic reductive decolorisation of azo dyes by Candida zeylanoides. Enzyme Microb. Technol. 31 : 848-854

[2] Chung KT , Cerniglia CE, 1992, Mutagenicity of azo dyes: structure activity relationships. MutatRes, 277(3), 201-20.

[3] Moosvi,S. Keharia,H . Madamwar, D. 2005 Decolourization of Textile dye reactive violet 5 by a newly isolated bacterial consortium RVM 11.1. World Journal of Microbiology and Biotechnology 21,667- 672.

[4] Mondal P, Baksi S, Bose D (2017) Study of environmental issues in textile industries and recent wastewater reatment technology. World Sci News 61(2):98–109.

[5] Ghaly A, Ananthashankar R, Alhattab M, Ramakrishnan V (2014) Production, characterization and treatment of textile effluents: a critical review. J Chem Eng Process Technol 5(1):1.

Comparison of Zeolite and Activated carbon as the bacterial media in biodecolorization of Azo dye

M. Shayestehvar[1,2], D. Poorasadollah[1,2], F.Sabbaghiyan[1,2], T. Bagheri Lotfabad [2,*], A. Heydarinasab [1], S. Yaghmaei[3]

[1] Department of Chemical Engineering, Science and Research branch, Islamic Azad University, Tehran, Iran.

[2] Department of Industrial and Environmental Biotechnology, National Institute of Genetic Engineering and Biotechnology (NIGEB), Tehran, Iran.

[3] Department of Chemical and Petroleum Engineering, Sharif University of Technology, Tehran, Iran.

[*] bagheril@nigeb.ac.ir

Abstract

Azo dyes as the widely used synthetic dyes found in many industrial wastewaters. Due to environmental concerns, they should be omitted from wastewaters before discharge into receiving waters. Among the different methods suggested for degradation of azo dyes, biological processes have received great attention to remove these contaminants because they are eco-friendly, cost-effective and highly efficient. This study aimed to compare two carriers, Extruded Activated Carbon (EAC) and Zeolite for bacterial cell growth to use in decolorization of carmoisine containing medium. Surface physicochemistry was measured for both EAC and Zeolite through the surface area and pore size analyses as well as the Fourier transform infrared spectroscopy (FTIR). Scanning electron microscopy (SEM) images illustrated the possibility of bacterial cell growth on the carriers. The decolorization process was performed in synthetic wastewater included azo dye carmoisine at a concentration of 50 ppm. Spectrophotometric analyses indicated that the cells immobilized on EAC and zeolite carriers could remove 96.4 ± 2.7 and 90.75 ± 3.35 of initial dye, respectively during the 9 h-process. Moreover, dye removal was confirmed by thin layer chromatography (TLC).

Keywords: Zeolite; Extruded Activated Carbon; Biodecolorization; Carmoisine; Azo dye

1. Introduction

The wastewater of textile industry contains various types of dyes, detergents, insecticides, pesticides, grease and oils, sulfide compounds, solvents, heavy metals, inorganic salts, and fibers, relying on the process [1]. Decolorization has been becoming one of the major concern considering aesthetic and environment [2]. Applying physicochemical, advanced oxidation, biological processes, and a combination of processes to treat wastewaters usually are used to meet regulatory discharge limits [3]. Anaerobic digestion of textile wastewater is a thriving procedure because not only does it reduce the costs but is more environmentally friendly. In reason of severing the Azo bonds are decomposed under anaerobic condition and consequently the color of wastewater is eliminated. The reduced products (aromatic amines) should then be further treated using aerobic biological treatment methods [4-8]. Azo-reductase activity leads to color removal under anaerobic conditions [9,10]. Nowadays, immobilization of microbial cells has grabbed lots of attention in field of wastewater treatment. In fact, it can be seen that

immobilized microbial systems has enormously developed bioreactor efficiency. Take increasing process stability and tolerance to shock loadings as example which allow higher treatment capacity per unit biomass and generating relatively less biological sludge. Furthermore, as high densities of specialized microorganisms are used in immobilized cell systems, they enjoy the potential to degrade toxic chemicals faster than conventional wastewater treatment systems [11-14]. The zeolites are porous materials with cavities of different pore sizes in their structure [15]. Activated carbon is used in wastewater treatment and drinking water purification [16]. The high applicability of activated carbon is related to its high porosity, rapid absorption, and thermal stability [17]. In this study, the Zeolite was compared with the activated carbon to use as the media for bacteria in order to employ in the biological removal of azo dye carmoisine.

2. Materials and methods

2.1. Materials

All the chemicals used in this research were purchased from the German company Merck. Activated carbon (Extruded, Jacoba, XH 4 mm, China) was purchased. Zeolite was prepared from local mines (30 kilometer of south east of Semnan) and donated by Afrazand company. Carmoisine dye was gifted by Vista Zar Co. (http://www.vistazar.com/).

2.2. Microorganisms and culture conditions

The microorganism used was an indigenous strain characterized as genus *Klebsiella*, which was previously isolated in Amalshi's research [18]. Culture medium was YTS included Yeast extract (10 g/L), Tryptone (20 g/L) and Sucrose (20 g/L). The decolorization process was performed in a liquid culture medium of Yeast extract and Sucrose containing dye at a concentration of 50 ppm. To prepare the pre-culture, a single colony of the desired microorganism was cultivated in liquid medium of YTS and incubated for 21 hours at 30 ° C and 180 rpm [19,20].

2.3. Physical surface properties

The surface area and pore size analyses were performed for zeolite and activated carbon using nitrogen gas adsorption analysis at 77 K. The sample was degassed with nitrogen gas at 300ºC for 3 h until its weight became stable before measurements were started. The analysis was conducted using Belsorp mini zII. Surface area was determined by BET (Brunauer, Emmett, Teller) analysis. Pore sizes were determined by BJH (Barrett-Joyner-Halenda) analysis.

2.4. Fourier Transform Infrared Spectroscopy (FTIR)

FTIR spectra were recorded on Thermo-Nicolate-Nexus-870FTIR between 4500-400 cm^{-1} for Zeolite and Extruded activated carbon. Samples were prepared according to the potassium bromide technique with the proportion of 1:3(w/w).

2.5. Immobilized cells and biodecolorization

In order to prepare the cell bed, 20 g of the Zeolite and Extruded Activated Carbon samples were individually transferred to 100 ml bottles, and 75 ml of the preculture in YTS was added. The bottles were statically incubated

at 30 ° C for 10 days. Carries were investigated using the scanning electron microscope (Seron AIS-2100, 5000x) to examine the growth of bacteria on the solid bed. Subsequently, the liquid phase was discarded and replaced with 75 ml of dye containing YS medium (carmoisine, 50 ppm) to study the decolorization process. The bottles were statically re-incubated at 30 ° C. The control experiments were performed without inoculation. Samples were taken at specified time intervals and examined for carmoisine concentrations via spectrophotometry method. Each sample was scanned by Beckman DU530 spectrophotometer in the range of 200 to 1000 nm and absorbance at maximum carmoisine wavelength (λ max = 515nm) was recorded.

The percentage of dye removal was calculated using the following equation.

$$\text{Dye removal (\%)} = \frac{A_0 - A_t}{A_0} \times 100$$

where, A_0 and A_t are the carmoisine absorbances at initial and specified time of incubation, respectively.

2.6. Thin layer chromatography (TLC)

Due to high accuracy and sensitivity of the TLC method, samples of 9h-decolorization process were evaluated by this technique and compared to initial point samples. To this end, the sample was examined by the method described by Kiayi et al. [19].

3. Results and discussion

3.1. Surface area and pore size analyses

The BET and BJH calculations through the nitrogen gas adsorption data estimated surface area for EAC and Zeolite (given in Table 1).

Carrier	Surface area (m^2/g)	Pore Radius (nm)
Extruded Activated Carbon	940.70	1.21
Zeolite	12.868	14.32

Table 1- BET test results

BET shows a much larger surface area for EAC (940.70 m^2/g) in comparison to zeolite (12.868 m^2/g) resulting in higher adsorption potency of EAC. However, BJH data indicated, pore radii of 1.21 nm and 14.32 nm for EAC and zeolite, respectively, which are not suitable to entrap the bacteria, due to this fact that bacteria have a minimum diameter of 0.5µm. Consequently, despite the higher porosity of EAC than zeolite, this does not lead to higher biomass entrapment by EAC to be more efficient in decolorization.

3.2. Fourier transform infrared spectroscopy (FT-IR)

FT-IR spectra of EAC and Zeolite is shown in Figure 1. Analyzing Zeolite FT-IR diagram (orange) illustrated that the bond associated with the symmetric and asymmetric stretching vibrations of the hydroxyl functional group is situated at 3461 cm^{-1}. Additionally, the bond located at 1639 cm^{-1} is due to the vibration of the bond O-H. The

generated stretching vibrations by Al-O bonds are described by the intensity located at 998cm^{-1}. The allotropic phase of SiO_2 is identified by the intensity observed in 796 cm^{-1}. It is important to mention that the intensities associated with the Si-O and O-Al bonds, which is typical of tectosilicates, are very strong. On the other hand, EAC FT-IR diagram (blue) showed the stretching vibration of O-H stood at 3400 cm^{-1}, and the symmetric and asymmetric bond of aliphatic CH3, CH2 and CH ranging from 2300 to 2400. Also, carbonyl group and aromatic cycles accounted for 1700 cm^{-1} and 1400-1560 cm^{-1} respectively. Whole analysis can be seen in table 2 and 3 attaching below.

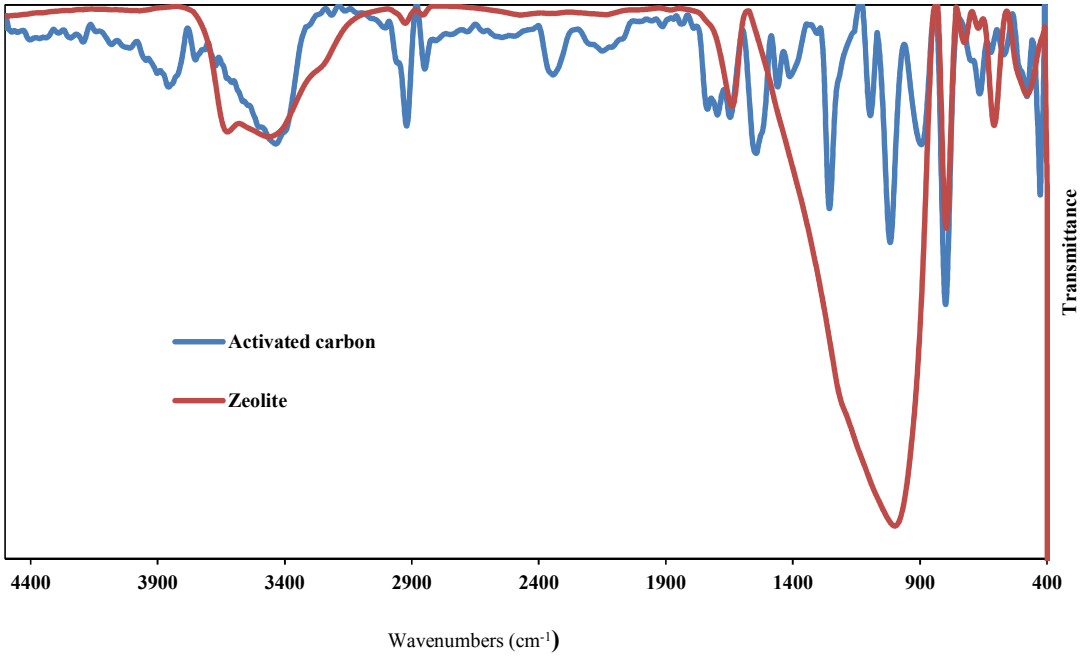

Figure1- Extruded Activated Carbon versus Zeolite FT-IR diagram

Chemical Bonds	Wavenumbers	
Stretching vibrations of **OH** group	3400	Extruded Activated Carbon
Stretching vibrations of aliphatic **CH** group	2800 - 2900	
Symmetric and asymmetric $\mathbf{CH_3}$bond of aliphatic and $\mathbf{CH_2}$،**CH**	2300 - 2400	
Carbonyl group **C=O**	1700	
Bending vibrations of water **OH** group	1636	
Stretching vibrations of aromatic cycles **C=C** or **C-C**	1400 - 1560	
Stretching vibrations **CH**	887.71 - 1049	

Table 2 - Analysis of activated Carbon carrier FT-IR results

Chemical Bonds	Wavenumbers (cm^{-1})	
Stretching vibration of absorbed water **OH** group	3461	Zeolite
Binding vibration of absorbed water **OH** group	1639	
Stretching vibration of **Si-O-Si** or **Al-O-Al** in quadrilateral structure	998	
Binding vibration of **Si-O-Si** or **Al-O-Al**	478-796	
Stretching vibration of absorbed water **OH** group	3461	
Stretching vibration of absorbed water **OH** group	1639	

Table 3 - Analysis of Zeolite carrier FT-IR results

FTIR studies show that the surface of zeolite contains Si-O-Si compounds that cause surface hydrophobicity of this adsorbent [21]. Also, activated carbon possesses a good surface hydrophobicity due to the presence of aromatic compounds on its surface, which is shown in FTIR [22]. On the other hand, gram-negative bacteria have high hydrophobicity due to the presence of lipopolysaccharide on the membrane surface [23]. Hence, the bacteria settle on the surface of zeolite and activated carbon as a result of hydrophobic interaction. Therefore, despite the higher porosity on EAC compared to zeolite, similar bacterial density are formed on EAC and Zeolite resulting in similar removal efficiency in biodecolorization experiments.

3.3. Investigation of bacteria grown on substrates

Observations showed that after 10 days of incubation (Figures 2 and 3), the mediums on EAC and Zeolite became clear. This revealed the hydrophobic attachment of bacteria to EAC and Zeolite particles.

Figure 2. The EAC particles (a) immediately after inoculation and (b) after 10 days of incubation at 30 ° C.

Figure 3. The Zeolite particles (a) immediately after inoculation and (b) after 10 days of incubation at 30 ° C.

SEM analysis was used to study the growth of bacteria on EAC and Zeolite particles. The SEM Images for EAC and Zeolite with 23.0 kV × 4.0 K magnification are shown in Figure 4. SEM images show a porous and heterogeneous surface illustrating many exchange sites on the adsorbent surface which are able to create a large contact surface for dye removal [24-25]. The images in Figure 4 also show that the bacteria grew on solid substrates of Zeolite and EAC after 10 days. Ramos et al., and Sich and Van Reijen had previously succeeded in

forming a biofilm on a solid substrate in their research, which had been demonstrated using SEM analysis [26-27]. Increasing substrate surface area and its porosity lead to better bacterial contact with the substrate [28-30]. Bacterial growth occurs better and more in the porous substrate and therefore denitrification in porous media is better than in non-porous ones [29].

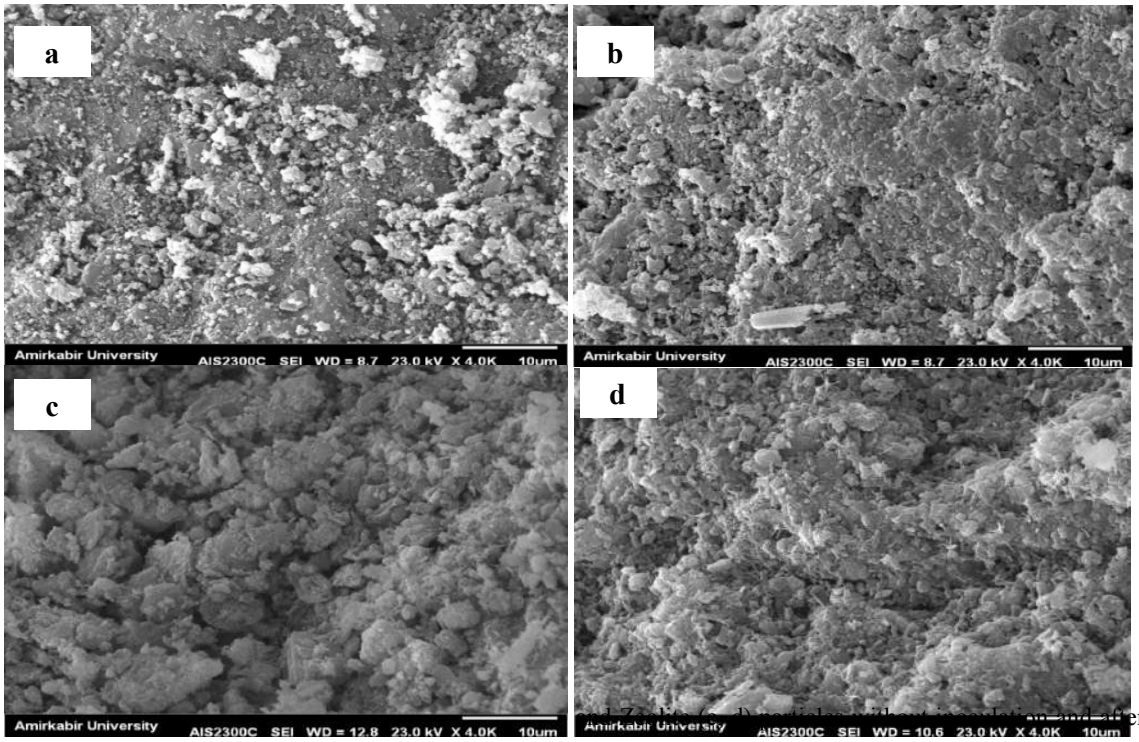

and Zeolite (c and d) particles without inoculation and after inoculation and 10 days of incubation at 30 °C, respectively from left to right. Images at 23.0 kV × 4.0 K.

3.4. The process of dye removal by microorganisms grown on a solid bed

As shown in Figures 5 and 6, the use of adsorbent without the presence of bacteria in the control samples did not play an effective role in removing the dye. Dye removal efficiency percentages while using immobilized cell on EAC carrier accounted for 81.1 ± 3.5 after 3 hours, 90.1 ± 7.1 after 6 hours and 96.4 ± 2.7 after 9 hours. Also, dye removal efficiency percentages while using immobilized cell on Zeolite carrier accounted for 32.7 ± 0.9 after 3 hours, 85.4 ± 5.1 after 6 hours and 90.75 ± 3.35 percentages after 9 hours. As can be seen in the graphs, with increasing the contact time, the percentage of dye removal for all samples containing cells immobilized on the adsorbent increased, which is consistent with the results of studies by Sohrabi et al. Rasulifard et al. By examining the dye removal from aqueous solution, they found that with increasing contact time, the collision of dye molecules with the adsorbent surface increased and as a result, the amount of dye removal also increased [31, 32]. In another study using *Pseudomonas luteola* stabilized on activated carbon adsorbent, the ability to remove reactive Azo red dye was 22.89% [33], and in [34] the results were 37-93% removal of reactive azo dye after 48 hours.

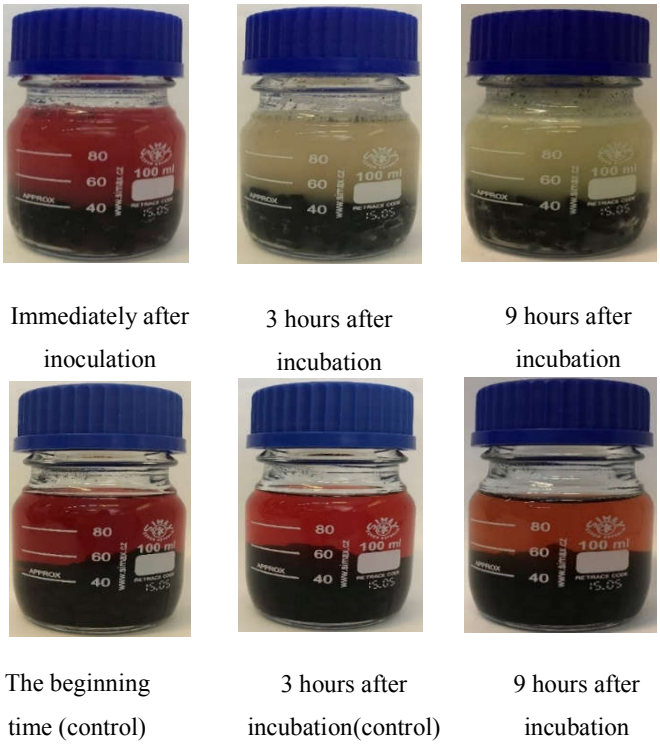

Figure 5 . Decolorizing by stabilized cells on the extruded activated Carbon carrier at different times

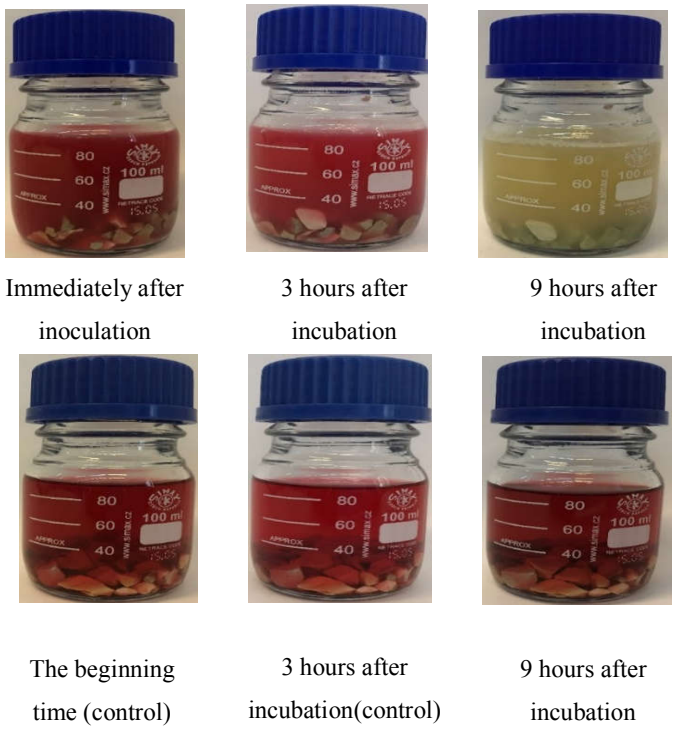

Figure 6 . Decolorizing by stabilized cells on the Zeolite carrier at different time

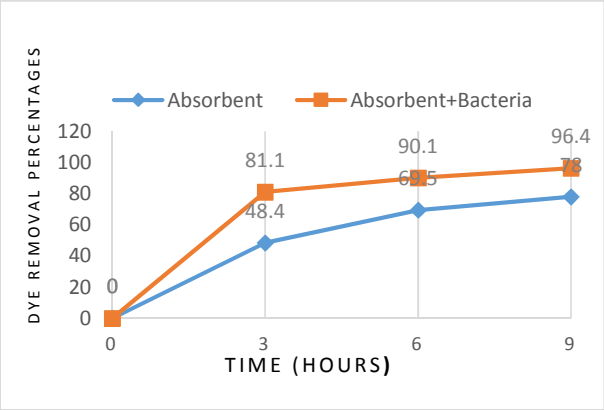

Figure 7 - Dye removal efficiency in YS medium containing 50 ppm carmoisine dye by cells on EAC compared to control sample

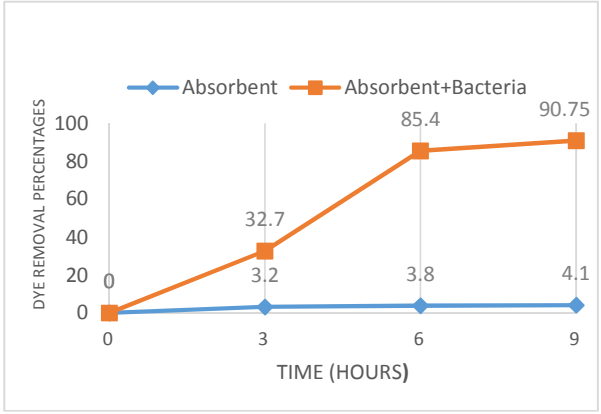

Figure 8 - Dye removal efficienvy in YS medium containing 50 ppm carmoisine dye by cells on Zeolite compared to control sample

3.5. Thin layer chromatography (TLC)

Thin-layer chromatography (TLC) was used to investigate the dye removal by bacteria immobilized on EAC and Zeolite. Figure 9 illustrates that the dye spot was completely disappeared for both samples prepared at the end of decolorization processes with cell attached-EAC and Zeolite (shown as ED point in Figure 9) during 9 h incubation. Whereas, TLC showed that carmoisine spot appeared for samples of 9h-incubation in control experiments (shown as EC point in Figure 9). Moreover, the lighter spot at point of EC on TLC sheets (Figure 9) for EAC in comparison to Zeolite may be assigned to higher porosity of EAC in comparison to Zeolite.

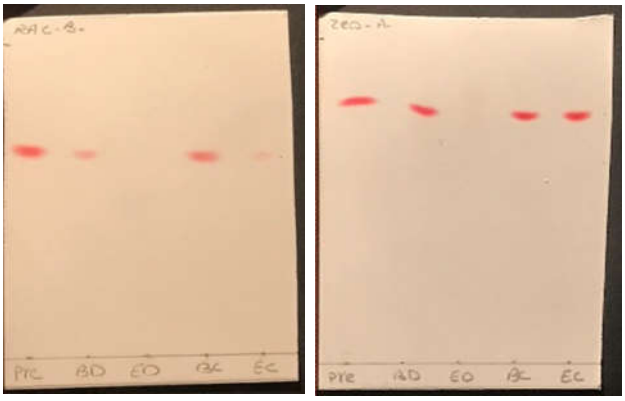

Figure 9. TLC of samples from decolorization process by EAC and Zeolite, respectively from left to right. Where, (Pre) is dye containing (50 ppm) YS medium, (BD) shows the beginning of decolorization process, (ED) shows the end of decolorization process, (BC) and (EC) are for beginning of and end of control experiments.

4. Conclusion

This study shows that despite the higher porosity of EAC than zeolite, they caused to similar removal efficiency when used as media for bacterial cells used in biodecolorization. This may probably attributed to surface chemistry of EAC and Zeolite rendering a similar situation for bacterial biomass. Therefore, considering the much lower price of Zeolite in comparison to EAC, zeolite may replace for activated carbon in biological removal of azo dyes.

5. References

[1] Lopez A, Ricco G, Cinnarella R, Di Pinto A C, Passino R, 1999. Textile wastewater reuse: ozonation of membrane concentrated secondary effluent. Water Sci Technol, 40(4-5): 99–105.

[2] Grau P, 1991. Textile industry wastewater treatment. Water Sci Technol, 24(1): 97–103.

[3] Banat I M, Nigam P, Marchant R, Singh D I, 1996. Microbial decolorization of textile-dye containing effluents: a review. Bioresource Technol, 58: 217–227.

[4] Chung K, Fulk B B E, Egan M, 1978. Reduction of azo dyes by intestinal anaerobes. Appl Environ Microbiol, 35: 558–562.

[5] Ong S A, Toorisaka E, Hirata M, Hano T, 2005. Decolorization of azo dye (Orange II) in a sequential UASB-SBR system. Sep Pur Technol,42(3): 297–302.

[6] LuangdilokW, Panswad T, 2000. Effect of chemical structures of reactive dyes on color removal by an anaerobic-aerobic process. Water Sci Technol, 42(3-4): 377–382.

[7] Bromley-Challenor K C A, Knapp J S, Zhang Z, Gray N C C, Hetheridge M J , Evans M R, 2000. Decolorization of an azo dye by unacclimated activated sludge under anaerobic conditions. Watert Res, 34(18): 4410–4418.

[8] Kudlich M, Bishop P L, Knackmuss H J, Stolz A, 1996. Simultaneous anaerobic and aerobic degradation of the sulfonated azo dye mordant yellow 3 by immobilized cells from a naphatlene sulfonate-degrading mixed culture. Appl Microbiol Biotechnol, 46: 597–603.

[9] Idaka E, Horitsu H, Ogawa T, 1987. Some properties of azoreductase produced by Pseudomonas cepacia. Bull Environ Contam Toxicol, 39: 982–989.

[10] Dubin P, Wrigth K L, 1975. Reduction of azo food dyes in cultures of Proteus vulgaris. Xenobiotica, 5: 563–571.

[11] Yang P Y, Nitisoravut S, Wu J Y S, 1995. Nitrate removal using a mixedculture entrapped microbial cell immobilization process under high salt conditions. Water Res, 29(6): 1525–1532.

[12] Zhou G M, Herbert H P F, 1997. Anoxic treatment of low-strength wastewater by immobilized sludge. Water Sci Technol, 36(12): 135–141.

[13] Christopher J, Owen P W, Ajay S, 2002. Biodegradation of dimethylphthalate with high removal rates in a packed-bed reactor. World J Microbiol Biotechnol, 18: 7–10.

[14] Ong S A, Toorisaka E, Hirata M, Hano T, 2007. Granular activated carbon-biofilm configured sequencing batch reactor treatment of C.I. Acid Orange 7. Dyes and Pigments, 76 (1): 142–146.

[15] M. Maretto, F. Blanchi, R. Vignola et al., "Microporous and mesoporousmaterials for the treatment ofwastewater produced by petrochemical activities," Journal of Cleaner Production, vol. 77, pp. 22‑34, 2014.

[16] Heijman, S. G. J., and Hopman, R. (1999). "Activated carbon filtration in drinking water production: Model prediction and new concepts" Colloids and Surfaces A: Physicochemical and Engineering Aspects 151, 303-310.

[17] Hosinzadeh Hesas, R., Wan Daud, W.M.A., Sahu, J.N., and Arami-Niya, A. (2013). "The effects of a microwave heating method on the production of activated carbon from agricultural waste: A review," Journal of Analytical and Applied Pyrolysis 100, 1-11.

[18]Amlashi,S.S., Lotfabad, T.B., Heidarinasab, A., Yaghmaei, S., 2019. Evaluation of the ability of native isolates to bio-removal of azo-methyl red dye from the dye medium. Sixth National Congress of Strategic Research in Chemistry and Chemical Engineering with Emphasis on Iranian Indigenous Technologies.

[19] Kiayi, Z., Lotfabad, T.B., Heidarinasab, A. and Shahcheraghi, F., 2019. Microbial degradation of azo dye carmoisine in aqueous medium using Saccharomyces cerevisiae ATCC 9763. Journal of hazardous materials, 373, pp.608-619.

[20] Vatandoostarani, S., Lotfabad, T.B., Heidarinasab, A. and Yaghmaei, S., 2017. Degradation of azo dye methyl red by Saccharomyces cerevisiae ATCC 9763. International Biodeterioration & Biodegradation, 125, pp.62-72.

[21] Tsutsumi.K., Kawai.T., Yanagihara.T., 1994. Adsorption characteristics of hydrophobic zeolites.

[22] Budarin.V.L., Clark. J.H., Mikhalovsky. S.V, Gorlova .A.A., Boldyreva. N.A.,.Yatsimirsky. V.K. 1999. The hydrophobisation of activated carbon surfaces by organic functional groups.

[23] Yuan. Y., Hays.M.P., Hardwidge.P.R., Kim. J., 2017. Surface characteristics influencing bacterial adhesion to polymeric substrates.

[24] Mousavi, A., Kashij, M., Shahbazi, P., 2016. Study of isotherms and effective factors on decolorization of methylene blue using activated carbon powder prepared from grape leaves., 4, pp.249-256.

[25] Sanadiv, O., Mirzaei, R., 2018. Removal of Direct Yellow 12 Dye from Aqueous Solutions using Hydrated Cement Powder., pp.33-48.

[26] Ramos, A.F., Gomez, M.A., Hontoria, E. and Gonzalez-Lopez, J., 2007. Biological nitrogen and phenol removal from saline industrial wastewater by submerged fixed-film reactor. Journal of hazardous materials, 142(1-2), pp.175-183.

[27] Sich, H. and Van Rijn, J., 1997. Scanning electron microscopy of biofilm formation in denitrifying, fluidised bed reactors. Water Research, 31(4), pp.733-742.

[28] Foglar, L., Sipos, L. and Bolf, N., 2007. Nitrate removal with bacterial cells attached to quartz sand and zeolite from salty wastewaters. World Journal of Microbiology and Biotechnology, 23(11), pp.1595-1603.

[29] Rajapakse, J.P. and Scutt, J.E., 1999. Denitrification with natural gas and various new growth media. Water research, 33(18), pp.3723-3734.

[30] Saliling, W.J.B., Westerman, P.W. and Losordo, T.M., 2007. Wood chips and wheat straw as alternative biofilter media for denitrification reactors treating aquaculture and other wastewaters with high nitrate concentrations. Aquacultural Engineering, 37(3), pp.222-233.

[31] Sohrabi, M.R., Amiri, S., Masoumi, H.R.F. and Moghri, M., 2014. Optimization of Direct Yellow 12 dye removal by nanoscale zero-valent iron using response surface methodology. Journal of Industrial and Engineering Chemistry, 20(4), pp.2535-2542.

[32] Rasoulifard, M., Khanmohammadi, M., Hatefi, H., Doust, M.S. and Heidari, A., 2012. Removal Of Anionic Dye Acid Blue 25 From Contaminated Water By Hardened Paste Of Portland Cement as a Low-cost Adsorbent.

[33] Y.-H. Lin, J.-Y. Leu. Kinetics of reactive azo-dye decolorization by Pseudomonas luteola in a biological activated carbon process. Biochemical Engineering Journal 39 (2008) 457-467. https://doi.org/10.1016/j.bej.2007.10.015

[34] T.L. Hu, Decolorization of reactive azo dyes by transformation with Pseudomonas luteola. Volume 49, Issue 1, 1994, pp 47-51.

Introduction the medicinal species of Boraginaceae family in Ilkhji and Sharafaldin regions of Esat Azarbaijan in Iran

Leila joudi

Department of agriculture, shabestar branch, Islamic Azad University, shabestar, Iran

Joudi.leila@yahoo.com

Abstract

As medicinal plants are suitable alternatives for synthetic and chemical drugs (Idu and Osemwegie) also because of medical and nutritional importance of Boraginaceae species, all plants of this family are collected in Ilkhji and sharafaldin regions during growth seasons. Plants were collected in 2 regions according to the classical method of regional floristical studies. Collected plants were recognized by valid references (Parsa and Reshinger). Then medical species are chosen by using pharmacopeias. The results of the current study demonstrated that at Ilkhji region 16 species belong to 10 genuses and at Sharafaldin region 8 species belong to 7 genuses that all of them belong to Boraginaceae family. Among these species, 8 species at Ilkhji region and 5 species at sharafaldin region had medicinal properties. Medicinal species of two regions consist of: *Alkanna orientalis, Alkanna bracteosa, Anchusa italica, Asperogo* procumbens, Heliotropicum ellipticum, Lappula microcarpa, Lappula barbata, Moltkia coerolea, Nonea caspica and *Rochelia persica*.The results of this study showed that the region has a great potential for producing respective medicinal plants species belong to those families. Medicinal plants recently become more important because of their medicinal uses.

Key words: Family – Floristical – Medicinal plan- Boraginaceae

Introduction

Today according to the World Health Organization (WHO), as many as 80% of the world's people depend on traditional medicine for their primary health care needs. There are considerable economic benefits in the development of indigenous medicines and in the use of medicinal plants for the treatment of various diseases (Azaizeh , Fulder and Khalil ,2003).Plants have been used in traditional medicine for several thousand years (Abu-Rabia,2007).The traditional culture worldwide are more or less endangered as a result of increasing legislative and moral supports accorded orthodox practice over native medicine(Ido,2007) Boraginaceae plants are considered to be a very good source of polyphenolic compounds that may act as chemo preventive agents, especially by their antioxidant properties.

Material and Methods

All the plant samples in this research, belong to Boraginaceae family, were gathered from Ilkhji and Sharafeddin areas which is located in East Azerbaijan province. Ilkhji area is located in 25 km south west of Tabriz and the geographic coordinates 45.59 to 12 and 46.3 eastern longitudes and 37.55 to 37.57 north latitude and Shabestar city is located in the north-west of Tabriz and the geographic coordinates 37 degrees and 42 minutes of north latitude and 45 degrees and 5 minutes and 46 degree and 9 minutes East longitude. Plant samples belong to Boraginaceae family from Yal, Khaselar, Kordlar and Chaman areas and from Sharafaddin area of Shabestar city as well, were obtained during vegetative period of year. All the plant samples were pressed according to standard methods. If the plant samples were too long, they were cut from several areas, so the sample contained the complete

plant. At the next stage, samples were stick to the herbarium Cardboards and then were identified using floras, keys, illustrations and explanations which are available for different sources of plant Species. Finally, the medicinal species belong to this family were introduced using valid standard pharmacological sources.

Result

Result of survey show that 16 species belong to 10 genera (Table 1) and 8species with 7 genera are in common practice in the traditional system of health care of 2 regions. From this study 10 species were introducing as a medicinal plant. Results showed in table 1, table 2 and table 3.

Table (1): plant species in *Boraginaceae* in Ilkhji

Genus	***Species***	**Growth Form**
Alkanna	***A. orientalis***	Hemicryptophyte
	A. brateosa	Hemicryptophyte
Anchusa	***A. italica***	Hemicryptophyte
Asperugo	***A. procumbens***	Trophyte
Heliotropium	***H. brevilimbe***	Trophyte
	H. swtanense	Hemicryptophyte
	H. szovitsianum	Trophyte
Lappula	***L. sinaica***	Trophyte
Lithospermum	***L. arvense***	Hemicryptophyte
Moltkia	***M.coerulea***	Camephyte
	M. grpsacea	Camephyte
Nonnea	***N. caspica***	Camephyte
	N. persica	Camephyte
Onosma	***K. kotschyi Boiss***	Camephyte
Rochelia	***R. disperma***	Camephyte
	R. persica	Camephyte

Table (2) plant species in *Boraginaceae* in Sharafaldin

Genus	***Species***	**Growth Form**
Alkanna	A.bracteosa	Hemicryptophyte
Anchusa	A.italica.var.italica	Hemicryptophyte
	A.ovata	Trophyte
Asperugo	A.procumbens L.	Trophyte
Heliotropium	H.ellipticum	Trophyte
Heterocarum	H.Szovitsianum(Fich.et.C.A.Mey)A.D.C	Trophyte
Lappula	L.barbata	Trophyte
Lappula	L.microcarpa	Trophyte

Table (3) Medicinal plant species in Leguminosae in 2 regions

Genus	*Species*	**Medical properties**
Alkanna	***A. orientalis***	antimicrobial
	A. bracteosa	Anti-inflammatory and analgesic activity
Anchusa	A.italica.var.italica	anticancer, antioxidant, antiviral
Asperugo	A.procumbens L.	Antidepressant
Heliotropium	H.ellipticum	Antibacterial and antifungal
Lappula	L.microcarpa	antimicrobial
Lappula	L.barbata	Hepatoprotective activities- antioxidant
Moltkia	***M.coerulea***	Antioxidant
Nonnea	***N. caspica***	***antimicrobial***
Rochelia	***R. persica***	antioxidant

Discussion

This report is based on the survey of medicinal plants from different communities in east Azerbaijan, Iran. The present study documents data regarding the availability of ethno medicinal plant resources, which have various potential uses. All the plants mentioned in this paper are very popular among the communities of east Azerbaijan and enjoys a good reputation in Trado- medicinal practice in the areas. From this study, it was found that plants are used to treat mostly as Antibacterial, Antioxidant, anticancer and antifungal and etc.We suggest a detail assessment of resource quantities productivity potential, sustainable harvesting methods, domestication possibilities, market value of potentially promising species and importantly, equitable benefit sharing regiments, this view is also shared by Shrestha and Dhillion (Shrestha and Dillon, 2003). Bhat recently reviewed diverse sources of such information in traditional abstracting services as well as in a variety of online electronic databases (Bhat 1997).

Properly studied and recorded, this traditional knowledge could revolutionize the world of medicine.

References:

[6] Abu-Rabia A: Urinary diseases and ethnobotany among pastoral nomads in the Middle East. *Journal of Ethnobiology and Ethnomedicine* 2005. **1:4.**

[7] Azaizeh H, Fulder S, Khalil K, Said O: Ethnomedicinal knowledge of local Arab practitioners in the Middle East Region. *Fitoterapia* 2003, **74:**98-108.

[8] Bhat,K.K.S., 1997. Medicinal and plant information Databases.In: Medicinal Plants for Forests Conservation and health Care.Brodeker, G. AND p.Vantomne (Eds.),FAO,Non – Wood Forests products Series No.11, FAO,Rome,pp:158.

[9] Dulger, B. Gonuz, A.2004. Antimicrobial activity of certain plants used in turkish traditional medicine. Asian Journal of Sciences 3(1):104-107

[10] Idu, M.and O.O. Osemwegie.2007. Some Medicinal Flora of Forest Reserve in Southern Nigeria. Research Journal of Medicinal Plant 1(1): 29-31.

[11] Parsa, A. 1943-1950. Flore de L, Iran.Vol.1-5.

[12] Reshinger, K.H. 1963-1990.

[13] Shrestha,P.M and Dhillion,S.S. 2003. Medicinal plants diversity and use in the highlands of Dolakkha district, Nepal.J.Ethnopharmacol. 86:81-96

Effects of cerium oxide nanoparticles on histomorphometry factors following sciatic nerve damage

Milad Soluki[1] ,Fariba Mahmoudi [*1],Arash Abdolmaleki [2,3], Asadolah Asadi[1], Abbas Sabahi Namini[2,3]

[1] Department of Biology, Faculty of Science, University of Mohaghegh Ardabili, Ardabil, Iran.

[2] Department of Engineering Sciences, Faculty of Advanced Technologies, University of Mohaghegh Ardabili, Namin, Iran.

[3] Bio Science and Biotechnology Research center (BBRC), Sabalan University of Advanced Technologies (SUAT), Namin, Iran.

Corresponding author: Fariba Mahmoudi, Email: f.mahmoudi@uma.ac.ir

Abstract

In general, regeneration of peripheral nerve injury (PNI) is not completely occurred and sensory and function recovery is incomplete. The aim of the present study was to assess the effect of cerium oxide nanoparticles on histomorphometry analysis following sciatic nerve crash in male Wistar rats.

Material and Methods: Fifty male Wistar rats were divided into five groups (n = 10 in each group) including intact control, negative control (Crush the nerve), sham-operated group (surgical procedure without the nerve crush), experimental group 1 and 2 (sciatic nerve was crushed and treated with 20 or 80 mg/kg cerium oxide nanoparticles respectively. Then, right the sciatic nerve was crushed one centimeter above the nerve branching site.

Results: The regeneration process rate and sensory function recovery significantly increased in rats receiving 20 or 80 mg/kg cerium oxide nanoparticles in comparison with negative control rats.

Conclusion: Cerium oxide nanoparticles may be an effective drug target for improving the regeneration process of sciatic nerve neurons.

*Key words***:** regeneration, sciatic nerve, cerium oxide nanoparticles

Introduction

Peripheral nerve injures may be due to the physical, chemical, mechanical and thermal factors and can lead to the sensory and motor function to be partially or completely lost [1]. Clinical and preclinical trials have demonstrated that peripheral nerves have the ability to regenerate and repair themselves after damage. Nonetheless, complete recovery of the nerve as one of the challenges of nerve repair still remains [2, 3]. In this regard, with today's clinical treatments a very small percentage of peripheral nerve injury patients regain full motor and sensory function [4]. Nanobiology means the application of the nanotechnology engineering principles to biomolecules that provides the new treatment for diseases [5]. Cerium oxide nanoparticles are used widely in the materials field. Besides their material applications, these nanoparticles show promising medical applications in the treatment of oxidative stress-related diseases, like neurodegenerative disease [6-8]. Recent reports demonstrated that cerium oxide nanoparticles can protect various types of mammalian cells such as neural, hepatic, and epidermal cells from inflammatory reactions and oxidative stresses [9-11]. Barbara and colleagues

demonstrated that cerium oxide nanoparticles have antioxidant properties and treatment with these nanoparticle can support neuronal cells from Alzheimer-induced cell death [5]. In another study, Eitan et al. evaluated the neuroprotective effects of cerium oxide nanoparticles against autoimmune encephalomyelitis in mouse animal model that is descriptive for human MS disease. Results of their study showed that treatment with these nanoparticles reduced the clinical signs, decreased the damage to white matter and diminished the CNS inflammation [12]. In stroke, the production of free radicals after injury is one of the most common symptoms hence Estevez et al. evaluated the cerium oxide nanoparticles in rat animal model of brain ischemia. Notably, cerium oxide nanoparticles administration up to 4 h post stroke increased the brain cells neuroprotection significantly [13]. While the protective effects of cerium oxide nanoparticles on central nervous system disease have been investigated in several studies, the neuroprotective role of cerium oxide nanoparticles on peripheral nerve regeneration remains uncertain. Therefore, this study was conducted to evaluate the role of cerium oxide nanoparticles on axonal regeneration and functional recovery of sciatic nerve after crush injury in the rat model.

Material and methods

Cerium oxide nanoparticles were purchased from Merck (Germany). Ketamine and xylazine were obtained from Bimeda (Canada). Cerium oxide nanoparticles were dissolved in deionized water daily and were injected intraperitoneally.

The 40 rats were randomly assigned to 4 groups each group having 10 individuals. In two experimental groups rats were treated intraperitoneally with cerium oxide nanoparticles at the dosage of 20 or 80 mg/kg daily for one week. These two doses of cerium oxide nanoparticles were selected because they showed the neuroprotective effects on central nerves system diseases according to previous reports [14, 15]. Also, in negative control group (crush only) deionized-water was injected to animals as vehicle. In sham-operated group rats underwent surgery without crushing the sciatic nerve.

Histomorphometry Analysis

Quantitative histologic analyses of regenerated sciatic nerve cross-sections 8 weeks after surgery are represented in table 1. Result of the morphometric analysis showed that number of myelinated fibers and myelin sheath thicknesses in cerium oxide nanoparticle groups was significantly greater than in the negative control group. Furthermore, results of morphometric analysis showed that the number of myelinated fibers in all groups where significantly higher than sham operated group but the myelin sheath thickness in negative control group and cerium oxide nanoparticle (20 mg/kg) group was decreased significantly compared to sham operated group. Also, there was no significant difference in the myelin sheath thickness between cerium oxide nanoparticle (80 mg/kg) group and sham operated group.

Discussion

The antioxidant properties of cerium oxide (CeO2) nanoparticles show promise in the treatment of such diseases. Recent reports suggest that CeO2 and other nanoparticles are potent, and probably regenerative, free radical scavengers in vitro and in vivo. The best known mechanism underlying the action of these nanoparticles

is generally thought to be their dual oxidation state .The loss of oxygen and the reduction of Ce4+ to Ce3+ are accompanied by creation of an oxygen vacancy.

References

[1] Abdolmaleki, A., S. Zahri, and A. Bayrami, Rosuvastatin enhanced functional recovery after sciatic nerve injury in the rat. European Journal of Pharmacology, 2020: p. 173260.

[2] Li, J., et al., Ketogenic Diet Potentiates Electrical Stimulation–Induced Peripheral Nerve Regeneration after Sciatic Nerve Crush Injury in Rats. Molecular Nutrition & Food Research, 2020. 64(7): p. 1900535.

[3] Grinsell, D. and C. Keating, Peripheral nerve reconstruction after injury: a review of clinical and experimental therapies. BioMed research international, 2014. 2014.

[4] Mohammad-Bagher, G., et al., Synergistic Effects of Acetyl-l-Carnitine and Adipose-Derived Stromal Cells on Improving Regenerative Capacity of Acellular Nerve Allograft in Sciatic Nerve Defect. Journal of Pharmacology and Experimental Therapeutics, 2019. 368(3): p. 490-502.

[5] D'Angelo, B., et al., Cerium oxide nanoparticles trigger neuronal survival in a human Alzheimer disease model by modulating BDNF pathway. Current Nanoscience, 2009. 5(2): p. 167-176.

[6] Liying, H., et al., Recent advances of cerium oxide nanoparticles in synthesis, luminescence and biomedical studies: a review. Journal of rare earths, 2015. 33(8): p. 791-799.

[7] Walkey, C., et al., Catalytic properties and biomedical applications of cerium oxide nanoparticles. Environmental Science: Nano, 2015. 2(1): p. 33-53.

[8] Kim, C.K., et al., Ceria nanoparticles that can protect against ischemic stroke. Angewandte Chemie International Edition, 2012. 51(44): p. 11039-11043.

[9] Das, M., et al., Auto-catalytic ceria nanoparticles offer neuroprotection to adult rat spinal cord neurons. Biomaterials, 2007. 28(10): p. 1918-1925.

[10] Amin, K.A., et al., The protective effects of cerium oxide nanoparticles against hepatic oxidative damage induced by monocrotaline. International journal of nanomedicine, 2011. 6: p. 143.

[11] Horie, M., et al., Cellular responses induced by cerium oxide nanoparticles: induction of intracellular calcium level and oxidative stress on culture cells. The Journal of Biochemistry, 2011. 150(4): p. 461-471.

[12] Eitan, E., et al., Combination therapy with lenalidomide and nanoceria ameliorates CNS autoimmunity. Experimental neurology, 2015. 273: p. 151-160.

[13] Estevez, A., et al., Neuroprotective mechanisms of cerium oxide nanoparticles in a mouse hippocampal brain slice model of ischemia. Free Radical Biology and Medicine, 2011. 51(6): p. 1155-1163.

[14] Najafi, R., et al., Neuroprotective effect of cerium oxide nanoparticles in a rat model of experimental diabetic neuropathy. Brain Research Bulletin, 2017. 131: p. 117-122.

[15] Heckman, K.L., et al., Custom cerium oxide nanoparticles protect against a free radical mediated autoimmune degenerative disease in the brain. ACS nano, 2013. 7(12): p. 10582-10596.

Cerium oxide nanoparticles effects on gastrocnemius muscle wet recovery following sciatic nerve crash

Milad Soluki[1], Fariba Mahmoudi [*1],Arash Abdolmaleki [2,3], Asadolah Asadi[1], Abbas Sabahi Namini[2,3]

[1]Department of Biology, Faculty of Science, University of Mohaghegh Ardabili, Ardabil, Iran.

[2] Department of Engineering Sciences, Faculty of Advanced Technologies, University of Mohaghegh Ardabili, Namin, Iran.

[3] Bio Science and Biotechnology Research center (BBRC), Sabalan University of Advanced Technologies (SUAT), Namin, Iran.

Corresponding author: Fariba Mahmoudi, Email: f.mahmoudi@uma.ac.ir

Abstract

In general, regeneration of peripheral nerve injury (PNI) is not completely occurred and muscle recovery is incomplete. The aim of the present study was to assess the effect of cerium oxide nanoparticles on gastrocnemius muscle math recovery following sciatic nerve crush in male Wistar rats.

Material and Methods: Fifty male Wistar rats were divided into five groups (n = 10 in each group) including intact control, negative control (Crush the nerve), sham-operated group (surgical procedure without the nerve crush), experimental group 1 and 2 (sciatic nerve was crushed and treated with 20 or 80 mg/kg cerium oxide nanoparticles respectively. Then, the right sciatic nerve was crushed one centimeter above the nerve branching site.

Results: The regeneration process rate of gastrocnemius muscle math significantly increased in rats receiving 20 or 80 mg/kg cerium oxide nanoparticles in comparison with negative control rats.

Conclusion: Cerium oxide nanoparticles may be an effective drug target for improving the regeneration process of muscle after damage.

Key words: regeneration, sciatic nerve, cerium oxide nanoparticles

Introduction

Peripheral nerve injures may be due to the physical, chemical, mechanical and thermal factors and can lead to the sensory and motor function to be partially or completely lost [1]. Clinical and preclinical trials have demonstrated that peripheral nerves have the ability to regenerate and repair themselves after damage. Nonetheless, complete recovery of the nerve as one of the challenges of nerve repair still remains [2, 3]. In this regard, with today's clinical treatments a very small percentage of peripheral nerve injury patients regain full motor and sensory function [4]. Nanobiology means the application of the nanotechnology engineering principles to biomolecules that provides the new treatment for diseases [5]. Cerium oxide nanoparticles are used widely in the materials field. Besides their material applications, these nanoparticles show promising medical applications in the treatment of oxidative stress-related diseases, like neurodegenerative disease [6-8]. Recent reports demonstrated that cerium oxide nanoparticles can protect various types of mammalian cells such as neural, hepatic, and epidermal cells from inflammatory reactions and oxidative stresses [9-11]. Barbara and colleagues demonstrated that cerium oxide nanoparticles have antioxidant properties and treatment with these nanoparticle

can support neuronal cells from Alzheimer-induced cell death [5]. In another study, Eitan et al. evaluated the neuroprotective effects of cerium oxide nanoparticles against autoimmune encephalomyelitis in mouse animal model that is descriptive for human MS disease. Results of their study showed that treatment with these nanoparticles reduced the clinical signs, decreased the damage to white matter and diminished the CNS inflammation [12]. In stroke, the production of free radicals after injury is one of the most common symptoms hence Estevez et al. evaluated the cerium oxide nanoparticles in rat animal model of brain ischemia. Notably, cerium oxide nanoparticles administration up to 4 h post stroke increased the brain cells neuroprotection significantly [13]. While the protective effects of cerium oxide nanoparticles on central nervous system disease have been investigated in several studies, the neuroprotective role of cerium oxide nanoparticles on peripheral nerve regeneration remains uncertain. Therefore, this study was conducted to evaluate the role of cerium oxide nanoparticles on axonal regeneration and functional recovery of sciatic nerve after crush injury in the rat model.

Material and methods

Cerium oxide nanoparticles were purchased from Merck (Germany). Ketamine and xylazine were obtained from Bimeda (Canada). Cerium oxide nanoparticles were dissolved in deionized water daily and were injected intraperitoneally.

The 40 rats were randomly assigned to 4 groups each group having 10 individuals. In two experimental groups rats were treated intraperitoneally with cerium oxide nanoparticles at the dosage of 20 or 80 mg/kg daily for one week. These two doses of cerium oxide nanoparticles were selected because they showed the neuroprotective effects on central nerves system diseases according to previous reports [14, 15]. Also, in negative control group (crush only) deionized-water was injected to animals as vehicle. In sham-operated group rats underwent surgery without crushing the sciatic nerve.

Gastrocnemius muscle wet weights

Gastrocnemius muscle wet weight was measured at eight weeks postoperative to assess denervation atrophy, as described previously [18]. The gastrocnemius muscles of the experimental and unoperated sides were harvested in each group. After the removal of the blood, the muscle was weighed immediately using a digital scale (Mettler Toledo, Switzerland). The gastrocnemius muscle mass ratio i.e., the weight of experimental side muscle /weight of muscle on the unoperated side was then calculated [19]

In all groups, the gastrocnemius muscle wet weight ratio (%) was calculated as the muscle

wet weight of the in- jured limb/the weight of the contralateral limb × 100%

(Fig. 3) [Li et al., 2018]. There was no statistically significant difference between the gastrocnemius muscle weight ratio of the sham group and the Cin 30 group ($p > 0.05$); however, there was a highly significant difference between the sham group and the other groups ($p < 0.001$). In addition, in the injury group, the gastrocnemius muscle ratio showed a marked decrease compared with the sham group; this decrease was attenuated by treatment

with different Cin doses (30 and 90 mg/kg/day). There was no significant difference in the muscle ratio between the Cin 30 group versus the sham group ($p > 0.05$), but both other doses were significantly different from the sham group ($p < 0.001$).

Discussion

The antioxidant properties of cerium oxide (CeO2) nanoparticles show promise in the treatment of such diseases. Recent reports suggest that CeO2 and other nanoparticles are potent, and probably regenerative, free radical scavengers in vitro and in vivo. The best known mechanism underlying the action of these nanoparticles is generally thought to be their dual oxidation state. The loss of oxygen and the reduction of Ce4+ to Ce3+ are accompanied by creation of an oxygen vacancy.

References

[1] Abdolmaleki, A., S. Zahri, and A. Bayrami, Rosuvastatin enhanced functional recovery after sciatic nerve injury in the rat. European Journal of Pharmacology, 2020: p. 173260.

[2] Li, J., et al., Ketogenic Diet Potentiates Electrical Stimulation–Induced Peripheral Nerve Regeneration after Sciatic Nerve Crush Injury in Rats. Molecular Nutrition & Food Research, 2020. 64(7): p. 1900535.

[3] Grinsell, D. and C. Keating, Peripheral nerve reconstruction after injury: a review of clinical and experimental therapies. BioMed research international, 2014. 2014.

[4] Mohammad-Bagher, G., et al., Synergistic Effects of Acetyl-l-Carnitine and Adipose-Derived Stromal Cells on Improving Regenerative Capacity of Acellular Nerve Allograft in Sciatic Nerve Defect. Journal of Pharmacology and Experimental Therapeutics, 2019. 368(3): p. 490-502.

[5] D'Angelo, B., et al., Cerium oxide nanoparticles trigger neuronal survival in a human Alzheimer disease model by modulating BDNF pathway. Current Nanoscience, 2009. 5(2): p. 167-176.

[6] Liying, H., et al., Recent advances of cerium oxide nanoparticles in synthesis, luminescence and biomedical studies: a review. Journal of rare earths, 2015. 33(8): p. 791-799.

[7] Walkey, C., et al., Catalytic properties and biomedical applications of cerium oxide nanoparticles. Environmental Science: Nano, 2015. 2(1): p. 33-53.

[8] Kim, C.K., et al., Ceria nanoparticles that can protect against ischemic stroke. Angewandte Chemie International Edition, 2012. 51(44): p. 11039-11043.

[9] Das, M., et al., Auto-catalytic ceria nanoparticles offer neuroprotection to adult rat spinal cord neurons. Biomaterials, 2007. 28(10): p. 1918-1925.

[10] Amin, K.A., et al., The protective effects of cerium oxide nanoparticles against hepatic oxidative damage induced by monocrotaline. International journal of nanomedicine, 2011. 6: p. 143.

[11] Horie, M., et al., Cellular responses induced by cerium oxide nanoparticles: induction of intracellular calcium level and oxidative stress on culture cells. The Journal of Biochemistry, 2011. 150(4): p. 461-471.

[12] Eitan, E., et al., Combination therapy with lenalidomide and nanoceria ameliorates CNS autoimmunity. Experimental neurology, 2015. 273: p. 151-160.

[13] Estevez, A., et al., Neuroprotective mechanisms of cerium oxide nanoparticles in a mouse hippocampal brain slice model of ischemia. Free Radical Biology and Medicine, 2011. 51(6): p. 1155-1163.

[14] Najafi, R., et al., Neuroprotective effect of cerium oxide nanoparticles in a rat model of experimental diabetic neuropathy. Brain Research Bulletin, 2017. 131: p. 117-122.

[15] Heckman, K.L., et al., Custom cerium oxide nanoparticles protect against a free radical mediated autoimmune degenerative disease in the brain. ACS nano, 2013. 7(12): p. 10582-10596.

[16] Bain, J., S. Mackinnon, and D. Hunter, Functional evaluation of complete sciatic, peroneal, and posterior tibial nerve lesions in the rat. Plastic and reconstructive surgery, 1989. 83(1): p. 137-138.

[17] Raimondo, S., et al., Methods and protocols in peripheral nerve regeneration experimental research: part II—morphological techniques. International review of neurobiology, 2009. 87: p. 81-103.

[18] Ghayour, M.B., A. Abdolmaleki, and M. Behnam-Rassouli, The effect of Riluzole on functional recovery of locomotion in the rat sciatic nerve crush model. European Journal of Trauma and Emergency Surgery, 2016: p. 1-9.

[19] Lewin, S.L., et al., Simultaneous treatment with BDNF and CNTF after peripheral nerve transection and repair enhances rate of functional recovery compared with BDNF treatment alone. The Laryngoscope, 1997. 107(7): p. 992-999.

New Extraction Techniques of Bioactive Compounds from Medicinal and Aromatic Plants

Zahra Mohebi*

Department of Natural Resources, Faculty of Agricultural Sciences & Natural Resources, Razi University, Kermanshah, Iran.

Email: z.mohebi@razi.ac.ir

Abstract

Natural products are chemical compounds or substances produced by living organisms found in nature. Those compounds that can be isolated or produced by plants are called phytochemicals. Medicinal and aromatic plants contain a large source of phytochemicals, which after their isolation can be used for different purposes and in different scientific fields. The study on medicinal plants started with extraction procedures that play a critical role to the extraction outcomes (e.g. yield and phytochemicals content) and also to the consequent assays performed. A wide range of technologies with different methods of extraction is available nowadays. Extraction, as the term is used pharmaceutically, involves the separation of medicinally active portions of plant or animal tissues from the inactive or inert components by using selective solvents in standard extraction procedures. Hence, this review aims to describe and compare the most commonly used methods based on their principles to help evaluating the suitability and economic feasibility of the methods

Keywords: phenolic groups, Soxhlet, extractor, essence.

1. Introduction

Natural products are chemical compounds or substances produced by living organisms found in nature. Those compounds that can be isolated or produced by plants are called phytochemicals. Medicinal and aromatic plants contain a large source of phytochemicals, which after their isolation can be used for different purposes and in different scientific fields. For example, medicinal plants are a great source of drugs for traditional systems of medicine, modern medicines, nutraceuticals, food supplements, folk medicines, pharmaceutical intermediates, and chemical entities for synthetic drugs. On the other hand, aromatic plants are a source of essential oils, concretes, absolutes, pomades, and resinoids, which can be used in fragrances, flavours, cosmetics, pharmaceuticals, health beverages, and chemical terpenes, since they consist of a wide range of chemical compounds, such as hydrocarbons, esters, terpenes, lactones, phenols, aldehydes, acids, alcohols, and ketones [1]. Medicinal plants have been used as a source of remedies since ancient times. The ancient Egyptians were familiar with many medicinal herbs and were aware of their usefulness in treatment of various diseases. The healing of sick persons was carried out by priest doctors who prescribed and prepared medicaments. The first recorded prescriptions were found in Ancient Egyptian tombs. The writing on the temple walls and in the papyri revealed that Ancient Egyptians used many herbal drugs for the same purposes as they are used today [[2],[3]]. Plants have

been the source of potential therapeutic agents ever since mankind has evolved. Although several active phytoconstituents and high activity profile drugs have been discovered from plants but the quality and safety related problems of herbal drugs have still been a challenge for researchers. The major reasons for these drawbacks are the lack of high performance, reliable extraction techniques and methodologies for establishing the purity and standard for herbal medicines [4]. Due to these factors, the herbal medicines have still to find their way in order to be accepted in global market. In research related to discovery of new active phytoconstituents, extraction is one of the important steps as it is the starting point for the isolation and purification procedures. An individual plant may consist of several active phytoconstituents existing in abundance along with certain constituents of low activity profile. Thus, there arises a need for the development of extraction and analysis techniques with high performance. There has been a need for better and newer extraction techniques, in the herbal drug industry so that the extraction time and the cost of solvent consumption is decreased [5].

2. Extracts

Extraction, as the term is used pharmaceutically, involves the separation of medicinally active portions of plant or animal tissues from the inactive or inert components by using selective solvents in standard extraction procedures. The products so obtained from plants are relatively impure liquids, semisolids or powders intended only for oral or external use. These include classes of preparations known as decoctions, infusions, fluid extracts, tinctures, pillar (semisolid) extracts and powdered extracts. Such preparations popularly have been called galenicals, named after Galen, the second century Greek physician. The purposes of standardized extraction procedures for crude drugs are to attain the therapeutically desired portion and to eliminate the inert material by treatment with a selective solvent known as menstruum.

The extract thus obtained may be ready for use as a medicinal agent in the form of tinctures and fluid extracts, it may be further processed to be incorporated in any dosage form such as tablets or capsules, or it may be fractionated to isolate individual chemical entities such as ajmalicine, hyoscine and vincristine, which are modem drugs. Thus, standardization of extraction procedures contributes significantly to the final quality of the herbal drug. Extraction is the treatment of plant or animal tissue through standard procedures with selective solvents, in order to dissolve the pharmaceutically active constituents, while most of the inert matter remains undissolved. Extraction of bioactive chemical compounds is the first step of the analysis of medical and aromatic plants and it plays a crucial role in their further separation and characterization. Nowadays, a wide range of extraction techniques are available. Apart from the conventional extraction techniques, a lot of novel procedures have been developed and they can be used for the production of natural extracts.

Due to the great variety of extraction procedures, no single method is regarded as standard for extracting phenolic compounds from plants and there is no universal extraction method that can be considered as an ideal method. The main parameters, which should be taken into account before choosing an extraction procedure, are the nature of the drug, the nature of the solvent, the cost of the drug taking into account its therapeutic value, the concentration of the product, and the stability of the drug. In general terms, among the conventional extraction procedures, maceration is used for cheaper drugs and drugs containing compounds that do not have high

therapeutic value and when water is required as solvent or the preparation of a diluted solution is required. On the other hand, for costly drugs and drugs that have considerable therapeutic value and when a volatile solvent is required or a concentrate is required, percolation is commonly used [1].

3. The Overview of Extraction Methods

Some of the major constraints in sustainable industrial exploitation of medicinal and aromatic plants (MAPs) are due to the fact that the developing countries including Egypt have poor agricultural practices for MAPs, unscientific and indiscriminate gathering practices from the wild, poor postharvest and post-gathering practices leading to poor quality raw material, lack of research for the development of high-yielding varieties of MAPs, poor propagation methods, inefficient processing techniques, poor quality control procedures, lack of research on process and product development, difficulty in marketing, non-availability of trained personnel, lack of facilities and tools to fabricate equipment locally, and finally lack of access to the latest technologies and market information [6]. This calls for co-operation and coordination among various institutes and organizations of the region, in order to develop MAPs for sustainable commercial exploitation. The process of extracting MAPs determines how efficiently we add value to MAP bioresources. In case of essential oils, the extraction process affects the physical as well as internal composition. External appearance, at times, can result in rejection of the batch even if the analytical results are within acceptable limits. Furthermore, essential oils are evaluated internationally for their olfactory properties by experienced perfumers and these olfactory qualities supersede analytical results. Variations in the chemical constituents of the extracts of medicinal plants may result by using non-standardized procedures of extraction. Efforts should be made to produce batches with quality as consistent as possible (within the narrowest possible range) [7].

4. Extraction Methods

Extraction is the separation of medicinally active portions of plant using selective solvents through standard procedures [1]. The purpose of all extraction is to separate the soluble plant metabolites, leaving behind the insoluble cellular marc (residue). The initial crude extracts using these methods contain complex mixture of many plant metabolites, such as alkaloids, glycosides, phenolics, terpenoids and flavonoids. Some of the initially obtained extracts may be ready for use as medicinal agents in the form of tinctures and fluid extracts but some need further processing. Several of the commonly used extraction methods are discussed below:

4.1 Maceration, infusion, percolation and decoction

Maceration is a technique use in wine making and has been adopted and widely used in medicinal plants research. Maceration involved soaking plant materials (coarse or powdered) in a stoppered container with a solvent and allowed to stand at room temperature for a period of minimum 3 days with frequent agitation [1]. The

processed intended to soften and break the plant's cell wall to release the soluble phytochemicals. After 3 days, the mixture is pressed or strained by filtration. In this conventional method, heat is transferred through convection and conduction and the choice of solvents will determine the type of compound extracted from the samples. Infusion and decoction use the same principle as maceration; both are soaked in cold or boiled water. However, the maceration period for infusion is shorter and the sample is boiled in specified volume of water (e.g. 1:4 or 1:16) for a defined time for decoction [1]. Decoction is only suitable for extracting heat-stable compounds, hard plants materials (e.g. roots and barks) and usually resulted in more oil-soluble compounds compared to maceration and infusion. Unique equipment called percolator (Figure 1) is used in percolation, another method that shares similar fundamental principle. Dried powdered samples are packed in the percolator, added with boiling water and macerated for 2 hours. The percolation process is usually done at moderate rate (e.g. 6 drops /min) until the extraction is completed before evaporation to get a concentrated extract [8].

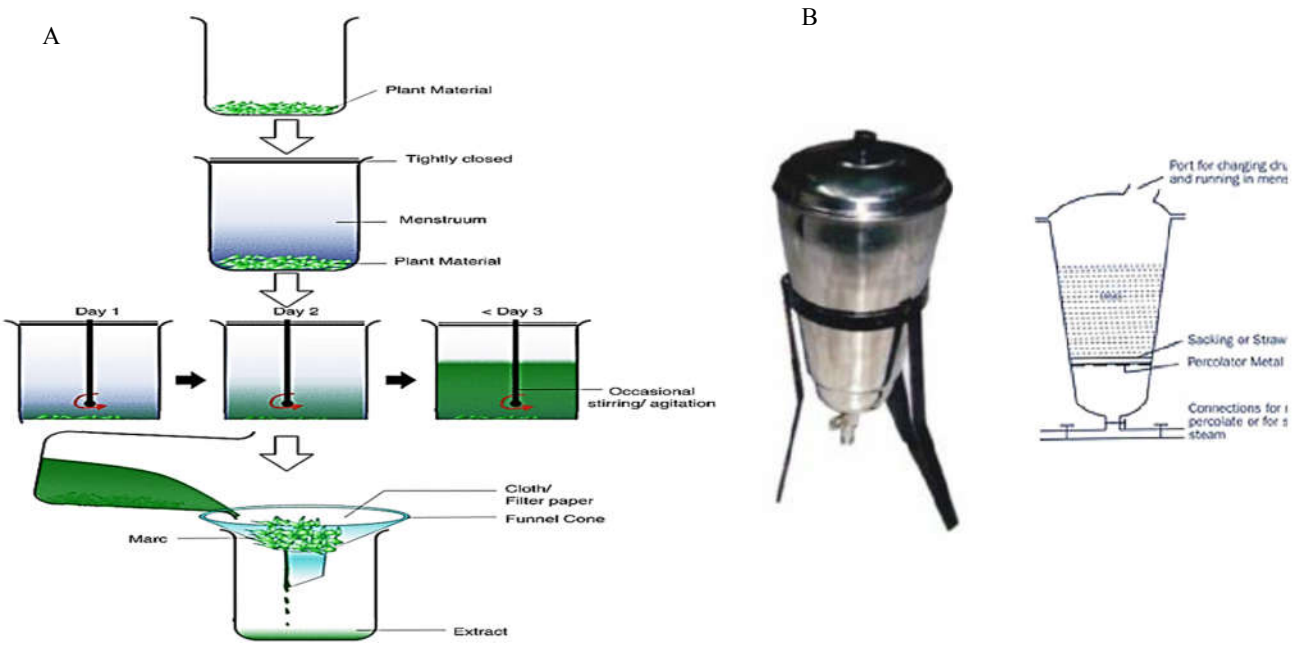

Fig. 1. Maceration (A) and percolation (B) methods

Another widely used conventional extraction procedure is maceration, which is considered as a steady-state extraction technique. In this process, the whole or powdered medicinal or aromatic plant sample is placed in a closed vessel with the solvent and it is allowed to stand at room temperature for a period of at least three days with frequent agitation until the soluble matter has dissolved. The closed vessel is used so that the evaporation of the extracting solvent could be prevented and no variation between different batches of the same plant can occur. The mixture is then strained, the marc that is the undissolved part after extraction is pressed to recover a large amount of occluded solutions and the two fractions of the liquids are combined. Finally, when equilibrium is

achieved the combined liquids are clarified by filtration or decantation after standing and the marc may be strained through a special press.

In order to increase the extraction yield, repeated maceration can be implemented. Double or triple maceration can be extremely useful, especially when the target components are of high value and in cases where the concentrated infusion contains oil that is considered volatile. Usually, evaporation of the second and the third extract is required before combination with the first extract, in order to decrease the total volume of solvent [1].

4.2 Soxhlet extraction or hot continuous extraction

In this method, finely ground sample is placed in a porous bag or "thimble" made from a strong filter paper or cellulose, which is place, is in thimble chamber of the Soxhlet apparatus (Figure 2). Extraction solvents is heated in the bottom flask, vaporizes into the sample thimble, condenses in the condenser and drip back. When the liquid content reaches the siphon arm (Figure 2), the liquid contents emptied into the bottom flask again and the process is continued. Soxhlet extraction is a general and well-established technique, which was firstly proposed by Franz Ritter von Soxhlet in 1879 and it was initially designed for extracting lipids. Nowadays, its use is not limited to lipid compounds, but it is also widely used for the extraction of active compounds from different natural sources [9].

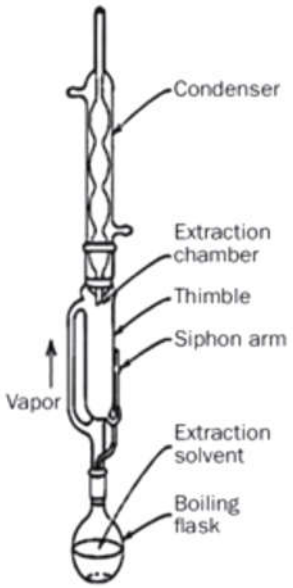

Fig. 2. Soxhlet apparatus

In this technique, the plant material is placed in a porous carrier made from filter paper or cellulose, which is known as "thimble." The carrier is placed in a thimble-holder, which is then filled with the extraction solvent. The solvent is heated in the bottom flask, vaporizes into the bag that contains the sample, condenses, and drops back. When the level of the liquid reaches the overflow level, a siphon is used to aspirate the liquid content of the thimble into the distillation flask, carrying the extracted solutes into the bulk liquid. The process is continued until complete extraction is achieved. The Soxhlet extraction procedure is considered to have many advantages. Firstly, compared to other conventional techniques, in this case a smaller quantity of extraction solvent is used for the

extraction of a large amount of the active components of medicinal and aromatic plants. This can result in high economy of treatment time and energy required for the extraction procedure. In addition, a relatively high extraction temperature is maintained with heat from the distillation flask and no filtration of the product after the extraction is needed.

4.3 Microwave assisted extraction (MAE)

Upon absorption by a material, electromagnetic energy of microwaves is converted to heat energy. 2450 MHz (2.45 GHz) is the most commonly used frequency for commercial microwave instruments, which has an energy output of 600-700 W [10]. MAE is a simple, environment friendly and economical technique for the extraction of biologically active compounds from different plant materials [11]. Samra et. al. had first time used microwave domestic ovens for the treatment of biological samples for metal analysis in 1975 [12]. The application of MAE for plant materials was first reported by Ganzler and co-workers in 1986 [13]. MAE utilizes microwave energy to facilitate partition of analytes from the sample matrix into the solvent [14]. Microwave radiation interacts with dipoles of polar and polarizable materials (e.g. solvents and sample) causes heating near the surface of the materials and heat is transferred by conduction. Dipole rotation of the molecules induced by microwave electromagnetic disrupts hydrogen bonding; enhancing the migration of dissolved ions and promotes solvent penetration into the matrix [13]. In non-polar solvents, poor heating occurs as the energy is transferred by dielectric absorption only [1]. MAE can be considered as selective methods that favor polar molecules and solvents with high dielectric constant.

Microwaves possess electric and magnetic fields which are perpendicular to each other. The electric field causes heating via two simultaneous mechanisms, namely, dipolar rotation and ionic conduction. Dipolar rotation is due to the alignment on the electric field of the molecules possessing a dipole moment in both the solvent and the solid sample. This oscillation produces collisions with surrounding molecules leading to liberation of thermal energy into the medium. With a frequency of 2.45 GHz, this phenomenon occurs 4.9×109 times faster and thus the resulting heating is very fast. Indeed, larger the dielectric constant of the solvent, more rapid the heating is. Consequently, unlike classical conductive heating methods, microwaves heat the whole sample simultaneously. In the case of extraction, the advantage of microwave heating is the disruption of weak hydrogen bonds promoted by the dipole rotation of the molecules [13].

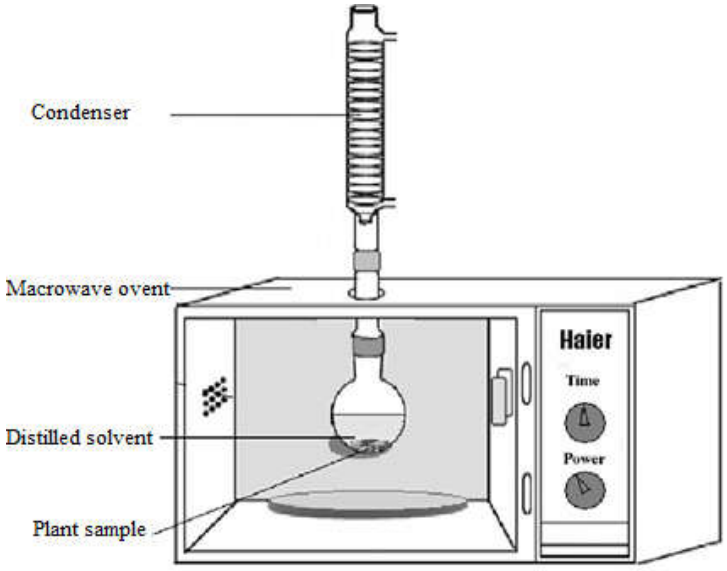

Fig. 3. The apparatus of MAE extraction

MAE can be practiced in two different modes- one is closed vessel operation, that is under controlled (elevated) pressure and temperature, another is open vessel operation performed at atmospheric pressure. These technologies are named as pressurized microwave assisted extraction (PMAE) and focused microwave assisted extraction (FMAE), respectively [15]. In closed vessel system the solvent may be heated much above their atmospheric boiling point. Both extraction speed and efficiency are enhanced in this procedure [13]. In closed vessels the temperature may be elevated by simply applying the correct pressure. The closed vessel system is most suitable for volatile compounds. In open vessel system the maximum temperature is determined by the boiling point of the solvent used [16]. Compared to closed vessel extractions, open cells offer increased safety in sample handling and, furthermore, they allow larger amounts to be extracted [13]. Open cells can accommodate multiple extraction vessels at a time. Advantage of improved mass transfer due to agitation is available in both modes of MAE. Though superheating has been indicated to occur during microwave processes [15], MAE is not likely to suffer from thermal degradation of phytoconstituents by superheating because superheating is reported to occur in homogenous systems, and not in heterogeneous ones -in which MAE falls.

4.4 Ultrasound-assisted extraction (UAE) or sonication extraction

UAE involves the use of ultrasound ranging from 20 kHz to 2000 kHz [1]. The mechanic effect of acoustic cavitation from the ultrasound increases the surface contact between solvents and samples and permeability of cell walls. Physical and chemical properties of the materials subjected to ultrasound are altered and disrupt the plant cell wall; facilitating release of compounds and enhancing mass transport of the solvents into the plant cells [17]. The procedure is simple and relatively low-cost technology that can be used in both small and larger scale of phytochemical extraction. UAE involves application of high-intensity, high-frequency sound waves and their

interaction with materials. UAE is a potentially useful technology as it does not require complex instruments and is relatively low-cost. It can be used both on small and large scale. UAE involves ultrasonic effects of acoustic cavitation. Under ultrasonic action solid and liquid particles are vibrated and accelerated and, because of that solute quickly diffuses out from solid phase to solvent [18]. Several probable mechanisms for ultrasonic enhancement of extraction, such as cell disruption, improved penetration, and enhanced swelling, capillary effect, and hydration process have been proposed [19]. If the intensity of ultrasound is increased in a liquid, then it reaches at a point at which the intramolecular forces are not able to hold the molecular structure intact, so it breaks down and bubbles are created, this process is called cavitation. Collapse of bubbles can produce physical, chemical and mechanical effects which result in the disruption of biological membranes to facilitate the release of extractable compounds and enhance penetration of solvent into cellular materials and improve mass transfer [[18],[20]. The beneficial effects of sound waves on extraction are attributed to the formation and asymmetrical collapse of microcavities in the vicinity of cell walls leading to the generation of microjets rupturing the cells. The pulsation of bubbles is thought to cause acoustic streaming which improves mass transfer rate by preventing the solvent layer surrounding the plant tissue from getting saturated and hence enhancement of convection.

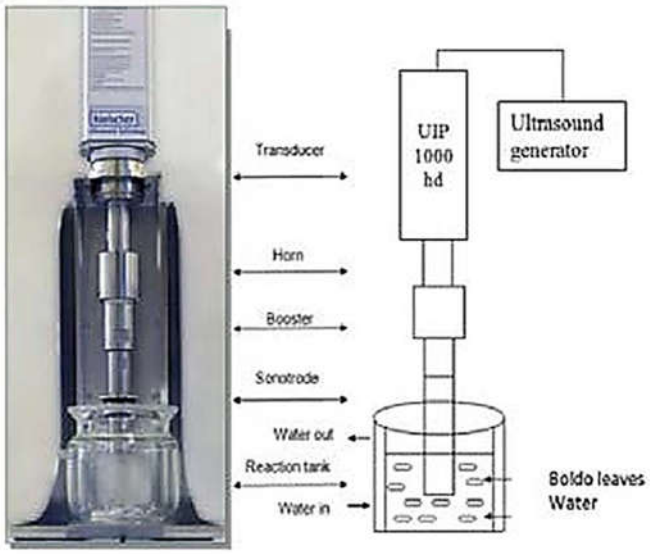

Fig. 4. Ultrasound-assisted extraction machine

4.5 Accelerated solvent extraction (ASE)

ASE is an efficient form of liquid solvent extraction compared to maceration and Soxhlet extraction as the method use minimal amount of solvent. Sample is packed with inert material such as sand in the stainless-steel extraction cell (Figure 3) to prevent sample from aggregating and block the system tubing [21]. Packed ASE cell includes layers of sand-sample mixture in between cellulose filter paper and sand layers. This automated extraction technology is able to control temperature and pressure for each individual sample and requires less than an hour for extraction. Similar to other solvent technique, ASE also critically depend on the solvent types.

Cyclohexaneacetone solution at the ratio of 6:4 v/v with 5-minute heating (50°C) showed to yield highest bixin from Bixa orellana with 68.16% purity [21], High recoveries (~94%) of flavonoids from Rheum palmatun were observed using 80% aqueous methanol by ASE, suggesting the suitability of this method for quality control evaluation.

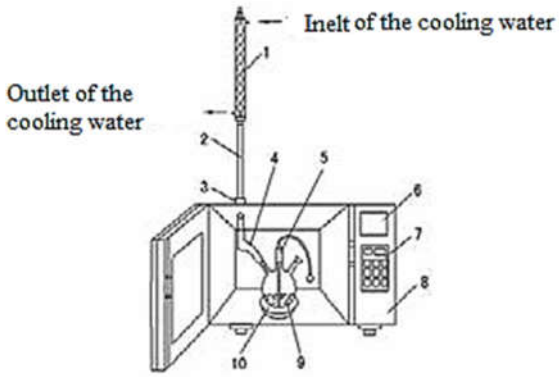

Fig. 5. Microwave equipment diagram; 1-water condenser; 2-air condenser; 3-copper tube; 4-tailored tube; 5-air agitator; 6 status display; 7-microwave timer; microwave oven; 8-flask; 10-base of flask

4.6 Supercritical fluid extraction (SFE)

SFE is a modern technique, which is nowadays used during the analysis of environmental, pharmaceutical, and polymer samples. The main reason for the interest in SFE was the possibility of carrying out extractions at temperature near to ambient, thus preventing the substance of interest from incurring thermal degradation, by stopping using conventional organic solvents and using supercritical fluids [22]. In 1980, SFE was firstly carried out on a commercial scale, while its industrial scale application includes processes such as decaffeination of coffee beans and tea, extraction of essential oils, oleoresins, and flavoring compounds from herbs and spices as well as extraction of high-valued bioactive compounds from a great variety of natural matrices [23]. Supercritical fluid (SF) or also called as dense-gas is a substance that shares the physical properties of both gas and liquid at its critical point. Factors such as temperature and pressure are the determinants that push a substance into its critical region. SF behaves more like a gas but have the solvating characteristic of a liquid. An example of SF is CO2 that become SF at above 31.1°C and 7380 kPa. Interest in Supercritical-CO2 (SC-CO2) extraction due to excellent solvent for nonpolar analytes and CO2 is readily available at low cost and has low toxicity. Even though SC-CO2 has poor solubility for polar compounds, modification such as adding small amount of ethanol and methanol enable it to extracts polar compounds. SC-CO2 also produces analytes at concentrate form as CO2 vaporizes at ambient temperature. SC-solvents strength can be easily altered by changing the temperature, pressure or by adding modifiers that lead to reduce extraction time. Optimization of SC-CO2 on *Wadelia calendulacea* achieved its optimum yield at 25 MPa, 25 ºC temperature, 10% modifier concentration and 90-minute extraction time [24]. A major drawback of this method is the initial cost of the equipment is very high [25].

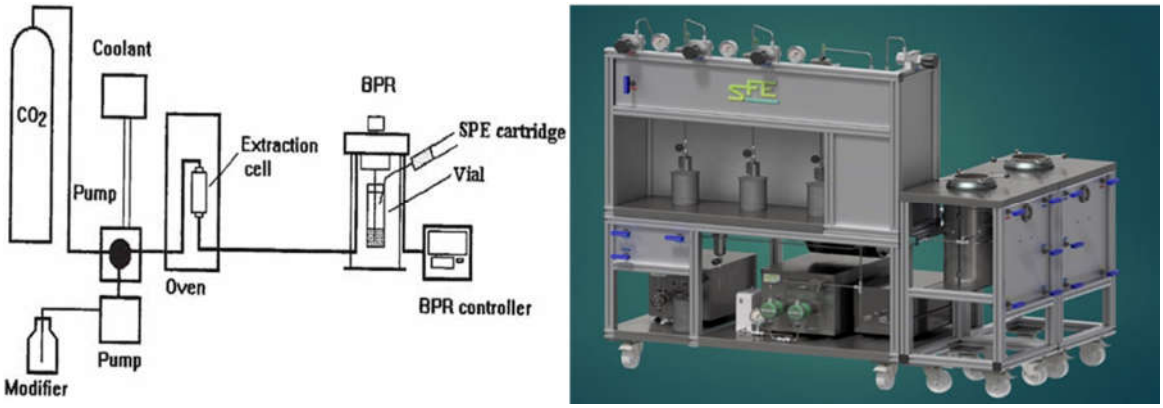

Fig. 6. Supercritical fluid extraction (SFE) diagram and apparatus

SFE can be used to extract certain compounds from plants at temperature near to ambient, thus preventing the substance from incurring in thermal denaturation. SFE is an old technique of solvent extraction but its commercial application happened slowly due to the sophisticated and expensive high-pressure equipment and technology required [26]. SFE is currently a well-established method for extraction and separation because its design and operating criteria are now fully understood. The favorable transport properties of fluids near their critical points allow deeper penetration into solid plant matrix and more efficient and faster extraction than with conventional organic solvents. The extraction is carried out in high-pressure equipment in batch or continuous manner. In both cases, the supercritical solvent is put in contact with the material from which a desirable product is to be separated. Generally cylindrical extraction vessels are used for sample preparation [1]. In batch processing solid is placed into extraction vessel and the supercritical solvent is fed in until the target extraction conditions are reached. And in semi batch processing the supercritical solvent is fed continuously through a high-pressure pump at a fixed flow rate, to precipitate solute from supercritical solution one or more separation stages are used. Supercritical fluid technology is now recognized as an effective analytical technique with efficiency comparable to existing chemical analysis methods. SFE is favorably applicable for the qualitative and quantitative identification of constituents of natural products, including heat-labile compounds [27].

4.7 Hydro-distillation

Another conventional extraction method is hydro-distillation, which is a traditional method widely used for the extraction of the active components and essential oils from plant samples. This procedure is good for the extraction of volatile active compounds, but since high extraction temperature is required it cannot be used for thermolabile compounds. Moreover, hydro-distillation is a technique that does not involve organic solvents and it can be applied both for dried and for wet plant samples. The four basic categories of hydro-distillation are: (a) water distillation, (b) water and steam distillation, (c) direct steam distillation, and (d) distillation with cohobating. The choice between the four modifications depends on the boiling point of the essential oil and the nature of the medicinal or aromatic plant. With direct steam distillation, extraction occurs with the use of steam generated

outside the tank in a steam generator or in a boiler. The plant is again supported above the steam inlet, as in the previous case of water and steam distillation. By using direct steam distillation, the extraction time can be significantly reduced and this is the reason why this extraction modification is recommended for distillation of high-boiling oils and hard materials such as roots and woods [[1],[28].

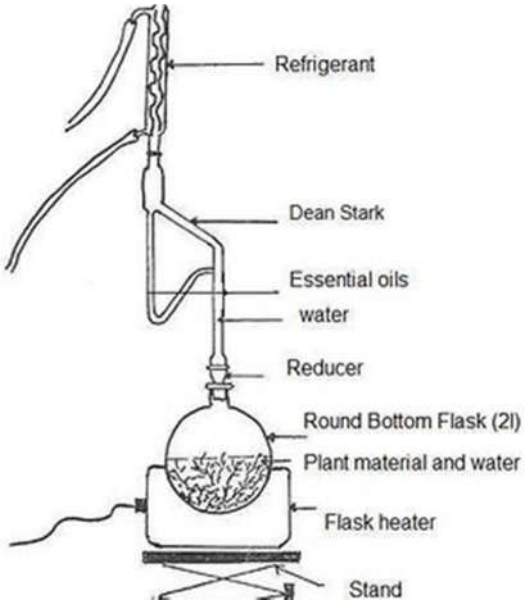

Fig. 7. Hydro-distillation apparatus

4.8 Steam Distillation

Steam distillation is a well-known extraction method, applied especially for the thermal sensitive plant materials. Considering these compounds tend to degrade at higher temperatures, steam distillation ensures that the plant material is not subjected to temperature higher than 100 °C as the hot steam is generated outside the still in a satellite steam generator known as the boiler and the amount of steam can also be promptly controlled. The flask containing plant material is placed in a heating mantle. When the boiling point of the solvent is reached, vapour generated is subsequently condensed through a condenser. The distillate which is the extract can be collected while the solvent can also be separated and reused again [29].

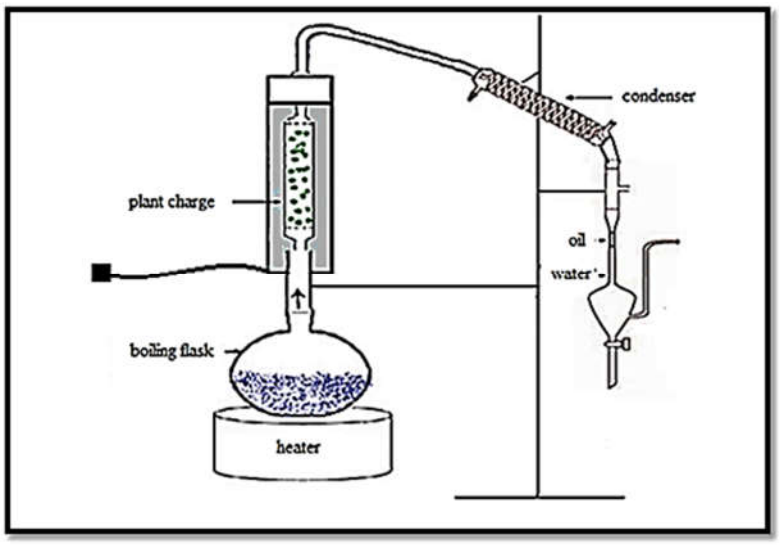

Fig. 8. Steam distillation apparatus

4.9 Enzyme-Assisted Extraction

Enzyme-assisted extraction suggests that the release of phytochemical constituents from aromatic and medicinal plant cells can be supported by using enzymes in order to provide cell disruption. Generally, enzymes can be used as catalysts to help the extraction, modification, or synthesis of bioactive compounds in medicinal and aromatic plants as they are able to catalyze reactions with exquisite specificity and regioselectivity and they are also able to be functional under mild processing conditions in aqueous solutions, in which extraction can take place.

There is quite a big variety of enzymes that can be used for extracting chemical compounds. Among them lactase, protease/lipase, lipase, and phospholipase are the enzymes that are more commonly reported in the literature. Moreover, pectinases, cellulases, and hemicellulases are also widely used for extracting bioactive compounds from medicinal and aromatic plants due to their catalytic property. These enzymes show the ability to degrade or disrupt the cell walls and membranes of plant materials resulting in better release and more efficient extraction of the active compounds. Therefore, these enzymes can be used particularly for the treatment of plant material

prior to other conventional extraction techniques. They often require particle-size reduction of the plant material in order to increase the contact surface and, as a result, the extraction efficiency of the whole process. Also, after choosing the appropriate enzyme, there are some parameters that should be optimized. Among them pH, time, temperature, and enzyme concentration are included. Temperature is considered significantly important and although enzymes have an optimal temperature at which they are flexible, they can still be used in a wide range of temperatures, which makes the selection of working temperature easier.

The enzyme-assisted extraction technique reduces solvent usage and decreases energy consumption and it is supposed to be a more green and more effective alternative procedure compared to conventional solvent extraction

techniques. Moreover, it reduces the required extraction time; thus, the use of enzymes makes the whole extraction procedure more rapid. However, enzyme-assisted extraction has some drawbacks such as its high cost for processing large volumes of raw plants, the difficulties that exists when the procedure has to be applied in industrial scale, and the limitation of the enzymes in order to hydrolyze the cell walls of the plant completely. Those facts should be overcome in order to increase not only the efficiency of the extraction but also the quality of the extracts obtained from medicinal and aromatic plants [30].

5. Discussion

All the methods that employ solvents in the procedures (maceration, MAE, UAE and ASE) are critically influenced by the solvent's types. However, no significant effect caused by the solvent volume used using three methods (maceration, MAE and UAE) on the biologically active compounds in the poplar type propolis at ratio (1:10 w: v), suggesting use of solvents at greater ratio is unnecessary. However, the finding is limited to assessment of phenolic, flavonoid content and total yield as comparison.

Maceration have been suggested as more applicable, convenient and less costly method for small and medium enterprises (SMEs) compared to other modern extraction methods [31]. However, chemical waste is a major issue in maceration technique as compared to MAE and UAE, which is known as the "Green method" [17]. Although, all these extraction methods resulted in crude extracts containing a mixture of metabolites, the efficacy of those crude extracts using nano-encapsulated processing in *Centella asiatica* showed to have similar efficacy as those purified [32]. This particular fact suggests that further isolation and purification of extracts, which is rather complex and time consuming is not necessary if proper preparation and extraction are done.

Suitable conditions for each extraction methods are also important. Certain factors such as temperature and light need to be evaluated to extracts thermo-labile compounds. Slightly acidic solvent (0.1% HCl-methanol v/v) was used to extract anthocyanin from the red and blue flowers, pointed the effect of pH in extraction procedures [33]. Hydrochloric acid in ethanol system was found to be more efficient than acetic acid in extraction of anthocyanin [34]. Among parameters such as solvent types, solvent strength, extraction time, agitation speed, sample-solvent ratio and temperature investigated using factorial design experiment; solvent strength, which is 70% ethanol, is the most influential factors in Curcuma longa extraction [35]. Similar observation of 70% ethanol as the most influential parameters was seen in triterpenoids extraction from *Jatropha curcas* leaves [36] and phenolic extractions from *Moringa oliefera* [31].

6. Conclusion

Medicinal plants are important for discovery and identification of new therapeutic compounds. Extraction method plays an important role in separation and characterization of different phytochemicals from herbs, and screening plant extracts for novel leads. Conventional methods are exhaustive and require more time, power, sample and solvent consumption is higher than their modern counterparts. The recovery, stability and overall quality of extract also can be improved by selection of a better method. Modern methods can be optimized for

extraction of a particular compound (or a certain class of plant metabolites) and the extract can be directly used for gas chromatography (GC) or high-pressure liquid chromatography (HPLC). Among the modern methods, MAE has been proposed as more amenable to be coupled with subsequent separation and characterization operations. The on-line continuous sampling dynamic microwave-assisted extraction (on-line CSDMAE) coupled with high performance liquid chromatographic separation and determination of the lignans in *Wuweizi* and naphthoquinones in *Zicao* is one such example [37]. Compared with the conventional extraction methods, such as off-line continuous microwave-assisted extraction, ultrasound-assisted extraction and Soxhlet extraction, this method is claimed to be quicker and more effective. Optimization of microwave assisted extraction for the characterization of olive leaf phenolic compounds by using high-performance liquid chromatography (HPLC) coupled to electrospray time-of-flight mass spectrometry (ESI-TOF-MS) and electrospray ion trap tandem mass spectrometry (ESI-IT-MS2) has also been reported recently [38]. As compared to the conventional method, MAE is shown to be a better alternative for the characterization of phenolic compounds from olive leaves due to its efficiency and speed.

Numerous extraction processes are widely used in order to extract phytochemical compounds from medicinal and aromatic plants. Those methods can be separated into conventional methods, which have been widely used till date and nonconventional methods, which are becoming more and more popular because of their substantial benefits. Conventional methods include Soxhlet extraction, maceration, and hydro-distillation. Those methods are well established for the extraction of chemical compounds of various plant samples; however, they have some drawbacks such as the long extraction time and the use of costly and high-purity solvents in big amounts. In addition, there is low extraction selectivity and there is thermal decomposition of thermolabile compounds, when high temperature is used.

Other extraction procedures include infusion, digestion, decoction, percolation, modified percolation, aqueous alcoholic extraction by fermentation, and CCE for the extraction of the active components of medicinal plants and expression, cold fat extraction (enfleurage), protoplast extraction, cohobation, and phytosol extraction or phytonics process with hydrofluorocarbon solvents for the various extract types of aromatic plants.

Another trend in the extraction procedure of medicinal and aromatic plants is the replacement of traditional extraction solvents such as water, alcohol, acetone, chloroform, ether, etc. with some “green” alternative solvents such as ILs, DESs, and NADESs. Taking into account that there is no ideal extraction technique, the selection should be based on both chemical and economical parameters and despite the fact that there are many developed extraction methods reported in the literature, a lot of progress can be made in the future in this scientific field.

References

[1] S.S. Handa, SPS. Khanuja, G. Longo, DD. Rakesh, Extraction Technologies for Medicinal and Aromatic Plants, (1stedn) no. 66. Italy: United Nations Industrial Development Organization and the International Centre for Science (2008).

[2] K. Prasad Acharya, A. Mohan, Extraction methods, Journal of Medicinal Plants Research 4(2) (2010) 235-239.

[3] M. Rajadurai, VG. Vidhya, M. Ramya, A. Bhaskar, Methodology in plant extraction, Ethno-Med 3(1) (2009) 39-41.

[4] V. Mandal, Y. Mohan, S. Hemalatha, Pharmacognosy Reviews, 1(1) (2007) 7-18.

[5] Shams, K.A., Abdel-Azim, N.S., Hegazy, S.M., El-Missiry, M., Hammouda, F.M., Green technology: Economically and environmentally innovative methods for extraction of medicinal & aromatic plants (MAP) in Egypt, Journal of Chemical and Pharmaceutical Research 7(5) (2015) 1050-1074.

[6] SS. Handa, DD. Rakesh K. Vasisht., Compendium of Medicinal and Aromatic Plants, Asia, Vol. II, ICS-UNIDO, Trieste, Italy (2006).

[7] U. Ghosh, MA. Badhul Haq, S. Chakraborty., International Journal of Chemical and Analytical Science, 2(9) (2011) 1153-1158.

[8] BS. Rathi, SL. Bodhankar, AM. Baheti., Evaluation of aqueous leaves extract of Moringa oleifera Linn for wound healing in albino rats, Indian J Exp Biol 44 (2006) 898-901.

[9] M.D. Luque de Castro, L.E. Garcia-Ayuso., Soxhlet extraction of solid materials: an outdated technique with a promising innovative future, Anal. Chim. Acta 369 (1998) 1–10.

[10] T. Jain, V. Jain, R. Panday, A. Vyas, SS. Shukla., Microwave assisted extraction for phytoconstituents - An overview, Asian J. Res. Chem. 2 (2009) 19-25.

[11] S. Hemwimon, P. Pavasant, A. Shotipruk., Microwave assisted extraction of antioxidative arthraquinones from roots of Morinda citrifolia, Sep. Purif. Technol. 54 (2007) 44-50.

[12] M. Letellier, H. Budzinski., Microwave assisted extraction of organic compounds. EDP Sciences, Wiley-VCH, Analysis 27 (1999) 251-271.

[13] B. Kaufmann, P. Christen., Recent extraction techniques for natural products: microwave-assisted extraction and pressurized solvent extraction, Phytochem. Anal 13 (2002) 105-113.

[14] B. Trusheva, D. Trunkova, V. Bankova., Different extraction methods of biologically active components from propolis: a preliminary study. Chem Cent J 1 (1) (2007) 13.

[15] F. Chemat, E. Esveld., Microwave assisted heterogeneous and homogeneous reactions, Fifth international electronic conference on synthetic organic chemistry (ECSOC-5) (2001). http://www.mdpi.org/ecsoc-5.htm.

[16] V. Camel., Recent extraction techniques for solid matrices-supercritical fluid extraction, pressurized fluid extraction and microwave-assisted extraction: their potential and pitfalls, The Royal Soc. Chem. Analyst 126 (2001)1182-1193.

[17] T. Dhanani, S. Shah, NA. Gajbhiye, S. Kumar., Effect of extraction methods on yield, phytochemical constituents and antioxidant activity of Withania somnifera Arab J Chem 10 (2013) 1193-1199.

[18] MG. Cares, Y. Vargas, L. Gaete, J. Sainz, J. Alarcon., Ultrasonically assisted extraction of bioactive principles from Quillaja Saponaria Molina. Physics, Procedia 3 (2009) 169-178.

[19] X. Huaneng, Z. Yingxin, H. Chaohong., Ultrasonically assisted extraction of isoflavones from stem of Pueraria Lobata (Willd.) Ohwi and its mathematical model, Chin J. Chem. Eng. 15 (2007) 861-867.

[20] AH. Metherel, AY. Taha, H. Izadi, KD. Stark., The application of ultrasound energy to increase lipid extraction throughput of solid matrix samples [flaxseed] Prostaglandins Leukot Essent Fatty Acids, 81 (2009) 417-23.

[21] M. Alu'datt, T. Rababah, M. Alhamad, M. Al-Mahasneh, A. Almajwal, S. Gammoh, K. Ereifej, A. Johargy, I. Alli., A review of phenolic compounds in oil-bearing plants: distribution, identification and occurrence of phenolic, Food Chem. 218 (2016) 99–106.

[22] W. Rahmalia, JF. Fabre, Z. Mouloungui., Effects of Cyclohexane/Acetone Ratio on Bixin Extraction Yield by Accelerated Solvent Extraction Method, Procedia Chem 14 (2015) 455-464.

[23] Zeković, Z., Bera, O., Đurović, S., Pavlić, B., 2017. Supercritical fluid extraction of coriander seeds: kinetics modelling and ANN optimization. J. Supercrit. Fluids 125, 88–95.

[24] AA. Patil, BS. Sachin, PS. Wakte, DB. Shinde., Optimization of supercritical fluid extraction and HPLC identification of wedelolactone from Wedelia calendulacea by orthogonal array design, J Adv Res 5 (2013) 629-635.

[25] Y. Naudé, WHJ. De Beer, S. Jooste, L. Van Der Merwe, SJ. Van Rensburg., Comparison of supercritical fluid extraction and Soxhlet extraction for the determination of DDT, DDD and DDE in sediment, Water SA 24 (1998) 205-214.

[26] P. Tonthubthimthong, S. Chuaprasert, P. Douglas, W. Luewisutthichat., Supercritical CO2 extraction of nimbin from neem seeds an experimental study, J. Food Eng. 47 (2001) 289-293.

[27] R.S. Mohamed, G.A. Mansoor, The use of supercritical fluid extraction technology in food processing. Food Technol Magazine, The World Markets Research Centre, London, UK (2002).

[28] J. Azmir, I. Zaidul, M. Rahman, K. Sharif, A. Mohamed, F. Sahen, M. Jahurul, K. Ghafoor, N. Norulaini, A. Omar, Techniques for extraction of bioactive compounds from plant materials: a review, J. Food Eng. 117 (2013) 426–436.

[29] L. Nahar, SD. Sarker., Supercritical fluid extraction in natural products analyses. In: Sarker SD, Nahar L (eds) Natural products isolation, Methods in molecular biology, Springer, New York, NY (2012) vol 864.

[30] M. Puri, D. Sharma, C. Barrow, Enzyme-assisted extraction of bioactives from plants, Trends Biotechnol. 30 (1) (2012) 37–44.

[31] B. Vongsak, P. Sithisarn, S. Mangmool, S. Thongpraditchote, Y. Wongkrajang., Maximizing total phenolics, total flavonoids contents and antioxidant activity of Moringa oleifera leaf extract by the appropriate extraction method, Ind. Crops Prod 44 (2013) 566-571.

[32] MC. Kwon, WY. Choi, YC. Seo, JS. Kim, CS. Yoon., Enhancement of the Skin-Protective Activities of Centella asiatica L. Urban by a Nanoencapsulation Process, J Biotechnol 157 (2012) 100-106.

[33] PS. Vankar, J. Srivastava., Evaluation of Anthocyanin Content in Red and Blue Flowers, Int J Food Eng 6 (2010) 4.

[34] Oancea S, Stoia M, Coman D (2012) Effects of extraction conditions on bioactive anthocyanin content of Vaccinium corymbosum in the perspective of food applications. Procedia Eng 42: 489-495.

[35] VP. Paulucci, RO. Couto, CCC. Teixeira, LAP. Freitas., Optimization of the extraction of curcumin from Curcuma longa rhizomes, Brazilian J Pharmacogn 23 (2013) 94-100.

[36] L. Wei, W. Zhang, L. Yin, F. Yan, Y. Xu., Extraction optimization of total triterpenoids from Jatropha curcas leaves using response surface methodology and evaluations of their antimicrobial and antioxidant capacities, Electron J Biotechnol 18 (2015) 88-95.

[37] S. Gao, J. You, Y. Wang, R. Zhang, H. Zhang., On-line continuous sampling dynamic microwave-assisted extraction coupled with high performance liquid chromatographic separation for the determination of lignans in Wuweizi and naphthoquinones in Zicao. Journal of Chromatography B 887 (2012) 35-42.

[38] A. Taamalli, RD. Arraez, E. Ibanez, M. Zarrouk, CA. Segura, GA. Fernández., Optimization of Microwave-Assisted Extraction for the Characterization of Olive Leaf Phenolic Compounds by Using HPLC-ESI-TOF-MS/IT-MS2, J. Agric. Food Chem. 60 (2012) 791-798. doi: 10.1021/jf204233u

Design of optical sensor to detect different types of blood groups in a non-invasive way based on photon radiation technology

Neda Azimian[1], Hamed Alipour Banai[2]*

1 Department of Medical Engineering, Tabriz Branch, Islamic Azad University, Tabriz, Iran

2 Department of Electrical Engineering, Tabriz Branch, Islamic Azad University, Tabriz, Iran

*Email: azimiyaaannedaa@gmail.com alipour@iaut.ac.ir

Abstract

Increasing medical needs and the urgent need for blood is one of the major challenges in the medical world. But time is always an important and vital factor in treatment. Diagnosis of blood type for acute and urgent cases, in addition to speed of response, requires high accuracy and trust, using different methods and techniques in a traditional and laboratory way leads to increased cost, response time and reduced reliability.

Therefore, using intelligent and non-invasive methods with high functional accuracy is a necessity. In fact, mechanized methods without human intervention is a new approach in the field of medicine and treatment.

The method presented in this paper consists of several different and interdependent steps. In the first step of the proposed approach with photon radiation analysis, initial images of the photon wave are obtained using the Maxwell function and other edge detection techniques. Also, the image obtained from the point of view of implicit features and conformity with the model data is examined. In the next step, according to the initial data, Selecting the selected time series model from Arma models. Arima, moving average is discussed, After selecting the selected model based on the low prediction error, the neural network technique has been used in two phases of learning and diagnosis. At this stage, the photon wave image data are matched with the learner and pattern data to determine the blood group. The proposed method is compared to similar methods.

Keywords: Blood type, photon radiation, time series error model, neural network

1. Introduction

It is necessary to determine the blood type before transfusion or blood transfusion, for example in emergency situations.

At present, these tests are performed manually by technicians, which can lead to human error. Various systems have been developed to automate these tests, but none of them have the ability to perform timely analysis for emergency situations.

The aim of the present study is to develop an automated sensor-based system for performing these tests in a short period of time in accordance with emergency situations. To achieve this, slide testing and image processing

techniques using IMAQ Vision are currently being used by national tools to reveal the slide test image and the occurrence of agglutination. Data mining is one of the recent advances in computer science for in-depth data exploration. Today, the health and medical sector is in the greatest need for data mining, and the move from traditional medicine to evidence-based medicine is one of the things I could emphasize. Nowadays, the interpretation of optical images, both microscopes and telescopes, has necessitated the use of intelligent image segmentation techniques. Therefore, data mining as a modern and intelligent approach in these matters has become the vanguard of all intelligent algorithms. But one of the most important challenges of blood type diagnosis is to take advantage of an approach with high functional accuracy and non-invasiveness. Various methods and standards have been proposed for this purpose. Most of the proposed methods are aggressive and have a human error rate. In this paper, to increase the reliability and use a non-invasive approach, an optical sensor-based approach with photon radiation technology has been used. The structure of the article is as follows: In the second part (2), the basic concepts related to blood group, image processing, image segmentation and photon crystal are explained. In the third part (3), useful excerpts from previous studies and researches similar to the subject of the article are briefly and usefully explained, and in the fourth part (4) the proposed method is described. Finally, the evaluation and model are discussed. ¬The construction of the proposed method is discussed.

2. Basic concepts

Nowadays, different definitions of concepts are mentioned according to the type of application and their efficiency. In this article, concepts are defined according to the application and type of use.

2-1 Blood type

It is a method of dividing blood based on the presence or absence of certain inherited antigens on the surface of red blood cells. Blood in humans occupies 5 liters of body volume. Blood types are different in different people, and this has led to different types of blood types among people. Each person's blood type is determined by transferring related genes from their parents. One of the well-known methods for identifying blood type is the ABO system. It is worth noting that in addition to the blood groups that can be identified by this method, there are other blood groups that are fewer in different populations. Blood type of each person directly to the parents and what they inherit from them. Reach, is relevant. Today, among more than 20 types of blood grouping systems, ABO and RH systems are the most important [1].

2-2 Image processing

Image processing is one of the most important issues in artificial intelligence. Image processing is a branch of computer science that deals with the processing of digital signals that represent images taken with a digital camera or scanned by a scanner. Image processing is any type of signal processing that is the input of an image, such as a photo or scene from a movie. The output of the image processor can be an image or a set of special symbols or

image-related variables. The earliest applications of digital image processing in the 1960s and 1970s were military and espionage aspects, which necessitated higher quality images [2].

2-3 image fragmentation

Fragmentation is the labeling of pixels in medical images. Fragmentation divides the image into separate sections, each of which has uniform brightness levels. In medical imaging, it is important to accurately identify the tissue boundary to view the tissues.

In addition, magnetic resonance imaging has many applications [3] .Imaging is a classic subject in the field of image processing and is also one of the key topics in this field. Image segmentation is often described as the process of dividing an image into its constituent parts, or extracting parts of the image in question.

2-4 photonic crystals

Photonic crystals are a set of wave motifs that are regularly placed next to each other to create an interference pattern of desired degrees. Thus there are many similarities between a photonic crystal and an array of uniform antennas, which is very instructive.

It can be said that a photon crystal is an array of very small antennas that are placed next to each other in a regular arrangement of one, two or three dimensions. If hypothetical isotropic antennas were used for this purpose, we would have a network of antennas that, due to the constructive and destructive interference of network members in different directions of space, could input power like an array of antennas in the direction of Disperses certains. However, if antennas with anisotropic scattering pattern are used (as is often the case), the scatter pattern of the product will be the pattern of the overlap of each antenna and the network interference pattern [4].

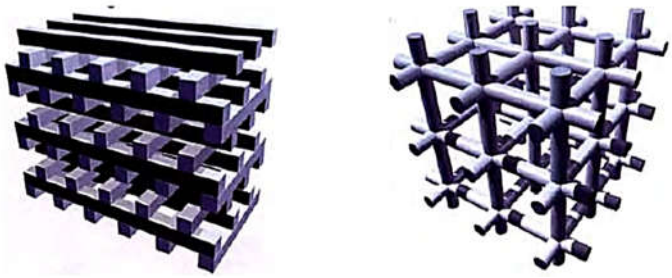

Figure 1: Two samples of cubic photon crystals (right figure) and structure (FCC left figure) [4].

3. Previous works

In this section, due to the breadth of the subject under study, several similar studies have been conducted. Most of the methods and research done here are focused on blood type detection using automated approaches and artificial intelligence with minimal human error. The following is a description of some of the research done.

Vijay A, Kanade A study entitled "Blood Type Determination Based on Image Processing Techniques Using Optical Sensor" was presented in 2017. In this study, the proposed idea is a non-invasive method to identify the patient's blood type without perforation of the skin. Using image processing algorithms, the paper provides a method for automatic determination of human blood using images taken from optical images of superficial capillaries under the skin. Based on image processing, it is possible to safely determine a patient's blood type in a short period of time without the need to take a blood sample, thereby eliminating the pain caused by the needle. This process is useful in emergencies, blood transfusions, etc. because it reduces the time and hassle of manual blood adaptation testing for the patient [5].

They presented a study entitled Non-invasive extraction and determination of blood sugar level in 2017. Significant research into the development of a system capable of non-invasive diagnosis and intelligent classification of hypoglycemia in diabetic patients.

Isotropic

In fact, the analytical method for controlling blood sugar levels without direct extraction of blood samples by examination and classification of acetone compounds in the breath is presented here. This classification is based on the measurement and desired amount of physical activity and for recommendations Lifestyle management is provided to the user. To address the identified research challenges, the authors propose a sensor-based solution that can detect and measure blood glucose levels by extracting acetone from the human breath without the use of blood sampling.

An algorithm for measuring processing, including considering the embedded relationship between acetone and blood sugar, is then designed and built for real-time, dynamic, and intelligent classification.

A decision support system that uses a combined NN and FLC method to process intelligent information that is patient-specific and compatible with the lifestyle of a diabetic provides a customized solution that affects the lives of diabetics[6].

An electronic system and an interface program are provided that can quickly and easily perform all pre-transfer tests in high security conditions, even in remote locations. For this purpose, this system is based on the screen test method and is small in size and easy to carry. Another advantage of this system is its low cost, which can be a factor in competing in the market. In addition, data mining is based on image processing techniques to obtain results and is developed using the C # programming language. The user interface was developed with the Xaml programming language, because the requirements of usability, compatibility with various operating systems, including computers, tablets and smartphones, have imposed this issue [7].

Hamedani et al. Presented a study entitled Non-invasive diagnosis of human fetal RhD genotype from serum sample of RhD-negative mothers using Heminested-PCR in 2006. RhD antigen plays an important role in the development of neonatal hemolytic diseases. Free fetal DNA in the serum of pregnant women should be determined non-invasively using Heminested PCR. Evaluation of the results of this study showed that in 37 of the 41 traceable samples, fetal RhD was 95.45% correctly determined. The results were for the remaining 4 samples, including one false negative and three false positives. This study showed that maternal serum samples are very

suitable for prenatal diagnosis of fetal RhD blood group in a non-invasive manner and with the lowest risk for the baby [8].

Ali Dolahaei and colleagues presented a study entitled "Investigation of the relationship between ABO and RH blood groups with hepatitis surface antigen stability in 2005". Hepatitis is a general term for inflammation of the liver, which can be caused by a variety of factors, including viruses. Data were analyzed by SPSS software using chi-square test. The distribution of ABO blood group was similar in both groups and no statistically significant difference was observed.

(97.9%) 232 people in the case group (90%) 226 people in the control group were Rh positive ($p < 0.0001$). Due to the lack of significant differences in the ABO system between the two groups, the system of this blood group probably does not play a role in contributing to the chronicity of the disease. However, considering the existence of significant differences in the Rh system, more extensive studies should be conducted in this field [9].

A study entitled The use of an automated system for determining blood type using image processing techniques was presented in 2013. This study introduces a new system that automatically determines blood type and at the same time human error in short Eliminates time. The system is based on a slide test to determine blood types and software developed with Using image processing techniques works. This method uses the possibility of analysis to determine the blood type in emergency situations and allows the management of a compatible blood type in the first unit of blood transfusion and elimination of possible blood incompatibilities. The goal of future work is to upgrade the system or make it smaller, so that it can be portable and use GSM technology, and to avoid unnecessary travel, a message is sent to the mobile technician of the trusted laboratory.
In addition, the goal is to use the other pre-injection tests required in the system to make the injection as safe as possible [10].

4. The proposed method

Before describing the method of the article, first its general trend is shown in Figure (2).

According to Figure (2), in the first step, the clients refer to the relevant centers to diagnose their blood type. In the relevant center, an optical sensor designed based on photon radiation is used. In fact, the sensor in question is assisted. The carrier force itself, which can be seen in the microscopic bed, should be analyzed and examined in order to determine the result based on the study and finally the grouping. The mechanism in question is defined as an image processing system in this article. At this stage, there are several different approaches to accurately detect and reduce errors in detection. Error checking is used with the help of time series methods. It becomes nervous. Finally, with the help of various indicators and parameters, the result and grouping are determined. This approach, in addition to reducing the amount of error in diagnosis, also increases the accuracy of diagnosis. Finally, the output of the processing and analysis is delivered to the medical staff.

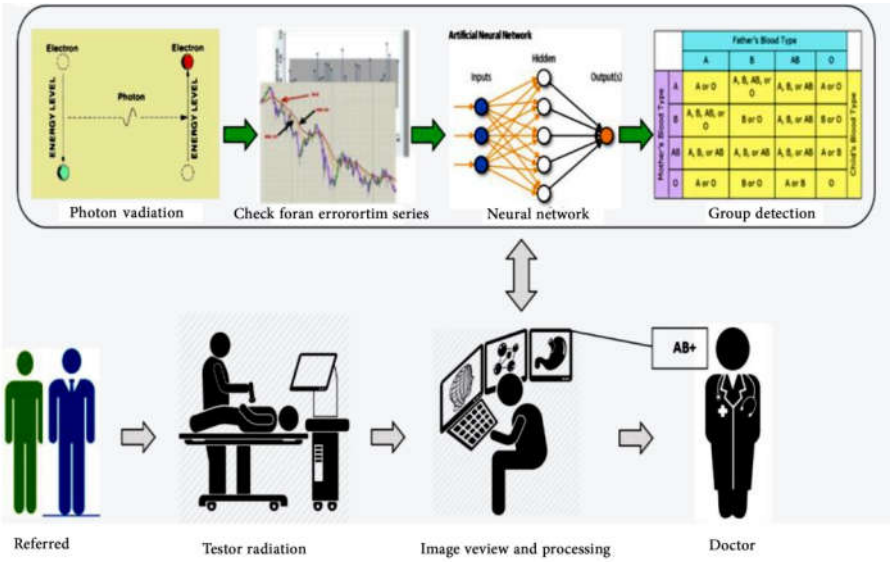

Figure 2 Process of the proposed method

1-4 Photon emission and application of scattering and absorption theory

In this section, considering that the purpose of blood group detection is based on the design of an optical sensor, the photon wave is used because it carries electromagnetic force. In fact, in photon wave analysis, different patterns of waves are drawn based on the theory of scattering and image absorption. In other words, photons pass through the skin in each blood group in different forms and this can be investigated by image processing. When light passes and cuts through capillaries for dynamic classification of blood cells based on antigen Special operations are performed on the surface of red blood cells using the dispersion technique. The advantage of using this theory to study dispersion is that the whole problem can be formulated as a first-order problem.

It is debatable that a photon, like other elementary particles, has a wave function (state vector) as a function of location, which still has no solid theoretical basis. The definition of the "wave function" of a photon is Equation (1)

$$\vec{\nabla} \times \vec{\psi} \equiv \mathrm{j}\frac{\mathrm{n}}{\mathrm{c}}\frac{\partial}{\partial \mathrm{t}}\vec{\psi} + \sigma\vec{\psi}$$

. In this regard, the σ coefficient of conductivity of the environment is in the general case of a place.

This means that conduction loss is intended for both electric and magnetic currents. In dispersion theory, the goal is to determine the specificity of the impaired hamilton function by not having the specific Hamilton function.Since the elastic scattering is considered (the photon energy does not change or equivalent to the wave frequency), the values corresponding to the mentioned functions are equal. Particle dispersion response Landing with mode vector $|\underline{\varphi}>$ Is given by the scattering disorder V by Lippmann-Schwinger equation, shown in Equation (2).

(2)

$$|\underline{\psi}> = |\underline{\varphi}> - \frac{1}{\underline{\underline{\hat{H}_0}} - E} V |\underline{\psi}>$$

In this equation φ Specific state of unchanged Hamiltonian (particle or landing wave) and They are $|\psi\rangle$ specific to the disturbed state of hemiltin (scattered particle or wave).

2-4 Error evaluation in time series methods

In this section, three models (Arma. Arima, mean moving average) are examined by determining how the error is evaluated in each of the models. Arma is the first model discussed. In this method, the analyst first designs an experimental model based on past information. It then estimates the coefficients of the variables of the model and controls the model with the help of available information to measure its predictive power. The overall structure of the model is in accordance with Equation (3).

$$Z_t = \emptyset_1 Z_{t-1} + \emptyset_2 Z_{t-2} + \cdots \emptyset Z_{t-pp} + a_t - \theta_1 a_{t-1} - \theta_2 a_{t-2} - \theta_p a_{t-p}$$

$\emptyset_1 . \emptyset_2 . \ldots . \emptyset_p$ Coefficients and parameters of AR model and a_t random and time-independent value that follows a normal distribution with a mean of zero. Shows the $\theta_1 . \theta_2 . \ldots . \theta_p$ coefficients and parameters of the MR model. Arima is one of the famous time series modeling methods that is mainly used to predict time series. In relation (4),:

$$\text{RMSE} = \sqrt{\sum_{i=1}^{n} (Q_{ci} - Q_{oi})^2 / n}$$

RMSE is the root mean square of the error,: MBE is the mean bias error i: Also, the Qci following i .Qoi three indicators have been used to determine the time error and determine the best forecast time.(5)

$$F_i = \sum_{i=1}^{n} E_i \ / iE_i = |Q_{ci} - Q_{oi}| \ / Q_{oi}$$

In the above relationships, RelativeE_i error in the I,F_i month Mean I, $\bar{E}$ comparative relative error per i month Mean $\bar{E}$ relative error and The coefficientC_v of variation is relative error. But the third model under consideration is the average moving average, which is constantly updated with new information. The simplest way to calculate the average moving average is to consider the actual statistics in the last period for the next period. Be. One of the drawbacks of choosing a course in calculating the moving average is that all the factors influencing the actual statistics of the previous course are reflected in the next course, and this may not always be true.

3-4 Neural network examination and evaluated features

One of the most basic neuronal models available is the multilayer perceptron model, or MLP, which mimics the translational function of the human brain. Therefore, in order to find the best network-building architecture, one must proceed with trial and error. The neural network is designed using MATLAB software in such a way that it is able to receive wave images prepared from photons available from the beginning of the experiment until time t. Slow and then trained using this data and able to predict blood type detection in the time interval t to less

than the threshold time. This prediction is designed as a test for the performance of the designed model. In fact, the various steps we have in this section are data separation, normalization, learning, and prediction. . To do this, three criteria of total error squares, mean absolute magnitude of error and criterion of mean percentage of absolute magnitude of error were used.

5. Results

According to the proposed method, first, with the help of photon radiation and important criteria in the detection of received signals, an image of the individual's blood group is received in the form of intermittent electrical pulses. And determining the type of blood group by means of light transmission, light cutting, scattering, absorption, Birolla and Silberstein theory define the Maxwell wave function and finally the final evaluation is done with the help of the model developed in MATLAB tool. (3) The output of the evaluation performed using a prototype reconstructed image is shown by photon irradiation.

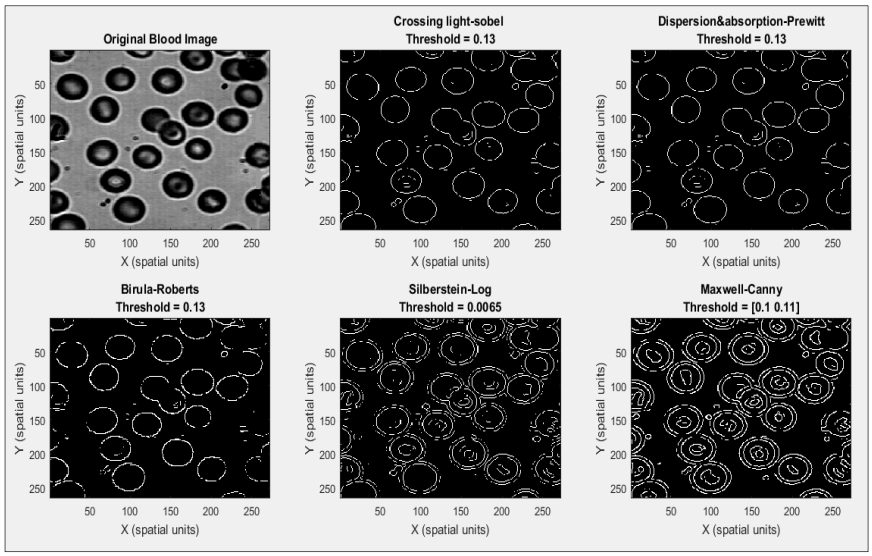

Figure 3 Photon wave edge detection on blood

In Figure 4, the output with higher resolution represents the dimensions and size of the cells by means of a photon wave.

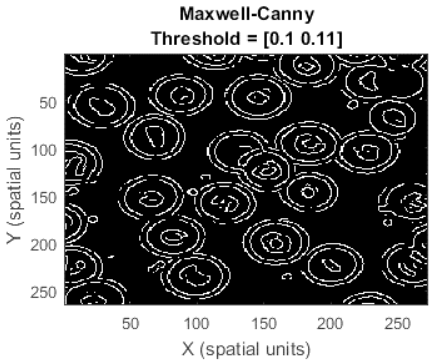

Figure 4 Detection of the final globule by photon wave radiation using the Maxwell function

The target database has 4888 records and 23 different indicators. In this section, to select the model, measure specific values of the conditions defined as MA (1), Ma (2), ARMA (1,1), ARMA (1,2), ARMA (2,1), ARMA (2,2), ARIMA (1,1,1), ARIMA (1,2,1) ARIMA (2,1,1), ARIMA (2,2,1), ARIMA (1,1,2), ARIMA (1,2,2) is performed. Among the studied models, ARMA (2,1) is more suitable for data production and has been selected as the final model. Table (1) shows the results of error detection of time series models.

Table 1 Results of experiments performed

Statistict	Standard Error	Value	Parameter
17.2312	599132	1.03E+07	MA(1,2)
78.5796	1551.17	121891	ARMA(1,1)
19.1145	56680.3	1.08E+06	ARMA(1,2)
79.1362	1526.36	120790	ARMA(2,1)
3.15E+06	0.353958	1.11E+06	ARMA(2,2)
75.2421	1706.18	128377	ARIMA(1,1,1)
77.9411	1635.81	1.27E+05	ARIMA(1,2,1)
79.3933	1531.95	121627	ARIMA(2,1,1)
78.6531	1603.65	1.26E+05	ARIMA(2,2,1)
78.9584	1547.47	122186	ARIMA(1,1,2)
78.2319	1588.9	1.24E+05	ARIMA(1,2,2)

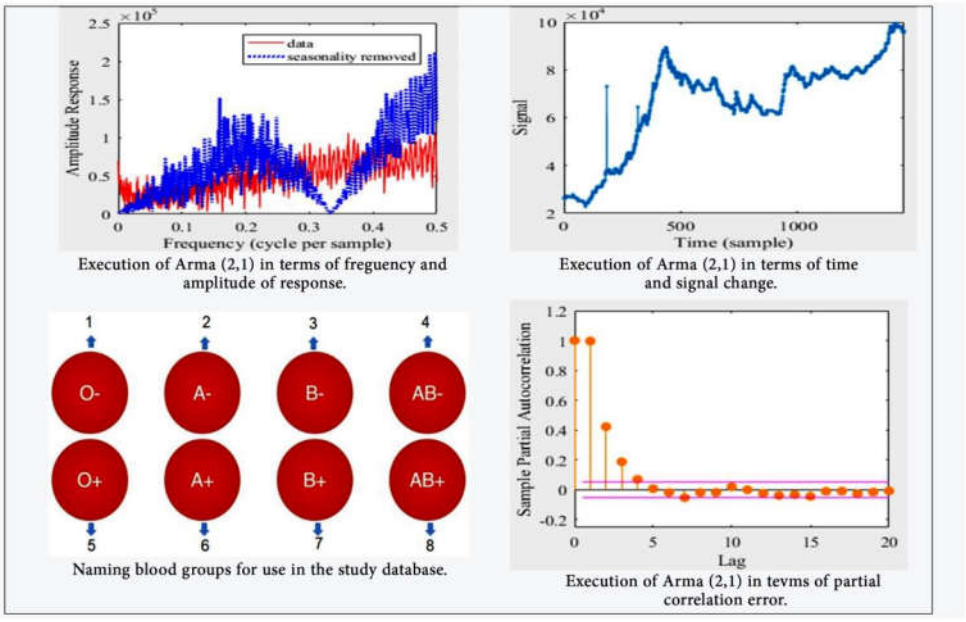

Figure (5) shows the output of the model performed to use the ARMA time series model in the MATLAB tool.

Figure 6 Results of ARMA implementation (2,1) using a model performed in MATLAB tool

There are several cases according to the intended output, which indicates the blood type for individuals, here the number 1 indicates a negative blood type o and other numbers each indicate a different blood type. Labeling to identify blood groups is to ensure that the data used for the neural network algorithm are uniform and that all

are numerical and usable data. Figure (7) shows the total square root of the error of each prediction by increasing the number of layers in the neural network on the studied system.

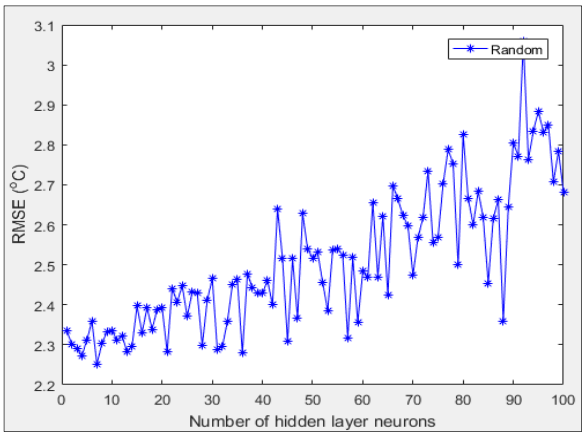

Figure 7 The sum of the square root of the error of each prediction with respect to the number of layers in the neural network

Figure (8) shows the best validation performance with the number of periods of 7. The number of iterations on one side and the average squares of the error are shown on the other.

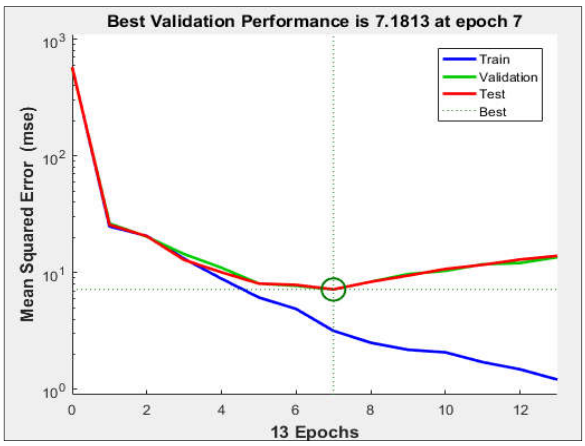

Figure 8 Chart of selecting the best validation performance according to the number of iterations

Figure (9) shows the error diagram with respect to the stop conditions.

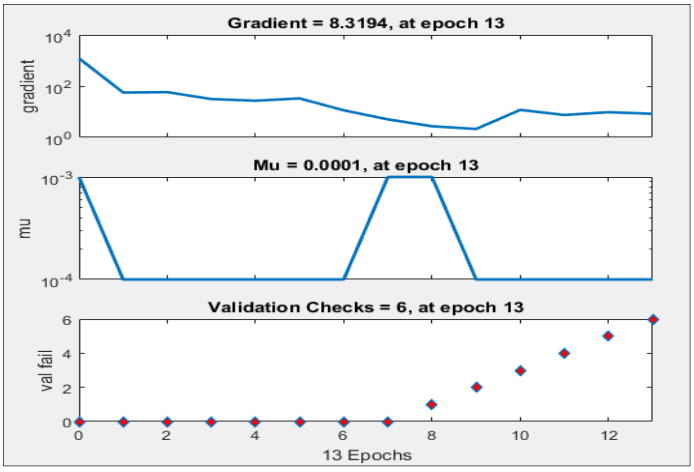

Figure 9 Graph of the amount of errors according to the optimization stop conditions

Figure (10) shows the degree to which each category of data belongs to different errors.

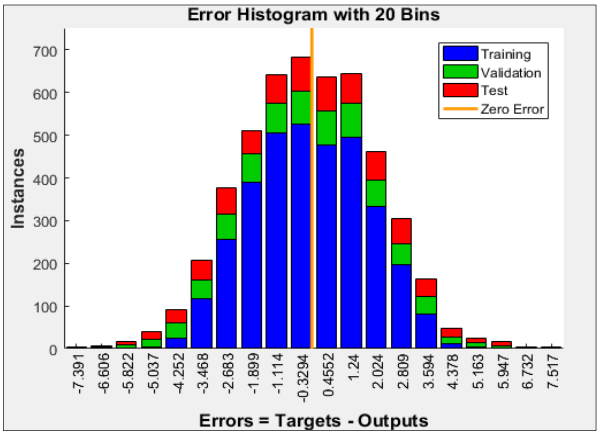

Figure 10 The degree to which each category of data belongs to different errors

In order to show the good quality of the use of the neural network, Figure (11) summarizes the output of the neural network and the real one, and if the two coincide, it indicates the good quality of the neural network.

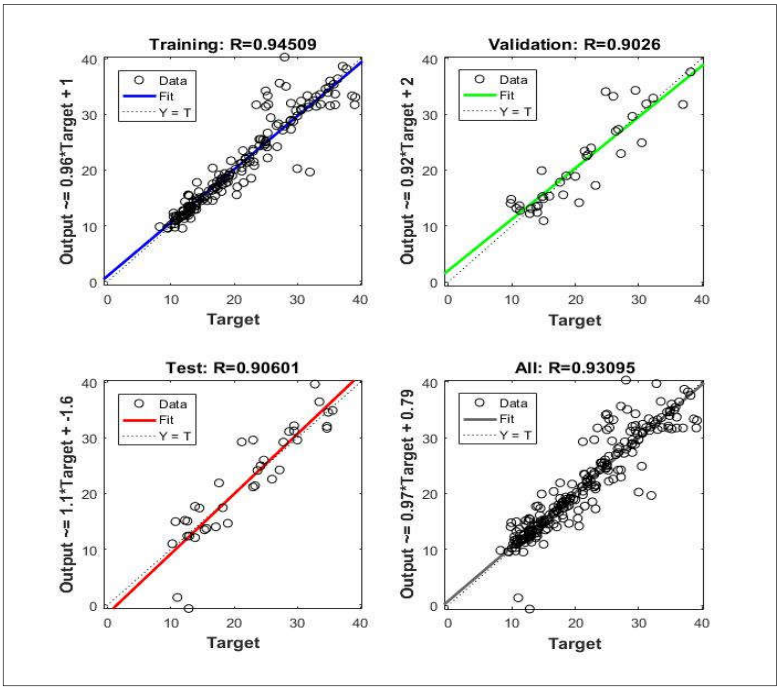

Figure 11 Comparison of neural network quality and actual with target adaptation

The output of the neural network algorithm for the effect of the characteristics on the prediction of blood group is obtained using the proposed method as shown in Figure (12).

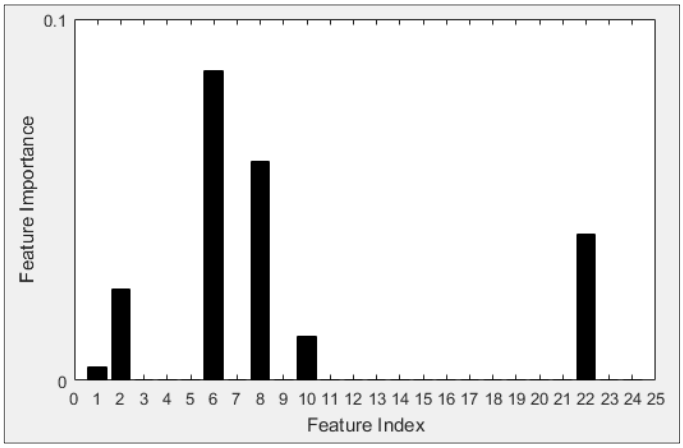

Figure 12 The effect of characteristics on blood group prediction using the proposed method

Figure (13) shows the three methods of ARMA, neural network and the combination of these two strategies in terms of prediction error with respect to the number of repetitions.

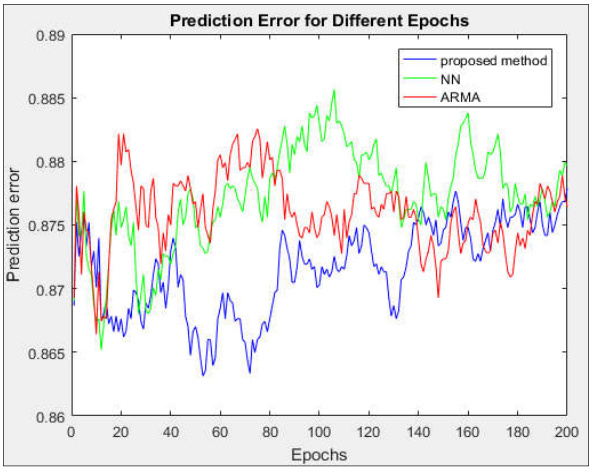

Figure 13 Comparison of three models in terms of prediction error with respect to the number of iterations

6. Conclusion

Automatic diagnosis of blood type can be useful and used in emergencies and in the absence of a knowledgeable technician in medical centers. Also, in research work and large sample size, an automated system will increase the speed of work. In this article, focusing on one of the non-invasive and intelligent methods for detecting blood type, image processing technique has been used. In this way, by photon irradiation and photon wave detection with low edge detection and measurement error and elimination of noise and other disturbances in photon wave detection, the Maxwell function was used, then the final image as a data and initial record to the data of Predefined was added to the system. In this way, the initial database is the result of experiments and experiments and laboratories of different people were examined and analyzed so that the data are integrated and uniform. In the next step, according to the nature of the algorithms used, the data The datasets used were normalized and numerically used to describe intelligible numbers. Then, different time series models were used to determine the prediction approach with low error rate, and finally, according to the results, a model was selected and finally, using a neural network algorithm in two stages of training and data-based testing. The study was performed. The results of the evaluation indicate the desirability of the proposed method for diagnosing blood type in a non-invasive and safe approach. One of the important innovations in this research is the reliance on image processing and detection techniques based on photon radiation analysis and initial drawing of red blood cells in the blood of individuals, which is identified and matched based on different size dimensions and pulses. Patterns are learning, as well as the use of a combined method based on time series model and neural network are other advantages of this article. Contained in it increased.

It also used a dynamic and concurrent evaluation mechanism to prove and validate the proposed method in critical and different situations, and the possibility to expand and develop hardware and software to apply the proposed method and enter the real environment. Dad. In fact, the proposed method for implementation in a real environment requires careful modeling and evaluation of important and different parameters before the

implementation and implementation phase, so providing a dynamic and workable model can be a quick way. Be considered in access to practical reality in hospitals and medical staff.

References

[1] Acevedo, A., Merino, A., AlférezJosé, S., (2020),"A dataset of microscopic peripheral blood cell images for development of automatic recognition systems", Data in BriefJune, Vol 6, pp.456-471.

[2] Ruberto, C., Loddo, A., Putzu, L., (2020),"Detection of red and white blood cells from microscopic blood images using a region proposal approach", Computers in Biology and Medicine, Vol 24, pp. 326-338.

[3] ترجمة ع. جعفرنژادقمی، ویرایش دوم، نشر علوم رایانه، بهار ۱۳۹۱MATLABر گنزالس، پردازش تصویر دیجیتال با زبان.

[4] Anilkumar, K.K., Manoj, V.J., (2020), "A survey on image segmentation of blood and bone marrow smear images with emphasis to automated detection of Leukemia", Biocybernetics and Biomedical Engineering, Vol 40, Issue 4, pp. 1406-1420.

[5] Babazadeh,N., Salehian, P., Arabalibeik, H., Setayeshi, S.,(2017), "MCV Measurement of Abnormal Red Blood Cells Using Adaptive Neuro-Fuzzy System with Image Processing", Sarem Journal of Reproductive Medicine, Vol 3, pp. 97-104.

[6] Dong Sung Kim, Se Hwan Lee, Chong H. Ahn, Jae Y. Lee, Tai Hun Kwon, (2005),"disposable integrated microfluidic biochip for blood typing by plastic microinjection moulding", Academic research paper on "Chemical sciences".

[7] Anderson, K., Prylutska, H., Ducharme, A., Harel, F.,(2014),"Evaluation of the right ventricle: Comparison of gated blood-pool single photon electron computed tomography and echocardiography with cardiac magnetic resonance", International Journal of Cardiology, Vol 171, Issue 1, pp. 1-8.

[8] Catherine Todd, Paola Salvetti, Katy Naylor, and Mohammad Albatat (2017), "Towards Non-Invasive Extraction and Determination of Blood Glucose Levels", Bioengineering (Basel), Vol 27, pp. 70-82.

[9] Rahmdani F, Mesbah-Namin S, Tarihi T., (2006), "Non-invasive fetalRhD genotyping by hemi-nested PCR of maternal serum in RhD-negative pregnancies", Sci J Iran Blood Transfus Organ, Vol 3, pp. 93-100.

[10]Ferraz, A., Carval, V., Machado, H.,(2020), "Determination of human blood type using image processing techniques", Measurement, Vol 97, pp. 165-173

Biocomposites containing bioactive glasses with potential application in wound repair and regeneration

Tina Mehrabi, Abdorreza S. Mesgar*

Biomaterials Laboratory, Division of Biomedical Engineering, Department of Life Science Engineering, Faculty of New Sciences and Technologies, University of Tehran, Tehran, Iran

*Email: asmesgar@ut.ac.ir

Abstract

The healing of burn injuries and chronic wounds associated with the prolonged hospital stay and mortality of patients following the extensive skin damages have always been among the healthcare issues. Despite the emerging of several advanced wound dressings and skin substitutes over time, shortcomings of these wound care products have led to the ongoing development of novel therapeutic strategies, specifically biomaterial-based approaches. Bioactive glasses are one of the most widely used subgroups of bioceramics that have been extensively studied for hard tissue replacement. In recent years, this class of materials has shown specific therapeutic effects on soft tissue regeneration, including skin tissue. The promising potential of bioactive glasses in distinct but overlapping stages of wound healing, including hemostasis, inflammation, proliferation, and remodeling, as well as participating in the early stages of repair with their antibacterial activity has been proved. The incorporation of bioactive glass nano/microparticles into the polymeric matrix enables the fabrication of multi-functional biocomposites, which may be used at the wound site to address the requirements of the wound healing process. This review highlights the biological effects of bioactive glasses in healing phases and summarizes the current progress of bioactive glass-containing composites in the field of wound healing.

Keywords: Biocomposites, Bioactive glass, Wound Healing, Skin Tissue Engineering.

1. Introduction

The skin is the largest and active immune organ in the human body, which functions as the outermost protective barrier against micro-organisms, ultraviolet radiation, and external physical and chemical insults [1,2]. Moreover, skin plays a key role in vitamin D synthesis, thermoregulation, sensory perception, and protecting the body against dehydration [3]. Skin wounds can be caused by trauma and surgical procedures but extensive skin damages in burn patients and the complications of healing in chronic wounds are among health issues that lead to the prolonged hospitalization of patients and mortality. The wound healing process, which initiates in damaged skin to restore the native structure, integrity, and functionality of the tissue, comprises four distinct but overlapping stages, including hemostasis, inflammation, proliferation, and remodeling, [4]. In some cases, the normal healing process may be delayed or impaired by local (e.g., infection and ischemia) and systemic factors (e.g., diabetes, malnutrition, and aging), and when the wound does not heal within a reasonable time (3-6 weeks) and stuck in one of the stages of healing, it would be considered as a chronic wound [5].

Over time, various types of wound dressings and skin tissue engineering scaffolds in the form of hydrogels, sponges, foams, fibers and films have been investigated and several advanced wound care products based on biomaterials, cells, and signaling molecules are under research and development [6–8].

Moreover, biocomposite wound care products composed of a natural/synthetic polymeric matrix (e.g., collagen, gelatin, alginate, chitosan, fibroin, polyvinyl alcohol, and polycaprolactone) and nano/microparticles as an additive (e.g., silver and gold nanoparticles, zinc oxide, cerium oxide, copper oxide, and bioactive glass) have been suggested to take advantage of the properties of both components. The invention of 45S5 bioactive glass by Professor Hench in 1969, revolutionized the field of biomaterials because of the ability of this man-made material to bond to living tissues [9,10]. Over the last decades, silicate, borate, and phosphate-based bioactive glasses exhibited possible potential in biomedical applications from soft to hard tissue repair and regeneration, including cardiac tissue regeneration [11], spinal cord injuries [12], gastrointestinal applications [13], lung tissue engineering [14], cancer treatment [15], and wound healing [16]. Consequently, the applications of bioactive glasses outside the skeletal system or hard tissues of the human body have extended the concept of "bioactivity", which arises from the formation of hydroxycarbonate apatite (HCA) at the surface of glasses in contact with physiological fluids [9,10].

The first bioactive glass-based wound care product is MIRRAGEN (also known as DermaFuse), which has received FDA clearance in 2016. MIRRAGEN is composed of 13-93B3 borate glass fibers with the formulation of $53B_2O_3$-20CaO-$2K_2O$-$6Na_2O$-5MgO-$4P_2O_5$ (wt.%). Interestingly, this dressing has a fibrous morphology that resembles the natural microstructure of fibrin clot and also it has increased the angiogenesis and migration of epidermal cells [17,18] Furthermore, other bioactive glass-based wound care products including Dermfactor in form of silicate-based glass powder and Arglaes composed of Ag-doped phosphate glass are also available [19,20]. Dermfactor has been used for burn wounds, diabetic foot ulcers, and bedsores; meanwhile, Arglaes is designed to control the infection of partial and full-thickness wounds by sustained release of Ag ions [19,21]. This review will discuss the structure, fabrication techniques, and biological behavior of bioactive glasses in the wound healing process and provides an overview of biocomposites containing bioactive glasses that have been used as a therapeutic strategy in wound repair and regeneration.

2. Bioactive glasses: structure, fabrication techniques and biological behaviour

2.1 Basics of bioactive glass structure and fabrication techniques

Understanding the basics of glass structure and structure-properties relationship can provide a tool to predict the glass properties, which may be useful for formulating bioactive glasses with specific biological behavior. Bioactive glasses are amorphous solid structures with short-range order, which lack periodic arrangement of atoms in their structure [22]. The structural components of bioactive glasses are network-forming oxides, network-modifying oxides, and intermediate oxides. Network forming oxides, including SiO_2, B_2O_3, and P_2O_5 are able to build the skeleton of glass, whereas network-modifying oxides such as CaO, K_2O, and Na_2O disrupt the glass network by altering the bridging oxygens between network forming elements to non-bridging oxygens.

Intermediate oxides such as ZnO, MgO, and TiO_2 act as a network former or network modifier depending on the glass composition [23,24]. According to the type of network forming oxides in bioactive glasses, they can be divided into the three groups of silicate, borate, and phosphate-based glasses, in which SiO_4^{4-} tetrahedron, BO_3 trigonal groups and PO_4^{3-} are basic structural units, respectively [25,26]. Upon changing the composition of glasses, the structural changes occur and the distribution of structural units in the glass network (structural units denoted as Q^n species, where Q defines network-forming polyhedron and n is the number of bridging oxygen atoms) can be determined by nuclear magnetic resonance (NMR) spectroscopy [27,28].

Melt-quenching and Sol-gel are two principal techniques for fabricating bioactive glasses. In the melt-quenching route, stoichiometric amounts of reagents such as oxides, nitrates, sulfates, or carbonates (commonly in the form of powders) are weighed and mixed, and the obtained powder is melted at high temperatures depending on the glass composition [29,30]. In the next step, the homogenous melt is poured into appropriate molds and cooled in order to produce desired bulk pieces (e.g., rods and monoliths) [31,32]. Additionally, small glass granules can be formed by quenching the melt in cold water and the obtained granules can be further dried, ground, and sieved to obtain glass powder. Finally, in order to remove the internal thermo-mechanical stresses in the glass, which are induced by rapid cooling, the glass undergoes a heat treatment step or annealing [33].

In 1991, another method for producing bioactive glasses called the "sol-gel" process was suggested by Professor Larry. Hench. The Sol-gel is a chemistry-based approach, which provides a more controlled and convenient route for developing homogeneous structures and overcomes the limitations of the melt-quenching method [25,34]. The most investigated type of bioactive glasses produced by the sol-gel method is silicate-based glass. Although, the synthesis of sol-gel derived borate and phosphate-based bioactive glasses has also been reported [35,36]. In the sol-gel technique, organometallic alkoxides such as tetraethyl orthosilicate (TEOS) are precursors of glass network formers and nitrate or carbonate salts are used as precursors of network modifiers. Processing steps of the sol-gel route are mixing, casting, gelation, aging, drying, stabilization, and densification [37]. In this method, mixing of alkoxide precursors, water, and/or ethanol as solvents and an acid or base catalyst (e.g., HNO_3 and NH_4OH) results in hydrolysis of the precursors associated with condensation reaction, which makes a homogenous solution named "Sol." Sols are dispersions of solid particles called "colloids" (with a diameter of <100 nm) in a liquid [37]. Considering the glass composition, precursors of network modifiers (e.g., calcium or phosphate salts) can be added during the hydrolysis and condensation of alkoxide precursor [38]. During the mixing step, colloidal particles agglomerate continuously, which leads to an increase in the viscosity of the sol and sol-gel transition or gelation. The polycondensation continues within the gel network during the next step called "aging", in which the gel is holding at temperatures of 25-80 °C for several hours or days. The aging step can increase the mechanical strength and densification of the gel that decreases the porosity of the material [27,39]. The drying step is carried out at temperatures of 120-180 °C to eliminate the liquid phase and physically adsorbed water from pores [39]. The stabilization step is the thermal treatment of dried gels at a temperature range of 500–900°C, in which sub-products such as nitrate ions decompose and eliminate from the glass [25]. If a nonporous final product with higher mechanical properties is required, the sintering or densification step is performed at higher temperatures to obtain a densified glass [27,40].

Melt-quenching is a less expensive method than sol-gel, due to the high cost of alkoxide precursors required in the sol-gel process. However, the relatively lower processing temperature of the sol-gel route enables the incorporation of temperature-sensitive molecules into the glass [27]. The other key advantages of the sol-gel method compared to melt-quenching are the high specific surface area of the obtained bioactive glass powders, the simpler equipment for glass synthesis and expanded compositional range of glasses. On the other hand, using a large amount of solvent, the difficulty of drying for structures with complex shapes and crack formation due to the shrinkage during the drying step are drawbacks of this method. Despite the advantage of large-scale production of bioactive glasses by melt-quenching route, this method has disadvantages, including compositional limitation, high-temperature processing, and inability to precisely control the properties of the resulting product (e.g., obtaining particles with regular shape and uniform size distribution) [38].

2.2 Biological behavior of bioactive glasses in wound healing process

In recent years, different silicate, borate, and phosphate-based bioactive glasses have been formulated to take advantage of their biological behavior for repairing and regenerating a target tissue. In this context, bioactive glasses can be considered as multifunctional materials because of their ability to release multiple therapeutic ions in contact with physiological environments, including wound bed. Several biologically active elements such as Au, Ag, B, Ca, Ce, Co, Cu, Ga, Se, Sr, and Zn can be incorporated into the glass network to obtain different glass compositions with specific properties [19]. Some of the above-mentioned chemical elements are required for maintaining a healthy state and proper functioning of the human body and some of them are known for their biological activities such as antibacterial and anti-inflammatory properties [32,41]. For example, the boron (B) element is involved in the inflammatory response [42] and extracellular matrix (ECM) synthesis [43]. It is reported that boron has a stimulatory effect on the migration of keratinocytes [44] and fibroblasts [45] and also angiogenesis [45]. As a clotting factor calcium (Ca) has a hemostatic effect and can regulate the proliferation of fibroblasts and collagen synthesis [46–48]. Cerium (Ce) and Zinc (Zn) are known for their antioxidant, anti-inflammatory [49] and antibacterial properties [50,51] and it may increase the migration and proliferation of fibroblasts, keratinocytes and vascular endothelial cells [52]. It is also suggested that cobalt (Co) [53], copper (Cu) [54], phosphorous (P) [53], and Strontium (Sr) [55] may stimulate angiogenesis.

Generally, the possible mechanisms of bioactive glasses, which considered as role players in promoting wound healing are as follows. Bioactive glasses can take part in the early stages of wound healing with their hemostatic potential and antibacterial properties [19]. Some of the major effective factors for the hemostatic ability of silicate-based bioactive glasses are glass morphology, porosity, surface area, pore-volume, Si/Ca ratio, and the presence of Ca^{2+} in the glass composition [56]. The antibacterial activity of bioactive glasses has sparked interest in using them in wound healing applications, because of the growing risk of wound infection and antibiotic resistance of bacterial strains. The antibacterial activity of bioactive glasses can be explained by the following mechanisms: 1) the release of alkali and alkaline earth ions as a result of glass dissolution in biological fluids, which can increase the pH and osmotic pressure of the local environment [57,58], 2) the bacterial cell wall damage induced by sharp glass debris, which can facilitate the penetration of antibacterial agents into the bacterial cytoplasm [58], and 3)

the incorporation of antibacterial metallic elements such as copper, zinc, silver, cerium, and gallium into the glass network [59].

It is investigated that bioactive glasses are able to regulate anti-inflammatory response, for example, ionic dissolution products of 45S5 bioactive glass have shown anti-inflammatory properties by activating the macrophages toward the M2 phenotype and up-regulating the expression of anti-inflammatory factors in macrophages [60]. Additionally, the results of in vivo studies on bioactive glass-treated full-thickness wounds of rats have also confirmed the reduction of inflammatory response due to the presence of fewer neutrophils and more M2 macrophages in the wound site [60]. The anti-inflammatory properties of bioactive glasses may further improve by introducing the metallic ions with inherent anti-inflammatory activity (e.g., zinc and cerium) into the glass network [61,62].

According to the in vitro and in vivo studies, cell functions such as cell migration, proliferation and cell viability have been affected by the ionic dissolution products of bioactive glasses, which may favor the new tissue formation in the wound bed. For example, the proliferation rate of keratinocytes increased by SiO_2-CaO-P_2O_5 glasses doped with gold nanoparticles [63]. In another investigation, the ions released from the Cu-doped borate glass microfibers increased the proliferation of fibroblasts and human umbilical vein endothelial cells [64].

Considering the fact that the regeneration of the damaged tissue relies on the formation of new blood vessels, which provide oxygen, nutrients and also immune cells in the wound bed, the development of wound dressings and skin substitutes with angiogenic potential is encouraging [65]. Furthermore, angiogenesis may be impaired in chronic wounds because of a decrease in expression of proangiogenic cytokines and overexpression of anti-angiogenic cytokines, consequently, treatment of chronic wounds requires therapeutic strategies that promote angiogenesis [65]. The angiogenic potential of bioactive glasses has attracted increasing interest to use them in soft tissue engineering, which arises from the potential of dissolution products of glasses in stimulating the secretion of proangiogenic growth factors such as basic fibroblast growth factor (bFGF) and vascular endothelial growth factor (VEGF) and proliferation of endothelial cells [53,66]. The approach of using bioactive glasses in the regeneration of skin tissue can be regarded as an effective inorganic ion delivery method that may overcome the limitations of growth factor-based therapeutic strategies.

3. **Biocomposites containing bioactive glass nano/microparticles: applications in wound repair and regeneration**

The idea of incorporating bioactive glass nano/microparticles as additives into the polymeric matrix is a strategic way to benefit from the advantages of polymers and bioactive glass for accelerating wound healing. A wide range of natural and synthetic polymers, including chitosan, alginate, gelatin, albumin, fibroin, cellulose, agarose, polyvinyl alcohol (PVA), polyhydroxybutyrate (PHB), and polycaprolactone (PCL), and different fabrication methods have been used to prepare polymer/bioactive glass biocomposites in the forms of electrospun composites, hydrogels, sponges and films as illustrated in Figure 1.

Table 1 summarizes the in vitro and in vivo studies of biocomposites containing bioactive glasses for wound healing applications.

The wound dressings and skin substitutes prepared by the electrospinning method have inherent advantages such as high porosity, high specific surface area and gas permeability and their morphology resembles the structure of natural ECM, which affects cell adhesion, proliferation, migration and differentiation [67,68]. Many researchers have studied electrospun composites containing bioactive glasses. For example, Chen et.al [69] fabricated chitosan/PVA/bioactive glass nanoparticles trilayer nanofibrous membrane via electrospinning for promoting chronic wound healing. The results of in vivo studies on full-thickness skin defect of rat and the diabetic chronic wounds of mice indicated that the composite membrane could enhance healing by complete re-epithelialization, improving the deposition and alignment of collagen and formation of skin appendages such as follicles and sebaceous glands [69]. Moreover, the composite accelerated wound closure in diabetic chronic wound by up-regulating VEGF and transforming growth factor-beta (TGF-β) growth factors and down-regulating inflammatory cytokines of tumor necrosis factor (TNF-α) and Interleukin 1 beta (IL-1β) that was attributed to the effect of bioactive glass [69]. Injectable hydrogels have become one of the most attractive candidates for treating wounds because of their inherent characteristics that mimic living tissues and are suitable for irregular shaped-wounds. Zhou et.al [70] designated an injectable albumin/45S5 composite hydrogel with adhesive property for stimulating wound healing. The amount of bioactive glass has regulated the gelation time of hydrogel and the ionic products of glass have promoted angiogenesis and wound healing [70]. The results of in vivo experiment indicated that composite hydrogels enhanced the collagen deposition, stimulated the migration of keratinocytes, differentiation of fibroblasts to myofibroblasts, and angiogenesis in chronic wounds [70]. Skin tissue engineering scaffolds in form of three-dimensional porous structures can provide a suitable microenvironment for skin regeneration, for

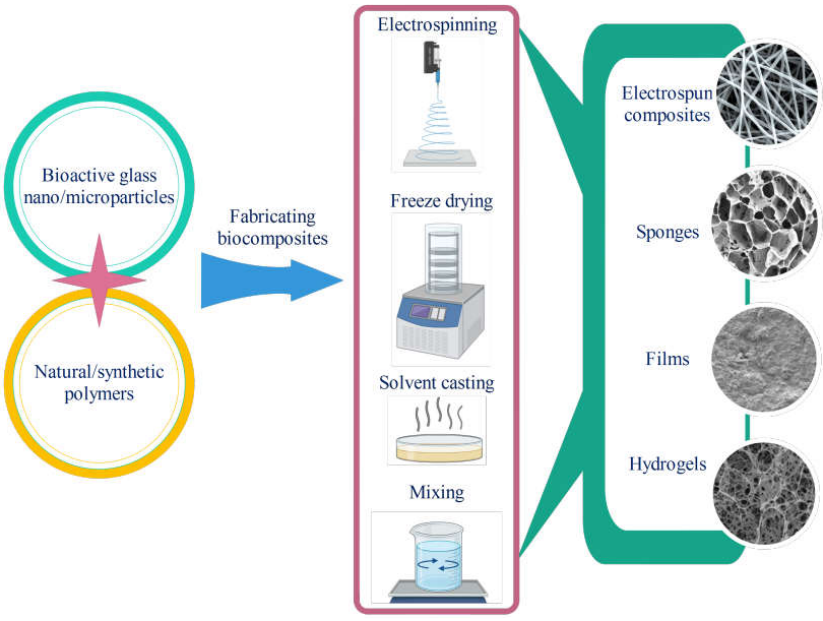

Figure 18. Schematic representation of different types of bioactive glass-containing biocomposites according to their fabrication method.

example, Li et.al [71] developed a hybrid composite composed of chitosan, silk fibroin and bioactive glass microparticles that promoted the formation of new blood vessels and accelerated wound regeneration. In another study methylcellulose/manuka honey/bioactive glass porous biocomposites improved the proliferation and migration of skin cells and showed antibacterial activity against E.coli and S.aureus bacteria [72].

Table 4. The summary of in vitro and in vivo studies of biocomposites containing bioactive glasses for wound healing applications

Type of biocomposite	Base composition	Glass system	Cell type (in vitro studies)	Animal model/type of wound (in vivo studies)	Ref.
Electrospun composite	Chitosan/PVA	SiO_2-CaO-P_2O_5	Mouse fibroblast cells (L929) and HDF	Rat and Mice/FT skin defects and diabetic chronic wound	[69]
	Gelatin/Chitosan	SiO_2–CaO–B_2O_3–P_2O_5–CuO–ZnO–K_2O–Na_2O	-	Rat/Chronic wound	[73]
	Polycaprolactone	SiO_2-CaO-P_2O_5	Human skin fibroblasts	-	[68]
Film	Soy protein isolate	1- SiO_2-CaO-Na_2O-P_2O_5 2- SiO_2-CaO-Na_2O-P_2O_5-K_2O-MgO 3- SiO_2-CaO-Na_2O- P_2O_5-K_2O-MgO-SrO	MEF	-	[74]
	P3HB	SiO_2-Na_2O-CaO-P_2O_5	Human keratinocyte	-	[75]
Hydrogel	Albumin	SiO_2-CaO-Na_2O-P_2O_5	-	Mice/FT Excisional chronic wound	[70]
	Alginate	SiO_2-CaO-Na_2O-P_2O_5	HUVEC	Rat/Diabetic wound	[76]
	Sodium alginate	SiO_2-CaO-Na_2O-P_2O_5	Murine-derived macrophage cell, L929 fibroblasts and mouse artery endothelial cells	Mice/FT Excisional wound	[77]
	PEGDA/Sodium alginate	SiO_2-CaO-P_2O_5-CuO	Endothelial progenitor cells	Mice/Diabetic wound	[78]
	Agarose/Alginate	SiO_2-CaO-Na_2O-P_2O_5	Fibroblast and HUVEC	Rabbit/Ischemic chronic wound	[79]
Sponge	Alginate/Agarose	SiO_2-B_2O_3-SeO_2	Normal skin fibroblast	-	[80]
	Silk fibroin/Chitosan	SiO_2-CaO-P_2O_5	NIH 3T3 fibroblast	Rat/FT burn wound	[71]
	Methyl cellulose/Manuka honey	1- Na_2O-K_2O-MgO-CaO-B_2O_3-P_2O_5 2- Na_2O-K_2O-MgO-CaO-B_2O_3-P_2O_5-CuO	MEF, HDF and Human keratinocyte cells	-	[72]

Abbreviations: FT: Full Thickness, MEF: Mouse Embryonic Fibroblasts, HDF: Human Dermal Fibroblasts, HUVEC: Human Umbilical Vein Endothelial Cells, PVA: Poly Vinyl Alcohol, PEGDA: Polyethylene glycol diacrylate, P3HB: Poly(3-hydroxybutyrate)

4. Conclusions

The present review has highlighted the therapeutic potential of bioactive glasses in wound healing applications and the possibility of developing biocomposite wound care products by combining bioactive glass micro/nanoparticles with natural/synthetic polymers. Bioactive glasses have shown the potential of use for soft tissue engineering due to their multifunctional properties, including hemostatic ability, anti-inflammatory properties, antibacterial properties, stimulatory effect on angiogenesis, and improving cell functions such as keratinocyte and fibroblast proliferation and migration. Consequently, these biological effects of bioactive glasses have inspired researchers to investigate novel formulations of glasses and incorporate them into the polymeric matrix to fabricate biocomposites for enhancing wound closure. However, more research still needs to be undertaken to tailor the biological, physicochemical, and mechanical properties of bioactive glass-containing composites according to the requirements of wound healing. Moreover, the addition of an optimal amount of bioactive glass in the polymeric matrix is another important aspect of designing biocomposites due to the importance of avoiding cytotoxicity as well as determining the optimum concentration of glass dissolution products for proper cellular functions in the healing process.

References

[1] D. Simões, S.P. Miguel, M.P. Ribeiro, P. Coutinho, A.G. Mendonça, I.J. Correia, Recent advances on antimicrobial wound dressing : A review, European Journal of Pharmaceutics and Biopharmaceutics. 127 (2018) 130–141. doi:10.1016/j.ejpb.2018.02.022.

[2] H. Savoji, B. Godau, M.S. Hassani, M. Akbari, Skin Tissue Substitutes and Biomaterial Risk Assessment and Testing, Frontiers in Bioengineering and Biotechnology. 6 (2018) 1–18. doi:10.3389/fbioe.2018.00086.

[3] A. Chaudhari, K. Vig, D. Baganizi, R. Sahu, S. Dixit, V. Dennis, S. Singh, S. Pillai, Future Prospects for Scaffolding Methods and Biomaterials in Skin Tissue Engineering: A Review, International Journal of Molecular Sciences. 17 (2016) 1974. doi:10.3390/ijms17121974.

[4] H. Sorg, D.J. Tilkorn, S. Hager, J. Hauser, U. Mirastschijski, Skin Wound Healing: An Update on the Current Knowledge and Concepts, European Surgical Research. 58 (2017) 81–94. doi:10.1159/000454919.

[5] K.G. Harding, Science, medicine, and the future: Healing chronic wounds, BMJ. 324 (2002) 160–163. doi:10.1136/bmj.324.7330.160.

[6] A.M. Writers, Select appropriate wound dressings by matching the properties of the dressing to the type of wound, Drugs & Therapy Perspectives. 30 (2014) 213–217. doi:10.1007/s40267-014-0125-5.

[7] R.F. Pereira, P.J. Bártolo, Traditional Therapies for Skin Wound Healing, Advances in Wound Care. 5 (2016) 208–229. doi:10.1089/wound.2013.0506.

[8] K. Vig, A. Chaudhari, S. Tripathi, S. Dixit, R. Sahu, S. Pillai, V. Dennis, S. Singh, Advances in Skin Regeneration Using Tissue Engineering, International Journal of Molecular Sciences. 18 (2017) 789. doi:10.3390/ijms18040789.

[9] L.L. Hench, R.J. Splinter, W.C. Allen, T.K. Greenlee, Bonding mechanisms at the interface of ceramic prosthetic materials, Journal of Biomedical Materials Research. 5 (1971) 117–141. doi:10.1002/jbm.820050611.

[10] L.L. Hench, Biomaterials: a forecast for the future, Biomaterials. 19 (1998) 1419–1423. doi:10.1016/S0142-9612(98)00133-1.

[11] Q. Chen, L. Jin, W.D. Cook, D. Mohn, E.L. Lagerqvist, D.A. Elliott, J.M. Haynes, N. Boyd, W.J. Stark, C.W. Pouton, E.G. Stanley, A.G. Elefanty, Elastomeric nanocomposites as cell delivery vehicles and cardiac support devices, Soft Matter. 6 (2010) 4715–4726. doi:10.1039/c0sm00213e.

[12] N.Y. Joo, J.C. Knowles, G.S. Lee, J.W. Kim, H.W. Kim, Y.J. Son, J.K. Hyun, Effects of phosphate glass fiber-collagen scaffolds on functional recovery of completely transected rat spinal cords, Acta Biomaterialia. 8 (2012) 1802–1812. doi:10.1016/j.actbio.2012.01.026.

[13] A.R. Boccaccini, J.J. Blaker, V. Maquet, R.M. Day, R. Jéróme, Preparation and characterisation of poly(lactide-co-grycolide) (PLGA) and PLGA/Bioglass® composite tubular foam scaffolds for tissue engineering applications, Materials Science and Engineering C. 25 (2005) 23–31. doi:10.1016/j.msec.2004.03.002.

[14] S. Verrier, J.J. Blaker, V. Maquet, L.L. Hench, A.R. Boccaccini, PDLLA/Bioglass® composites for soft-tissue and hard-tissue engineering: an in vitro cell biology assessment, Biomaterials. 25 (2004) 3013–3021. doi:10.1016/j.biomaterials.2003.09.081.

[15] M. Miola, Y. Pakzad, S. Banijamali, S. Kargozar, C. Vitale-Brovarone, A. Yazdanpanah, O. Bretcanu, A. Ramedani, E. Vernè, M. Mozafari, Glass-ceramics for cancer treatment: So close, or yet so far?, Acta Biomaterialia. 83 (2019) 55–70. doi:10.1016/j.actbio.2018.11.013.

[16] R.L. Gillette, S.F. Swaim, E.A. Sartin, D.M. Bradley, S.L. Coolman, Effects of a bioactive glass on healing of closed skin wounds in dogs, American Journal of Veterinary Research. 62 (2001) 1149–1153. doi:10.2460/ajvr.2001.62.1149.

[17] P. Taylor, "Cotton candy" that heals ?, American Ceramic Society Bulletin. 90 (2010) 25–29.

[18] S. Naseri, W.C. Lepry, S.N. Nazhat, Bioactive glasses in wound healing: hope or hype?, Journal of Materials Chemistry B. 5 (2017) 6167–6174. doi:10.1039/C7TB01221G.

[19] T. Mehrabi, A.S. Mesgar, Z. Mohammadi, Bioactive Glasses: A Promising Therapeutic Ion Release Strategy for Enhancing Wound Healing, ACS Biomaterials Science & Engineering. 6 (2020) 5399–5430. doi:10.1021/acsbiomaterials.0c00528.

[20] S. Chen, Z. Huan, L. Zhang, J. Chang, The clinical application of a silicate-based wound dressing (DermFactor®) for wound healing after anal surgery: A randomized study, International Journal of Surgery. 52 (2018) 229–232. doi:10.1016/j.ijsu.2018.02.036.

[21] F. Baino, S. Hamzehlou, S. Kargozar, Bioactive Glasses: Where Are We and Where Are We Going?, Journal of Functional Biomaterials. 9 (2018) 25. doi:10.3390/jfb9010025.

[22] R.K. Brow, Structures of glasses, in: J.E. Shelby (Ed.), Introduction to Glass Science and Technology, Royal Society of Chemistry, Cambridge, 2007: pp. 72–110. doi:10.1039/9781847551160-00072.

[23] D.C. Boyd, P.S. Danielson, D.A. Thompson, M. Velez, S.T. Reis, R.K. Brow, Glass, in: Kirk-Othmer Encyclopedia of Chemical Technology, Wiley, Hoboken, NJ, USA, 2004: pp. 284–319. doi:10.1002/0471238961.0712011902152504.a01.pub2.

[24] A.C. da Silva, Structure and Percolation of Bioglasses, in: J. Marchi (Ed.), Biocompatible Glasses From Bone Regeneration to Cancer Treatment, Springer, Switzerland, 2016: pp. 49–84. doi:10.1007/978-3-319-44249-5_3.

[25] D.S. Brauer, D. Möncke, Introduction to the Structure of Silicate, Phosphate and Borate Glasses, in: A.R. Boccaccini, D.S. Brauer, L. Hupa (Eds.), Bioactive Glasses: Fundamentals, Technology and Applications, The Royal Society of Chemistry, Cambridge, UK, 2017: pp. 61–88. doi:10.1039/9781782622017-00061.

[26] R.K. Brow, Review: the structure of simple phosphate glasses, Journal of Non-Crystalline Solids. 263–264 (2000) 1–28. doi:10.1016/S0022-3093(99)00620-1.

[27] A.C. Julian Jones, ed., Bio-Glasses: An Introduction, Wiley, 2012.

[28] H.R. Fernandes, A. Gaddam, A. Rebelo, D. Brazete, G.E. Stan, J.M.F. Ferreira, Bioactive Glasses and Glass-Ceramics for Healthcare Applications in Bone Regeneration and Tissue Engineering, Materials. 11 (2018) 2530. doi:10.3390/ma11122530.

[29] M. Bengisu, Borate glasses for scientific and industrial applications: a review, Journal of Materials Science. 51 (2016) 2199–2242. doi:10.1007/s10853-015-9537-4.

[30] D.S. Brauer, Phosphate Glasses, in: Bio-Glasses, John Wiley & Sons, Ltd, Chichester, UK, 2012: pp. 45–64. doi:10.1002/9781118346457.ch4.

[31] J.R. Jones, Reprint of: Review of bioactive glass: From Hench to hybrids, Acta Biomaterialia. 23 (2015) S53–S82. doi:10.1016/j.actbio.2015.07.019.

[32] G. Kaur, O.P.O.P. Pandey, K. Singh, D. Homa, B. Scott, G. Pickrell, A review of bioactive glasses: Their structure, properties, fabrication and apatite formation, Journal of Biomedical Materials Research Part A. 102 (2014) 254–274. doi:10.1002/jbm.a.34690.

[33] G. Palareti, C. Legnani, B. Cosmi, E. Antonucci, N. Erba, D. Poli, S. Testa, A. Tosetto, Comparison between different D-Dimer cutoff values to assess the individual risk of recurrent venous thromboembolism: analysis of results obtained in the DULCIS study, International Journal of Laboratory Hematology. 38 (2016) 42–49. doi:10.1111/ijlh.12426.

[34] R. Li, A.E. Clark, L.L. Hench, An investigation of bioactive glass powders by sol-gel processing, Journal of Applied Biomaterials. 2 (1991) 231–239. doi:10.1002/jab.770020403.

[35] W.C. Lepry, S.N. Nazhat, Highly Bioactive Sol-Gel-Derived Borate Glasses, Chemistry of Materials. 27 (2015) 4821–4831. doi:10.1021/acs.chemmater.5b01697.

[36] F. Foroutan, B.A. Kyffin, I. Abrahams, A. Corrias, P. Gupta, E. Velliou, J.C. Knowles, D. Carta, Mesoporous Phosphate-Based Glasses Prepared via Sol–Gel, ACS Biomaterials Science & Engineering. 6 (2020) 1428–1437. doi:10.1021/acsbiomaterials.9b01896.

[37] L.L. Hench, J.K. West, The sol-gel process, Chemical Reviews. 90 (1990) 33–72. doi:10.1021/cr00099a003.

[38] K. Zheng, A.R. Boccaccini, Sol-gel processing of bioactive glass nanoparticles: A review, Advances in Colloid and Interface Science. 249 (2017) 363–373. doi:10.1016/j.cis.2017.03.008.

[39] L.L. Hench, J. Wilson, Introduction, in: L.L. Hench (Ed.), An Introduction to Bioceramics, 2nd ed., Imperial College Press, London, UK, 2013: pp. 1–26. doi:10.1142/p884.

[40] J.R. Jones, L.M. Ehrenfried, L.L. Hench, Optimising bioactive glass scaffolds for bone tissue engineering, Biomaterials. 27 (2006) 964–973. doi:10.1016/j.biomaterials.2005.07.017.

[41] R. Chitturi, V.R. Baddam, L. Prasad, L. Prashanth, K. Kattapagari, A review on role of essential trace elements in health and disease, Journal of Dr. NTR University of Health Sciences. 4 (2015) 75. doi:10.4103/2277-8632.158577.

[42] I. Uluisik, H.C. Karakaya, A. Koc, The importance of boron in biological systems, Journal of Trace Elements in Medicine and Biology. 45 (2018) 156–162. doi:10.1016/j.jtemb.2017.10.008.

[43] R.M. Nzietchueng, B. Dousset, P.P. Franck, M. Benderdour, P. Nabet, K. Hess, Mechanisms implicated in the effects of boron on wound healing, Journal of Trace Elements in Medicine and Biology. 16 (2002) 239–244. doi:10.1016/S0946-672X(02)80051-7.

[44] N. Chebassier, E.H. Ouijja, I. Viegas, B. Dreno, Stimulatory Effect of Boron and Manganese Salts on Keratinocyte Migration, Acta Dermato-Venereologica. 84 (2004) 191–194. doi:10.1080/00015550410025273.

[45] S. Demirci, A. Doğan, E. Karakuş, Z. Halıcı, A. Topçu, E. Demirci, F. Sahin, Boron and Poloxamer (F68 and F127) Containing Hydrogel Formulation for Burn Wound Healing, Biological Trace Element Research. 168 (2015) 169–180. doi:10.1007/s12011-015-0338-z.

[46] A.B.G.G. Lansdown, Calcium: a potential central regulator in wound healing in the skin, Wound Repair and Regeneration. 10 (2002) 271–285. doi:10.1046/j.1524-475X.2002.10502.x.

[47] T. Wang, Q. Gu, J. Zhao, J. Mei, M. Shao, Y. Pan, J. Zhang, H. Wu, Z. Zhang, F. Liu, Calcium alginate

enhances wound healing by up-regulating the ratio of collagen types I/III in diabetic rats., International Journal of Clinical and Experimental Pathology. 8 (2015) 6636–6645. http://www.ncbi.nlm.nih.gov/pubmed/26261545.

[48] C. Navarro-Requena, S. Pérez-Amodio, O. Castaño, E. Engel, O. Castano, E. Engel, Wound healing-promoting effects stimulated by extracellular calcium and calcium-releasing nanoparticles on dermal fibroblasts, Nanotechnology. 29 (2018) 395102. doi:10.1088/1361-6528/aad01f.

[49] C. Xu, X. Qu, Cerium oxide nanoparticle: a remarkably versatile rare earth nanomaterial for biological applications, NPG Asia Materials. 6 (2014) e90–e90. doi:10.1038/am.2013.88.

[50] H. Kaygusuz, E. Torlak, G. Akın-Evingür, İ. Özen, R. von Klitzing, F.B. Erim, Antimicrobial cerium ion-chitosan crosslinked alginate biopolymer films: A novel and potential wound dressing, International Journal of Biological Macromolecules. 105 (2017) 1161–1165. doi:10.1016/j.ijbiomac.2017.07.144.

[51] C. Lang, C. Murgia, M. Leong, L.-W. Tan, G. Perozzi, D. Knight, R. Ruffin, P. Zalewski, Anti-inflammatory effects of zinc and alterations in zinc transporter mRNA in mouse models of allergic inflammation, American Journal of Physiology-Lung Cellular and Molecular Physiology. 292 (2007) L577–L584. doi:10.1152/ajplung.00280.2006.

[52] S. Chigurupati, M.R. Mughal, E. Okun, S. Das, A. Kumar, M. McCaffery, S. Seal, M.P. Mattson, Effects of cerium oxide nanoparticles on the growth of keratinocytes, fibroblasts and vascular endothelial cells in cutaneous wound healing, Biomaterials. 34 (2013) 2194–2201. doi:10.1016/j.biomaterials.2012.11.061.

[53] S. Kargozar, F. Baino, S. Hamzehlou, R.G. Hill, M. Mozafari, Bioactive Glasses: Sprouting Angiogenesis in Tissue Engineering, Trends in Biotechnology. 36 (2018) 430–444. doi:10.1016/j.tibtech.2017.12.003.

[54] A.P. Kornblatt, V.G. Nicoletti, A. Travaglia, The neglected role of copper ions in wound healing, Journal of Inorganic Biochemistry. 161 (2016) 1–8. doi:10.1016/j.jinorgbio.2016.02.012.

[55] F. Zhao, B. Lei, X. Li, Y. Mo, R. Wang, D. Chen, X. Chen, Promoting in vivo early angiogenesis with sub-micrometer strontium-contained bioactive microspheres through modulating macrophage phenotypes, Biomaterials. 178 (2018) 36–47. doi:10.1016/j.biomaterials.2018.06.004.

[56] T.A. Ostomel, Q. Shi, C.-K.K. Tsung, H. Liang, G.D. Stucky, Spherical Bioactive Glass with Enhanced Rates of Hydroxyapatite Deposition and Hemostatic Activity, Small. 2 (2006) 1261–1265. doi:10.1002/smll.200600177.

[57] D. Zhang, O. Leppäranta, E. Munukka, H. Ylänen, M.K. Viljanen, E. Eerola, M. Hupa, L. Hupa, Antibacterial effects and dissolution behavior of six bioactive glasses, Journal of Biomedical Materials Research Part A. 93A (2009) 475–483. doi:10.1002/jbm.a.32564.

[58] L. Drago, M. Toscano, M. Bottagisio, Recent Evidence on Bioactive Glass Antimicrobial and Antibiofilm Activity: A Mini-Review, Materials. 11 (2018) 326. doi:10.3390/ma11020326.

[59] S. Pourshahrestani, E. Zeimaran, N. Adib Kadri, N. Gargiulo, S. Samuel, S.V. Naveen, T. Kamarul, M.R. Towler, Gallium-containing mesoporous bioactive glass with potent hemostatic activity and antibacterial efficacy, Journal of Materials Chemistry B. 4 (2016) 71–86. doi:10.1039/C5TB02062J.

[60] X. Dong, J. Chang, H. Li, A. Manuscript, X. Dong, J. Chang, H. Li, Bioglass promotes wound healing through modulating the paracrine effects between macrophages and repairing cells Xin, Journal of Materials Chemistry B. 5 (2017) 5240–5250. doi:10.1039/C7TB01211J.

[61] H. Agarwal, V. Shanmugam, A review on anti-inflammatory activity of green synthesized zinc oxide nanoparticle: Mechanism-based approach, Bioorganic Chemistry. 94 (2020) 103423. doi:10.1016/j.bioorg.2019.103423.

[62] K. Zheng, E. Torre, A. Bari, N. Taccardi, C. Cassinelli, M. Morra, S. Fiorilli, C. Vitale-Brovarone, G. Iviglia, A.R. Boccaccini, Antioxidant mesoporous Ce-doped bioactive glass nanoparticles with anti-inflammatory and pro-osteogenic activities, Materials Today Bio. 5 (2020) 100041. doi:10.1016/j.mtbio.2020.100041.

[63] S.M. Mârza, K. Magyari, S. Bogdan, M. Moldovan, C. Peştean, A. Nagy, F. Tăbăran, E. Licarete, S. Suarasan, A. Dreanca, L. Baia, I. Papuc, Skin wound regeneration with bioactive glass-gold nanoparticles ointment, Biomedical Materials. 14 (2019) 025011. doi:10.1088/1748-605X/aafd7d.

[64] S. Zhao, L. Li, H. Wang, Y. Zhang, X. Cheng, N. Zhou, M.N. Rahaman, Z. Liu, W. Huang, C. Zhang, Wound dressings composed of copper-doped borate bioactive glass microfibers stimulate angiogenesis and heal full-thickness skin defects in a rodent model, Biomaterials. 53 (2015) 379–391. doi:10.1016/j.biomaterials.2015.02.112.

[65] R.J. Bodnar, Chemokine Regulation of Angiogenesis During Wound Healing, Advances in Wound Care. 4 (2015) 641–650. doi:10.1089/wound.2014.0594.

[66] A.A. Gorustovich, J.A. Roether, A.R. Boccaccini, D. Ph, Effect of Bioactive Glasses on Angiogenesis: A Review of In Vitro and In Vivo Evidences, Tissue Engineering Part B: Reviews. 16 (2010) 199–207. doi:10.1089/ten.teb.2009.0416.

[67] W. Ma, X. Yang, L. Ma, X. Wang, L. Zhang, G. Yang, C. Han, Z. Gou, Fabrication of bioactive glass-introduced nanofibrous membranes with multifunctions for potential wound dressing, RSC Adv. 4 (2014) 60114–60122. doi:10.1039/C4RA10232K.

[68] Z. Lin, W. Gao, L. Ma, H. Xia, W. Xie, Y. Zhang, X. Chen, Preparation and properties of poly(ε-caprolactone)/bioactive glass nanofibre membranes for skin tissue engineering, Journal of Bioactive and Compatible Polymers. 33 (2018) 195–209. doi:10.1177/0883911517715659.

[69] Q. Chen, J. Wu, Y. Liu, Y. Li, C. Zhang, W. Qi, K.W.K. Yeung, T.M. Wong, X. Zhao, H. Pan, Electrospun chitosan/PVA/bioglass Nanofibrous membrane with spatially designed structure for accelerating chronic wound healing, Materials Science and Engineering: C. 105 (2019) 110083. doi:10.1016/j.msec.2019.110083.

[70] Y. Zhou, L. Gao, J. Peng, M. Xing, Y. Han, X. Wang, Y. Xu, J. Chang, Bioglass Activated Albumin Hydrogels for Wound Healing, Advanced Healthcare Materials. 7 (2018) 1800144. doi:10.1002/adhm.201800144.

[71] D. Li, G. Jiao, W. Zhang, X. Chen, R. Ning, C. Du, Hybrid scaffolding strategy for dermal tissue reconstruction: a bioactive glass/chitosan/silk fibroin composite, RSC Advances. 6 (2016) 19887–19896. doi:10.1039/C5RA26871K.

[72] K. Schuhladen, P. Mukoo, L. Liverani, Z. Neščáková, A.R. Boccaccini, Manuka honey and bioactive glass impart methylcellulose foams antibacterial effects for wound healing applications, Biomedical Materials. in press (2020) 1–31. doi:10.1088/1748-605X/ab87e5.

[73] W. Ma, X. Yang, L. Ma, X. Wang, L. Zhang, G. Yang, C. Han, Z. Gou, Fabrication of bioactive glass-introduced nanofibrous membranes with multifunctions for potential wound dressing, RSC Advances. 4 (2014) 60114–60122. doi:10.1039/c4ra10232k.

[74] S. Tansaz, M. Schulte, U. Kneser, D. Mohn, W. Stark, J.A. Roether, I. Cicha, A.R. Boccaccini, Soy protein isolate/bioactive glass composite membranes: Processing and properties, European Polymer Journal. 106 (2018) 232–241. doi:10.1016/j.eurpolymj.2018.07.003.

[75] L. Francis, D. Meng, I.C. Locke, J.C. Knowles, N. Mordan, V. Salih, A.R. Boccaccini, I. Roy, Novel poly(3-hydroxybutyrate) composite films containing bioactive glass nanoparticles for wound healing applications, Polymer International. 65 (2016) 661–674. doi:10.1002/pi.5108.

[76] L. Kong, Z. Wu, H. Zhao, H. Cui, J. Shen, J. Chang, H. Li, Y. He, Bioactive Injectable Hydrogels Containing Desferrioxamine and Bioglass for Diabetic Wound Healing, ACS Applied Materials & Interfaces. 10 (2018) 30103–30114. doi:10.1021/acsami.8b09191.

[77] Y. Zhu, Z. Ma, L. Kong, Y. He, H.F. Chan, H. Li, Modulation of macrophages by bioactive glass/sodium alginate hydrogel is crucial in skin regeneration enhancement, Biomaterials. 256 (2020) 120216. doi:10.1016/j.biomaterials.2020.120216.

[78] Y. Li, T. Xu, Z. Tu, W. Dai, Y. Xue, C. Tang, W. Gao, C. Mao, B. Lei, C. Lin, Bioactive antibacterial silica-based nanocomposites hydrogel scaffolds with high angiogenesis for promoting diabetic wound healing and skin repair, Theranostics. 10 (2020) 4929–4943. doi:10.7150/thno.41839.

[79] Q. Zeng, Y. Han, H. Li, J. Chang, Design of a thermosensitive bioglass/agarose–alginate composite hydrogel for chronic wound healing, Journal of Materials Chemistry B. 3 (2015) 8856–8864. doi:10.1039/C5TB01758K.

[80] A.M. El-Kady, A.A. Ali, A. El-Fiqi, Controlled delivery of therapeutic ions and antibiotic drug of novel

alginate-agarose matrix incorporating selenium-modified borosilicate glass designed for chronic wound healing, Journal of Non-Crystalline Solids. 534 (2020) 119889. doi:10.1016/j.jnoncrysol.2020.119889.